PATENT

IN THE UNITED STATES PATENT AND TRADEMARK OFFICE

Applicants	Rajagopalan et al.
Serial No.	10/808,184
Filing Date	March 24, 2004
Art Unit	1612
Confirmation No.	4580
Examiner	Packard, Benjamin J
Title	NOVEL AROMATIC AZIDES FOR TYPE I PHOTOTHERAPY
Attorney Docket No.	1486.1 H US (073979.68)

December 23, 2009

THIRD DECLARATION OF JOHN K. BUOLAMWINI, Ph.D.
UNDER 37 C.F.R. §1.132

I, John K. Buolamwini, declare as follows:

My credentials have been provided in my previous Declarations.

I understand that the Examiner holds the opinion that my June 29, 2009 Declaration was unconvincing because "there is no assertion as to what was known at the time of filing" and instead "is directed to what is now known".

This is inaccurate. In each of my June 29, 2009 and October 10, 2008 Declarations, I specifically noted the requirement that, for what I asserted was known, the relevant date of this knowledge was the filing date of the application:

> I understand that the Examiner holds the opinion that the specification does not disclose sufficient information so that one skilled in the art can reasonably conclude that the inventor had possession of the claimed invention at the time the application was filed, which is referred to as the "written description" requirement in the Office Action. (emphasis added)

I now reassert that the "required function" for the "E" portion of the formula is targeting, and that any compound that targets the claimed formula to a tissue or site containing a bombesin receptor, and hence that can be photoactivated at that site to effect therapy, meets the claimed limitation. A person of ordinary skill in this art, for example, a medicinal chemist, would have

known or could easily find, at the time the parent application, of which this application is a Division, was filed on January 19, 2001, the identity, characteristics, etc. of such molecules that bind the bombesin receptor. In the claims, such molecules are referred to as a "receptor binding molecules". I have described examples of such molecules on p. 3 of my October 10, 2008 Declaration. I understand that what is generally known in the art need not be detailed in the application.

In my opinion, Applicants' description of "bombesin (or other) receptor binding molecules" would have allowed me, at the time the application was filed, to quickly envisage compounds that would fit the definition of E in the claimed formula. It provides me with the identity of compounds that have the required structure, and it provides me with a "link" to distinguish those compounds that will target the compound to a bombesin-receptor, from those compounds that will not target the compound to a bombesin receptor. Thus, their use of the term "bombesin receptor binding molecules" indicates to me that the inventors were in possession of compounds that target and bind to the bombesin receptor at the time they filed the parent application. I stated this in another way in my October 10, 2008 Declaration, with new emphasis added to note the fact that I did address what was known at the time of the invention:

> I assert that the structure of the targeting group was sufficiently definite at the time of the invention. As a medicinal chemist who makes molecules that bind primarily to receptors or enzymes, I cannot immediately profane a molecule that binds to a receptor unless I have seen that molecule described as a ligand for the receptor, or I myself have made such a molecule. In the former case I can propose a potential ligand that will be a derivative or analog of an already known molecule. That does not mean that the molecule does not exist, however, and it does not mean that I cannot, by a single literature search, uncover it. It is reasonable that a chemist or medicinal chemist will perform a literature search to find a molecule that will bind a receptor. I assert that a bombesin receptor binding molecule is an art-recognized structural term. When one hears these as a medicinal chemist, one can envision such molecules [or identify them by a quick literature search]. For example, E could be an antibody or part of a monoclonal antibody–FAB fragment, there are methods for linking antibodies to other compounds, etc. (see Zhou et al., Clin. Cancer Res. 9 (2003) 4953).

To substantiate my opinion, my previous Declaration listed compounds that I would have known, at the time the application was filed, would bind the bombesin receptor, and thus fit the description of a "bombesin receptor binding molecule" These provided several such compounds, and I noted a review by Jensen et al., Pharmacol. Rev. 60 ((2008) 1-42. The 2008 review cited numerous references, only a few of which I have listed below (emphasis added and internal citations omitted), and attach to this Declaration, that predate the January 19, 2001 filing date of the parent of the pending application that support my assertion, e.g.,

> **Benya et al., 1995b, Expression and characterization of cloned human bombesin receptors. Mol. Pharmacol 47:10-20.**
>
> The human BB1 receptor as well as the rat BB1 receptor has a >100-fold higher affinity for NMB than for GRP (cited at Jensen p. 7, section E).

Both the human and rat BB1 receptors are rapidly internalized with receptor activation of the BB1 receptor (cited at Jensen p. 10 bottom right column, internal citations omitted).

...[GRP] had greater selectivity than bombesin analogs for the BB2 over the BB1...With the development of selective BB2 receptor antagonists and the increased use of BB2 selective ligands such as GRP, it became clear that a separate GRP-preferring receptor existed, even before the cloning of the mouse and human BB2 receptor in the early 1990s (cited at Jensen p. 12 bridging columns and top right column, internal citations omitted).

The human BB2 receptor and the rat, mouse, and guinea pig BB2 receptors have >50-fold higher affinity for GRP than for NMB (Fig. 2) (cited at Jensen p. 14 Section E).

Subsequent studies [to Coy's pseudopeptide studies] demonstrated that this [Ψ 13-14 bombesin] analog had 50- to 100-fold higher selectivity for the BB2 receptor in human or rat than the BB1 receptor (cited at Jensen p. 15 bottom right column).

A number of these [[desMet^{14}]Bn or [desMet^{27}]GRP] analogs have high potency for the BB2 receptor in all species studied and have high selectivity for the BB2 over the BB1 receptor. Two widely used antagonists in this class are [D-Phe^{8}]Bn$_{6-13}$ methyl ester or its analogs and *Ac-N*-GRP$_{20-26}$ ethyl ester with each having high affinity for the BB2 receptor (K_i 2-5 nM) ... (cited at Jensen p. 16 middle right column).

[D-pentafluoro-Phe^{6}, D-Ala^{11}]Bn$_{6-13}$ methyl ester not only retained high affinity for the BB2 receptor (K_i human BB2 0.9 nM; rat BB2 5 nM) but it also had >400- to 10,000-fold selectivity for the BB2 over the BB1 receptor in rat and human and 15-fold longer duration of action in vivo (Fig. 1).

Coy et al., (1988) Probing peptide backbone function in bombesin, a reduced peptide bond analogue with potent and specific receptor antagonist activity. J. Biol. Chem 263:5056-5060.

Binding studies and the development of highly selective antagonists established unequivocally the existence of two different classes of receptors in mammalian tissues mediating the actions of these peptides (cited at Jensen p. 4, bottom left column).

In 1988 Coy and coworkers reported a new class of BB2 receptor antagonists by substituting pseudopeptide bonds (Ψ bonds) (i.e., each CONH group one at a time replaced by CH_2NH) into the COOH terminus of bombesin, a strategy that had been used successfully to make antagonists for gastrin, secretin, and substance P (Fig. 1; Table 2). Two of the pseudopeptides were antagonists with the Ψ 13-14 analogs having a higher affinity than the Ψ 9-10 bond analog. This Ψ 13-14 bombesin analog was the first bombesin receptor antagonist described with an affinity <0.1 μM (cited at Jensen p. 15 bottom left column).

This [Ψ 13-14 bombesin analog] antagonist was shown to inhibit a number of BB2 receptor-stimulated processes including bombesin-stimulated enzyme secretion from isolated acini and growth of Swiss 3T3 cells as well as of various small cell lung cancer cell lines (cited at Jensen p. 15 bottom right column).

de Castiglione and Gozzini (1996) Bombesin receptor antagonists. Crit. Rev. Oncol. Hematol. 23:117-151.

Whereas the search for high-affinity receptor antagonists for the BB2 receptor has been very successful,... (cited at Jensen p. 7, section E.2. bottom right column)

There have been a large number of different compounds reported to function as BB2 receptor antagonists. They can be divided into six general classes of BB2 receptor antagonists (cited at Jensen p. 15 bridging columns).

The fourth class of BB2 receptor antagonists are all [desMet^{14}]Bn or [desMet^{27}]GRP analogs...

Eden et al., (1996) PD 1659 – the first high affinity non-peptide neuromedin-B (NMB) receptor selective antagonist. Bioorg Med Chem 6:2617-2622

Peptide antagonists of BB1 have been described, including PD 165929 and PD 168368, which have high affinity and selectivity for BB1 (cited at Jensen p. 15, left column, section 2.a.).

Frucht et al., (1992) Characterization of functional receptors for gastrointestinal hormones on human colon cancer cells. Cancer Res 52:1114-1122.

Bombesin and various frog peptides, including ranatensin, litorin, PG-L, and [Phe^{13}]bombesin also have high affinities for the BB2 receptor, whereas other frog peptides such as phyllolitorin, [Leu8] phyllolitorin, [Ser^{3}, Arg^{10}, Phe^{13}]-bombesin and *Xenopus* NMB have low affinities for this receptor (cited at Jensen bridging pp. 14-15).

Regarding my previous Declaration, the Examiner states that my

assertion that the skilled artisan would know or can easily find the identity, characteristics, etc of such molecules that target the bombesin receptor seems to be rebutted by the art submitted which antedate the application priority date, where at pg 33 last paragraph of the art, the Authors note unresolved issues including knowing what the structure of the natural ligand of the BB3 receptor is and even question whether an equivalence to the frog BB3 exists in humans and mammals. Where it is unclear what receptors exist, it is unclear how one can immediately envision targeting molecules for that general class of receptors.

I respectfully disagree. The section to which the Examiner refers is "Unresolved Nomenclature Issues". The first sentence, "The principal unresolved issue is that the natural ligand of the BB3 receptor remains unknown, and therefore its pharmacology and roles in normal physiology or pathological process is unknown", encompasses only one type of bombesin receptor (i.e., BB3). Because the article covers other types of bombesin receptors (e.g., BB1 and BB2), the lack of knowledge of the natural ligand for one type of receptor does not alter my position. The fact is that receptors that bind bombesin in human tissues and cells such as 3T3 cells, small cell lung cancer cells and breast cancer cells were known to exist, as well as

molecules that bound to those receptors, at the time the application was filed (Castiglione and Gozzini, Crit. Rev. Oncol. Hematol. 23 (1996) 117-151.

The Examiner's reference to the article's questioning "whether an equivalence to the frog BB3 exists in humans and mammals" also does not alter my position. Quoting from p. 33:

> Another unresolved issue is whether a receptor equivalent to the frog BB4 [not BB3] exists in human and mammals. Two studies have sought additional members of the bombesin receptor family, and none were found in mammals.

The fact that BB4 may not exist in human and mammals, and that further "additional members" may or may not exist in mammals, does not negate the presence of other bombesin receptor binding compounds for, e.g., BB1, BB2, and BB3. In my opinion, even "where it is unclear what receptors exist", as the Examiner states, is not an accurate representation of the authors' statement. The title of the review is "Mammalian Bombesin Receptors: Nomenclature, Distribution, Pharmacology, Signaling, and Functions in Normal and Disease States". In my opinion, the authors in the last section are noting, in the midst of myriad known facts about the bombesin receptor, some specific unresolved issues.

I understand the Examiner questions other terms of the pending claims which he states are not described, namely, somatostatin receptor binding molecules, ST receptor binding molecules, neurotensin receptor binding molecules, carbohydrate receptor binding molecules, steroid receptor binding molecule, and CCK receptor binding molecules. The Examiner states that, with respect to these binding molecules:

> ...the claims are directed to functional limitations with no structural description which might lead one of skill in the art to believe Applicant's [*sic*] were in possession of the genus instantly claimed.

I respectfully disagree, and provide support for my opinion that the inventors were in possession of the claimed method because binding molecules for each of these receptors were known as of January 19, 2001, the date the parent of the present application was filed. All references I cite are attached.

Somatostatin receptor binding molecules include somatostatin and somatostatin receptor analogs, octreotide, glycosylated somatostatin-14 (somatostatin-dextran^{70}), seglitide, peptides P587 and P829 (Vallabhajosula et al., J. Nuclear Med., 37 (1996) 1016).

ST receptor binding molecules include heat stable enterotoxin (ST) (Kuno, J. Biol Chem. 261 (1986) 1470; SEQ ID NOS.:2, 3, 4, 5, and 12 from Waldman U.S. Patent No. 5,518,888; and guanylin (Currie et al., Proc. Natl. Acad. Sci. USA, 89 (1992) 947.

Neurotensin receptor binding molecules include neurotensin, neuromedin N, JMV449 (*H*-Lysψ(CH_2NH)-Lys-Pro-Tyr-Ile-Leu), the non-peptide antagonist SR142948A (2-([5-(2,6-dimethoxyphenyl)-1-(4-(*N*-[3-dimethylaminopropyl]-*N*-methylcarbamoyl)-2-isopropylphenyl)-1*H*-pyrazole-3-carbonyl)amino)adamantine-2-carboxylic acid hydrochloride) (Betancur et al., Eur. J. Pharmacol. 343 (1998) 67, SR 48692 (2-[1-(7-chloro-4-quinolinyl)-5-(2,6-

dimethoxyphenyl)pyrazol-3-yl)carbonylamino]tricycle[3.3.1.1.^{3,7}]decan-2-carboxylic acid) (Gully et al., Biochem. Pharmacol. *Proc. Natl. Acad. Sci. USA* 90 (1993) 65) and levocobastine (Kitabgi et al. Eur. J. Pharmacol. 140 (1987) 285). There are neurotensin receptor binding kits to evaluate potential neurotensin receptor binding compounds (e.g., DELFIA Neurotensin Receptor Binding Kit, PerkinElmer (Boston MA)).

One example of a carbohydrate receptor is a glucose receptor. The glucose conjugate N-palmitoyl glucosamine [NPG] was known to bind the glucose receptor (Dufes et al., Pharm. Res. 17 (2000) 1250). The glycoprotein hormone receptor is another example of a carbohydrate receptor to which carbohydrate receptor binding molecules bind. Follicle stimulating hormone (FSH) is known to bind the glycoprotein hormone receptor (Tilly et al., Endocrinology 131 (1992) 799). Other compounds known to bind the carbohydrate receptor, and hence examples of carbohydrate receptor binding molecules, are polysialic acid, bacterial adhesins (specialized surface proteins that mediate binding of many pathogenic bacteria, such as enterohemorrhagic *E. coli* (EHEC) and *Shigella dysenteria*, to host cells, which allows these bacteria to colonize host cell surfaces), soluble carbohydrate receptor analogs, artificial glycopolymers and other multivalent glycoconjugates such as an acrylamide copolymer carrying -L-fucopyranoside and 3-sulfo--D-galactopyranoside in clusters, isomeric carbohydrates, synthetic derivatives, neoglycoproteins, neoglycolipids, glycosidases, and glycosyltransferases. Carbohydrate binding proteins can be screened with phage display libraries.

One example of a steroid receptor is an estrogen receptor. The following compounds were known to bind to the estrogen receptor as of January 19, 2001: estratriol, 17β-aminoestrogen (AE) derivatives such as prolame and butolame; drugs such as tamoxifen, ICI-164384, raloxifene, genistein; 17β-estradiol; glucocorticoids, progesterone, estrogens, retinoids, fatty acid derivatives, phytoestrogens, etc. Commercially available kits identify compounds specific for binding to the estrogen receptor (e.g., Estrogen Receptor-alpha Competitor Assay Kit, Red; Estrogen Receptor-beta Competitor Assay Kit, Red (Invitrogen Corp., Carlsbad CA).

Cholecystokinin receptor binding molecules include the endogenous peptides cholecystokinin (CCK)-4, CCK-8, CCK-33, and gastrin; antagonists devazepide and lorglumide (Bishop et al., Br. J. Pharmacol. 106 (1992) 61; agonists BC264 [Tyr(SO_3H)-gNle-mGly-Trp-(NMe)Nle-Asp-Phe-NH_3] (Ladurelle et al., Brain Res. 628 (1993) 254), and desulfated CCK-8; Kinevac (synthetic cholecystekinin, sincalide); and CCK analogues modified at the sulfated tyrosyl at position 27. Other benzodiazepine CCK receptor binding molecules have also been reported (Semple et al., J. Med. Chem. 40 (1997) 331).

Finally, in the Office Action at p. 4 ¶2, the Examiner makes the point that the term "derives" has been used to modify aromatic and heteroaromatic radicals, and it is unclear how far the radicals can be derived and still have sufficient written description. The word "derives" as used in that context, to my understanding, refers to the specific chemical structural classes of the

aromatic or heteroaromatic radical from which to choose the Ar radical. Thus, the defined chemical structural classes from which the aromatic radical is chosen are indicated. The essential thing is the extended conjugated systems in these structures that make them chromophores and able to absorb light energy from irradiation. As a medicinal chemist, I understand to choose an Ar from any of the defined structural classes indicated by the designations.

For at least the reasons I have set forth, I respectfully assert that the inventors were in possession of their invention at the time they filed their application and that the claims are sufficiently described.

I hereby declare that all statements made herein of my own knowledge are true and that all statements made on information and belief are believed to be true; and further that these statements were made with the knowledge that willful false statements and the like so made are punishable by fine or imprisonment or both, under §1001 of Title 18 of the United States Code and that such willful false statements may jeopardize the validity of the subject application or any patent issued thereon.

12/23/09
Date

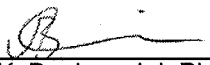

John K. Buolamwini, Ph.D.

752292

0026-895X/95/010010-11$03.00/0

MOLECULAR PHARMACOLOGY, 47:10-20, 1995.

Expression and Characterization of Cloned Human Bombesin Receptors

RICHARD V. BENYA, TAKASHI KUSUI, TAPAS K. PRADHAN, JAMES F. BATTEY, and ROBERT T. JENSEN

Digestive Diseases Branch, National Institute of Diabetes and Digestive and Kidney Diseases (R.V.B., T.K., T.K.P., R.T.J.), and Laboratory of Biological Chemistry, Developmental Therapeutics Program, National Cancer Institute (J.F.B.), National Institutes of Health, Bethesda, Maryland 20892

Received June 6, 1994; Accepted October 20, 1994

SUMMARY

Little is known about the pharmacology or cell biology of human bombesin (Bn) receptors, because they are usually present at low levels and both subtypes are frequently present in the same tissues. Human gastrin-releasing peptide (GRP) receptors (huGRP-R) and human neuromedin B (NMB) receptors (huNMB-R) were stably transfected into BALB/3T3 fibroblasts. Both receptor types were glycosylated, with 35% of the huGRP-R and 38% of the huNMB-R representing carbohydrate residues. The extent of glycosylation of the transfected huGRP-R was the same as that seen in the human glioblastoma cell line U-118. Radiolabeled agonist ligands were rapidly internalized, whereas noninternalized ligand readily dissociated in a temperature-dependent fashion. The affinities of various agonists for binding to the huGRP-R were Bn (K_i = 1.4 ± 0.2 nM) = 4 × GRP = 300 × NMB. In contrast, affinities for the huNMB-R were NMB (K_i = 8.1 ± 5.2 nM) = 4 × Bn = 600 × GRP. [F_5-D-Phe^6,D-Ala^{11}]Bn(6–13)methyl ester was the most potent huGRP-R antagonist, whereas D-Nal-Cys-Tyr-D-Trp-Lys-Val-Cys-Nal-NH_2 was the most potent huNMB-R antagonist. Agonist binding to either receptor type caused activation of phospholipase C and increased cellular [^{3}H]inositol phosphate levels. GRP was potent at increasing [^{3}H]inositol phosphate generation in cells expressing the huGRP-R (EC_{50} = 13.6 ± 1.3 nM), whereas NMB was similarly potent when acting upon cells expressing the huNMB-R (EC_{50} = 9.3 ± 1.4 nM). However, neither receptor type, when stimulated with agonist, caused an increase in cAMP levels. These data show that stably transfected huGRP-R exhibit similar pharmacology for agonists and antagonists, are appropriately glycosylated, and function similarly with respect to their ability to alter biological activity, compared with natively expressed receptors. Minimal native huNMB-R data are available for comparison, but in general the huNMB-R is similar to the rat NMB receptor in its pharmacology and cell biology.

Bn-related peptides act on diverse tissues, including the central nervous system [regulating satiety (1), thermoregulation (2), and circadian rhythm (3)] and the gastrointestinal tract [regulating pancreatic secretion (4), smooth muscle contractility (5), and the release of other gastrointestinal peptides (6)], and are involved in development [stimulating growth of chondrocytes *in utero* (7) and participating in normal lung development (8)]. Bn-related peptides also are involved in the regulation of thyrotropin release (9) and in immune function [stimulating chemotaxis and increasing natural killer cell activity and antibody-dependent cellular cytoxicity (10)] and function as potent growth factors for both normal and neoplastic tissues (11, 12).

In mammals the actions of the amphibian peptides Bn, litorin, and ranatensin are mediated by GRP and NMB. By pharmacological, functional, and cloning studies, these actions are now known to be mediated by two classes of receptors, the GRP-R and the NMB-R, which are widely expressed in the central nervous system and peripheral tissues (13). Each of these receptors is linked to activation of phospholipase C, whereas activation of the GRP-R in some cell types also acts to increase cAMP levels (12, 14). Activation of both receptor subtypes results in receptor internalization, down-regulation, and desensitization (12, 15). Recently, the huGRP-R and huNMB-R have been cloned and sequenced (16).

Although extensive information is available on the effects of this family of peptides in various species, including their possible physiological functions and pharmacological actions (11), relatively few such studies exist for humans. Recent studies show that Bn-related peptides in humans are potent satiety factors (17), can stimulate the release of different peptides (6), and can function as potent growth factors in various human tumors, including human small cell lung cancer cells, breast cancer cells, and prostatic adenocarcinoma cells (11, 18, 19).

ABBREVIATIONS: Bn, bombesin; GRP, gastrin-releasing peptide; NMB, neuromedin B; GRP-R, gastrin-releasing peptide receptor(s); NMB-R, neuromedin B receptor(s); huGRP-R, human gastrin-releasing peptide receptor(s); huNMB-R, human neuromedin B receptor(s); PNGase F, peptide-*N*^{4}-(acetyl-β-glucosaminyl)asparagine amidase; DSS, disuccinimidyl suberate; MBS, *m*-maleimidobenzoyl-*N*-hydroxysuccinimide; DMEM, Dulbecco's modified essential medium; cyclo-SS-octa, D-Nal-Cys-Tyr-D-Trp-Lys-Val-Cys-Nal-NH_2; IP, inositol phosphates; [Ca^{2+}]$_i$, intracellular calcium concentration; SDS, sodium dodecyl sulfate; EGTA, ethylene glycol bis(β-aminoethyl ether)-*N*,*N*,*N*′,*N*′-tetraacetic acid; HEPES, 4-(2-hydroxyethyl)-1-piperazineethanesulfonic acid.

However, little else is known about the action of GRP and NMB in humans. Understanding the pharmacological and cellular bases of action of these peptides and their receptors in humans, and not relying on data derived from nonhuman animals, is important for a number of reasons. Recent studies demonstrate that a number of gastrointestinal peptides may have different structure-function relationships in different species, with a given compound functioning as an agonist in one species but as an antagonist in another (20); therefore, extrapolation of animal-derived data to human tissues is not always correct. Furthermore, existing cell lines expressing human Bn receptors usually express both Bn receptor types, thus limiting their usefulness for exploring the specific characteristics of either the huGRP-R or the huNMB-R. The availability of cells possessing a homogeneous population of either huGRP-R or huNMB-R would allow their pharmacology, regulation, signal transduction properties, and cell biology to be explored. In addition, cells expressing such a homogeneous population of receptors would be useful for the screening of potential human Bn receptor antagonists.

In the current study we have stably expressed the huGRP-R and huNMB-R in murine BALB/3T3 cells, thereby facilitating the exploration of their pharmacology as well as the cellular basis of their action. We selected BALB/3T3 cells as hosts for the huGRP-R and huNMB-R because these cells do not express Bn receptors (14, 21) before transfection. Furthermore, recent detailed studies have demonstrated that, for both the murine GRP-R and the rat NMB-R, stable transfection of these receptors into this cell line yields receptors that are pharmacologically indistinguishable from their natively expressed counterparts (14, 21).

Experimental Procedures

Materials

Rat glioblastoma C_6 cells, human glioblastoma U-118 cells, and BALB/3T3 fibroblasts were obtained from the American Type Culture Collection (Rockville, MD), Swiss 3T3 fibroblasts were a gift from Dr. John Taylor (Biomeasure, Medford, MA), and DMEM, fetal bovine serum, and aminoglycoside G-418 were obtained from GIBCO (Waltham, MA).

Bovine serum albumin (fraction V) and HEPES were obtained from Boehringer Mannheim Biochemicals (Indianapolis, IN); soybean trypsin inhibitor, EGTA, trypsin, and bacitracin were obtained from Sigma Chemical Co. (St. Louis, MO); Bn, GRP, and NMB were obtained from Peninsula Laboratories (Belmont, CA); $Na^{125}I$ was from Amersham (Arlington Heights, IL); *myo*-[2-^{3}H]inositol (16–20 Ci/mmol) and cAMP radioimmunoassay reagents were from New England Nuclear (Boston, MA); Dowex AG 1-X8 anion exchange resin (100–200 mesh, formate form), SDS, and 2-mercaptoethanol were from Bio-Rad (Richmond, CA); Hydro-Fluor scintillation fluid, methanol, acetic acid, and hydrochloric acid were from the J. T. Baker Chemical Co. (Phillipsburg, NJ); PNGase F was from Genzyme (Cambridge, MA); cholera toxin and forskolin were from Calbiochem (San Diego, CA); and MBS and DSS were from Pierce Chemical Co. (Rockville, IL).

Methods

Transfection of cell lines. BALB/3T3 fibroblasts devoid of GRP-R and NMB-R were selected by clonal expansion after assaying for GRP-R or NMB-R by RNase protection and binding studies, as described previously (21). These BALB/3T3 cells were stably transfected using a full length huGRP-R clone (huGRP-R-transfected cells) (16) or using a full length huNMB-R clone (huNMB-R-transfected cells) (16). In both cases the receptor was subcloned into a modified version of the pCD2 plasmid and transfected using calcium phosphate precipitation. Stable transfectants were isolated in the presence of 800 μg/ml aminoglycoside G-418, identified by binding studies, and then maintained in DMEM containing 10% fetal bovine serum and 270 μg/ml G-418. Cells were passaged every 3–5 days at confluence by splitting 1:4.

Preparation of peptides. [D-Tyr^0]NMB, [F_5-D-Phe^6,D-Ala^{11}]-Bn(6–13)methyl ester, [Leu^{14},Ψ13–14]Bn, and cyclo-SS-octa were synthesized using solid-phase methods, as described previously. Peptides were purified on a 2.5- × 90-cm Sephadex G-25 column, followed by elution with a linear gradient consisting of acetonitrile and 0.1% trifluoroacetic acid, using an Eldex Chromatrol gradient controller and 1.5- × 50-cm Vydac C_{18} silica (10–15-mm) columns. Peptides were further purified by rechromatography on the same column when necessary, to >97% purity.

Binding studies. [^{125}I-D-Tyr^0]NMB (2200 Ci/mmol), ^{125}I-GRP (2200 Ci/mmol), and [^{125}I-Tyr^4]Bn (2000 Ci/mmol) were prepared using Iodo-Gen and purified using high pressure liquid chromatography, according to previously published methods (22). Binding studies were performed by suspending disaggregated cells in binding buffer containing 75 pM levels of either [^{125}I-D-Tyr^0]NMB or [^{125}I-Tyr^4]Bn and 3 × 10^6 cells/ml, for 30 min at 22°. Nonsaturable binding of either radiolabeled peptide was the amount of radioactivity associated with transfected cells when the incubation mixture contained either 1 μM NMB or 1 μM Bn. Nonsaturable binding was <10% of total binding in all experiments, and all values in this paper are reported as saturable binding.

Internalization of [^{125}I-D-Tyr^0]NMB or [^{125}I-Tyr^4]Bn. Cells were disaggregated, washed, and resuspended in binding buffer as described above, and then 3 × 10^6 cells/ml were incubated with 75 pM radiolabeled peptide for various times at 4°, 22°, or 37°. After incubation, 100-μl samples were added to 1.0 ml of 0.2 M acetic acid in 0.5 M NaCl, pH 2.5, for 5 min at 4°, to remove surface-bound radioligand, as described previously (14, 21, 22). In all cases, parallel incubations were conducted in the presence of 1 μM NMB or 1 μM Bn to determine changes in nonsaturable binding. Results are expressed as the percentage of saturably bound radiolabeled peptide that is internalized.

Cross-linking of huGRP-R and huNMB-R. Cell membranes were prepared by growing huGRP-R-transfected cells or huNMB-R-transfected cells to confluence, washing them once in binding buffer, and then resuspending them in homogenization buffer (50 mM Tris, pH 7.4, 5 mM $MgCl_2$, 0.2 mg/ml soybean trypsin inhibitor, 100 mM phenylmethylsulfonyl fluoride). Cells were homogenized on ice using a Polytron homogenizer (Beckman Instruments, Fullerton, CA) at speed 6 for 30 sec. The homogenate was then centrifuged at 1500 rpm for 10 min in a Sorval RC-5B Superspeed centrifuge (DuPont, Wilmington, DE); the supernatant was removed and recentrifuged at 20,000 rpm for 20 min. The pellet was resuspended in homogenization buffer and stored at −70°.

Cell homogenates were diluted to the concentration of 0.5 mg of protein/ml with homogenization buffer supplemented with 0.2% bovine serum albumin and 0.1% bacitracin. Aliquots (500 μl) were preincubated with 0.5 nM [^{125}I-D-Tyr^0]NMB or 0.5 nM ^{125}I-GRP at 22°, in 1.6-ml polypropylene tubes. After a 15-min incubation, the reaction mixture was centrifuged at 10,000 × *g* for 3 min. The pellet was washed twice in 1 ml of cross-linking buffer (50 mM HEPES, pH 7.5, 5 mM $MgCl_2$) (at 4°) and resuspended in 200 μl of cross-linking buffer containing 1 mM MBS as the cross-linking agent for huNMB-R or 1 mM DSS as the cross-linking agent for huGRP-R. After cross-linking at 22° for 30 min, the reaction was stopped by addition of 25 μl of 1 M glycine. After 10 min on ice, the sample was centrifuged at 10,000 × *g* for 3 min. The supernatant was aspirated and the pellet was resuspended in 100 μl of 120 mM Tris·HCl, pH 6.8. A 6-μl aliquot of the mixture was reserved to determine protein concentration. Cross-linked membranes were solubilized by addition of 25 μl of gel loading buffer (0.4 M Tris·HCl, pH 6.8, 20%, w/v, SDS, 50%, v/v, glycerol, 0.05%, w/v, bromphenol blue, 0.5 M dithiothreitol) at 22° for 60 min. After adjustment of the protein concentration, cell membranes (10 μg of

protein/lane) of either type were applied to the gel and were subjected to SDS-polyacrylamide gel electrophoresis. For the GRP-R-transfected cell membranes, the Laemmli buffer system (375 mM Tris·HCl, pH 8.8, 0.1% SDS, 10% acrylamide, for the gel; 25 mM Tris, 192 mM glycine, 0.1% SDS, for electrodes) was used, whereas for the NMB-R-transfected cell membranes the Weber and Osborn buffer system was used [100 mM sodium phosphate, 0.1% SDS, for the gel (6% acrylamide) and the electrodes] as described previously (23). In both cases electrophoresis was carried out at a constant current of 40 mA/gel. Gels were stained with 0.1% (w/v) Coomassie blue R-250 in 40% (v/v) ethanol/10% (v/v) acetic acid and destained with 10% (v/v) ethanol/7.5% (v/v) acetic acid. After overnight destaining, gels were equilibrated in 45% (v/v) ethanol/5% (v/v) glycerol for 30 min and dried in a slab gel drier (model SE 540; Hoefer Scientific Instruments, San Francisco, CA). Dried gels were exposed to storage phosphor screens for 3 days at 22° and processed using a PhosphorImager (Molecular Dynamics, Sunnyvale, CA).

PNGase F treatment of membrane receptor proteins. Cross-linked membrane proteins were denatured by a 3-min incubation at 95° in 80 μl of 50 mM Tris·HCl, pH 7.7, containing 50 mM EDTA, 50 mM 2-mercaptoethanol, and 0.5% (w/v) SDS. To a 20-μl aliquot containing 40 μg of membrane protein, 10 μl of 7.5% Nonidet P-40 were added. The mixture was incubated with 10 units/ml PNGase F, in a volume of 60 μl, for 18 hr at 37°. The reaction was halted using 4% SDS, and the samples were subsequently analyzed by SDS-polyacrylamide gel electrophoresis.

Measurement of phosphoinositides. Total phosphoinositides in cells transfected with either the huNMB-R or huGRP-R were determined as described previously, with minor modifications (14, 21, 22). Cells were grown to confluence in 24-well plates in regular medium and then were loaded for 24 hr at 37° with 100 Ci/ml *myo*-[2-^{3}H]inositol in DMEM containing 2% fetal bovine serum. Cells were washed and incubated in phosphoinositide buffer (binding buffer additionally containing 10 mM $LiCl_2$) for 15 min and then for 60 min at 37° with agonists at various concentrations. Reactions were halted by addition of 1% HCl in methanol, and total [^{3}H]IP were isolated by anion exchange chromatography as described previously (14, 21, 22).

Measurement of cAMP levels. Cells were mechanically disaggregated and washed twice in binding buffer. Cells (5×10^6/ml) were incubated with various peptides for 60 min at 37°, after which cAMP was solubilized by the addition of 2 volumes of ice-cold ethanol. Peptide effects were measured in the presence of 30 μM forskolin or 100 ng/ml cholera toxin. When forskolin was used cells were preincubated for 30 min with forskolin, and when cholera toxin was used cells were preincubated for 60 min with cholera toxin before exposure to peptide. cAMP was measured by radioimmunoassay as described previously (14), with all samples diluted so that the values remained in the linear portion of the standard curve.

Results

Initial studies were performed to confirm the presence of huGRP-R on huGPR-R-transfected cells and huNMB-R on huNMB-R-transfected cells and to structurally compare the receptors in the two cell types (Figs. 1 and 2). In huGRP-R-transfected cells a single broad protein band of 60 ± 1 kDa was cross-linked using ^{125}I-GRP (Fig. 1, *middle*), whereas for huNMB-R-transfected cells a single band of 72 ± 1 kDa was cross-linked using [^{125}I-D-Tyr^0]NMB (Fig. 2, *left*). Recently, some human small cell lung cancer cells and glioma and glioblastoma cell lines have been shown to possess GRP-R (24). To structurally compare the transfected huGRP-R with the native receptor, similar cross-linking studies were performed using the human glioblastoma cell line U-118. Similarly to the cells stably transfected with the huGRP-R, a single band of 60 ± 1 kDa was seen (Fig. 1, *left*). In contrast to the huGRP-R,

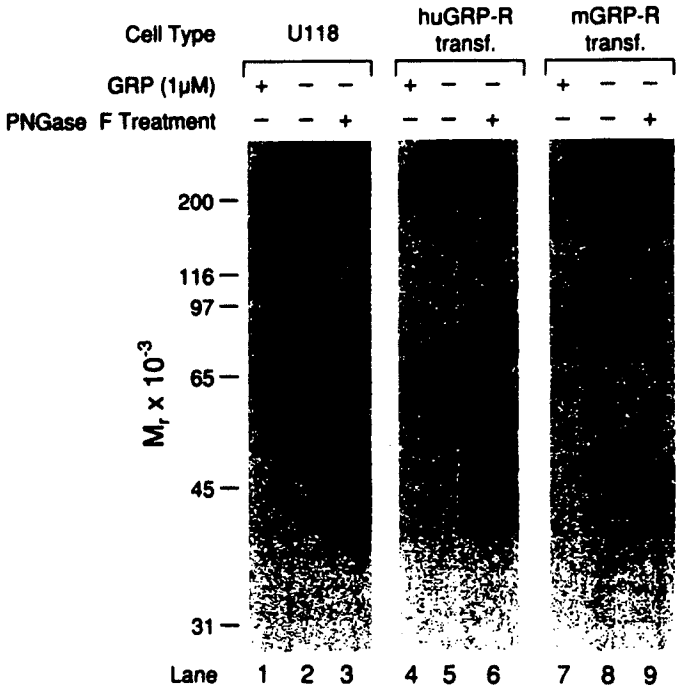

Fig. 1. Affinity labeling and deglycosylation of the huGRP-R on huGRP-R-transfected cells (*middle*) and human glioblastoma U-118 cell membranes (*left*) and of the mouse GRP-R on mouse GRP-R-transfected cell membranes (*right*). Membranes were prepared as outlined in Experimental Procedures. GRP-R cross-linking was performed using ^{125}I-GRP and radiolabeled peptide was cross-linked using 1 mM DSS, as described in Experimental Procedures, after binding in the presence or absence of 1 μM GRP. This experiment is representative of two others.

the mouse GRP-R transfected into the same BALB/3T3 cells gave a broad protein band of 822 kDa (Fig. 1, *right*), which is identical to the molecular mass of the GRP-R found in native murine Swiss 3T3 cells (14, 24). Although some human small cell lung cancer cell lines, including NCI-H209, NCI-510, and NCI-H1373, are reported to possess huNMB-R (16, 25), because of low receptor numbers an insufficient amount of binding of [^{125}I-D-Tyr^0]NMB to these cell lines was observed (data not shown) to allow cross-linking to be carried out, and therefore comparative data for a nontransformed, natively expressed, huNMB-R could not be obtained. With the rat NMB-R transfected into the same BALB/3T3 cells, a single broad protein band of 631 kDa was seen (Fig. 2, *right*), which was similar to the value reported for the native rat NMB-R on rat C_6 glioma cells. Treatment with PNGase F resulted in a deglycosylated receptor, with a molecular mass of 43 ± 1 kDa for the huGRP-R and mouse GRP-R for both the transfected cells and the glioblastoma cell line U-118 (Fig. 1) and with a molecular mass of 43 ± 1 kDa for the huNMB-R and rat NMB-R on transfected cells (Fig. 2). These values agree closely with the molecular masses of these receptors predicted from the amino acid sequence (16).

The time and temperature dependence of [^{125}I-Tyr^4]Bn binding to huGRP-R-transfected cells (Fig. 3, *left*) and that of [^{125}I-D-Tyr^0]NMB binding to huNMB-R-transfected cells (Fig. 3, *right*) were similar. For both cell types ligand binding was rapid at both 37° and 22°. Binding decreased with time for both cell types at 37°, whereas it remained relatively constant between 30 and 60 min of incubation at 22°. Half-maximal binding of radiolabeled ligand at 37° or 22° was observed

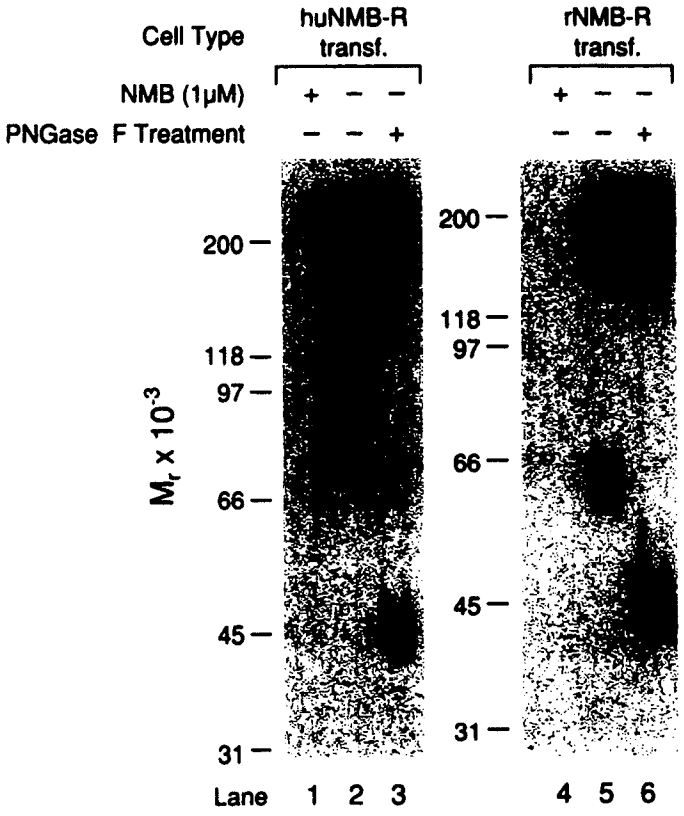

Fig. 2. Affinity labeling and deglycosylation of the hNMB-R on huNMB-R-transfected cells (*left*) and the rat NMB-R on rat NMB-R-transfected cells (*right*). NMB-R cross-linking was performed using [^{125}I-D-Tyr^0]NMB with 1 mM MBS, in the presence or absence of 1 μM NMB. After cross-linking, membranes were deglycosylated by incubation with 10 units/ml PGNase F, as described in Experimental Procedures. The experiment is representative of two others.

between 4 and 5 min for both cell types (Fig. 3). Reducing the incubation temperature to 4° resulted in a decreased rate and amount of binding to both cell types (Fig. 3). Addition of 1 μM Bn to huGRP-R-transfected cells incubated with [^{125}I-Tyr^4]Bn or addition of 1 μM NMB to huNMB-R-transfected cells incubated with [^{125}I-D-Tyr^0]NMB at 4°, 22°, or 37° reduced binding by >90% (Fig. 3).

To compare the ability of huNMB-R-transfected cells and huGRP-R-transfected cells to interact with the two naturally occurring mammalian Bn-related peptides, GRP and NMB, complete dose-inhibition studies for these agonists (Fig. 4) were performed. For huGRP-R-transfected cells, GRP was the most potent at inhibiting binding of [^{125}I-Tyr^4]Bn, causing detectable inhibition at 100 pM, half-maximal inhibition at approximately 3 nM, and complete inhibition at 1 μM (Fig. 4, *left*). To determine receptor affinity and number of binding sites, a saturation analysis was performed by adding increasing amounts of unlabeled peptide to a fixed concentration of radioligand. Analysis of the ability of Bn to inhibit [^{125}I-Tyr^4]Bn binding using the least-squares curve-fitting program LIGAND demonstrated that the data were best fit by a single binding site model (K_i = 1.4 ± 0.2 nM). Bn was 4-fold more potent than GRP (K_i = 6.2 ± 1.3 nM) (Table 1) and was >300-fold more potent than NMB (K_i = 437 ± 30 nM) (Table 1). In contrast, for huNMB-R-transfected cells NMB was the most potent at inhibiting the binding of [^{125}I-D-Tyr^0]NMB, with detectable inhibition being observed at 0.1 nM, half-maximal inhibition at approximately 8 nM, and complete inhibition at 1 μM (Fig. 4, *left*). Analysis of the binding data using the least-squares curve-fitting program LIGAND demonstrated that the data were best fit by a single-binding site model. NMB (K_i = 8.1 ± 5.2 nM) was 4-fold more potent than Bn (K_i = 32 ± 3 nM) (Table 1) and was 650-fold more potent than GRP (K_i = 5080 ± 770 nM) (Table 1).

Numerous classes of Bn receptor antagonists have been described (20). The abilities of three peptides, representing different classes of antagonists, to interact with the GRP-R on huGRP-R-transfected cells and with the NMB-R on huNMB-R-transfected cells were determined (Fig. 5). For huGRP-R-transfected cells, [F$_5$-D-Phe^6,D-Ala^{11}]Bn(6–13)methyl ester was the most potent at inhibiting the binding of [^{125}I-Tyr^4]Bn, with half-maximal inhibition being observed at 0.9 ± 0.1 nM. This antagonist was >8-fold more potent than [Leu^{14},Ψ13–14]Bn (K_i = 7.7 ± 0.3 nM) and was >5000-fold more potent than cyclo-SS-octa (K_i = 4570 ± 230 nM). In contrast, only cyclo-SS-octa was potent at inhibiting the binding of [^{125}I-D-Tyr^0]-NMB to huNMB-R-transfected cells (K_i = 605 ± 23 nM). Both [F$_5$-D-Phe^6,D-Ala^{11}]Bn(6–13)methyl ester and [Leu^{14},Ψ13–14]-Bn, at the maximal concentration used (10 μM), displaced <30% of [^{125}I-D-Tyr^0]NMB binding to huNMB-R-transfected cells (K_i > 10,000 nM).

The kinetics of binding were further examined by investigating the reversibility of binding of [^{125}I-Tyr^4]Bn to huGRP-R-transfected cells (Fig. 6, *left*) and of [^{125}I-D-Tyr^0]NMB to huNMB-R-transfected cells (Fig. 6, *right*). At 37° the dissociation of [^{125}I-Tyr^4]Bn bound to huGRP-R-transfected cells was slower than the dissociation of [^{125}I-D-Tyr^0]NMB bound to huNMB-R-transfected cells (Fig. 6). Specifically, by 15 min approximately 20% of bound ligand dissociated from huGRP-R-transfected cells, increasing to 53% by 60 min. In contrast, 58% of bound ligand dissociated from huNMB-R-transfected cells by 15 min, and this increased to 76% by 60 min. Lowering the temperature to 4° slowed the dissociation of bound ligand from either cell type, with <10% being dissociated by 60 min (Fig. 6). The incompleteness of dissociation at 37° suggested the possibility of peptide internalization in each of the cell types.

To determine whether internalization of ligand was occurring, acid-stripping experiments were performed to remove surface-bound ligand at various times and temperatures (Fig. 7). After incubation for 5 min at 37°, the time of half-maximal binding for both cell types (Fig. 3), 46 ± 3% of bound radiolabel was internalized by huGRP-R-transfected cells (Fig. 7, *left*), whereas 27 ± 3% of radiolabel was internalized by huNMB-R-transfected cells (Fig. 7, *right*). Maximal internalization at 37° was achieved by approximately 60–90 min in both cell types (Fig. 7). Internalization at 22° similarly was more rapid and complete with the huGRP-R-transfected cells (62 ± 1% internalized by 15 min and 75 ± 4% internalized by 90 min) than with the huNMB-R-transfected cells (29 ± 5% internalized by 15 min and 63 ± 3% internalized by 90 min). In both cell systems receptor internalization rates were markedly inhibited at 4°, with >90% of bound ligand existing in an acid-strippable form after a 90-min incubation (Fig. 7).

To determine whether transfected human Bn receptors activated phospholipase C, we determined the ability of the two mammalian Bn-related peptides to increase [^{3}H]IP in both cell types (Fig. 8). In huGRP-R-transfected cells a maximally effective dose of GRP (i.e., 1 μM) caused a 3.2-fold increase in

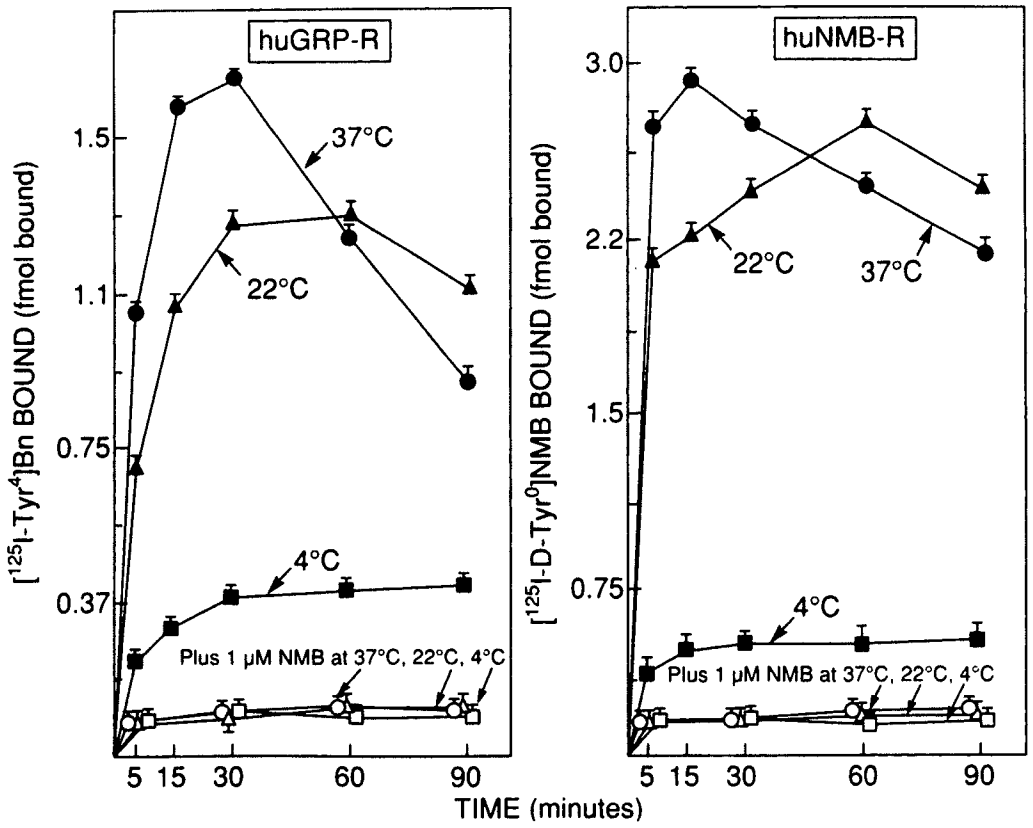

Fig. 3. Time- and temperature-dependent binding of [^{125}I-Tyr^4]Bn to huGRP-R-transfected cells (*left*) and [^{125}I-D-Tyr^0]NMB to huNMB-R-transfected cells (*right*). For both cell types, 3 × 10^6 cells/ml were incubated with 75 pM radiolabeled peptide alone (*closed symbols*) or with 1 μM unlabeled peptide (*open symbols*). At the indicated times and temperatures, 100-μl samples were taken and processed as described in Experimental Procedures. Results are expressed as fmol bound at each time point. In each experiment each value was determined in triplicate, and the results are given as the means ± standard errors of at least three separate experiments.

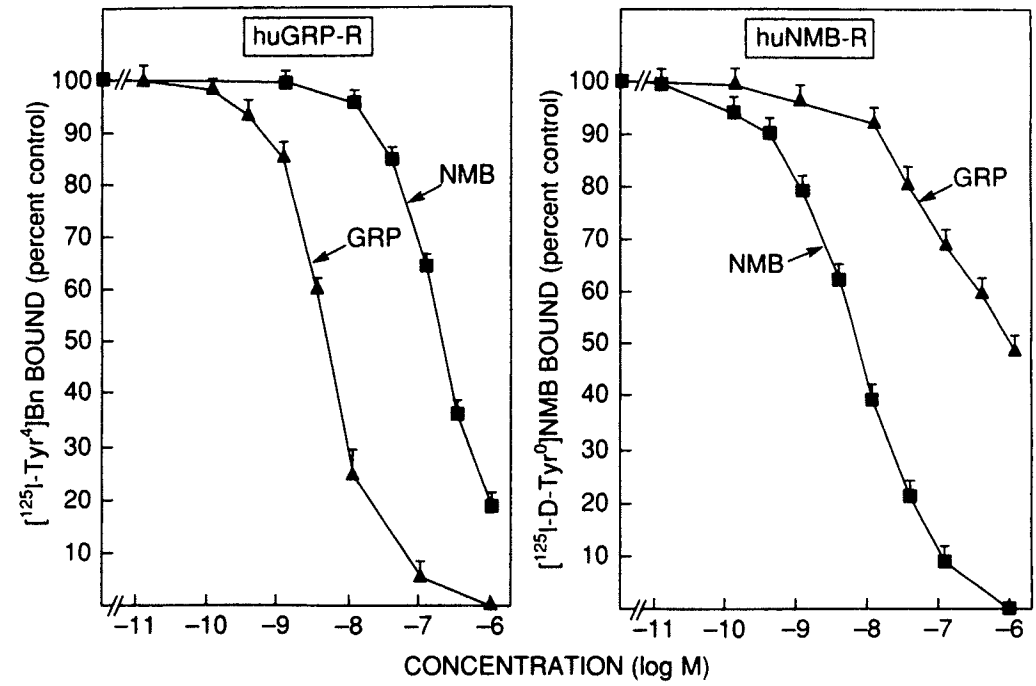

Fig. 4. Comparison of the ability of various Bn-related agonists to inhibit the binding of [^{125}I-Tyr^4]Bn to huGRP-R-transfected cells (*left*) and [^{125}I-D-Tyr^0]NMB to huNMB-R-transfected cells (*right*). For both cell types, 3 × 10^6 cells/ml were incubated with 75 pM radiolabeled peptide alone or with the indicated concentrations of the unlabeled Bn-related peptide. Data are expressed as the percentage of saturably bound radioactivity in the absence of nonradioactive peptide. For each experiment each value was determined in duplicate, and the results are the means ± standard errors of at least three separate experiments.

[^{3}H]IP. GRP was the most potent (EC_{50} = 13.6 ± 1.3 nM) at increasing [^{3}H]IP and was 100-fold more potent than NMB (EC_{50} = 1410 ± 171 nM) (Fig. 8, *left*). In huNMB-R-transfected cells a maximally effective concentration of NMB (i.e., 1 μM) caused a 19-fold increase in [^{3}H]IP. NMB (EC_{50} = 9.3 ± 1.4 nM) was 96-fold more potent than GRP (EC_{50} = 891 ± 67 nM) at increasing [^{3}H]IP in the huNMB-R-transfected cells (Fig. 8, *right*).

In addition to activating phospholipase C, Bn stimulation of the murine GRP-R expressed on Swiss 3T3 cells results in increased cellular cAMP levels (12, 14). However, the same receptor transfected into murine BALB/3T3 cells fails to increase cAMP levels (14). Therefore, we determined whether either transfected human Bn receptor type increased cellular cAMP levels when activated. When huNMB-R- or huGRP-R-transfected cells were preincubated with 30 mM forskolin or 100 ng/ml cholera toxin, basal cAMP levels were increased approximately 2-fold (Table 2). Whereas further incubation

TABLE 1

Binding affinities of various Bn-related agonists and receptor antagonists for different mammalian Bn receptors

Binding was performed as detailed in Experimental Procedures. Data for rat NMB-R-transfected BALB/3T3 cells (14, 21), C_6 glioblastoma cells (29), rat pancreatic acini (20, 35), mouse GRP-R-transfected BALB/3T3 cells (14), mouse pancreatic acini (20, 28), Swiss 3T3 cells (12, 14, 29), and guinea pig pancretic acini (4, 20) have been published previously or were obtained from binding studies with these cells. All values represent the mean ± standard error of at least three separate experiments, with each experiment performed in duplicate.

	NMB-R			GRP-R					
	Human	Rat		Human	Mouse			Rat	Guinea pig
	transfected cells	Transfected cells	C_6 Cells	transfected cells	Transfected cells	Pancreas	Swiss 3T3 cells	pancreas	pancreas
					K_i (nM)				
Agonists									
NMB	8.1 ± 5.2	4.2 ± 0.6	3.3 ± 0.8	437 ± 30	174 ± 4	230 ± 80	42 ± 5	248 ± 5	1,500 ± 150
Bn	32 ± 3	34 ± 2	21 ± 7	1.4 ± 0.2	0.9 ± 0.3	6.8 ± 1.3	1.3 ± 0.2	4.1 ± 1.0	3.6 ± 0.5
GRP	5,080 ± 770	439 ± 66	403 ± 58	6.2 ± 1.3	3.1 ± 1.4	6.0 ± 2.0	1.6 ± 0.2	18 ± 5	11 ± 2
Antagonists									
[F_5-D-Phe^6-D-Ala^{11}]Bn(6-13)-methyl ester	>10,000	>10,000	620 ± 120	0.9 ± 0.1	ND*	ND	0.2 ± 0.1	5.5 ± 1.4	6 ± 1
[Leu^{14},ψ13-14]Bn	>10,000	>10,000	>10,000	7.7 ± 0.3	87 ± 11	ND	65 ± 6	434 ± 65	60± 6
Cyclo-SS-octa	605 ± 23	220 ± 36	60 ± 9	4,570 ± 230	ND	ND	>10,000	>10,000	ND

* ND, no data.

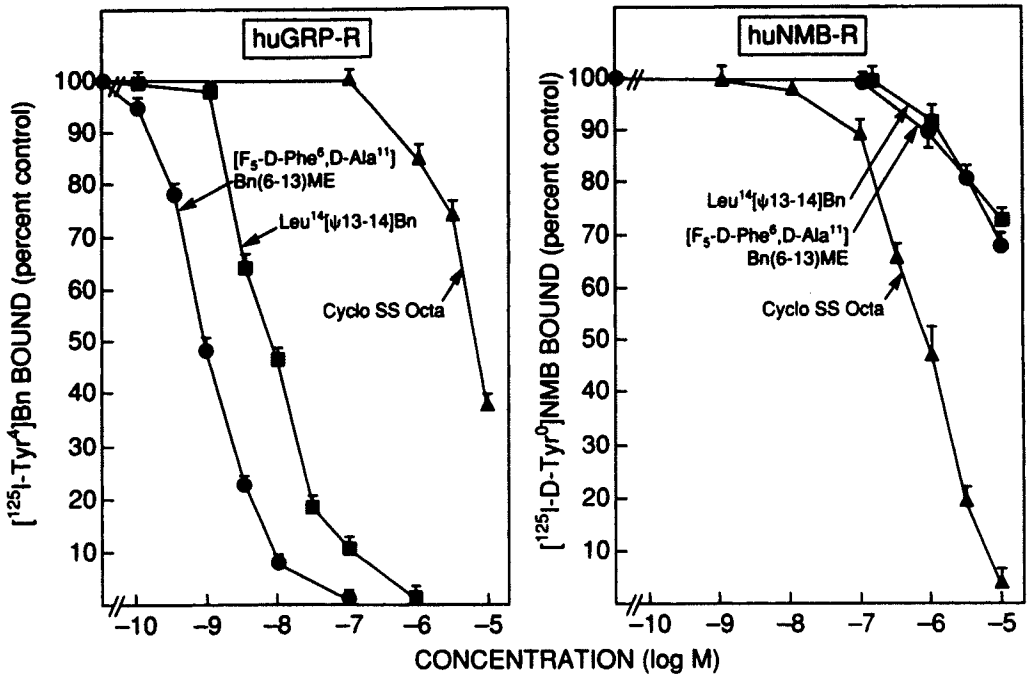

Fig. 5. Ability of various Bn receptor antagonists to inhibit the binding of [^{125}I-Tyr^4]Bn to huGRP-R-transfected cells (*left*) and [^{125}I-D-Tyr^0] NMB to huNMB-R-transfected cells (*right*). Experimental conditions were similar to those described in the legend to Fig. 3. For each experiment, each value was determined in duplicate, and the results are the means ± standard errors of at least three separate experiments.

with Bn increased cAMP levels 10.8-fold in Swiss 3T3 cells, Bn, GRP, and NMB failed to significantly increase cAMP levels further in the huNMB-R- and huGRP-R-transfected cell lines (Table 2).

Discussion

This study provides the first systematic characterization of the pharmacology and cell biology of human Bn receptors using huGRP-R and huNMB-R stably transfected into BALB/3T3 cells and demonstrates that they are a good model system for such studies of human Bn receptors. Previous cross-linking studies have demonstrated that the huGRP-R expressed by small cell lung cancer cells and by a human duodenal tumor cell line (24, 26) has a molecular weight of 62,000. After PNGase F treatment, a single band of M_r 40,000 (24) was seen, demonstrating that the huGRP-R was approximately 35% glycosylated. Similarly, in the present study we found that in the human glioblastoma cell line U-118 the natively expressed huGRP-R had a molecular weight of 60,000 and that 34% of this weight was due to glycosylation. An identical result was found with the transfected huGRP-R, demonstrating that in BALB/3T3 cells this receptor is glycosylated to a similar extent as the natively expressed receptor. Species-appropriate glycosylation also was observed with the mouse GRP-R transfected into the same cell type (27), demonstrating that GRP-R glycosylation in BALB/3T3 cells appears to be similar to that observed in native tissues, regardless of the species origin of the receptor. The mouse GRP-R has four potential glycosylation sites, all of which are utilized (13, 27), and is 47% glycosylated in pancreatic acinar cells (28) and Swiss 3T3 cells (12, 26, 27) and when expressed in stably transfected BALB/3T3 cells (27). In contrast, the huGRP-R has only two potential *N*-linked glycosylation sites (16), which likely explains the difference in percentage glycosylation between the mouse GRP-R and the huGRP-R. No comparable data exist for natively

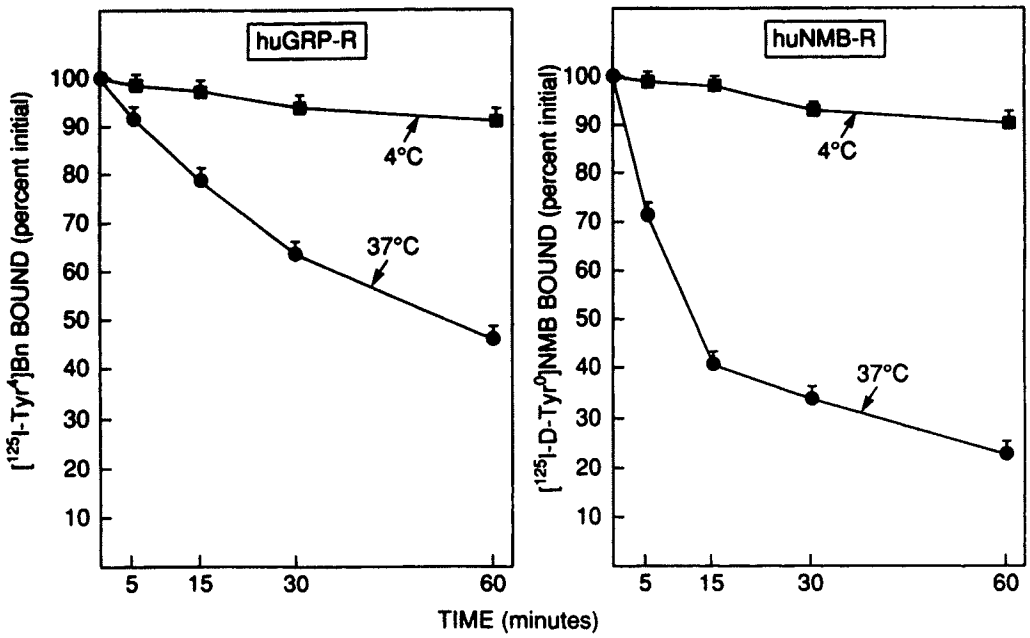

Fig. 6. Dissociation of [^{125}I-Tyr^4]Bn bound to huGRP-R-transfected cells (*left*) and [^{125}I-D-Tyr^0]NMB bound to huNMB-R-transfected cells (*right*). For both transfected cell types, 3×10^6 cells/ml were incubated in binding buffer with 75 pM radiolabeled peptide at 22° for 60 min. At that time, aliquots were diluted 50-fold with binding buffer at 4° or 37° and incubated at the indicated temperature for the indicated times. Results are expressed as the percentage of saturable binding at the beginning of the second incubation. In each experiment each value was determined in triplicate, and each data point is the mean ± standard error of at least three separate experiments.

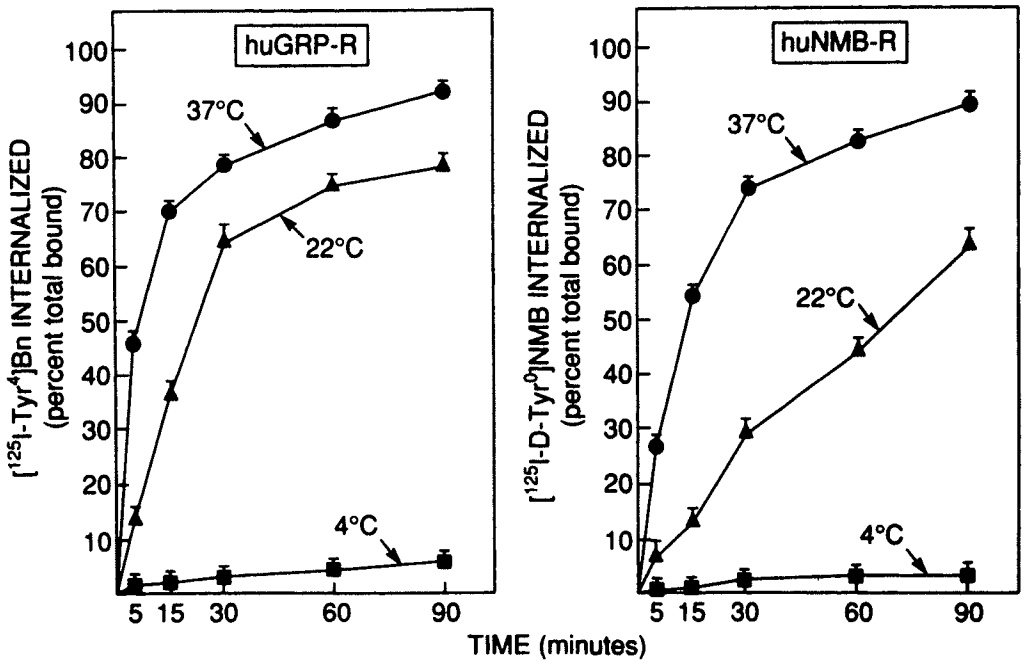

Fig. 7. Time and temperature dependence of internalization of the huGRP-R in huGRP-R-transfected cells (*left*) and the huNMB-R in huNMB-R-transfected cells (*right*). Surface-bound ligand was the proportion of saturably bound counts removed by acid stripping, as described in Experimental Procedures, whereas the internalized ligand was the proportion not removed. Results are expressed as the proportion of total saturable ligand at any time point and temperature that was not acid strippable. For each experiment each value was determined in triplicate, with each data point representing the mean ± standard error of at least three separate experiments.

expressed huNMB-R. In the present study with the transfected huNMB-R, a single cross-linked protein band of M_r 72,000 was seen. Deglycosylation studies demonstrated that 38% of the molecular weight of the huNMB-R was due to glycosylation. Similarly, in recent cross-linking studies the rat NMB-R was shown to have a molecular weight of 63,000, with 32% of the weight being due to glycosylation of the natively expressed NMB-R either by rat C_6 glioblastoma cells or by the stably transfected BALB/3T3 cells. The difference in glycosylation between species is again likely due to the fact that the huNMB-R has three potential *N*-linked glycosylation sites (16), whereas the rat NMB-R has only two such sites (13). In a recent study it was demonstrated that each potential glycosylation site on the rat NMB-R was glycosylated (23); therefore, the additional potential glycosylation site in the huNMB-R also is likely glycosylated, thus accounting for the greater degree of glycosylation of the huNMB-R versus the rat NMB-R.

Previous studies have provided evidence that GRP, NMB, and other Bn-related peptides can activate either GRP-R or NMB-R but differ in their relative affinities in different species (20, 22, 29). In the present study, the transfected huGRP-R had the highest affinity for the amphibian peptide Bn, whereas GRP was 4-fold less potent and NMB was >300-fold less potent. A similar result was seen in rat pancreas, guinea pig pancreas, and rat pancreatic AR-42J cells, where Bn was 3–10 times more potent than GRP and >60 times more potent than NMB (see Table 1). In contrast, with the mouse GRP-R (expressed by either mouse pancreas, mouse Swiss 3T3 cells, or stably transfected BALB/3T3 cells), Bn and GRP have almost equal high affinity and have only a 30–40-fold higher affinity

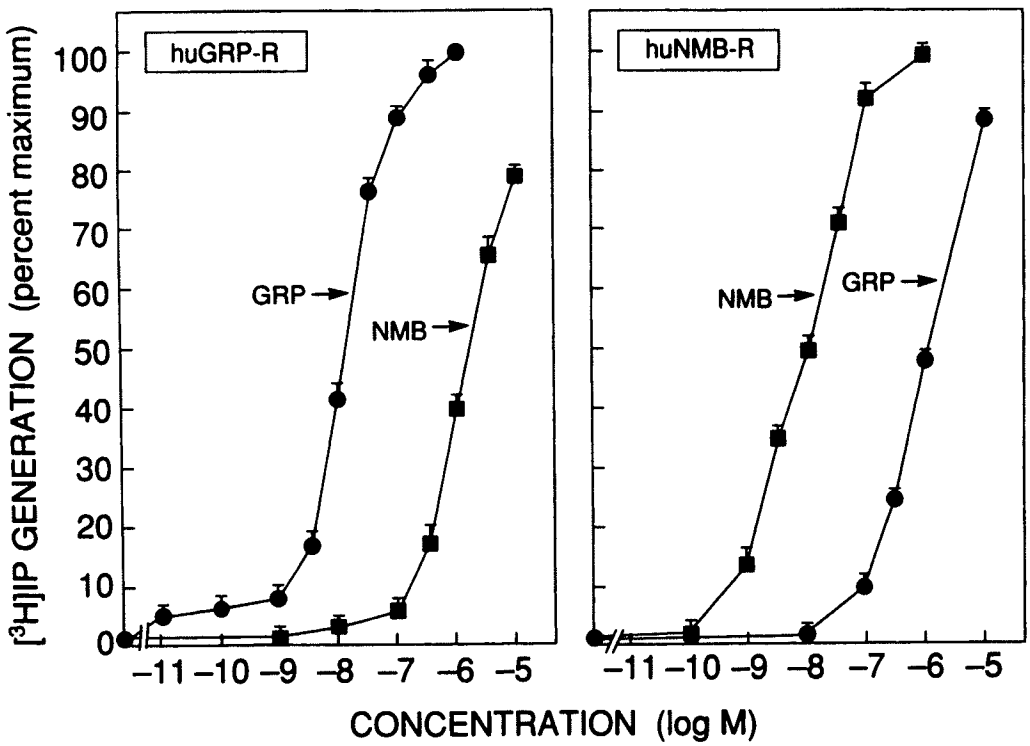

Fig. 8. Ability of Bn-related peptides to stimulate [^{3}H]IP generation in huGRP-R-transfected cells (*left*) or in huNMB-R-transfected cells (*right*). Confluent cells were incubated with 100 Ci/ml *myo*-[2-^{3}H]inositol for 24 hr, after which they were exposed to the indicated Bn-related peptides at the indicated concentrations for 60 min. Data are expressed as the percentage of maximal increase obtained using 1 μM Bn in huGRP-R-transfected cells or 1 μM NMB in huNMB-R-transfected cells. For huGRP-R-transfected cells, control and 1 μM Bn-stimulated values for [^{3}H]IP were 7,100 ± 1,100 dpm and 23,000 ± 2,200 dpm, respectively. For huNMB-R-transfected cells, control and 1 μM NMB-stimulated values for [^{3}H]IP were 9,800 ± 900 dpm and 185,000 ± 20,000 dpm, respectively. For each experiment, each value was determined in duplicate, with each data point representing the mean ± standard error of at least three separate experiments.

TABLE 2

Ability of Bn-related agonists to increase cAMP levels in huNMB-R- and huGRP-R-transfected cells and in Swiss murine 3T3 cells

For all cell types, 3 × 10^6 cells/ml were preincubated with 100 ng/ml cholera toxin for 60 min at 37° or with 30 μM forskolin for 30 min at 37°. After forskolin preincubation, the cells were further stimulated with the indicated peptides for 30 min. Basal cAMP levels were 18 pmol/10^6 cells for Swiss 3T3 cells, 27 pmol/10^6 cells for huNMB-R-transfected cells, and 139 pmol/10^6 cells for huGRP-R-transfected cells. Each value represents the fold increase (mean ± standard error) from three separate experiments, with each experiment performed in triplicate.

	Relative cAMP level		
	huNMB-R-transfected cells	huGRP-R-transfected cells	Murine Swiss 3T3 cells
No additions	1	1	1
Cholera toxin (100 ng/ml)	1.6 ± 0.4	1.4 ± 0.3	2.2 ± 0.4
Forskolin (30 μM)	2.1 ± 0.6	2.2 ± 0.4	2.9 ± 0.3
Forskolin (30 μM) + NMB (1 μM)	2.8 ± 0.6	3.3 ± 0.6	3.6 ± 0.9
Forskolin (30 μM) + Bn (1 μM)	2.5 ± 0.7	3.3 ± 0.5	10.8 ± 1.1*
Forskolin (30 μM) + GRP (1 μM)	2.9 ± 0.7	3.1 ± 0.6	6.3 ± 0.5*

* Value is significantly different from the value obtained in the presence of forskolin alone; $p < 0.05$.

than NMB (12, 14, 28). At present, the basis for this difference in the relative affinities and selectivity of these three naturally occurring agonists for the GRP-R in mice, compared with humans and other species, is unclear. The affinities of these three agonists for the transfected huGRP-R are in reasonable agreement with results from studies on human cells containing native huGRP-R. In human pancreatic acinar membranes Bn was the most potent at inhibiting binding (IC_{50} = 1 nM) and was 8-fold more potent than GRP-R (30). In the human colon cancer cell line NCI-H716 Bn was 3-fold more potent than GRP and 350-fold more potent than NMB (31), in the small cell lung cancer cell line NIH-H345 Bn was 5-fold more potent than GRP, and with the huGRP-R in the human gastric cancer cell line St42 (32) Bn was 2-fold more potent than GRP and 100-fold more potent than NMB. In biological studies assessing the ability of Bn-related peptides to cause contraction of isolated human circular jejunal smooth muscle cells, Bn was 20 times more potent than GRP (33). However, in the human duodenal tumor cell line HuTu-80 Bn and GRP were equipotent and >100-fold more potent than NMB (26), whereas in the human breast cancer cell line T-47D (19) GRP was reported to be 10-fold more potent than Bn. At present, it is unclear whether the differences in the relative affinities of these three Bn-related peptides for the huGRP-R reported in these various studies are due to different experimental conditions, intrinsic differences of these multiple tumor cell lines due to alterations in G protein coupling or glycosylation, or some other factors. The degree of glycosylation may represent a hitherto underappreciated reason for alterations in receptor affinity for ligands. Indeed, in a recent study (27) the extent of glycosylation of the mouse GRP-R was shown to affect receptor affinity and G protein coupling. Furthermore, in a study of the huGRP-R in T-47D breast cancer cells (19), which has a higher affinity for GRP than Bn, the cross-linked receptor had a molecular weight of 75,000. This molecular weight is similar to that reported for human glioma cells (24) and thus supports the contention that differences in glycosylation may represent an important factor contributing to the differing affinities of the huGRP-R for GRP and Bn in different human cell lines.

In contrast, few cell lines express sufficient huNMB-R to permit a systematic comparison of the data obtained herein using the stably transfected huNMB-R cells with data on cells natively expressing this receptor. In general, however, the pharmacology of the huNMB-R was similar to data obtained from rats, where this receptor has been extensively characterized (21, 22, 29). Indeed, the huNMB-R had relatively high affinity for both NMB and Bn, with GRP having a >800-fold lower affinity for this receptor than the huGRP-R. The only comparable data for natively expressed huNMB-R is from the NCI-

H345 small cell lung cancer cell line (25). For this cell line, one pharmacological analysis revealed that NMB had a 100-fold higher affinity than Bn and a 50-fold higher affinity than GRP (25), whereas in a study evaluating changes in $[Ca^{2+}]_i$ in the same cell line NMB was only 3-fold more potent than Bn (16). The reasons accounting for the differences in relative affinities of GRP and NMB for the huNMB-R, as well as their differing abilities to alter $[Ca^{2+}]_i$, between NCI-H345 cells and the stably huNMB-R-transfected cells studied herein are unclear but are likely multifactorial. Potential factors include noncomparable experimental conditions, alterations in peptide degradation, and different G protein populations in the different cell types. However, it also is important to realize that NCI-H345 cells express both huNMB-R and huGRP-R and that both classes of receptors can interact with both peptides. Earlier studies of the huNMB-R on NCI-H345 cells were not performed on cells possessing a pure population of receptors and are therefore difficult to interpret. However, in terms of selectivity for Bn receptors, the pharmacology of the human receptors is similar to that reported in various animal studies (22, 29), with NMB having >50-fold higher selectivity for the NMB-R than the GRP-R. In contrast, Bn interacts with high affinity with both transfected human Bn receptor subtypes, whereas GRP is >400-fold more selective for the huGRP-R than the huNMB-R. Because GRP and Bn share a similar carboxyl-terminal heptapeptide, with nine of the 10 carboxyl-terminal amino acids being identical in the biologically active portion of the molecule (34), this increased selectivity of GRP over Bn for huGRP-R suggests that the amino-terminal amino acids of GRP are important for determining this selectivity for the various human Bn receptors.

Previous studies have demonstrated, with Bn receptors from rats, mice, and guinea pigs (12, 14, 21, 29), that the radiolabeled agonist ligands are rapidly internalized and degraded. Results in the present study suggest that similar phenomena occur with huGRP-R and huNMB-R. With both human receptors, rapid temperature-dependent internalization was seen. Furthermore, with both human receptors binding decreased with time at 37°, which in animal studies was shown to be due to degradation of the radiolabeled agonists. In those studies the broad-spectrum protease inhibitor bacitracin, which was included in the incubation medium in the present study, was shown to markedly inhibit this degradation, whereas neutral endopeptidase or amino peptidase inhibitors were largely without effect (29).

In previous studies, six chemically different classes of Bn receptor antagonists have been described (20, 35). Almost no data are available on the ability of these antagonists to interact with human Bn receptors. In the present study, representative compounds from three of these classes of antagonists were examined for their abilities to interact with and distinguish the two human Bn receptor subtypes. Similarly to studies in other species (20), the [des-Met^{13}]Bn analogue [F_5-D-Phe^6,D-Ala^{11}]-Bn(6–13)methyl ester had high affinity for huGRP-R and had >10,000-fold selectivity for the huGRP-R over the huNMB-R. A recent study has demonstrated that this analogue functions as a GRP-R antagonist in humans *in vivo* and inhibits Bn-stimulated enzyme secretion and gastric emptying (36). Closely related [des-Met^{13}]Bn antagonists have been shown to inhibit Bn-stimulated increases in $[Ca^{2+}]_i$ in NCI-H345 small cell lung cancer cells (25) and to inhibit GRP-stimulated chloride currents in *Xenopus* oocytes after injection of huGRP-R mRNA but do not inhibit NMB-stimulated changes in chloride currents after injection of huNMB-R mRNA (16). These results, coupled with their marked selectivity for the huGRP-R, suggest that this class of antagonists will be useful for exploring the role of the GRP-R in mediating various physiological functions. The pseudopeptide analogue [Leu^{14},Ψ13–14]Bn also had high affinity for the huGRP-R and a 1000-fold selectivity for this receptor over the huNMB-R. This analogue has been shown to inhibit Bn-stimulated increases in [^{3}H]IP levels, $[Ca^{2+}]_i$, and proliferation of NCI-H345 cells (37). In contrast to these two antagonists, but similarly to results reported recently for rats, the somatostatin octapeptide analogue cyclo-SS-octa was more selective for the NMB-R than the GRP-R. However, it was pointed out that the use of this particular analogue may be limited because it has both somatostatin agonist activity and some μ-opioid antagonist activity, although structure-function studies suggest that these can be separated from the NMB-R inhibitory activity. The present study suggests that an additional problem also exists for this class of antagonists in humans, in that cyclo-SS-octa has a much lower affinity for the huNMB-R (K_i = 605 nM) than the rat NMB-R (K_i = 40–220 nM), as well as being less selective for this receptor than for the huGRP-R.

In all species examined, GRP-R and NMB-R activation results in activation of phospholipase C, which results in an increase in IP and mobilization of cellular calcium (12, 22, 38). In the present study we found that both huGRP-R and huNMB-R activate phospholipase C and increase [^{3}H]-IP levels. These results are similar to studies using human small cell lung cancer cells possessing either GRP-R or NMB-R (25, 37, 39), in which the addition of Bn-related peptides increases phosphatidylinositol turnover and $[Ca^{2+}]_i$. Furthermore, the GRP-R antagonist [D-Phe^6]Bn(6–13)methyl ester inhibited GRP-stimulated increases in $[Ca^{2+}]_i$ without altering the increase caused by NMB in the human small cell lung cancer cell line NCI-H345 (16). This demonstrates that activation of both huGRP-R and huNMB-R activates phospholipase C. Similarly, activation of the GRP-R on the human pancreatic tumor cell line Capan (40) and the human duodenal cancer cell line HuTu 80 (26) also has been shown to activate phospholipase C, whereas stimulation of GRP-R on human endometrial stromal cells (41) has been shown to increase the activity of phospholipase C and to increase $[Ca^{2+}]_i$ and IP levels. Thus, activation of both huGRP-R and huNMB-R, either stably transfected in BALB/3T3 cells or in human tissues, results in phospholipase C activation. The ability to readily detect changes in [^{3}H]IP consequent to receptor activation, coupled with the ability to easily measure binding to huGRP-R or huNMB-R in the present study, suggests that these two transfected cell lines should be excellent systems for exploring additional ligand or receptor structure-function relationships for the human Bn receptors.

In some cell systems, such as Swiss 3T3 cells (12, 14), activation of the GRP-R also increases cAMP levels. In contrast, activation of the rat NMB-R natively expressed by C_6 glioblastoma cells (22) or by rat pancreatic acini, or of the rat NMB-R transfected into BALB/3T3 cells (21), does not result in an increase in cAMP levels. In the present study activation of neither the huGRP-R nor the huNMB-R resulted in increases in cAMP levels. The failure to observe an increase in cAMP levels with activation of either human Bn receptor could be either due to altered G protein-

receptor coupling or due to the fact that neither human Bn receptor type natively acts to increase cAMP levels. In a recent study (14), BALB/3T3 cells stably transfected with the mouse GRP-R derived from Swiss 3T3 cells, which increases cAMP levels in Swiss 3T3 cells (12, 14, 42), did not show increased cAMP levels. That study demonstrated that BALB/3T3 cells possessed abundant G_s; thus, the failure to increase cAMP levels could not be explained on the basis of inadequate G protein availability. Also, forskolin and cholera toxin increased cAMP levels in the transfected BALB/3T3 cells, further demonstrating that adenylate cyclase could be directly activated in these cells (14). This suggests that mouse GRP-R activation of cAMP production may be peculiar to Swiss 3T3 cells and that the failure of this same receptor to increase cAMP levels in BALB/3T3 cells cannot be blamed on the lack of appropriate machinery necessary to generate this cyclic nucleotide. At present, however, the possibility still cannot be completely excluded that activation of either human Bn receptor may be coupled to adenylate cyclase, in addition to activating phospholipase C, and that this dual activation pathway was not detected in the present study because of differences in G protein coupling between the transfected cells and cells natively expressing these receptors.

In conclusion, in the present study we demonstrate that huGRP-R and huNMB-R can be stably transfected into BALB/3T3 cells. We show that the transfected receptors exhibit similar pharmacology for agonists and antagonists, that they undergo identical glycosylation, and that they function similarly with respect to their ability to alter biological activity, compared with natively expressed receptors. The availability of these cells should greatly facilitate further studies of human Bn receptor pharmacology and receptor modulation.

References

1. McCoy, J. G., and D. D. Avery. Bombesin: potential integrative peptide for feeding and satiety. *Peptides* **11**:595–607 (1990).
2. Brown, M. R., K. Carver, and L. A. Fisher. Bombesin: central nervous system actions to affect the autonomic nervous system. *Ann. N. Y. Acad. Sci.* **547**:174–182 (1988).
3. Albers, H. E., S. Y. Liou, E. G. Stopa, and R. T. Zoeller. Interaction of colocalized neuropeptides: functional significance in the circadian timing system. *J. Neurosci.* **11**:846–851 (1991).
4. Jensen, R. T., D. H. Coy, Z. A. Saeed, P. Heinz-Erian, S. Mantey, and J. D. Gardner. Interaction of bombesin and related peptides with receptors on pancreatic acini. *Ann. N. Y. Acad. Sci.* **547**:138–149 (1988).
5. Severi, C., R. T. Jensen, V. Erspamer, L. D'Arpino, D. H. Coy, A. Torsoli, and G. Delle Fave. Different receptors mediate the action of bombesin-related peptides on gastric smooth muscle cells. *Am. J. Physiol.* **260**:G683–G690 (1991).
6. Ghatei, M. A., R. T. Jung, J. C. Stevenson, C. J. Hillyard, T. E. Adrian, Y. C. Lee, N. D. Christofides, D. L. Sarson, K. Mashiter, I. MacIntyre, and S. R. Bloom. Bombesin action on gut hormones and calcium in man. *J. Clin. Endocrinol. Metab.* **54**:980–985 (1982).
7. Hill, D. J., and T. J. McDonald. Mitogenic action of gastrin-releasing polypeptide on isolated epiphyseal growth plate chondrocytes from the ovine fetus. *Endocrinology* **130**:2811–2819 (1992).
8. Sunday, M. E., J. Hua, B. Reyes, H. Masui, and J. S. Torday. Anti-bombesin monoclonal antibodies modulate fetal mouse lung growth and maturation *in utero* and in organ cultures. *Anat. Rec.* **236**:25–32 (1993).
9. Rettori, V., C. C. Pazos-Moura, E. G. Moura, J. Polak, and S. M. McCann. Role of neuromedin B in control of the release of thyrotropin in hypothyroid and hyperthyroid rats. *Proc. Natl. Acad. Sci. USA* **89**:3035–3039 (1992).
10. De la Fuente, M., M. Del Rio, and A. Hernanz. Stimulation of natural killer and antibody-dependent cellular cytotoxicity activities in mouse leukocytes by bombesin, gastrin-releasing peptide and neuromedin C: involvement of cyclic AMP, inositol 1,4,5-trisphosphate and protein kinase C. *J. Neuroimmunol.* **48**:143–150 (1993).
11. Tache, Y., P. Melchiorri, and L. Negri. Bombesin-like peptides in health and disease. *Ann. N. Y. Acad. Sci.* **547**:1–541 (1988).
12. Rozengurt, E. Bombesin-induction of cell proliferation in 3T3 cells: specific receptors and early signaling events. *Ann. N. Y. Acad. Sci.* **547**:277–292 (1988).
13. Battey, J., and E. Wada. Two distinct receptors for mammalian bombesin-like peptides. *Trends Neurosci.* **14**:524–527 (1991).
14. Benya, R. V., Z. Fathi, T. Pradhan, J. F. Battey, T. Kusui, and R. T. Jensen. Gastrin-releasing peptide receptor-induced internalization, down-regulation, desensitization and growth: possible role of cAMP. *Mol. Pharmacol.* **46**:235–245 (1994).
15. Benya, R. V., T. Kusui, J. F. Battey, and R. T. Jensen. Desensitizaton of neuromedin B receptors (NMB-R) on native and NMB-R transfected cells involves down-regulation and internalization. *J. Biol. Chem.* **269**:11721–11728 (1994).
16. Corgay, M. H., D. J. Dobrzanski, J. M. Way, J. Viallet, H. Shapira, P. Worland, E. A. Sausville, and J. F. Battey. Two distinct bombesin receptor subtypes are expressed and functional in human lung carcinoma cells. *J. Biol. Chem.* **266**:18771–18779 (1991).
17. Lieverse, R. J., J. B. Jansen, A. van de Zwan, L. Samson, A. A. Masclee, L. C. Rovati, and C. B. Lamers. Bombesin reduces food intake in lean man by a cholecystokinin-independent mechanism. *J. Clin. Endocrinol. Metab.* **76**:1495–1498 (1993).
18. Bologna, M., C. Festuccia, P. Muzi, L. Biordi, and M. Ciomei. Bombesin stimulates growth of human prostatic cancer cells *in vitro*. *Cancer (Phila.)* **63**:1714–1720 (1989).
19. Giacchetti, S., C. Gauville, P. de Cremoux, L. Bertin, P. Berthon, J. P. Abita, F. Cuttitta, and F. Calvo. Characterization, in some human breast cancer cell lines, of gastrin-releasing peptide-like receptors which are absent in normal breast epithelial cells. *Int. J. Cancer* **46**:293–298 (1990).
20. Jensen, R. T., and D. H. Coy. Progress in the development of potent bombesin receptor antagonists. *Trends Pharmacol. Sci.* **12**:13–19 (1991).
21. Benya, R. V., E. Wada, J. F. Battey, Z. Fahti, L. H. Wang, S. A. Mantey, D. H. Coy, and R. T. Jensen. Neuromedin B receptors retain functional expression when transfected into BALB/3T3 fibroblasts: analysis of binding, kinetics, stoichiometry, modulation by guanine nucleotide binding proteins, signal transduction and comparison with natively expressed receptors. *Mol. Pharmacol.* **42**:1058–1068 (1992).
22. Wang, L. H., J. F. Battey, E. Wada, J. T. Lin, S. Mantey, D. H. Coy, and R. T. Jensen. Activation of neuromedin B-preferring bombesin receptors on rat glioblastoma C_6 cells increases cellular Ca^{2+} and phosphoinositides. *Biochem. J.* **286**:641–648 (1992).
23. Kusui, T., R. V. Benya, J. F. Battey, and R. T. Jensen. Glycosylation of bombesin receptors: characterization, effect on binding and G protein coupling. *Biochemistry* **33**:12968–12980 (1994).
24. Kris, R. M., R. Hazan, J. Villines, T. W. Moody, and J. Schlessinger. Identification of the bombesin receptor on murine and human cells by cross-linking experiments. *J. Biol. Chem.* **262**:11215–11220 (1987).
25. Moody, T. W., J. Staley, F. Zia, D. H. Coy, and R. T. Jensen. Neuromedin B binds with high affinity, elevates cytosolic calcium and stimulates the growth of small cell lung cancer cell lines. *J. Pharmacol. Exp. Ther.* **263**:311–317 (1992).
26. Williams, B. Y., and A. Schonbrunn. Bombesin receptors in a human duodenal tumor cell line: binding properties and function. *Cancer Res.* **54**:818–824 (1994).
27. Benya, R. V., T. Kusui, Z. Fathi, J. F. Battey, and R. T. Jensen. Glycosylation location and its functional significance in the gastrin-releasing peptide receptor (GRP-R) (Abstract). *Dig. Dis. Sci.* **39**:1765 (1994).
28. Huang, S. C., D. H. Yu, S. A. Wank, J. D. Gardner, and R. T. Jensen. Characterization of bombesin receptors on mouse pancreatic acini by chemical cross-linking. *Peptides* **11**:1143–1150 (1990).
29. Wang, L. H., S. A. Mantey, J. T. Lin, H. Frucht, and R. T. Jensen. Ligand binding, internalization, degradation and regulation by guanine nucleotides of bombesin receptor subtypes: a comparative study. *Biochim. Biophys. Acta* **1175**:232–242 (1993).
30. Scemama, J. L., A. Zahidi, D. Fourmy, P. Fagot-Revurat, N. Vaysse, L. Pradayrol, and A. Ribet. Interaction of [^{125}I]-Tyr^4-bombesin with specific receptors on normal human pancreatic membranes. *Regul. Peptides* **13**:125–132 (1986).
31. Frucht, H., A. F. Gazdar, J. A. Park, H. Oie, and R. T. Jensen. Characterization of functional receptors for gastrointestinal hormones on human colon cancer cells. *Cancer Res.* **52**:1114–1122 (1992).
32. Preston, S. R., L. F. Woodhouse, S. Jones-Blackett, J. I. Wyatt, and J. N. Primrose. High affinity binding sites for gastrin releasing peptide on human gastric cancer and Menetrier's mucosa. *Cancer Res.* **53**:5090–5092 (1993).
33. Micheletti, R., J. R. Grider, and G. M. Makhlouf. Identification of bombesin receptors on isolated muscle cells from human intestine. *Regul. Peptides* **21**:219–226 (1988).
34. Broccardo, M., G. F. Erspamer, P. Melchiorri, L. Negri, and R. De Castiglione. Relative potency of bombesin-like peptides. *Br. J. Pharmacol.* **55**:221–227 (1976).
35. Jensen, R. T., J. E. Mrozinski, Jr., and D. H. Coy. Bombesin receptor antagonists: different classes and cellular basis of action. *Recent Results Cancer Res.* **129**:87–113 (1993).
36. Hildebrand, P., L. Rossi, M. Meyer, S. Mossi, S. Ketterer, and C. Beglinger. Effect of BIM26226, a potent and specific bombesin/GRP receptor antagonist, on gastrointestinal functions in man. *Gastroenterology* **104**:A308 (1993).
37. Trepel, J. B., J. D. Moyer, F. Cuttitta, H. Frucht, D. H. Coy, R. B. Natale, J. L. Mulshine, R. T. Jensen, and E. A. Sausville. A novel bombesin receptor antagonist inhibits autocrine signals in a small cell lung carcinoma cell line. *Biochem. Biophys. Res. Commun.* **156**:1383–1389 (1988).
38. Jensen, R. T. Receptors on pancreatic acinar cells, in *Physiology of the Gastrointestinal Tract* (L. R. Johnson, E. D. Jacobsen, J. Christensen, D. H. Alpers, and J. H. Walsh, eds.), Ed. 3. Raven Press, New York, 1377–1446 (1994).
39. Heikkila, R., J. B. Trepel, F. Cuttitta, L. M. Neckers, and E. A. Sausville. Bombesin-related peptides induce calcium mobilization in a subset of human small cell lung cancer cell lines. *J. Biol. Chem.* **262**:16456–16460 (1987).

40. Avis, I., M. Jett, P. G. Kasprzyk, F. Cuttitta, A. M. Treston, R. Maneckjee, and J. L. Mulshine. Effect of gastrin-releasing peptide on the pancreatic tumor cell line (CAPAN). *Mol. Carcinog.* 8:214–220 (1993).
41. Endo, T., H. Fukue, M. Kanaya, M. Mizumuma, M. Fujii, H. Yamamoto, S. Tanaka, and M. Hashimoto. Bombesin and bradykinin increase inositol phosphates and cytosolic free Ca^{2+} and stimulate DNA synthesis in human endometrial stomal cells. *J. Endocrinol.* 131:313–318 (1991).
42. Millar, J. B. A., and E. Rozengurt. Bombesin enhancement of cAMP accumulation in Swiss 3T3 cells: evidence of a dual mechanism of action. *J. Cell. Physiol.* 137:214–222 (1988).

Send reprint requests to: Robert T. Jensen, National Institutes of Health, Building 10, Room 9C-103, 10 Center Dr., MSC 1804, Bethesda MD 20892-1804.

THE JOURNAL OF BIOLOGICAL CHEMISTRY

Vol. 263, No. 11, Issue of April 15, pp. 5056-5060, 1988
Printed in U.S.A.

Probing Peptide Backbone Function in Bombesin

A REDUCED PEPTIDE BOND ANALOGUE WITH POTENT AND SPECIFIC RECEPTOR ANTAGONIST ACTIVITY*

(Received for publication, October 7, 1987)

David H. Coy‡, Peter Heinz-Erian§, Ning-Yi Jiang‡, Yusuke Sasaki‡¶, John Taylor‖, Jacques-Pierre Moreau‖, William T. Wolfrey§, Jerry D. Gardner§, and Robert T. Jensen§

From the ‡Department of Medicine, Peptide Research Laboratories, Tulane University Medical Center, New Orleans, Louisiana 70112, the §Digestive Diseases Branch, National Institute of Diabetes and Digestive and Kidney Diseases, National Institutes of Health, Bethesda, Maryland 20892, and ‖Biomeasure, Inc., Hopkinton, Massachusetts 01748

Each peptide bond CONH group in the most important COOH-terminal octapeptide region of [Leu^{14}]bombesin was replaced by a CH_2NH group using recently developed rapid solid-phase methods. The resulting analogues were then examined for amylase releasing activity in guinea pig pancreatic acini and for their ability to inhibit binding of [^{125}I-Tyr^4]bombesin to acinar cells. Replacement of the Trp^8-Ala^9, Gly^{11}-His^{12}, and His^{12}-Leu^{13} peptide bonds resulted in about 1000-, 200-, and 300-fold losses in both amylase releasing activity and binding affinity. The Val^{10}-Gly^{11} replacement, however, retained 30% potency relative to the parent peptide. Ala^9-Val^{10} and Leu^{13}-Leu^{14} bond replacement analogues exhibited no detectable amylase releasing activity but were still able to bind to acini with K_d values of 1060 and 60 nM, respectively (compared to 15 nM for [Leu^{14}]bombesin itself). Subsequently, both analogues were demonstrated to be competitive inhibitors of bombesin-stimulated amylase release with IC_{50} values of 937 and 35 nM, respectively. [Leu^{14}-ψ-CH_2NH-Leu^{13}]Bombesin exhibits a 100-fold improvement in binding affinity compared to previously reported bombesin receptor antagonists and showed no affinity for substance P receptors. It was also a potent inhibitor of bombesin-stimulated growth of murine Swiss 3T3 cells with an IC_{50} of 18 nM. In terms of a bombesin receptor-binding conformation, these results may aid in the delineation of intramolecular hydrogen-bonding points and the eventual design of improved, conformationally restricted analogues.

There has been considerable interest in the design and development of competitive bombesin receptor antagonists as possible antimitotic agents since the discovery that bombesin (*p*Glu-Gln-Arg-Leu-Gly-Asn-Gln-Trp-Ala-Val-Gly-His-Leu-Met-NH_2) and related peptides (1) act as potent autocrine growth factors in human small cell lung carcinoma systems *in vitro* and *in vivo* (2, 3). These cells also contain high levels of bombesin immunoreactivity (4) and high affinity receptors for the peptide (5, 6).

There have been two published reports concerning peptide analogues capable of blocking the actions of bombesin. The first of these (7) described the ability of a substance P receptor antagonist to prevent bombesin-stimulated pancreatic amylase release with an IC_{50} in the millimolar range. The second (8) report concerned a bombesin analogue in which D-Phe replacement for His^{12} resulted in a competitive antagonist. Although this latter compound was specific for pancreatic bombesin receptors, it also had a relatively high IC_{50} of 4 mM.

In the present paper, rather than using the classical side chain modification strategies, we have adopted a more unusual peptide backbone modification approach to bombesin analogue design and antagonist discovery. This was prompted by a recent report (9) in which the tetragastrin pseudopeptide, *t*-butoxycarbonyl-Trp-Leu-ψ[CH_2NH]-Asp-Phe-NH_2, was found to be an effective gastrin receptor antagonist and our own work (10) on ψ-CH_2NH pseudooctapeptide somatostatin analogues which were helpful in examining potential peptide bond involvement in intramolecular hydrogen bonding and peptide conformation. Although the reduced peptide bond is only one of many possible alternatives (11) for altering the CONH linkage, it also has the advantage of being easily incorporated (12) by reductive alkylation with sodium cyanoborohydride and the appropriate protected amino acid aldehyde during the rapid solid-phase synthesis of a peptide. Synthetic work was concentrated on the COOH-terminal half of the bombesin peptide chain which earlier structure-activity studies (13) indicate to be primarily responsible for receptor binding and triggering of the biological signal. To eliminate the readily oxidized Met^{14} residue, the analogues described here were based on [Leu^{14}]bombesin which retains about 33% of the biological potency and binding affinity of bombesin itself (Table I).

EXPERIMENTAL PROCEDURES

Materials

Protected amino acids and other synthetic reagents were obtained from Advanced ChemTech, Louisville, KY. NIH strain guinea pigs (175-225 g) were obtained from the Small Animals Section, Veterinary Resources Branch, National Institutes of Health. HEPES[1] was from Boehringer Mannheim; purified collagenase (type CLSPA, 440 units/mg) from Worthington; sodium borate, soybean trypsin inhibitor, carbamylcholine, theophylline, bacitracin, and 8-bromo-cAMP from Sigma; essential vitamin mixture (100× concentrated) from Microbiological Associates; glutamine and gastrin-I(2-17) from Research Plus; ^{125}I-labeled *N*-succinimydyl-3-(4-hydroxyphenyl)propionate (1500 Ci/mmol) and Na^{125}I from Amersham Corp.; [^{3}H]thymidine from Du Pont-New England Nuclear; Phadebas amylase test reagent from Pharmacia LKB Biotechnology Inc.; bovine plasma albumin (Fraction V) from Miles Laboratories; A23187 from

* The costs of publication of this article were defrayed in part by the payment of page charges. This article must therefore be hereby marked "*advertisement*" in accordance with 18 U.S.C. Section 1734 solely to indicate this fact.

¶ Present address: Tohuku College of Pharmacy, Sendai, Miyagi 983, Japan.

[1] The abbreviations used are: HEPES, 4(2-hydroxyethyl)-1-piperazineethanesulfonic acid; ^{125}I-BH-SP, ^{125}I-labeled Bolton-Hunter-substance P; LH-RH, luteinizing hormone-releasing hormone.

Behring Diagnostics; vasoactive intestinal polypeptide and substance P from Peninsula Laboratories. COOH-terminal octapeptide of cholecystokinin was a gift from M. Ondetti, Squibb Institute for Biomedical Research, Princeton, NJ.

The standard incubation solution used in experiments involving pancreatic acini contained 24.5 mM HEPES (pH 7.4), 6 mM, NaCl, 2.5 mM, KCl, 5 mM NaH_2PO_4, 5 mM Na pyruvate, 5 mM, Na fumarate, 5 mM Na glutamate, 2 mM glutamine, 11.5 mM glucose, 0.5 mM $CaCl_2$, 1.0 mM $MgCl_2$, 5 mM theophylline, 1% (w/v) albumin, 0.01% (w/v) trypsin inhibitor, 1% (v/v) amino acid mixture, and 1% (v/v) essential vitamin mixture. The incubation solution was equilibrated with 100% O_2 and all incubations were carried out with O_2 as the gas phase.

Methods

Preparation of Peptides—Solid-phase syntheses, including introduction of each reduced peptide bond, were carried out by the standard methods recently described by Sasaki and Coy (12). The crude hydrogen fluoride-cleaved peptides were purified on a column (2.5 × 90 cm) of Sephadex G-25 which was eluted with 2 M acetic acid, followed by preparative medium pressure chromatography on a column (1.5 × 45 cm) of Vydac C_{18} silica (15–20 μm) which was eluted with a linear gradient of 15–55% acetonitrile in 0.1% trifluoroacetic acid using an Eldex Chromatrol gradient controller (flow rate 1 ml/min). Analogues were further purified by re-chromatography on the same column with slight modifications to the gradient conditions when necessary. Homogeneity of the peptides was assessed by thin layer chromatography and analytical reverse-phase high pressure liquid chromatography, and purity was 97% or higher. Amino acid analysis gave the expected amino acid ratios. The presence of the reduced peptide bond was demonstrated by fast atom bombardment mass spectrometry. Each of the 6 analogues gave good recovery of the molecular ion corresponding to the calculated molecular mass of 1587.

Tissue Preparation—Dispersed acini from guinea pig pancreas were prepared as described previously (14).

Amylase Release—Dispersed acini from one guinea pig pancreas were suspended in 150 ml of standard incubation solution and samples (250 μl) were incubated for 30 min at 37 °C. Amylase activity was determined by the method of Ceska *et al.* (15, 16) using the Phadebas reagent. Amylase release was calculated as the percentage of amylase activity in the acini at the beginning of the incubation that was released into the extracellular medium during the incubation.

Binding of [^{125}I-Tyr^4]Bombesin—[^{125}I-Tyr^4]Bombesin (2000 Ci/mmol) was prepared using a modification (17) of the chloramine-T method of Hunter and Greenwood (18). [^{125}I-Tyr^4]Bombesin was separated from ^{125}I using a Sep-Pak and separated from unlabeled peptide by reverse-phase high pressure liquid chromatography on a column (0.46 × 25 cm) of μBondspak C_{18}. The column was eluted isocratically with acetonitrile (22.5%) and triethylammonium phosphate (0.25 M, pH 3.5) (77.5%) at a flow rate of 1 ml/min. Incubations contained 0.05 nM [^{125}I-Tyr^4]bombesin and were for 30 min at 37 °C. Nonsaturable binding of [^{125}I-Tyr^4]bombesin was the amount of radioactivity associated with the acini when incubation contained 0.05 nM [^{125}I-Tyr^4]bombesin plus 1 mM bombesin. All values shown are for saturable binding, *i.e.* binding measured with [^{125}I-Tyr^4]bombesin alone (total) minus binding measured in the presence of 1 mM unlabeled bombesin (nonsaturable binding). Nonsaturable binding was <20% of total binding in all experiments.

Binding of ^{125}I-Bolton-Hunter-Substance P (^{125}I-BH-SP)—^{125}I-BH-SP (1500 Ci/mmol) was prepared using a modification (19) of the method of Bolton and Hunter (20) and purified by reverse-phase high pressure liquid chromatography on a C_{18} column (21). Binding of ^{125}I-BH-SP to dispersed pancreatic acini was measured as described previously (19). Nonsaturable binding of ^{125}I-BH-SP was the amount of radioactivity associated with the acini when the incubation contained 0.06 nM ^{125}I-BH-SP plus 1 mM unlabeled substance P. All values given are for saturable binding, *i.e.* binding measured with ^{125}I-BH-SP alone (total) minus binding measured with 1 mM unlabeled substance P (nonsaturable). Nonsaturable binding was <20% of total binding in all experiments.

Growth of Swiss 3T3 Fibroblasts—Stock cultures of Swiss 3T3 cells (American Type Culture Collection CCL 92) were grown in Dulbecco's modified Eagle's medium supplemented with 10% fetal calf serum in an atmosphere of 10% CO_2, 90% air at 37 °C. The cells were seeded into 24-well cluster trays and used 4 days after the last change of medium. The cells were arrested in the G_1/G_0 phase of the cell cycle by changing to serum-free medium prior to thymidine uptake determinations.

Assays of DNA Synthesis—3T3 cells were washed twice with 1-ml aliquots of medium (without serum) and then incubated with medium, 0.5 mM [^{3}H]thymidine (20 Ci/mmol), bombesin (1 nM), and several concentrations of bombesin analogue in a final volume of 0.5 ml. After 28 h at 37 °C, [^{3}H]thymidine incorporation into acid-insoluble pools was then determined. Cells were washed twice with ice-cold 0.9% saline (1-ml aliquots) and acid-soluble radioactivity was removed by a 30-min (4°) incubation with 5% trichloroacetic acid. The cultures were washed once with 95% ethanol (1 ml) and solubilized by a 30-min incubation with 0.1 N NaOH. The solubilized material was measured for radioactivity on the scintillation counter.

RESULTS

We were interested in quantitating both the agonist and potential antagonist activity of the 6 analogues which were synthesized. They were, therefore, initially examined for stimulating effects on pancreatic amylase release, which is a major biological activity of bombesin peptides, and the dose-response curves obtained are shown in Fig. 1 in comparison to bombesin and [Leu^{14}]bombesin standards. EC_{50} values calculated from half-maximal stimulation concentration are given in Table I. Only [Val^{10}-ψ-CH_2NH-Gly^{11},Leu^{14}]bombesin retained high potency, being about three times less active than [Leu^{14}]bombesin itself. Analogues with 11–12, 12–13, and, particularly, 8–9 peptide bond replacement were several orders of magnitude less potent, but were full agonists. In contrast, 9–10 and 13–14 bond replacement completely destroyed detectable amylase releasing activity. The analogues were then tested for their abilities to inhibit binding of [^{125}I-Tyr^4]bombesin to pancreatic acini and inhibition curves are shown in Fig. 2 with calculated K_d values given in Table I. All analogues displayed affinities that correlated completely with their biopotencies with the exception of the 9–10 and 13–14 replacement peptides which were able to bind with K_d values of 1060 and 60 nM, respectively, despite having no amylase releasing activity.

The 9–10 and 13–14 replacement peptides were tested for inhibition of the amylase release produced by a 0.2 nM dose of bombesin (Fig. 3). Both gave concentration-dependent inhibition of the activity of bombesin and the calculated IC_{50} values were 937 ± 8 and 35 ± 7 nM, respectively. Finally, the antagonists were examined for their specificity towards bom-

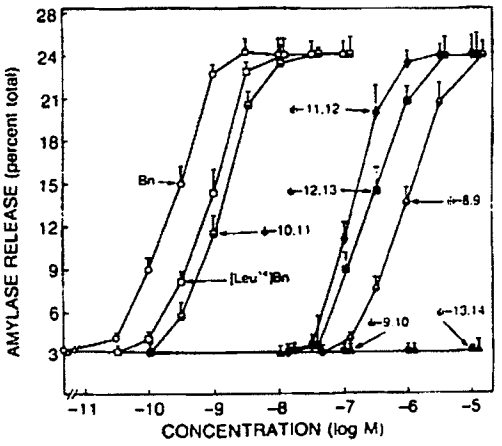

FIG. 1. **Effect of various concentrations of bombesin and [Leu^{14}]bombesin standards and 6 reduced-peptide bond replacement analogues on amylase release from dispersed guinea pig pancreatic acinar cells under conditions described in the text.** Values are the means from five experiments ± standard error.

TABLE I

Comparison of the ability of bombesin and [Leu^{14}]peptide bond replacement analogues to stimulate dispersed acinar amylase release and displace [^{125}I-Tyr^4]bombesin from intact cells

K_d values for binding of the analogues were calculated by the method of Cheng and Prusoff (28). The K_d value for bombesin was determined by Scatchard analysis. EC_{50} and IC_{50} values are from data shown in Figs. 2 and 3 and represent concentrations of peptide causing half-maximal amylase release or half-maximal inhibition of 0.2 nM bombesin-stimulated release, respectively. Each value is the mean ± S.E. of five experiments.

Bond replaced	Amylase release (EC_{50})	Binding (K_d)
	nM	
8 9 10 11 12 13 14 -Trp-Ala-Val-Gly-His-Leu-Met-NH_2 Leu	0.2 ± 0.1	4.4 ± 0.6
	0.8 ± 0.3	15.1 ± 2.9
~[a]	1060.5 ± 14.5	15500.6 ± 2040
~	ND[b]	1060.7 ± 140.8
~	2.1 ± 0.3	38.9 ± 5.9
~	140.6 ± 20.5	2410.8 ± 154.5
~	251.8 ± 36.6	4512.6 ± 1132.3
~	ND[c]	59.6 ± 5.8

[a] ~, Peptide bond replaced.
[b] Antagonist, IC_{50} = 937 ± 8 nM.
[c] Antagonist, IC_{50} = 35 ± 7 nM (see Fig. 3).

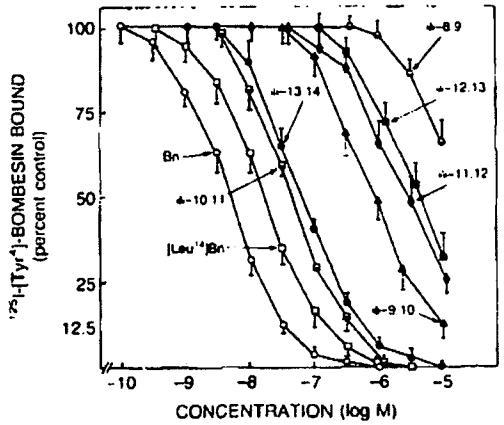

FIG. 2. **Displacement of ^{125}I-labeled bombesin from intact guinea pig pancreatic acinar cells by various concentrations of bombesin, [Leu^{14}]bombesin, and 6 peptide bond replacement analogues under conditions described in the text.** Values are the means from five experiments ± standard error.

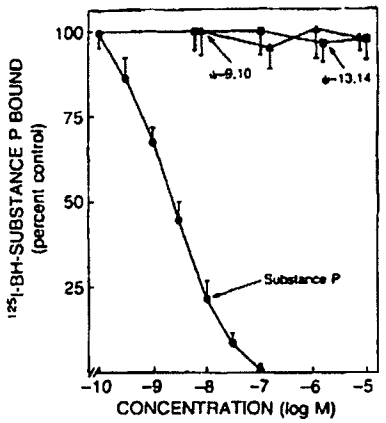

FIG. 4. **Displacement of ^{125}I-labeled Bolton-Hunter-substance P from guinea pig pancreatic acinar cells by a substance P standard and [Leu^{13}-ψ-CH_2NH-Leu^{14}]- and [Ala^9-ψ-CH_2NH-Val^{10}]bombesin under conditions described in the text.** Values are the means from five experiments ± standard error.

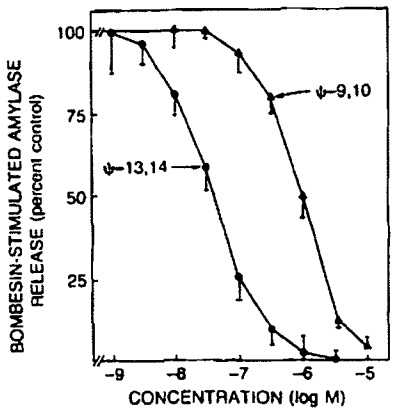

FIG. 3. **Inhibitory effects of various concentrations of [Leu^{13}-ψ-CH_2NH-Leu^{14}]- and [Ala^9-ψ-CH_2NH-Val^{10}]bombesin on guinea pig pancreatic acinar amylase release stimulated by 0.2 nM bombesin under conditions described in the text.** Values are the means from five experiments ± standard error.

besin receptors. Importantly, no inhibition of the binding of ^{125}I-labeled substance P could be achieved at concentrations up to 10 mM (Fig. 4). No inhibition of amylase release stimulated by substance P, cholecystokinin 8, vasoactive intestinal polypeptide, 8-bromo-cAMP, or A21837 was evident at the concentrations tested (Table II). The dose-response curve for bombesin-stimulated amylase release was shifted in a parallel fashion to the right by increasing concentrations of either the 13–14 (data not shown) or 9–10 bond replacement peptide. Schild plots for both peptides demonstrated a slope not significantly different from unity with a K_d of 22 ± 6 nM for the 13–14 and 473 ± 60 nM for the 9–10 bond replacement analogue.

The antagonist activity of [Leu^{13}-ψ-CH_2NH-Leu^{14}]bombesin was also examined in a totally different biological system, murine Swiss 3T3 fibroblast cells, the growth of which is stimulated by bombesin agonists (22) and which are known to contain bombesin receptors (23). Excellent inhibition of bombesin-stimulated growth was demonstrated and data from three experiments based on [^{3}H]thymidine incorporation are shown in Fig. 5. An average IC_{50} of 18 nM (Table III) was obtained from these experiments, which agrees very well with that derived from the acinar cell system. For comparison, a

TABLE II

Effect of [Leu[13]-ψ-CH$_2$NH-Leu[14]]- and [Ala[9]-ψ-CH$_2$NH-Val[10], Leu[14]]bombesin on guinea pig pancreatic acinar amylase release stimulated by various agents

Secretagogue	Amylase release		
	Alone	+0.3 mM 13–14 analogue	+10 mM 9–10 analogue
		% total[a]	
None	3.9 ± 0.7	4.1 ± 0.3	4.0 ± 0.2
Bombesin (0.2 nM)	17.1 ± 2.3	4.3 ± 0.3[b]	5.1 ± 1.0[b]
Substance P (3 nM)	10.3 ± 1.1	10.8 ± 0.3	11.2 ± 0.7
Cholecystokinin 8 (0.1 nM)	35.6 ± 2.2	33.9 ± 2.1	36.7 ± 3.0
Carbachol (10 mM)	28.4 ± 2.2	28.0 ± 2.9	30.0 ± 3.6
Vasoactive intestinal polypeptide (0.1 nM)	20.2 ± 2.4	20.4 ± 0.9	22.1 ± 1.1
8-Bromo-cAMP (1 mM)	24.0 ± 2.1	23.8 ± 2.5	25.1 ± 7.3
A21837 (3 mM)	13.2 ± 1.9	12.3 ± 0.3	13.0 ± 1.3

[a] Results are the means ± S.E. from five separate experiments.
[b] $p < 0.01$ compared to bombesin alone.

TABLE III

Comparison of the effectiveness of inhibition of 3T3 cell growth by two bombesin antagonists and a substance P antagonist

Peptide	IC_{50}
	nM
[D-Phe[12]]Bombesin	>5000
[D-Arg[1], D-Pro[2], D-Trp[7,9], Leu[11]] Substance P	2900
[Leu[13]-ψ-CH$_2$NH-Leu[14]]Bombesin	18 ± 12[a]

[a] Calculated from the data shown in Fig. 5.

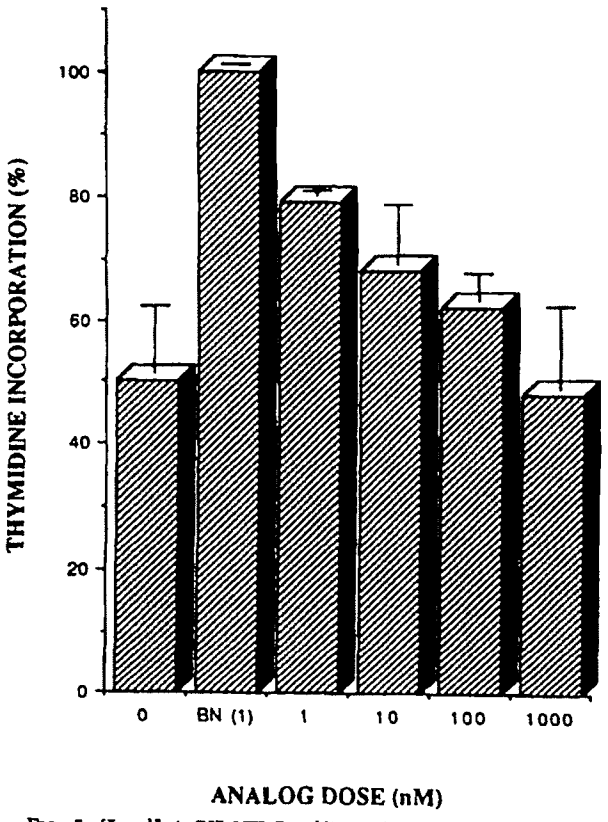

FIG. 5. [Leu[13]-ψ-CH$_2$NH-Leu[14]]Bombesin inhibition of bombesin-stimulated [^{3}H]thymidine incorporation into murine Swiss 3T3 cells in culture. Values are the means from three experiments ± standard error.

substance P receptor antagonist exhibited an IC_{50} of 2600 nM and our previous [D-Phe[12]]bombesin antagonist was not effective at concentrations up to 5000 nM.

DISCUSSION

Although modifications to a peptide bond have long been considered an interesting approach to structure-activity relationships, it was not until recently that the chemistry for introducing one of them, the CH$_2$NH group, was simplified by adapting it to rapid solid-phase methods (12). Therefore, we are only just beginning to build a sufficiently large data base for this type of analogue with which to eventually derive some indication of what can be expected in terms of effects on biological activity generally. Thus far, reduced peptide bond somatostatin (10), gastrin (9), and bombesin analogues have not yielded any compounds with increased biopotency caused by increased receptor affinity. Likewise, in a reduced peptide bond series of luteinizing hormone-releasing hormone (LH-RH) antagonists (24), no analogues were found with improved antagonist activity. On the other hand, both the gastrin and the present bombesin studies resulted in the discovery of more than one antagonist analogue in each case. It is tempting to conclude, therefore, that this may be the design approach of choice for antagonist discovery.

Generally, the tendency for loss of potency in a peptide agonist series is probably explained by the profound effects which elimination of a peptide bond CO group will have on conformation due to both loss of a potential intramolecular hydrogen-bonding point and increased rotation about the C–N bond. In a folded peptide conformation, hydrogen bonding is a prime factor stabilizing the structure and in our previously reported somatostatin octapeptide series (10), for which much physicochemical data existed, replacement of hydrogen bonds not involved in this process tended to retain the most activity.

With [Leu[13]-ψ-CH$_2$NH-Leu[14]]bombesin it is entirely possible that the 13–14 peptide bond CO group, although clearly not necessary for binding, is directly responsible for triggering the receptor response. However, this does not account for the antagonist activity also produced by 9–10 bond replacement. We suggest that another explanation could reside in destabilization of a folded, extensively hydrogen-bonded conformation similar to those present in somatostatin analogues (25), LH-RH (26), and several other peptides. Fig. 6 attempts to show this. We have placed the beginning of a β-turn at Val[10] so that Gly[11] occupies a pivotal position. The rest of the chain, modeled on the known solution conformation of conformationally restricted somatostatin octapeptides (25), is arranged in the form of an antiparallel β-pleated sheet. It should be

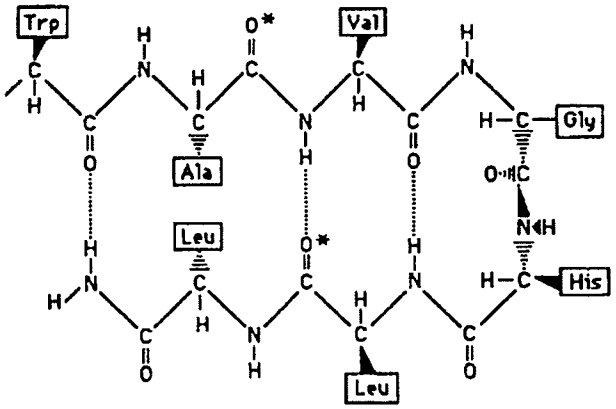

FIG. 6. **Possible conformation for the COOH-terminal octapeptide region of [Leu^{14}]bombesin with a type II′ β-bend involving the Val-Gly-His-Leu tetrapeptide.** Carbonyl groups (*) which produce antagonists when replaced by CH_2 and putative intramolecular hydrogen bonding interactions along the chain are shown.

noted that Gly^{11} in bombesin can be replaced by D-Ala with complete retention of activity, which prompted Rivier and Brown (13) and, more recently, Erne and Schwyzer (27) to discuss a similar β-bend. Also, the β-bends in somatostatin and LH-RH are similarly characterized by residues (Trp and Gly in positions 8 and 6, respectively) which can be replaced by D-amino acids with, in these cases, actual improvements in potency. In the β-pleated sheet area of the model, hydrogen bonding between the Leu^{13}-Leu^{14}-CO group and the Ala^{9}-Val^{10}-NH group assumes some importance and we propose that its destruction in the 13–14 analogue could result in a conformational shift responsible for loss of biological activity. Additionally, the 9–10 NH group would be adjacent to the Ala^{9}-CO group which, when replaced by CH_2 also results in an antagonist. It is thus conceivable that the same hydrogen bond could also be inhibited by the 9–10 peptide bond replacement since bond angles and rotational freedom would all be significantly affected. Also noteworthy in relation to this model are the loss of activity caused by replacement of the Trp^{8}-CO group which, could also be involved in another hydrogen bond, and the previously described importance of the COOH-terminal amide (13) which would also contribute to the same interaction. There is also loss of activity, although much less dramatic, associated with the Val^{10}-CO replacement which constitutes part of the hydrogen bond integral to the β-bend. It should be emphasized that no direct physicochemical evidence from solution studies exists to support this hypothesis and, indeed, a recent infrared spectroscopic study of bombesin in phospholipid bilayer membranes (27) points to a α-helical structure in this environment. However, as Erne and Schwyzer (27) point out, the helical structure of the membrane-bound peptide could actually facilitate a second conformational transition caused by interaction with the receptor which could well involve the proposed β-turn and hydrogen bonding points. In any event, the model does provide a useful starting point for the design of additional, conformationally covalently restricted linear and cyclic analogues in the future.

An additional advantage to this type of analogue design strategy appears to lie in the absence of multiple side chain modifications which are so often needed for development of potent antagonists by standard approaches. This can often result in the introduction of undesirable properties, such as the loss of specificity with the substance P antagonists (7), introduction of enhanced histamine releasing activity with the LH-RH antagonists (28), and the poor solubility properties of the [D-Phe^{12}]bombesins. In contrast, both of the present antagonists exhibited physical properties almost identical to bombesin and thus far both appear to be highly specific for bombesin receptors.

It is encouraging that the high antagonist activity of [Leu^{13}-ψ-CH_2NH-Leu^{14}]bombesin extended to an assay system examining bombesin-stimulated cellular growth where it is about 200 times more potent than the substance P inhibitor spantide, which is the only other compound reported capable of blocking the actions of bombesin in the 3T3 cell system. This indicates that there are no significant differences in receptor recognition requirements between acinar and 3T3 cells and suggests that the probability of this antagonist inhibiting bombesin-stimulated growth of human small cell lung carcinoma strains should be quite good. The development of a bombesin receptor antagonist with useful therapeutic properties may require additional synthetic work aimed at improving receptor affinity even further and particularly at improving *in vivo* pharmacokinetic properties. The present compound offers an excellent lead structure for this type of research.

REFERENCES

1. Erspamer, V. (1980) in *Gastrointestinal Hormones* (Glass, G. B. J., ed) pp. 343–361, Raven Press, New York
2. Minna, J. D., Carney, D. N., Cuttitta, F., Gazdar, A. F., Ihde, G. C., Mulshine, J., and Nau, M. (1984) in *Adjuvant Therapy of Cancer IV* (Jones, S. E., and Salmon, S. E., eds) pp. 168–182, Grune and Stratton, New York
3. Cuttitta, F., Carney, D. N., Mulshine, J., Moody, T. W., Fedorko, J., Fischler, A., And Minna, J. D. (1985) *Nature* **316**, 823–826
4. Moody, T. W., Pert, C. B., Gadzer, A. F., Carney, D. N., and Minna, J. D. (1981) *Science* **214**, 1246–1248
5. Moody, T. W., Bertness, V., and Carney, D. N. (1983) *Peptides* **4**, 683–686
6. Moody, T. W., Carney, D. N., Cuttitta, F., Quattroochi, K., and Minna, J. D. (1985) *Life Sci.* **37**, 105–113
7. Jensen, R. T., Jones, S. W., Folkers, K., and Gardner, J. D. (1984) *Nature* **309**, 61–63
8. Heinz-Erian, P., Coy, D. H., Tamura, M., Jones, S. W., Gardner, J. D., and Jensen, R. T. (1987) *Am. J. Physiol.* **252**, G439–G442
9. Martinez, J., Bali, J. P., Rodriguez, M., Castro, B., Magous, R., Laur, J., and Ligon, M. F. (1985) *J. Med. Chem.* **28**, 1874–1879
10. Sasaki, Y., Murphy, W. A., Heiman, M., Lance, V. A., and Coy, D. H. (1987) *J. Med. Chem.* **30**, 1162–1166
11. Spatola, A. F. (1983) in *Chemistry and Biochemistry of Amino Acids and Proteins* (Weinstein, B., ed) pp. 267–357, Marcel Dekker, Basel
12. Sasaki, Y., and Coy, D. H. (1986) *Peptides* **8**, 119–121
13. Rivier, J. E., and Brown, M. R. (1978) *Biochemistry* **17**, 1766–1771
14. Jensen, R. T., Lemp, G. F., and Gardner, J. D. (1982) *J. Biol. Chem.* **257**, 5554–5559
15. Ceska, M., Birath, K., and Brown, B. (1969) *Clin. Chim. Acta* **26**, 437–444
16. Ceska, M., Brown, B., and Birath, K. (1969) *Clin. Chim. Acta* **26**, 445–453
17. Jensen, R. T. T., Moody, T., Pert, C., Rivier, J. E., and Gardner, J. D. (1978) *Proc. Natl. Acad. Sci. U. S. A.* **75**, 6139–6143
18. Hunter, W. M., and Greenwood, F. C. (1962) *Nature* **194**, 495–496
19. Jensen, R. T., Jones, S. W., Lu, Y-A., Xu, J-C., Folkers, K., and Gardner, J. D. (1984) *Biochim. Biophys. Acta* **804**, 181–191
20. Bolton, A. E., and Hunter, W. M. (1973) *Biochem. J.* **133**, 529–539
21. Shults, C. W., Find, R., Jensen, R. T., Moody, T. W., O'Donohue, T. L., and Chase, T. M. (1982) *Peptides* **3**, 1073–1075
22. Rozengurt, E., and Sinnet-Smith, J. (1983) *Proc. Natl. Acad. Sci. U. S. A.* **80**, 2936–2940
23. Zachary, I., and Rozengurt, E. (1985) *Proc. Natl. Acad. Sci. U. S. A.* **82**, 7616–7620
24. Hocart, S. J., Nekola, M. V., and Coy, D. H. (1988) in *Peptides: Chemistry and Biology, Proceedings of the 10th American Peptide Symposium* (Marshall, G. R., ed) ESCOM Science Publishers, Leiden, The Netherlands, in press
25. Wynants, C., Van Binst, G., and Loosli, H. R. (1985) *Int. J. Peptide Protein Res.* **25**, 615–621
26. Monahan, M. W., Amoss, M. S., Anderson, H. A., and Vale, W. (1973) *Biochemistry* **12**, 4616–4620
27. Erne, D., and Schwyzer, R. (1987) *Biochemistry* **26**, 6316–6319
28. Morgan, J. E., O'Neil, C. E., Coy, D. H., Hocart, S. J., and Nekola, M. V. (1986) *Int. Arch. Allergy Appl. Immun.* **80**, 70–75

ELSEVIER

Critical Reviews in Oncology/Hematology 24 (1996) 117–151

Critical Reviews in
ONCOLOGY/
HEMATOLOGY

Bombesin receptor antagonists

Roberto de Castiglione[a,1,*], Luigia Gozzini[b]

[a]*Farmitalia Carlo Erba (now Pharmacia), Research Centre, Via Giovanni XXIII, 23, 20014 Nerviano (MI), Italy*
[b]*Bracco S.p.A., Milano Research Centre, Via Folli, 50, 20134 Milano, Italy*

Accepted 25 June 1996

Contents

Abbreviations: ACTH, adrenocorticotropic hormone; 8-Br-cAMP, 8-bromo-cyclic-adenosin-monophosphate; A23187, calcimycin; Ac, acetyl; AN, alytesin; AVP, arginine-vasopressin; β-Leu β-homo-L-leucine; b.i.d., twice a day; BN, bombesin; Boc, *t*-butoxycarbonyl; BRS-3, BN receptor subtype 3; Cab, 4-[bis(2-chloroethylamino)]benzoic acid; CCK, cholecystokinin; CGRP, calcitonin gene related peptide; CNS, central nervous system; Cpa, *p*-chlorophenylalanine; DMBA, 9,10-dimethyl-1,2-benzanthracene; Dnp, 2,4-dinitrophenyl; Δ^2Phe, (z)-dehydrophenylalanine; ED_{50}, dose that is effective in 50% of test subjects; EGF, epidermal growth factor; EGF-R, epidermal growth factor receptor; ET, endothelin; Et, ethyl; FICE, Farmitalia Carlo Erba; FSH, follicle stimulating hormone; Glp, pyroglutamic acid; GIP, gastric inhibitory peptide; GH, growth hormone; GHRH, growth hormone releasing hormone; GHRP, growth hormone releasing peptide; GRP, gastrin releasing peptide; GRP-R, GRP-preferring bombesin receptor; h, hour; Hz, Hertz; i.c.v., intracerebroventricular(ly); i.p., intraperitoneal(ly); i.t., intrathecal(ly); i.v., intravenous(ly); IC_{50}, concentration of the antagonist to produce 50% inhibition; ICI, Imperial Chemical Industries; ID_{50}, dose inhibiting the response in 50% of the test subjects; IGF-I, insulin-like growth factor I; IP, inositol phosphates; K_d, equilibrium dissociation constant; K_i, inhibition constant; LH, luteinizing hormone; LHRH, luteinizing hormone releasing hormone; LLBN, [Leu[13]ψ(CH_2NH)Leu[14]]bombesin; LN, litorin; Me, methyl; Mel, 4-[bis(2-chloroethylamino)]-L-phenylalanine, Melphalan®; MeLeu, *N*-methylleucine; MePhe, *N*-methylphenylalanine; mMel, 3-[bis(2-chloroethylamino)]-L-phenylalanine; M_r, relative molecular mass; mRNA, messanger RNA; MS&D, Merck Sharp and Dohm; n.a., not available; n.t., not tested; Nal, 3-(2-naphthyl)alanine; NCI, National Cancer Institute; NMB, neuromedin B; NMB-R, NMB-preferring bombesin receptor; NMC, neuromedin C; NSCLC, non-small cell lung carcinoma; p115, 115 kDa protein; p90, 90 kDa protein; PDGF, platelet-derived growth factor; Ph, phenyl; PKC, protein kinase C; PI, phosphatidylinositol; PN, phyllolitorin; PP, pancreatic peptide; PRL, prolactin; ψ, peptide bond modification (the amide bond replacement is indicated in parenthesis or in the footnotes to the tables); PYY, peptide with N-terminal tyrosine and C-terminal tyrosinamide; RN, ranatensin; s.c., subcutaneous(ly); SCLC, small cell lung cancer; SP, substance P; SS, somatostatin; Sta, statine, (3*S*,4*S*)-4-amino-6-methyl-3-hydroxyheptanoic acid; TGFα, transforming growth factor α; Tic, 1,2,3,4-tetrahydroisoquinoline-3-carboxylic acid; TPA, 12-*o*-tetradecanoylphorbol-13-acetate; Tpi, 2,3,4,9-tetrahydro-1H-pyrido[3,4-b]indol-3-carboxylic acid; VIC, vasointestinal contractor; VIP, vasoactive intestinal peptide; Z, benzyloxycarbonyl; wt, weight.

* Corresponding author. Tel.: + 39 331 583832, fax: + 39 331 583833.

[1] Presently retired.

PII S1040-8428(96)00220-X

1. Introduction

Bombesin (BN) and its natural analogue alytesin (AN) are tetradecapeptides isolated in 1970 from the skins of the European discoglossid frogs *Bombina bombina*, *Bombina variegata* and *Alytes obstetricans* [1]. Other BN-like peptides are present in amphibian skins, the most representative being litorin (LN) [2], ranatensin (RN) [3] and phyllolitorin (PN) [4]. On the basis of their chemical structure and differential receptor affinity these peptides have been subdivided into three subfamilies: bombesin/alytesin, litorin/ranatensin and phyllolitorin. So far, mammalian counterparts have been found only for the first two subfamilies: gastrin-releasing peptide (GRP) [5] and neuromedin B (NMB) [6], respectively. GRP exists also in a shorter form, GRP-10 or GRP(18–27) (formerly neuromedin C, NMC) [7]. Recently, however, an amphibian GRP has been identified [8], which puts the present classification into question. There is some evidence for the presence of a phyllolitorin-like peptide in extracts of lymphoblasts from human leukemic bone marrow [9] and in certain human small cell lung cancer (SCLC) cell lines [10]. The sequences of these peptides are shown in Table 1; the human GRP and NMB structures are reported [11,12].

Binding studies with different BN-related peptides suggest that there are at least two distinct BN receptor subtypes: a receptor with higher affinity for GRP and BN than for NMB (GRP-preferring bombesin receptor; GRP-R) and a receptor with higher affinity for NMB than for either GRP or BN (NMB-preferring bombesin receptor; NMB-R) [13–19]. More recently, evidence for the existence of a separate receptor for phyllolitorin has been put forward [20], and a novel bombesin receptor subtype (BN receptor subtype 3; BRS-3) has been cloned [21].

Bombesin receptors, like the receptors for other neuropeptide mitogens such as angiotensin, endothelin (ET), substance P (SP) and substance K, are members of the G protein-coupled receptor family which are characterised by having seven transmembrane domains which cluster to form the ligand-binding pocket. Among the early events following BN binding in 3T3 cells are rapid activation of the phosphatidylinositol (PI) turnover and Ca^{2+} mobilisation, stimulation of protein kinase C (PKC) and phosphorylation of an acidic M_r 80 000 cellular protein, and epidermal growth factor (EGF) receptor transmodulation [22]. Tyrosine phosphorylation of a 115 kDa protein (p115) [23,24] and a 90 kDa protein (p90) [24] has also been observed.

The wide spectrum of biological activities of BN-like peptides has been extensively reviewed [25–29]. These activities include regulation of the release of gastrointestinal peptide hormones, stimulation of secretion by various exocrine glands, contraction of smooth musculature, and effects on the central nervous system (CNS). In addition, they can function as growth factors in Swiss 3T3 murine fibroblasts and have been implicated as autocrine growth factors in the pathogenesis of some human small cell lung carcinomas.

Whereas a number of BN analogues have been synthesised and the structural requirements for agonistic activity defined [30–32], no specific BN-receptor antagonists were known until quite recently. The search for such antagonists was stimulated by the finding that BN-like peptides could play a role as autocrine growth factors in promoting the growth of small cell lung

Table 1
Amino-acid sequences of some natural BN-like peptides

	1	2	3	4	5	6	7	8	9	10	11	12	13	14	
Bombesin (BN) [1]	Glp	Gln	Arg	Leu	Gly	Asn	Gln	Trp	Ala	Val	Gly	His	Leu	Met	NH_2
Alytesin (AN) [1]	Glp	Gly	Arg	Leu	Gly	Thr	Gln	Trp	Ala	Val	Gly	His	Leu	Met	NH_2
Human gastrin-releasing peptide (h-GRP) [11]	R	Tyr	Pro	Arg	Gly	Asn	His	Trp	Ala	Val	Gly	His	Leu	Met	NH_2
		15	16	17	18	19	20	21	22	23	24	25	26	27	
					⊢				GRP-10, NMC					⊣	
Litorin (LN) [2]						Glp	Gln	Trp	Ala	Val	Gly	His	Phe	Met	NH_2
Ranatensin (RN) [3]				Glp	Val	Pro	Gln	Trp	Ala	Val	Gly	His	Phe	Met	NH_2
Human neuromedin B (h-NMB) [12]	R'	His	Ser	Arg	Gly	Asn	Leu	Trp	Ala	Thr	Gly	His	Phe	Met	NH_2
					⊢				NMB-10				⊣		
Phyllolitorin (PN) [4]						Glp	Leu	Trp	Ala	Val	Gly	Ser	Phe	Met	NH_2

R = Val Pro Leu Pro Ala Gly Gly Gly Thr Val Leu Thr Lys Met

R' = Ala Pro Leu Ser Trp Asp Leu Pro Glu Pro Arg Ser Arg Ala Ser Lys Ile Arg Val

Amino acid residues different from bombesin are in bold type.

cancers and by the potential of these antagonists in the treatment of these tumours [33–35]. The medical interest in these antagonists was further enhanced with the subsequent discovery of a possible autocrine/paracrine role of BN-like peptides in other tumoural forms, such as cancers of the breast [36,37], colon [38,39], pancreas [40–42], and prostate [43].

A number of receptor antagonists for bombesin-like peptides have been synthesised and assayed both in vitro and in vivo in different test preparations and animal species. These antagonists can be classified in different groups according to their chemical structure Some of them have already been reviewed [44–47], and will not be mentioned here except for a short introduction and for new studies. The present review covers the literature until the end of 1993.

2. Bombesin receptor antagonists

2.1. Substance P-derived antagonists and SP/BN hybrids

2.1.1. Substance P analogues

The history of bombesin receptor antagonists began in 1984 with the discovery that the substance P receptor antagonist [D-Arg^1,D-Pro^2,D-Trp^{7,9},Leu^{11}]SP was able to reverse, in a competitive manner, the BN-stimulated release of amylase from dispersed guinea-pig pancreatic acini [48]. Since then, other multiple D-amino acid-substituted analogues of SP, SP(4–11) or SP(6–11) have similarly been found to behave as competitive BN receptor antagonists. However, all these peptides suffered from lack of potency (activity in the 0.1–100 μM range) and selectivity, antagonising also the effects of vasopressin and angiotensin. The literature on this class of BN antagonists has been covered to mid-1990 by Houben and Denef [46]. Structures of the analogues discussed in this review are reported in Table 2.

In murine Swiss 3T3 cells, [D-Arg^1,D-Phe^5,D-Trp^{7,9},Leu^{11}]SP (2), at 10 μM concentration, was found to completely inhibit Ca^{2+} mobilisation induced by 10 nM bradykinin, cholecystokinin (CCK), arginine-vasopressin (AVP) and galanin, and by 2 nM GRP and neurotensin [49]. Under the same test conditions, [Arg^6,D-Trp^{7,9},MePhe^8]SP(6–11) (5) had potency similar to antagonist 2 in competitively inhibiting vasopressin-stimulated DNA synthesis. However, it was a less potent antagonist of GRP and bradykinin in these cells and did not block the effects of other mitogens [49]. In SCLC cell lines, antagonists 2 and 5 almost completely suppressed the growth of cell lines H345 and H69 in liquid culture, with half-maximal inhibition of growth at about 20 μM. The antagonism was reversible. In the clonogenic assay (cell line H510A) both antagonists inhibited colony formation in a dose-depen-

Table 2
Substance P-derived bombesin receptor antagonists (1-5) and SP/BN hybrids (6-11)

					1	2	3	4	5	6	7	8	9	10	11	
	SP				Arg	Pro	Lys	Pro	Gln	Gln	Phe	Phe	Gly	Leu	Met	NH_2
1					arg	Pro	Lys	Pro	Gln	Gln	trp	Phe	trp	Leu	Leu	NH_2
2					arg	Pro	Lys	Pro	phe	Gln	trp	Phe	trp	Leu	Leu	NH_2
3					arg	pro	Lys	Pro	Gln	Gln	trp	Phe	trp	Leu	Leu	NH_2
4								pro	Gln	Gln	trp	Phe	trp	trp	Met	NH_2
5										Arg	trp	MePhe	trp	Leu	Met	NH_2
6					Arg	Pro	Lys	Pro	*Trp*	*Ala*	*Val*	*Gly*	trp	*Leu*	*Leu*	NH_2
7		*Glp*	*Gln*	*Arg*	*Leu*	*Gly*	*Asn*	*Gln*	□		trp	Phe	trp	Leu	Met	NH_2
8							*Boc*	*gln*	*Trp*	*Ala*	trp	Phe	trp	*Leu*	*Nle*	NH_2
9							*Asn*	*gln*	*Trp*	*Ala*	trp	Phe	trp	*Leu*	*Nle*	NH_2
10								*Glp*	*Trp*	*Ala*	trp	Phe	trp	*Leu*	*Nle*	NH_2
11							*Boc*	*Gln*	*Trp*	*Ala*	trp	Phe	*his*	*Leu*	*Nle*	NH_2
	BN	*Glp*	*Gln*	*Arg*	*Leu*	*Gly*	*Asn*	*Gln*	*Trp*	*Ala*	*Val*	*Gly*	*His*	*Leu*	*Met*	NH_2
		1	2	3	4	5	6	7	8	9	10	11	12	13	14	

Different graphic types are used for SP (roman) and BN (italic); substituted residues are in bold type; residues of D-amino acids and deleted amino acids are represented by small letters and an open box, respectively.

dent manner, but antagonist 2 was slightly more potent than 5. Both antagonists, at 10 μM, inhibited Ca^{2+} mobilisation due to 10 nM bradykinin, CCK and vasopressin (cell line H510A). At the same concentration each antagonist inhibited the effect of 2 nM GRP, 2 nM neurotensin and 10 nM galanin (cell lines NCI-H345 and NCI-H69), although incomplete suppression of responses was seen with antagonist 5 at this dose. As in the model Swiss 3T3 cell system, less antagonist was required to block Ca^{2+} mobilisation than mitogenesis. Moreover, the inhibition of SCLC growth induced by antagonist 5 could be reversed by washing the cells, but not by the addition of these agonists at 100 nM concentrations [49]. (However, 200 nM galanin was subsequently reported to reverse the inhibitory effect on SCLC colony formation induced by 20 μM antagonist 5 [50]). The potency of these two antagonists contrasts with the weak effects of other SP antagonists in SCLC. The fact that antagonist 5 is about 10-fold less potent than antagonist 2 in blocking BN/GRP-mediated mitogenesis but is almost as potent as 2 in inhibiting SCLC proliferation, and that their antagonism in SCLC is not reversed by BN, suggests that the mechanism of the inhibitory action of 2 and 5 cannot be ascribed solely to the interruption of a BN-driven autocrine loop, but rather to multiple autocrine or paracrine loops and possibly to an as yet unidentified neuropeptide growth factor. These considerations have lead to the proposition that broad-spectrum antagonists, such as antagonists 2 and 5, could constitute a logical new approach to the treatment of complex tumours in which multiple growth factors are known to interact to stimulate proliferation [51], as recently evidenced for antagonist 5. In fact, this antagonist, given peritumourally once a day for 1 week to nude mice bearing fragments of NCI-H69 SCLC xenograft implanted for 6 weeks (when the tumours had reached a mean volume of 30 mm^3), profoundly inhibited the growth of the tumour beyond the duration of administration. Moreover, antagonist 2, at 10 μM, completely abolished the Ca^{2+} mobilising effect of 100 nM BN in SCLC cells, and that of 1 nM but not 100 nM BN in Swiss 3T3 cells. The antagonist at this concentration effectively inhibited the mitogenic action of 1 nM BN in Swiss 3T3 cells; however, much higher doses ($\sim$ 100 μM) were needed to inhibit DNA synthesis in SCLC cells. In addition, the antagonist inhibited DNA synthesis with a similar dose dependency both in BN/GRP-nonproducing and -producing cells. These results indicate that BN/GRP and other calcium mobilising peptides (such as tachykinins) do not always act as growth factors in SCLC cells, and that the BN antagonist could inhibit growth of SCLC cells through a mechanism other than BN antagonism [52]. In human lung tumour cell lines, antagonist 2, as

well as LLBN (see Section 2.4.1), inhibited Ca^{2+} responses stimulated by GRP (SCLC), NMB and phyllolitorin (both SCLC and NSCLC) [20]. Antagonist 2 also blocked the calcium response to BN, bradykinin and AVP in several human SCLC cell lines, but had only a partial inhibitory effect on the calcium response induced by CCK-8. A 20-fold higher concentration, however, was required to inhibit [^{3}H]thymidine incorporation, indicating once again that there is no direct correlation between peptide effects on intracellular calcium and cell proliferation [53]. The broad spectrum of action of this class of antagonists was further extended with the discovery that antagonist 2 blocked binding, Ca^{2+}-mobilising and mitogenic effects of endothelin and vasoactive intestinal contractor (VIC) in mouse 3T3 cells [54], while [D-Arg^1,D-Trp^{7,9},Leu^{11}]SP (1) inhibited naloxone binding to mouse spinal cord and brain membranes, and its antinoceptive effects (i.t. and i.c.v.) were antagonised by pretreatment with naloxone [55].

Antagonist 1, [D-Arg^1,D-Pro^2,D-Trp^{7,9},Leu^{11}]SP (3) and antagonist 2 inhibited in a dose-dependent manner the growth hormone (GH) release from rat anterior pituitary cells stimulated with 2.08×10^{-8} M His-D-Trp-Ala-Trp-D-Phe-Lys-NH_2 (a synthetic GH releasing peptide, GHRP) with IC_{50}'s of 0.2, 0.85, and 6 μM, respectively, but had only a 10–15% inhibitory effect on the GH release stimulated with 3.71×10^{-9} M rGHRH (the natural rat GH releasing hormone) [56].

In anaesthetised dogs, antagonist 3 inhibited the dose-dependent increase of pancreatic protein secretion induced by GRP (i.v.). The fact that a similar inhibition was observed also with a CCK antagonist, suggested that GRP-stimulated secretion was, at least in part, mediated by endogenously released CCK [57].

In the human breast cancer cell line MCF-7 both antagonists 2 and 3 antagonised BN-stimulated inositol lipid hydrolysis, as did the selective BN antagonist [Leu$^{13}\psi$(CH$_2$NH)Leu^{14}]BN (LLBN) (see Section 2.4.1.). However, antagonist 2 (60 and 80 μM) also exhibited considerable agonist activity which was not antagonised by LLBN. Indeed, a subthreshold dose of antagonist 2 (40 μM) in the presence of LLBN (10 μM) potentiated the inositol lipid hydrolysis response. BN, GRP, LLBN and antagonist 2 inhibited 43 pM [^{125}I]GRP binding to MCF-7 cells with IC_{50}'s of 150 pM, 150 pM, 150 nM and 600 nM, respectively. These data are consistent with the presence of separate receptors or binding sites for BN and SP analogues, which are coupled to a common signal pathway in human breast cancer cells [58].

On rat pancreatic tissue, where BN/GRP have higher affinity than NMB for BN receptors, both [D-Pro^4,D-Trp^{7,9,10}]SP (4) and antagonist 1 functioned as agonists at concentrations > 1 μM. On rat oesophageal muscle strips (where the BN receptor has higher affinity for NMB than for BN, GRP and NMC) neither antagonist, at concentrations up to 100 μM, caused muscle contraction. However, they were the most potent antagonists for inhibiting 3 nM NMB-stimulated oesophageal muscle contractions, with IC_{50}'s of 9 ± 1 and 35 ± 12 μM, respectively. Other BN-related antagonists (except [Tyr^4,D-Phe^{12}]BN) showed no inhibition up to the maximal doses tested [59].

2.1.2. Substance P/bombesin hybrids

Structural features responsible for the lack of selectivity were examined after the preparation of two mixed BN/SP sequences [60]. [D-Trp^{12},Leu^{14}]SP(1–4)BN(8–14) (6) retained some bombesin antagonistic activity on guinea-pig pancreatic acini (IC_{50} of 10 μM; concentration of agonist not reported); however, the presence of the SP amino terminus did not produce any affinity for SP receptors. BN(1–7)-D-Trp-Phe-D-Trp-Leu-Met-NH_2 (7), containing a bombesin amino terminus and an SP-antagonist carboxyl terminus, was an antagonist of both BN and SP (IC_{50} of 10 and 2 μM, respectively; concentration of agonists not reported). Therefore, it was concluded that receptor selectivity and recognition requirements for both receptor types reside totally in the carboxyl-terminal pentapeptide regions of each peptide.

In the search for more potent and specific BN receptor antagonists as antimitogenic agents in SCLC tumours, a series of carboxyl-terminal BN analogues (from 8 to 14 amino-acid residues), incorporating some of the characteristic features of SP antagonists, were synthesised and screened on 3T3 fibroblasts [61]. Antagonists 8–11 inhibited [^{125}I]GRP (0.2 nM) binding with IC_{50}'s of 6.0 ± 1.7, 4.0 ± 0.5, 5.3 ± 0.2 and 3.8 ± 0.8 μM, respectively; slightly better than antagonists 1 and 3 under the same experimental conditions (IC_{50}'s of 11.1 and 14.0 μM, respectively). All six antagonists were practically equipotent in inhibiting DNA synthesis ($IC_{50} \sim 5$ μM) induced by 25 nM BN. Antagonist 8, at a 5 μM concentration, significantly antagonised rat urinary bladder contraction (in vitro) induced by 5 nM BN. At a dose of 10 μg/rat i.c.v., antagonist 8 also significantly antagonised the grooming behaviour induced by 0.01 μg BN, without any of the toxic effects observed with spantide (antagonist 1) [62]. However, at a 1 μM concentration, the compound only marginally reduced amylase secretion from dispersed rat pancreatic acini induced by 0.3 nM BN, as observed also for the other members of this series of hybrid peptides. In view of their poor receptor binding affinities and antimitogenic activities in 3T3 cells, none of these derivatives was considered worthy of study in SCLC cell lines or in selectivity tests versus other neuropeptides [61].

2.2. BN antagonists by modifications at positions 10 12 and 14

2.2.1. [D-Phe^{12}] and [des-His^{12}]BN analogues

[D-Phe^{12}]bombesin analogues were the first BN-related peptides that functioned as selective receptor antagonists, [D-Phe^{12},Leu^{14}]BN being the prototype [63]. Other D-amino acids were subsequently introduced in

position 12, alone or in combination with other modifications in other parts of the molecule, but, as already reviewed, the efficacy of all these derivatives was limited by low solubility and potency [45,46]. Among the new findings, fourth ventricular injection of 25 ng [D-Phe[12],Leu[14]]BN reliably facilitated milk intake in nondeprived rats (suggesting that endogenous BN-like peptides contribute to the termination of feeding) [64]. Another analogue, [D-Phe[25]]GRP(18–27) (corresponding to [His[7],D-Phe[12]]BN(5–14)), was found to reduce to 15.4% the release of insulin from isolated canine pancreas stimulated by 1 nM GRP(18–27), when previously infused at a 10 μM concentration [65].

Just as replacement of His[12] by D-amino acids gave rise to derivatives with antagonistic properties, so did its deletion [66]. On Swiss 3T3 fibroblasts, two alytesin derivatives, [Boc-Thr[6],des-His[12]]BN(6–14) and [Thr[6],des-His[12]]BN(6–14), were practically devoid of agonistic activity, but inhibited [^{125}I]GRP binding (0.2 nM) with much higher affinity than [D-Phe[12],Leu[14]]BN (IC_{50}'s of 1.00 ± 0.1 and 3.19 ± 0.21 μM, respectively, versus 22.8 ± 8 μM). Furthermore, they also inhibited, by 53 ± 14 and 32 ± 9%, respectively, the incorporation of [^{3}H]thymidine induced by 25 nM bombesin. Under the same experimental conditions [D-Phe[12],Leu[14]]BN did not show any antagonism. In addition, [Boc-Thr[6],des-His[12]]BN(6–14), at a concentration of twice its binding IC_{50}, inhibited, by 84%, inositol phosphate production induced by 5 nM bombesin (the other analogue was not tested).

2.2.2. [Ala[10]]BN analogues

Replacement of Val[8] of GRP-10 (corresponding to Val[23] of GRP or Val[10] of BN) by Ala also gave rise to BN receptor antagonists. [Ala[8]]GRP-10 was shown to inhibit insulin secretion stimulated by GRP-10 in a dose-dependent manner both in vivo and in vitro. In the dog the inhibition was almost complete at a dose 100 times higher than that of GRP-10 [67]. By prior infusion of 10 and 100 nM, the analogue reduced to 85.2 and 33.0%, respectively, the insulin release from isolated canine pancreas induced by 1 nM GRP-10 [65]. Glucagon secretion was inhibited only in vivo [65,67] while the stimulation of gastrin secretion was potentiated, suggesting the presence of different types of receptors for BN-like peptides on gastric G- and pancreatic B-cells [67].

2.2.3. [D-Pro[11]] and [D-Tic[11]]BN analogues

Very recently, a series of side chain restricted analogues of BN receptor agonist [D-Phe[6],Leu[14]]BN(6–14) (equipotent with BN) has been prepared. Only alteration of Gly[11] gave rise to antagonists. Among these, [D-Phe[6],D-Pro[11],Leu[14]]BN(6–14) and [D-Phe[6],D-Tic[11],Leu[14]]BN-(6–14) (Tic = 1,2,3,4-tetrahydroisoquinoline-3-carboxylic acid), in the dispersed rat pancreatic acini test, inhibited both [^{125}I-Tyr[4]]BN binding (IC_{50}'s ~ 100 nM) and 0.3 nM BN-stimulated amylase release (IC_{50}'s ~400 nM). The antagonism was competitive and highly selective for GRP receptors [68].

2.2.4. [Δ[5]Phe[14]]BN analogues

Another bombesin analogue containing a conformationally constrained C-terminal dehydrophenylalanine methyl ester, Ac[D-Phe[6],Δ[5]Phe[14]]BN-OMe, was shown to be a competitive BN-receptor antagonist in mouse pancreas (PI turnover), with a K_d of 0.78 nM (concentration of labeled ligand not reported) [69].

2.3. [Des-Met[14]]BN analogues

This class of bombesin receptor antagonists was independently developed by several research groups, based on previous knowledge that receptor antagonists of cholecystokinin or gastrin could have been obtained by removal of their C-terminal amino acid residue [70,71] or by restoring its side-chain by an alkylamide [72] or ester [73].

2.3.1. FICE's products

During a structure-activity study carried out at Farmitalia Carlo Erba (FICE), mainly on the carboxyl-terminal nonapeptide of alytesin (that differs from bombesin only in having the Asn[6] residue replaced by Thr), and which was addressed particularly at the mitogenic effects, it was found that removal of Met[14] markedly impaired bioactivity (Table 3) [66]. On Swiss 3T3 cells peptides 12–15 displayed some binding affinity for BN receptors but, at concentrations up to 5 μM, the same peptides did not stimulate thymidine incorporation. Moreover, they neither induced phosphorylation of a p115 protein associated with the BN receptor, nor stimulated inositol phosphate production (not shown). In competition experiments, peptides 12–15 (but not peptide 16) at 5 μM concentrations were able to inhibit thymidine incorporation induced by 25 nM BN. Peptide 16, alone, stimulated both thymidine incorporation and p115 phosphorylation, suggesting that a pentyl amide residue could replace Met-NH_2 without loss of activity (in other words, a carboxyamide group is not required in position 14 of bombesin). Therefore, the weak antagonism of peptides 14 and 15 could be ascribed to the concomitant presence of a Dnp-protected His[12] residue. In addition, peptides 13–15 (peptide 12 was not tested), at concentrations of twice their binding IC_{50}'s, inhibited by 91, 87 and 82%, respectively, the inositol phosphate production induced by 5 nM BN [66].

2.3.2. Coy's products

Almost at the same time, a series of des-Met[14] bombesin derivatives (terminating either as primary or secondary amides, alkyl esters or hydrazides) were developed by Coy at Tulane University. As they have already been reviewed [44–47], they will be only briefly summarised here. While

Table 3
Structure and biological activities of FICE's [des-Met[14]]BN analogues in Swiss 3T3 fibroblasts [66]

No.	Structure	Inhibition of 0.2 nM [^{125}I]GRP binding IC_{50} (nM)	Inhibition of [^{3}H]thymidine incorporation induced by 25 nM BN at 5 μM peptide concentration %
	Bombesin	12.6 ± 0.6	agonist
12	Boc - Thr - Gln - Trp - Ala - Val - Gly - His - Leu - NH_2	566 ± 128	13 ± 5
13	Boc — (Dnp His) — NH_2	770 ± 13	14 ± 4
14	Boc — (Dnp His) — $NH(CH_2)_4CH_3$	508 ± 112	22 ± 6
15	H — (Dnp His) — $NH(CH_2)_4CH_3$	335 ± 101	31 ± 13
16	H — $NH(CH_2)_4CH_3$	76 ± 30	0

Residues identical to the parent compound are represented by a line.

[des-Met[14]]BN amide was as potent an antagonist as [Leu[13]ψ(CH_2NH)Leu[14]]BN (the prototype of another class of receptor antagonist discussed in Section 2.4.1.) in inhibiting amylase release from guinea-pig pancreatic acini, shortening of the peptide length at the amino-terminus, as in BN(6–13)amide, resulted in a 20-fold decrease in potency. However, the substitution of Asn[6] with D-Phe compensated for the shortening of the peptide sequence: [D-Phe[6]]BN(6–13)amide was even more potent than BN(1–13)amide in inhibiting 50 pM [^{125}I-Tyr[4]]BN binding and 0.3 nM BN-stimulated amylase release in both guinea-pig pancreatic acini (K_i and IC_{50} values of 96 ± 21 and 24 ± 11 nM vs. 216 ± 30 and 33 ± 10 nM, respectively) and rat pancreatic acini (27 ± 6 and 100 ± 20 nM vs. 296 ± 28 and 2300 ± 230 nM, respectively), and in inhibiting 50 pM labeled BN binding and [^{3}H]thymidine incorporation in 3T3 cells stimulated with 1 nM BN (K_i and IC_{50} values of 23 ± 1 and 29 ± 16 nM vs. 226 ± 70 and 88 ± 21 nM, respectively) [45]. It was also observed that the requirements for position 6 were not narrow. D-Phe[6] could be replaced by either natural or unnatural aromatic D-amino acids and by D-Leu with retention of potent antagonistic activity [74]. On the basis of these results the [D-Phe[6]]BN(6–13) sequence was selected for studying the effects of derivatization of the carboxyl-terminal function [75]. [D-Phe[6]]BN(6–13)propyl amide turned out to be the most potent antagonist, being 30-fold more potent than [Leu[13]ψ(CH_2NH)Leu[14]]BN in 3T3 cells (K_i of 1.7 ± 0.2 nM; IC_{50} of 0.8 ± 0.1 nM) and 40-fold more potent in guinea-pig pancreatic acini (K_i of 5.3 ± 0.9 nM; IC_{50} of 1.6 ± 0.3 nM) (concentration of the labeled ligand and of the agonist as above) [74,75]. The chain length of the alkyl amide was crucial for antagonistic/agonistic activity. In fact, while in guinea-pig pancreatic acini [D-Phe[6]]BN(6–13)ethyl, propyl and heptyl amides were pure antagonists, the butyl and hexyl amides behaved as partial agonists. In rat pancreatic acini only the ethyl amide was a pure antagonist, whereas the propyl and heptyl amides behaved as partial agonists, and the butyl and hexyl amides as agonists [75]. This observation is in line with the results of FICE's investigators who found that the pentyl amide could confer agonistic properties to [des-Met[14]]BN analogues [66]. Replacement of the amide by the hydrazide or alkyl ester function also resulted in potent antagonistic activity [75], whereas the free acid analogue was a very weak antagonist [74]. From these studies it was also evident that BN receptors in different species do not necessarily have the same requirements for agonistic activity. For example, [D-Phe[6]]-BN(6–13)propyl amide was a pure antagonist in the Swiss 3T3 and guinea-pig acinar cell preparations [74–76], as well as in guinea-pig airways in vivo, in which a transient inhibition of BN-induced bronchoconstriction was produced [77]. However, it was a partial antagonist in rat pancreatic acini [75,78], in human antral G cells (where at 1.0 μM concentration it stimulated gastrin release 3-fold over the basal value and only partially inhibited BN-stimulated gastrin release) [79], and in rats

in vivo (where enhanced BN-provoked gastrin release) [80]. On the other hand, this bombesin analogue bound to the BN/GRP receptors in the SCLC cell line NCI-H720 with an affinity (IC_{50}, 3 nM vs. 0.25 nM [^{125}I]GRP) comparable to that of BN and GRP (IC_{50}'s of 1 and 5 nM, respectively), and higher than [D-Phe^6]BN(6–13)butyl amide (IC_{50}, 5 nM) and [D-Phe^6]BN(6–13)amide (IC_{50}, 12 nM). These observations confirmed that the optimal length of the alkyl amide side chain at the carboxyl-terminus of [des-Met^{14}]BN analogues is three carbon atoms [81]. In SCLC cell lines, at 1 μM concentration, [D-Phe^6]BN(6–13)propyl amide had no effect on cytosolic Ca^{2+} but significantly antagonised the increase in Ca^{2+} caused by 10 nM bombesin. In contrast, [D-Phe^6]BN(6–13)butyl amide behaved in the same assay as a mixed agonist/antagonist [81]. Both peptides inhibited dose-dependently the clonal growth of several SCLC cell lines induced by 10 nM BN. However, at 1 μM concentration, [D-Phe^6]BN(6–13)propyl amide inhibited while [D-Phe^6]BN(6–13)butyl amide stimulated the basal colony count, suggesting that the propyl amide analogue is a better BN receptor antagonist than the butyl amide derivative, in that it is also able to stop the growth induced by endogenous BN/GRP [81]. [D-Phe^6]BN(6–13)propyl amide also inhibited radiolabeled BN (50 pM) and GRP (20 pM) binding to human colon cancer cell line NCI-H716 (K_i of 5.9 ± 0.8 nM) [39] and to MC-26 mouse colon tumour membranes (IC_{50} of 4.5 ± 0.5 nM) [76], respectively. Moreover, the peptide blocked 50 nM BN-induced growth of the MC-26 cell line (IC_{50} ~ 65 nM), but not the growth effects of conditioned medium. This indicated that GRP is not an autocrine growth factor for these tumoural cells. This was confirmed by an absence of BN-like peptides and the GRP gene in these cells [76].

The specificity of this class of BN-receptor antagonists was demonstrated by the finding that both [D-Phe^6]BN(6–13)amide and propyl amide completely inhibited amylase release from guinea-pig pancreatic acini stimulated by BN, GRP and NMC (which stimulate secretion by interacting with bombesin receptors), but not by CCK-8, carbamylcholine, SP, vasoactive intestinal peptide (VIP), secretin, or calcitonin gene related peptide (CGRP) (each of which interacts with its receptor on pancreatic acini), or by TPA or A23187 which stimulate amylase secretion by post-receptor mechanisms [74].

A protected carboxyl-terminus is required for both agonistic and antagonistic activity. des-amidated bombesin being at least 100-fold less potent an agonist than bombesin [31,32], and [D-Phe^6]BN(6–13)OH an antagonist 40-fold less active than [D-Phe^6]BN(6–13)amide [74]. Hydrazide or methyl and ethyl esters of [D-Phe^6]BN(6–13) were as potent antagonists as [D-Phe^6]BN(6–13)propyl amide in guinea-pig pancreatic acini and pure antagonists also in the rat pancreatic acini, where the last one behaved as a partial agonist [75]. Unlike the propyl amide derivative, [D-Phe^6]BN(6–13)OMe and [D-Phe^6]BN(6–13)NH-NH$_2$, at 1.0 μM concentrations, did not stimulate gastrin release from isolated human G-cells but rather inhibited, by 99 ± 2.4 and 85 ± 3.8%, respectively, gastrin release induced by 10 nM BN [79]. In isolated rat stomach, [D-Phe^6]BN(6–13)OMe, at 1 μM concentration, did not affect basal gastrin secretion but inhibited gastrin release stimulated vagally at 10 Hz but not 2 Hz [82]. In unanaesthetised rats, the antagonist did not alter basal gastrin, GIP, PP, and PYY levels but completely antagonised the release of these hormones, through primarily the GRP/NMC-preferring receptor [83]. In the SCLC cell line NCI-H720, [D-Phe^6]BN(6–13)OMe inhibited the binding of 0.25 nM [^{125}I]GRP to its receptor with an IC_{50} value of 5 nM [81], while in human colon cancer cell line NCI-H716 it totally blocked, at 1 μM concentration, $[Ca^{2+}]_i$ increase induced by 0.1 μM [Tyr^4]BN [39]. After injection in rats, the methyl ester derivative was clearly the most potent antagonist and, at 20 μmol/kg (i.v. bolus), completely inhibited the amylase release stimulated with continuous i.v. infusion of 2 nmol BN/kg/h for 2 h [78]. However, the lack of an effect of this BN-receptor antagonist on basal pancreatic secretion, on the response to liquid food intake or on the diversion of bile-pancreatic juice in rats suggested that endogenous BN-like peptides do not act either directly or indirectly to mediate these responses [84]. In contrast to that, fourth ventricular injection of [D-Phe^6]BN(6–13)OMe (5 ng), as well as [D-Phe^{12},Leu^{14}]BN (25 ng), reliably facilitated milk intake in rats by inhibiting satiety induced by endogenous BN-like peptides [64]. [D-Phe^6]BN(6–13)OMe antagonised in a competitive manner the bombesin-induced, concentration-dependent contraction of the guinea-pig isolated bladder (GRP-R) but failed to inhibit the contraction of isolated rat bladder (NMB-R), behaving as a partial agonist [85]. The same antagonist inhibited BN-induced guinea-pig lung contraction with high potency (in contrast to the lower potency of the less specific antagonist [Leu$^{13}\psi$(CH$_2$NH)Leu^{14}]BN), providing evidence that BN-induced bronchoconstriction results from a direct effect of BN on bronchial smooth muscle GRP-preferring receptors [86]. In line with these findings, the radiolabeled antagonist [^{125}I-D-Tyr^6]BN(6–13)OMe was recently found to have a > 10 000-fold higher affinity for GRP receptors (rat pancreatic membranes) than for NMB receptors (rat oesophageal membranes). In comparison with the radiolabeled agonist [^{125}I-Tyr^4]BN, binding of the antagonist more rapidly reached equilibrium and was more rapidly reversible. Unlike [^{125}I-Tyr^4]BN, binding of the antagonist was not affected by guanine nucleotides and the ligand was not internalised [87].

It was suggested that, although the potency and biological half-life of these short BN antagonists were significantly improved over that of [Leu$^{13}\psi$-(CH_2NH)Leu^{14}]BN, their degradation rates were still quite high. It was thought that [D-Phe^6]BN(6–13)OMe derivatives carrying further modifications to the peptide chain might combine high receptor affinity and inhibitory potency with improved enzymatic stability. The modifications tested were the replacement of Gly^{11} by D-Ala and the introduction of more lipophilic residues at the amino-terminus. The new analogues, [D-Phe^6,D-Ala^{11}]BN(6–13)OMe, [D-pentafluoro-Phe^6,D-Ala^{11}]BN(6–13)OMe and N^{α}-propionyl-[D-Ala^{24}]GRP(20–26)OMe (corresponding to N^{α}-propionyl-[His^7,D-Ala^{11}]BN(7–13)OMe), behaved as the parent compound with regard to receptor selectivity (BN vs. NMB) and inhibition of amylase release from and binding to rat pancreatic acini. The most lipophilic analogue (the D-F_5Phe derivative) inhibited BN-stimulated protein secretion in rats to basal values for 15 times longer than an equivalent dose of any of the other three analogues [88]. All of the antagonists of this class had significantly higher affinity for the GRP-preferring receptor subtype than for the NMB-preferring subtype in rat brain [89,90]. At the GRP-preferring site [D-F_5Phe^6,D-Ala^{11}]BN(6–13)OMe was the most potent, with a K_i of 2 nM vs. 40 pM labeled GRP [89]. The same behaviour was also noticed in rat urinary bladder membranes, where these antagonists were almost ineffective in displacing radiolabeled [Tyr^4,Leu^{14}]BN from putative NMB receptor sites [91].

In an in vitro binding assay vs. 0.25 nM labeled GRP, in the SCLC cell line NCI-H345, [D-F_5Phe^6,D-Ala^{11}]BN(1–13)OMe had an IC_{50} value (9 nM) of the same order of magnitude as [D-Phe^6]BN(6–13)propyl amide (3 nM). However, when incubated with intact cells, the two peptides had a quite different half-lives (1338 and 559 min, respectively) [92]. In the rat brain each member of this class of antagonists displayed the greatest potency and highest degree of selectivity for the GRP-preferring subtype over the NMB-preferring one [79].

Antagonists such as [D-Phe^6]BN(6–13)OMe and [D-Tyr^6]BN(6–13)propyl amide bound with the same high affinity (1–5 nM) to both solubilized and cellular BN/GRP receptors on human glioblastoma (U-118) and lung carcinoid (NCI-H720) cell lines. On the contrary, agonists bound to cellular receptors with the same high affinity as antagonists, but with lower affinity to solubilized receptors [93]. This, together with the observation that binding of radiolabeled GRP to purified Swiss 3T3 BN/GRP receptors was insensitive to guanine nucleotides (contrary to the binding situation in intact membranes) [94], suggested that a guanine nucleotide binding protein had dissociated from the solubilized receptors during purification, thus impairing the ability of agonists (but not that of antagonists) to bind to these receptors [93].

Following a similar approach, a series of [des-Met^9]litorin (litorin = [Glp^6,Phe^8]BN(6–14)) were prepared [95]. The replacement of Phe^8 in [des-Met^9]LN by statine (Sta = (3*S*,4*S*)-4-amino-6-methyl-3-hydroxyheptanoic acid) produced a peptide endowed with antagonistic activity in thymidine uptake (3T3 cells) and amylase release (isolated guinea-pig pancreatic acini). Surprisingly, the same modification in the bombesin sequence resulted in a product that behaved as an agonist. The potency of the [Sta^8]LN(1–8)NH_2 was further increased by the additional replacement of the N-terminal Glp residue by D-Phe or D-*p*-chlorophenylalanine (D-Cpa). The two compounds inhibited [^{125}I]GRP binding (concentration not reported) to Swiss 3T3 cells with K_i values of 7.2 and 4.5 nM, respectively. These values are several times lower than the value for the corresponding analogue unmodified in position 1 (K_i of 150 nM). A similar affinity was retained when position 8 was occupied by other uncommon substituted γ-amino acids. In preliminary experiments in vivo with human SCLC cell line NCI-H69 transplanted in athymic nude mice, [Sta^8]LN(1–8)NH_2, administered s.c. around the tumours at a dose of 50 μg b.i.d., produced a significant reduction of tumour size [95]. Another analogue, [D-Cpa^1,β Leu^5]LN(1–8)NH_2, inhibited both BN/GRP binding and thymidine incorporation in BN/GRP receptor-positive SCLC cell lines. In addition, it delayed the growth of xenografts of these cell lines in nude mice (showing a cytostatic effect) when administered at a dose of 50 μg twice a day by peritumoural s.c. injection. The peptide was ineffective both in vitro and in vivo in SCLC cell lines not expressing BN/GRP receptors [96].

2.3.3. MS&D's products

In the meantime, Merck Sharp and Dohme's (MS&D) investigators, while elucidating the minimal GRP sequence required for mitogenic activity in Swiss 3T3 fibroblasts, had identified *N*-acetyl-GRP(20–27)amide as the smallest peptide exhibiting full agonistic activity [97]. This confirmed what had previously been observed for temperature and glucose regulation [98] and gastric secretion [99] in rats. Deletion of Met^{27} from *N*-acetyl-GRP(20–27)amide, however, generated a peptide which preserved some binding affinity (IC_{50} of 1.57 μM) but did not stimulate a mitogenic response [97]. This observation prompted MS&D's investigators to study a series of carboxyl-terminal esters of *N*-acetyl-GRP(20–26). Each of the esters proved to be a mitogenic antagonist, with the ethyl and propyl derivatives having IC_{50} values of approximately 4 nM in the binding inhibition assay vs. 2 nM [^{3}H-Phe^{15}]GRP(15–27) [100]. Larger aliphatic substituents on the ester linkage gave rise to less potent compounds. The ethyl amide

derivative of *N*-acetyl-GRP(20–26) was prepared for comparison with the corresponding ethyl ester. Despite the fact that the carboxyl-terminus of this compound more closely mimicked the peptide bond between Leu^{26}-Met^{27} of GRP, the ethyl amide exhibited lower antagonistic potency than the ethyl ester [100]. The same trend, although less pronounced, was observed for the pair [D-Phe^6]BN(6–13)ethyl amide and [D-Phe^6]BN(6–13)ethyl ester [75]. Also for this new series of analogues the methyl ester was again less potent than the ethyl ester [100]. It is worth noting that Ac-GRP(20–26)OEt had been synthesised and tested both at Tulane University and at MS&D. In the binding assay with Swiss 3T3 cells the affinity values reported by the two groups were, respectively, 1.5 nM [75] and 3.9 nM [100]. This discrepancy, which can perhaps be ascribed to small differences in experimental conditions (such as cells, challenge dose of radioligand, etc.) indicates the difficulties in comparing data obtained from different laboratories. Another striking example is [$Leu^{13}\psi(CH_2NH)Leu^{14}$]BN, for which, in the same binding assay, IC_{50} values of 18 nM (Tulane University) [101], 190 nM (MS&D) [100] and 214 nM (FICE) [102] have been reported.

In SCLC cell line NCI-H345, Ac-GRP(20–26)OEt not only failed to elicit any calcium response but also inhibited $[Ca^{2+}]_i$ increase induced by 100 nM GRP with an IC_{50} of approximately 400 nM [100]. Moreover, in the rat the same peptide significantly reduced the GRP-dependent release of gastrin [100]. Intracisternal administration (1 nmol) of Ac-GRP(20–26)OMe, but not Ac-GRP(20–26)OEt, reversed the inhibitory effect of an intracisternal injection of bombesin (19 pmol) on gastric acid output and concentration in the rat [103]. Both antagonists reduced or blocked the effects of BN-related peptides in vitro on GRP receptor systems while being completely inactive on rat urinary bladder (NMB-R system) [104]. Intravenous administration of Ac-GRP(20–26)NH_2 specifically inhibited GRP-stimulated insulin and glucagon secretion in mice [105].

Unfortunately, Ac-GRP(20–26)OEt was found to be rapidly degraded by human serum esterases, which severely limited the peptide's potential clinical utility. To overcome this drawback, MS&D's investigators introduced modifications to the C-terminal portion of the molecule, resulting in novel antagonists with improved receptor binding potency and antimitogenic activity in Swiss 3T3 fibroblasts (Table 4) and improved stability in human serum [106]. Replacement of the C-terminal carbonyl of Ac-GRP(20–26)OEt (17) by a methylene group yielded an ethyl ether derivative 19 which was almost as potent as the parent compound in 3T3 cells, but completely stable to degradation in human serum in vitro.

Substitution of Gly^{24} by D-Ala, which should not interfere with the formation of a β-turn (unlike substitution with L-Ala), gave compound 22 which had complete retention of binding and antagonistic activity. A similar substitution in the agonist sequence Ac-GRP(20–27)NH_2 had a potentiating effect. On the other hand, replacement by L-Ala dramatically reduced the binding affinity of both peptides, without changing their biological profile (not shown). These results suggest that a β-turn structure may be important in high-affinity binding of both GRP agonists and antagonists to GRP receptors on murine fibroblasts [106].

Replacement of the ether oxygen of the methyl ether derivative 18 by a methylene group gave the pair of alkyl amide derivatives 23 and 24 in which, depending upon the presence of heteroatoms, the stereochemical nomenclature is reversed compared to the nomenclature of the ether antagonists and Leu^{26} of GRP itself [106]. Chain length variation of the alkyl amide slightly modified binding and mitogenic inhibition, the optimal length being, in this case, four carbon atoms. (*R*)-Alkyl amide derivatives were always more potent than the corresponding *S* isomers. Replacement of the *N*-acetyl by the *N*-pivaloyl group (potentially more stable in vivo) gave a compound (29) with similar binding affinity and higher antimitogenic activity [106]. The ethyl ether (19) and the (*R*)-2-methyl-4-nonylalkylamide (26) blocked the GRP-dependent elevation of $[Ca^{2+}]_i$ in SCLC cell line H345 with IC_{50}'s of 250 and 150 nM, respectively, when stimulated with 100 nM GRP [106]. Similar results were obtained for the pair of isomers 23 and 24 in Cos-7 monkey cells [107]. Not surprisingly, compound 26 was ineffective in inhibiting the growth of SCLC cell lines NCI-H345, NCI-N592 and NCI-H69, which were insensitive to stimulation of colony formation by *N*-acetyl-GRP(20–27) [108]. In rats, the pivaloyl alkyl amide (29) dose-dependently inhibited the NMC-stimulated (1 nM) GH and PRL release from perifused anterior pituitary cell aggregates (with IC_{50}'s of 0.20 and 0.16 nM, respectively) [109], while the ethyl ether (19) reduced in a dose-dependent fashion the GRP-induced elevation of serum gastrin after i.p. administration [106].

2.3.4. ICI's products

Investigators at ICI obtained potent [des-Met^{14}]BN receptor antagonists as a result of a systematic synthesis of truncated and side-chain deletion analogues of the Ac-GRP(18–27) sequence, and from a screening of a previous collection of SP analogues. A hybrid between the weak SP antagonist (belonging to the class of [des-Met^{11}]SP) Z-Arg-Pro-Lys(Z)-Pro-Gln-Gln-Phe-Phe-Gly-Leu-OMe and GRP(18–26) provided the first potent specific in vitro BN antagonist, Z-Arg-Pro-Lys(Z)-His-Trp-Ala-Val-Gly-His-Leu-OMe (30) (Table 5). This had IC_{50}'s of 2–3 nM for both binding and mitogenic assays in 3T3 cells [110]. Further structural modifications led to the identification of $(CH_3)_2CHCO$-

Table 4
Structure and biological activities of MS&D's GRP(20-25) alkylether and alkylamide derivatives in Swiss 3T3 fibroblasts [106]

No.	Structure	Inhibition of 2 nM [^{3}H-Phe^{15}]GRP(15-27)NH_2 IC_{50} (nM)	Inhibition of [^{3}H]thymidine incorporation induced by 3 nM Ac-GRP(20-27)NH_2 IC_{50} (nM)
	$CH_2CH(CH_3)_2$		
17	Ac-His-Trp-Ala-Val-Gly-His-NH-CH-C-OCH_2CH_3 (Ac-GRP(20-26)OEt)	3.9	20
18	CH_2OCH_3	8.3	91
19	$CH_2OCH_2CH_3$	6.2	31
20	$CH_2O(CH_2)_2CH_3$	3.2	18
21	$CH_2O(CH_2)_2CH(CH_3)_2$	11.0	32
22	ala — $CH_2OCH_2CH_3$	5.0	35
23	$(CH_2)_2CH_3$ (R)	2.6	10
24	$(CH_2)_2CH_3$ (S)	4.9	35
25	$(CH_2)_2CH_3$ (R)	1.4	3
26	$(CH_2)_4CH_3$ (R)	2.0	4
27	$(CH_2)_4CH_3$ (S)	11.0	22
28	$(CH_2)_5CH_3$ (R)	2.8	7
29	$(CH_3)_3C$-C(=O)- $(CH_2)_4CH_3$ (R)	1.8	0.6

Residues identical to the parent compound are represented by a line. ala, D-Ala.

His-Trp-Ala-Val-D-Ala-His-Leu-NHMe (ICI 216140) (31), which reduced BN-stimulated (5 μg/kg, i.v.) rat pancreatic amylase secretion to basal levels when administered s.c. at 2.0 mg/kg [110], and produced a statistically significant inhibition of turkey pancreatic fluid and protein output when administered at the dose of 50 μg/kg i.v. 2 min before the stimulation with 6-100 pmol/kg chicken GRP [111]. In a study aimed at defining its pharmacological profile, compound 31 was also found to inhibit BN-stimulated mobilisation of calcium in Swiss 3T3 fibroblasts and contraction of the rat gastric fundal strip, and to attenuate, in rats (up to 10 μg i.c.v.), the fall in rectal temperature associated with bombesin (0.10 μg i.c.v.). However, it was shown not to antagonise grooming/scratching but rather to act as an agonist [112]. Antagonist 31, as well as [D-Phe^{6}]BN(6-13)ethyl amide, competitively inhibited BN-induced Ca^{2+} mobilisation in SCLC cell line NCI-H345. In contrast, these compounds antagonised NMB-stimulated Ca^{2+} transients in a noncompetitive manner, thus supporting receptor heterogeneity for BN-like peptides in this SCLC cell line [113]. Subsequently, each position of compound 31 was modified. Compounds identified in vitro for their ability to inhibit 0.2-0.4 nM GRP(18-27)-induced mitogenesis in Swiss 3T3 cells were also tested in vivo for their ability to inhibit BN-induced (5 μg/kg i.v.) amylase secretion in rats. The Trp-Ala-Val sequence was found to be a very important feature of the antagonist activity. In contrast, amino-acid replacements in other parts of the molecule were more tolerated and sometimes led to marked increases in the in vitro and in vivo activity. The most potent analogues were obtained by replacing Leu^{26} by MeLeu and His^{25} by Lys(X) where X = Z, PhCO, $PhCH_2CO$ or $Ph(CH_2)_2CO$. Thus, 4-pyridylcarbonyl-His-Trp-Ala-Val-D-Ala-His-Lys($COCH_2CH_2Ph$)-Leu-NHMe (32) inhibited mitogenesis with an IC_{50} of 0.022 nM. In vivo, compound 32, its Lys($COCH_2Ph$) derivative (33) and 4-pyridylcarbonyl-His-Trp-Ala-Val-D-Ala-Lys(Z)-MeLeu-OMe (34) had IC_{50} values of less than 20 μg/kg s.c., and their effects lasted for more than 3 h [114].

The same investigators, after observing that a number of antagonists of both substance P and luteinizing

Table 5
Structure and biological activities of ICI's GRP(20–26) analogues [110,114,115]

No.	Structure	Mouse 3T3 fibroblasts: Receptor binding[a] (IC_{50}, nM)	Mouse 3T3 fibroblasts: Inhibition of mitogenesis[b] (IC_{50}, nM)	Amylase output in rats[c]: Dose (mg/kg s.c.)	Amylase output in rats[c]: Time before i.v. BN (min)	Amylase output in rats[c]: Inhibition (%)
30	Z - Arg - Pro - Lys - His - Trp - Ala - Val - Gly - His - Leu - OMe (GRP (20-26))	2.85 ± 0.53	2.6 ± 0.66	20.0	250	20
31	$(CH_3)_2CHC$(O) — ala — NHMe	4.13 ± 0.82	3.4, 5.3	2.0 0.5 0.1	60 60 60	100 65 58
32	4-Pyridyl-C(O) — ala - Lys($COCH_2CH_2Ph$) — NHMe	n.a.	0.022	0.02	150	77
33	4-Pyridyl-C(O) — ala - Lys($COCH_2Ph$) — NHMe	n.a.	0.103	0.02	150	88
34	4-Pyridyl-C(O) — ala - Lys(Z) - MeLeu-OMe	n.a.	0.22	0.1 0.02	150 150	91 76
35	Ac - nal - Pro - cpa — ala — OMe	2.94 ± 1.7	1.1, 0.8	20	150	inactive
36	4-Pyridyl-C(O) — ala — OMe	0.99 ± 0.31	0.67, 0.9	2.0 0.5 0.1	150 150 150	92 57 39

Residues identical to the parent compound are represented by a line; ala, D-Ala; cpa, D-Cpa; nal, D-Nal.
[a] Vs 1.5 nM [^{125}I]GRP.
[b] Stimulated with 0.4 nM GRP(18-27).
[c] Stimulated with 5 μg BN/kg i.v.

hormone-releasing hormone (LHRH) were at the same time weak antagonists of bombesin, synthesised a few hybrids of LHRH and BN/GRP antagonists [115]. Some of these new analogues, e.g. Ac-D-2-naphthylalanyl-Pro-D-Cpa-His-Trp-Ala-Val-D-Ala-His-Leu-OMe (35), were potent inhibitors of bombesin in the in vitro test systems, but were inactive in vivo following subcutaneous injection. The high lipophilicity of these compounds, due to the presence of very hydrophobic and bulky amino-acid residues, and their high molecular weight, could possibly have prevented them from diffusing from the site of injection. It was also possible that they were absorbed but excreted very rapidly. In fact, one of these derivatives, administered intravenously to rat along with 5 μg BN/kg, at a dose of 0.5 mg/kg, inhibited BN-stimulated amylase secretion very significantly (80%). Further modifications of the N-terminus of the His-Trp-Ala-Val-D-Ala-His-Leu heptapeptide, aiming at reducing size and hydrophobicity of the previous derivatives, led to analogues that displayed potent and prolonged antagonist activity in vivo. One of these, 4-pyridylcarbonyl-His-Trp-Ala-Val-D-Ala-His-Leu-OMe (36, IC_{50} of 0.99 nM in the binding assay vs. 0.25 nM labeled GRP), inhibited BN-stimulated amylase secretion in rats at dose levels ranging from 0.1 to 2 mg/kg s.c. [115].

2.4. BN analogues with a reduced peptide bond

2.4.1. [Leu$^{13}\psi$(CH_2NH)Leu^{14}]BN

The strategy of modifying the peptide bond to obtain peptide hormone antagonists was originally applied to gastrin analogues, in which an amino-acid linkage (–CONH–) was changed into a reduced peptide bond ($-CH_2NH-$) [116]. At the time of its discovery, [Leu$^{13}\psi$(CH_2NH)Leu^{14}]BN (LLBN), with a reported IC_{50} value of 18 nM for the inhibition of 1 nM BN-stimulated DNA synthesis in Swiss 3T3 fibroblasts [101], was the first BN receptor antagonist which was active in the nanomolar range. It was hoped, therefore, that this product would be the peptide or the lead structure for the treatment of human small cell lung carcinoma.

To explain the mechanism by which [Leu$^{13}\psi$-(CH$_2$NH)Leu^{14}]BN functions as an antagonist, the authors referred to the hypothesis that the C-terminal BN sequence exists in a β-turn conformation stabilised by hydrogen bonds (Fig. 1). The switch from agonistic to antagonistic activity was consequently ascribed to the destruction of the hydrogen bond between the Leu^{13}-CO group and the Val^{10}-NH group. Such a theory also explained why [Ala$^{9}\psi$(CH$_2$NH)Val^{10},Leu^{14}]BN behaved as a weak antagonist, while other analogues, in which the reduced peptide bond is in other positions, did not. In this case it is conceivable that the same hydrogen bond could also be inhibited by the replacement of the 9–10 peptide bond since bond angles and rotational freedom would all be significantly affected [101]. However, conformational studies on bombesin and analogues favour random coil and α-helix conformations for the molecule in solution and in a membrane-like environment, respectively [117–120]. Nevertheless, the hypothesis of disruption of a stabilised structure still holds [121,122].

Since its discovery [Leu$^{13}\psi$(CH$_2$NH)Leu^{14}]BN has been studied by several groups and has proved to be an excellent compound for investigating the various cellular growth-promoting and neurohormonal effects of BN-like peptides. In Swiss 3T3 cells, LLBN blocked BN-stimulated DNA synthesis with IC_{50} values in the submicromolar range (18 nM [101]; 214 nM [102]; 250 nM [122]; 240 nM [123]; 199 nM [124]) but not that induced by other mitogens such as platelet-derived growth factor (PDGF), epidermal growth factor (EGF), phorbol-12,13-dibutyrate, and cholera toxin [123]. Unlike substance P antagonists, LLBN failed to inhibit mitogenesis induced by bradykinin [125]. Moreover, this antagonist inhibited receptor associated signals induced by BN, such as release of arachidonic acid [126], and phosphorylation of an M_r 80 000 cellular protein [127] (subsequently named MARCKS, Myristoylated Alanine-Rich C Kinase Substrate [128]), as well as decreasing the levels of mRNA encoding this protein [128], and down-regulating the receptor [129].

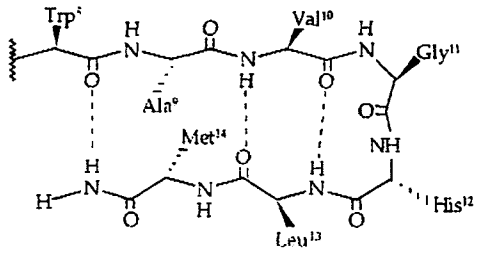

Fig. 1. Possible conformation of the C-terminal BN sequence (modified from Ref. [101]).

[Leu$^{13}\psi$(CH$_2$NH)Leu^{14}]BN was also able to inhibit transmembrane signals associated with autocrine growth control in human SCLC. In SCLC cell line NCI-H345 the peptide showed high binding affinity with a K_i value of 80.4 vs. 0.05 nM [^{125}I-Tyr^{4}]BN [130] and displaced 0.25 nM [^{125}I]GRP with an IC_{50} of 15 nM [131] which is similar to that reported by Coy for Swiss 3T3 cells [101]. Subsequently, this value was modified to 30 nM by the same group [132]. In the same cell line the antagonist blocked BN-induced PI turnover [130,133] and transient increase in [Ca^{2+}]$_i$ [130–132,92]. The IC_{50} values reported by the different groups are different for the two assays; nevertheless, the data suggest that there are differences in the sensitivity of the antagonist to the various BN-evoked responses. In vitro, in the clonogenic assay, LLBN antagonised both the BN/GRP-stimulated and basal growth of SCLC cell lines NCI-H345 [92,130,132], NCI-N592 [131,132,134], NCI-H720 [132], and NCI-H69 [134]. In contrast, it did not alter the growth of cell lines NCI-H520 (squamous carcinoma) and NCI-H727 (bronchial carcinoid) [132]. In SCLC cell line NCI-H345 the antagonistic potency of the peptide was enhanced by the simultaneous presence of the protease inhibitor thiorphan, suggesting that the peptide may be degraded by endogenous, membrane-associated enzymes. The LLBN half-life, after incubation with NCI-H345 cells, was 646 min; addition of 100 μM thiorphan increased this value to 907 min [92]. When injected subcutaneously into the tissue adjacent to the tumour, at a dose of 10 μg/day starting 1 week after cell implantation, LLBN inhibited NCI-N592 xenograft formation in nude mice. The effect was dose-dependent, in that 0.1 μg/day had no effect [92,132]. The maximum inhibition value reported was 72% [132]. In another study, the peptide was given s.c. twice a day for 20 days in the contralateral flank, at a nominal dose of 100 μg/day (actual dose: 72 μg/day). Treatment started on day 18 when the average tumour weight was about 100 mg. Under such drastic conditions, NCI-N592 tumour growth inhibition accounted for only 21% [134]. Biodistribution experiments with ^{125}I-labeled LLBN in nude mice showed that only 1% of the peptide injected intravenously localised to the tumour. Low percentages were associated with other organs and tissues, confirming that the peptide undergoes rapid degradation [92].

LLBN inhibited binding of 43 pM [^{125}I]GRP to human breast cancer cell line MCF-7 with an IC_{50} value of 150 nM [58] and binding of ~ 20 pM labeled GRP to mouse colon cancer MC-26 cells with an IC_{50} value of 87 nM [76]. In the MCF-7 cell line the peptide, at a 1 μM concentration, had no effect on inositol phosphate production and displaced the bombesin dose-response curve to the right, resulting in a tenfold increase in the ED_{50} for bombesin. The increase in Ca^{2+} efflux in response to 10 nM BN was also reduced

by approximately 50% by 1 μM LLBN and completely blocked at 10 μM LLBN [58]. In MC-26 cells this peptide inhibited the clonal growth induced by the maximal effective dose of BN (50 nM) in a dose-dependent manner; in the absence of BN, the peptide had no effect on clonal growth [76]. It was also demonstrated that in several human tumour cell lines, LLBN inhibited the Ca^{2+} response, induced not only by GRP and NMB, but also by phyllolitorin [20].

[Leu$^{13}\psi$(CH$_2$NH)Leu^{14}]BN has been tested in several other in vitro and in vivo systems, and has proved to be an interesting tool for investigating the role of endogenous BN-like peptides. This peptide inhibited 1 nM BN-stimulated contraction of isolated smooth muscle cells from guinea-pig stomach with an IC_{50} value of 0.8 nM, and acted as a competitive BN-receptor antagonist with a calculated IC_{50} value of 70 nM [135]. In isolated perfused porcine antrum, at 0.5 μM concentration, the peptide inhibited somatostatin and gastrin secretion, and abolished the motility induced by both GRP infusion and vagus stimulation [136]. Gastric secretion was also inhibited in vivo in pentobarbital-anaesthetised rats in a dose-dependent fashion, exhibiting an ID_{50} of 0.66 μg/250 g [137]. In isolated mouse gastric fundus, LLBN dose-dependently antagonised BN-induced inhibition of both basal and histamine-stimulated acid secretion and reduced somatostatin secretion to below the basal level [138,139]. In isolated vascularly perfused rat duodeno-jejunum, the antagonist was a potent inhibitor of BN-stimulated CCK release. At 1 μM concentration this compound completely abolished the CCK release mediated by 1 nM BN, but failed to suppress food-induced CCK release [140]. In isolated canine G-cells, at 1 μM concentration, LLBN did not affect basal gastrin secretion and completely blocked the BN-activated gastrin secretion over the BN range 0.01–1 pM. Inhibition of gastrin release induced by 10 and 100 pM BN was 74.8 and 56.2%, respectively [141]. In brain slices, pretreatment with LLBN inhibited the stimulatory effects of BN on suprachiasmatic neurons [142]. In perifused anterior pituitary reaggregate cell cultures from adult male rats, LLBN (500 μM) blocked the GH release stimulated by NMC (1 μM), GRP (1 μM) and NMB (10 μM), but not the stimulation of GH release by GHRH. PRL responses were also inhibited [143]. In cultured human retinal pigment epithelium LLBN blocked, by > 90%, the BN-enhanced PI hydrolysis [144].

In the rat, i.c.v. administration of [Leu$^{13}\psi$-(CH$_2$NH)Leu^{14}]BN blocked the suppressive effects on food intake of both i.c.v. [145] and i.p. [146] bombesin, and, in satiated animals, enhanced food intake [145]. In gastric fistula cat, the antagonist abolished the dose-related stimulation of luminal gastric somatostatin output and the concomitant dose-dependent inhibition of food intake produced by intravenous BN [147]. Infusion of the peptide (2.5 μg) in the preoptic area prior to bombesin (25 ng) injection also prevented BN-induced hypothermia [148]. However, in the anaesthetised rat, the peptide failed to antagonise the inhibitory effect of bombesin on GH release and, given alone, mimicked BN behaviour [137]. Moreover, at 1 and 10 μg i.c.v., rather than preventing grooming/scratching induced by BN (0.01 and 0.1 μg), it stimulated such behaviour in rats [149]. All these data taken together support the hypotheses that: (i) [Leu$^{13}\psi$(CH$_2$NH)Leu^{14}]BN may act also as a partial agonist; and (ii) different types of binding sites exist for BN-like peptides. These hypotheses are further corroborated by the observation that LLBN stimulated pepsinogen secretion from frog oesophageal peptic cells, with an intrinsic efficacy which was 36% of that of BN, and with an IC_{50} of 30 nM [150] and, contrary to what occurred with guinea-pig pancreatic acini (pure antagonist, with an IC_{50} of 31 $\pm$ 4 nM against stimulation with 0.3 nM BN), it behaved as partial agonist (11% of BN efficacy) in stimulating amylase release from rat pancreatic acini (IC_{50} of 300 $\pm$ 60 nM) [75].

It is known that BN receptors in rat pancreatic tissue have a high affinity for GRP and BN, but a low affinity for NMB. The opposite is true for BN receptors in rat oesophageal muscle. In such preparation LLBN was unable to inhibit 3 nM NMB-stimulated muscle contraction, while it was able to antagonise 0.3 nM BN-stimulated amylase release with an IC_{50} of 0.21 $\pm$ 0.05 μM [59]. BN/GRP-preferring and NMB-preferring receptors are also present in rat uterus and urinary bladder, respectively, whereas receptors on seminal vesicles show similar affinities to BN and NMB. [Leu$^{13}\psi$(CH$_2$NH)Leu^{14}]BN was much more potent in displacing saturable [^{125}I-Tyr^4]BN binding from uterus than from bladder and seminal vesicle membranes [19].

2.4.2. *Analogues of [Leu$^{13}\psi$(CH$_2$NH)Leu^{14}]BN*

Among the various amino-acid replacements to increase binding affinity and antagonistic potency of the LLBN parent compound, only substitution of Phe for Leu^{14} and D-Phe for Asn^6 gave better or comparable results, as measured in the dispersed guinea-pig pancreatic acini for amylase release and by displacement of radiolabeled [Tyr^4]BN [151].

2.4.3. *Short-chain BN analogues with a reduced peptide bond*

2.4.3.1. Coy's derivatives. Another approach to improve the biological profile of [Leu$^{13}\psi$(CH$_2$NH)Leu^{14}]BN was to shorten the peptide chain from the amino-terminus. Short-chain pseudopeptides were prepared based on bombesin, neuromedin C and litorin sequences [151]. In the guinea-pig pancreatic acini test, BN(5–14)-, BN(6–14)-, and NMC-analogues were all at least five times

less potent than the full-length parent peptide. Two notable exceptions were the litorin pseudopeptides [Phe^{8} ψ(CH$_2$NH)Met^{9}]LN and [Leu$^{8}\psi$(CH$_2$NH)Met^{9}]-LN, which were just as potent as [Leu$^{13}\psi$(CH$_2$NH)-Leu^{14}]BN. Since the latter litorin analogue corresponds to BN(6-14) in which Asn^{6} is replaced by Glp, it was apparent that the pyroglutamic acid residue at position 1 was directly instrumental in producing these much improved inhibitory potencies. With this in mind, the position was examined in much greater detail. D-Amino acids were again a logical choice: a 30-fold increase in potency was obtained with [D-Phe^{6},Leu$^{13}\psi$(CH$_2$NH)Leu^{14}]BN(6-14) compared to [Leu$^{13}\psi$(CH$_2$NH)Leu^{14}]BN(6-14), and a 10-fold increase with [D-Phe^{2},Leu$^{9}\psi$(CH$_2$NH)Leu^{10}]NMC(2-10) (= [D-Phe^{6},His^{7},Leu$^{13}\psi$(CH$_2$NH)Leu^{14}]BN(6-14)) over [Leu$^{9}\psi$(CH$_2$NH)Leu^{10}]NMC [151]. Thus, the D-Phe residue mimicked the effects of the N-terminal 5 amino acids of bombesin, either in terms of a direct interaction with the BN-receptor or by influencing the folded conformation of the analogue chain. That a D-Phe residue could compensate for the loss of the N-terminal sequence was observed also in the series of short-chain [des-Met^{14}]BN antagonists (see Section 2.3.2.). Replacement of the Gly^{1} residue in NMC by D-Ala led to a substantial increase of potency. In fact, [Leu$^{9}\psi$(CH$_2$NH)Leu^{10}]NMC antagonised 1 nM NMC-induced amylase release from isolated rat pancreatic acini with an IC$_{50}$ of 13.4 μM. This value was lowered to 1.5 μM when the N-terminal amino acid was replaced by D-Ala to give [D-Ala^{1},Leu$^{9}\psi$(CH$_2$NH)-Leu^{10}]NMC [152]. The same trend was observed for guinea-pig pancreatic acini [151]. In vitro, this increase in activity is often attributable to a conformational enhancement of receptor affinity but in vivo it can also be the result of an increased resistance to proteolytic breakdown.

The substitution of Phe for Leu^{14} in the parent peptide gave [Leu$^{13}\psi$(CH$_2$NH)Phe^{14}]BN which was about twice as potent in the amylase release and pancreatic acinar binding assays [151] (see Section 2.4.2.). The same modification to D-Phe^{6} short-chain analogues gave rise to [D-Phe^{6},Leu$^{13}\psi$(CH$_2$NH)Phe^{14}]BN(6-14) which was particularly effective in inhibiting Swiss 3T3 cell growth induced by 3 nM BN (IC$_{50}$ = 0.72 ± 0.29 nM; K_i = 3.1 ± 0.6 nM) and amylase release stimulated with 0.1 nM BN from guinea-pig pancreatic acini (IC$_{50}$ = 7.5 ± 0.5 nM; K_i = 10.0 ± 1.5 nM). The requirement for a D-Phe residue in position 6 of short pseudopeptides does not seem to be too strict in that this residue could be replaced by D-Cpa and D-Nal with little effect on potency. A loss of potency was, however, observed when D-Phe was replaced by D-MePhe [151].

When examined in murine Swiss 3T3 cells, two other analogues proved more active than the parent peptide [Leu$^{13}\psi$(CH$_2$NH)Leu^{14}]BN, namely [D-Phe^{6},Leu$^{13}\psi$-(CH$_2$NH)Leu^{14}]BN(6-14) (IC$_{50}$ = 9.2 ± 3.9 nM; K_i = 7.1 ± 0.6 nM) and [D-Nal^{6},Leu$^{13}\psi$(CH$_2$NH)Phe^{14}]-BN(6-14) (IC$_{50}$ = 3.3 ± 1.6 nM; K_i = 14.6 ± 6.9 nM) [151]. However, as observed for LLBN, these short-chain derivatives also showed partial agonistic activity in rat pancreatic acini [153]. Several structural modification strategies were developed to remove these partial agonistic properties. The most effective of these was the substitution of the C-terminal residue with Cpa to give [D-Phe^{6},Leu$^{13}\psi$(CH$_2$NH)Cpa^{14}]BN(6-14) which, in both guinea-pig and rat pancreatic acini, behaved as pure antagonist in inhibiting 0.3 nM BN-stimulated amylase release with IC$_{50}$ values of 2.4 ± 0.5 and 10.4 ± 1.4 nM, respectively. Another effective method was the alteration of the stereochemistry of the amino acid in position 14. [D-Phe^{6},Leu$^{13}\psi$(CH$_2$-NH)D-Phe^{14}]BN(6-14) had somewhat lowered binding affinities but pure antagonistic properties. [D-Phe^{6,14}]BN(6-14) itself, however, was a strong full agonist in the rat and a partial agonist in the guinea-pig [153].

[D-Phe^{6},Leu$^{13}\psi$(CH$_2$NH)Leu^{14}]BN(6-14) at a 1 μM concentration completely inhibited amylase release from guinea-pig pancreatic acini stimulated by 0.3 nM BN, 1 nM GRP, 1 nM NMC and NMB (all these peptides acting through the BN-receptor) but not by 0.1 nM CCK-8, 10 μM carbamylcholine, 3 nM SP, 0.3 nM VIP, 0.1 μM secretin or 0.1 μM CGRP (each of which interacts with its own receptor), or by 0.1 μM TPA, 1 μM A23187, or 8-Br-c-AMP (which have post-receptor mechanisms) [151]. However, this compound, as well as [D-Cpa^{6},Leu$^{13}\psi$(CH$_2$NH)Phe^{14}]BN(6-14), was almost ineffective in displacing radiolabeled bombesin from rat urinary bladder membranes [91].

[D-Cpa^{6},Leu$^{13}\psi$(CH$_2$NH)Phe^{14}]BN(6-14) competitively blocked bombesin stimulatory effects on pancreatic amylase and total protein secretion when continuously infused into anaesthetised rats. However, this analogue, despite being a long-lasting BN antagonist, was incapable of lowering amylase to basal levels even at 50 times the BN dose, and, probably because in vivo it behaved as a mixed agonist/antagonist, was less potent than the full antagonist [D-Phe^{6}]BN(6-13)OMe [78]. A residual agonist activity of 7% was also observed in vitro in rat pancreatic acini [153].

With regard to the antiproliferative effects of the peptides of this series, it was observed that [D-Phe^{6},Leu$^{13}\psi$(CH$_2$NH)D-Cpa^{14}]BN(6-14) bound to human colon cancer cell line NCI-H716 with a K_i of 7 ± 0.8 nM vs. 50 pM [^{125}I-Tyr^{4}]BN [39]. In SCLC cell line NCI-H345, [D-Phe^{6},Leu$^{13}\psi$(CH$_2$NH)Cpa^{14}]-BN(6-14) and [D-Nal^{6},Leu$^{13}\psi$(CH$_2$NH)Phe^{14}]BN-(6-14) inhibited 0.25 nM [^{125}I]GRP binding with IC$_{50}$'s of 10 and 5 nM, respectively, and at 1 μM dose inhibited both [Ca^{2+}]$_i$ release and growth response induced by 10 nM bombesin [92]. [D-

Phe[6],Leu[13]ψ(CH_2NH)Cpa[14]]BN(6–14) was examined for its ability to inhibit DNA synthesis in vitro in four SCLC cell lines. Two of these (SCLC 6 and SCLC 74R) did not possess receptors for BN/GRP, whereas the other two lines (SCLC 41 and SCLC 75) not only had receptors for these growth factors but also expressed prepro-GRP mRNA. The peptide inhibited DNA synthesis in cell line SCLC 41 but, surprisingly, had no effect in SCLC 75. Likewise, no effect was observed in cell line SCLC 74R. In SCLC 6, however, a weak stimulation was observed, suggesting a different mechanism of interaction [96]. In vivo, with xenografts of SCLC 41 in nude mice, the peptide significantly decreased the rate of tumour growth after s.c. administration around the tumour at a dose of 50 μg twice a day for 10 days. Treatment started when the tumour had reached 30–100 mm^3. However, after day 20 the tumour started to regrow. A stronger inhibitory effect was observed when the dose was increased to 250 μg twice a day. No effect was seen with the other transplanted cell lines [96].

A study aimed at examining the long term consequences of a neonatal blockade of bombesin was carried out using [D-Phe[6],Leu[13]ψ(CH_2NH)Cpa[14]]BN-(6–14) [154]. The results of this study indicated that, under the dose regimen and testing conditions employed, subchronic treatment of infant rats with the antagonist did not appear to have consequences in terms of adult sensitivity to central or systemic bombesin. To what extent this result is the reflex of a limited in vivo stability of the peptide remains to be clarified. In fact, in a different study, it was shown that this peptide, as well as [D-Nal[6],Leu[13]ψ-(CH_2NH)Phe[14]]BN(6–14), had a short half-life when incubated with intact SCLC cell line NCI-H345 [90]. In rats, [D-Phe[6],Leu[13]ψ(CH_2NH)Cpa[14]]BN(6–14), which had no effect on food intake when administered alone even at high doses (20 mg/kg), selectively reduced BN-induced satiety but had no effect on satiety induced by [D-Phe[1],βLeu[8],Leu[9]]LN, a synthetic bombesin agonist [155].

2.4.3.2. Schally's derivatives. As an extension of the work of Coy et al., on short-chain pseudopeptide BN receptor antagonists, culminating in the discovery of [D-Phe[6],Leu[13]ψ(CH_2NH)Phe[14]]BN(6–14) [153], the Schally's group at Tulane University developed a series of analogues with the general formula [A[6],Leu[13]ψ(CH_2NH)B[14]]BN(6–14), in which A is D-Phe, D-Trp or D-Tpi (Tpi = 2,3,4,9-tetrahydro-1H-pyrido[3,4-b]indol-3-carboxylic acid, a Trp analogue) and B either Leu or Phe [156]. Antagonist [D-Trp[6],Leu[13]ψ(CH_2NH)Phe[14]]BN(6–14) (RC-3420) was the most potent of the analogues tested: it inhibited the amylase release induced by 10 nM GRP(14–27) from superfused rat pancreatic acini (60% inhibition of the maximal response and 80% inhibition of the net-integral response at 100 nM concentration) and showed the highest binding affinity to Swiss 3T3 and NCI-H345 SCLC cells (K_d of 1.0 and 4.6 nM vs. 50 and 80 pM [^{125}I-Tyr[4]]BN, respectively). This analogue was also the most active antagonist of mitogenesis induced by 3 nM GRP(14–27) in Swiss 3T3 cells (IC_{50} of 0.8 nM) [156], behaving in all respects as Coy's parent compound (RC-3100) [153,156].

A second series of bombesin analogues with the same general formula were subsequently developed. In this series A was still D-Phe, D-Trp, D-Tpi or Tpi, and B was Trp or Tpi. The two best antagonists of this series, [D-Trp[6],Leu[13]ψ(CH_2N)Tpi[14]]BN(6–14) (RC-3415) and [Tpi[6],Leu[13]ψ(CH_2N)Tpi[14]]BN(6–14) (RC-3440), inhibited 3 nM GRP-stimulated growth of Swiss 3T3 cells with IC_{50} values of less than 1 nM. RC-3440 was also active in vivo, suppressing GRP(14–27)-stimulated serum gastrin secretion in rats [157]. In spite of these encouraging results, the analogue most extensively studied was [D-Tpi[6],Leu[13]ψ(CH_2NH)Leu[14]]BN(6–14) (RC-3095). This antagonist (as well as RC-3100) inhibited in a concentration-dependent manner 1 nM BN-induced amylase release in vitro from isolated rat pancreatic acini (IC_{50} 10^{-7} M) [158,159], and protein secretion in vivo in chronic pancreatic fistula rats (ID_{50} about 20 nmol/kg/h for a BN stimulation of 1 nmol/kg/h s.c.) [158] and cats (almost complete suppression by RC-3100 at 10 nmol/kg/h for a GRP stimulation of 620 pmol/kg/h i.v.) [160]. RC-3095, administered to fasted rats by i.p. injection, blocked DNA synthesis induced by bombesin but not by gastrin or CCK [159]. The same antagonist also significantly suppressed GRP(14–27)-stimulated gastrin secretion in rats when administered subcutaneously or by the pulmonary inhalation route, 60 min prior to GRP(14–27). The bioavailability of RC-3095 by inhalation was about 69% of the s.c. route [161]. In the rat, antagonist RC-3095, at the doses of 5 and 25 μg/100 g body wt, completely suppressed (glucagon) or significantly inhibited (gastrin, at the higher dose) the response of these two hormones to GRP(14–27) administered i.v. at the dose of 5 μg/100 g body wt [162]. The fact that other antagonists of this series inhibited the two hormones to varying degrees supports the suggestion that different subtypes of BN/GRP receptors exist in gastrin cells and the target sites for glucagon release [162]. I.c.v. injection of RC-3095 (10 μg), immediately before GRP(14–27) (1 μg), completely prevented agonist-induced serum GH suppression, suggesting that this action is mediated through specific BN/GRP receptors located in the CNS [162]. Similarly, its i.c.v. (but not i.v.) administration rapidly and significantly lowered serum LH (but not FSH) levels. The suppressive effect was completely prevented by prior i.c.v. administration of GRP(14–27) [163].

The potential antitumour activity of RC-3095 was evaluated in various in vitro and in vivo models. The antagonist displayed significant inhibitory effects on nitrosamine-induced pancreatic cancers in hamsters after 2 months s.c. treatment with implanted osmotic mini pumps which released 20 μg/day of the product. No significant down-regulation of BN/GRP receptors was found on the tumoural membranes. However, the significant down-regulation of EGF receptors in these membranes after treatment with RC-3095 might explain, at least in part, the inhibition of the tumour growth [164]. This is in agreement with the observation that GRP enhanced EGF-induced protein phosphorylation in membrane extracts from several cancer cell lines and cancer samples, while RC-3095 inhibited all these phosphorylations, suggesting that GRP works by up-regulating EGF-R and that RC-3095 prevents this up-regulation [165]. In apparent contrast with this hypothesis, however, was the recent finding that a greater inhibition of this pancreatic tumour (which is always accompanied by a decrease in the binding capacity of EGF receptors) was observed after administration of RC-3095 together with bombesin or GRP, than with RC-3095 alone. Moreover, administration of bombesin alone caused a down-regulation of EGF-R, while the greatest decrease in binding capacity was observed after treatment with RC-3095 in combination with GRP [166]. In another study, carried out on MIA PaCa-2 human pancreatic cancer cell line xenografted in nude mice, RC-3095 was without effect on the tumour growth. The compound was also inactive in vitro in the same cell line which, however, did not show specific binding for [^{125}I-Tyr^4]BN [167].

Binding of [^{125}I-Tyr^4]BN to human colon cancer membranes (binding sites were present in 40% of the specimens but not in specimens of normal colonic mucosa) was inhibited by nanomolar concentrations of the BN antagonists of this first series [168]. Antagonist RC-3095, at a dose of 20 μg/day, administered by s.c. injections or by continuous infusion using Alzet osmotic mini pumps, significantly inhibited tumour growth in nude mice bearing xenografts of HT-29 human colon cancer cell line [169].

Bombesin antagonist RC-3095 was also tested in nude mice bearing xenografts of the hormone-dependent human prostate tumour PC-82. Treatment started one month after implantation, when the tumour size was still small (10 mm^3), by daily s.c. injection at a dose of 20 μg. Tumour growth was significantly decreased, as well as serum prostatic-specific antigen, insulin-like growth factor I (IGF-I) and GH levels; EGF receptors were also significantly down-regulated [170]. In the androgen-dependent Dunning R-3327H rat prostate cancer model, RC-3095 infusion significantly reduced tumour volume and weight. This effect was enhanced by the simultaneous treatment with the LH-RH agonist, [D-Lys^6]LH-RH. Specific high-affinity binding sites for BN/GRP, EGF and IGF-I were found on the tumour membranes. The concentration of EGF receptors was significantly reduced by the BN/GRP antagonist [171]. In nude mice bearing xenografts of the androgen-independent human prostate cancer cell lines PC-3 [172] or DU-145 [173], tumour growth was significantly reduced by RC-3095 when the tumours measured approximately 10 mm^3 but not when they measured about 90 mm^3. In these mice too, EGF receptors were significantly down-regulated.

RC-3095 inhibited BN-stimulated cell growth of human breast cancer cell lines MDA-MB-231 and MCF-7 MIII (but not MCF-7) [174]. In female mice bearing estrogen-dependent or estrogen-independent MXT mammary carcinomas, 20 μg/d of RC-3095 administered from osmotic mini pumps significantly inhibited tumour growth. In the estrogen-independent cancer, tumour inhibition was associated with a decreased EGF-R number [175]. Moreover, RC-3095, infused s.c. at 2 μg/d via osmotic mini pumps, delayed the development of malignancies in hamsters with premalignant disease induced by DMBA (9,10-dimethyl-1,2-benzanthracene) [176].

2.4.3.3. Wellcome's derivatives. A further extension to the approach of BN-receptor antagonists based on reduced peptide bond derivatives was carried out at the Wellcome Research Laboratories. In a first paper [122], the combined insertion of a carboxyl-terminal leucine residue and a reduced peptide bond between the last two amino acids in the bombesin, GRP(15–27) and [D-Pro^{16}]GRP(15–27) sequences (Table 6) gave rise to compounds 37–39 which behaved as partial agonists/antagonists when examined for the ability to stimulate [^{3}H]thymidine incorporation into quiescent Swiss 3T3 cells (agonist activity) and to diminish the agonist response to GRP (antagonist activity). The agonist dose-response of the Leu-insertion peptides (EC_{50} values of 1–10 nM) paralleled GRP and bombesin, but their maximal response, even at concentrations as high as 10^{-4} M, was half the maximal value of GRP or bombesin. Computer-generated molecular modeling studies indicated that the novel structures could adopt the energy minimised conformations of either an agonist or an antagonist [122] as proposed earlier [101]. As expected, the introduction of a reduced peptide bond between the last two amino-acid residues of these sequences without a Leu insertion afforded pure antagonists [122]. In a subsequent paper [177], the observation that an octapeptide C-terminal GRP analogue having D-Pro adjacent to the C-terminal amino acid was antagonistic, with an IC_{50} value of 40 nM, prompted the Wellcome investigators to combine such a feature with the 'classical' reduced peptide bond modification. A series of extremely potent and specific GRP/BN recep-

Table 6
Structures of new BN/GRP analogues with a modified peptide bond

No.	Formula		
BN	Glp - Gln - Arg - Leu - Gly - Asn - Gln - Trp - Ala - Val - Gly - His - Leu - Met - NH_2		
37	Leu ψ Leu-NH_2	ψ = ψ(CH_2NH)	[122]
38	Tyr - Pro - Arg —— His —— Leu ψ Leu-NH_2	"	"
39	Tyr - pro - Arg —— phe - His —— Leu ψ Nle-NH_2	"	"
40	(des-NH_2) Tyr - Pro - Arg —— His —— ala —— pro ψ Phe-NH_2	"	[177]
41	1-naphthoyl - Pro - Arg —— His —— ala —— pro ψ Phe-NH_2	"	"
42	phe - His —— Leu ψ $COCH_3$	"	[178]
43	phe —— Leu ψ $COCH_3$	"	"
44	Ac - His —— Leu ψ Leu-NH_2	ψ = ψ(CH_2O)	[124]
45	Glp —— Phe ψ Leu-NH_2	ψ = ψ(CH_2S)	[69]
46	Glp —— Phe ψ Leu-NH_2	ψ = ψ(CH_2SO)	"

Residues identical to the parent compound are represented by a line; (des-NH_2)Tyr, 3-(4'-hydroxyphenyl)propanoyl; ala, D-Ala; phe, D-Phe; pro, D-pro.

tor antagonists were obtained, e.g., 3-(4-hydroxyphenyl)propanoyl-His-Trp-Ala-Val-D-Ala-His-D-Proψ(CH_2NH)Phe-NH_2 (40) and 1-naphthoyl-His-Trp-Ala-Val-D-Ala-His-D-Proψ(CH_2NH)Phe-NH_2 (41), which, in Swiss 3T3 cells, antagonised [^{3}H]thymidine incorporation stimulated with 6 nM BN with IC_{50} values of ~0.3 nM and inhibited the binding of 50 pM ^{125}I-labeled GRP with IC_{50} values of ~1 pM.

2.4.3.4. Mokotoff's derivatives. By combining two modifications to give BN/GRP receptor antagonists, i.e., deletion of the C-terminal Met and incorporation of a reduced peptide bond between the last two amino-acid residues, Mokotoff et al., at Pittsburgh University have synthesised a series of [des-Met^{14}]BN and [des-Met^{27}]GRP analogues containing a C-terminal ψ($CH_2NHCOCH_3$) group [178]. The two most active compounds, [D-Phe^{19},Leu^{26}ψ(CH_2-$NHCOCH_3$)]GRP(19–26) (42) and [D-Phe^6,Leu^{13}ψ-($CH_2NHCOCH_3$)]BN(6–13) (43) (Table 6), inhibited 0.2 nM BN-stimulated amylase release from dispersed rat pancreatic acini and 10 nM BN-stimulated [^{3}H]thymidine uptake in Swiss 3T3 cells with IC_{50}'s, respectively, of 46 and 55 nM in the first test, and 2.7 and 32.5 nM in the second test [178]. In suckling rats, compound 42, at 2.4 mg/kg body weight, partially blocked the trophic effect of bombesin (20 μg/kg twice a day for 9 days) on the pancreas and stomach, and the increase in trypsinogen in the pancreas [179].

2.5. BN analogues with other modifications in the peptide bond

Given that the ethyl ester Ac-GRP(20–26)OEt was a better ligand in Swiss 3T3 cells than the corresponding amide analogue Ac-GRP(20–26)NHEt, MS&D's investigators tested a similar substitution of oxygen for nitrogen in reduced carbonyl derivatives. Of these, Ac-[Leu^{26}ψ(CH_2O)Leu^{27}]GRP(20–27) (44, Table 6) was found to be a more potent inhibitor of 3 nM [^{3}H-Phe^{15}]GRP(15–27) binding (IC_{50} = 30 nM) and 3 nM Ac-GRP(20–27)-induced mitogenesis (IC_{50} = 100 nM) in Swiss 3T3 fibroblasts than the related nitrogen analogue [Leu^{13}ψ(CH_2NH)Leu^{14}]BN, possibly because of increased hydrophobicity and a reduced tendency of the oxygen derivative to form hydrogen bonds [124].

The introduction of a ψ(CH_2S) at the 8–9 peptide bond position of [Leu^9]litorin (Table 6) gave an antagonist (45) which was 2–3 times more potent than the corresponding derivative with a ψ(CH_2NH) substitution when measured by binding affinity and PI turnover in mouse pancreas. The replacement by one of the two possible sulfoxide isomers ψ(CH_2SO) (46) gave a further 3-fold increase in binding over the ψ(CH_2S) substituted compound [69].

2.6. Cyclic and dimeric BN analogues

Head-to-tail cyclization between positions 6 and 14 of bombesin and its analogues, through either an amide bond or a disulphide bridge, was found to give com-

Table 7
Effect of the introduction of an alkylating moiety on the receptor binding affinity of BN analogues [102,181]

Peptide	Inhibition of 0.25 nM [^{125}I]GRP binding expressed as IC_{50} (nM)			
	X = Thr	X = Mel	X = mMel	X = Cab-Thr
Asn - Gln - Trp - Ala - Val - Gly - His - Leu - Met - NH_2 BN(6-14)				
Boc - X — OH	>100,000	12,000 ± 400	8,200 ± 680	-
X —	12.0 ± 5.2	60 ± 12	95 ± 8	0.7 ± 0.2
Boc - X —	10.7 ± 0.1	48 ± 0.2	40 ± 8	-
X — Dnp His —	5,800 ± 525	660 ± 105	148 ± 19	1,815 ± 330
Boc - X — □ —	1,000 ± 100	69 ± 5	60 ± 3	-
X — □ —	3,190 ± 210	406 ± 49	n.t.	1,636 ± 266
Boc - X — phe —	19,500 - 2,600	5,240 ± 1,809	n.t.	-

Residues identical to the parent compound are represented by a line; deleted residue is represented by an open box; phe, D-Phe; —, non-existing structure.

pounds that retained some of the agonistic activity of the parent compounds. Introduction of a reduced peptide bond in 13–14 of the cystine derivatives, however, gave rise to antagonists. In dispersed rat pancreatic acini, cyclo[D-Cys^6,D-Ala^{11},Leu$^{13}\psi$(CH_2NH)Cys^{14}]BN-(6–14) had a K_i value for binding of 2.2 ± 0.3 μM vs. 50 pM [^{125}I-Tyr^4]BN, and an IC_{50} of 5.7 ± 2.7 μM for inhibition of 0.3 nM BN-stimulated amylase release [121]. These results seem to provide support for the proposal that both bombesin agonists and antagonists adopt folded conformations at their receptor(s) [101].

A [Lys^3]BN glutaraldehyde homodimer specifically inhibited [^{125}I]GRP (4 ng/ml) binding to Swiss 3T3 cells with an IC_{50} of 52 nM. The same compound also antagonised 10 nM bombesin-induced mitogenic activity and intracellular Ca^{2+} mobilisation with potencies 100- and 1000-fold higher than [D-Phe^{12},Leu^{14}]BN and [D-Phe^{12}]BN, respectively. The dimer also inhibited growth of bombesin receptor-positive NCI-H345 SCLC cells in vitro in a dose-dependent fashion [180].

2.7. Alkylating BN analogues

A completely unique approach to the search for BN/GRP receptor antagonists was followed at FICE. In order to increase the weak binding affinity of some BN analogues modified in positions 12 and 14, endowed with weak antagonistic activity [66], an alkylating moiety was introduced that, by irreversibly binding to the receptor, was able to shift the equilibrium of the ligand towards the bound form. Several alkylating moieties, located in different positions along the peptide sequence, were tested: nitrogen mustards such as 4-[bis(2-chloroethylamino)]-L-phenylalanine (Melphalan®, Mel), 3-[bis(2-chloroethylamino)]-L-phenylalanine (mMel) [102,181], 4-[bis(2-chloroethylamino)]benzoic acid (Cab) [181], 2-chloroethylnitrosourea [182], and chloromethylketones [182]. Such modifications were also applied to inactive BN analogues that showed undetectable binding and to BN analogues with good binding affinity that had agonistic properties. The reasoning behind such an approach was that a permanent blockade of the receptor could give antagonism rather than mitogenic stimulation. The introduction of an alkylating moiety had a marked effect on receptor binding in 3T3 cells, particularly for analogues displaying very weak affinity (Table 7). In addition, while the agonistic profile (as measured by thymidine incorporation and p115 phosphorylation) was unaltered, competitive antagonism vs. bombesin was dramatically increased (Table 8), even in compounds (like 47) which seemed devoid of any biological activity. The antagonism was assayed according to two paradigms: contemporaneous treatment, i.e. when the tested compound was given simultaneously with BN, and sequential treatment: when cells were first incubated for 24 h with the tested compound, and then washed and stimulated with BN. A 25 nM BN concentration was chosen for the competition experiments, as this corresponded to the concentration which maximally increased thymidine incorporation. A similar low responsiveness was ob-

Table 8
Bioassays of selected alkylating BN analogues in 3T3 fibroblasts: receptor binding, mitogenic activity (thymidine incorporation and p115 phosphorylation), and inhibition of BN-stimulated mitogenic activity [102,181]

No.	Peptide	A	B	C	D	E
BN	Glp - Gln - Arg - Leu - Gly - Asn - Gln - Trp - Ala - Val - Gly - His - Leu - Met - NH_2	12.6 ± 0.65	6.6 (25 nM)	3	agonist	agonist
47	Boc - Mel —— OH	12,000 ± 400	1.3 (5 μM)	>10,000	64 ± 10	39 ± 7
48	H - Mel ——	60 ± 14	4.7 (50 nM)	1	17 ± 4	61 ± 9
49	Boc - Mel —— His(Dnp) ——	1,170 ± 280	2.3 (5 μM)	50	67 ± 3	68 ± 5
50	Boc - mMel —— □ ——	60 ± 3	1.5 (0.5 μM)	>500	68 ± 8	35 ± 3
51	Boc - Mel —— □ ——	69 ± 5	1.0 (0.5 μM)	>100	85 ± 2	61 ± 5
52	Boc - Lys(Boc) —— Mel —— □ ——	103 ± 1	1.2 (0.5 μM)	>1,000	91 ± 2	89 ± 4
53	Boc - mMel —— Thr —— His(Dnp) —— $NH(CH_2)_4CH_3$	445 ± 60	1.3 (0.5 μM)	>1,000	85 ± 4	93 ± 1
54	Boc - Mel —— Leu ψ Met ——	28 ± 1	0.8 (0.5 μM)	n.t.	90 ± 3	86 ± 6
55	Boc - Mel —— His(Dnp) - Leu ψ Met ——	839 ± 178	1.8 (0.5 μM)	n.t.	75 ± 4	84 ± 3
56	Ac - Mel —— His(Dnp) - Leu ψ Met ——	2,340 ± 291	0.8 (0.5 μM)	n.t.	86 ± 1	61 ± 16
57	Cab —— His(Dnp) - Leu ψ Met ——	2.3 ± 1.0	1.3 (5 μM)	n.t.	78 ± 12	84 ± 6
58	Cab —— Leu ψ Met ——	0.9 ± 0.5	1.1 (0.5 μM)	n.t	85 ± 7	39 ± 7
LLBN	—— Leu ψ Met ——	214 ± 30	1.0 (0.5 μM)	200	56 ± 4	0

A, inhibition of 0.25 nM [^{125}I]GRP binding (IC_{50}, nM); B, maximal fold increase of [^{3}H]thymidine incorporation over basal value, at the indicated concentration; C, minimal active dose (μM) for p115 phosphorylation; D and E, % inhibition of [^{3}H]thymidine incorporation induced by 25 nM BN in the contemporaneous and sequential treatment, respectively, at 5 μM concentration. In the sequential treatment, cells were incubated with the antagonist and after 24 h washed and challenged with BN.
Residues identical to the parent compound are represented by a line; deleted residue is represented by an open box; ψ = $\psi(CH_2NH)$.

served in the binding assay in which BN displaced radiolabeled GRP with an IC_{50} of 12.6 ± 2.8 nM, a value which is about 10 times higher than that reported by others [183–185]. In the competition experiments, alkylating BN analogues with intrinsic 'antagonistic' features (47,49–58) displayed comparable antagonism to BN in both treatments. Analogues with intrinsic 'agonistic' features (like 48), on the other hand, showed better antagonism in the sequential treatment [102,181]. As expected, the reference peptide [Leu$^{13}\psi$(CH_2NH)Leu^{14}]BN (LLBN), being a reversible antagonist, was completely inactive in the sequential studies [102]. The mechanism of action of these alkylating derivatives was not investigated. However, it was observed (Table 9) that, after 24 h treatment with BN analogues belonging to different classes, the number of GRP receptors on 3T3 fibroblasts was greatly reduced (up to complete suppression) only with the alkylating analogues 62 and 50. These compounds were the only active antagonists in the sequential treatment. The percent inhibition of thymidine incorporation was inversely related to the number of residual receptors. The receptor number was completely restored only 48 h after cell washing [102].

Owing to their specificity for BN receptors (they did not bind to other growth factor receptors, such as the EGF receptor in human epidermoid A431 cell line) and reduced cytotoxicity (IC_{50}'s > 50 μM, vs. an IC_{50} of 3.3 μM for Melphalan®) [102], these alkylating analogues were ideal candidates for in vitro and in vivo studies in SCLC. A selected number of analogues were tested in the clonogenic assay, using SCLC cell lines NCI-N592 and NCI-H69, which were previously found to have BN receptors and to produce BN-like peptides (Table 10). A few of the analogues proved to be much better antagonists than the reference peptide LLBN, and specific for these cells, in that they did not inhibit the clonal growth of two cell lines (LoVo adenocarcinoma and M14 melanoma) which were devoid of BN receptors [134]. The reference compound LLBN and a representative of the Mel (51) and Cab (57) derivatives were then tested in nude mice xenografted with cell line N592. In the hands of FICE's investigators, this particular cell line was the most sensitive to BN antagonists

Table 9
Effect of different classes of BN analogues (at 5 μM concentration) on receptor number and DNA synthesis in Swiss 3T3 fibroblasts [102]

No.	Formula	GRP receptor number per cell after 24 h treatment	% Inhibition of [^{3}H]thymidine incorporation	
			contemporaneous treatment	sequential treatment
	(control, no treatment)	(12,000)	(0)	(0)
59	H - Thr - Gln - Trp - Ala - Val - Gly - His - Leu - Met - NH_2	9,000	0	n.t.
60	H - Thr — Dnp His —	9,000	0	n.t.
61	Boc - Thr — □ —	7,300	53 ± 14	n.t.
BBLN	R - Asn — Leu ψ Leu —	10,500	56 ± 4	0
62	H - Mel — Dnp His —	undetectable	44 ± 12	83 ± 6
50	Boc - mMel — □ —	3,000	68 ± 8	35 ± 3

Residues identical to the parent compound are represented by a line; deleted residues are represented by an open box; R, Glp-Gln-Arg-Leu-Gly; ψ, ψ(CH_2NH).

but, nevertheless, was 10 times less sensitive than reported by others [131]. The peptides were administered s.c. at a dose of about 100 μg twice a day for 20 days in the flank contralateral to the tumour. Treatment began when the tumour weight was about 100 mg (Table 11). The Cab derivative 57 was completely inactive while the Mel derivative 51 showed a moderate activity (33–45% of tumour growth inhibition) which was higher than the reference peptide LLBN (21%) and without any toxicity. The low solubility prevented the administration of higher doses [134].

2.8. Substituted somatostatin analogues

Recently it was reported that somatostatin-14 (SS-14) inhibited the cross-linking of [^{125}I]GRP to a 120-kDa protein in Triton extract of 3T3 cells and human SCLC cells [186], which are known to possess BN receptors [18]. Previous studies demonstrated that SS-14 could also weakly inhibit binding of opioid ligands to opiate receptors [187,188], and subsequent studies led to the identification of various D-amino acid-substituted and constrained amino acid-substituted cyclo-SS analogues that functioned as potent μ-opioid receptor antagonists [189,190]. Therefore, the ability of SS-14, SS-28, and various cyclo-SS octapeptides to function as GRP or NMB receptor antagonists was explored [191]. It was found that some SS analogues functioned as NMB-R antagonists, having > 100-fold selectivity for NMB-R over GRP-R. None of them, at a concentration of 10 μM, had agonist activity and stimulated increases of [^{3}H]IP in NMB-R-transfected cells (BALB 3T3) or amylase release from rat pancreatic acini, which have GRP receptors. Similarly, none of these peptides at this concentration altered the increase in amylase release caused by 3 nM BN in rat pancreatic acini. Whereas some octapeptide analogues caused some inhibition of the 14-fold increase in [^{3}H]IP induced by 3 NMB in NMB-R transfected cells, D-Nal^1-*cyclo*-(Cys^2-Thr^3-D-Trp^4-Lys^5-Val^6-Cys^7)-Nal^8-NH_2(cyclo-SS-octa), [D-Cys^2]-cyclo-SS-octa, [D-Cys^7]-cyclo-SS-octa, [His^5]-cyclo-SS-octa and [D-Nal^4]-cyclo-SS-octa at 10 μM completely inhibited the NMB-stimulated increase in [^{3}H]IP. Cyclo-SS-octa was the most potent, causing detectable inhibition at 0.3 μM, half-maximal inhibition at 885 nM, and complete inhibition at 10 μM. In NMB-R transfected cells, cyclo-SS-octa was functioning as a competitive antagonist, with an affinity for NMB-R of 59 ± 9 nM. However, it had only a 10-fold higher affinity for NMB-R than for μ-opioid receptors and a 40-fold higher affinity for SS receptors than for NMB-receptors. Alteration in either the stereochemistry or the nature of the substitutions in positions 4, 7 and 8 as well as position 5, of cyclo SS-octa were particularly important for retaining high affinity NMB-R interaction and decreasing SS or μ-opioid receptor interaction, suggesting that modifications in these positions in the future will likely lead to a much more selective NMB-R antagonist.

Table 10
Binding affinity and clonal growth inhibition of selected BN receptor antagonists in SCLC cell lines [134]

No.	Formula	Inhibition of 0.25 nM [^{125}I]GRP binding (IC_{50}, nM)	Inhibition of clonal growth (IC_{50}, nM)	
		SCLC N592	SCLC N592	SCLC H69
BN	Glp - Gln - Arg - Leu - Gly - Asn - Gln - Trp - Ala - Val - Gly - His - Leu - Met - NH_2	810	-	-
49	Boc - Met — His(Dnp) —	68,000	240	580
51	Boc - Met — □ —	4,250	50	110
52	Boc - Lys(Boc) — Met — □ —	n.t.	60	690
53	Boc - mMet — Thr — His(Dnp) — $NH(CH_2)_4CH_3$	n.t.	> 5,000	2,518
54	Boc - Met — Leu ψ Met —	n.t.	110	940
57	Cab — His(Dnp) - Leu ψ Met —	166	700	783
LLBN	— Leu ψ Leu —	6,000	520	1,660

Residues identical to the parent compound are represented by a line; deleted residues are represented by an open box: ψ, ψ(CH_2NH).

2.9. Non-peptide BN antagonists

At Pfizer, in the course of screening to discover non-peptide GRP antagonists, two related compounds, CP-70,030 and CP-75,998 (Fig. 2), were identified. These compounds were able to displace [^{125}I]GRP from rat brain BN receptors with IC_{50} values of 1.5–3 μM, and to inhibit 10 nM BN-induced PI turnover in rat pituitary GH_3 cells with IC_{50} values of 1.5 ± 0.1 μM [192]. However, neither compound (at concentrations up to 32 μM) displaced labeled GRP from its receptors in the bombesin-responsive human SCLC cell line N592. This confirmed what had previously been observed with non-peptide substance P antagonists [193], that relatively rigid non-peptide antagonists can reveal receptor differences between species that are not apparent when using peptides [192].

Table 11
Antitumour activity of selected BN receptor antagonists in advanced SCLC in nude mice [134]

Peptide	Dose	% Tumour growth inhibition[a]		Mortality
	μg/treat.[c]	1st exp.[b]	2nd exp.	
51	100	45	33	0/12
57	100	2		0/12
LLBN	100	21	—	0/12
Melphalan[d]	25	—	97	0/12

[a] 1 week after the last treatment, refers to animals treated with solvent.
[b] In the first experiment the actual doses of the administered peptides, determined by amino-acid analysis after sterilisation by filtration, were 78, 82, and 72 μg, respectively.
[c] Treatments: s.c. twice a day for 20 days in the flank contralateral to the tumour, when the tumour weight was about 100 mg.

3. Antitumour activity of BN receptor antagonists

In the preceding section, BN receptor antagonists belonging to different classes were reviewed. All of them were screened in in vitro tests, and usually the

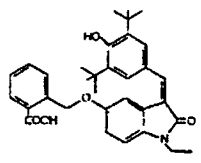

CP-70,030

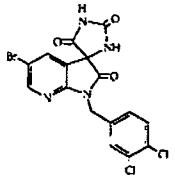

CP-75,998

Fig. 2. Chemical structures of two non-peptide BN/GRP receptor antagonists.

most active were assayed in experimental animals. Some proved to be potent and long-acting agents, for example, in inhibiting amylase release [114] or gastrin secretion [161]. In this section we focus our attention on the in vivo antitumour activity of these antagonists and will present all the positive results that have appeared in the literature up to December 1993. For a better understanding, Table 12 reports the results in human SCLC (for which the original interest in BN-R antagonists was stimulated) xenografted into nude mice while in Table 13 the results on other tumoural models are summarised.

As can be seen from Table 12, all the reported BN-receptor antagonists were able to inhibit in vivo tumour growth. Positive results were also obtained with [D-Nal^6,Leu$^{13}\psi$(CH$_2$NH)Phe^{14}]BN(6–14) [132] which is not reported in the table. In the literature, negative results in such experiments are rare: [D-Arg^1,D-Pro^2,D-Trp^{7,9},Leu^{11}]SP (3) [132], BN(1–12) [132] and [Cab^6,His(Dnp)^{12},Leu$^{13}\psi$(CH$_2$NH)Met^{14}]BN(6–14) [134] are the only peptides described that are devoid of inhibitory activity. In addition, [D-Cpa^1,βLeu^5]LN(1–8)NH$_2$ and [D-Phe^6,Leu$^{13}\psi$(CH$_2$NH)Cpa^{14}]BN(6–14) were practically inactive towards cell lines SCLC 74R and SCLC 6 which, however, have no or few GRP/BN receptors [96]. In general, all the BN-receptor antagonists inhibited tumour growth but with different degrees of potency, the efficacy of the treatment depending probably also on the size of the tumour when treatment started. Different percentages of inhibition were even reported for the same peptide. In fact, [Leu$^{13}\psi$(CH$_2$NH)Leu^{14}]BN (LLBN) inhibited in vivo the growth of SCLC cell line NCI-N592 to comparable extent in two experiments [92,132] but gave only a 21% reduction of tumour growth in another case [134], despite the fact that the peptide was administered at higher doses (100 μg b.i.d. vs. 10 μg/d). Such differences can partially be explained by the fact that the tumour size was measured not during treatment but 1 week after the last injection. It is likely such a behaviour can be ascribed to the fact that the peptide was given s.c. in the contralateral flank (and not adjacently to the tumour) with the result that it underwent degradation before reaching the site of the tumour. If this is the case, much higher percentages of inhibition could have been observed for LLBN as well as for [Boc-Met^6,des-His^{12}]BN(6–14) had they been tested under the same favourable experimental conditions [134]. On the other hand, since it is impractical in therapeutic treatment to inject the agent directly into the tumour, this poses the problem of developing (peptidic or non-peptidic) stable antagonists.

Two other observations need to be mentioned here: (i) the inhibition was incomplete; and (ii) in several cases tumours started to regrow, although with lower doubling times than the controls. It is known that there is a considerable heterogeneity between different SCLC cell lines in terms of production, binding and growth activity of peptides and growth factors. Three types of SCLC cell lines, namely NCI-H169, NCI-N592 and SCLC-41 were used in in vivo studies in nude mice. NCI-H69 and NCI-N592 were isolated, respectively, from pleural effusion and bone marrow specimens that were taken from male patients before undergoing therapeutic treatment [194]. Both cell lines display bombesin-like immunoreactivity [33,195–197]. However, NCI-H69 does not express detectable membrane receptors for GRP [196,197] despite the fact that traces of the corresponding mRNA were detected [18]. On the contrary, SCLC NCI-N592 cells do possess GRP receptors [18,197]. Ciomei et al., measured 1000 and 3500 BN receptors/cell for cell lines NCI-H69 and NCI-N592, respectively [134]. Low levels of NMB [10,198] were detected for both cell lines although in both cases no NMB receptor mRNA was found [18]. The two cell lines also show a slightly different pattern towards the production and sensitivity for other peptides and growth factors [197]. Less is known about the SCLC-41 cell line which expresses prepro-GRP mRNA and has GRP receptors [96]. Taking all these considerations together it is possible to envisage that alternative approaches such as broad spectrum antagonists [51] or BN analogues coupled with cytotoxic agents [102,134,181,182] could be more promising than the 'classic' ones. Indeed, [Arg^6,D-Trp^{7,9},MePhe^8]SP(6–11) produced a marked reduction of tumour volume and the inhibitory effect was maintained beyond the duration of the treatment [51].

Unlike Table 12, which collates the results of different antagonists on a single tumour form (SCLC), Table 13 shows the effects of a single compound, [D-Tpi^6,Leu$^{13}\psi$(CH$_2$NH)Leu^{14}]BN(6–14) (RC-3095), on different types of tumours. In each tumour model, the compound displayed antiproliferative activity. In nitrosamine-induced pancreatic cancer, two values were reported for the same dose, namely 87% [164] and 31% [166]. In the same model a dose-response curve was observed, ranging from 31 to 65% at a maximal dose of 60 μg/d [166]. In addition, the combined administration of 30 μg/d of the antagonist with 10 μg/d of either BN or GRP produced a tumour growth inhibition greater than when the antagonist was administered alone. This surprising finding, together with the observation that a correlation exists between tumour inhibition and decrease of binding capacity of EGF receptors [166], fits with the occasional inhibition of pancreatic tumour growth induced by chronic treatment with BN or GRP [199,200]. These findings are possibly explained by a down-regulation of both GRP and EGF receptors, and/or by the BN.GRP-induced release of somatostatin. Down-regulation of the EGF-receptors was also observed in breast and prostate tumours (no such infor-

Table 12
Effect of BN receptor antagonists on the growth of SCLC implanted in nude mice[a]

Peptide	Cell line	Dosage	Injection site	Treatment	Results	Refs.
[Arg^6,D-Trp^{7,9},MePhe^8]SP(6–11)	NCI-H69	900 μg/d	Adjacent to the tumour	Started 6 weeks after tumour implantation when tumour size was 30 mm^3 and continued for 7 days	Marked reduction of tumour volume; the inhibitory effect was maintained beyond the duration of treatment	[51]
[Sta^5]LN(1–8)	NCI-H69	50 μg b.i.d.	Adjacent to the tumour	Started 4 days after tumour implantation and continued for 30 days	Significant tumour size reduction	[95]
[D-Cpa^1,βLeu^8]LN(1–8)	SCLC-41	50 μg b.i.d.	Adjacent to the tumour	Started when tumour size was 30–100 mm^3 and continued for 10 days	Almost complete reduction of tumour growth during treatment	[96]
[Leu$^{13}\psi$(CH$_2$NH)Leu^{14}]BN	NCI-N592	10 μg/d	Adjacent to the tumour	Started 1 week after tumour implantation and continued for 3 weeks	About 50% reduction in tumour volume during treatment	[92]
	NCI-N592	10 μg/d	Adjacent to the tumour	Started 1 week after tumour implantation and continued for 4 weeks	72% reduction of tumour growth at week 2 and about 50% at weeks 3, 4 and 5	[132]
	NCI-N592	100 μg b.i.d.	Contralateral flank	Started 18 days after tumour implantation and continued for 20 days	21% reduction of tumour growth 1 week after last treatment	[134]
[Glp^6,Phe$^{13}\psi$(CH$_2$NH)Leu^{14}] BN(6–14)	NCI-H69	50 μg/d	Adjacent to the tumour	Started 1 week after tumour implantation and continued for 4 weeks	20%, 24% and 13% reduction of tumour growth after 2, 3 and 4 weeks, respectively	[132]
[D-Phe^6,Leu$^{13}\psi$(CH$_2$NH)Cpa^{14}] BN(6–14)	SCLC-41	50 μg b.i.d.	Adjacent to the tumour	Started when tumour size was 30–100 mm^3 and continued for 10 days	Almost complete reduction of tumour growth during treatment	[96]
[Boc-Mel^6,des-His^{12}]BN(6–14)	NCI-N592	100 μg b.i.d.	Contralateral flank	Started 18 days after tumour implantation and continued for 20 days	45–33% reduction in tumour growth 1 week after last treatment	[134]

[a] All peptides were given s.c., see text for further details.

Table 13
In vivo activity of RC-3095 on different tumour models[a]

Tumour origin	Experimental model	Dosage	Treatment	Results	Refs.
Pancreas	Nitrosoamine induced pancreatic cancer in female hamsters	20 μg/d by osmotic mini pumps	Started 18 weeks after last nitrosoamine treatment and continued for 8 weeks	87 and 31% inhibition of tumoural pancreas weight	[164,166]
Colon	HT-29 human colon cancer cell line xenografted in male nude mice	20 μg/d by continuous infusion or by s.c. injection b.i.d.	Started 2 weeks after transplantation (tumour volume, about 20 mm^3) and continued for 4 weeks	40–50% inhibition of tumour growth	[169]
Breast	Estrogen-dependent or estrogen-independent MXT mammary tumour in female nude mice	20 μg/day by osmotic mini pump	Estrogen-independent: started 2 days after transplantation and continued for 15–16 days; estrogen-dependent: started 4 weeks after transplantation and continued for 5 weeks	45–65% reduction in tumour volume and 35–58% reduction in tumour weight for both type of tumours	[175]
Prostate	Androgen-dependent PC-82 human prostatic cancer cell line xenografted in male nude mice	20 μg/day s.c.	Started 1 month after tumour implantation (tumour volume, about 10 mm^3) and continued for 5 weeks	86% reduction of tumour volume	[170]
	Androgen-dependent dunning R-3327H rat prostatic cancer	100 μg/day by osmotic mini pump	Started when tumour was well developed and continued for 7 weeks	50% reduction in tumour volume	[171]
	Androgen-independent PC-3 human cancer cell line xenografted in male nude mice	20 μg/day s.c.	Started 2 weeks after tumour transplantation (tumour volume, about 10 mm^3) and continued for 4 weeks	40% reduction in tumour volume or tumour weight; no tumour growth inhibition was observed when the starting tumour measured about 90 mm^3	[172]
	Androgen-independent DU-145 human prostate cell line xenografted in male nude mice	20 μg/day s.c.	Started 2 weeks after transplantation (tumour volume, about 10 mm^3) and continued for 4 weeks	Significant reduction of tumour growth (about 25%)	[173]

[a] See text for further details.

mation was given for colon adenocarcinoma) following treatment with RC-3095, and this might explain, at least in part, the inhibition of tumour growth. Interference with EGF might, therefore, be the common mechanism behind the inhibitory effects of both BN/GRP agonists and antagonists. In addition, somatostatin release in response to RC-3095 may also contribute to tumour inhibition, as, in animals with nitrosamine-induced pancreatic cancer that are treated with this compound, the GH levels are decreased [168].

4. BN-receptor subtypes

Since the discovery of BN, several other BN-like peptides have been identified such that now there is a large family of these peptides. As mentioned earlier, this family can be further divided into three subfamilies on the basis of amino-acid sequence similarities and pharmacological activity. It is worth mentioning that only differences in the carboxyl-terminal portion of the peptide account for differences in receptor interaction and biological activity.

Early studies on several smooth muscle preparations showed that different bombesin-like peptides elicited varying degrees of potency. These studies provided the first evidence for the presence of multiple BN-receptor subtypes [9,13]. The existence of at least two classes of bombesin receptors was for the first time demonstrated by von Schrenck et al. [14] who showed that rat oesophageal muscle possesses a class of BN receptors with a higher affinity for NMB than for BN (NMB-preferring bombesin receptor, NMB-R). These differed from the pancreatic BN receptors which, like all other BN receptors described previously, display much higher affinity for GRP than for NMB (GRP-preferring bombesin receptor, GRP-R). Subsequently, it was shown that the two receptor subtypes were widely distributed and could be expressed either in distinct tissues or in the same tissue [201]. NMB-R were found in rat urinary bladder [19,91] and in rat seminal vesicle [19], whereas GRP-R was found in rat uterus [19]. As in the peripheral tissues, two pharmacologically distinct populations of BN receptors have been identified in rat central nervous system [15,201]: again, some brain regions bind BN with higher affinity than NMB, while binding sites in other regions show higher affinity for NMB than for BN. The distinct distribution suggests that both receptor subtypes may play independent roles in mediating many of the effects of BN-like peptides [201]. SCLC cell lines likewise express both BN receptor subtypes. NMB, like GRP, binds with high affinity to SCLC cells, provoking elevation of cytosolic Ca^{2+} and stimulation of colony formation [202]. NMB immunoreactivity and NMB gene expression were detected in SCLC cell lines suggesting that NMB also functions as an autocrine growth factor [10,198]. In general, the distribution of NMB was more widespread than was that of GRP, the levels of GRP being much higher in positive cell lines. Moreover, it was found that complementary DNA (cDNA) clones isolated from human cell line SCLC NCI-H345 encoded both GRP-R and NMB-R, and that the antagonist [D-Phe^{6}]BN(6–13)ethyl ester was effective in blocking the response elicited from the cloned GRP-R but not from the cloned NMB-R [18].

Molecular cloning, expression and characterisation of GRP- and NMB-preferring BN receptors added further support to the notion of two structurally and pharmacologically separated receptors for mammalian BN-like peptides [18,203]. By these techniques it was also possible to characterise human genomic and cDNA clones encoding a third BN-receptor subtype (BRS-3) with a functional role distinct from either GRP-R and NMB-R [21]. BN receptors, like receptors of other peptide hormones, are members of the G protein-coupled receptor superfamily, characterised by having seven transmembrane domains. Comparison of the human GRP-R, NMB-R and BRS-3 amino-acid sequences shows a high degree of overall amino-acid identity. In particular, the third transmembrane domain is extremely well conserved among the three BN-receptor subtypes, although different from that of other known G protein-coupled receptors. As a consequence, this region may be involved in ligand binding or in functional roles that would be expected to be similar among closely related receptor subtypes but not common to all members of the G protein-coupled receptor family. It is not yet known whether they use the same G protein subtypes [21,203].

Despite the high similarity, the three receptors have distinct features. Expression of BRS-3 cDNA in *Xenopus* oocytes encoded a functional receptor which is activated by the naturally occurring BN-like peptides (BN, GRP, NMB, [Phe^{8}]phyllolitorin, and ranatensin), but not by other structurally unrelated peptides (substance P, bradykinin or CCK) and, strangely enough, not by other natural BN-like peptides (alytesin, litorin, and [Leu^{8}]phyllolitorin) [21]. It is worth noting that binding was observed only at 10^{-5} M concentration whereas the other two BN-receptor subtypes had binding affinities in the nanomolar range. The peculiarity of this third BN-receptor subtype is that, in normal rat tissue, BRS-3 mRNA was detected in the testis but not in the thymus, stomach, jejunum, colon, lung, kidney, spleen, prostate, brain and retina. This suggests that, contrary to GRP-R and NMB-R, BRS-3 is restricted to a limited area [21].

Before the discovery of BRS-3, GRP-R and NMB-R mRNAs were detected in SCLC cell lines at low levels. The levels were, however, consistent with the low number of GRP/NMB binding sites present on SCLC cell

lines [18]. The expression of the two receptors in non-SCLC cells was rare. BRS-3 mRNA was instead detected in human cell lines from all histological types of lung carcinoma examined (SCLC, NSCLC, and carcinoid). Expression of BRS-3 mRNA in some carcinoma cell lines overlapped with either GRP-R or NMB-R mRNA expression, or both. In view of the limited expression of BRS-3 in normal rat tissue, it is striking that BRS-3 mRNA is expressed in over half of the human lung carcinoma cell lines examined. If the limited distribution of expression in normal rat tissues is representative of the expression patterns in normal human tissues, BRS-3 may prove to be a useful cell surface target for specifically detecting antiproliferative agents to lung carcinoma cells [21].

The search for BN antagonists as putative antiproliferative agents for SCLC treatment was stimulated by the discovery of the autocrine role for GRP in the development of such a malignancy. On the wave of the enthusiasm following this observation, new peptides were synthesised that were targeted to the GRP receptor and all screening was performed using pharmacological models that, as we now know, were representative of the GRP-preferring receptor. The early observation that substance P antagonists could block pancreatic amylase release induced by BN was taken into consideration mainly as a starting point for the development of more specific antagonists: in other words, more BN-like antagonists. This approach was not intensively pursued because all the antagonists of this class failed to possess sufficient potency and specificity. Other approaches, on the other hand, turned out to be more promising. Indeed, potent BN antagonists were found.

The discovery of different BN-receptor subtypes which have different distribution and which are present in several lung tumour histological types opened up new possibilities. The retesting of the BN receptor antagonists so far developed in in vitro models for the NMB-R showed that potent antagonists of the des-Met and reduced peptide bond classes (which are endowed with potent antagonism toward the GRP-R) were practically inactive or several orders of magnitude less potent toward NMB-R than GRP-R [17,19,88–91,113,202,204]. This indicated that they were highly selective for GRP-R. Indeed, examination of the binding affinities showed that the two receptor subtypes share common requirements but also display distinct features. In particular, deletion and L-alanine replacement of the C-terminal Met is better tolerated at the GRP site than at the NMB one [90]. Interestingly, the less potent BN receptor antagonists belonging to the class of SP analogues (see Section 2.1.1.) and of [D-Phe^{12}] analogues (see Section 2.2.1.) display the same degree of potency toward both BN-receptor subtypes. [D-Pro^{2},D-Trp^{7,9,10}]SP(4–11) (4), [D-Arg^{1},D-Trp^{7,9},Leu^{11}]SP (1) and [Trp^{4},D-Phe^{12}]BN, in fact, inhibited NMB-induced contraction of rat oesophageal muscle strips where most potent GRP antagonists were inactive [17]. Similarly, the SP antagonist [D-Arg^{1},D-Pro^{2},D-Trp^{7,9},Leu^{11}]SP (3) but not [D-Phe^{6}]BN(6–13)methyl ester, at 1 μM concentration, reversed the increase in cytosolic Ca^{2+} caused by 10 nM NMB in SCLC cell line NCI-H345. At 1 μM concentration, the same SP antagonist inhibited the NMB-induced clonal growth of the SCLC cell lines NCI-H209 and NCI-H345. The mechanism of action of antagonist 3 remains unclear but may involve G-protein interaction [202] (see Section 5). The recently discovered cyclo-somatostatin octapeptides (see Section 2.8), although non specific, function as BN-receptor antagonists with a > 100-fold selectivity for NMB-R over GRP-R.

5. Peptide receptors in human small cell lung cancer

The presence of an autocrine circuit for BN-like peptides in SCLC cells gave great impetus to the search for BN-receptor antagonists as potential curative agents for this highly malignant disease. However, it was soon evident that other mitogenic peptides were produced and other receptors expressed by these cell lines, suggesting that additional autocrine loops or paracrine influences might be present [205]. An updated list of such peptides and receptors is reported in Table 14 [205,206] where only new entries are referenced. As shown in the table, not all human SCLC cells express receptors for the ligands they produce and vice versa. There is a great heterogeneity of responses to various neuropeptides both within individual lung cancer cell lines and among different lung cancer cell lines. In most instances a minority of cells within a cell line responds to an individual peptide. It is not clear whether this is due to a lack of expression of the receptors for the other peptides in the non-responsive cells or whether there is an autocrine secretion of these peptides and some cells are self down-regulated at the time of peptide administration. In fact, during tumour progression, the cells may become independent of autocrine growth factor stimulation [53].

While most of the ligands for the receptors expressed by SCLC cell lines are mitogenic, others (like somatostatin and enkephalins) are inhibitors of cell growth. In the case of VIP, which stimulates release of BN-like peptides from SCLC cell lines through elevation of intracellular cAMP [207], both stimulatory and inhibitory effects on SCLC clonal growth have been reported. In fact, VIP has been shown to slightly stimulate the proliferation of cell lines NCI-H82 and NCI-H417 (which belong to the variant subclasses of SCLC) by a factor of 1.3 and 1.2, respectively, at 1 nM concentrations [197], and to stimulate the clonal growth

Table 14
Peptides produced and receptor expressed by human SCLC cell lines and mitogenic activity in vitro [205,206]

Peptide	Peptide production	Peptide receptor expression	Mechanism of action
			↑ stimulation ↓ inhibition
GRP	-	+	↑
NMB [10,18,198]	-	+	↑
IGF-I	-	+	↑
Transferrin	-	+	↑
Calcitonin	-	+	?
AVP	-	+	↑
β-Endorphin	-	+	↑
Enkephalins	-	+	↓
Neurotensin	-	+	↑
Glucagon	-	?	?
Substance P	-	?	?
Somatostatin [212,213]	-	+	↓
CCK/gastrin [214,215]	-	+	↑
TGF-α/EGF	-	+	?
VIP [208,209]	-	+	↑↓
ACTH	-	?	?
Galanin	?	+	↑
Bradykinin	?	+	↑

of the classic SCLC cell line NCI-H345 approximately two-fold at 100 nM [208]. On the other hand, VIP, in a concentration range from 1,0 nM to 1.0 μM, dose-dependently inhibited the growth and multiplication of both NCI-H345 and NCI-H69 cells up to 75 and 84%, respectively [209].

Many of the neuropeptides listed in Table 14 (such as GRP, NMB, bradykinin, AVP, CCK, neurotensin, and galanin) act via G protein-coupled receptors through mobilisation of Ca^{2+} and stimulation of protein kinase C [210]. Substance P antagonists can block the mitogenic effects of these peptides but have no effect on mitogenesis induced by VIP (which acts by stimulating cAMP accumulation) or by a wide range of other mitogens including polypeptide growth factors and pharmacological agents. This suggests that these antagonists can recognise a domain common to the receptors of these neuropeptides that is essential for the coupling of the G-proteins required for Ca^{2+} mobilisation. This common domain, which is separate from the ligand binding site (because the ligands are structurally unrelated and the ligand-specific antagonists show no cross-reactivity) could reside on the G proteins themselves [211]. Consistent with this hypothesis is the finding that [D-Pro^4,D-Trp^{7,9,10}]SP(4-11) (antagonist 5) and, to a major extent, the new antagonist [Glp^5,D-Trp^{7,9,10}]SP(5-11) compete with the M_2 subtype of muscarinic cholinergic receptor for the interaction with G proteins (G_i and G_o), and one or two molecules of antagonist need to bind per G protein to inhibit the effects of receptor activation (GTP hydrolysis). The same peptides appear to interact with the G_s protein of the β-adrenergic receptor as well, suggesting that the binding site of these peptides might include the βγ subunits of G proteins. Such subunits seem to be common to all G proteins [211].

Although SCLC growth has been hypothesised to be regulated by multiple autocrine and/or paracrine circuits involving Ca^{2+}-mobilising neuropeptides, Ca^{2+} mobilisation is only one of the components of a complex array of signalling events rather than the signal that promotes cell growth [51]. This was evidenced in some SCLC cell lines by bombesin and tachykinin neuropeptides which mobilised Ca^{2+} without stimulating DNA synthesis [52].

6. Concluding remarks

As a result of a large screening programme on BN receptor antagonists, a number of analogues have been found which display good in vivo antiproliferative activity not only in small cell lung carcinomas but also in other types of cancer characterised by the presence of BN receptors. Tumour reduction was observed both during treatment and 1 week after the last administration of the peptide drug, and was largely dependent of the initial tumour size. Anticancer activity was greatly affected by the site of injection being more pronounced when the antagonists were administered directly into tumour. This suggests that peptide instability and bioavailability are crucial for efficacy, and still remain an unsolved problem. Moreover, it should be noted that most of the antagonists tested in vivo were specific

for GRP receptors. We now know that NMB, as well as other neuropeptides act as autocrine/paracrine growth factors. As a consequence, a therapeutic approach based on specific GRP receptor antagonists will probably be safer but inadequate. Broad spectrum antagonists (as alternatives to a combination of selected, specific neuropeptide receptor antagonists) or GRP analogues covalently linked to cytotoxic molecules (a similar approach was followed at FICE, although mainly with the aim of increasing receptor binding) may be more suitable. More stable derivatives (either peptidic or non peptidic) have to be developed for practical use, while awaiting further progress in drug delivery techniques which will allow for more convenient routes of administration.

Neuropeptides such as GRP play an important role in SCLC carcinogenesis (probably as well as in other malignancies), favouring the development of multiple genetic anomalies. When tumours are established, the use of antagonists will not be as efficient as in the early stages of the disease. Nevertheless, BN receptor antagonists may, all the same, be of interest as adjuvants to chemotherapy or surgery in all forms of tumours where BN receptors are present.

Acknowledgements

The authors wish to thank Mrs A. Picciocchi for typing the manuscript and Dr M. Kirchin for English language revision.

Reviewers

This paper was reviewed by Dr Robert T. Jensen, NIH/NIDDK/DDB, 10/9C103, 10 Center DR MSC 1804, Bethesda, MD20892-1804, USA and Jean Martinez, C.P.M.I.B., Faculté de Pharmacie, 15, avenue Charles Flahault, 34060 Montpellier Cedex 1, France.

References

[1] Anastasi A, Erspamer V, Bucci M. Isolation and structure of bombesin and alytesin, two analogous active peptides from the skin of the European amphibian *Bombina* and *Alytes*. Experientia 27:166–167, 1971.

[2] Anastasi A, Erspamer V, Endean R. Amino acid composition and sequence of litorin, a bombesin-like nonapeptide occurring in methanol extracts of the skin of the Australian leptodactylid frog *Litoria aurea*. Experientia 31:510, 1975.

[3] Nakajima T, Tanimura T, Pisano JJ. Isolation and structure of a new vasoactive polypeptide. Fed Proc 29:282, 1970.

[4] Yasuhara T, Nakajima T, Nokihara C, Yanaihara N, Erspamer V, Falconieri Erspamer G. Two new frog skin peptides, phyllolitorins, of the bombesin-ranatensin family Phyllomedusa sauvagei. Biomed Res 4:407–412, 1983.

[5] McDonald TJ, Jörnvall H, Ghatei M, et al. Characterization of a gastrin releasing peptide from porcine non-antral gastric tissue. FEBS Lett 122:45–48, 1979.

[6] Minamino R, Kangawa K, Matsuo H. Neuromedin B: a novel bombesin-like peptide identified in porcine spinal cord. Biochem Biophys Res Commun 114:541–548, 1983.

[7] Minamino N, Kangawa L, Matsuo H. Neuromedin C: a bombesin-like peptide identified in porcine spinal cord. Biochem Biophys Res Commun 119:14–20, 1984.

[8] Nagalla SR, Gibson BW, Tang D, Reeve JR Jr, Spindel ER. Gastrin-releasing peptide (GRP) is not mammalian bombesin. Identification and molecular cloning of a true amphibian GRP distinct from amphibian bombesin in *Bombina orientalis*. J Biol Chem 267:6916–6922, 1992.

[9] Falconieri Erspamer G, Severini C, Erspamer V, Melchiorri P, Delle Fave G, Nakajima T. Parallel bioassay of 27 bombesin-like peptides on 9 smooth muscle preparations. Structure-activity relationships and bombesin receptor subtypes. Regul Pept 21:1–11, 1988.

[10] Cardona C, Rabbitts PH, Spindel ER, et al. Production of neuromedin B and neuromedin B gene expression in human lung tumor cell lines. Cancer Res 51:5205–5211, 1991.

[11] Spindel ER, Chin WW, Price J, Rees LH, Besser GM, Habener JF. Cloning and characterization of cDNAs encoding human gastrin-releasing peptides. Proc Natl Acad Sci USA 81:5699–5703, 1984.

[12] Krane IM, Naylor SL, Helin-Davis D, Chin WW, Spindel ER. Molecular cloning of cDNAs encoding the human bombesin-like peptide neuromedin B. J Biol Chem 263:13 317–13 332, 1988.

[13] Regoli D, Dion S, Rhaleb N-E, Drapeau G, Rouissi N, D'Orleans-Juste P. Receptors for neurokinins, tachykinins, and bombesin: a pharmacological study. Ann NY Acad Sci 547:158–173 1988.

[14] von Schrenck T, Heinz-Erian P, Moran T, Mantey SA, Gardner JD, Jensen RT. Neuromedin B receptor in esophagus: evidence for subtypes of bombesin receptor. Am J Physiol 256:G747–G758, 1989.

[15] Ladenheim EE, Jensen RT, Mantey SA, Mc Hugh PR, Moran TH. Receptor heterogeneity for bombesin-like peptides in the rat central nervous system. Brain Res 537:223–240, 1990.

[16] Lee MC, Jensen RT, Coy DH, Moody TW. Autoradiographic localization of neuromedin B binding sites in rat brain. Mol Cell Neurosci 1:161–167, 1990.

[17] von Schrenck T, Wang L-H, Coy DH, Villanueva ML, Mantey S, Jensen RT. Potent bombesin receptor antagonists distinguish receptor subtypes. Am J Physiol 259:G468–G473, 1990.

[18] Corjay MH, Dobrzanski DJ, Way JM, et al. Two distinct bombesin receptor subtypes are expressed and functional in human lung carcinoma cells. J Biol Chem 266:18 771–18 779, 1991.

[19] Kilgore WR, Mantyh PW, Mantyh CR, McVey DC, Vigna SR. Bombesin/GRP-preferring and neuromedin B-preferring receptors in the rat urogenital system. Neuropeptides 24:43–52, 1993.

[20] Cardona C, Reeve JG, Blochen NM. Evidence for the existence of separate receptors for gastrin releasing peptide, neuromedin B and phyllolitorin in human tumour cell lines. Br J Cancer 63 (suppl 13):14, 1991.

[21] Fathi Z, Corjay MH, Shapira H, et al. BRS-3: a novel bombesin receptor subtype selectively expressed in testis and lung carcinoma. J Biol Chem 268:5979–5984, 1993.

[22] Rozengurt E. Bombesin stimulation of mitogenesis. Specific receptors, signal transduction, and early events. Am Rev Respir Dis 142:S11–S15, 1990.
[23] Cirillo DM, Gaudino G, Naldini L, Comoglio PM. Receptor for bombesin with associated tyrosine kinase activity. Mol Cell Biol 6:4641–4649, 1986.
[24] Zachary I, Gil J, Lehman W, Sinnett-Smith J, Rozengurt E. Bombesin, vasopressin, and endothelin rapidly stimulate tyrosine phosphorylation in intact Swiss 3T3 cells. Proc Natl Acad Sci USA 88:4577–4581, 1991.
[25] Erspamer V. Peptides of the amphibian skin active on the gut. II. Bombesin-like peptides: isolation, structure, and basic functions. In: Glass GBJ, ed. Gastrointestinal Hormones. New York: Raven Press, 1980; 343–361.
[26] Taché Y, Brown M. On the role of bombesin in homeostasis. Trends Neurosci 5:431–433, 1982.
[27] Walsh JH. Bombesin-like peptides. In: Kieger DT, Brownstein MJ, Martin JB, eds. Brain Peptides. New York: Wiley-Interscience, 1983; 941–960.
[28] Zachary I, Woll PJ, Rozengurt E. A role for neuropeptides in the control of cell proliferation. Dev Biol 124:295–308, 1987.
[29] Lebacq-Verheyden, Trepel J, Sausville EA, Battey JF. Bombesin and gastrin-releasing peptide: neuropeptides, secretogogues, and growth factors. In: Sporn MB, Roberts AB, eds. Peptide Growth Factors and Their Receptors II. New York: Springer-Verlag, 1991; 71–124.
[30] Broccardo C, Falconieri Erspamer G, Melchiorri P, Negri L, de Castiglione R. Relative potency of bombesin-like peptides. Br J Pharm 55:221–227, 1975.
[31] Rivier JE, Brown MR. Bombesin, bombesin analogues, and related peptides: effects on thermoregulation. Biochemistry 17:1766–1771, 1978.
[32] Moody TW, Crawley JN, Jensen RT. Pharmacology and neurochemistry of bombesin-like peptides. Peptides 3:559–563, 1982.
[33] Cuttitta F, Carney DN, Mulshine J, et al. Bombesin-like peptides can function as autocrine growth factors in human small-cell lung cancer. Nature (Lond) 316:823–826, 1985.
[34] Sunday ME, Kaplan LM, Motoyama E, Chin WW, Spindel ER. Gastrin-releasing peptide (mammalian bombesin) gene expression in health and disease. Lab Invest 59:5–24, 1988.
[35] Moody TW, Korman LY. The release of bombesin-like peptides from small cell lung cancer cells. Ann NY Acad Sci 547:351–359, 1988.
[36] Giacchetti S, Gauvillé C, de Crémoux P, et al. Characterization, in some human breast cancer cell lines, of gastrin-releasing peptide-like receptors which are absent in normal breast epithelial cells. Int J Cancer 46:293–298, 1990.
[37] Pagani A, Papotti M, Sanfilippo B, Bussolati G. Expression of the gastrin-releasing peptide gene in carcinomas of the breast. Int J Cancer 47:371–375, 1991.
[38] Narayan S, Guo Y-S, Townsend CM Jr, Singh P. Specific binding and growth effects of bombesin-related peptides on mouse colon cancer cells in vitro. Cancer Res 50:6772–6778, 1990.
[39] Frucht H, Gazdar A, Park J-A, Oie H, Jensen RT. Characterization of functional receptors for gastrointestinal hormones on human colon cancer cells. Cancer Res 52:1114–1122, 1992.
[40] Avis FP, Maneckjee R, Cuttitta F, Nakanishi Y, Mulshine J, Avis I. The role of gastrin releasing peptide in a pancreatic tumor cell line (Capan). Proc Am Cancer Res 29:54, 1988.
[41] Hajri A, Balboni G, Garaud JC, Aprahamian M, Damgé C. Gastrin-releasing-peptide stimulates growth of a pancreatic acinar cell carcinoma in vitro and in vivo. Regul Pept 40:165, 1992.
[42] Hajri A, Koenig M, Balboni G, Damgé C. Expression of GRP receptors in normal and cancerous pancreatic cells. Regul Pept 40:165, 1992.
[43] Bologna M, Festuccia C, Muzi P, Biordi L, Clomei M. Bombesin stimulates growth of human prostatic cancer cells in vitro. Cancer 63:1714–1720, 1989.
[44] Coy DH, Taylor JE, Jiang N-Y, et al. Developing receptor antagonists of neuropeptides: the bombesin/GRP and substance P systems. In: Schwartz TW, Hilsted LM, Rehfeld JR, eds. Neuropeptides and Their Receptors. Copenhagen: Munksgaard, 1990; 376–388.
[45] Jensen RT, Coy DH. Progress in the development of potent bombesin receptor antagonists. Trends Pharmacol Sci 12:13–19, 1991.
[46] Houben H, Denef C. Bombesin receptor antagonists and their use in the evaluation of paracrine and autocrine intercellular communication. Front Horm Res 19:176–195, 1991.
[47] Coy DH, Jensen RT, Jiang N-Y, Lin J-T, Bogden AE. Systematic development of bombesin/gastrin-releasing peptide antagonists. J Natl Cancer Inst Monogr 13:133–139, 1992.
[48] Jensen RT, Jones SW, Folkers K, Gardner JD. A synthetic peptide is a bombesin receptor antagonist. Nature (Lond) 309:61–63, 1984.
[49] Woll PJ, Rozengurt E. A neuropeptide antagonist that inhibits the growth of small cell lung cancer in vitro. Cancer Res 50:3968–3973, 1990.
[50] Sethi T, Rozengurt E. Galanin stimulates Ca^{2+} mobilization, inositol phosphate accumulation, and clonal growth in small cell lung cancer cells. Cancer Res 51:1674–1679, 1991.
[51] Sethi T, Langdon S, Smyth J, Rozengurt E. Growth of small cell lung cancer cells: stimulation by multiple neuropeptides and inhibition by broad spectrum antagonists in vitro and in vivo. Cancer Res (Suppl) 52:2737s–2742s, 1992.
[52] Takuwa N, Takuwa Y, Ohue Y, et al. Stimulation of calcium mobilization but not proliferation by bombesin and tachykinin neuropeptides in human small cell lung cancer cells. Cancer Res 50:240–244, 1990.
[53] Bunn PA, Dienhart DG, Chan D, Tagawa M, Jewett P. Effects of neuropeptides on human lung and breast cancer cells. J Natl Cancer Inst Monogr 13:145–151, 1992.
[54] Fabregat I, Rozengurt E. [D-Arg^1,D-Phe^5,D-$Trp^{7,9}$,Leu^{11}] substance P, a neuropeptide antagonist, blocks binding, Ca^{2+}-mobilizing, and mitogenic effects of endothelin and vasoactive intestinal contractor in mouse 3T3 cells. J Cell Physiol 145:88–94, 1990.
[55] Tan-No K, Sakurada T, Yamada T, Sakurada S, Kisara K. Spantide-induced antinociception in the opioid mechanism. Regul Pept 46:343–345, 1993.
[56] Bitar KG, Bowers CY, Coy DH. Effect of substance P/bombesin antagonists on the release of growth hormone by GHRP and GHRH. Biochem Biophys Res Commun 180:156–161, 1991.
[57] Iwatsuki K, Horiuchi A, Ren LM, Chiba S. Effects of gastrin releasing peptide (GRP) on pancreatic exocrine secretion in anaesthetized dogs. Asia Pac J Pharmacol 7:129–134, 1992.
[58] Patel KV, Schrey MP. Modulation of inositol lipid hydrolysis in human breast cancer by two classes of bombesin antagonists. J Mol Endocrinol 6:71–78, 1991.
[59] von Schrenck T, Wang L-H, Coy DH, Villanueva ML, Mantey S, Jensen RT. Potent bombesin receptor antagonists distinguish receptor subtypes. Am J Physiol 259:G468–G473, 1990.
[60] Coy DH, Heinz-Erian P, Jiang N-Y, et al. Progress in the development of competitive bombesin antagonists. Ann NY Acad Sci 547:150–157, 1988.
[61] Rusconi L, de Castiglione R, Gozzini L, et al. Bombesin receptor antagonists. 2. Analogues based on substance P antagonists. Farmaco 46:725–742, 1991.
[62] Cowan A, Khunawat P, Zhu XZ, Omerek DE. Effects of bombesin on behavior. Life Sci 37:135–145, 1985.

[63] Jensen RT, Heinz-Erian P, Gardner JD, Tamura M, Lance V, Coy DH. (D-Phe[12],Leu[13])-bombesin: a new class of bombesin receptor antagonist. Can J Physiol Pharmacol 64 (Suppl): 175, 1986.
[64] Flynn FW. Fourth ventricular injection of selective bombesin receptor antagonists facilitates feeding in rats. Am J Physiol 264:R218–R221, 1993.
[65] Mukai H, Kawai K, Suzuki S, Yamashita K, Munekata E. Antagonism by GRP(18–27) and substance P analogues on insulin release stimulated by GRP(18–27). Peptides 11:173–175, 1990.
[66] de Castiglione R, Gozzini L, Mena R, et al. Bombesin receptor antagonists. I. Analogues with deleted, inverted or substituted amino acid residues. Farmaco 45:1251–1263, 1990.
[67] Mukai H, Kawai K, Suzuki S, Ohmori H, Yamashita K, Munekata E. [Ala[6]]gastrin-releasing peptide-10: an analogue with dissociated biological activities. Am J Physiol 257:E235–E240, 1989.
[68] Mrozinski J Jr, Coy D, Neya M, Mantey S, Jensen R. Sidechain restricted analogues. A new class of bombesin receptor antagonists. Gastroenterology 104 (Suppl): A323, 1993.
[69] Edwards JV, Fanger BO, Cashman EA, Eaton SR, McLean LR. Amide bond substitutions and conformational constraints applied to bombesin antagonists. In: Smith JA, Rivier JE, eds. Peptides. Chemistry and Biology. Leiden: ESCOM, 1992; 52–53.
[70] Spanarkel M, Martinez J, Briet C, Jensen RT, Gardner JD. Cholecytokinin-27-32-amide. A member of a new class of cholecystokinin receptor antagonists. J Biol Chem 258:6746–6749, 1983.
[71] Martinez J, Magous R, Lignon M-F, Laur J, Castro B, Bali J-P. Synthesis and biological activity of new peptide segments of gastrin exhibiting gastrin antagonist property. J Med Chem 27:1597–1601, 1984.
[72] Martinez J, Rodriguez M, Bali J-P, Laur J. Phenylethylamide derivatives of the C-terminal tetrapeptide of gastrin. Int J Peptide Protein Res 28:529–535, 1986.
[73] Martinez J, Rodriguez M, Bali J-M, Laur J, Phenethyl ester derivative analogues of the C-terminal tetrapeptide of gastrin as potent gastrin antagonists. J Med Chem 29:2201–2206, 1986.
[74] Wang L-H, Coy DH, Taylor JE, et al. Desmethionine alkylamide bombesin analogues: a new class of bombesin receptor antagonists with potent antisecretory activity in pancreatic acini and antimitotic activity in Swiss 3T3 cells. Biochemistry 29:616–622, 1990.
[75] Wang L-H, Coy DH, Taylor JE, et al. Des-Met carboxyl terminal modified analogues of bombesin function as potent bombesin receptor antagonists, partial agonists, or agonists. J Biol Chem 265:15695–15703, 1990.
[76] Narayan S, Spindel ER, Rubin NH, Singh P. A potent bombesin receptor antagonist inhibits bombesin-stimulated growth of mouse colon cancer cells in vitro: absence of autocrine effects. Cell Growth Differentiation 3:111–118, 1992.
[77] Belvisi MG, Stretton CD, Barnes PJ. Bombesin-induced bronchoconstriction in the guinea pig: mode of action. J Pharmacol Exp Ther 258:36–41, 1991.
[78] Alptekin N, Yagci RV, Ertan A, et al. Comparison of prolonged in vivo inhibitory activity of several potent bombesin (BN) antagonists on BN-stimulated amylase secretion in the rat. Peptides 12:749–753, 1991.
[79] Buchan AMJ, Meloche M, Coy DH. Inhibition of bombesin-stimulated gastrin release from isolated human G cells by bombesin analogs. Pharmacol 41:237–245, 1990.
[80] Singh P, Guo Y-S, Kull FC, Leban JJ. A novel bombesin receptor antagonist (2258U89) potently inhibits bombesin evoked release of gastrointestinal hormones from rats and dogs, in vitro and in vivo. Regul Pept 40:75–86, 1992.
[81] Staley J, Coy D, Taylor JE, Kim S, Moody TW. [Des-Met[14]] bombesin analogues function as small cell lung cancer bombesin receptor antagonists. Peptides 12:145–149, 1991.
[82] Weigert N, Madaus S, Alexiou C, et al. Effect of bombesin antagonist D-Phe^-BN(6-13)OMe on vagally induced gastrin release from perfused rat stomach. Life Sci 52:725–732, 1993.
[83] Varga G, Adrian TE, Coy DH, Reidelberger RD. Effect of potent bombesin receptor antagonist on release of gut hormones in rats. Regul Pept 40:267, 1992.
[84] Varga G, Reidelberger RD, Liehr R-M, Bussjaeger LJ, Coy DH, Solomon TE. Effects of potent bombesin antagonist on exocrine pancreatic secretion in rats. Peptides 12, 493–497, 1991.
[85] Maggi CA, Coy DH, Giuliani S. Effect of [D-Phe^]bombesin (6–13)methylester, a bombesin receptor antagonist, towards bombesin-induced contractions in the guinea-pig and rat isolated urinary bladder. J Auton Pharmacol 12:215–222, 1992.
[86] Lach E, Haddad E-B, Gies J-P. Contractile effect of bombesin on guinea pig lung in vitro: involvement of gastrin-releasing peptide-preferring receptors. Lung Cell Mol Physiol 264:L80–L86, 1993.
[87] Mantey S, Frucht H, Coy DH, Jensen RT. Characterization of bombesin receptors using a novel, potent, radiolabeled antagonist that distinguishes bombesin receptor subtypes. Mol Pharmacol 43:762–774, 1993.
[88] Coy DH, Mungan Z, Rossowski WJ, et al. Development of a potent bombesin receptor antagonist with prolonged in vivo inhibitory activity on bombesin-stimulated amylase and protein release in the rat. Peptides 13:775–781, 1992.
[89] Ladenheim EE, Jensen RT, Mantey SA, Taylor JA, Coy DH, Moran TH. Bombesin receptor antagonists differentiate receptor subtypes in rat brain. Eur J Pharmacol 235:121–125, 1993.
[90] Guard S, Watling KJ, Howson W. Structure-activity requirements of bombesin for gastrin-releasing peptide- and neuromedin B-preferring bombesin receptors in rat brain. Eur J Pharmacol 240:177–184, 1993.
[91] Bitar KG, Coy DH. Identification and initial characterization of a putative neuromedin B-type receptor from rat urinary bladder membranes. Eur J Pharmacol 219:117–122, 1992.
[92] Davis TP, Crowell S, Taylor J, et al. Metabolic stability and tumor inhibition of bombesin/GRP receptor antagonists. Peptides 13:401–407, 1992.
[93] Staley J, Coy DH, Jensen RT, Moody TW. Solubilization and purification of bombesin/gastrin releasing peptide receptors from human cell lines. J Mol Neurosci 4:29–40, 1993.
[94] Feldman RI, Wu JM, Jensen JC, Mann E. Purification and characterization of the bombesin/gastrin releasing peptide receptor from Swiss 3T3 cells. J Biol Chem 265:17364–17372, 1990.
[95] Kim SH, Taylor JE, Jensen RT, Coy DH, Bogden AE, Moreau J-P. C-terminal modified bombesin and litorin analogs with potent in vitro and in vivo antiproliferative activity. In: Rivier JE, Marshall GR, eds. Peptides. Chemistry, Structure and Biology. Leiden: ESCOM, 1990; 182–184.
[96] Thomas F, Arvelo F, Antoine E, Jacrot M, Poupon MF. Antitumoral activity of bombesin analogues on small cell lung cancer xenografts: relationship with bombesin receptor expression. Cancer Res 52:4872–4877, 1992.
[97] Heimbrook DC, Boyer ME, Garsky VM, et al. Elucidation of a novel gastrin releasing peptide antagonist by minimal ligand analysis. In: Tam J, Kaiser ET, eds. Synthetic Peptides: Approaches to Biological Problems. New York: Alan R Liss, 1989; 295–307.
[98] Märki W, Brown M, Rivier JE. Bombesin analogs: effects on thermoregulation and glucose metabolism. Peptides 2 (Suppl 2):169–171, 1981.

[99] Tuché Y, Mārki W, Rivier J, Vale W, Brown M. Gastrin releasing peptide (GRP): central nervous system (CNS) action to inhibit gastric secretion in rats. Regul Pept 1 (Suppl 1):S112, 1980.

[100] Heimbrook DC, Saari WS, Balishin NL, et al. Carboxyl-terminal modification of a gastrin releasing peptide derivative generates potent antagonists. J Biol Chem 264:11 258–11 262, 1989.

[101] Coy DH, Heinz-Herian P, Jiang N-Y, et al. Probing peptide backbone function in bombesin. A reduced peptide bond analogue with potent and specific receptor antagonist activity. J Biol Chem 263:5056–5060, 1988.

[102] de Castiglione R, Gozzini L, Galantino M, et al. Bombesin receptor antagonists. 3. Irreversible alkylating analogues: melphalan derivatives. Farmaco 46:743–757, 1991.

[103] Stephens RL Jr, Horner P, Drapeau G. N-Acetyl-GRP(20-26)-O-CH_3 reverses intracisternal bombesin-induced inhibition of gastric acid secretion in rats. Peptides 12:665–667, 1991.

[104] Rouissi N, Rhaleb N-E, Nantel F, Dion S, Drapeau G, Regoli D. Characterization of bombesin receptors in peripheral contractile organs. Br J Pharmacol 103:1141–1147, 1991.

[105] Karlsson S, Ahrén B. Peptide receptor antagonists in the study of insulin and glucagon secretion in mice. Eur J Pharmacol 191:457–464, 1990.

[106] Heimbrook DC, Saari WS, Balishin NL, et al. Gastrin releasing peptide antagonists with improved potency and stability. J Med Chem 34:2102–2107, 1991.

[107] Heimbrook DC, Wallen JW, Balishin NL, Friedman A, Oliff A. High-density functional gastrin releasing peptide receptors on primate cells. J Natl Cancer Inst 82:402–407, 1990.

[108] Heimbrook DC, Saari WS, Balishin NL, et al. Design and evaluation of novel gastrin-releasing peptide antagonists for the treatment of small cell lung cancer. In: Rivier JE, Marshall GS, eds. Peptides. Chemistry, Structure and Biology. Leiden: ESCOM, 1990; 56–59.

[109] Houben H, Denef C. Effect of the bombesin receptor blockers [Leu^{13},$\psi$$CH_2$NH-Leu^{14}]bombesin and N-pivaloyl GRP(20–25) alkylamide (L 686,095-001C002) on basal and neuromedin C-stimulated PRL and GH release in pituitary cell aggregates. Peptides 12:371–374, 1991.

[110] Camble R, Cotton R, Dutta AS, et al. N-Isobutyryl-His-Trp-Ala-Val-D-Ala-His-Leu-NHMe (ICI 216140) a potent in vivo antagonist of bombesin/gastrin releasing peptide (BN/GRP) derived from the C-terminal sequence lacking the final methionine residue. Life Sci 45:1521–1527, 1989.

[111] Campbell B, Garner A, Dimaline R, Dockray GJ. Hormonal control of avian pancreas by gastrin-releasing peptide from the proventriculus. Am J Physiol 261:G16–G21, 1991.

[112] Cowan A, Daniel JL, Ryan RR, Wheeler-Aceto H. Pharmacological profile of ICI 216140, a novel bombesin antagonist. Eur J Pharmacol 183:235–236, 1990.

[113] Ryan RR, Daniel JL, Cowan A. Two bombesin analogues discriminate between neuromedin B- and bombesin-induced calcium flux in a lung cancer cell line. Peptides 14:1231–1235, 1993.

[114] Best JR, Cotton R, Dutta AS, et al. Antagonists of bombesin/gastrin releasing peptide based on [D-Ala^{24}] GRP(20–26)-heptapeptide. Modifications leading to potent analogues with prolonged duration of action. Drug Des Deliv 6:255–271, 1990.

[115] Best JR, Byrne P, Cotton R, et al. Antagonists of bombesin/gastrin-releasing peptide based on GRP(21–26)-heptapeptide. Effects of N- and C-terminal modifications. Drug Des Deliv 5:267–280, 1990.

[116] Martinez J, Bali J-P, Rodriguez M, Castro B, Magous R, Laur J. Synthesis and biological activities of some pseudo-peptide analogues of tetragastrin: the importance of the peptide backbone. J Med Chem 28:1874–1879, 1985.

[117] Carver JA. The conformation of bombesin in solution as determined by two-dimensional ^{1}H-NMR techniques. Eur J Biochem 168:193–199, 1987.

[118] Erne D, Schwyzer R. Membrane structure of bombesin studied by infrared spectroscopy. Prediction of membrane interactions of gastrin-releasing peptide, neuromedin B, and neuromedin C. Biochemistry 26:6316–6319,1987.

[119] Di Bello C, Scatturin A, Vertuani G, et al. Conformational studies on bombesin antagonists: CD and NMR characterization of [Thr^6,Leu^{13}ψ(CH_2NH)Met^{14}]bombesin(6–14). Biopolymers 31:1397–1408, 1991.

[120] Malikayil JA, Edwards JV, McLean LR. Micelle-bound conformations of a bombesin/gastrin releasing peptide receptor agonist and an antagonist by two-dimensional NMR and restrained molecular dynamics. Biochemistry 31:7043–7049, 1992.

[121] Coy DH, Jiang N-Y, Kim SH, et al. Covalently cyclized agonist and antagonist analogues of bombesin and related peptides. J Biol Chem 266:16 441–16 447, 1991.

[122] Kull FC Jr, Leban JJ, Landavazo A, Stewart KD, Stockstill B, McDermed JD. Conveyance of partial agonism/antagonism to bombesin/gastrin-releasing peptide analogues on Swiss 3T3 cells by a carboxyl-terminal leucine insertion. J Biol Chem 267:21 132–21 138, 1992.

[123] Woll PJ, Coy DH, Rozengurt E. [Leu^{13}-ψ(CH_2NH)Leu^{14}]bombesin is a specific bombesin receptor antagonist in Swiss 3T3 cells. Biochem Biophys Res Commun 155:359–365, 1988.

[124] Saari WS, Heimbrook DC, Friedman A, Fisher TW, Oliff A. A gastrin-releasing peptide antagonist containing a ψ(CH_2O) amide bond surrogate. Biochem Biophys Res Commun 165:114–117, 1989.

[125] Woll PJ, Rozengurt E. Two classes of antagonist interact with receptors for the mitogenic neuropeptides bombesin, bradykinin, and vasopressin. Growth Factors 1:75–83, 1988.

[126] Millar JBA, Rozengurt E. Arachidonic acid release by bombesin. A novel postreceptor target for heterologous mitogenic desensitization. J Biol Chem 265:19 973–19 979, 1990.

[127] Erusalimsky JD, Friedberg I, Rozengurt E. Bombesin, diacylglycerols, and phorbol esters rapidly stimulate the phosphorylation of an M_r = 80 000 protein kinase C substrate in permeabilizes 3T3 cells. Effect of guanine nucleotides. J Biol Chem 263:19 188–19 194, 1988.

[128] Brooks SF, Herget T, Broad S, Rozengurt E. The expression of 80 K/MARCKs, a major substrate of protein kinase C (PKC), is down-regulated through both PKC-dependent and -independent pathways. Effect of bombesin, platelet-derived growth factor, and cAMP. J Biol Chem 267:14 212–14 218, 1992.

[129] Millar JBA, Rozengurt E. Chronic desensitization to bombesin by progressive down-regulation of bombesin receptors in Swiss 3T3 cells. Distinction from acute desensitization. J Biol Chem 265:12 052–12 058, 1990.

[130] Trepel JB, Moyer JD, Cuttitta F, et al. A novel bombesin receptor antagonist inhibits autocrine signals in a small cell lung carcinoma cell line. Biochem Biophys Res Commun 156:1383–1389, 1988.

[131] Mahamoud S, Palaszynski E, Fiskum G, Coy DH, Moody TW. Small cell lung cancer bombesin receptors are antagonized by reduced peptide bond analogues. Life Sci 44:367–373, 1989.

[132] Mahmoud S, Staley J, Taylor J, et al. [Psi^{13,14}] bombesin analogues inhibit growth of small cell lung cancer in vitro and in vivo. Cancer Res 51:1798–1802, 1991.

[133] Sausville EA, Trepel JB, Moyer JD. Inhibitors of bombesin-stimulated intracellular signals: interruption of an autocrine pathway as a therapeutic strategy in small cell lung carcinoma. In: Ragaz J, et al., eds. Effects of Therapy on Biology and Kinetics of the Residual Tumor. Part A: Pre-Clinical Aspects. New York: Wiley-Liss, 1990; 193–207.

[134] Ciomei M, Pastori W, Pastori A, de Castiglione R, Gozzini L, Corradi F. In vitro and in vivo activity of alkylating bombesin receptor antagonists on small cell lung carcinoma. Anticancer Res 13:75–80, 1993.

[135] Severi C, Coy DH, Jensen RT, Boschero L, Anania MC, Delle Fave G. Pharmacological characterization of [Leu-^{13}-ψ-CH_2NH-Leu^{14}]-bombesin as a specific bombesin receptor antagonist on isolated smooth muscle cells. J Pharmacol Exp Ther 251:713–717, 1989.

[136] Holst JJ, Harling H, Messell T, Coy DH. Identification of the neurotransmitter/neuromodulator functions of the neuropeptide gastrin-releasing peptide in the porcine antrum, using the antagonist (Leu^{13}-ψ-CH_2NH-Leu^{14})-bombesin. Scand J Gastroenterol 25:89–96, 1990.

[137] Rossowski WJ, Murphy WA, Jiang N-J, Yeginsu O. Effects of a novel antagonist analogue on bombesin-stimulated gastric acid secretion and growth hormone release in the pentobarbital-anesthetized rat. Scand J Gastroenterol 24:121–128, 1989.

[138] Schubert ML, Hightower J, Coy DH, Makhlouf GM. Regulation of acid secretion by bombesin/GRP neurons of the gastric fundus. Am J Physiol 260:G156–G160, 1991.

[139] Schubert ML, Coy DH, Makhlouf GM. Peptone stimulates gastrin secretion from the stomach by activating bombesin/GRP and cholinergic neurons. Am J Physiol 262:G685–G689, 1992.

[140] Cuber JC, Bernard G, Coy DH, Bernard C, Chayvialle JA. Blockade of bombesin receptors with [Leu^{14}-ψ(CH_2NH)-Leu^{13}]bombesin fails to suppress nutrient-induced CCK release from rat duodenojejunum. Peptides 11:255–258, 1990.

[141] Campos RV, Buchan AMJ, Pederson RA, McIntosh CHS, Coy DH. Inhibition of bombesin-stimulated gastrin release from isolated canine G cells by bombesin antagonists. Can J Pharmacol 67:1520–1524, 1989.

[142] Tang K-C, Pan J-T. Stimulatory effects of bombesin-like peptides on suprachiasmatic neurons in brain slices. Brain Res 614:125–130, 1993.

[143] Houben H, Denef C, Vranckx C. Stimulation of growth hormone release and prolactin release from rat pituitary cell aggregates by bombesin- and ranatensin-like peptides is potentiated by estradiol, 5α-dihydrotestosterone, and dexamethasone. Endocrinology 126:2257–2266, 1990.

[144] Feldman EL, Randolph AE. Peptides stimulate phospho-inositide hydrolysis in human retinal pigment epithelium. Invest Ophthalmol Visual Sci 34:431–437, 1993.

[145] Merali Z, Moody TW, Coy DH. Blockade of brain bombesin/GRP receptors increases food intake in satiated rats. Am J Physiol 264:R1031–R1034, 1993.

[146] Motamedi F, Rashidi-Pour A, Zarrindast MR, Badavi M. Bombesin-induced anorexia requires central bombesin receptor activation: independence from interaction with central catecholaminergic systems. Psychopharmacol 110:193–197, 1993.

[147] Bado A, Moizo L, Laigneau J-P, Gauthier M, Dubrasquet M, Lewin MJM. Possible mediation by luminal somatostatin of bombesin-induced satiety in the cat. Am J Physiol 263:R84–R88, 1992.

[148] Babcock AM, Baker DA, Moody TW. Bombesin-induced hypothermia: a dose-response and receptor antagonist study. Pharmacol Biochem Behav 43:957–960, 1992.

[149] Cowan A, Wheeler H, Coy DH. Studies in vivo with Leu^{13}-ψ[CH_2NH]-Leu^{14}-bombesin, a proposed competitive antagonist of bombesin. FASEB J 2:A784, 1988.

[150] Dickinson KEJ, Uemura N, Sekar MC. Partial agonist activity of the bombesin-receptor antagonist [Leu^{13}-ψ-CH_2-NH-Leu^{14}]-bombesin in frog peptic cells. Biochem Biophys Res Commun 157:1154–1158, 1988.

[151] Coy DH, Taylor JE, Jiang N-Y, et al. Short-chain pseudo-peptide bombesin receptor antagonists with enhanced binding affinities for pancreatic acinar and Swiss 3T3 cells display strong antimitotic activity. J Biol Chem 264:14691–14697, 1989.

[152] Wisner JR Jr, Xue BG, Coy DH, Renner IG. [D-Ala^1,Leu^4-ψ-CH_2NH/(ψ-CH_2NH)-Leu^{10}]neuromedin C antagonizes neuromedin C-stimulated amylase release by acini isolated from the rat pancreas. Pancreas 5:408–414, 1990.

[153] Coy D, Wang L-H, Jiang N-Y, Jensen R. Short chain bombesin pseudopeptides with potent bombesin receptor antagonist activity in rat and guinea pig pancreatic acinar cells. Eur J Pharmacol 190:31–38, 1990.

[154] Piggins HD, Moody TW, Merali Z. Effects of neonatal blockade of bombesin (BN) receptors with [D-Phe^6,ψLeu^{13}-Cpa^{14}]BN(6–14) on adult behavior and sensitivity to BN. Peptides 14:845–848, 1993.

[155] Laferrère B, Leroy F, Bonhomme G, Le Gall A, Basdevant A, Guy-Grand B. Effects of bombesin, of a new bombesin agonist (BIM187) and a new antagonist (BIM189) on food intake in rats, in relation to cholecystokinin. Eur J Pharmacol 215:23–28, 1992.

[156] Radulovic S, Cai R-Z, Serfozo P, et al. Biological effects and receptor binding affinities of new pseudononapeptide bombesin/GRP receptor antagonists with N-terminal D-Trp or D-Tpi. Int J Pept Protein Res 38:593–600, 1991.

[157] Cai R-Z, Radulovic S, Pinski J, et al. Pseudononapeptide bombesin antagonists containing C-terminal Trp or Tpi. Peptides 13:267–271, 1992.

[158] Jaworek J, Konturek PK, Konturek SJ, Cai R-Z, Schally AV. Actions of novel bombesin receptor antagonists on pancreatic secretion in rats. Eur J Pharmacol 214:239–245, 1992.

[159] Konturek SJ, Dembinski A, Warzecha Z, et al. Antagonism of receptors for bombesin, gastrin and cholecystokinin in pancreatic secretion and growth. Digestion 48:89–97, 1991.

[160] Konturek SJ, Bilski J, Hladij M, Krzyzek E, Cai R-Z, Schally AV. Role of cholecystokinin, gastrin and gastrin-releasing peptide in the regulation of pancreatic secretion in cats. Digestion 49:97–105, 1991.

[161] Pinski J, Yano T, Rekasi Z, Cai R-Z, Radulovic S, Schally AV. High potency of a new bombesin antagonist (RC-3095) in inhibiting serum gastrin levels; comparison of different routes of administration. Regul Pept 41:185–193, 1992.

[162] Pinski J, Yano T, Groot K, Cai R-Z, Radulovic S, Schally AV. Endocrine effects of new bombesin/gastrin-releasing peptide antagonists in rats. Am J Physiol 263:E712–E717, 1992.

[163] Pinski J, Yano T, Schally AV. Inhibitory effects of the new bombesin receptor antagonist RC-3095 on the luteinizing hormone release in rats. Neuroendocrinol 56:831–837, 1992.

[164] Szepeshazi K, Schally AV, Cai R-Z, Radulovic S, Milovanovic S, Szoke B. Inhibitory effects of bombesin/gastrin-releasing peptide antagonist RC-3095 and high dose of somatostatin analogue RC-160 on nitrosamine-induced pancreatic cancers in hamsters. Cancer Res 51:5980–5986, 1991.

[165] Liebow C, Lee MT, Krebs L, Schally AV. Bombesin may stimulate growth through up-regulation of EGF receptors. Pancreas 7:746, 1992.

[166] Szepeshazi K, Schally AV, Groot K, Halmos G. Effect of bombesin, gastrin-releasing peptide (GRP) (14–27) and bombesin/GRP receptor antagonist RC-3095 on growth of nitrosamine-induced pancreatic cancers in hamsters. Int J Cancer 54:282–289, 1993.

[167] Radulovic S, Comaru-Schally AM, Milovanovic S, Schally AV. Somatostatin analogue RC-160 and LH-RH antagonist SB-75 inhibit growth of MIA PaCa human pancreatic cancer xenografts in nude mice. Pancreas 8:88–97, 1993.

[168] Radulovic SS, Milovanovic SR, Cai R-Z, Schally AV. The binding of bombesin and somatostatin and their analogs to human colon cancers. Proc Soc Exp Biol Med 200:394–401, 1992.

[169] Radulovic S, Miller G, Schally AV. Inhibition of growth of HT-29 human colon cancer xenografts in nude mice by treatment with bombesin/gastrin releasing peptide antagonist (RC-3095). Cancer Res 51:6006–6009, 1991.

[170] Milovanovic SR, Radulovic S, Groot K, Schally AV. Inhibition of PC-82 human prostate cancer line xenografts in nude mice by bombesin antagonist RC-3095 or combination of agonist [D-Trp^6]-luteinizing hormone-releasing hormone and somatostatin analog RC-160. Prostate 20:269–280, 1992.

[171] Pinski J, Halmos G, Szepeshazi K, Schally AV. Antagonists of bombesin/gastrin-releasing peptide as adjuncts to agonists of luteinizing hormone-releasing hormone in the treatment of experimental prostate cancer. Cancer 72:3263–3270, 1993.

[172] Pinski J, Schally AV, Halmos G, Szepeshazi K. Effect of somatostatin analog RC-160 and bombesin/gastrin releasing peptide antagonist RC-3095 on growth of PC-3 human prostate-cancer xenografts in nude mice. Int J Cancer 55:963–967, 1993.

[173] Pinski J, Halmos G, Schally AV. Somatostatin analog RC-160 and bombesin/gastrin-releasing peptide antagonist RC-3095 inhibit the growth of androgen-independent DU-145 human prostate cancer line in nude mice. Cancer Lett 71:189–196, 1993.

[174] Yano T, Pinski J, Groot K, Schally AV. Stimulation by bombesin and inhibition by bombesin/gastrin-releasing peptide antagonist RC-3095 of growth of human breast cancer cell lines. Cancer Res 52:4545–4547, 1992.

[175] Szepeshazi K, Schally AV, Halmos G, Groot K, Rudulovic S. Growth inhibition of estrogen-dependent and estrogen-independent MXT mammary cancers in mice by the bombesin and gastrin-releasing peptide antagonist RC-3095. J Natl Cancer Inst 24:1915–1922, 1992.

[176] Libow C, Crean DH, Schally AV, Mang TS. Peptide analogues alter the progression of premalignant lesions, as measured by Photofrin fluorescence. Proc Natl Acad Sci USA 90:1897–1901, 1993.

[177] Leban JJ, Kull FC Jr, Landavazo A, Stockstill B. Development of potent gastrin-releasing peptide antagonists having a D-Pro-ψ(CH$_2$NH)-Phe-NH$_2$ C terminus. Proc Natl Acad Sci USA 90:1922–1926, 1993.

[178] Mokotoff M, Ren K, Wong LK, LeFever AV, Lee PC. Synthesis and biological evaluation of novel potent antagonists of the bombesin/gastrin releasing peptide receptor. J Med Chem 35:4696–4703, 1992.

[179] Borysewicz R, Ren KJ, Mokotoff M, Lee PC. Direct effect of bombesin on pancreatic and gastric growth in suckling rats. Regul Pept 41:157–169, 1992.

[180] Gawlak SL, Kiener PA, Braslawsky GR, Greenfield RS. Homodimeric forms of bombesin act as potent antagonists of bombesin on Swiss 3T3 cells. Growth Factors 5:159–170, 1991.

[181] de Castiglione R, Gozzini L, Galantino M, et al. Bombesin receptor antagonists. 5. New irreversible alkylating analogues. Farmaco 47:855–867, 1992.

[182] Lucietto P-L, de Castiglione R, Gozzini L, Ciomei M. Bombesin receptor antagonists. 4. Chloromethylketone and chloroethylnitrosourea derivatives. Farmaco 46:1111–1120, 1991.

[183] Zachary I, Rozengurt E. High-affinity receptors for peptide of the bombesin family in Swiss 3T3 cells. Proc Natl Acad Sci USA 82:7616–7620, 1985.

[184] Kris RM, Hazan R, Villines J, Moody TW, Schlessinger J. Identification of the bombesin receptor on murine and human cells by cross-linking experiments. J Biol Chem 262:11215–11220, 1987.

[185] Layton JE, Scanlon DB, Soveny C, Morstyn G. Effects of bombesin antagonists on the growth of small cell lung cancer cells in vitro. Cancer Res 48:4783–4789, 1988.

[186] Fanger BO, Wade AC. Somatostatin competes with the central portion of gastrin-releasing peptide for binding to a 120 kDa protein. Neurochem Int 18:185–189, 1991.

[187] Terenius L. Somatostatin and ACTH are peptides with partial antagonist-like selectivity for opiate receptor. Eur J Pharmacol 38:211–213, 1976.

[188] Rezek M, Havlicedk V, Leybin L, La Bella FS, Friesen H. Opiate-like naloxone-reversible actions of somatostatin given intracerebrally. Can J Pharmacol 56:227–231, 1978.

[189] Gulya K, Pelton JT, Hruby VJ, Yamamura HI. Cyclic somatostatin octapeptide analogues with high affinity and selectivity towards *mu* opioid receptors. Life Sci 38:2225–2229, 1986.

[190] Walker JM, Bowen WD, Atkins ST, Hemstreet MK, Coy DH. *Mu*-opiate binding and morphine antagonism by octapeptide analogs of somatostatin. Peptides 8:869–875, 1987.

[191] Orbuch M, Taylor JE, Coy DH, et al. Discovery of a novel class of neuromedin B receptor antagonists, substituted somatostatin analogues. Mol Pharmacol 44:841–850, 1993.

[192] Valentine JJ, Nakanishi S, Hageman DL, Snider RM, Spencer RW, Vinick FJ. CP-70,030 and CP-75,998: the first non-peptide antagonists of bombesin and gastrin releasing peptide. Biorg Med Chem Lett 2:333–338, 1992.

[193] Snider RM, Constantine JW, Lowe III JA, et al. A potent nonpeptide antagonist of the substance P (NK$_1$) receptor. Science 251:435–439, 1991.

[194] Carney DN, Gazdar AF, Bepler G, et al. Establishment and identification of small cell lung cancer cell lines having classic and variant features. Cancer Res 45:2913–2923, 1985.

[195] Carney DN, Cuttitta F, Moody TW, Minna JD. Selective stimulation of small cell lung cancer clonal growth by bombesin and gastrin-releasing peptide. Cancer Res 47:821–825, 1987.

[196] Kado-Fong H, Malfroy B. Effects of bombesin on human small cell lung cancer cells: evidence for a subset of bombesin non-responsive cell lines. J Cell Biochem 40:431–437, 1989.

[197] Bepler G, Rotsch M, Jaques G, Haeder M, Heymanns J, Hartogh G, Kiefer P, Havemann K. Peptides and growth factors in small cell lung cancer: production, binding sites, and growth effects. J Cancer Res Clin Oncol 114:235–244, 1988.

[198] Giaccone G, Battey J, Gazdar AF, Oie H, Draoui M, Moody TW. Neuromedin B is present in lung cancer cell lines. Cancer Res 52:2732s–2736s, 1992.

[199] Alexander RW, Upp JR Jr, Poston GJ, Townsend CM Jr, Singh P, Thompson JC. Bombesin inhibits growth of human pancreatic adenocarcinoma in nude mice. Pancreas 3:297–302, 1988.

[200] Meijers M, Van Garderen-Hoetmer A, Lamers CBHW, Rovati LC, Jensen JBMJ, Woutersen RA. Effects of bombesin on the development of N-nitrosobis(2-oxopropyl)amine-induced pancreatic lesions in hamsters. Cancer Lett 59:45–50, 1991.

[201] Battey J, Wada E. Two distinct receptor subtypes for mammalian-like peptides. Trends Neurosci 14:524–528, 1991.

[202] Moody TW, Staley J, Zia F, Coy DH, Jensen RT. Neuromedin B binds with high affinity, elevates cytosolic calcium and stimulates the growth of small-cell lung cancer cell lines. J Pharmacol Exp Ther 263:311–317, 1992.

[203] Giladi E, Nagalla SR, Spindel ER. Molecular cloning and characterization of receptors for the mammalian bombesin-like peptides. J Mol Endocrinol 4 (1):41–54, 1993.

[204] Shapira H, Wada E, Jensen R, Battey J. Distinguishing bombesin receptor subtypes. In: Conn PM, ed. Methods in Neurosciences. New York: Academic Press, 1993; 13:220–237.

[205] Viallet J, Minna JD. Gastrin-releasing peptide (GRP, mammalian bombesin) in the pathogenesis of lung cancer. Prog Growth Factor Res 1:89–97, 1989.

[206] Moody TW, Cuttitta F. Growth factor and peptide receptors in small cell lung cancer. Life Sci 52:1161–1173, 1993.

[207] Korman LY, Carney DN, Citron ML, Moody TW. Secretin/vasoactive intestinal peptide-stimulated secretion of bombesin/gastrin releasing peptide from human small cell carcinoma of the lung. Cancer Res 46:1214–1218, 1986.
[208] Moody TW, Zia F, Makhejia A. Pituitary adenylate cyclase activating polypeptide receptors are present on small cell lung cancer cells. Peptides 14:241–246, 1993.
[209] Maruno K, Said SI. Small-cell lung carcinoma: inhibition of proliferation by vasoactive intestinal peptide and helodermin and enhancement of inhibition by anti-bombesin antibody. Life Sci 52:PL267–PL271, 1993.
[210] Woll PJ, Rozengurt E. Neuropeptides as growth regulators. Br Med Bull 45:492–505, 1989.
[211] Mukai H, Munekata E, Higashijima T. G protein antagonists. A novel hydrophobic peptide compete with receptor for G protein binding. J Biol Chem 267:16237–16243, 1992.
[212] Reubi JC, Waser B, Sheppard M, Macaulay V. Somatostatin receptors are present in small-cell but not in non-small-cell primary lung carcinomas: relationship to EGF-receptors. Int J Cancer 45:269–274, 1990.
[213] Sagman U, Mullen B, Kovacs K, Kerbel R, Ginsberg R, Reubi J-C. Identification of somatostatin receptors in human small cell lung carcinoma. Cancer 66:2129–2133, 1990.
[214] Rehfeld JF, Bardrum L, Hilsted L. Gastrin in human bronchogenic carcinoma: constant expression but variable processing of progastrin. Cancer Res 49:2840–2843, 1989.
[215] Geijer T, Folkesson R, Rehfeld JF, Monstein H-J. Expression of cholecystokinin gene in a human (small-cell) lung carcinoma cell line. FEBS Lett 270:30–32, 1990.

Biographies

Roberto de Castiglione is a consultant in the peptide field. Formerly head of the Peptide Chemistry Unit at Farmitalia Carlo Erba (Milan) he worked for more than 30 years on biologically active peptides, mainly of non-mammalian origin. *Luigia Gozzini* is presently head of the Biochemistry Department at Bracco (Milan). Formerly she worked for several years on peptides and proteins of pharmaceutical interest at Farmitalia Carlo Erba.

Pergamon

Bioorganic & Medicinal Chemistry Letters, Vol. 6, No. 21, pp. 2617-2622, 1996

0960-894X/96 $15.00 + 0.00

PII: S0960-894X(96)00481-7

PD 165929 - The First High Affinity Non-peptide Neuromedin-B (NMB) Receptor Selective Antagonist

J. M. Eden, M. D. Hall, M. Higginbottom, D. C. Horwell, W. Howson, J. Hughes, R. E. Jordan, R. A. Lewthwaite, K. Martin, A. T. McKnight, J. C. O'Toole, R. D. Pinnock, M. C. Pritchard,* N. Suman-Chauhan and S. C. Williams.

Parke-Davis Neuroscience Research Centre, Cambridge University Forvie Site, Robinson Way, CAMBRIDGE, CB2 2QB, UK.

Abstract : In this paper we describe the development of a novel series of non-peptide neuromedin-B (NMB) receptor ligands as exemplified by PD 165929. PD 165929, which exhibits nanomolar affinity for the NMB receptor (Ki=6.3nM), has been demonstrated to be a competitive antagonist at this receptor (appK_B=7.6nM) and is selective over the corresponding gastrin-releasing peptide (GRP) receptor type (Ki>10000nM).

INTRODUCTION

We have previously published on our interest in the development of non-peptide ligands for neuropeptide receptors as exemplified by the identification of non-peptide agonists[1] and antagonists for cholecystokinin[2] and tachykinin[3] receptors. This has been *via* the application of a so-called "peptoid" drug design strategy.[4] The basic premise behind the peptoid structure-based approach to drug design involves the rational development of non-peptide receptor ligands starting from, and utilising the information contained within, the endogenous peptide of the targeted receptor.In brief[5] this peptoid drug design strategy consists of the following discrete steps :

i) identification of a **minimum active peptide fragment** of the endogenous peptide,
ii) recognition of key residues contained within the **minimum active fragment** with respect to receptor binding - achieved by carrying out an alanine scan on the peptide fragment,
iii) incorporation of the side chains of the three[6] most important residues identified from the alanine scan onto a **small molecule template**
iv) **exploration of conformational space** of amino acid side chains and,
v) optimisation of the side chains to provide a **high affinity, non-peptide receptor ligand.**

In this paper we describe how the peptoid drug design strategy has been adapted to the development of a series of non-peptide neuromedin-B receptor selective antagonists.

BOMBESIN, NEUROMEDIN-B AND GASTRIN-RELEASING PEPTIDE

The amphibian tetradecapeptide bombesin (BB) belongs to a class of peptides which share structural homology in their C-terminal decapeptide region.[7] At present two mammalian bombesin-

email address : martyn.pritchard@camb.wl.com
fax number : 01223-416712

like peptides have been identified and characterised,[8] the decapeptide neuromedin- B (NMB) and a 27 residue amino acid, gastrin-releasing peptide (GRP). NMB and GRP peptides are believed to mediate a variety of biological actions such as on autocrine growth, satiety, thermoregulation and stereotyped behaviour[9] via an action upon the corresponding NMB-preferring (BB_1) and GRP-preferring (BB_2) receptors. Although there are a number of peptide-based selective ligands for both the NMB and GRP receptors,[10] the precise physiological roles of these neuropeptides remain unclear partly due to a lack of high affinity non-peptide bombesin antagonists.[11]

RESULTS AND DISCUSSION

i) Identification of a minimum active peptide fragment of the endogenous peptide.

In employing our peptoid drug design strategy to the development of non-peptide bombesin antagonists, we first carried out an alanine scan study on the previously published[12] bombesin peptide fragment AcBB (7-14). This octapeptide derivative exhibited nanomolar affinity (see table I) for both receptor types and thus, we felt, would serve as an appropriate minimum active fragment in the design of both NMB and GRP receptor ligands.

ii) Recognition of the key residues contained within the minimum active fragment.

The largest decreases in NMB and GRP receptor binding affinity ensuing from the alanine scan study occurred when the Trp-8 (>1000 fold decrease), Leu-13 (>5000 fold) and Val-10 (>100 fold) residues of the minimum active fragment were replaced by Ala.[13] These findings reveal the primary importance of the side chains of these residues in the molecular recognition of AcBB(7-14) at bombesin receptors.

iii) Incorporation of the side chains of the three most important residues onto a small molecule template

In accord with the peptoid design strategy, the next step was to append the side chains of the three most important residues, in this case Trp, Leu/Phe[14] and Val, onto appropriate small molecule templates. A variety of small molecule templates were investigated including, for example, urea and secondary amide moieties (unpublished results). The highest affinity lead, however, proved to be a mono amino acid ligand [(S)-1] identified from a limited search of a company compound collection using the Trp, Leu/Phe and Val side chains as search queries. Compound (S)-1 (Table I) is a simple alanine derivative small molecule template on to which is appended Trp, Phe and Val side chains and exhibits excellent affinity and selectivity for the human NMB receptor type (NMB, Ki=95nM). As compound 1 contains the side chain of Phe as opposed to a Leu residue,[14] it is, as anticipated, selective for the NMB receptor type (GRP, Ki>10000nM).

The relative proximity of these key amino acid side chain surrogates is consistent with previous modeling studies[13] carried out on AcBB(7-14) which indicate that the heptapeptide adopts a γ-turn conformation which acts to bring the Trp, Leu and Val side chains close together in space (distances between α-carbons <7 Angstrom).

In attempting to reduce the bulk and complexity of the C-terminal phenyl serinol moiety of 1, we subsequently prepared a limited number of less structurally complex C-terminal derivatives (Table I). Removal of the whole of the phenyl serinol moiety (2, Ki=3700nM) from the C-terminal proved to have a detrimental effect on NMB receptor binding as did, to a lesser extent, exclusion of the phenyl (3, Ki=630nM) and dioxane (4, Ki=450nM) groups. Optimal among this data set of compounds proved to be the simple cyclohexyl derivatives 5 (Ki=310nM) and 6 (Ki=125nM) with the latter retaining much of the NMB receptor affinity and selectivity displayed by 1. We felt the cyclohexyl methylamine derivative 6 was a more appropriate lead than 1 to carry onto the next step

Table I : SAR of C-Terminal Phenyl Serinol Moiety of Compound 1.

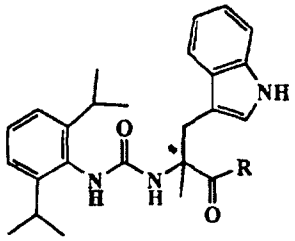

Compound No.	*	R	NMB, Ki(nM)[a]	GRP, Ki(nM)[a]
(S) - 1	S	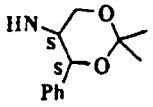	95	>10000
(R) - 1	R		420	>10000
2	RS	NHMe	3700	>10000
3	RS	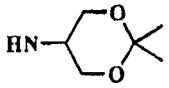	630	>10000
4	RS	$NH(CH_2)_2Ph$	450	>10000
5	RS	NHC_6H_{11}	310	>10000
6	RS	$NHCH_2C_6H_{11}$	125	>10000
NMB			0.068	56
GRP			9.1	0.040
Bombesin			2.0	0.15
AcBB(7-14)			2.1	0.70

a) Values shown represent the geometric mean of at least 3 separate experiments carried out using [^{125}I][Tyr^4] bombesin to label cloned human NMB or GRP receptors stably expressed in CHO cells.[15]

of the peptoid design strategy since this NMB receptor ligand exhibited equal affinity to its parent (1) whilst, importantly, being less structurally complex.

iv) Exploration of conformational space of amino acid side chains.

With this promising lead in hand the next priority was to explore the spatial arrangement of the amino acid side chains of the NMB receptor ligand 6. One means of achieving this objective, and a strategy that has previously proved particularly successful,[2,3] is to incorporate a single methyl group at key positions, eg. on nitrogen and α-carbon atoms, on the molecule thus introducing conformational constraint. Table II lists the derivatives of compound 6 that were prepared in following this strategy. With the exception of the "non-methylated" compound (11, Ki=120nM), all of the methylated derivatives showed reduced NMB receptor affinity when compared to 6. Although the optimal compound from this study with respect to NMB receptor binding affinity proved to be the non-methylated derivative 11, we decided to proceed with the marginally lower

Table II : Exploration of Conformational Space of Amino Acid Side Chains of Compound 6.

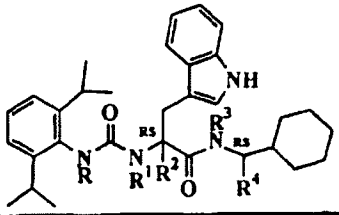

Compd.	R	R^1	R^2	R^3	R^4	NMB, Ki(nM)	GRP, Ki(nM)
7	Me					260	>10000
8		Me				760	1500
6			Me			125	>10000
9				Me		490	>10000
10					Me	440	>10000
11						120	>10000

Table III : C-Terminal Derivatives of Compound 6.

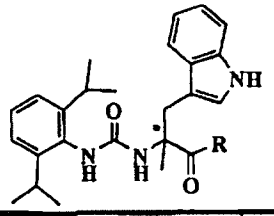

Compound No.	*	R	NMB, Ki (nM)	GRP, Ki (nM)
12	S	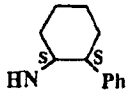	76	>10000
13	RS	(RS)-2-aminotetralin	310	>10000
14	RS	(RS)-1-aminotetralin	72	>10000
15	R	(S)-1-aminotetralin	14	>10000
16	RS	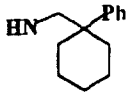	7.8	>10000
17 (PD165929)	S	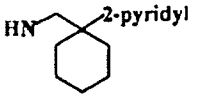	6.3	>10000

affinity parent compound 6 due to the advantageous properties the α-methyl group may confer on *in vivo* stability.[16]

v) Optimisation of the side chains to provide a high affinity, non-peptide receptor ligand.

Having decided upon the optimal spatial arrangement of the side chains surrounding the substituted alanine small molecule template, we then proceeded to optimise, individually, each of the three peripheral side chains. We first turned our attention towards investigating the SAR of the C-terminal cyclohexyl methylamine moiety of compound 6. A selection of key compounds prepared for this study are listed in Table III. Compounds 12 through 14 were prepared in an attempt to further understand the dimensions of the NMB receptor binding pocket that interacts with the C-terminal of this class of compound. The similar NMB receptor binding affinity achieved with the 1,2-substituted cyclohexyl derivative 12 (Ki=76nM) in comparison to the dioxane derivative 1, implied that the hydrophilic oxygen atoms were not contributing to NMB receptor binding to any great extent. This initial view was reinforced by the good receptor binding affinity exhibited by the racemic tetralin derivatives 13 (Ki=310nM) and, most notably, 14 (Ki=72nM). The preferred stereochemistry of the 1-substituted tetralin derivative was found to be R,S with this particular isomer (15) binding to the NMB receptor with an affinity of 14nM. Further high affinity compounds were obtained by appending aryl moieties to the 1-position of the cyclohexyl group in compound 6. For example the simple racemic phenyl derivative 16 displayed excellent affinity and selectivity for the NMB receptor (Ki=7.8nM). However, our preferred compound from this series is the resolved 2-pyridyl variant 17 (PD 165929) since in addition to having good affinity for the NMB receptor (Ki=6.3nM) this S-configured derivative (S stereochemistry was found to be optimal in this series) has improved aqueous solubility over 16.

In vitro functional assays demonstrate that compound 17 (PD 165929) acts as a competitive antagonist at the human NMB receptor exhibiting appK$_B$ values in line with its binding affinity in two separate bioassays (Table IV).

Table IV : Species Selectivity and *In Vitro* Functional Activity of 17 (PD 165929).

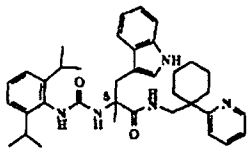

NMB Receptor Binding Affinities		In Vitro Functional Assays	
Human	Rat[a]	Cytosensor[b]	*Xenopus Oocytes*[c]
Ki, nM	IC_{50}, nM	appK$_B$, nM	appK$_B$, nM
6.3	150	7.6	7.5
(3.5-11)	(130-170)	(5.3-11)	(4.2-10)

a) Values shown represent the geometric mean of 3 separate experiments carried out using [^{125}I][Tyr^4] bombesin in the presence of [D-Phe^6] bombesin (6-13) ethyl ester to label NMB receptor binding sites in rat olfactory bulb.[17]

b) Inhibition of NMB-induced acidification response at the human NMB receptor expressed in CHO cells. Values are the means of at least 3 determinations.[18]

c) Inhibition of NMB-evoked increases in chloride currents in xenopus oocytes expressing human NMB receptors. Values represent the mean of at least three separate experiments.[19]

[CANCER RESEARCH 52, 1114–1122, March 1, 1992]

Characterization of Functional Receptors for Gastrointestinal Hormones on Human Colon Cancer Cells

H. Frucht,[1] A. F. Gazdar, J-A. Park, H. Oie, and R. T. Jensen[2]

National Institute of Diabetes, Digestive and Kidney Diseases, National Institutes of Health [H. F., R. T. J.], and National Cancer Institute-Navy Medical Oncology Branch, National Institutes of Health, Bethesda, Maryland 20892 [A. F. G., J-A. P., H. O.]

ABSTRACT

Studies demonstrate that some colon cancers possess receptors for various gastrointestinal hormones or neurotransmitters, the occupation of which can affect growth. These results are limited because frequently only a small number of tumors are studied, only 1 or 2 receptors are sought, and the effect on cell function is not investigated. In the present study, 10 recently characterized human colon cancer cell lines were studied to determine whether they possess receptors for any of 12 different gastrointestinal hormones or neurotransmitters and to determine whether these receptors mediate changes in cellular function. Each of the cell lines exhibited receptors for at least one radioligand. Receptors for vasoactive intestinal peptide (VIP) and muscarinic cholinergic agents occurred on 60%, bombesin and gastrin on 30%, β-adrenergic agents and gastrin-releasing peptide (GRP) on 20%, and somatostatin, opiates, neuromedin B, and substance P on 10%. Analysis of [^{3}H]*N*-methylscopolamine binding revealed a K_d of 0.2 nM for *N*-methylscopolamine with a binding capacity of 2500 sites/cell. With the agonist carbamylcholine, the receptor exhibited 2 classes of binding sites: one of high affinity (K_d 55 μM) representing 75% of the binding sites and one of low affinity (K_d 0.3 mM) representing 25% of the binding sites. Analysis of ^{125}I-[Tyr^4]bombesin binding revealed a receptor of high affinity (K_d 2.1 μM) with a binding capacity of 3300 sites/cell. Inhibition of binding by agonists revealed relative potencies of ^{125}I-[Tyr^4]bombesin > GRP >> neuromedin B, and two recently described antagonists were similar in potency to GRP. Analysis of ^{125}I-VIP binding revealed a receptor having 2 classes of binding sites: one of high affinity (K_d 3.6 nM) and one of low affinity (K_d 1.7 μM) which represented the majority of the 5.5 × 10^6 binding sites/cell. The relative potencies of agonists were VIP > helodermin > peptide histidine methionine > secretin. Evaluation of biological activity mediated by the muscarinic cholinergic and bombesin receptors revealed an increase of intracellular calcium and of inositol triphosphate by specific receptor agonists. The presence or absence of receptors detected by binding correlated closely with the ability of selective receptor agonists to alter cell function. These results demonstrate the presence of several different receptors for gastrointestinal hormones or neurotransmitters, some described for the first time, on human colon cancer cell lines, including bombesin-related peptides, VIP, somatostatin, substance P, β-adrenergic agents, calcitonin gene-related peptide, gastrin, muscarinic cholinergic agents, and opiates. These receptors are functional because occupation by selective agonists altered intracellular mediators. These results suggest that it will be important to extend these studies to evaluate growth effects.

INTRODUCTION

Colon cancer is one of the most common solid tumors in the United States, second in frequency only to lung cancer (1). Although great strides have been made in the early detection and prevention of colon cancer using occult blood testing and colonoscopic polypectomy (2), the therapeutic options for advanced disease are limited in their efficacy. At present, the 5-year survival of patients with advanced colon cancer remains low (3). This has prompted investigators to seek new modalities of treatment effective in controlling the growth and degree of differentiation of these tumors.

Recently, receptors for a number of gastrointestinal hormones have been found on several tumors such as breast and prostate and small cell lung carcinoma (4–6). The occupation of some of these receptors by agonists or antagonists has been shown to modulate tumor cell growth and function (7). Several reports have demonstrated the presence of receptors for various gastrointestinal hormones on human colon cancer cell lines (8–11), and a few have demonstrated the biological activity of these receptors by studying increases in cAMP[3] or phospholipid turnover (10–12). In addition, a number of reports have demonstrated that some of these hormones can affect the growth of colon cancer cells (13–16). For example, gastrin has a trophic effect on several human colon cancer cell lines, and some authors have suggested that gastrin may be an autocrine growth factor for colon cancer cell lines (13–17). Somatostatin has been reported to inhibit the trophic effects of gastrin (15). These reports are limited because only a small number of cell lines were examined, the presence of only a few specific receptors was investigated, the effect of receptor-ligand interaction on cell function was not always examined, and there was often no attempt to correlate the presence or absence of receptors with an effect on cell function. This has made it difficult to determine whether the presence of gastrointestinal receptors on colon cancer cell lines is common or not, whether all colon cancer cell lines possess a number of different classes of receptors for gastrointestinal hormones, or whether there is one particular receptor that is present on all colon tumors.

To address these uncertainties, we studied 10 newly characterized human colon cancer cell lines for the presence of hormone receptors using 12 different radiolabeled ligands. These receptors are characterized pharmacologically on these cell lines, their binding characteristics compared to similar receptors on normal physiological tissues, and the effect of receptor occupation on cell function examined by studying intracellular mediators. These data provide information for future studies examining these hormones in modulating colon tumor cell growth or differentiation.

MATERIALS AND METHODS

^{125}I-BH-CCK-8 (2200 Ci/mmol), ^{125}I-BH-SP (2200 Ci/mmol), ^{125}I-gastrin 17-1 (2200 Ci/mmol), ^{125}I-VIP (2200 Ci/mmol), ^{125}I-OH-BZP (2200 Ci/mmol), and [^{3}H]*N*-methylscopolamine (70–87 Ci/mmol) were

Received 7/30/91; accepted 12/13/91.

The costs of publication of this article were defrayed in part by the payment of page charges. This article must therefore be hereby marked *advertisement* in accordance with 18 U.S.C. Section 1734 solely to indicate this fact.

[1] Present address: Division of Oncologic Gastroenterology, Department of Medicine, Fox Chase Cancer Center, 7701 Burholme Avenue, Philadelphia, PA 19111.

[2] To whom requests for reprints should be addressed, at National Institute of Diabetes, Digestive and Kidney Diseases, National Institutes of Health, Building 10, Room 9C-103, Bethesda, MD 20892.

[3] The abbreviations used are: cAMP, cyclic AMP; CCK-8, cholecystokinin octapeptide; ^{125}-BH-CCK-8, ^{125}I-Bolton Hunter-labeled CCK-8; ^{125}I-BH-SP, ^{125}I-Bolton Hunter-labeled substance P; VIP, vasoactive intestinal peptide; ^{125}I-OH-BZP, ^{125}I-hydroxybenzylpindolol; NMB, neuromedin B; ^{125}I-BH-NMB, ^{125}I-Bolton Hunter-labeled NMB; GRP, gastrin-releasing peptide; CGRP, calcitonin gene-related peptide; NMS, methylscopolamine bromide; IC_{50}, 50% inhibitory concentration; $[Ca^{2+}]_i$, concentration of intracellular cytosolic calcium; IP_3, inositol trisphosphate.

obtained from New England Nuclear (Boston, MA). ^{125}I-[Tyr^4]bombesin (2200 Ci/mmol), ^{125}I-BH-NMB (2200 Ci/mmol), ^{125}I-secretin (2200 Ci/mmol), and ^{125}I-CGRP (2200 Ci/mmol) were prepared using the methods described previously (18–21). ^{125}I-Tyr^{11}-somatostatin-14 (2000 Ci/mmol) and [15,16-^{3}H]etorphine (30–60 Ci/mmol) were obtained from Amersham Corp. (Arlington Heights, IL). CCK-8 was obtained from Research Plus (Bayonne, NJ); [Tyr^4]bombesin and GRP were obtained from Bachem, Inc. (Torrance, CA); gastrin-I, NMB, VIP, secretin, substance P, somatostatin, helodermin, peptide histidine methionine-27, and CGRP were obtained from Peninsula Laboratories (Belmont, CA); pindolol, carbamylcholine chloride (carbachol), and NMS were obtained from Sigma Chemical Co. (St. Louis, MO). The bombesin analogues were synthesized and characterized as described previously (22–24). Etorphine was from the Laboratory of Chemistry, NIH, Bethesda, MD. Media and sera were obtained from Grand Island Biological Co. (Grand Island, NY).

Cell Culture. Ten human colon cancer cell lines, recently established as previously described, were examined (25). Relevant clinical information regarding the primary site of tumors, culture site of tumors, and degree of tumor differentiation is provided in Table 1. Cell lines were grown in RPMI 1640 medium supplemented with 5% heat-inactivated fetal bovine serum. Adherent cultures were passaged weekly at subconfluence after trypsinization. Nonadherent cultures were passaged weekly by transfer of floating multicellular aggregates. Cultures were maintained in incubators at 37°C in an atmosphere of 5% CO_2 and 95% air.

Binding of Radiolabeled Ligand. Adherent cells were scraped from the flask with a rubber policeman at least 72 h after last passage using trypsin. Cells were washed twice in five-fold volume % of media, spun down at 1000 × *g* for 5 min, and resuspended in standard incubation buffer consisting of 50 mM Tris buffer, 0.1% bacitracin, 5 mM $MgCl_2$, 130 mM NaCl, 7.7 mM KCl, 1 mM ethyleneglycol bis(β-aminoethyl ether)-*N,N,N',N'*-tetraacetic acid, 4 μg/ml leupeptin, 2 μg/ml chymostatin, and 0.1% bovine serum albumin at pH 7.4. After washing, the viability of the cells was assessed by trypan blue exclusion and was >90%, with no evidence of cell lysis. Cells at a concentration of 15 × 10^6 cells/ml (range, 5–25 × 10^6 cells/ml), in a volume of 0.5 ml were incubated with radioligand at a concentration of 50 pM for ^{125}I-BH-CCK-8, ^{125}I-[Tyr^4]bombesin, ^{125}I-BH-NMB, ^{125}I-VIP, ^{125}I-secretin, and ^{125}I-OH-BZP; 100 pM for ^{125}I-gastrin 17–1 and ^{125}I-[Tyr^{11}]somatostatin-14; 125 pM for ^{125}I-BH-SP and ^{125}I-CGRP; 0.6 nM for [^{3}H]NMS; and 1.5 nM for [15,16-^{3}H]etorphine, for the times and temperatures indicated. After incubation with iodinated radioligand, 0.133 ml of cells were sampled, spun down through standard incubation buffer containing 4% bovine serum albumin in a Beckman microfuge at 10,000 × *g* for 1 min, and then washed twice. The pellet was then counted in an Auto-Gamma 5000 series gamma counter (Packard Instrument Corp., Sterling, VA). After incubation with a tritiated radioligand, cells were sampled, filtered using glass microfiber filters (GF/C; Whatman International Ltd., Maidstone, England), and then counted in a liquid scintillation spectrometer (Packard Instrument Corp., Sterling, VA).

Nonsaturable binding was the amount of radioactivity associated with the cells when the incubation contained radioligand plus the unlabeled peptide in concentrations of 1–10 μM. Values shown for saturable binding are those measuring binding with radioligand alone (total binding) minus the nonsaturable binding. All values are for saturable binding unless stated otherwise. Dissociation constants were determined by the nonlinear, least-squares curve-fitting program (LIGAND) (26). The inhibitory constant values for antagonist binding and their relationship to the IC_{50} were calculated by the method of Cheng and Prusoff (27). The number of binding sites were determined by the curve-fitting program (LIGAND) (26) and expressed as binding sites/cell.

To establish that the ligands would bind to the appropriate receptor, the activity of all radioligands were tested for binding in cell systems known to exhibit receptors for the ligand. Dispersed cells from guinea pig pancreatic acini were used for the following ligands: with ^{125}I-[Tyr^4]Bn, 8% of the total counts added bound with a nonsaturable binding of <20% of the total counts bound; with ^{125}I-VIP, 26% of the total counts added bound with a nonsaturable binding of <10%; with ^{125}I-BH-SP, 9% of the total counts added bound with a nonsaturable binding of <20% of the total counts bound; with ^{125}I-secretin 20% of the total counts added bound with a nonsaturable binding of <15% of the total counts bound; with ^{125}I-gastrin 4% of the total counts added bound with a nonsaturable binding of <30% of the total counts bound; with ^{125}I-CCK-8, 10% of the total counts added with a nonsaturable binding of <15% of the total counts bound; and with ^{125}I-[Tyr^{11}]somatostatin, 10% of the total counts added bound with a nonsaturable of <20% of the total counts bound. Guinea pig gastric smooth muscle cells were used for the following ligands: with ^{125}I-OH-BZP, 3% of the total counts added bound with a nonsaturable binding of <15% of the total counts bound; with ^{125}I-CGRP, 4% of the total counts added bound with a nonsaturable binding of <15%; and with [^{3}H]etorphine, 1.2% of the total counts added bound with a nonsaturable binding of <25% of the total counts bound. Chief cells from guinea pig stomach were used for [^{3}H]NMS, which bound 5% of the total counts added with a nonspecific binding of <10% of the total counts bound. Tissue sections from rat esophagus were used for ^{125}I-BH-NMB, which bound 2000 cpm/section (50 pM radioligand added) with a nonsaturable binding of <15% of the total counts bound.

Table 1 *Characteristics of human colon cancer cell lines examined*

The primary tumor site, site used for cell culture, and degree of tumor differentiation are shown. All cell lines were adherent except for NCI-H498, NCI-H716, and SNU-C1. Full characterization of each cell line is in Ref. 25.

Cell line	Primary site	Culture site	Tumor differentiation
NCI-H498	Ileocecum	Peritoneum	Mucinous
NCI-H508	Cecum	Abdominal wall	Moderate
NCI-H548	Sigmoid	Colorectal	Well
NCI-H630	Rectum	Liver	Well
NCI-H716	Cecum	Ascites	Poor
NCI-H747	Cecum	Lymph node	Moderate
NCI-H768	Cecum	Colorectal	Moderate
SNU-C1	Descending colon	Peritoneum	Moderate
SNU-C4	Transverse colon	Colorectal	Poor
SNU-C5	Cecum	Colorectal	Poor

The human colon cancer cell lines studied exhibited a nonsaturable binding of <15% in all cases in which binding was significant for all radioligands except pindolol, for which the nonsaturable binding was <30% of the total counts bound.

Intracellular Calcium Mobilization. Intracellular calcium concentrations were measured using the fluorescence indicator fura-2/AM. Cells were loaded with fura-2/AM (Molecular Probes, Inc., Eugene, OR) at 2 μM in a volume containing 3.5 × 10^6 cells/ml. The cells were incubated in the dark for 40 min at 37°C, washed in standard incubation buffer at pH 7.4 three times, and resuspended in standard incubation buffer in the original volume. The fluorescence of fura-2-containing cells was measured with a dual wavelength excitation fluorimeter (Photon Technology International, Inc., So. Brunswick, NJ). The wavelengths were 340 and 380 nm for excitation and 500 nm for emission. $[Ca^{2+}]_i$ was calculated as previously described by Grynkyewicz *et al.* (28), using the formula:

$$[Ca^{2+}]_i = K_d \times (R - R_{min}) \times \frac{S_f}{S_b} / (R_{max} - R)$$

where K_d is the affinity of fura-2 for Ca^{2+}, determined to be 225 nM, $R = F_{340}/F_{380}$ is the ratio of the fluorescence with the two excitation wavelengths, R_{max} is the ratio of F_{340}/F_{380} in a saturated calcium environment after addition of 0.1% Triton, R_{min} is the fluorescence ratio at virtually zero calcium by the addition of 25 mM ethyleneglycol bis(β-aminoethyl ether)-*N,N,N', N'*-tetraacetic acid, S_f is the F_{380} at zero $[Ca^{2+}]_i$ and S_b the F_{380} at saturated $[Ca^{2+}]_i$. All experiments were performed with constant mixing by a magnetic stirrer under the cuvette holder.

IP_3 Determination. Changes in IP_3 (1, 4, 5) were measured using the IP_3 (1, 4, 5) radioreceptor assay system from Amersham, as described previously (29). Cells were incubated at a concentration of 20 × 10^6 cells/ml in 4-(2-hydroxyethyl)-1-piperazineethanesulfonic acid buffer at pH 7.4. Incubations were at 37°C and were terminated by adding

trichloroacetic acid. After centrifugation for 15 min at 1000 × *g*, 0.5 ml of the samples was extracted five times with 2.5 ml of water-saturated diethyl ether and neutralized with $KHCO_3$, and 100 μl of the samples was analyzed in the radioreceptor assay.

DNA Determination. Cellular DNA was determined using the diphenylamine method described by Burton (30). Duplicate samples of cell suspension were assayed for DNA.

Statistical Analysis. Differences were analyzed using Student's *t* test. Differences of $P < 0.05$ were considered significant.

RESULTS

Radiolabeled Ligand-binding Studies. Six of the 10 cell lines exhibited a significant amount of binding of ^{125}I-VIP with a mean value of 67 fmol/μg DNA (range, 19–111 fmol/μg DNA), and six cell lines exhibited a significant amount of binding of [^{3}H]NMS with a mean value of 1332 fmol/μg DNA (range, 314–3443 fmol/μg DNA) (Table 2). Three cell lines exhibited a significant amount of binding of ^{125}I-[Tyr^4]bombesin with a mean value of 126 fmol/μg DNA (range, 17–294 fmol/μg DNA), and three cell lines exhibited a significant amount of binding of ^{125}I-BH-CCK-8 with a mean value of 52 fmol/μg DNA (range, 16–70 fmol/μg DNA). Two cell lines exhibited a significant amount of binding of ^{125}I-OH-BZP with values of 55 and 294 fmol/μg DNA, and two cell lines exhibited a significant amount of binding of ^{125}I-CGRP with values of 4 and 44 fmol/μg DNA. One cell line exhibited a significant amount of binding to ^{125}I-BH-NMB with a value of 3 ± 0.002 fmol/μg DNA (mean ± SEM), one cell line exhibited a significant amount of binding to ^{125}I-[Tyr^{11}]somatostatin with a value of 246 ± 1.5 fmol/μg DNA, one cell line exhibited significant binding to ^{125}I-BH-SP with a value of 22 ± 0.1 fmol/μg DNA, one cell line exhibited significant binding to ^{125}I-gastrin 17–1 with a value of 43 ± 0.2 fmol/μg DNA, and one cell line exhibited significant binding to [^{3}H]etorphine with a value of 6784 ± 115 fmol/μg DNA. None of the 10 cell lines exhibited significant binding to ^{125}I-secretin.

All of the cell lines exhibited binding for at least one of the radioligands studied (Table 2). Cell lines NCI-H630 and SNU-C4 exhibited binding for only one radioligand each, cell lines NCI-H508, NCI-H768, and SNU-C1 exhibited binding for 2 radioligands each, cell lines NCI-H498, NCI-H548, NCI-H747, and SNU-C5 exhibited binding for 3 radioligands each, and NCI-H716 exhibited binding for 7 of the radioligands studied.

To further examine the interaction of [^{3}H]NMS with receptors on these cell lines, we studied the binding characteristics of this radioligand on cell line H-508. At 22°C, binding was maximal by 45 min, remained constant for the next 45 min, and then decreased thereafter (Fig. 1). Increasing the incubation temperature from 22 to 37°C caused a more rapid time course with maximal binding by 10 min and a progressive decrease thereafter, such that, after 120 min of incubation, binding was 50% that at 22°C. At 4°C, binding was maximal at 45 min, at which time it was 50% that of binding at 22°C, and was constant for an additional 75 min. Adding 10 μM NMS reduced binding of [^{3}H]NMS by 88, 93, and 93% of maximal binding at 4, 22, and 37°C, respectively.

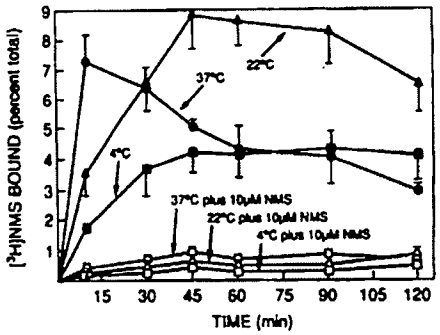

Fig. 1. Time course of binding of [^{3}H]NMS to colon cell line NCI-H508. Cells were incubated with 0.6 nM [^{3}H]NMS for the times indicated at 4, 22, or 37°C alone or with 10 μM NMS. Results are the percentages of the added radioligand bound at the times indicated. *Points*, means from 4 separate experiments; *vertical bars*, SEM.

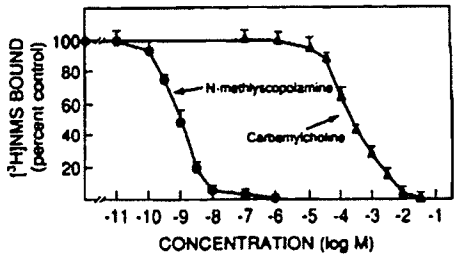

Fig. 2. Ability of NMS and carbamylcholine to inhibit binding of [^{3}H]NMS to colon cell line NCI-H508. Cells were incubated at 22°C for 45 min with 0.6 nM [^{3}H]NMS plus the indicated concentrations of ligands. Binding is expressed as percentage of [^{3}H]NMS that was saturably bound in the absence of ligand. *Points*, means from at least 4 experiments; *vertical bars*, SEM.

The muscarinic cholinergic agonist, carbamylcholine, and the muscarinic cholinergic antagonist, NMS, were tested for their abilities to inhibit binding of [^{3}H]NMS. With NMS, detectable inhibition occurred at a concentration of 100 pM, half-maximal inhibition at 1 nM, and complete inhibition of [^{3}H]NMS binding at 1 μM (Fig. 2). With carbamylcholine, detectable inhibition occurred at 10 μM, half-maximal inhibition at 300 μM, and

Table 2 *Radiolabeled peptides saturably bound to human colon cancer cell lines*

The number of radiolabeled peptides bound to each cell line is shown, as well as the peptide bound and of binding expressed as fmol/μg DNA ± SEM (in parentheses). All binding results in which there was significant ($P < 0.05$) saturable binding detected are listed.

	Radiolabeled peptide saturably bound	
Cell line	No.	Radiolabeled peptide bound (fmol/μg DNA)
NCI-H498	3	^{125}I-[Tyr^4]bombesin (67 ± 1), ^{125}I-BH-CCK-8 (16 ± 1), [^{3}H]NMS (399 ± 3)
NCI-H508	2	^{125}I-VIP(111 ± 2), [^{3}H]NMS (1561 ± 22)
NCI-H548	3	^{125}I-gastrin 17-1 (43 ± 1), ^{125}I-BH-CCK-8 (70 ± 2), [^{3}H]NMS (314 ± 1)
NCI-H630	1	^{125}I-VIP (76 ± 3)
NCI-H716	7	^{125}I-[Tyr^4]bombesin (294 ± 7), ^{125}I-BH-NMB (3.5 ± 0.1), ^{125}I-[Tyr^{11}]somatostatin (246 ± 2) ^{125}I-BH-SP (22 ± 1), ^{125}CGRP (44 ± 1), ^{125}I-BH-CCK-8 (69 ± 1), [^{3}H]NMS (3443 ± 58)
NCI-H747	3	^{125}I-VIP (19 ± 1), ^{125}I-OH-BZP (55 ± 1), [^{3}H]etorphine (6784 ± 115)
NCI-H768	2	^{125}I-OH-BZP (294 ± 16), [^{3}H]NMS (1002 ± 24)
SNU-C1	2	^{125}I-VIP (38 ± 1), [^{3}H]NMS (1270 ± 41)
SNU-C4	1	^{125}I-VIP (99 ± 1)
SNU-C5	3	^{125}I-[Tyr^4]bombesin (17 ± 1), ^{125}I-VIP (61 ± 2), ^{125}I-CGRP (4.4 ± 0.1)

Table 3 *Results of computer analysis of the ability of the muscarinic cholinergic antagonist, N-methylscopolamine, or agonist, carbamylcholine, to inhibit binding of [³H]NMS to the human colon cancer cell line NCI-H508*

Values are means ± SEM of at least 4 experiments. K_d values and number of binding sites were obtained by analysis of the dose-inhibition curves of [³H]NMS binding shown in Fig. 2 using the nonlinear, least-squares curve fitting program, LIGAND (26). The number of binding sites was converted to sites/cell after determining the number of cells/ml of incubation volume. Numbers in parentheses, % of total.

Agent	Affinity		No. of binding sites/cell	
	K_d high	K_d low	High affinity	Low affinity
NMS	0.2 ± 0.04 nM	0.20 ± 0.04 nM	2499 ± 153 (100)	
Carbamylcholine	55.3 ± 6.5 μM	0.33 ± 0.03 nM	1874 ± 178 (75)	625 ± 18 (25)

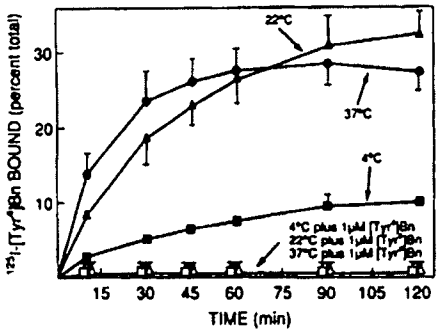

Fig. 3. Time course of binding of ^{125}I-[Tyr^4]bombesin to colon cell line NCI-H716. Cells were incubated with 50 pM ^{125}I-[Tyr^4]bombesin for the times indicated at 4, 22, or 37°C alone or with 1 μM [Tyr^4]bombesin. Results are the percentages of the added radioligand bound at the times indicated. *Points*, means from 5 separate experiments; *vertical bars*, SEM.

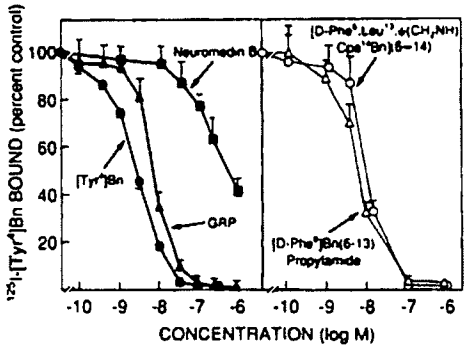

Fig. 4. Abilities of bombesin agonists (*left*) and antagonists (*right*) to inhibit binding of ^{125}I-[Tyr^4]bombesin to colon cell line NCI-H716. Cells were incubated at 22°C for 30 min with 50 pM ^{125}I-[Tyr^4]bombesin plus the indicated concentrations of ligands. Binding is expressed as percentage of ^{125}I-[Tyr^4]bombesin that was saturably bound in the absence of ligand. *Points*, means from at least 4 separate experiments; *vertical bars*, SEM.

Table 4 *Ability of various bombesin-related peptides to inhibit binding of ^{125}I-[Tyr^4]bombesin to human colon cancer cell line NCI-H716*

Values are means ± SEM of at least 4 experiments. K_i values were calculated according to the method of Cheng and Prusoff from the experiments shown in Fig. 4.

Peptide	K_i (nM)
[Tyr⁴]bombesin	2.1 ± 0.1
GRP	6.6 ± 1.3
Neuromedin B	700.0 ± 200.0
[D-Phe⁶]Bn(6-13)propylamide	5.9 ± 0.8
[D-Phe⁶,Leu¹³ψ(CH₂NH),Cpa¹⁴]Bn(6-14)	7.0 ± 0.8

complete inhibition at 30 mM (Fig. 2). Computer analysis of the broad dose-inhibition curve of [³H]NMS binding by carbamylcholine was best fit with a model having 2 classes of binding sites. Computer analysis demonstrated 2499 ± 153 binding sites/cell (mean ± SEM, n = 6) of which 75% had a high affinity for carbamylcholine (K_d 55 ± 7 μM) and 25% had a low affinity (K_d 0.33 ± 0.03 mM) (Table 3). The computer analysis of the dose-inhibition curve of [³H]NMS binding by NMS was best fit by a model having a single class of binding sites, demonstrating that the antagonist could not distinguish between the muscarinic cholinergic receptors having high and low affinities for the agonists. The analysis demonstrated 2499 ± 153 binding sites/cell (n = 6) having a K_d of 0.20 ± 0.04 nM (Table 3).

To examine the interaction of ^{125}I-[Tyr^4]bombesin on these human colon cancer cells, we studied the binding characteristics of this radioligand on cell line NCI-H716 (Fig. 3). [Tyr^4] bombesin, an analogue, has previously been shown (18) to be a high-affinity radioligand useful for identifying receptors that interact with bombesin and structurally related peptides. At 22°C, there was a steady increase in binding such that maximal binding occurred at 90 min. Increasing the incubation temperature to 37°C caused a more rapid time course with a leveling off of binding at 45 min for the next 75 min, such that the amount of binding at 120 min was 85% that at 22°C. Decreasing the incubation temperature to 4°C caused a decrease in binding such that maximal binding was not reached until 120 min, at which time it was 30% that at 22°C. Adding 1 μM [Tyr^4] bombesin to the incubation reduced binding of ^{125}I-[Tyr^4]bombesin by >95% at all temperatures (Fig. 3).

To characterize the subtype of bombesin receptor present, various bombesin receptor agonists and antagonists were tested for their abilities to inhibit binding of ^{125}I-[Tyr^4]bombesin. Of the agonists tested, [Tyr^4]bombesin was the most potent (Fig. 4). Detectable inhibition of ^{125}I-[Tyr^4]bombesin binding occurred with 0.1 nM [Tyr^4]bombesin, half-maximal inhibition with 3 nM, and complete inhibition with 100 nM (Fig. 4). Computer analysis of the dose-inhibition curve of ^{125}I-[Tyr^4] bombesin binding by [Tyr^4]bombesin was best fit by a model having a single class of binding sites. The analysis demonstrated 3312 ± 301 binding sites/cell (n = 3) of hign affinity (K_d 2.1 nM). For inhibiting binding of ^{125}I-[Tyr^4]bombesin, [Tyr^4]bombesin was 3-fold more potent than GRP (K_i 6.6 ± 1.3 nM, n = 3; Table 4) and 300-fold more potent than NMB (K_i 700 ± 200 nM, n = 3; Table 4). Of the two recently described (23) bombesin receptor antagonists tested, [D-Phe^6]Bn(6–13)propylamide was the more potent, having a K_i of 5.9 ± 0.8 nM, which is only 3-fold less potent than [Tyr^4]bombesin in inhibiting the binding of ^{125}I-[Tyr^4]bombesin. [D-Phe^6,Leu^{13}, ψ(CH$_2$NH)Cpa^{14}]Bn(6–14) was also potent, having a K_i of 7.0 ± 0.8 nM (n = 3; Fig. 5, Table 4), which is 3.3-fold less potent than [Tyr^4]bombesin (Table 4).

To examine the interaction of ^{125}I-VIP on these human colon cancer cell lines, we studied the binding characteristics of this radioligand on cell line SNU-C4. At 37°C, there was a steady increase of binding, reaching a plateau at 45 min, remaining stable for an additional 45 min, and then decreasing (Fig. 5). Decreasing the incubation temperature to 22°C slowed the time course such that a plateau was reached at 60 min, at which point binding was 96% that at 37°C. Decreasing the incubation temperature to 4°C caused a decrease in the rate of binding

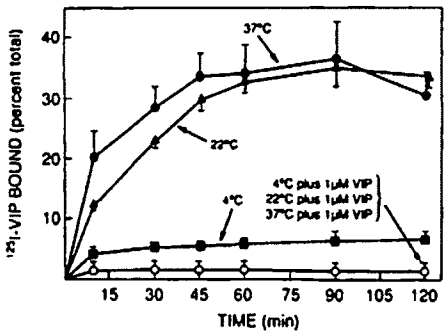

Fig. 5. Time course of binding of ^{125}I-VIP to colon cell line SNU-C4. Cells were incubated with 50 pM ^{125}I-VIP for the times indicated at 4, 22, or 37°C alone or with 1 μM VIP. Results are percentages of the added radioligand bound at the times indicated. *Points*, means from 5 separate experiments; *vertical bars*, SEM.

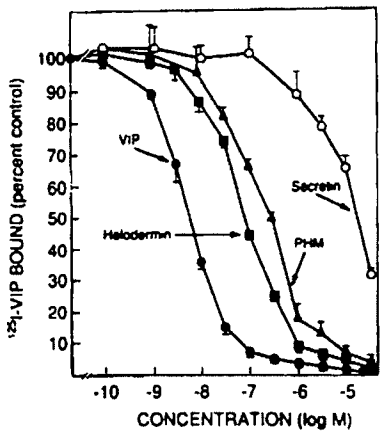

Fig. 6. Abilities of various VIP receptor agonists to inhibit binding of ^{125}I-VIP to colon cell line SNU-C4. Cells were incubated at 22°C for 45 min with 50 pM ^{125}I-VIP plus the indicated concentrations of agonists. Binding is expressed as percentage of ^{125}I-VIP that was saturably bound in the absence of unlabeled agonist. *Points*, means from at least 5 experiments; *vertical bars*, SEM.

Table 5 *Ability of VIP-secretin-related peptides to interact with VIP receptors on colon cancer cell line SNU-C4*

Values are means ± SEM of at least 5 experiments. IC_{50} is the concentration of agonist required to inhibit saturable binding of ^{125}I-VIP by 50%. Values were calculated from the experiments shown in Fig. 6 by the method of Cheng and Prusoff (27).

Agent	Binding of ^{125}I-VIP IC_{50} (nM)
VIP	5.4 ± 1.0
Helodermin	20.2 ± 0.8
Peptide histidine methionine	139 ± 7
Secretin	2121 ± 82

such that the amount of binding at 120 min was only 17% that at 37°C. Adding 1 μM VIP to the incubation reduced binding of ^{125}I-VIP by 97, 96, and 80% at 37, 22, and 4°C, respectively (Fig. 5).88

To characterize the ^{125}I-VIP binding sites further, various VIP-related peptides were tested for their abilities to inhibit binding of ^{125}I-VIP (Fig. 6). VIP was the most potent with detectable inhibition at 1 nM, half-maximal inhibition at 6 nM, and complete inhibition at 30 μM. Computer analysis of this broadly based dose-inhibition curve of ^{125}I-VIP binding by VIP was best fit with a model having 2 classes of binding sites. The analysis demonstrated 5.5×10^6 binding sites/cell ($n = 6$) of which 20,000 ± 4,200 binding sites/cell ($n = 6$) had a high affinity for VIP (K_d 3.6 nM) and the remainder had a low affinity for VIP (K_d 1.7 μM). Helodermin caused a detectable inhibition of ^{125}I-VIP binding at 3 nM (Fig. 6, Table 5) and was 4-fold less potent than VIP (IC_{50}, 20.2 nM, Table 5), peptide histidine methionine was 25-fold less potent than VIP with an IC_{50} of 139 nM and secretin as 400-fold less potent than VIP with an IC_{50} of 2121 nM (Table 5).

Studies of Changes in Cytosolic Calcium Concentration. Immunoreactive bombesin-like peptides, as well as other gastrointestinal peptides and neurotransmitters, have been localized to intestinal epithelial cells as well as other gastrointestinal tissues (31–40). Binding of a number of these agents such as bombesin, CCK-8, or muscarinic cholinergic agents to their specific receptors has been shown to alter intracellular calcium (7, 33, 35). To examine whether occupation of these various receptors on human colon carcinoma cell lines resulted in similar biological activity, we studied the ability of [Tyr^4]bombesin or carbamylcholine to alter intracellular calcium in the human cancer cell line, NCI-H716. [Tyr^4]bombesin caused a rapid transient increase in $[Ca^{2+}]_i$ (Fig. 7). The increase was detectable at 0.1 nM with a 12 ± 3% ($n = 6$) increase of $[Ca^{2+}]_i$ above baseline (Fig. 8). Maximal $[Ca^{2+}]_i$ mobilization was detected with 1 μM [Tyr^4] bombesin, giving a 266 ± 15% ($n = 6$) increase above baseline, and half-maximal stimulation was detected at 20 nM (Fig. 8). Receptors for muscarinic cholinergic agents were also found on

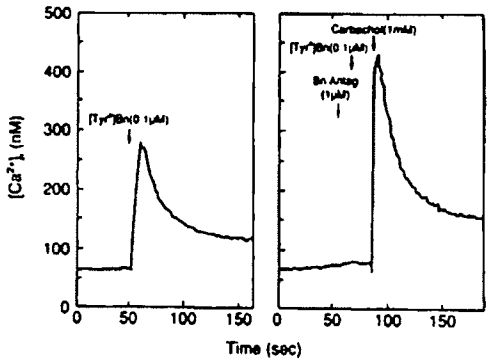

Fig. 7. Ability of the bombesin and muscarinic cholinergic receptor agonists or antagonists to alter intracellular calcium in NCI-H716 human colon cancer cells. NCI-H716 cells were loaded with 2 μM fura-2/AM, washed, and resuspended in standard incubation buffer. [Tyr^4]bombesin (0.1 μM) was either added alone (*left*) or 10 s after the bombesin antagonist [D-Phe^6]Bn(6–13)methyl ester (*right*). Carbachol (1 mM) was added 10 s after the [Tyr^4]bombesin (*right*). This experiment is representative of 4 others.

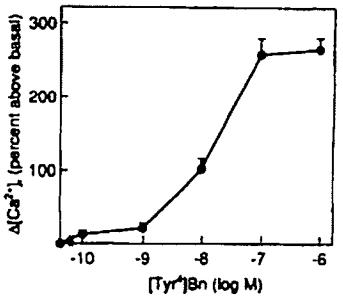

Fig. 8. Dose-response effect of [Tyr^4]bombesin on the intracellular calcium concentration in NCI-H716 cells. Results are expressed as the percentages of increase. In these experiments, the basal calcium concentration was 67 ± 8 and increased to 248 ± 34 with 1 μM [Tyr^4]bombesin (mean ± 1 SEM). Colon cells were loaded with 2 μM fura-2/AM, washed, and resuspended in standard incubation buffer. *Points*, means from at least 4 separate experiments; *vertical bars*, SEM.

NCI-H716 cells, and carbachol was therefore studied to determine whether occupation of the cholinergic receptor altered $[Ca^{2+}]_i$. At a concentration of 1 mM carbamylcholine, there was a rapid transient increase in $[Ca^{2+}]_i$ of 279 ± 22% ($n = 6$) above baseline (Fig. 7).

To establish that [Tyr⁴]bombesin was in fact mediating its effects on intracellular calcium by interacting with bombesin receptors, we tested the ability of the specific bombesin receptor antagonist, [D-Phe⁶]bombesin(6–13)methyl ester (24) to inhibit the action of bombesin (Fig. 7). When 0.1 μM [Tyr⁴]bombesin was added to NCI-H716 cells, the $[Ca^{2+}]_i$ increased by 259 ± 21% ($n = 6$) above baseline (Figs. 7 and 8). The addition of the specific bombesin receptor antagonist, [D-Phe⁶]Bn(6–13)methyl ester, caused no increase in $[Ca^{2+}]_i$ but totally blocked the increase in cytosolic calcium caused by 0.1 μM [Tyr⁴]bombesin added immediately after the antagonist (Fig. 7). The inhibitory action of the antagonist was specific for the bombesin receptor because the antagonist did not effect the increase in cytosolic calcium caused by carbamylcholine (Fig. 7).

To determine whether a cell line without detectible bombesin or muscarinic cholinergic receptors responded to these agents, we examined cell line SNU-C4 which does not exhibit receptors for either bombesin or muscarinic cholinergic agents. There was no increase in $[Ca^{2+}]_i$ detected in this cell line with 1 μM [Tyr⁴]bombesin or 1 mM carbamylcholine (data not shown).

Cellular Inositol Triphosphate Studies. Bombesin and muscarinic cholinergic agents have been reported to activate phospholipase C, cause the breakdown of phospholipids, and increase phosphoinositides in intestinal epithelial and other cells (7, 10, 11). To determine whether receptor occupation by these agents had a similar effect on human colon cancer cell lines, we studied the ability of the bombesin receptor agonist, [Tyr⁴]bombesin, or the muscarinic cholinergic receptor agonist, carbamylcholine, to increase IP_3(1, 4, 5), the biologically active IP_3 isomer which alters cellular calcium. Also, to assess whether the presence of receptors for these agents correlated with the ability to alter IP_3(1, 4, 5), colon cell lines with and without detected receptors for these agents were tested. [Tyr⁴]bombesin (1 μM) in NCI-H716 cells, which possess bombesin receptors, caused a 4-fold increase above baseline in IP_3(1, 4, 5) within 5 s (Table 6). Carbamylcholine (1 mM) in NCI-H716 cells, which also have receptors for muscarinic cholinergic agents, also caused a 4-fold increase in IP_3(1, 4, 5) within 5 s (Table 6). The human colon cell line, NCI-H508, which has receptors for muscarinic cholinergic agents but not for bombesin, responded to 1 mM carbamylcholine with a 2-fold increase in IP_3(1, 4, 5) within 5 s but did not respond to 1 μM [Tyr⁴]bombesin (Table 6). SNU-C4 cells, which do not have receptors for muscarinic cholinergic agents or for bombesin, did not respond to these agents with an increase in IP_3(1, 4, 5) (Table 6).

Table 6 Ability of the muscarinic cholinergic receptor agonist, carbamylcholine, or the bombesin receptor agonist, [Tyr⁴]bombesin, to stimulate the generation of IP_3 (1,4,5) in human colon cancer cell lines

Concentrations of IP_3 (1,4,5) for three cell lines are shown in the absence of added peptide and after stimulation by 1 μM [Tyr⁴]bombesin or by 1 mM carbamylcholine for 5 s. Values are means ± SEM of at least 5 experiments.

	IP_3 (1,4,5) (pmol/μg DNA)		
Cell line	No addition	[Tyr⁴]bombesin (1 μM)	Carbamylcholine (1 mM)
NCI-H716	1.1 ± 0.2	4.4 ± 0.8*	4.5 ± 1.1*
NCI-H508	1.3 ± 0.2	1.4 ± 0.2	2.4 ± 0.4*
SNU-C4	1.0 ± 0.2	1.2 ± 0.3	1.0 ± 0.1

* Significantly different from corresponding value with no addition ($P < 0.05$).

DISCUSSION

The present results demonstrate that human colon cancer cell lines frequently possess functional receptors for a number of gastrointestinal hormones or neurotransmitters. Prior studies (8–11) of the presence of these receptors on human colon cell lines or colon cancers were limited in a number of ways. Frequently, only one receptor on an individual human colon cancer cell line or cancer tissue was studied, making it difficult to determine whether the presence of these receptors was a common or an uncommon finding. The effect of receptor occupation by agonists on cell function was not always examined, and there was often no attempt to correlate the presence or absence of receptors with an effect on cell function. With the recent availability of a number of well-characterized human colon cancer cell lines, it has become possible to systematically address each of these points. Ten well-characterized human colon cell lines were examined for the presence of functional receptors for gastrointestinal peptides or neurotransmitters.

Each of the 10 cell lines tested exhibited binding sites for at least one ligand, and the only ligand that did not exhibit a binding site on any of the cell lines was radiolabeled secretin. The binding of the 12 radiolabeled ligands tested on the 10 colon cancer cell lines could, theoretically, reveal a maximum of 120 receptors if all of the cell lines bound all of the ligands. A total of 27 receptors of a possible 120 (23%) were exhibited, demonstrating that the presence of receptors for gastrointestinal hormones and neurotransmitters on human colon cancer cell lines is not an uncommon occurrence.

The binding characteristics of [³H]NMS support the presence of a specific receptor for muscarinic cholinergic agents which is similar to muscarinic cholinergic receptors previously described on intestinal epithelium (35, 36, 40). Although there are at least 5 different muscarinic cholinergic receptor subtypes, in the present study we did not attempt to distinguish these subtypes. The binding of [³H]NMS was temperature dependent, saturable, and specific. Similar to these other gastrointestinal tissues (33, 34), computer analysis of the binding revealed 2 classes of binding sites which interacted with different affinities with the muscarinic, cholinergic agonist, carbamylcholine, and with the same high affinity with the muscarinic cholinergic antagonist, *N*-methylscopolamine, or quinuclidinyl benzilate (40). Seventy-five % of these sites had a high affinity for carbachol (K_d 55 μM), and 25% had a low affinity for the agonist (K_d 0.3 mM). These characteristics are very similar to those reported for the muscarinic cholinergic receptor found in a highly enriched preparation of chief cells prepared from guinea pig stomach (34). The muscarinic cholinergic chief cell receptor also exhibits 2 classes of binding sites, 73% with a high affinity (K_d 53 μM) and 27% with a low affinity (K_d 4.6 mM) for carbachol. Further evidence supporting the conclusion that the binding was to a muscarinic cholinergic receptor on human colon cell lines was the ability of the muscarinic cholinergic receptor agonists to elicit biological response. Carbachol only stimulated a change in cytosolic calcium or inositol trisphosphates in those cells in which the muscarinic cholinergic receptor was identified by binding studies.

The binding results with ^{125}I-[Tyr⁴]bombesin support the conclusion that it is binding to a bombesin receptor in that the binding was time and temperature dependent, saturable, and specific. Interaction was with a single class of high-affinity binding sites (K_d 2.1 nM), exhibiting 3312 binding sites/cell. Although the bombesin receptor has not been previously de-

scribed on human gastrointestinal colon cancer cell lines, it has been extensively studied in a number of other tumor cell systems (6, 7, 41, 42). Similar to the bombesin receptor here, the receptor described on various tumor cell lines, such as on small cell lung cancer and prostatic adenocarcinoma, has a high affinity for bombesin (K_d 1.1 nM) with 6444 binding sites/cell and 2 nM, respectively, and is similar to that in normal tissue such as the mouse fibroblast 3T3 cells which has an affinity of 0.5 nM or in dispersed acini from normal guinea pig pancreas of 4.4 nM with 5400 binding sites/cell (7, 18, 41, 42). Further evidence of the presence of the bombesin receptor was shown by the ability of 2 newly described bombesin antagonists (23, 24), having a high affinity and specificity, to inhibit the binding of ^{125}I-[Tyr^4]bombesin. In recent studies (19, 43), two subtypes of bombesin receptors have been described. One has a high affinity for the mammalian bombesin-related peptide GRP and low affinity for NMB, and the other has a high affinity for NMB and lower affinity for GRP. These bombesin receptor antagonists have a high affinity only for the GRP-preferring subtype (43), demonstrating that the bombesin receptors identified on human colon cancer cells are of this subtype and similar to those identified on 3T3 cells, the pancreatic tumor cell line AR42J, and normal pancreatic acinar cells, as well as some areas of the central nervous system (43–45). The ability of bombesin to cause an increase of cytosolic calcium and inositol phosphates in human colon cancer cells exhibiting binding of ^{125}I-[Tyr^4]bombesin was additional evidence of the presence of a specific bombesin receptor which was functional. That the bombesin binding site identified represented the receptors mediating biological activity was suggested by the result that there was a close correlation between the ability of bombesin to occupy the bombesin receptor and inhibit binding of ^{125}I-[Tyr^4]bombesin and to increase intracellular calcium. In addition, the fact that bombesin was altering biological activity through the bombesin receptor was demonstrated, in that the increase of cytosolic calcium was blocked by specific bombesin receptor antagonists which did not effect a subsequent response elicited by carbachol.

The binding sites identified using ^{125}I-VIP suggest that they represent an interaction with a VIP receptor in that it is saturable, specific, and time and temperature dependent. Furthermore, there are 2 classes of VIP-binding sites, one having a high affinity for VIP (K_d 3.6 nM) and the other having a low affinity for VIP (K_d 1.7 μM). The binding characteristics of this receptor are very similar to those described in a number of other tissues such as dispersed pancreatic acini from guinea pig pancreas which exhibits 2 classes of binding sites, 90% having a low affinity (K_d 0.5 μM) and 10% having a high affinity (K_d 1.1 nM) for VIP (46). Receptors for VIP have also been described on human colon and human gastric cancer cell lines (9, 47). In both of these cases, as well as in a human intestinal cell line (38), the receptor was of high affinity (K_d 0.12 nM in colon, 2.5 nM in gastric, and 0.13 nM in intestine), but only one binding site was exhibited. This difference raises the possibility that the VIP receptors previously described on human colon cancers (9), which exhibit only a single site, are in fact different from the VIP receptors described here that exhibit 2 sites, but it is more likely that these differences are due to methodological differences. The low-affinity VIP-binding site would not have been demonstrated if a nonsaturable concentration of 0.01–1 μM VIP was used as in the previous studies (9, 38, 47), as opposed to a nonsaturable concentration of 10 μM VIP as was used in these experiments and in the study of pancreatic acini, which demonstrated a 2-site model (46). The biological activity of the VIP receptor on these cell lines has not yet been studied. However, previous reports have described the presence of functional VIP receptors on the human colon cancer cell line, HT-29, that exhibits an increase in cAMP in response to VIP (9, 12).

Because of the limited availability of gastrointestinal tumor cell lines of human origin, only occasional reports of the presence of receptors for gastrointestinal peptides on human tumor cell lines have been published (8–11, 47–50). Human colon cancer cell lines have been reported to exhibit high-affinity receptors for VIP demonstrated by radioligand binding and a cAMP response on the human colon cell line HT-29 (9, 12). In addition, receptors for muscarinic cholinergic agents were demonstrated by radioligand binding and inositol phosphate turnover on the human colon cell line HT-29 (10, 11), and receptors for gastrin were demonstrated by radioligand binding on the human colon cell line LoVo (8). Human gastric cancer cell lines have been reported to exhibit receptors for muscarinic cholinergic agents, demonstrated by radioligand binding on 2 of 4 newly established cell lines (47), receptors for VIP, demonstrated by radioligand binding, and a cAMP response on the cell line HGT-1 (50) and 4 of 4 newly established cell lines (47), receptors for gastrin demonstrated by radioligand binding on several cell lines (51), and receptors for histamine H_2-receptor agonists, gastric inhibitory peptide and glucagon by a cAMP response on cell line HGT-1 (52, 53). Human pancreatic cancer cell lines have been reported to exhibit receptors for VIP by radioligand binding and a cAMP response on cell line capan-1 (54) and receptors for muscarinic cholinergic agents by radioligand binding and inositol phosphate formation (55). Of the receptors studied, only those for VIP, gastrin, and muscarinic cholinergic agents have been previously described on human colon cancer cell lines. The present study is the first to demonstrate the presence of receptors for bombesin, CGRP, NMB, somatostatin, substance P, β-adrenergic agents, and opiates on human colon cancer cell lines.

During the past several years, much attention has been given to the role of gastrin in promoting the growth of human colon and gastric cancer (8, 13–15). Gastrin has been reported to increase the growth of various human colon cancers or gastric cancers implanted into nude mice and the gastrin/cholecystokinin receptor antagonist, proglumide, to inhibit the growth (15, 16, 56). Gastrin receptor content of colonic neoplasms has been reported to have prognostic significance (57). In other studies, gastrin receptors have been identified by radioligand binding on some human colon and gastric cancer cell lines (8, 51). Although a number of the reports demonstrated the presence of these receptors on only one or 2 cell lines (13, 56), at least 2 reports demonstrated gastrin receptors on 4 or 5 cell lines (14, 51). In our study, gastrin receptors occurred on only 10% of the human cancer cell lines, suggesting that they occur relatively infrequently. These results are in agreement with reports describing gastrin receptors on a small number of tumors (13, 15, 56) but are at variance with reports describing gastrin receptors on a number of human colon cancer cell lines (14, 51). Several explanations could account for this difference. It is possible that receptors were present but not detected because of the methodology, loss of receptors during cell preparation for binding studies such as due to cell lysis and loss of membranes, or the conditions were not optimal for binding. These possibilities seem unlikely because cell integrity was assessed by trypan blue exclusion, cells were rapidly processed,

and the ligands bound well to control cells using similar conditions. In both previous reports, as well as the present study (14, 51), the human colon cancer cell lines were maintained in media containing 5–10% fetal bovine serum; however, different media with different supplementation were used in the different studies, and this possibly may have an effect on the number of receptors present on the cell surface at any given time. We studied 7 cell lines which originated in the United States and 3 which originated in Korea, while Weinstock and Baldwin (51) studied human colon cancer cell lines originating in Japan and Australia, and Watson *et al.* (14) studied cell lines originating in the United Kingdom as well as other origins. Thus, it is possible that the human colon cancer cell lines derived from tumors in different geographic locations have different biological characteristics. Another possibility could be the length of time that the cell lines have remained in culture. In the report by Watson *et al.* (14), 4 freshly disaggregated human adenocarcinomas responded to gastrin, 2 newly established colon cancer cell lines responded to gastrin at passage 2 but not passage 6, and 8 established colon cancer cell lines did not respond to gastrin, but 1 of these lines responded to gastrin during synchronization of the cell cycle. The established cell lines in the report by Watson *et al.* (14) were passaged >500 times, a substantially high number of passages. This latter study suggests that the ability of some colon tumor cell lines to respond to a peptide and perhaps the presence of its receptor is a dynamic process that may change during the course of the cell line. This raises the possibility that the percentage of human colon cancer cell lines demonstrating gastrin receptors in this study may actually be an underestimate of the presence of gastrin receptors in the original human colon cancer tissue from which the tumor cell line was derived. A recent study of surgical specimens from 67 patients with primary colon cancer supports this possibility (57). In this study (57), 57% of the specimens examined were reported to possess gastrin receptors. Of further interest is the number and variety of receptors for gastrointestinal hormones or neurotransmitters demonstrated on the human colon cancer cell lines, compared to those previously reported on the human gastric cancer cell lines, using the same ligands as in the present study (47). A greater number of receptors for hormones and neurotransmitters were exhibited on human colon cancer cell lines, *i.e.*, 11 of the 12 (92%) different receptors sought were present on at least one colon cell line, compared to only 2 of 9 (22%) receptors found on human gastric cancer cell lines. At present, the basis for this difference is unclear, as is the possibility that gastrointestinal hormones may have a greater effect on colon cancer cell growth.

As mentioned earlier, one of the prime interests in establishing the presence of receptors for gastrointestinal peptides or neurotransmitters on gastrointestinal tumor cell lines is to determine whether they exhibit biological activity and to establish whether alteration of intracellular mediators has a mitogenic effect on cell differentiation. This has been shown to be the case for the gastrointestinal peptide, bombesin, which interacts with high-affinity receptors on small cell lung carcinoma (7, 58). Many of the classic small cell lung carcinoma cell lines exhibit receptors for bombesin, and bombesin has been shown to modulate an autocrine growth effect which can be inhibited by bombesin receptor antagonists or by bombesin antibodies (6, 7, 59, 60). The present study demonstrates that bombesin receptors and muscarinic cholinergic receptors on the human colon cancer cell lines could alter intracellular mediators in the tumor cells. This suggests that occupation of the GRP-preferring bombesin receptors or muscarinic cholinergic receptors by agonists causes a similar cascade of changes in intracellular mediators in human colon cancer cell lines as that reported in other neoplastic as well as normal tissues (7, 33). Previous studies have demonstrated that bombesin as well as muscarinic cholinergic agents activates phospholipase C and causes the breakdown of polyphosphoinositides and mobilization of cytosolic calcium (7, 33, 55). Agonists for each of these receptors increased the biologically active inositol trisphosphate, IP_3(1, 4, 5), and caused increases in cytosolic calcium. Previous studies have demonstrated that occupation of VIP receptors on some human colon cell lines can activate adenylate cyclase and increase cellular cyclic AMP (50); however, this was not determined in the present study. It is not established whether occupation of these receptors in the present human colon cancer cell lines will alter growth or differentiation.

In conclusion, we demonstrated the presence of several different receptors for gastrointestinal peptides or neurotransmitters on human colon cancer cell lines including receptors for bombesin, neuromedin B, VIP, somatostatin, substance P, β-adrenergic agents, CGRP, gastrin, CCK, muscarinic cholinergic agents, and opiates. Occupation of these receptors altered intracellular mediators. The binding characteristics of these receptors are very similar to receptors described on normal physiological tissues in their affinities, specificities, and response to agonists and antagonists. The results provide a basis to examine the effect of occupation of these receptors by agonists or antagonists in cell growth or differentiation.

REFERENCES

1. Selected cancer sites. *In:* Cancer Facts and Figures, pp. 9–15. New York: American Cancer Society, 1990.
2. Boland, C. R., Itzkowitz, S. H., and Kim, Y. S. Colonic polyps and the gastrointestinal polyposis syndromes. *In:* M. H. Sleisenger and J. A. Fordran (eds.), Gastrointestinal Disease—Pathophysiology, Diagnosis, Management, Ed. 4, pp. 1483–1518. Philadelphia: W. B. Saunders, 1989.
3. Cohen, A. M., Shank, B., and Friedman, M. A. Colorectal cancer. *In:* V. T. DeVita, Jr., S. Hellman, and S. A. Rosenberg (eds.), Cancer—Principles and Practice of Oncology, Ed. 3, pp. 895–964. Philadelphia: J. B. Lippincott, 1989.
4. Lippman, M. E., Dickson, R. B., Bates, S., Knabbe, C., Huff, K., Swain, S., McManaway, M., Bronzert, D., Kasid, A., and Gelmann, E. P. Autocrine and paracrine growth regulation of human breast cancer. Breast Cancer Res. Treat., *7:* 59–70, 1986.
5. Prostate cancer and hormone receptors. *In:* P. Ekman and A. A. Snochowski (eds.), Progress in Clinical and Biological Research, Vol. 23. New York: Alan R. Liss, Inc., 1979.
6. Moody, T. W., Carney, D. N., Cuttitta, F., Quattrocchi, K., and Minna, J. D. High affinity receptors for bombesin/GRP-like peptides on human small cell lung cancer. Life Sci., *37:* 105–113, 1985.
7. Trepel, J. B., Moyer, J. D., Cuttitta, F., Frucht, H., Coy, D. H., Natale, R. B., Mulshine, J. L., Jensen, R. T., and Sausville, E. A. A novel bombesin receptor antagonist inhibits autocrine signals in a small cell lung carcinoma cell line. Biochem. Biophys. Res. Commun., *156:* 1383–1389, 1988.
8. Singh, P., Rae-Venter, B., Townsend, C. M., Jr., Khalil, T., and Thompson, J. C. Gastrin receptors in normal and malignant gastrointestinal mucosa: age associated changes. Am. J. Physiol., *249:* G761–G769, 1985.
9. Couvineau, A., Rousset, M., and LaBurthe, M. Molecular identification and structural requirement of vasoactive intestinal peptide (VIP) receptors in the human colon adenocarcinoma cell line, HT-29. Biochem. J., *231:* 139–143, 1985.
10. Kopp, R., Lambrecht, G., Mutschler, E., Moser, U., Tacke, R., and Pfeiffer, A. Human HT-29 colon carcinoma cells contain muscarinic M3 receptors coupled to phosphoinositide metabolism. Eur. J. Pharmacol., *172:* 397–405, 1989.
11. Kopp, R., Mayer, P., and Pfeiffer A. Agonist-induced desensitization of cholinergically stimulated phosphoinositide breakdown is independent of endogenously activated protein kinase C in HT-29 human colon carcinoma cells. Biochem. J., *269:* 73–78, 1990.
12. LaBurthe, M., Rousset, M., Boissard, C., Chevalier, G., Zweibaum, A., and Rosselin, G. Vasoactive intestinal peptide: a potent stimulator of adenosine 3':5'-cyclic monophosphate accumulation in gut carcinoma cell lines in culture. Proc. Natl. Acad. Sci. USA, *75:* 2772–2775, 1978.
13. Sumiyoshi, H., Yasui, W., Ochiai, A., and Tahara, E. Effects of gastrin on

tumor growth and cyclic nucleotide metabolism in xenotransplantable human gastric and colonic carcinomas in nude mice. Cancer Res., *44:* 4276–4280, 1984.
14. Watson, S. A., Durrant, L. G., and Morris, D. L. Growth-promoting action of gastrin on human colonic and gastric tumour cells cultured *in vitro*. Br. J. Surg., *75:* 342–345, 1988.
15. Palmer-Smith, J., and Solomon, T. E. Effects of gastrin, proglumide, and somatostatin on growth of human colon cancer. Gastroenterology, *95:* 1541–1548, 1988.
16. Hoosein, N. M., Kiener, P. A., Curry, R. C., Rovati, L. C., McGilbra, D. K., and Brattain, M. G. Antiproliferative effects of gastrin receptor antagonists and antibodies to gastrin on human colon carcinoma cell lines. Cancer Res., *48:* 7179–7183, 1988.
17. Hoosein, N. M., Kiener, P. A., Curry, R. C., and Brattain, M. G. Evidence for autocrine growth stimulation of cultured colon tumor cells by a gastrin/cholecystokinin-like peptide. Exp. Cell Res., *186:* 15–21, 1990.
18. Jensen, R. T., Moody, T., Pert, C., Rivier, J. E., and Gardner, J. D. Interaction of bombesin and litorin with specific membrane receptors on pancreatic acinar cells. Proc. Natl. Acad. Sci. USA, *75:* 6139–6143, 1978.
19. Von Schrenck, T., Heinz-Erian, P., Moran, T., Mantey, S. A., Gardner, J. D., and Jensen, R. T. Neuromedin B receptor in esophagus: evidence for subtypes of bombesin receptors. Am. J. Physiol., G747–G758, 1989.
20. Jensen, R. T., Charlton C. G., Adachi, H., Jones, S. W., O'Donohue, T. L., and Gardner, J. D. Use of ^{125}I-secretin to identify and characterize high-affinity secretin receptors on pancreatic acini. Am. J. Physiol., G186–G195, 1983.
21. Zhou, Z. C., Villanueva, M. L., Noguchi, M., Jones, S. W., Gardner, J. D., and Jensen, R. T. Mechanism of action of calcitonin gene-related peptide in stimulating pancreatic enzyme secretion. Am. J. Physiol., *251:* G391–G397, 1986.
22. Coy, D. H., Heinz-Erian, P., Jiang, N. Y., Sasaki, Y., Taylor, J., Moreau, J. P., Wolfrey, W. T., Gardner, J. D., and Jensen, R. T. Probing peptide backbone function in bombesin. J. Biol. Chem., *263:* 5056–5060, 1988.
23. Wang, L. H., Coy, D. H., Taylor, J. E., Jiang, N. Y., Kim, S. H., Moreau, J. P., Huang, S. C., Mantey, S. A., Frucht, H., and Jensen, R. T. Desmethionine alkylamide bombesin analogues: a new class of bombesin receptor antagonists with potent antisecretory activity in pancreatic acini and antimitotic activity in Swiss 3T3 cells. Biochemistry, *29:* 616–622, 1990.
24. Wang, L. H., Coy, D. H., Taylor, J. E., Jiang, N. Y., Moreau, J. P., Huang, S. C., Frucht, H., Haffar, B. M., and Jensen, R. T. Des-met carboxyl-terminally modified analogues of bombesin function as potent bombesin receptor antagonists, partial agonists, or agonists. J. Biol. Chem., *265:* 15695–15703, 1990.
25. Park, J. G., Herbert, K. O., Sugarbaker, P. H., Henslee, J. G., Chen, T. R., Johnson, B. E., and Gazdar, A. Characteristics of cell lines established from human colorectal carcinoma. Cancer Res., *47:* 6710–6718, 1987.
26. Munson, P. J., and Rodbard, D. A versatile computerized approach for characterization of ligand-binding systems. Anal. Biochem., *107:* 220–239, 1980.
27. Cheng, Y. C., and Prusoff, W. H. Relationship between the inhibition constant (K_i) and the concentration of inhibitor which causes 50 per cent inhibition (I_{50}) of an enzymatic reaction. Biochem. Pharmacol., *22:* 3099–3108, 1973.
28. Grynkiewicz, G., Poenie, M., and Tsien, R. Y. A new generation of Ca^{2+} indicators with greatly improved flurescence properties. J. Biol. Chem., *260:* 3440–3450, 1985.
29. Rowley, W. H., Sato, S., Huang, S. C., Collado-Escobar, D. M., Beaven, M. A., Wang, L. H., Martinez, J., Gardner, J. D., and Jensen, R. T. Cholecystokinin-induced formation of inositol phosphates in pancreatic acini. Am. J. Physiol., G655–G665, 1990.
30. Burton, K. Determination of DNA concentration with diphenylamine. Methods Enzymol., *12:* 163–166, 1968.
31. Polak, J. M., Bloom, S. R., Hobbs, S., Solcia, E., and Pearse, A. G. E. Distribution of a bombesin-like peptide in human gastrointestinal tract. Lancet, 1109–1110, 1976.
32. Ferri, G-L., Adrian, T. E., Ghatei, M. A., O'Shaughnessy, D. J., Probert, L., Lee, Y. C., Buchan, A. M. J., Polak, J. M., and Bloom, S. R. Tissue localization and relative distribution of regulatory peptides in separated layers from the human bowel. Gastroenterology, *84:* 777–786, 1983.
33. Gardner, J. D., and Jensen, R. T. Secretagogue receptors on pancreatic acinar cells. *In:* L. R. Johnson (ed.), Physiology of the GI Tract, Ed. 2, pp. 1109–1127. New York: Raven Press, 1987.
34. Sutliff, V. E., Rattan, S., Gardner, J. D., and Jensen, R. T. Characterization of cholinergic receptors mediating pepsinogen secretion from chief cells. Am. J. Physiol., G226–G234, 1989.
35. Yada, T., Oiki, S., Ueda, S., and Okada, Y. Intestinal secretagogues increase cytosolic free Ca^{2+} concentration and K^+ conductance in a human intestinal epithelial cell line. J. Membr. Biol. *112:* 159–167, 1989.
36. Lepor, H., Rigaud, G., Shapiro, E., Baumann, M., Kodner, I. J., and Fleshman, J. W. Muscarinic cholinergic and alpha 2-adrenergic receptors in the epithelium and muscularis of the human ileum. Surgery (St. Louis), *107:* 461–467, 1990.
37. Rouyer-Fessard, C., Augeron, C., Grasset, E., Maorett, J. J., Laboisse, C. L., and Laburthe, M. VIP receptors and control of short circuit current in the human intestinal clonal cell line C1. 19A. Experientia (Basel), *45:* 1102–1105, 1989.
38. Laburthe, M., Augeron, C., Rouyer-Fessard, C., Roumagnac, I., Maorett, J. J., Grasset, E., and Laboisse, C. Functional VIP receptors in the mucus-secreting colonic epithelial cell line Cl. 16E. Am. J. Physiol *256:* G443–450, 1989.
39. Couvineau, A., and Laburthe, M. The human vasoactive intestinal peptide receptor: molecular identification by covalent cross-linking in colonic epithelium. J. Clin. Endocrinol. Metab., *61:* 50–55, 1985.
40. Rimele, T. J., O'Dorisio, M. S., and Gaginella, T. S. Evidence for muscarinic receptors on rat colonic epithelial cells: binding of [^{3}H]quinuclidinyl benzilate. J. Pharmacol. Ther., *218:* 426–434, 1981.
41. Bologna, M., Festuccia, C., Muzi, P., Biordi, L., and Ciomei, M. Bombesin stimulates growth of human prostatic cancer cells *in vitro*. Cancer (Phila.), *63:* 1714–1720, 1989.
42. Zachary, I., and Rozengurt, E. High-affinity receptors for peptides of the bombesin family in Swiss 3T3 cells. Proc. Natl. Acad. Sci. USA, *82:* 7616–7620, 1985.
43. Von Schrenck, T., Wang, L-H., Coy, D. H., Villanueva, M. L., Mantey, S., and Jensen, R. T. Potent bombesin receptor antagonists distinguish receptor subtypes. Am. J. Physiol., *259:* G468–G473, 1990.
44. Moody, T. W., Pert, C. B., Rivier, J., and Brown, M. R. Bombesin: Specific binding to rat brain membranes. Proc. Natl. Acad. Sci. USA, *75:* 5372–5376, 1978.
45. Jensen, R. T., and Coy, D. H. Progress in the development of potent bombesin receptor antagonists. Trends Pharmacol. Sci., *12:* 13–18, 1991.
46. Zhou, Z-C., Gardner, J. D., and Jensen, R. T. Receptors for vasoactive intestinal peptide and secretin on guinea pig pancreatic acini. Peptides, *8:* 633–637, 1987.
47. Park, J-G., Frucht, H., LaRocco, V., Bliss, D. P., Kurita, Y., Chen, T-R., Henslee, J. G., Trepel, J. B., Jensen, R. T., Johnson, B. E., Bang, Y-J., Kim, J-P., and Gazdar, A. F. Characteristics of cell lines established from human gastric carcinoma. Cancer Res., *50:* 2773–2780, 1990.
48. Liehr, R-M., Melnykovych, G., and Solomon, T. E. Growth effects of regulatory peptides on human pancreatic cancer lines PANC-1 and MIA PaCa-2. Gastroenterology, *98:* 1666–1674, 1990.
49. Reyl-Desmars, F., Laboisse, C., and Lewin, M. J. M. A somatostatin receptor negatively coupled to adenylate cyclase in the human gastric cell line HGT-1. Regul. Pept., *16:* 207–215, 1986.
50. Gespach, C., Emami, S., and Rosselin, G. Gastric inhibitory peptide (GIP), pancreatic glucagon and vasoactive intestinal peptide (VIP) are cAMP-inducing hormones in the human gastric cancer cell line HGT-1. Homologous desensitization of VIP receptor activity. Biochem. Biophys. Res. Commun., *120:* 641–649, 1984.
51. Weinstock, J., and Baldwin, G. S. Binding of gastrin$_{17}$ to human gastric carcinoma cell lines. Cancer Res., *48:* 932–937, 1988.
52. Laboisse, C. L., Augeron, C., Couturier-Turpin, M-H., Gespach, C., Cheret, A-M., and Potet, F. Characterization of a newly established human gastric cancer cell line HGT-1 bearing histamine H_2-receptors. Cancer Res., *42:* 1541–1548, 1982.
53. Emami, S., Chastre, E., Bodere, H., Gespach, C., Bataille, D., and Rosselin, G. Functional receptors for VIP, GIP, glucagon-29 and -37 in the HGT-1 human gastric cancer cell line. Peptides, *7:* 121–127, 1986.
54. Ruellan, C., Scemama, J. L., Clerc, P., Fagto-Revurat, P., Clemente, F., and Ribet, A. VIP regulation of a human pancreatic cancer cell line: capan-1. Peptides, *1:* 267–271, 1986.
55. Ackerman, M. S., Roeske, W. R., Heck, R. J., and Korc, M. Identification and characterization of muscarinic receptors in cultured human pancreatic carcinoma cells. Pancreas, *4:* 363–370, 1989.
56. Beauchamp, R. D., Townsend, C. M., Singh, P., Glass, E. J., and Thompson, J. C. Proglumide, a gastrin receptor antagonist, inhibits growth of colon cancer and enhances survival in mice. Ann. Surg., 303–309, 1985.
57. Upp, J. R., Singh, P., Townsend, C. M., and Thompson, J. C. Clinical significance of gastrin receptors in human colon cancers. Cancer Res., *49:* 488–492, 1989.
58. Viallet, J., Sharoni, Y., Frucht, H., Jensen, R. T., Minna, J. D., and Saurville, E. A. Cholera toxin inhibits signal transduction by several mitogens and the *in vitro* growth of human small-cell lung cancer. J. Clin. Invest., *86:* 1904–1912, 1990.
59. Carney, D. N., Cuttitta, F., Moody, T. W., and Minna, J. D. Selective stimulation of small cell lung cancer clonal growth by bombesin and gastrin-releasing peptide. Cancer Res., *47:* 821–825, 1987.
60. Cuttitta, F., Carney, D. N., Mulshine, J., Moody, T. W., Fedorko, J., Fischler, A., and Minna, J. D. Bombesin-like peptides can function as autocrine growth factors in human small-cell lung cancer. Nature (Lond.), *316:* 823–826, 1985.

Preclinical Evaluation of Technetium-99m-Labeled Somatostatin Receptor-Binding Peptides

Shankar Vallabhajosula, Brian R. Moyer, John Lister-James, Bill J. McBride, Helena Lipszyc, Hiram Lee, Diago Bastidas and Richard T. Dean

Division of Nuclear Medicine, Department of Radiology, The Mount Sinai Medical Center, New York, New York; and Diatide, Inc., Londonderry, New Hampshire

We report here the results of studies on the in vitro receptor binding affinity, in vivo tumor uptake and biodistribution of two ^{99m}Tc-labeled peptides. **Methods:** Peptides P587 and P829 were synthesized by N-α-Fmoc peptide chemistry, purified by reversed-phase HPLC and characterized by fast-atom bombardment mass spectrometry. The peptides were labeled with ^{99m}Tc by ligand exchange from ^{99m}Tc-glucoheptonate. In vitro somatostatin receptors (SSTR)-binding affinities of P587, P829 and their oxorhenium complexes, [DTPA]octreotide and In-[DTPA]octreotide were determined in an inhibition assay using AR42J rat pancreatic tumor cell membranes and ^{125}I-[Tyr^3]somatostatin-14 as the probe. In vivo single- and dual-tracer studies of ^{99m}Tc peptides and ^{111}In-[DTPA]octreotide were carried out using Lewis rats bearing CA20948 rat pancreatic tumor implants. **Results:** Technetium-99m-P587 and ^{99m}Tc-P829 of high-specific activity (>60 Ci (2.2 TBq)/mmole) were prepared in >90% radiochemical yield. P587 and P829 had a Ki = 2.5 n*M* and 10 n*M*, respectively. [ReO]P587 and [ReO]P829, representing the ^{99m}Tc complexes, had Ki = 0.15 n*M* and 0.32 n*M*, respectively. In comparison, [DTPA]octreotide and In-[DTPA]octreotide had Ki = 1.6 and 1.2 n*M*, respectively. In vivo tumor uptake of ^{99m}Tc-P587 and ^{99m}Tc-P829 was high (4.1 and 4.9%ID/g at 90 min postinjection compared to 2.9% for ^{111}In-[DTPA]octreotide). Tumor/blood and tumor/muscle ratios at 90 min postinjection were 6 and 33 for ^{99m}Tc-P587, 21 and 68 for ^{99m}Tc-P829, and 22 and 64 for ^{111}In-[DTPA]octreotide. **Conclusion:** The high SSTR-binding affinity and high, receptor-specific and saturable in vivo tumor uptake indicate that ^{99m}Tc-P587 and ^{99m}Tc-P829 are promising radiotracers for the clinical detection of SSTR-expressing tumors and other tissues by ^{99m}Tc gamma scintigraphy.

Key Words: tumor imaging; somatostatin receptor imaging; technetium-99m; peptide; receptor binding

J Nucl Med 1996; 37:1016–1022

Natural somatostatin, also known as somatotropin release inhibiting factor (SRIF or SRIF-14), is a cyclic tetradecapeptide (Table 1) which is produced by the hypothalamus and pancreas and which, through binding to specific receptors and possibly through subsequent induced reduction in cellular cyclic AMP, inhibits the secretion of many hormones and growth factors (*2,3*). Receptors for SRIF have been found in the central nervous system, pituitary, pancreas and in the mucosa of the gastrointestinal tract. Five subtypes of human SRIF receptors, conventionally termed somatostatin-type receptors or SSTRs, hence SSTR1, SSTR2, SSTR3, SSTR4 and SSTR5, have been cloned (*4–7*).

Most neuroendocrine tumors and their metastases express SSTRs to a much greater extent than do normal tissues (*8–11*). The types of tumors which have been found to express SSTRs include tumors of the amine-precursor-uptake-and-decarboxylation (APUD) cell system (APUDomas) such as small-cell lung cancer, endocrine pancreatic tumors, metastatic carcinoids, growth hormone-producing pituitary adenomas, paragangliomas, lymphomas (mainly Hodgkins), astrocytomas and meningiomas as well as some colorectal, breast and prostate cancers (as determined by ^{125}I-[Tyr^3]octreotide autoradiography (*9*)). SSTR2 appears to be the predominant SSTR sub-type expressed by these tumors (*10,11*).

SSTR-expressing tumors can be treated with SRIF or synthetic analogs to either reduce hypersecretion of hormones or inhibit tumor growth, or both (*8*). However, because SRIF undergoes rapid in vivo enzymatic degradation, SRIF analogs which are more resistant to in vivo degradation have been prepared (*12–16*). Octreotide (Sandostatin®; SMS 201-995) (Table 1) is a synthetic SRIF analog which is currently in clinical use for treating the hypersecretion of hormones symptomatic of gastroenteropancreatic (GEP) tumors, and acromegaly and is approved in the US for treatment of carcinoid tumors and VIPomas (*12*).

Lamberts and Krenning et al. (*1,8,17,18*) and Kvols et al. (*19*) have shown the radiolabeled octreotide derivatives, ^{123}I-[Tyr^3]octreotide and ^{111}In-[DTPA]octreotide, to be very useful for detecting small neuroendocrine tumors and metastases not detected by conventional means and for identifying tumors that respond to therapeutic doses of octreotide. Nevertheless, a ^{99m}Tc-labeled SSTR-binding radiotracer is highly desirable for routine nuclear medicine studies because ^{99m}Tc is considerably less expensive than ^{111}In and because ^{99m}Tc provides a greater photon flux, and hence better quality images, per unit of absorbed radiation dose.

We have developed a number of unique, high-affinity SSTR-binding peptides which can be radiolabeled readily with ^{99m}Tc with retention and, in many cases, enhancement of SSTR-binding affinity (*20*). Of these, ^{99m}Tc-P587 and ^{99m}Tc-P829 were selected for clinical studies and we describe their preclinical evaluation.

MATERIALS AND METHODS

Peptide Synthesis

Peptides P587, P829, octreotide and [DTPA]octreotide (see Table 1 for sequences) were synthesized at Diatide, Inc. (Londonderry, NH) using both solution and solid-phase peptide synthesis techniques and N-α-Fmoc chemistry. Details of the syntheses will appear elsewhere. The peptides were purified by preparative, C_{18} reversed-phase HPLC using a Delta-Pak C_{18}, 15 μm, 300 Å, 47 × 300-mm column and 0.1% trifluoroacetic acid in water (0.1% TFA/H_2O) modified with 0.1% trifluoroacetic acid in 90% acetonitrile/10% water (0.1% TFA/(90% CH_3CN/H_2O)) as eluents, and then lyophilized. The purified peptides were lyophilized and their purity and identity were confirmed by analytical C_{18} reversed-

Received Jan. 19, 1995; revision accepted Nov. 3, 1995.

For correspondence or reprints contact: Shankar Vallabhajosula, PhD, Associate Professor of Radiology, Mount Sinai Medical Center, One Gustave L. Levy Pl., New York, NY 10029.

TABLE 1
Peptide Sequences*

Somatostatin: Ala-Gly-Cys-Lys-Asn-Phe-Phe-Trp-Lys-Thr-Phe-Thr-Ser-Cys
P587: cyclo-(N-Me)Phe-Tyr-(D-Trp)-Lys-Val-Hcy(CH_2CO-Gly-Gly-Cys-Lys-NH_2)
P829: cyclo-(N-Me)Phe-Tyr-(D-Trp)-Lys-Val-Hcy(CH_2CO-(β-Dap)-Lys-Cys-Lys-NH_2)
octreotide: (D-Phe)-Cys-Phe-(D-Trp)-Lys-Thr-Cys-Thr(ol)
[DTPA]octreotide: [DTPA]-(D-Phe)-Cys-Phe-(D-Trp)-Lys-Thr-Cys-Thr(ol)

*Cys ... Cys underline indicates cyclic disulfide; cyclo and underline indicates cyclic peptide.
Ala = L-alanine, Asn = L-asparagine, Cys = L-cysteine, β-Dap = β-(L-1,2-diaminopropionic acid), DTPA = diethylenetriaminepentaacetic acid, Gly = glycine, Hcy = L-homocysteine, Lys = L-lysine, (N-Me)Phe = N-α-methyl-L-phenylalanine, Phe = L-phenylalanine, D-Phe = D-phenylalanine, Ser = L-serine, Thr = L-threonine, Thr(ol) = L-threoninol, Trp = L-tryptophan, D-Trp = D-tryptophan, Tyr = L-tyrosine, Val = L-valine.

phase HPLC, C_{18}, 5 μm, 300 Å, 3.9 × 150-mm column and binary gradient elution with 0.1% TFA/H_2O as Solvent A and 0.1% TFA/(90% CH_3CN/H_2O) as Solvent B) and fast-atom bombardment mass spectrometry.

Peptide Metal Complexes

The oxorhenium complexes of P587 ([ReO]P587) and P829 ([ReO]P829) were prepared by ligand exchange using $Bu_4NReOBr_4$ (*21*) in DMF, followed by purification by preparative HPLC and confirmation of composition by electrospray mass spectrometry (ESMS). Indium-[DTPA]octreotide was prepared from In-chloride dissolved in 0.1 m citrate buffer at pH 5 and [DTPA]octreotide followed by purification by preparative HPLC and confirmation of composition by ESMS.

Preparation of Technetium-99m-Labeled Peptides

P587 and P829 were labeled with ^{99m}Tc by ligand exchange from ^{99m}Tc-glucoheptonate. P587 was dissolved to 1 mg/ml in 50% aqueous ethanol and P829 was dissolved to 1 mg/ml in normal saline. One quarter of a Glucoscan™ Kit (DuPont Pharma, N. Billerica, MA) that had been reconstituted with 1 ml ^{99m}Tc generator eluate (200–300 mCi; 7.4–11.1 GBq), was added to peptide solution. In the case of P587 the solution was heated at 100°C for 15 min. For P829, the reaction mixture was allowed to incubate at room temperature for 20 min. The radiochemical purity of the ^{99m}Tc-peptide complexes was determined by ITLC (ITLC-SG, Gelman Sciences, Ann Arbor, MI) developed in saturated saline (^{99m}Tc-peptide immobile, $^{99m}TcO_4$ and ^{99m}Tc-glucoheptonate mobile), ITLC-SG developed in 5:3:1.5 pyridine: acetic acid: water (^{99m}Tc-peptide, $^{99m}TcO_4$ and ^{99m}Tc-glucoheptonate mobile) and analytical reversed-phase HPLC, performed using an HPLC equipped with an in-line gamma detector linked to an integrating recorder, a Delta-Pak C_{18}, 5 μm, 300 Å, 3.9 × 150-mm column eluted at 1.2 ml/min with a gradient of 0.1% TFA/H_2O modified with 0.1% TFA/(90% CH_3CN/H_2O).

Preparation of Indium-111-[DTPA]Octreotide

Indium-111-[DTPA]octreotide was prepared by reacting ^{111}In-$InCl_3$ (1-2 mCi, 37-74 MBq) in 0.2 m HCl (1 ml) containing 25 mg trisodium citrate with 10 μg [DTPA]octreotide for 30 min at room temperature. The radiochemical purity of the ^{111}In-[DTPA]octreotide was determined by ITLC-SG developed in 0.1 m citrate buffer at pH 5.0.

In Vitro Assay

Peptides P587, P829 and [DTPA]octreotide and their metal complexes [ReO]P587, [ReO]P829 and In-[DTPA]octreotide were assayed in vitro for SSTR binding affinity by J.E. Taylor of Biomeasure, Inc., using AR42J rat pancreatic carcinoma cell membranes (expressing predominantly SSTR2 (*10*)) and ^{125}I-[Tyr^{11}]SRIF-14 as the probe. Briefly, AR42J cells were cultured in Dulbecco's Minimum Essential Medium supplemented with 10% fetal bovine serum and 8 mm L-glutamine maintained in a humidified 5% CO_2 atmosphere at 37°C in T-flasks. Harvested cells were homogenized in cold Tris buffer and the homogenate was centrifuged at 39,000 × g for 10 min at 4°C. The pellet was washed once using the same buffer then suspended in ice-cold 10 mm Tris HCl. Equal aliquots of cell membrane were incubated with ^{125}I-[Tyr-11]SRIF-14 (0.05 nm; 750,000 cpm/ml; 2000 Ci/mmole) and peptide at a final concentration of 10^{-11} to 10^{-6} m in 50 mm HEPES, pH 7.4 containing 1% bovine serum albumin, fraction V, 5 mm $MgCl_2$, Trasylol (200 KIU/ml), bacitracin (0.02 mg/ml) and phenylmethylsulfonyl fluoride (0.02 mg/ml) for 25 min at 30°C. Using a filtration manifold, the mixture was then filtered through a polyethylenimine-washed GF/C filter, and the residue was washed three times with 5 ml ice-cold buffer. The pellet/filter and filtrate/washings were counted in a well- counter to give the fractions of radioactivity bound and free. To assess nonspecific binding, the assay was run in the presence of 200 nm SRIF-14. Analysis of the data gave inhibition constants (Ki) via Hill plots (*22*).

Animal Model

The animal tumor model was essentially that described by Lamberts and Krenning et al. (*23*) and was prepared by A. Bogden, Biomeasure, Inc. CA20948 rat pancreatic tumor brei (0.05 to 0.1 ml) was inoculated into the subcutaneous space of the lateral aspect of the right thighs of 6-wk-old, male Lewis rats (175–225 g). The tumors were allowed to grow to approximately 0.5 to 2 g (2–3 wk) before serial passaging. The tumor-bearing animals used for the in vivo studies were from the fourth to the eleventh passage and carried 0.2 to 2 g (mean 1.2 ± 0.7 g) tumors. The tumors had a stable SSTR density of 80–100 fmole/mg tumor cell protein (assayed using ^{125}I-[Tyr^{11}]SRIF-14) through passages 4 to 9.

For studies of in vivo specificity of radiotracer localization in the tumors, selected animals were given a subcutaneous SSTR-blocking dose of 4 mg/kg octreotide 30 min prior to injection of the radiotracer. This protocol has been shown by Lamberts and Krenning et al. to result in a lowering of ^{111}In-[DTPA]octreotide tumor uptake by 40% (*23*).

In Vivo Tumor Uptake and Kinetics Studies

In all studies, CA20948 tumor-bearing Lewis rats were restrained and injected via the dorsal tail vein with radiolabeled peptides in a 0.2–0.4-ml volume containing 0.20 mCi (7.4 Mbq) of ^{99m}Tc-labeled P587 or P829 (2–8 μg) peptide and/or 0.10 mCi (3.7 MBq) of ^{111}In-[DTPA]octreotide (0.3–1 μg). For imaging studies, the animals were sedated with a mixture of ketamine and xylazine and whole-body images were obtained using a gamma camera (Technicare, Omega 500) fitted with a high-resolution collimator. Images were acquired for 5 min and the data were stored in 128 × 128-image matrix on a Summit image computer system.

Twenty-four Hour Pharmacokinetic Study. Fifteen tumor-bearing rats were injected with ^{99m}Tc-P587 and three animals each were sacrificed at 0.5, 1.5, 3, 6 and 24 hr. Selected tissue samples were excised, weighed and, along with an aliquot of the injected dose, were counted in a gamma well-counter set to count in the ^{99m}Tc window. The results were expressed as percent injected dose per gram (% ID/g) of tissue.

Dual-Tracer Comparison of Technetium-99m-P587 and Indium-111-[DTPA]Octreotide and In Vivo Receptor Specificity Study. Nine of 22 CA20948 tumor-bearing rats were injected subcutaneously with an SSTR-blocking dose of 4 mg/kg octreotide 30 min prior to injection of the radiotracers. All animals were injected with

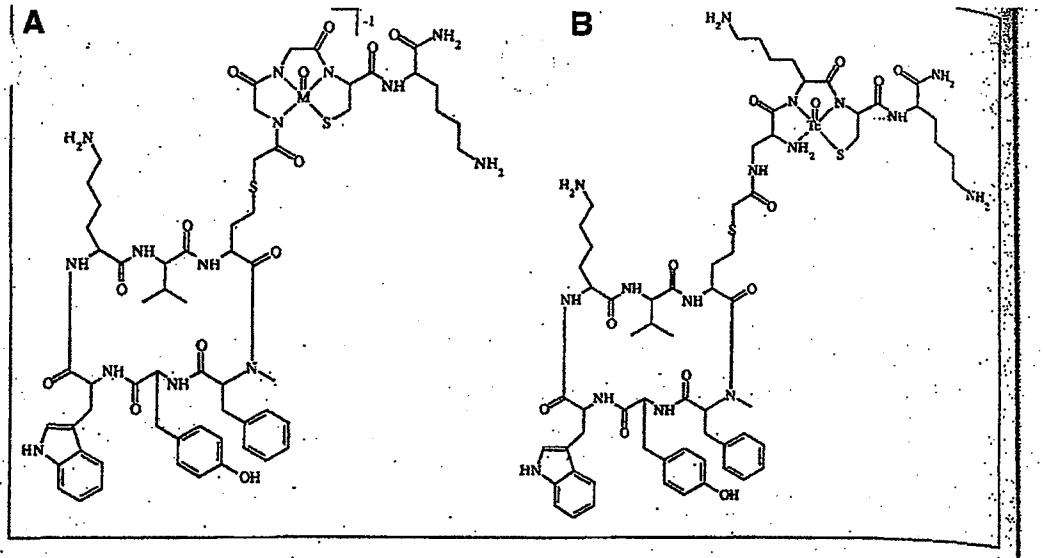

FIGURE 1. Proposed oxotechnetium/oxorhenium complexes of (A) P587 and (B) P829.

^{99m}Tc-P587 followed approximately 1 min later by ^{111}In-[DTPA]octreotide. At 30, 60 and 90 min, three SSTR-blocked and three nonblocked animals were killed by cervical dislocation and selected necropsy was performed. At 180 min the remaining four nonblocked animals were also killed and necropsied. Harvested tissue samples were weighed and, along with aliquots of both injected doses, were counted in a gamma well-counter set to count in both ^{99m}Tc and ^{111}In windows. Technetium-99m counts were corrected for ^{111}In spillover and 3 days later the samples were recounted for ^{111}In only. At 30, 60, 90 and 180 min selected animals also were imaged.

Dual-Tracer Comparison of Technetium-99m-P829 and Indium-111-[DTPA]Octreotide. The tumor uptake of ^{99m}Tc-P829 was compared with ^{111}In-DTPA-octreotide in a dual-tracer study using an additional five tumor-bearing rats. All animals were injected with ^{99m}Tc-P829 followed approximately 1 min later by ^{111}In-[DTPA]octreotide. The animals were killed at 90 min postinjection and % ID/g of tumor, blood, muscle, pancreas and gastrointestinal tract were determined as before for ^{99m}Tc and ^{111}In tracers.

Saturability Study. To assess the effect of specific activity on tumor uptake, ^{99m}Tc-P587 was studied in six groups of three tumor-bearing rats each. The animals were co-injected with either 0, 25, 100, 300, 600, 1000 or 4000 μg/kg of P587 peptide added to the standard dose of ^{99m}Tc-P587 (0.2 mCi; 7.4 MBq; 4 μg peptide). The animals were sacrificed at 90 min postinjection and % ID/g of tumor, blood, muscle, pancreas and gastrointestinal tract were determined as before. A similar study was performed with ^{99m}Tc-P829.

Biodistribution of Technetium-99m Peptides

The biodistributions of ^{99m}Tc-P587 and ^{99m}Tc-P829 were studied noninvasively in normal rabbits by gamma-camera imaging over a period of 4 hr. For the first 1 hr, serial static images (5 min per frame) were acquired and subsequent images were obtained at 2, 3 and 4 hr.

RESULTS

P587 peptide, P829 peptide, [DTPA]octreotide, [ReO]P587, [ReO]P829 and In-[DTPA]octreotide were all prepared and purified to >90% purity by HPLC analysis. The amino acid sequences of all of the peptides are shown in Table 1. The structures for P587 and P829 are shown in Figure 1. The proposed structures of the oxotechnetium and oxorhenium complexes of P587 and P829 are shown in Figures 1A and B, respectively. Selected analytical data are shown in Table 2.

The ^{99m}Tc-labeling of P587 and P829 were routinely obtained in >90% radiochemical yield and of >90% radiochemical purity by ITLC and HPLC analysis. No HPLC purification was required. Residual pertechnetate was <1% and ^{99m}Tc species immobile on ITLC analysis (^{99m}Tc-microcolloid or reduced, hydrolysed ^{99m}Tc) was <3%. HPLC analysis of ^{99m}Tc-P587 showed two, closely eluting radioactive components as expected for syn- and anti-oxotechnetium complexes of the -Gly-Gly-Cys-chelating sequence. HPLC analysis of ^{99m}Tc-P829 showed a single species. The ^{99m}Tc-labeled peptides were routinely prepared of high specific activity (50 mCi (2 GBq)/mg peptide; 60 Ci (2.2 TBq)/mmole peptide) but even higher specific activity (1000 Ci (37 TBq)/mmole P587) was readily achievable without significant loss of radiochemical yield. As discussed below, the effective specific activity was likely even higher.

[ReO]P587 was isolated as a mixture of two closely eluting components by HPLC analysis, presumed to be the expected two isomeric complexes. FABMS analysis showed only MH^+ peaks at m/z = 1458 corresponding to the expected mass (P587 − 4H + ReO + H^+) and 1258 corresponding to P587 itself. [ReO]P829 was isolated as a single peak by HPLC analysis. The HPLC analysis of oxorhenium complexes and ^{99m}Tc-labeled peptides showed that the corresponding rhenium and technetium complexes had virtually identical retention times (see Table 2). These data support the use of the oxorhenium complex(es) as a nonradioactive surrogate for ^{99m}Tc-peptides.

TABLE 2
Peptide and Peptide-Metal Complex Data

Peptide	Calc. MW	MH±(FABMS)	HPLC R_t (min)
P587	1257.7	1258	7.2[1]
[ReO]P587	1455.7	1458	14.6[4]
^{99m}Tc-P587	—	—	14.7, 14.9[4]
P829	1357.7	1358	5.8[3]
[ReO]P829	1556.9	1558	12.2[1]
^{99m}Tc-P829	—	—	12.3[1]
[DTPA]octreotide	1392.6	1394	7.1[1]
In-[DTPA]octreotide	1504.4*	1507	9.4[2]

*Assumed formula: [DTPA]octreotide + In − 3H

HPLC elution conditions: (a) 0 to 100% Solvent B in 10 min (Delta-Pak column); (b) 10 to 60% Solvent B in 10 min (Delta-Pak column); (c) 20–50% Solvent B in 10 min (NovaPak column).

TABLE 3
Inhibition Constants for Peptides and Metal Complexes Iodine-125-[Tyr[11]]SRIF-14/AR42J Rat Pancreatic Cell Membrane Assay

Peptide	Inhibition constant, Ki (nM) Peptide	Metal-peptide complex	Ratio*
P587	2.5	0.15[a]	20
P829	10	0.32[a]	30
DTPA-octreotide	1.6	1.20[b]	1

*Ratio of Ki of peptide to peptide-metal complex (to one significant figure). a = [ReO]peptide complex; b = In-DTPA-octreotide.

The in vitro inhibition constants obtained for P587 peptide, P829 peptide and their corresponding oxorhenium complexes and [DTPA]octreotide, and In-[DTPA]octreotide are shown in Table 3. It is noted that [ReO]P587 has a Ki approximately 20 times lower than that of P587 peptide and [ReO]P829 has a Ki 30 times lower than that of P829 peptide. This indicates that the rhenium complexes (and by inference, the ^{99m}Tc complexes) have a SSTR binding affinities that are an order of magnitude higher than those of the parent peptides. In-[DTPA]octreotide and [DTPA]octreotide did not share this property.

Kinetics of Tumor Uptake

Tumor and selected tissue uptake data of ^{99m}Tc-P587 over the course of the 24-hr pharmacokinetic study are presented in Table 4. Technetium-99m-P587 showed rapid, high tumor uptake, maximizing to 5.0 %ID/g at 3 hr, and only slow (68% of maximum remaining at 6 hr) clearance of radioactivity from the tumor over 24 hr. Tumor-to-blood ratio increased throughout the study, reflecting the initial tumor retention and subsequent much faster clearance of radiotracer from the blood than from the tumor. Tumor-to-muscle increased to 6 hr then showed insignificant change over 24 hr.

Tumor Uptake of Technetium-99m-P587 and Technetium-99m-P829 and Comparison with Indium-111-[DTPA]Octreotide

Data from the ^{99m}Tc-P587 and ^{111}In-[DTPA]octreotide dual-tracer study are presented in Table 5. The tumor uptake of both radiotracers was high and although not significantly different over the course of the 3-hr study, in general ^{99m}Tc-P587 and ^{99m}Tc-P829 gave higher tumor uptake than did ^{111}In-[DTPA]octreotide. Although ^{111}In-[DTPA]octreotide had faster blood clearance than ^{99m}Tc-P587 resulting in higher tumor-to-blood and tumor-to-muscle ratios for ^{111}In-[DTPA]octreotide, the ratios of 6.3 and 29, respectively, obtained with ^{99m}Tc-P587 at 90 min were more than sufficient to predict good imaging.

Data from the ^{99m}Tc-P829 and ^{111}In-[DTPA]octreotide dual-tracer study are presented in Table 6. Technetium-99m-P829 also showed high tumor uptake which was higher than that of ^{111}In-[DTPA]octreotide. Moreover, the blood clearance of ^{99m}Tc-P829 was faster than that of ^{99m}Tc-P587 resulting in tumor-to-blood and tumor-to-muscle ratios which were essentially equivalent to those of ^{111}In-[DTPA]octreotide.

The studies in SSTR-blocked animals (Table 5) showed that the tumor uptake of ^{99m}Tc-P587 was reduced by 86% (at 90 min) in SSTR-blocked versus nonblocked animals. Indium-111-[DTPA]octreotide tumor uptake was similarly reduced by 94%. Blood levels did not change significantly and therefore tumor-to-blood and tumor-to-muscle ratios were concomitantly reduced in SSTR-blocked animals. Notably pancreatic uptake was substantially diminished in blocked animals, indicating that the pancreatic uptake was also substantially receptor-mediated.

As a negative control, a much weaker affinity peptide P443 ([DTPA]-(D-Phe)-(4-chlorophenylalanyl)-Tyr-(D-Trp)-Lys-Thr-Phe-Thr-(ε-Lys)-Gly-Cys-NH_2) having a Ki of 7.9 nm as the oxorhenium complex, was also studied in CA20948 tumor-bearing rats. At 90 min postinjection, ^{99m}Tc-P443 gave only 0.42 %ID/g in the tumor and tumor-to-blood and tumor-to-muscle ratios of 0.9 and 2.7, respectively.

Tumor Uptake of Technetium-99m-Peptides: Imaging Studies

Representative gamma camera images (anterior view) of CA20948 tumor-bearing rats 90 min after injection with ^{99m}Tc-P587 are presented in Figure 2. The radiotracer uptake in the tumor in the right hind leg of each animal is clearly seen. Also seen are kidneys and bladder and some gastrointestinal tract uptake. The images show the obvious difference in tumor uptake in an SSTR-blocked animal (left image) and a non-SSTR-blocked animal (right image). Gamma camera images of ^{99m}Tc-P829 in two animals are shown in Figure 3. Again the high tumor uptake of the ^{99m}Tc-labeled peptide is clearly seen.

Effect of Specific Activity on the Tumor Uptake of the Technetium-99m-Peptides

The effect of increasing the amount of co-injected P587 peptide on ^{99m}Tc-P587 tumor uptake is shown in Figure 4A. P587 peptide was added to a standard preparation of ^{99m}Tc-P587 (0.2 mCi; 7.4 MBq; 5 μg P587 peptide), effectively lowering the specific activity. Tumor uptake decreased substantially when >100 μg P587 peptide was co-injected. Thus 100 μg co-injected P587 resulted in a 50% decrease in tumor uptake. Pancreatic uptake was also reduced by increasing amounts of co-injected P587 peptide. Similarly, the effect of decreasing specific activity on the uptake of ^{99m}Tc-P829 by tumor and pancreas is shown in Figure 4B. Blood, muscle and gastrointestinal tract uptake did not change significantly in either the ^{99m}Tc-P587 or ^{99m}Tc-P829 study.

Biodistribution of Technetium-99m-P587 versus Technetium-99m-P829

The gamma-camera images showing the relative distribution of ^{99m}Tc-P587 and ^{99m}Tc-P829 in normal rabbits are presented in Figure 5. The images show that ^{99m}Tc-P587 has substantial

TABLE 4
Technetium-99m-P587 Pharmacokinetic Study in CA20948 Tumor-Bearing Rats*

Time (hr)	%ID/g Tumor	Blood	Muscle	Tumor: Blood	Tumor: Muscle	%ID GI Tract
1.5	4.0 ± 0.64	0.67 ± 0.048	0.13 ± 0.0067	6.0 ± 0.80	30 ± 4.5	45 ± 1.9
3	5.0 ± 0.066	0.35 ± 0.013	0.076 ± 0.0070	14 ± 0.49	66 ± 6.7	49 ± 2.6
6	3.4 ± 0.59	0.075 ± 0.013	0.029 ± 0.0045	46 ± 8.7	120 ± 4.6	60 ± 17
24	0.80 ± 0.13	0.011 ± 0.0011	0.0084 ± 0.0023	69 ± 5.0	97 ± 12	31 ± 11

*Three animals per time point; mean ± s.d.

TABLE 5

Technetium-99m-P587 and Indium-111-[DTPA]Octreotide Dual-Tracer Study in CA 20948 Tumor-Bearing Rats Data from SSTR-Blocked and Nonblocked Animals*

Time (min)		%ID/g			Tumor: Blood	Tumor: Muscle	%ID	
		Tumor	Blood	Muscle			Pancreas	GI Tract
				^{99m}Tc-P587				
30	n	3.8 ± 0.18	1.4 ± 0.45	0.36 ± 0.055	2.3 ± 0.030	11 ± 1.0	3.0 ± 0.23	22 ± 1.7
	b	0.69 ± 0.050	1.5 ± 0.29	0.27 ± 0.070	0.48 ± 0.060	2.6 ± 0.6	0.66 ± 0.38	16 ± 2.5
60	n	2.7 ± 0.68	0.93 ± 0.23	0.19 ± 0.028	3.0 ± 0.61	15 ± 2.6	3.2 ± 0.50	25 ± 3.8
	b	0.70 ± 0.052	1.2 ± 0.18	0.25 ± 0.053	0.61 ± 0.060	2.9 ± 0.49	0.32 ± 0.004	27 ± 5.3
90	n	4.1 ± 0.56	0.64 ± 0.030	0.14 ± 0.010	6.3 ± 1.0	29 ± 2.9	3.2 ± 0.060	33 ± 0.8
	b	0.57 ± 0.08	0.74 ± 0.10	0.14 ± 0.025	0.77 ± 0.080	4.1 ± 0.45	0.27 ± 0.030	35 ± 2.2
180	n	3.0 ± 0.66	0.27 ± 0.030	0.050 ± 0.008	11 ± 2.6	61 ± 14	3.1 ± 0.49	36 ± 3.3
				^{111}In-[DTPA]octreotide				
30	n	3.1 ± 0.72	0.76 ± 0.13	0.29 ± 0.22	4.3 ± 1.6	16 ± 10	2.1 ± 0.91	5.6 ± 1.3
	b	0.62 ± 0.17	0.92 ± 0.38	0.27 ± 0.11	0.71 ± 0.11	2.5 ± 1.0	0.38 ± 0.15	5.1 ± 1.0
60	n	3.1 ± 0.46	0.27 ± 0.040	0.071 ± 0.004	12 ± 0.13	43 ± 4.0	2.4 ± 0.080	5.5 ± 0.23
	b	0.33 ± 0.030	0.31 ± 0.050	0.010 ± 0.015	1.1 ± 0.080	3.3 ± 0.54	0.18 ± 0.11	3.2 ± 0.66
90	n	2.9 ± 1.8	0.13 ± 0.070	0.045 ± 0.024	22 ± 3	64 ± 4.3	2.1 ± 0.92	6.5 ± 0.53
	b	0.18 ± 0.017	0.10 ± 0.004	0.031 ± 0.004	1.8 ± 0.19	5.9 ± 0.61	0.075 ± 0.02	2.8 ± 0.06
180	n	2.7 ± 0.57	0.024 ± 0.004	0.014 ± 0.006	120 ± 39	240 ± 120	2.6 ± 0.12	7.0 ± 0.39

*n = 3 for each group except four in 180-min group; mean ± s.d.
† n = nonblocked; b = SSTR-blocked with 4 mg/kg octreotide s.c. 30 min before dosing.

uptake in the gastrointestinal tract compared to ^{99m}Tc-P829 which is cleared mostly by the kidneys. A quantitative analysis of the images at 1 hr indicated that about 40% of ^{99m}Tc-P587 activity was in the gastrointestinal tract, 25% in the urinary bladder and only 6% in the kidneys. In contrast, 30% of ^{99m}Tc-P829 activity was in the kidneys, 20% in the urinary bladder and less than 5% in the gastrointestinal tract.

DISCUSSION

The presence of the disulfide bridge of octreotide means that labeling this molecule with ^{99m}Tc is problematic because the reducing agent (usually stannous ion) used in ^{99m}Tc labeling can reduce (open) the disulfide bond with consequent considerable loss of receptor-binding affinity. Macke et al. (*24*) has recently reported a ^{99m}Tc-labeled PnAO conjugate of octreotide. They reported, however, using essentially the same tumor model as we have used, only 0.38% ID/g in the tumor, a tumor-to-blood ratio <1 and only 30% reduction of tumor uptake in SSTR-blocked versus unblocked animals. In contrast, very high tumor uptake (4–5% ID/g), tumor-to-blood (6–21) and tumor-to-muscle ratios (21–68) were seen with ^{99m}Tc-labeled P587 and P829. In addition, 85% reduction in tumor uptake in SSTR-blocked animals was seen with ^{99m}Tc-P587 and both ^{99m}Tc-P587 and ^{99m}Tc-P829 tumor uptake was 80–90% by co-injection of large amounts of the respective peptides. These differences suggest that the ^{99m}Tc-labeled PnAO conjugate of Macke et al. did not retain high receptor-binding affinity and gave mainly nonspecific tumor uptake in vivo.

Inspection of the literature reveals that in order to maintain high SSTR-binding affinity, the pharmacophore of an SSTR ligand needs to be conformationally constrained (*25*). Expressly in order to avoid the incompatibility of having a disulfide in a molecule that is to be radiolabeled with ^{99m}Tc under reducing conditions, we designed peptide P587 and P829 to hold the pharmacophore, that is the key four SSTR-binding amino acid residues -Tyr-(D-Trp)-Lys-Val-, in a cyclic configuration that was not susceptible to reductive cleavage. The sequence -Gly-Gly-Cys- of P587, which constitutes a triamide-thiol chelator which would be expected to form a kinetically stable oxotechnetium (+5) complex (*26*), was appended to the thiol group of the side-chain of a the noncritical homocysteine residue of the molecule. The result was that P587 peptide had an in vitro inhibition constant (Ki) of 2.5 nm, showing it to be a high-affinity ligand for the SSTR. Similarly, with P829 comprises the same SSTR binding cyclic peptide with the novel monoamine, bisamide, monothiol chelating sequence -(β-Dap)-Lys-Cys- appended to the homocysteine side-chain. The Ki for P829 was 10 nm but the oxorhenium complex had a Ki of 0.32 nm.

In order to assess the SSTR-binding affinity of the ^{99m}Tc complex of P587 and ^{99m}Tc-P829, we chose to use the oxorhenium (+5) complexes of these two peptides as a ^{99m}Tc

TABLE 6

Technetium-99m-P829 and Indium-111-[DTPA]Octreotide Dual-Tracer Study in CA 20948 Tumor-Bearing Rats (90-Minute Data)*

%ID/g			Tumor: Blood	Tumor: Muscle	%ID	
Tumor	Blood	Muscle			Pancreas	GI Tract
			^{99m}Tc-P829			
4.8 ± 1.1	0.29 ± 0.14	0.078 ± 0.015	21 ± 11	68 ± 26	2.4 ± 0.34	8.4 ± 0.5
			^{111}In-[DTPA]octreotide			
2.8 ± 0.43	0.10 ± 0.024	0.048 ± 0.044	29 ± 5.9	90 ± 57	1.6 ± 0.10	5.0 ± 0.50

*n = 3 for each group.

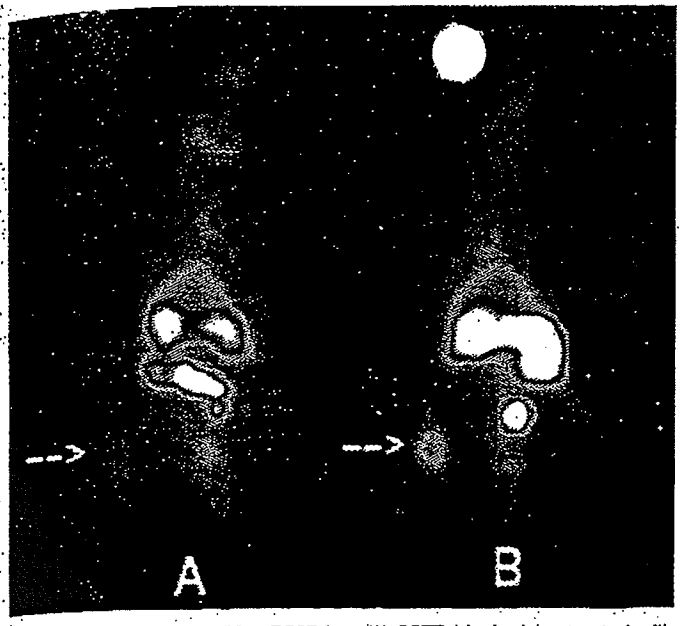

FIGURE 2. Technetium-99m-P587 in a (A) SSTR-blocked (pretreated with octreotide 4 mg/kg) and (B) a nonblocked CA20948 tumor-bearing rat at 90 min postinjection (anterior).

complex surrogate so as to avoid having to use the long-lived isotope ^{99m}Tc in the receptor-binding assay. It has been well-established that technetium and rhenium form configurationally equivalent, albeit not identical, oxometal (+5) complexes of triamide-thiol and bisamide-bisthiol ligands (*27*). As the results show, [ReO]P587 and [ReO]P829 have an even higher SSTR-binding affinity than the parent peptides. The higher affinity of the labeled peptides has important consequences in regard to specific activity. That is that co-injected peptides (P587 or P829) will compete poorly with the ^{99m}Tc-peptide complexes for the somatostatin receptors. Thus a readily achievable specific activity of 1000 Ci/mmole based on total injected P587 may be effectively an order of magnitude higher. In contrast the Kis of [DTPA]octreotide (1.6 nM) and In-[DTPA]octreotide (1.2 nm) which were similar to the previously reported values (*28*), showed that the unlabeled [DTPA]octreotide will compete equally with the ^{111}In-[DTPA]octreotide for the SSTRs.

The in vivo studies in CA20948 tumor-bearing rats showed

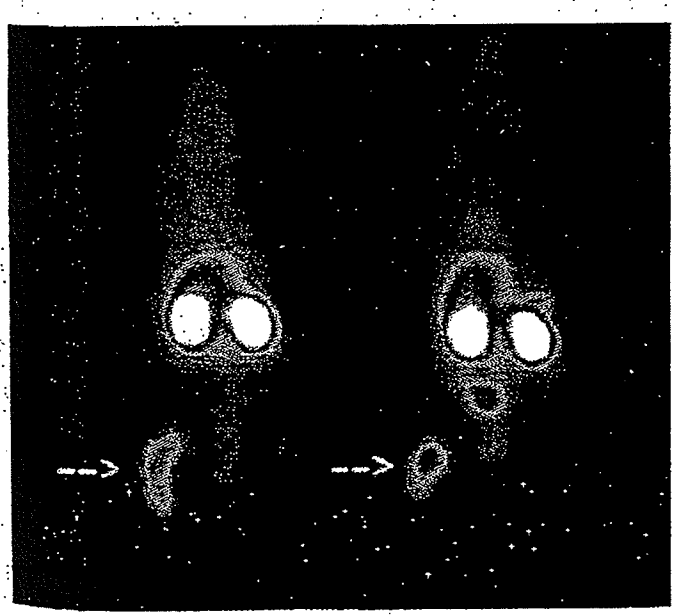

FIGURE 3. Technetium-99m-P829 in CA20948 two tumor-bearing rats (at 90 min postinjection, anterior views).

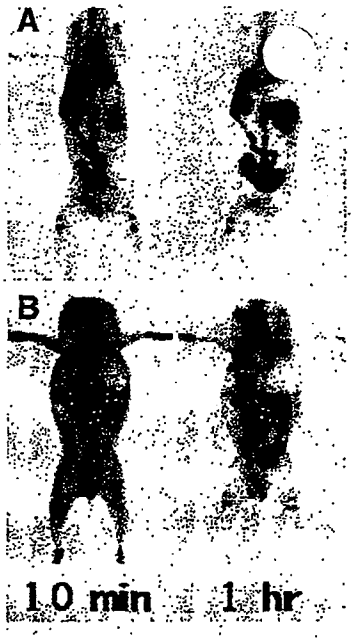

FIGURE 5. Gamma-camera images showing the relative distribution of (A) ^{99m}Tc-P587 and (B) ^{99m}Tc-P829 in normal rabbits at 10 min and 1 hr postinjection.

that the tumor uptake of ^{99m}Tc-P587 and ^{99m}Tc-P829 is at least, and perhaps a little higher than, that of ^{111}In-[DTPA]octreotide, that the tumor uptake of the labeled peptides is specific (blocked by octreotide) and that the tumor uptake of ^{99m}Tc-P587 and ^{99m}Tc-P829 is saturable (diminished by large amounts of co-injected parent peptide).

Regarding the biodistribution of ^{99m}Tc-P587 in normal animals, the biphasic nature of the blood clearance suggested hepatobiliary recycling which was supported by the observed progressive uptake from 15 min to 5 hr in the gastrointestinal tract. Significant reabsorption is probable since less than 6% ID remained in the large intestine at 5 hr and less than 5% ID remained in the entire gastrointestinal tract at 24 hr. Interestingly, the tumor-bearing animals showed greater and more persistent gastrointestinal uptake than did the normal animals. It is noted that as rats do not have gall bladders, biliary secretion is continuous as opposed to being controlled in other species including humans. Thus the gastrointestinal tract uptake seen maximally at from 3 to 6 hr in the rat may occur much later in the human leaving an early window in which the abdomen would be relatively clear of nonspecific radiotracer uptake. The retention of a fraction of the dose in the kidneys indicates proximal tubular reabsorption as has been observed for ^{111}In-[DTPA]octreotide. The primary route of excretion was the renal system as expected for a small peptide and as desirable for a radiopharmaceutical of this type. In comparison, the biodistribution of ^{99m}Tc-P829 showed almost no gastrointestinal uptake, with predominantly renal excretion.

These preclinical results have now been verified in initial clinical studies (*29*) with both agents in which SSTR-expressing tumors were detected as early as 5 min postinjection. Because it has showed both high tumor uptake and low gastrointestinal uptake, ^{99m}Tc-P829 has been selected for clinical studies.

CONCLUSION

Both ^{99m}Tc-P587 and ^{99m}Tc-P829 have been shown to have high SSTR-binding affinity and high, receptor-specific and saturable in vivo tumor uptake, and biodistribution characteristics favorable to early imaging. These observations support the clinical investigation of ^{99m}Tc-P587 and ^{99m}Tc-P829 as radiotracers for the detection of SSTR-expressing tumors and other tissues by gamma scintigraphy.

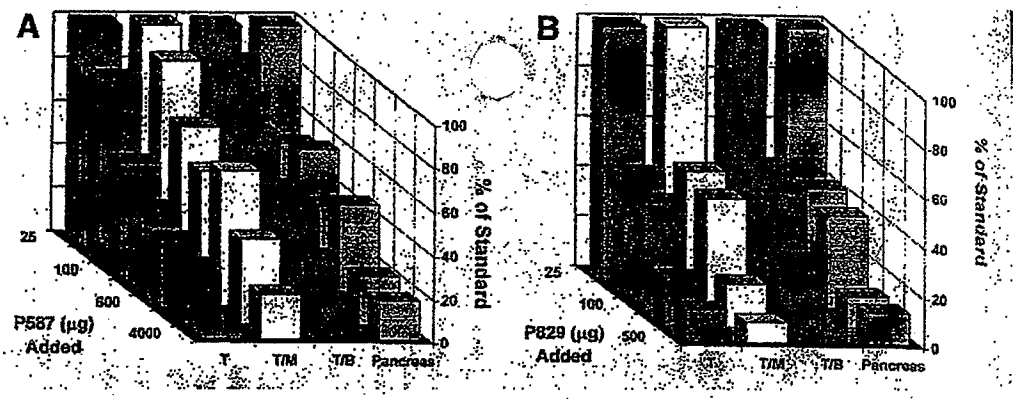

FIGURE 4. Effect of increasing amounts of co-injected cold peptide on the tumor uptake of ^{99m}Tc-peptides in CA20948 tumor-bearing rats. (A) ^{99m}Tc-P587 (top) and (B) ^{99m}Tc-P829. Tumor % ID/g (T), tumor:muscle (T/M), tumor:blood (T/B) and %ID in pancreas were plotted as percent of value observed with a standard (no additional cold peptide) ^{99m}Tc-peptide preparation.

ACKNOWLEDGMENTS

We thank Dr. John E. Taylor, of Biomeasure, Inc., for performing the in vitro assays and Dr. Arthur E. Bogden, also of Biomeasure, Inc., for preparing the animal model.

REFERENCES

1. Kremning EP, Kwekkeboom DW, Bakker WH, et al. Somatostatin receptor scintigraphy with [^{111}In-DTPA-D-Phe^1]- and [^{123}I-Tyr^3]-octreotide: the Rotterdam experience with more than 1000 patients. *Eur J Nucl Med* 1993;20:716–731.
2. Brazeau P, Vale W, Burgus R, et al. Hypothalamic polypeptide that inhibits the secretion of immunoreactive pituitary growth hormone. *Science* 1973;179:77–79.
3. Vale W, Brazeau P, Rivier C, et al. Somatostatin. *Recent Prog Horm Res* 1975;31: 365–397.
4. Yamada Y, Post SR, Wang K, et al. Cloning and functional characterization of a family of human and mouse somatostatin receptors expressed in brain, gastrointestinal tract and kidney. *Proc Natl Acad Sci USA* 1992;89:251–255.
5. Rens-Domiano S, Law SF, Yamada Y, et al. Pharmacological properties of two cloned somatostatin receptors. *Mol Pharmacol* 1992;42:28–34.
6. Raynor K, Murphy WA, Coy DH, et al. Cloned somatostatin receptors: identification of subtype-selective peptides and demonstration of high affinity binding of linear peptides. *Mol Pharmacol* 1993;43:838–844.
7. Raynor K, O'Carroll A-M, Kong H, et al. Characterization of cloned somatostatin receptors SSTR4 and SSTR5. *Mol Pharmacol* 1993;44:385–392.
8. Lamberts SWJ, Krenning EP, Reubi J-C. The role of somatostatin and its analogs in the diagnosis and treatment of tumors. *Endocrine Rev* 1991;12:450–482.
9. Reubi J-C, Krenning E, Lamberts SWJ, Kvols L. Somatostatin receptors in malignant tissues. *J Steroid Biochem Molec Biol* 1990;37:1073–1077.
10. Eden PA, Taylor JE. Somatostatin receptor subtype gene expression in human and rodent tumors. *Life Sci* 1993;53:85–90.
11. Reubi JC, Schaer JC, Waser B, Mengod G. Expression and localization of somatostatin receptor SSTR1, SSTR2 and SSTR3 messenger RNAs in primary human tumors using in situ hybridization. *Cancer Res* 1994;54:3455–3459.
12. Bauer W, Briner U, Doepfner W, et al. SMS 201-995: a very potent and selective octapeptide analog of somatostatin with prolonged action. *Life Sci* 1982;31:1133–1140.
13. Pless J, Bauer W, Briner U, et al. Chemistry and pharmacology of SMS 201-995, a long-acting octapeptide analog of somatostatin. In: Molinatti GM, Martinin L, Elsevier, eds. *Endocrinology '85*. New York, NY: 1986:319–333.
14. Murphy W, Lance VA, Moreau S, et al. Inhibition of rat prostate tumor growth by an octapeptide analog of somatostatin. *Life Sci* 1987;40:2515–2522
15. Veber DF, Saperstein R, Nutt RF, et al. *Science* 1984;34:1371.
16. Veber DF, Saperstein R, Nutt RF, et al. A super active cyclic peptide analog of somatostatin. *Life Sci* 1984;34:1371–1378.
17. Bakker WH, Kreening EP, Breeman WAP, et al. In vivo use of a radiolabeled somatostatin analog: dynamics, metabolism and binding to somatostatin receptor-positive tumors in man. *J Nucl Med* 1991;32:1184–1189.
18. Krenning EP, Bakker WH, Kooij PPM, et al. Somatostatin receptor scintigraphy with In-111-DTPA-D-Phe-1-octreotide in man: metabolism, dosimetry and comparison with I-123-Tyr-3-octreotide. *J Nucl Med* 1992;33:652–658.
19. Kvols LK, Brown ML, O'Connor MK, et al. Evaluation of a radiolabeled somatostatin analog (I-123 octreotide) in the detection and localization of carcinoid and islet cell tumors. *Radiology* 1993;187:129–133.
20. Lister-James J, McBride WJ, Moyer BR, et al. A structure-activity-relationship (SAR) study of somatostatin receptor-binding peptides radiolabeled with Tc-99m. *J Nucl Med* 1994;35:257P.
21. Cotton FA, Lippard SJ. Chemical and structural studies of the rhenium(V) oxyhalide complexes. I. Complexes from rhenium(III) bromide. *Inorg Chem* 1966;5:9–16.
22. Bylund DB, Yamamura HI. Methods for receptor binding. In: Yamamura HI, et al. eds. *Methods in neurotransmitter receptor analysis* New York, NY: Raven Press; 1990:1–35.
23. Bakker WH, Krenning EP, Reubi JC, et al. In vivo application of [^{111}In-DTPA-D-Phe^1]-octreotide for the detection of somatostatin receptor-positive tumors in rats. *Life Sci* 1991;49:593–1601.
24. Maina T, Stolz B, Albert H, et al. Synthesis, radiochemistry and biological evaluation of a new somatostatin analog (SDZ 219-387) labeled with technetium-99m *Eur J Nucl Med* 1994;21:437–444.
25. Huang Z, He Y-B, Raynor K, et al. Main chain and side chain chiral methylated somatostatin analogs: syntheses and conformational analyses. *J Am Chem Soc* 1992;114:9390–9401.
26. Fritzberg AR, Kasina S, Eshima D, Johnson DL. Synthesis and biological evaluation of technetium-99m MAG_3 as a hippuran replacement. *J Nucl Med* 1986;27:111–116.
27. Rao TN, Adhikesavalu D, Camerman A, Fritzberg AR. Technetium (V) and rhenium (V) complexes of 2,3-bis(mercaptoacetamido)propanoate. Chelate ring stereochemistry and influence on chemical and biological properties. *J Am Chem Soc* 1990;112: 5798–5804.
28. Bakker WH, Albert R, Bruns C, et al. [^{111}In-DTPA-D-Phe^1]-octreotide, a potential radiopharmaceutical for imaging of somatostatin receptor-positive tumors: synthesis, radiolabeling and in vitro validation. *Life Sci* 1991;49:1583–1591.
29. Lastoria S, Muto P, Acampa S, et al. Imaging of human tumors expressing somatostatin receptors with a novel synthetic peptide P587 labeled with ^{99m}Tc *Radiology* 1994;193P:300.

THE JOURNAL OF BIOLOGICAL CHEMISTRY

Vol. 261, No. 3, Issue of January 25, pp. 1470–1476, 1986
Printed in U.S.A.

Characterization of the Receptor for Heat-stable Enterotoxin from *Escherichia coli* in Rat Intestine*

(Received for publication, April 1, 1984)

Takayoshi Kuno‡, Yoshinori Kamisaki, Scott A. Waldman, Jean Gariepy, Gary Schoolnik, and Ferid Murad

From the Departments of Medicine, Pharmacology, and Microbiology, Stanford University School of Medicine, Palo Alto Veterans Administration Medical Center, Palo Alto, California 94304

The receptor for the heat-stable enterotoxin (ST) from *Escherichia coli* was solubilized with Lubrol-PX from rat intestinal brush-border membranes and characterized. The binding kinetics and analog specificity of the solubilized receptor were virtually identical to those obtained with the membrane-bound receptor. Furthermore, the regulation of the receptor's affinity by cations was also maintained after solubilization, indicating a conservation of the toxin-binding site after removal of the receptor from its membrane environment.

Gel filtration and sucrose density gradient sedimentation studies gave a Stokes radius of 5.5 nm and a sedimentation coefficient of 7.0 S for the solubilized receptor. The isoelectric point of the receptor was determined as 5.5 using Sephadex isoelectric focusing electrophoresis. In all of these separation techniques, the ST receptor showed a single peak of activity that was clearly separated from that of guanylate cyclase. When ^{125}I-ST was cross-linked to brush-border membranes with disuccinimidyl suberate, the affinity-labeled receptor solubilized with 0.1% Lubrol-PX eluted at a similar position as the native receptor on gel filtration chromatography. Analysis of the affinity-labeled receptor by sodium dodecyl sulfate-polyacrylamide gel electrophoresis in the presence of reducing agent and by autoradiography revealed the presence of three specifically labeled polypeptides with apparent molecular weights of 80,000, 68,000, and 60,000.

These results suggest that the ST receptor is solubilized by Lubrol-PX in an active form with preservation of its regulation by cations. Also, the ST receptor is separable from particulate guanylate cyclase indicating that the receptor is coupled to the activation of guanylate cyclase by an as yet undefined mechanism. Three subunit peptides may constitute a binding region of the receptor.

Heat-stable enterotoxins (ST[1]) produced by pathogenic strains of *Escherichia coli* are low molecular weight peptides that cause watery diarrhea by stimulating intestinal secretion (1–5). Several studies have provided evidence in favor of the concept that binding of ST to its specific receptor leads to the activation of particulate guanylate cyclase that initiates a cascade of reactions culminating in changes in ion and fluid transport in the brush-border membrane of intestinal epithelial cells (6–9). Although most mammalian tissues contain both soluble and particulate forms of guanylate cyclase, the enzyme in intestinal mucosa is predominantly particulate (10, 11). ST activates only the particulate form of the enzyme in intestinal mucosa (6–9). Recently, a high-affinity receptor for ST associated with rat intestinal epithelial cells and brush-border membranes has been detected (12–14) and solubilized (15). However, little is known about the coupling mechanism between the ST receptor and particulate guanylate cyclase. It remains to be determined whether the ST receptor and particulate guanylate cyclase are separate macromolecules or constitute a single protein that has an ST-binding site and guanylate cyclase activity. de Jonge (16) proposed that these activities reside in a single protein.

In this report, we describe the solubilization of the ST receptor with the nonionic detergent Lubrol-PX. Using several techniques, solubilized ST receptor and particulate guanylate cyclase can be separated indicating that they are different macromolecules. The structure of the ST receptor was also studied using an affinity cross-linking method. Some of these observations have been presented in abstract form (17).

EXPERIMENTAL PROCEDURES

Materials—Native ST purified from *E. coli* strain 431 was generously provided by Dr. D. C. Robertson, University of Kansas, Lawrence (13–15, 18). Synthetic analogs of ST used in this study included a 19-amino acid analog, a 14-amino acid analog (residues 6–19) and a 6-amino acid peptide (residues 10–15). The structure and synthesis of these peptides were described previously (19). Synthetic conotoxin GI was purchased from Peninsula Laboratories. Native ST or a synthetic 19-amino acid analog was radiolabeled with ^{125}I by the lactoperoxidase method ((13) Enzymobeads, Bio-Rad) to a specific activity of 300–700 Ci/mmol. Iodinated native toxin and synthetic 19-amino acid analog gave similar binding kinetics and were used interchangeably in these experiments. Disuccinimidyl suberate was purchased from Pierce Chemical Co., and bacitracin was obtained from Sigma. All other reagents were of analytical reagent grade and obtained as described previously (6, 8, 9, 20).

Membrane Preparation and Solubilization Procedure—Brush-border membranes were isolated from the small intestines of male Sprague-Dawley rats (weight 200–250 g) by a modification of the procedure described by Hauser *et al.* (21). Briefly, small intestine (jejunum and upper ileum) was removed and rinsed with ice-cold 50 mM Tris-HCl buffer, pH 7.6, containing 1 mM EDTA, 1 mM dithiothreitol, 0.25 M sucrose and 0.1 mM phenylmethanesulfonyl fluoride (buffer A). Mucosal scrapings were obtained with a glass slide. Mucosal tissue from four rats was homogenized with a Polytron homogenizer (Brinkmann) in 60 ml of ice-cold buffer A. The homogenate

* This work was supported by National Institutes of Health Grants AM30787 and HL28474 and by grants from the Veterans Administration and the Council for Tobacco Research-U.S.A. Inc. The costs of publication of this article were defrayed in part by the payment of page charges. This article must therefore be hereby marked "*advertisement*" in accordance with 18 U.S.C. Section 1734 solely to indicate this fact.

‡ To whom reprint requests should be addressed.

[1] The abbreviations used are: ST, heat-stable enterotoxin; CHAPS, 3-[(3-cholamidopropyl)dimethylammonio)-1-propanesulfonate.

was diluted 6-fold with ice-cold distilled water and adjusted to 10 mM Mg^{2+} by the addition of solid $MgCl_2$. After incubation at 4 °C for 15 min with mixing, the diluted extract was centrifuged at 1,000 × g for 20 min at 4 °C. The pellet was discarded, and the supernatant fraction was centrifuged at 100,000 × g for 60 min. The supernatant fraction was discarded. The pellet was resuspended in ice-cold buffer A and was washed twice with buffer A by repeating the resuspension and centrifugation. The final suspension was used fresh or stored at −80 °C until used.

Preparations of brush-border membranes were homogenized with a glass-Teflon homogenizer in 50 mM Tris-HCl buffer, pH 7.6, containing 1 mM EDTA, 1 mM dithiothreitol, 0.1 mM phenylmethanesulfonyl fluoride, and 0.1% (w/v) Lubrol-PX (buffer B) at a protein concentration of 1 mg/ml. The homogenate was kept on ice for 2 h prior to centrifugation at 200,000 × g for 60 min. The supernatant fraction containing approximately 0.3–0.4 mg of protein/ml was used as a solubilized preparation.

Receptor-binding Assay—Reaction mixtures contained 20 μl of sample (membrane or solubilized preparations), 50 mM Tris-HCl, pH 7.6, 0.1 mM EDTA, 150 mM NaCl, 0.67 mM cystamine, 0.1% (w/v) bacitracin, ^{125}I-ST, and the competing ligand, when used, in a final volume of 60 μl. Sodium chloride was omitted or substituted by other cations in some experiments. Cystamine was included in these reactions because samples contained dithiothreitol which inhibits the binding of ST to its receptor. Cystamine was used as a sink for the dithiothreitol and has no effect on receptor binding of toxin (data not shown). ^{125}I-ST and the competing ligand, when used, were combined in the assay tube followed by addition of samples to initiate the binding reaction. Nonspecific binding was determined using 1 μM nonradioactive 14-amino acid analog of ST. Reactions were allowed to proceed for 15 min at 37 °C to equilibrium. Bound ^{125}I-ST was separated from the free ligand by immediate filtration through polyethyleneimine-treated (22) Whatman GF/B or GF/C filters under vacuum. The reaction tube and filters were washed three times with 5 ml of ice-cold 20 mM phosphate-buffered saline, pH 7.0. Radioactivity on the filter was determined by counting in a Beckman Gamma 4000. The recovery of the solubilized receptor to the polyethyleneimine-treated filters in the binding assay was 95–105% when that of the gel filtration assay was assumed 100%. In some experiments, a cell harvester (M-24, Brandel, Gaithersburg, MD) was adapted for use in binding studies, and similar results were obtained.

Guanylate Cyclase Assay—Guanylate cyclase activity was assayed as described previously (8, 9, 20). Reaction mixtures contained 10 mM theophylline, 50 mM Tris-HCl, pH 7.6, 0.1% (w/v) bovine serum albumin, and a GTP-regenerating system consisting of 15 mM creatine phosphate and 20 μg (135 units/mg) of creatine phosphokinase. Assays (100 μl) were initiated by the addition of substrate (1 mM GTP and 4 mM $MnCl_2$), incubated for 10 min at 37 °C, and terminated by the addition of 50 mM sodium acetate, pH 4.0, followed by immersion in boiling water for 3 min. Generated cyclic GMP was quantified by radioimmunoassay (23) as described previously (8, 9, 20).

Gel Filtration—Gel filtration chromatography of the solubilized ST receptor was accomplished in two ways. The solubilized preparation (100 μl) or standard marker proteins (ferritin, catalase, lactate dehydrogenase, and bovine serum albumin) in a total volume of 100 μl were applied to a Spherogel-TSK G3000 SW column (7.5 × 300 mm; Beckman) that had been previously equilibrated and was then eluted with buffer B. The column was eluted with buffer B at 0.2 ml/min, and 0.2-ml fractions were collected. Each fraction was assayed for ^{125}I-ST binding and guanylate cyclase activity as described above. The elution positions of marker proteins were monitored by the absorbance at 280 nm.

Alternatively, the solubilized preparation (50 μl) was incubated with 1 nM ^{125}I-ST in the absence or the presence of 1 μM nonradioactive 14-amino acid analog of ST (as described in the binding assay above) in a final volume of 150 μl. After incubation at 37 °C for 15 min, 100 μl of the solution containing ^{125}I-ST-receptor complex was applied to the Spherogel TSK G3000 SW column, which was previously equilibrated and was eluted with buffer B without dithiothreitol at a flow rate of 0.2 ml/min. Each 0.2-ml fraction was assayed for radioactivity to locate the ^{125}I-ST-receptor complex.

Sucrose Density Gradient Centrifugation—Linear gradients (33 ml) were prepared with 5–20% (w/v) sucrose in buffer B. The solubilized preparation (1 ml) or standard marker proteins (β-galactosidase, catalase, lactate dehydrogenase, malate dehydrogenase, and cytochrome *c*) in a total volume of 1 ml were applied to the top of each gradient. Centrifugation was carried out at 4 °C in the Beckman SW 27 rotor at 135,000 × g for 24 h. After centrifugation, a capillary was lowered to the bottom of the centrifuge tube, and fractions of 0.85 ml were collected. Each fraction was assayed for ^{125}I-ST binding and guanylate cyclase activity as described above. Marker enzymes were assayed as described by Hall *et al.* (24).

Isoelectric Focusing Electrophoresis—The solubilized preparations (1 ml) were applied to a plate of Sephadex IEF (10 cm × 23 cm × 2 mm, Pharmacia) swollen with 6.3% (w/v) Pharmalyte (pH 5–8, Pharmacia) and 0.1% (w/v) Lubrol-PX and subjected to electrophoresis (30 watts for 2 h) at 4 °C, using a cathode solution of 0.5 M NaOH and an anode solution of 0.1 M H_3PO_4. After focusing, the Sephadex gels were cut into sections 7.5 mm wide, and each sample was extracted with 2 ml of buffer B containing 20% (v/v) glycerol. Samples were assayed for ^{126}I-ST binding and guanylate cyclase activity as described above. A part of each gel sample was extracted with distilled water for measuring pH.

Cross-linking Procedure and Analysis of Affinity-labeled Protein—Purified rat intestinal brush-border membranes prepared as described above were washed three times with ice-cold 20 mM phosphate-buffered saline, pH 7.0, by repeating the dilution and centrifugation. The washed membranes (1–2 mg of protein/ml) in 20 mM phosphate-buffered saline, pH 7.0, containing 0.1% (w/v) bacitracin were incubated for 15 min at 37 °C with 4 nM ^{125}I-ST in the presence or absence of 1 μM nonradioactive 14-amino acid analog of ST. After incubation, disuccinimidyl suberate (in dimethyl sulfoxide) was added to a final concentration of 1 mM, and the cross-linking reaction was allowed to occur for 15 min at 25 °C. Reactions were terminated by the addition of 0.05 volume of 1 M Tris-HCl buffer, pH 7.6. Lubrol-PX and phenylmethanesulfonyl fluoride were added to aliquots of quenched cross-linking reaction mixtures to final concentrations of 0.1% (w/v) and 0.1 mM, respectively. The samples were centrifuged at 200,000 × g for 60 min at 4 °C. Supernatant fractions (100 μl) were applied to the Spherogel TSK G3000 SW column, and each 0.2-ml fraction was collected and assayed for radioactivity to locate the ^{125}I-ST-cross-linked protein. Furthermore, affinity-labeled membrane and Lubrol-PX-solubilized preparations were analyzed by sodium dodecyl sulfate-polyacrylamide gel electrophoresis of 0.75-mm slab gels containing 5–15% or 7.5% acrylamide by the method of Laemmli (25). Samples were boiled for 3 min in the buffer containing 1.2% sodium dodecyl sulfate and 350 mM 2-mercaptoethanol prior to application to the gel. After electrophoresis, the gels were stained, destained, and dried for autoradiography. Molecular weight standards were phosphorylase *b*, bovine serum albumin, ovalbumin, carbonic anhydrase, soybean trypsin inhibitor, and α-lactalbumin.

Proteins were determined by a modification (26) of the procedure described by Lowry *et al.* (27).

RESULTS

Conditions for Solubilization—We evaluated a wide range of detergents for use in solubilizing the ST receptor and particulate guanylate cyclase. Lubrol-PX was superior in extracting ST receptor and guanylate cyclase from rat intestinal brush-border membranes when compared with sodium deoxycholate, sodium cholate, CHAPS, Triton X-100, or digitonin. When intestinal brush-border membranes were solubilized at a protein concentration of 1 mg/ml, sodium deoxycholate (5 mM) and sodium cholate (25 mM) solubilized 75 and 38% of the ST receptor, respectively. However, both of them inhibited the particulate guanylate cyclase activity to less than 10% of the Lubrol-PX-solubilized preparations. CHAPS (10 mM) and Triton X-100 (0.3%) solubilized 21 and 23% of the ST receptor, respectively. However, they solubilized less than 10% of the particulate guanylate cyclase from the original brush-border membrane. Digitonin (1%) solubilized 38% of the ST receptor and 22% of the particulate guanylate cyclase. (The values are the means of two independent experiments that were done with triplicate determinations.) On the other hand, Lubrol-PX (0.1%) solubilized 54 ± 8% of ST receptor and 42 ± 6% of the particulate guanylate cyclase. (The values are mean ± S.E. of five independent experiments.) Higher detergent concentrations did not significantly increase the total activity solubilized; however, lower specific activities were

The Journal of Biological Chemistry

found due to an increase in total protein extracted from membranes (data not shown).

Binding Characteristics of Solubilized Receptor—Specific binding of ^{125}I-ST to purified brush-border membrane preparations was measured in the presence of increasing concentrations of ^{125}I-ST. As shown in Fig. 1, Scatchard analysis gave a linear relationship indicating a single class of specific binding sites. The B_{max} and K_D values obtained by computer fitting of data to a Scatchard plot were 5.4 ± 0.6 pmol/mg protein and 1.4 ± 0.2 nM, respectively. ^{125}I-ST binding to solubilized preparations resembled very closely the binding to membranes. Scatchard analysis of binding of ^{125}I-ST to solubilized preparations also revealed a single class of binding sites (Fig. 1). The solubilized receptor had a B_{max} value of 6.2 ± 0.5 pmol/mg protein and K_D value of 1.4 ± 0.2 nM, respectively.

To determine whether ^{125}I-ST binding sites in the membrane and solubilized preparations represent biologically relevant ST receptors, we evaluated the effects of several ST analogs to compete for ^{125}I-ST binding. As shown in Fig. 2*A*, the 19-amino acid synthetic analog and 14-amino acid synthetic analog of ST, which retain enterotoxic activity (9, 19), inhibited ^{125}I-ST binding to brush-border membrane preparations at concentrations of 1–100 nM. Conotoxin GI shares a partial sequence homology with ST, representing a common antigenic determinant, but has no enterotoxic activity (19). Conotoxin GI did not inhibit ^{125}I-ST binding. Similarly, a 6-residue synthetic peptide encompassing the region common to ST and conotoxin GI, which also has no enterotoxic activity, did not inhibit ^{125}I-ST binding. Inhibition curves of ^{125}I-ST binding to solubilized preparations by these four synthetic peptides were identical to those obtained with membrane preparations (Fig. 2*B*).

Specific ^{125}I-ST binding to membrane and solubilized preparations from rat intestinal brush border was altered by the

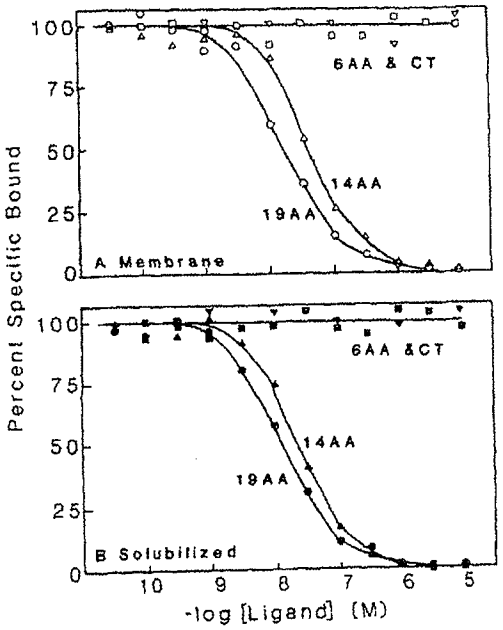

FIG. 2. **Inhibition of ^{125}I-ST binding to membrane (*A*) and solubilized (*B*) preparations from rat intestinal brush border.** Varying concentrations of peptides were incubated with 1 nM ^{125}I-ST and membrane (*open symbols*) or solubilized (*closed symbols*) preparations as described under "Experimental Procedures." Percentage values (*Percent Specific Bound*) were calculated by dividing the specific ^{125}I-ST binding at each point by maximum specific binding. Nonspecific binding was determined with 1 μM 14-amino acid analog of ST. The data presented are representative of three experiments with similar results. *19AA* (○, ●), 19-amino acid analog of ST; *14AA* (△, ▲), 14-amino acid analog of ST; *6AA* (□, ■), 6-amino acid residue of ST; *CT* (▽, ▼), conotoxin GI.

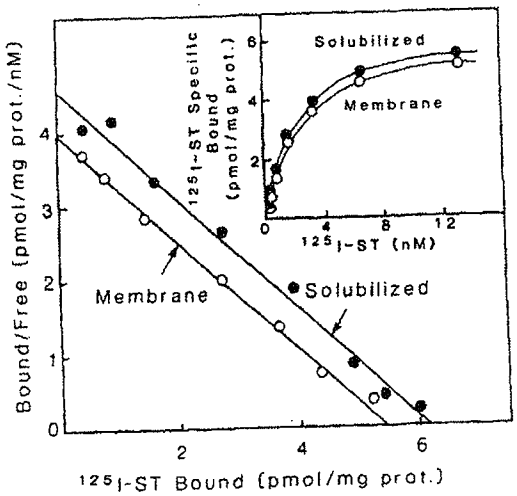

FIG. 1. **^{125}I-ST binding to membrane and solubilized preparations from rat intestinal brush border.** Scatchard plots and binding saturation curves (*inset*) for membrane (*open circles*) and solubilized (*closed circles*) preparations are shown. Aliquots (20 μl) of membrane or solubilized preparations containing 2 μg of protein were incubated with increasing concentrations of ^{125}I-ST for 15 min at 37 °C. Nonspecific binding was determined by parallel incubations in the presence of 1 μM 14-amino acid analog of ST. Binding data were plotted after correction for nonspecific binding. B_{max} and K_D values were 5.4 ± 0.6 pmol/mg protein and 1.4 ± 0.2 nM, respectively, for the membrane preparations and 6.2 ± 0.5 pmol/mg protein and 1.4 ± 0.2 nM, respectively, for the solubilized preparations. The values are mean ± S.E. of three experiments.

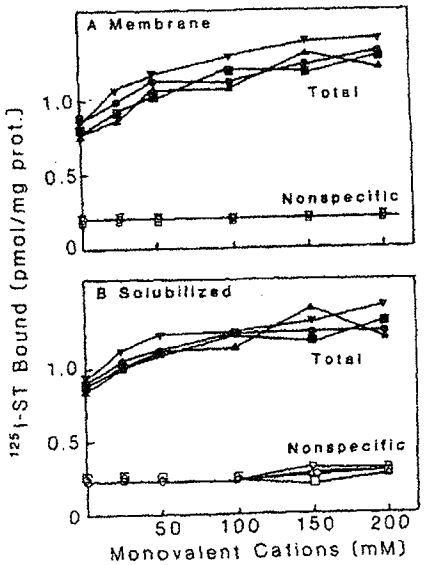

FIG. 3. **Effect of monovalent cations on ^{125}I-ST binding to membrane (*A*) and solubilized (*B*) preparations from rat intestinal brush border.** The figure displays total binding (*closed symbols*) and nonspecific binding (*open symbols*) of 1 nM ^{125}I-ST measured in the absence and in the presence of 1 μM 14-amino acid analog of ST. The results are the average of two separate experiments. ●, ○, Na; ▲, △, K; ■, □, Li; ▼, ▽, NH_4.

addition of various cations. Fig. 3 shows that inclusion of high concentrations of monovalent cations improved specific binding of ^{125}I-ST predominantly by increasing total binding without affecting nonspecific binding. All four (Li^+, Na^+, K^+, and NH_4^+) monoalent cations when tested at 150 mM almost equally increased specific binding by about 80% in the membrane and by 60% in the solubilized preparations. As shown in Fig. 4, low concentration of divalent cations similarly enhanced specific binding of ^{125}I-ST. Addition of 8 mM Mn^{2+}, Mg^{2+}, and Ca^{2+} increased specific binding by 81, 67, and 37%, respectively, in the membrane preparations and 62, 29, and 17%, respectively, in the solubilized preparations. In contrast to monovalent cations, divalent cations increased nonspecific binding both in the membrane and solubilized preparations. In the absence of cation, B_{max} and K_D values obtained by fitting data to a Scatchard plot were 5.6 ± 0.5 pmol/mg protein and 2.9 ± 0.3 nM, respectively, for the membrane preparations and 6.4 ± 0.6 pmol/mg protein and 2.2 ± 0.2 nM, respectively, for the solubilized preparations (mean ± S.E. of three independent experiments). These results in the absence and presence of 150 mM NaCl (Fig. 1) indicate that these cations increased the affinity of the ST receptor for ^{125}I-ST without altering the receptor number. The divalent cations also affected only the K_D values, and the effects of divalent and monovalent cations on the specific binding were not additive (data not shown). In subsequent experiments binding was conducted in the presence of 150 mM NaCl, a concentration that was maximally effective. Divalent cations were not included because this increased nonspecific binding.

Characterization of the Solubilized ST Receptor—Some properties of the solubilized ST receptor and particulate guanylate cyclase were compared to determine if these activities reside on the same or different proteins.

To determine the Stokes radius of the ST receptor on gel filtration, the solubilized receptor was treated in two ways. In some experiments, the solubilized preparation was applied to a Spherogel-TSK G3000SW column, followed by elution in the presence of 0.1% Lubrol-PX. The collected fractions were assayed for ^{125}I-ST binding and guanylate cyclase activity (Fig. 5A). In other experiments, ^{125}I-ST was bound first to the solubilized receptor followed by application of the receptor-^{125}I-ST complex to the column (Fig. 5B). The time required for completion of chromatography was less than 1 h, during which there was minimal dissociation of ^{125}I-ST from the receptor. The peak of receptor-binding activity eluted at the same position relative to standard proteins in both types of experiments (Fig. 5). The Stokes radius was estimated at 5.5 ± 0.1 nm (mean ± S.E. of three experiments). In contrast, as shown in Fig. 5A, solubilized particulate guanylate cyclase activity eluted earlier than the ST receptor peak and migrated as a protein with a Stokes radius of 5.8 ± 0.1 nm (mean ± S.E. of three experiments).

Sedimentation coefficients of the ST receptor and particulate guanylate cyclase were estimated using a gradient of 5–20% sucrose (Fig. 6). Solubilized fractions were layered onto

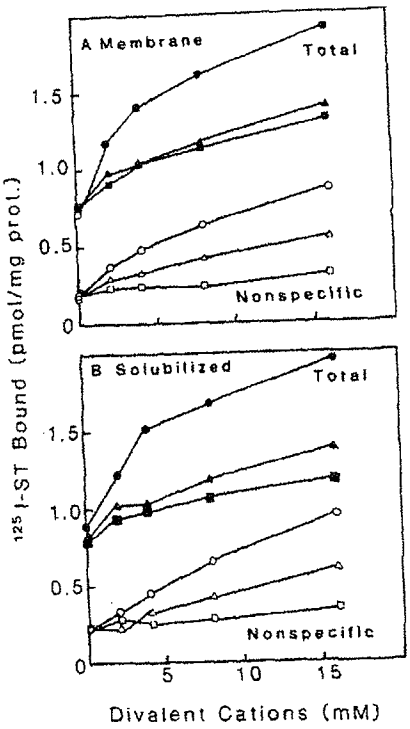

FIG. 4. **Effect of divalent cations on ^{125}I-ST binding to membrane (*A*) and solubilized (*B*) preparations from rat intestinal brush border.** The figure displays total binding (*closed symbols*) and nonspecific binding (*open symbols*) of 1 nM ^{125}I-ST measured in the absence and in the presence of 1 μM 14-amino acid analog of ST. The results are the average of two separate experiments performed in the absence of added monovalent cations. ●, ○, Mn; ▲, △, Ca; ■, □, Mg.

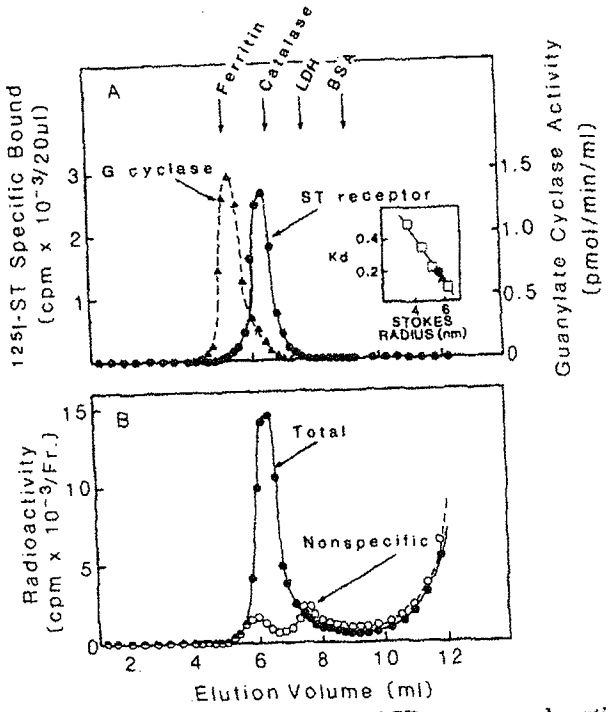

FIG. 5. **Gel filtration of solubilized ST receptor and particulate guanylate cyclase.** *A*, gel filtration of a solubilized preparation from rat intestinal brush border was followed by assay of fractions for specific ^{125}I-ST binding (*^{125}I-ST Specific Bound*, ●) and guanylate cyclase (▲) activities as described under "Experimental Procedures." The Stokes radii of ST receptor and guanylate cyclase were estimated at 5.5 ± 0.1 and 5.8 ± 0.1 nm, respectively. *B*, a solubilized fraction was incubated with 1 nM ^{125}I-ST in the presence (○, nonspecific) or absence (●, total) of 1 μM 14-amino acid analog of ST and then subjected to gel filtration. The Stokes radius of specifically labeled protein was estimated at 5.5 ± 0.1 nm. Markers were bovine serum albumin (*BSA*, 3.6 nm), lactate dehydrogenase (*LDH*, 4.5 nm), catalase (5.2 nm), and ferritin (6.1 nm). The values are mean ± S.E. of three experiments. The *inset* shows a standard curve of the distribution coefficient, K_d, *versus* Stokes radius of the calibrating proteins.

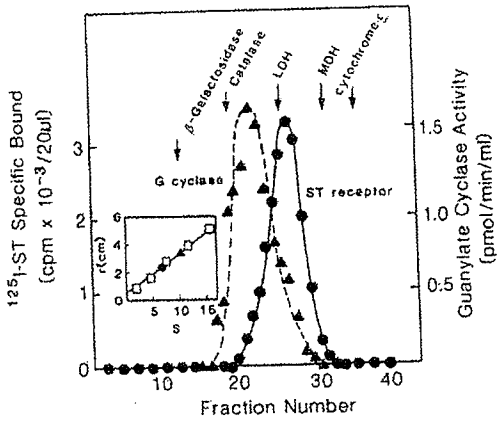

FIG. 6. **Sucrose density gradient centrifugation of solubilized ST receptor and particulate guanylate cyclase.** Sucrose density gradient centrifugation was carried out as described under "Experimental Procedures." Each fraction was assayed for specific ^{125}I-ST binding (*^{125}I-ST Specific Bound*, ●) and guanylate cyclase (▲) activities. The sedimentation coefficients of ST receptor and guanylate cyclase were calculated as 7.0 ± 0.4 and 10.0 ± 0.3 S, respectively. The markers were cytochrome *c* (1.9 S), malate dehydrogenase (*MDH*, 4.6 S), lactate dehydrogenase (*LDH*, 7.3 S), catalase (11.4 S), and β-galactosidase (16 S). The values are mean ± S.E. of three experiments. The *inset* shows a calibrating curve of distances (*r (cm)*) traveled by proteins *versus* S.

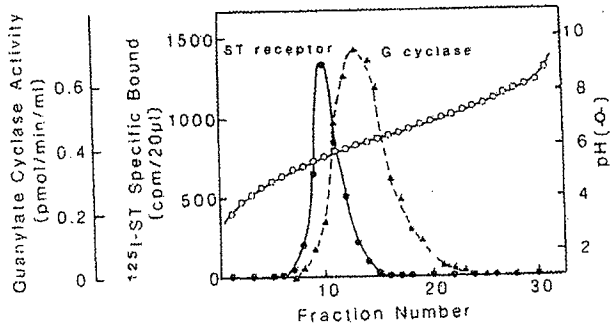

FIG. 7. **Isoelectric focusing of solubilized ST receptor and particulate guanylate cyclase.** Isoelectric focusing was carried out as described under "Experimental Procedures." Each fraction was assayed for ^{125}I-ST binding (●) and guanylate cyclase (▲) activities. The ST receptor and guanylate (*G*) cyclase had isoelectric points of 5.5 ± 0.2 and 5.9 ± 0.1, respectively. The values are mean ± S.E. of three experiments.

the gradients, and after centrifugation each fraction was assayed for ^{125}I-ST binding and guanylate cyclase activity. The peak of ^{125}I-ST binding with a sedimentation coefficient of 7.0 ± 0.4 S was clearly separated from the peak of guanylate cyclase with a coefficient of 10.0 ± 0.3 S (mean ± S.E. of three experiments) (Fig. 6).

The isoelectric points of the ST receptor and particulate guanylate cyclase were determined by isoelectric focusing of the Lubrol-PX-solubilized rat intestinal brush-border preparations as described above. The mobilities of the ST receptor and particulate guanylate cyclase are summarized in Fig. 7. The peak of ST receptor had an isoelectric point of 5.5 ± 0.2 and was separated from that of guanylate cyclase which had an isoelectric point of 5.9 ± 0.1 (mean ± S.E. of three experiments).

Affinity Cross-linking of ST Receptor—Analysis of affinity-labeled receptor was performed in two ways. Membranes containing cross-linked ^{125}I-ST were solubilized with 0.1% Lubrol-PX, and solubilized ^{125}I-ST-receptor complexes were applied to gel filtration as described above. The cross-linked ^{125}I-ST-receptor complex behaved similarly to its noncross-linked counterpart (see Fig. 5) and had a stokes radius of 5.5 ± 0.1 nm (mean ± S.E. of three experiments) (Fig. 8*A*). Furthermore, when cross-linked receptor was mixed with the noncross-linked control, a single peak was observed at the same elution position (data not shown).

With the receptor covalently linked to the labeled toxin, samples were also analyzed by sodium dodecyl sulfate-polyacrylamide gel electrophoresis in the presence of reducing agent and by autoradiography as described above. As shown in Fig. 8*B*, the pattern of labeled polypeptides obtained with either cross-linked membranes or cross-linked Lubrol-PX-solubilized preparations were identical. Three specifically labeled protein bands with apparent molecular weights of 80,000, 68,000, and 60,000 were observed (Fig. 8*B*). Incubation of samples with an increasing amount of unlabeled ligand

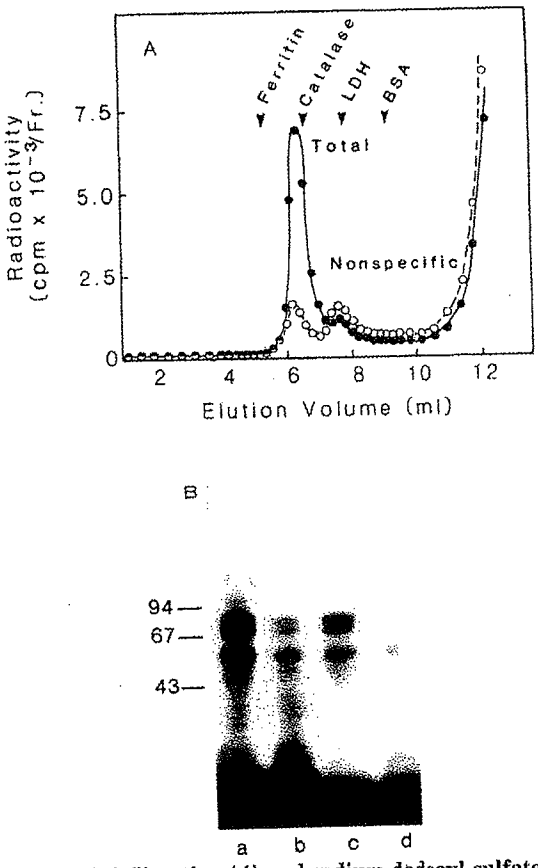

FIG. 8. **Gel filtration (*A*) and sodium dodecyl sulfate-polyacrylamide gel electrophoresis (*B*) of affinity-labeled ST receptor.** *A*, membranes were cross-linked with 4 nM ^{125}I-ST in the presence (○, nonspecific) or in the absence (●, total) of 1 μM 14-amino acid analog of ST. Samples solubilized with 0.1% Lubrol-PX were subjected to gel filtration as described under "Experimental Procedures." The Stokes radius of cross-linked protein was estimated at 5.5 ± 0.1 nm (mean ± S.E. of three experiments). *B*, autoradiography of affinity-labeled ST receptor on sodium dodecyl sulfate-polyacrylamide gel electrophoresis. Cross-linking and solubilization of the membrane were performed as described above. The membrane suspension (*a*, *b*) and the Lubrol-PX solubilized fraction (*c*, *d*) were subjected to electrophoresis using 5–15% gradient gels and to autoradiography as described under "Experimental Procedures." *Lanes b* and *d* show the nonspecific labeling that was observed in the presence of 1 μM 14-amino acid analog of ST. Molecular weight markers were phosphorylase *b* (94,000), bovine serum albumin (67,000) and ovalbumin (43,000). This experiment was repeated three times with similar results.

during cross-linking could not demonstrate an apparent difference in the relative affinities of the three protein bands (Fig. 9). The addition of various protease inhibitors to the buffers used for homogenization and other procedures also did not affect these labeling patterns (data not shown).

DISCUSSION

Dreyfus and Robertson (15) reported the use of CHAPS, a dipolar ionic detergent, for the solubilization of the ST receptor. We found that the yields of solubilized ST receptor and particulate guanylate cyclase with Lubrol-PX was higher than that obtained with CHAPS. Furthermore, sharper separations in various chromatographic procedures were achieved with Lubrol-PX (data not shown). Therefore, in the present study, with an aim being the chromatographic separation of the ST receptor and particulate guanylate cyclase, we used Lubrol-PX as a solubilizing agent. Saturation isotherms of ^{125}I-ST binding to membrane and solubilized preparations were identical (Fig. 1), and displacement patterns of ^{125}I-ST binding to membrane and solubilized preparations by synthetic analogs of ST were also identical (Fig. 2). These results indicate that the toxin-binding site retains its original binding characteristics after its extraction from a lipid-rich membrane environment.

As summarized in Figs. 3 and 4, binding of ^{125}I-ST to membrane and solubilized preparations of receptor was enhanced by various cations. It is noteworthy that similar effects on ligand binding by cations were also observed with specific receptor for atriopeptins (28). To date, ST (7–9) and atriopeptins (29, 30) are the only peptides that specifically activate particulate guanylate cyclase in cell-free systems. The effects of cations on the binding of these heat-stable peptides to their receptors may suggest that the coupling mechanisms of these receptors and particulate guanylate cyclase share some common features. However, this remains to be determined.

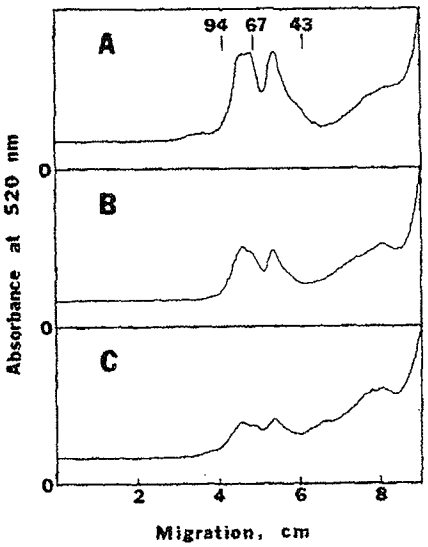

FIG. 9. **Densitometric analysis of the inhibition of the labeling with increasing amount of unlabeled ST.** Membranes were incubated with 4 nM ^{125}I-ST in the absence (*A*) and the presence of 10 nM (*B*) or 100 nM (*C*) 14-amino acid analog of ST. Sodium dodecyl sulfate-polyacrylamide gel electrophoresis and autoradiography of the labeled membranes were performed as described in the legend of Fig. 8. Two bands (80,000 and 68,000 daltons) were not resolved well by the densitometer and appeared as a single broad peak. The labeling of the three bands with ^{125}I-ST was inhibited to a similar extent by unlabeled ST.

With all of the techniques employed the solubilized ST receptor and particulate guanylate cyclase were readily separable (Figs. 5, 6, and 7). Furthermore, the ST receptor migrated as a single peak with all the methods used. These results and the linear Scatchard plots in Fig. 1 indicate that there is a single class of ST receptors and that this macromolecule is separate from particulate guanylate cyclase. We have evidence from studies with adsorption to Con A-agarose and elution with α-methyl mannoside that the solubilized ST receptor is a glycoprotein (data not shown). As reported previously, particulate guanylate cyclase from mammalian tissue (20) and sea urchin sperm (31) is also a glycoprotein. This suggests that both the guanylate cyclase receptor and particulate guanylate cyclase are separate transmembrane glycoproteins that are closely coupled. Although the coupling mechanism between the ST receptor and particulate guanylate cyclase is not presently known, cytoskeletal elements appear to play an important role in this interaction. The evidence in support of this hypothesis is that solubilized preparations fail to increase cyclic GMP synthesis with the addition of ST. However, residual membranes after detergent extraction contains some functionally coupled ST receptor and guanylate cyclase (*i.e.* increased cyclic GMP synthesis with the addition of ST) (15).[2]

When ^{125}I-ST was cross-linked to intestinal brush-border membranes followed by solubilization and analysis on gel filtration chromatography (Fig. 8*A*), the ^{125}I-ST-receptor complex migrated as a sharp single peak similar to the experiments without cross-linking. Mixing experiment with cross-linked and non-cross-linked receptor also exhibited a single peak at the same position (data not shown). These results indicated that the cross-linking procedure did not produce gross alterations in the molecular size of the receptor and that ^{125}I-ST was covalently attached to its receptor and not to some other membrane protein in close proximity. From the gel filtration and sedimentation data the size of the ST receptor is estimated to be about 200,000 daltons. Three peptides (about 80,000, 68,000, and 60,000 daltons) were labeled when cross-linked membrane preparations were subjected to sodium dodecyl sulfate-polyacrylamide gel electrophoresis (Fig. 8*B*). Similar results were obtained when Lubrol-PX-solubilized preparations were used. Incubation of samples with increasing amounts of cold ligand during the cross-linking procedure indicated that these three bands have similar affinities for ST (Fig. 9). These experiments suggest that the ST receptor contains three peptides with binding domains for the toxin. The possibility of receptor heterogeneity with similar affinities cannot be excluded. While similar results were obtained when various protease inhibitors were included in the buffers, we cannot exclude the possibility that these peptides are derived proteolytically from a larger peptide. Previous reports suggesting that binding of ST to its receptor is irreversible presented autoradiographic patterns of ^{125}I-ST-labeled ST receptor using sodium dodecyl sulfate-polyacrylamide gel electrophoresis in the absence of cross-linking (13, 15). In contrast, we observed that the binding of ST to its receptor is reversible and the dissociation of bound ^{125}I-ST can be increased by addition of a large excess of unlabeled ST, as reported by Giannella *et al.* (12). Furthermore, covalent cross-linking of ST to its receptor was required to prevent dissociation of ^{125}I-ST during electrophoresis (data not shown). Although the reasons for these discrepancies are unclear, it is apparent from the present studies that covalent

[2] T. Kuno, Y. Kamisaki, S. A. Waldman, J. Gariepy, G. Schoolnik, and F. Murad, unpublished observations.

affinity labeling of the ST receptor is necessary to study the binding subunit structure of the toxin receptor.

REFERENCES

1. Gyles, C. L. (1971) *Ann. N. Y. Acad. Sci.* **176,** 314–322
2. Banwell, J. G., and Sherr, H. (1973) *Gastroenterology* **65,** 467–497
3. Sack, D. A., Merson, M. H., Wells, J. G., Sack, R. B., and Morris, G. K. (1975) *Lancet* **2,** 239–241
4. Sack, R. B. (1975) *Annu. Rev. Microbiol.* **29,** 333–353
5. Giannella, R. A. (1981) *Annu. Rev. Med.* **32,** 341–357
6. Hughes, J. M., Murad, F., Chang, B., and Guerrant, R. L. (1978) *Nature* **271,** 755–756
7. Field, M., Graf, L. H., Jr., Laird, W. J., and Smith, P. L. (1978) *Proc. Natl. Acad. Sci. U. S. A.* **75,** 2800–2804
8. Guerrant, R. L., Hughes, J. M., Chang, B., Robertson, D. C., and Murad, F. (1980) *J. Infect. Dis.* **142,** 220–228
9. Waldman, S. A., O'Hanley, P. D., Falkow, S., Schoolnik, G., and Murad, F. (1984) *J. Infect. Dis.* **149,** 83–89
10. Kimura, H., and Murad, F. (1974) *J. Biol. Chem.* **249,** 6910–6919
11. Quill, H., and Weiser, M. M. (1975) *Gastroenterology* **69,** 470–478
12. Giannella, R. A., Luttrell, M., and Thompson, M. (1983) *Am. J. Physiol.* **245,** 492–498
13. Frantz, J. C., Jaso-Freidman, L., and Robertson, D. C. (1984) *Infect. Immun.* **43,** 622–630
14. Dreyfus, L. A., Jaso-Freidman, L., and Robertson, D. C. (1984) *Infect. Immun.* **44,** 493–501
15. Dreyfus, L. A., and Robertson, D. C. (1984) *Infect. Immun.* **46,** 537–543
16. de Jonge, H. R. (1984) *Biochem. Soc. Trans.* **12,** 180–184
17. Kuno, T., Waldman, S. A., Kamisaki,Y., Gariepy, J., Schoolnik, G., and Murad, F. (1985) *Fed. Proc.* **44,** 1798
18. Alderete, J. F., and Robertson, D. C. (1978) *Infect. Immun.* **19,** 1021–1030
19. Gariepy, J., O'Hanley, P. D., Waldman, S. A., Murad, F., and Schoolnik, G. K. (1984) *J. Exp. Med.* **160,** 1253–1258
20. Waldman, S. A., Lewicki, J. A., Chang, L. Y., and Murad, F. (1983) *Mol. Cell. Biochem.* **57,** 155–166
21. Hauser, H., Howell, K., Dawson, R. M. C., and Bower, D. E. (1980) *Biochim. Biophys. Acta* **602,** 567–577
22. Bruns, R. F., Lawson-Wendling, K., and Pugsley, T. A. (1983) *Anal. Biochem.* **132,** 74–81
23. Steiner, A. L., Parker, C. W., and Kipnis, D. M. (1972) *J. Biol. Chem.* **247,** 1106–1113
24. Hall, J. M., Frankham, P. A., and Strange, P. G. (1983) *J. Neurochem.* **41,** 1526–1532
25. Laemmli, U. K. (1970) *Nature* **227,** 680–685
26. Peterson, G. L. (1977) *Anal. Biochem.* **83,** 346–356
27. Lowry, O. H., Rosebrough, N. J., Farr, A. L., and Randall, R. J. (1951) *J. Biol. Chem.* **193,** 265–275
28. De Lean, A., Gutkowska, J., McNicoll, N., Schiller, P. W., and Cantin, M., and Genest, J. (1984) *Life Sci.* **35,** 2311–2318
29. Waldman, S. A., Rapoport, R. M., and Murad, F. (1984) *J. Biol. Chem.* **259,** 14332–14334
30. Winquist, R. J., Faison, E. P., Waldman, S. A., Schwartz, K., Murad, F., and Rapoport, R. M. (1984) *Proc. Natl. Acad. Sci. U. S. A.* **81,** 7661–7664
31. Radany, E. W., Gerzer, R., and Garbers, D. L. (1983) *J. Biol. Chem.* **258,** 8346–8351

US005518888A

United States Patent [19]

Waldman

[11] Patent Number: 5,518,888

[45] Date of Patent: May 21, 1996

[54] **ST RECEPTOR BINDING COMPOUNDS AND METHODS OF USING THE SAME**

[75] Inventor: **Scott A. Waldman**, Ardmore, Pa.

[73] Assignee: **Thomas Jefferson University**, Philadelphia, Pa.

[21] Appl. No.: **141,892**

[22] Filed: **Oct. 26, 1993**

[51] **Int. Cl.**[6] **G01N 33/574**; A61K 51/00; A61K 51/08

[52] **U.S. Cl.** **435/7.23**; 424/1.69; 424/9.1; 424/9.341

[58] **Field of Search** 424/1.49, 1.69, 424/9, 85.8, 9.1, 9.341; 435/7.21, 7.23; 530/388.22, 388.26, 388.8, 389.7, 324, 325, 326, 327

[56] **References Cited**

U.S. PATENT DOCUMENTS

5,160,723 11/1992 Welt et al. 424/1.69

OTHER PUBLICATIONS

Almenoff et al., "Ligand–based Histochemical Localization and Capture of Cells Expressing Heat–Stable Enterotoxin Receptors", *Molecular Microbiology* 8: 865–873 (1993).

Bjorn et al., "Antibody–Pseudomonas Exotoxin A Conjugates Cytotoxic to Human Breat Cancer Cells In Vitro", *Cancer Research* 46: 3262–3267 (1986).

Bjorn et al., "Evaluation of Monoclonal Antibodies for the Development of Breast Cancer Immunotoxins", *Cancer Research* 45: 1214–1221 (1985).

Bodansky et al., "Peptide Synthesis", John Wiley and Sons, 2d Ed. (1976).

Burgess et al., "Biological Evaluation of a Methanol–Soluble, Heat–Stable *Escherichia coli* Enterotoxin in Infant Mice, Pigs, Rabbits, and Calves", *Infection and Immunity* 21: 526–531 (1978).

Cawley and Herschman, "Epidermal Growth Factor–Toxin A Chain Conjugates: EGF–Ricin A is a Potent Toxin While EGF–Diphtheria Fragment A is Nontoxic", *Cell* 22: 563–570 (1980).

Chan and Giannella, "Amino Acid Sequence of Heat–stable Enterotoxin Produced by *Escherichia coli* Pathogenic for Man", *J. Biol. Chem.* 256: 7744–7746 (1981).

Chung and Collier, "Enzymatically Active Peptide from the Adenosine Diphosphate–Ribosylating Toxin of *Pseudomonas Aeruginosa" Infection and Immunity* 16: 832–841 (1977).

Eckelman et al., "Comparison of ^{99m}Tc and ^{111} In Labeling of Conjugated Antibodies", *Nucl. Med. Biol.* 13: 335–343 (1986).

Gros, O., "Biochemical Aspects of Immunotoxin Preparation", *J. Immunol. Melth.* 81: 283–297 (1985).

Gyles, C. L., "Discussion: Heat–Labile and Heat–Stable Forms of the Enterotoxin form *E. coli* Strains Enteropathogenic For Pigs", *Ann N.Y. Acad. Sci.* 16: 314–321 (1979).

Hakki et al., "Solubilization and Charaterization of Functionally Coupled *Escherichia coli* Heat–Stable Toxin Recpeptors and Particulate Guanylate Cyclas Associated with the Cytoskeleton Compartment of Intestinal Membranes", *Int. J. Biochem* 25: 557–566 (1993).

Magerstadt, M., *"Antibody Conjugates and Malignant Disease" Baca Raton: CRC Press, 110–152 (1991).*

Richardson et al., "Astatine (^{211}At) as a Therapeutic Radionuclide. The Plasma: Blood Cell distribution in Vitro", *Nucl. Med. Biol.* 13: 583–584 (1986).

Cumber et al., "Preparation of Antibody–Toxin Conjugates", *Methods in Enzymology* 112: 207–225 (1985).

Currie et al., "Guanylin: An Endogenous Activator of Intestinal Guanylate Cyclase", *Proc. Natl. Acad. Sci. USA* 89: 947–951 (1992).

Dreyfus et al, "Chemical Properties of Heat–Stable Enterotoxins Produced by Enterotoxigenic *Escherichia coli* of different Host Origins", *Infection and Immunity* 42: 539–548 (1983).

Evans et al., "Differences in the Response of Rabbit Small Intestine to Heat–Labile and Heat–Stable Enterotoxins of *Escherichia coli", Infection and Immunity* 7: 873–880 (1973).

Fitzgerald et al., "Adenovirus–Induced Release of Epidermal Growth Factor and Pseudomonas Toxin into the Cytosol of KB Cells during Receptor–Mediated Endocytosis", *Cell* 32: 607–617 (1983).

(List continued on next page.)

Primary Examiner—Toni R. Scheiner
Assistant Examiner—Lora M. Green
Attorney, Agent, or Firm—Woodcock Washburn Kurtz Mackiewicz & Norris

[57] **ABSTRACT**

Conjugated compounds which comprises an ST receptor binding moiety and a radiostable active moiety are disclosed. Pharmaceutical compositions comprising a pharmaceutically acceptable carrier or diluent, and a conjugated compound which comprises an ST receptor binding moiety and a radiostable active moiety or an ST receptor binding moiety and a radioactive active moiety are disclosed. Methods of treating an individual suspected of suffering from metastasized colorectal cancer comprising the steps of administering to said individual a pharmaceutical composition comprising a pharmaceutically acceptable carrier or diluent, and a therapeutically effective amount of a conjugated compound which comprises an ST receptor binding moiety and a radiostable active moiety or an ST receptor binding moiety and a radiostable active moiety are disclosed. Methods of radioimaging metastasized colorectal cancer cells comprising the steps of first administering to an individual suspected of having metastasized colorectal cancer cells, a pharmaceutical composition that comprises a pharmaceutically acceptable carrier or diluent, and conjugated compound that comprises an ST receptor binding moiety and a radioactive active moiety wherein the conjugated compound is present in an amount effective for diagnostic use in humans suffering from colorectal cancer and then detecting the localization and accumulation of radioactivity in the individual's body are disclosed.

22 Claims, No Drawings

OTHER PUBLICATIONS

Fitzgerald, "Construction of Immunotoxins Using Pseudomonas Exotoxin A", *Methods in Enzymology* 151: 139–145 (1987).

Giannella et al., "Development of a Radioimmunoassay for *Escherichia coli* Heat–Stable Enterotoxin: Comparison with the Suckling Mouse Bioassay", *Infection and Immunity* 33: 186–192 (1981).

Hugues et al., "Identification and Characterization of a New Family of High–Affinity Receptors for *Escherichia coli* Heat–Stable Enterotoxin in Rat Intestinal Membranes", *Biochemistry* 30: 10738–10745 (1991).

Humm et al., "Dosimetric Aspects of Radiolabeled Antibodies for Tumor Therapy", *Journal of Nuclear Medicine* 27: 1490–1497 (1986).

Klipstein et al., "Development of a Vaccine of Cross–Linked Heat–Stable and HeatLabile Enterotoxins that Protects Against *Escherichia coli* Producing Either Enterotoxin", *Infection and Immunity* 37: 550–557 (1982).

Krejcarek and Tucker, "Covalent Attachment of Chelating Groups to Macromolecules", *Biochemical and Biophysical Research Communications* 77: 581–585 (1977).

Kwok, "Calculation of Radiation Doses for Nonuniformly Distributed β and γ Radionuclides in Soft Tissue", *Med. Phys.* 12: 405–412 (1985).

Leonard et al., "Kinetics of Protein Synthesis Inactivation in Human T–Lymphocytes by Selective monoclonal Antibody–Ricin Conjugates", *Cancer Research* 45: 5263–5269 (1985).

Masuho et al., "Importance of the Antigen–Binding Valency and the Nature of the Cross–Linking Bond in Ricin A–Chain Conjugates with Antibody", *J. Biochem* 91: 1583–1591 (1982).

Merrifield, "Solid Phase Peptide Synthesis. I. The Synthesis of a Tetrapeptide", *J. Am. Chem. Society* 15: 2149–2154 (1963).

Michel and Dirkx, "Fluorescence Studies of Nucleotides Binding to Diphtheria Toxin and Its Fragment A", *Biochimica et Biophysia Acta* 365: 15–27 (1974).

Moseley et al., "Isolation and Nucleotide Sequence Determination of a Gene Encoding a Heat–Stable Enterotoxin of *Escherichia coli", Infection and Immunity* 39: 1167–1174 (1983).

Okamoto et al., "Substitutions of Cysteine Residues of *Escherichia coli* Heat–Stable Enterotoxin By Oligonucleotide–Directed Mutagenesis", *Infection and Immunity* 55: 2121–2125 (1987).

Sack, "Human Diarrheal Disease Caused by Enterotoxigenic *Escherichia coli"Ann Rev. Microbiol.* 29: 333–353 (1975).

Shimonishi et al., "Mode of Disulfide Bond Formation of a Heat–Stable Enterotoxin (ST_h) Produced by a Human Strain of Enterotoxigenic *Escherichia coli", FEBS LETTERS* 215: 165–170 (1987).

So and McCarthy, "Nucleotide Sequence of the Bacterial Transposon Tn1681 Encoding a Heat–Stable (ST) Toxin and Its Identification in Enterotoxigenic *Escherichia coli* Strains", *Proc. Natl. Acad. Sci. USA* 77: 4011–4015 (1980).

Spitler et al., "Therapy of Patients with Malignant Melanome Using a monoclonal Antimelanoma Antibody–Ricin A Chain Immunotoxin", *Cancer Research* 47: 1717–1723 (1987).

Steinsträsser et al., "Selection of Nuclides for Immunoscintigraphy/Immunotherapy", *J. Nucl. Med.* 5: 875 (1988).

Thompson et al, "Biological and Immunological Characteristics of ^{125}I–4Tyr and —18Tyr *Escherichia coli* Heat–Stable Enterotoxin Species Purified by High–Performance Liquid Chromatography", *Analytical Biochemistry* 148: 26–36 (1985).

Thorpe et al., "New Coupling Agents for the Synthesis of Immunotoxins Containing a Hindered Disulfide Bond with Improved Stability In Vivo", *Cancer Research* 47: 5924–5931 (1987).

Waldman and O'Hanley, "Influence of a Glycine or Proline Substitution on the Functional Properties of a 14–Amino–Acid Analog of *Escherichia coli* Heat–Stable Enterotoxin", *Infection and Immunity* 57: 2420–2424 (1989).

Wessels and Rogus, "Radionuclide Selection and Model Absorbed Dose Calculations for Radiolabeled Tumor Associated Antibodies", *Med. Phys.* 11: 638–645 (1984).

Worrell et al., "Effect of Linkage Variation on Pharmacokinetics of Ricin A Chain–Antibody Conjugates in Normal Rats", *Anti–Cancer Drug Design* 1: 179–188 (1966).

Yoshimura et al, "Essential Structure for Full Enterotoxigenic Activity of Heat–Stable Enterotoxin Produced by Enterotoxigenic *Escherichia coli", FEBS* 2232 vol. 181: 138–142 (1985).

Franz et al., "The Production of ^{99m}Tc–Labeled Conjugated Antibodies Using A Cyclam–Based Bifunctional Chelating Agent", *J. Nucl. Med. Biol.* 14: 569–572 (1987).

Cohen, M., et al., "Receptors for *Escherichia coli* Heat Stable Enterotoxin in Human Intestine and in a Human Intestinal Cell Line (Caco–2)", *J. of Cellular Physicol.* 1993, 156, 138–144.

Guarino, A. et al., "T^{84} Cell Receptor Binding and Guanyl Cyclas Activaiton by *Escherichia coli* Heat–Stable Toxin", *Am. J. Physiol.* 253 (Gastrointest. Liver Physiol. 16): G775–780, 1987.

Vaandrager, A. et al, "Atriopeptins and *Escherichia coli* Enterotoxin ST^a Have Different Sites of Aciton in Mammalian Intestine", *Gastroenterology* 1992, 102(4), 1161–1169.

deSauvage, F. J. et al., "Primary Structure and Functional Expression of the Human Receptor for *Escherichia coli* Heat–stable Enterotoxin" J. Biol. Chem 266: 17912–17918 (1991).

Corstens et al., J. Nucl. Med., vol. 32, #3 pp. 491–494 (1991) "Chemotactic Peptides: New Locomotion for Imaging Infection?".

Thompson, Pathol. Immunopathol. Res., vol. 6, pp. 103–116 (1987) "*Escherichia coli* Heat–stable Enterotoxins and Their Receptors".

Fischman et al., J. Nucl. Med., vol. 34, pp. 2253–2263 (1993) "A Ticket to Ride: Peptide Radiopharmaceuticals".

ST RECEPTOR BINDING COMPOUNDS AND METHODS OF USING THE SAME

ACKNOWLEDGEMENT OF GOVERNMENT RIGHTS

This invention was made with Government support under grant number DK43805-01A2 awarded by the National Institutes of Health. The Government has certain rights in this invention.

FIELD OF THE INVENTION

The present invention relates to compounds which comprise a receptor ligand moiety conjugated to an active agent. More particularly, the present invention relates to compounds which comprise a moiety that binds to the ST receptor conjugated to a therapeutic or imaging moiety.

BACKGROUND OF THE INVENTION

Colorectal cancer is the third most common neoplasm worldwide and the second most common in the United States, representing about 15% of the newly diagnosed cases of cancer in the United States. The large intestine or large bowel is the third leading site for the development of new cancer and is diagnosed in about 150,000 patients each year. Colorectal cancer is the second leading cause of cancer-related deaths and is responsible for about 12% of cancer deaths in the United States. The mortality rate of newly diagnosed large bowel cancer approaches 50% and there has been little improvement over the past 40 years. Most of this mortality reflects local, regional and distant metastases. About thirty percent of patients with colorectal cancer have unresectable disease at presentation and about 40% develop metastases during the course of their disease. Distant metastatic disease is seen in liver (about 12%), lung (about 3%), bone (about 0.9%), brain (about 0.7%), nodes (about 4%), and peritoneum (about 2%) at the time of initial diagnosis. In 1987, the large bowel cancers found regionally or at distant sites at the time of diagnosis were about 26% and about 18%, respectively.

Surgery is the mainstay of treatment for colorectal cancer but recurrence is frequent. Colorectal cancer has proven resistant to chemotherapy, although limited success has been achieved using a combination of 5-fluorouracil and levamisole. Surgery has had the largest impact on survival and, in some patients with limited disease, achieves a cure. However, surgery removes bulk tumor, leaving behind microscopic residual disease which ultimately results in recrudescence. Overall recurrence rates for colonic tumors are about 33% and for rectal cancer about 42%. Of these recurrences, about 9% are local, about 13% are systemic metastatic disease, and the remaining 88% are a combination of local and systemic disease. Fifty percent of patients with recurrent colorectal cancer have hepatic metastases.

Early detection of primary, metastatic, and recurrent disease can significantly impact the prognosis of individuals suffering from colorectal cancer. Large bowel cancer diagnosed at an early stage has a significantly better outcome than that diagnosed at more advanced stages. The 5 year relative survival rates for patients with regional or distant metastases are 48% and 5%, compared with 90% and 77% for disease which is in situ or local, respectively, at the time of diagnosis. Similarly, diagnosis of metastatic or recurrent disease earlier potentially carries with it a better prognosis.

Although current radiotherapeutic agents, chemotherapeutic agents and biological toxins are potent cytotoxins, they do not discriminate between normal and malignant cells, producing adverse effects and dose-limiting toxicities. Over the past decade, a novel approach has been employed to more specifically target agents to tumor cells, involving the conjugation of an active agent to molecules which binds preferentially to antigens that exist predominantly on tumor cells. These conjugates can be administered systemically and specifically bind to the targeted tumor cells. Theoretically, targeting permits uptake by cells of cytotoxic agents at concentrations which do not produce serious toxicities in normal tissues. Also, selective binding to targeted tumor cells facilitates detection of occult tumor and is therefore useful in designing imaging agents. Molecular targeting predominantly has employed monoclonal antibodies generated to antigens selectively expressed on tumor cells.

Immunoscintigraphy using monoclonal antibodies directed at tumor-specific markers has been employed to diagnose colorectal cancer. Monoclonal antibodies against carcinoembryonic antigen (CEA) labeled with ^{99}Technetium identified 94% of patients with recurrent tumors. Similarly, ^{111}Indium-labeled anti-CEA monoclonal antibodies successfully diagnosed 85% of patients with recurrent colorectal carcinoma who were not diagnosed by conventional techniques. ^{125}Iodine-labeled antibodies have been effective in localizing more than 80% of the pathologically-confirmed recurrences by intraoperative gamma probe scanning.

Monoclonal antibodies have also been employed to target specific therapeutic agents in colorectal cancer. Preclinical studies demonstrated that anti-CEA antibodies labeled with ^{90}Yttrium inhibited human colon carcinoma xenografts in nude mice. Antibodies generated to colorectal cancer cells and coupled to mitomycin C or neocarzinostatin demonstrated an anti-tumor effect on human colon cancer xenografts in nude mice and 3 patients with colon cancer. Similar results in animals were obtained with monoclonal antibodies conjugated to ricin toxin A chain.

Due to the sensitivity, specificity, and adverse-effect profile of monoclonal antibodies, the results obtained using monoclonal antibody-based therapeutics have shown them to be less than ideal targeting tools. Although monoclonal antibodies have been generated to antigens selectively expressed on tumors, no truly cancer-specific antibody has been identified. Most antigens expressed on neoplastic cells appear to be quantitatively increased in these compared to normal cells but the antigens are nonetheless often present in normal cells. Thus, antibodies to such determinants can react with non-neoplastic tissues, resulting in significant toxicities. Also, antibodies are relatively large molecules and consequently, often evoke an immune response in patients. These immune responses can result in significant toxicities in patients upon re-exposure to the targeting agents and can prevent targeting by the monoclonal due to immune complex formation with degradation and excretion. Finally, binding of antibodies to tumor cells may be low and targeted agents may be delivered to cells in quantities insufficient to achieve detection or cytotoxicity.

There remains a need for compositions which can specifically target metastasized colorectal cancer cells. There is a need for imaging agents which can specifically bind to metastasized colorectal cancer cells. There is a need for improved methods of imaging metastasized colorectal cancer cells. There is a need for therapeutic agents which can specifically bind to metastasized colorectal cancer cells. There is a need for improved methods of treating individuals who are suspected of suffering from colorectal cancer cells,

especially individuals who are suspected of suffering from metastasis of colorectal cancer cells.

SUMMARY OF THE INVENTION

The present invention relates to conjugated compounds which comprises an ST receptor binding moiety and a radiostable active moiety.

The present invention relates to a pharmaceutical composition comprising a pharmaceutically acceptable carrier or diluent, and a conjugated compound which comprises an ST receptor binding moiety and a radiostable active moiety.

The present invention relates to a method of treating an individual suspected of suffering from metastasized colorectal cancer comprising the steps of administering to said individual a pharmaceutical composition comprising a pharmaceutically acceptable carrier or diluent, and a therapeutically effective amount of a conjugated compound which comprises an ST receptor binding moiety and a radiostable active moiety.

The present invention relates to a pharmaceutical composition comprising a pharmaceutically acceptable carrier or diluent, and conjugated compound that comprises an ST receptor binding moiety and a radioactive active moiety wherein the conjugated compound is present in an amount effective for therapeutic or diagnostic use in humans suffering from colorectal cancer.

The present invention relates to a method of radioimaging metastasized colorectal cancer cells comprising the steps of first administering to an individual suspected of having metastasized colorectal cancer cells, a pharmaceutical composition that comprises a pharmaceutically acceptable carrier or diluent, and conjugated compound that comprises an ST receptor binding moiety and a radioactive active moiety wherein the conjugated compound is present in an amount effective for diagnostic use in humans suffering from colorectal cancer and then detecting the localization and accumulation of radioactivity in the individual's body.

The present invention relates to a method of treating an individual suspected of suffering from metastasized colorectal cancer comprising the steps of administering to said individual a pharmaceutical composition comprising a pharmaceutically acceptable carrier or diluent, and a therapeutically effective amount of a conjugated compound which comprises an ST receptor binding moiety and a radioactive active moiety.

DESCRIPTION OF PREFERRED EMBODIMENTS OF THE INVENTION

As used herein, the terms "ST" and "native ST" are used interchangeably and are meant to refer to heat-stable toxin (ST) which is a peptide produced by *E. coli*, as well as other organisms. STs are naturally occurring peptides which 1) are naturally produced by organisms, 2) which bind to the ST receptor and 3) which activate the signal cascade that mediates ST-induced diarrhea.

As used herein, the term "ST receptor" is meant to refer to the receptors found on colorectal cells, including local and metastasized colorectal cancer cells, which bind to ST. In normal individuals, ST receptors are found exclusively in cells of intestine, in particular in cells in the duodenum, small intestine (jejunum and ileum), the large intestine, colon (cecum, ascending colon, transverse colon, descending colon and sigmoid colon) and rectum.

As used herein, the term "ST receptor ligand" is meant to refer to compounds which specifically bind to the ST receptor. ST is an ST receptor ligand. An ST receptor ligand may be a peptide or a non-peptide.

As used herein, the term "ST receptor binding peptide" is meant to refer to ST receptor ligands that are peptides.

As used herein, the term "ST peptides" is meant to refer to ST receptor binding peptides selected from the group consisting of SEQ ID NO:2, SEQ ID NO:3, SEQ ID NOS:5–54 and fragments and derivatives thereof.

As used herein, the term "fragment" is meant to refer to peptide a) which has an amino acid sequence identical to a portion of an ST receptor binding peptide and b) which is capable of binding to the ST receptor.

As used herein, the term "derivative" is meant to refer to a peptide a) which has an amino acid sequence substantially identical to at least a portion of an ST receptor binding peptide and b) which is capable of binding to the ST receptor.

As used herein, the term "substantially identical" is meant to refer to an amino acid sequence that is the same as the amino acid sequence of an ST peptide except some of the residues are deleted or substituted with conservative amino acids or additional amino acids are inserted.

As used herein, the term "active agent" is meant to refer to compounds that are therapeutic agents or imaging agents.

As used herein, the term "radiostable" is meant to refer to compounds which do not undergo radioactive decay; i.e. compounds which are not radioactive.

As used herein, the term "therapeutic agent" is meant to refer to chemotherapeutics, toxins, radiotherapeutics, targeting agents or radiosensitizing agents.

As used herein, the term "chemotherapeutic" is meant to refer to compounds that, when contacted with and/or incorporated into a cell, produce an effect on the cell including causing the death of the cell, inhibiting cell division or inducing differentiation.

As used herein, the term "toxin" is meant to refer to compounds that, when contacted with and/or incorporated into a cell, produce the death of the cell.

As used herein, the term "radiotherapeutic" is meant to refer to radionuclides which when contacted with and/or incorporated into a cell, produce the death of the cell.

As used herein, the term "targeting agent" is meant to refer compounds which can be bound by and or react with other compounds. Targeting agents may be used to deliver chemotherapeutics, toxins, enzymes, radiotherapeutics, antibodies or imaging agents to cells that have targeting agents associated with them and/or to convert or otherwise transform or enhance coadministered active agents. A targeting agent may include a moiety that constitutes a first agent that is localized to the cell which when contacted with a second agent either is converted to a third agent which has a desired activity or causes the conversion of the second agent into an agent with a desired activity. The result is the localized agent facilitates exposure of an agent with a desired activity to the metastasized cell.

As used herein, the term "radiosensitizing agent" is meant to refer to agents which increase the susceptibility of cells to the damaging effects of ionizing radiation. A radiosensitizing agent permits lower doses of radiation to be administered and still provide a therapeutically effective dose.

As used herein, the term "imaging agent" is meant to refer to compounds which can be detected.

As used herein, the term "ST receptor binding moiety" is meant to refer to the portion of a conjugated compound that constitutes an ST receptor ligand.

As used herein, the term "active moiety" is meant to refer to the portion of a conjugated compound that constitutes an active agent.

As used herein, the terms "conjugated compound" and "conjugated composition" are used interchangeably and meant to refer to a compound which comprises an ST receptor binding moiety and an active moiety and which is capable of binding to the ST receptor. Conjugated compounds according to the present invention comprise a portion which constitutes an ST receptor ligand and a portion which constitutes an active agent. Thus, conjugated compounds according to the present invention are capable of specifically binding to the ST receptor and include a portion which is a therapeutic agent or imaging agent. Conjugated compositions may comprise crosslinkers and/or molecules that serve as spacers between the moieties.

As used herein, the terms "crosslinker", "crosslinking agent", "conjugating agent", "coupling agent", "condensation reagent" and "bifunctional crosslinker" are used interchangeably and are meant to refer to molecular groups which are used to attach the ST receptor ligand and the active agent to thus form the conjugated compound.

As used herein, the term "colorectal cancer" is meant to include the well-accepted medical definition that defines colorectal cancer as a medical condition characterized by cancer of cells of the intestinal tract below the small intestine (i.e. the large intestine (colon), including the cecum, ascending colon, transverse colon, descending colon, and sigmoid colon, and rectum). Additionally, as used herein, the term "colorectal cancer" is meant to further include medical conditions which are characterized by cancer of cells of the duodenum and small intestine (jejunum and ileum). The definition of colorectal cancer used herein is more expansive than the common medical definition but is provided as such since the cells of the duodenum and small intestine also contain ST receptors and are therefore amenable to the methods of the present invention using the compounds of the present invention.

As used herein, the term "metastasis" is meant to refer to the process in which cancer cells originating in one organ or part of the body relocate to another part of the body and continue to replicate. Metastasized cells subsequently form tumors which may further metastasize. Metastasis thus refers to the spread of cancer from the part of the body where it originally occurs to other parts of the body. The present invention relates to methods of delivering active agents to metastasized colorectal cancer cells.

As used herein, the term "metastasized colorectal cancer cells" is meant to refer to colorectal cancer cells which have metastasized; colorectal cancer cells localized in a part of the body other than the duodenum, small intestine (jejunum and ileum), large intestine (colon), including the cecum, ascending colon, transverse colon, descending colon, and sigmoid colon, and rectum.

ST, which is produced by *E. coli*, as well as other organisms, is responsible for endemic diarrhea in developing countries and travelers diarrhea. ST induces intestinal secretion by binding to specific receptors, ST receptors, in the apical brush border membranes of the mucosal cells lining the intestinal tract. Binding of ST to ST receptors is non-covalent and occurs in a concentration-dependent and saturable fashion. Once bound, ST-ST receptor complexes appear to be internalized by intestinal cells, i.e. transported from the surface into the interior of the cell. Binding of ST to ST receptors triggers a cascade of biochemical reactions in the apical membrane of these cells resulting in the production of a signal which induces intestinal cells to secrete fluids and electrolytes, resulting in diarrhea.

ST receptors are unique in that they are only localized in the apical brush border membranes of the cells lining the intestinal tract. Indeed, they are not found in any other cell type in placental mammals. In addition, ST receptors are almost exclusively localized to the apical membranes, with little being found in the basolateral membranes on the sides of intestinal cells.

Mucosal cells lining the intestine are joined together by tight junctions which form a barrier against the passage of intestinal contents into the blood stream and components of the blood stream into the intestinal lumen. Therefore, the apical location of ST receptors isolates these receptors from the circulatory system so that they may be considered to exist separate from the rest of the body; essentially the "outside" of the body. Therefore, the rest of the body is considered "outside" the intestinal tract. Compositions administered "outside" the intestinal tract are maintained apart and segregated from the only cells which normally express ST receptors.

In individuals suffering from colorectal cancer, the cancer cells are often derived from cells that produce and display the ST receptor and these cancer cells continue to produce and display the ST receptor on their cell surfaces. Indeed, T84 cells, which are human colonic adenocarcinoma cells isolated from lung metastases, express ST receptors on their cell surface. Similarly, HT29glu-cells, which are human colonic adenocarcinoma cells, express receptors for ST. Thus, in individuals suffering from colorectal cancer, some metastasized intestinal cancer cells express ST receptors.

An effort was undertaken to determine the proportion of colorectal tumors which have the ST receptor. Sixteen colorectal cancer tumors, including ten local colorectal tumors and six metastasized tumors (3 liver, 1 lung, 1 lymphnode, 1 peritoneum), were tested and each possessed ST receptors. In each case, the affinity and density of receptors was amenable for targeting. That is, the cells possessed at least 10^4–10^6 receptors per cell and demonstrated an affinity of 10^{-7} or better (that is preferably between 10^{-8} to 10^{-9} or less; the lower number indicating a tighter bond, thus a higher affinity). Normal liver, lymphnode, peritoneum and lung cells were found not to possess ST receptors.

When such cancer cells metastasize, the metastasized cancer cells continue to produce and display the ST receptor. The expression of ST receptors on the surfaces of metastatic tumors provides a target for selective binding of conjugated compositions. ST receptors permit the absolutely specific targeting of therapeutic and diagnostic agents that are conjugated to ST receptor ligands to metastatic colorectal cancer cells.

The conjugated compositions of the present invention are useful for targeting cells that line the inner intestine wall including those cancer cells derived from such cells, particularly metastasized cancer cells derived from such cells. The conjugated compositions of the present invention which are administered outside the intestinal tract such as those administered in the circulatory system will remain segregated from the cells that line the intestinal tract and will bind only to cells outside the intestinal tract which are derived from the intestinal tract such as metastasized colorectal cells. The conjugated compositions will not bind to noncolorectal derived cells. Thus, the active moieties of conjugated compositions administered outside the intestinal tract are delivered to cells which are derived from the intestinal tract such

as metastasized colorectal cells but will not be delivered to any other cells.

Therapeutic and diagnostic pharmaceutical compositions of the present invention include conjugated compounds specifically targeted to metastatic disease. These conjugated compounds include ST receptor binding moieties which do not bind to cells of normal tissue in the body except cells of the intestinal tract since the cells of other tissues do not possess ST receptors. Unlike normal colorectal cells and localized colorectal cancer cells, metastasized colorectal cancer cells are accessible to substances administered outside the intestinal tract, for example administered in the circulatory system. The only ST receptors in normal tissue exist in the apical membranes of intestinal mucosa cells and these receptors are effectively isolated from the targeted cancer chemotherapeutics and imaging agents administered outside the intestinal tract by the intestinal mucosa barrier. Thus, metastasized colorectal cells may be targeted by conjugated compounds of the present invention by introducing such compounds outside the intestinal tract such as for example by administering pharmaceutical compositions that comprise conjugated compounds into the circulatory system.

One having ordinary skill in the art can readily identify individuals suspected of suffering from colorectal cancer and metastasized colorectal cells. In those individuals diagnosed with colorectal cancer, it is standard therapy to suspect metastasis and aggressively attempt to eradicate metastasized cells. The present invention provides pharmaceutical compositions and methods for imaging and thereby will more definitively diagnose metastasis. Further, the present invention provides pharmaceutical compositions comprising therapeutic agents and methods for specifically targeting and eliminating metastasized colorectal cancer cells. Further, the present invention provides pharmaceutical compositions that comprise therapeutics and methods for specifically eliminating colorectal cancer cells.

The pharmaceutical compositions which comprise conjugated compositions of the present invention may be used to diagnose or treat individuals suffering from localized colorectal tumors, that is primary or non-metastatic colorectal tumors if these have penetrated the basement membrane underlying the mucosa into the submucosa where there is abundant blood supply to which they have access. Penetration into the submucosa circumvents the mucosal barrier resulting in the ability of conjugated compositions introduced into the circulatory system to interact with these tumors.

The present invention relies upon the use of an ST receptor binding moiety in a conjugated composition. The ST receptor binding moiety is essentially a portion of the conjugated composition which acts as a ligand to the ST receptor and thus specifically binds to these receptors. The conjugated composition also includes an active moiety which is associated with the ST receptor binding moiety; the active moiety being an active agent which is either useful to image, target, neutralize or kill the cell.

According to the present invention, the ST receptor binding moiety is the ST receptor ligand portion of a conjugated composition. In some embodiments, the ST receptor ligand may be native ST.

Native ST has been isolated from a variety of organisms including *E. coli*, Yersinia, Enterobacter, and others. In nature, the toxins are generally encoded on a plasmid which can "jump" between different species. Several different toxins have been reported to occur in different species. These toxins all possess significant sequence homology, they all bind to ST receptors and they all activate guanylate cyclase, producing diarrhea.

ST has been both cloned and synthesized by chemical techniques. The cloned or synthetic molecules exhibit binding characteristics which are similar to native ST. Native ST isolated from *E. coli* is 18 or 19 amino acids in length. The smallest "fragment" of ST which retains activity is the 13 amino acid core peptide extending toward the carboxy terminal from cysteine 6 to cysteine 18 (of the 19 amino acid form). Analogues of ST have been generated by cloning and by chemical techniques. Small peptide fragments of the native ST structure which include the structural determinant that confers binding activity may be constructed. Once a structure is identified which binds to ST receptors, non-peptide analogues mimicking that structure in space are designed.

SEQ ID NO:1 discloses a nucleotide sequence which encodes 19 amino acid ST, designated ST Ia, reported by So and McCarthy (1980) *Proc. Natl. Acad. Sci. USA* 77:4011, which is incorporated herein by reference.

The amino acid sequence of ST Ia is disclosed in SEQ ID NO:2.

SEQ ID NO:3 discloses the amino acid sequence of an 18 amino acid peptide which exhibits ST activity, designated ST I*, reported by Chan and Giannella (1981) *J. Biol. Chem.* 256:7744, which is incorporated herein by reference.

SEQ ID NO:4 discloses a nucleotide sequence which encodes 19 amino acid ST, designated ST Ib, reported by Mosely et al. (1983) *Infect. Immun.* 39:1167, which is incorporated herein by reference.

The amino acid sequence of ST Ib is disclosed in SEQ ID NO:5.

A 15 amino acid peptide called guanylin which has about 50% sequence homology to ST has been identified in mammalian intestine (Currie, M. G. et al. (1992) *Proc. Natl. Acad Sci. USA* 89:947–951, which is incorporated herein by reference). Guanylin binds to ST receptors and activates guanylate cyclase at a level of about 10- to 100-fold less than native ST. Guanylin may not exist as a 15 amino acid peptide in the intestine but rather as part of a larger protein in that organ. The amino acid sequence of guanylin from rodent is disclosed as SEQ ID NO:6.

SEQ ID NO:7 is an 18 amino acid fragment of SEQ ID NO:2. SEQ ID NO:8 is a 17 amino acid fragment of SEQ ID NO:2. SEQ ID NO:9 is a 16 amino acid fragment of SEQ ID NO:2. SEQ ID NO:10 is a 15 amino acid fragment of SEQ ID NO:2. SEQ ID NO:11 is a 14 amino acid fragment of SEQ ID NO:2. SEQ ID NO:12 is a 13 amino acid fragment of SEQ ID NO:2. SEQ ID NO:13 is an 18 amino acid fragment of SEQ ID NO:2. SEQ ID NO:14 is a 17 amino acid fragment of SEQ ID NO:2. SEQ ID NO:15 is a 16 amino acid fragment of SEQ ID NO:2. SEQ ID NO:16 is a 15 amino acid fragment of SEQ ID NO:2. SEQ ID NO:17 is a 14 amino acid fragment of SEQ ID NO:2.

SEQ ID NO:18 is a 17 amino acid fragment of SEQ ID NO:3. SEQ ID NO:19 is a 16 amino acid fragment of SEQ ID NO:3. SEQ ID NO:20 is a 15 amino acid fragment of SEQ ID NO:3. SEQ ID NO:21 is a 14 amino acid fragment of SEQ ID NO:3. SEQ ID NO:22 is a 13 amino acid fragment of SEQ ID NO:3. SEQ ID NO:23 is a 17 amino acid fragment of SEQ ID NO:3. SEQ ID NO:24 is a 16 amino acid fragment of SEQ ID NO:3. SEQ ID NO:25 is a 15 amino acid fragment of SEQ ID NO:3. SEQ ID NO:26 is a 14 amino acid fragment of SEQ ID NO:3.

SEQ ID NO:27 is an 18 amino acid fragment of SEQ ID NO:5. SEQ ID NO:28 is a 17 amino acid fragment of SEQ

ID NO:5. SEQ ID NO:29 is a 16 amino acid fragment of SEQ ID NO:5. SEQ ID NO:30 is a 15 amino acid fragment of SEQ ID NO:5. SEQ ID NO:31 is a 14 amino acid fragment of SEQ ID NO:5. SEQ ID NO:32 is a 13 amino acid fragment of SEQ ID NO: 5. SEQ ID NO: 33 is an 18 amino acid fragment of SEQ ID NO:5. SEQ ID NO:34 is a 17 amino acid fragment of SEQ ID NO:5. SEQ ID NO:35 is a 16 amino acid fragment of SEQ ID NO:5. SEQ ID NO:36 is a 15 amino acid fragment of SEQ ID NO:5. SEQ ID NO:37 is a 14 amino acid fragment of SEQ ID NO:5.

SEQ ID NO:27, SEQ ID NO:31, SEQ ID NO:36 AND SEQ ID NO:37 are disclosed in Yoshimura, S., et al. (1985) *FEBS Lett.* 181:138, which is incorporated herein by reference.

SEQ ID NO:38, SEQ ID NO:39 and SEQ ID NO:40, which are derivatives of SEQ ID NO:3, are disclosed in Waldman, S. A. and O'Hanley, P. (1989) *Infect. Immun.* 57:2420, which is incorporated herein by reference.

SEQ ID NO:41, SEQ ID NO:42, SEQ ID NO:43, SEQ ID NO:44 and SEQ ID NO:45, which are a derivatives of SEQ ID NO:3, are disclosed in Yoshimura, S., et al. (1985) *FEBS Lett.* 181:138, which is incorporated herein by reference.

SEQ ID NO:46 is a 25 amino acid peptide derived from *Y. enterocolitica* which binds to the ST receptor.

SEQ ID NO:47 is a 16 amino acid peptide derived from *V. cholerae* which binds to the ST receptor. SEQ ID NO:47 is reported in Shimonishi, Y., et al. *FEBS Lett.* 215:165, which is incorporated herein by reference.

SEQ ID NO:48 is an 18 amino acid peptide derived from *Y. enterocolitica* which binds to the ST receptor. SEQ ID NO:48 is reported in Okamoto, K., et al. *Infec. Immun.* 55:2121, which is incorporated herein by reference.

SEQ ID NO:49, is a derivative of SEQ ID NO:5.

SEQ ID NO:50, SEQ ID NO:51, SEQ ID NO:52 and SEQ ID NO:53 are derivatives.

SEQ ID NO:54 is the amino acid sequence of guanylin from human.

In some preferred embodiments, conjugated compounds comprise ST receptor binding moieties that comprise amino acid sequences selected from the group consisting of SEQ ID NO:2, SEQ ID NO:3, SEQ ID NOS:5–54 and fragments and derivatives thereof.

Those having ordinary skill in the art can readily design and produce derivatives having substantially identical amino acid sequences of ST peptides with deletions and/or insertions and/or conservative substitutions of amino acids. For example, following what are referred to as Dayhof's rules for amino acid substitution (Dayhof, M. D. (1978) *Nat. Biomed. Res. Found.*, Washington, D.C. Vol. 5, supp. 3), amino acid residues in a peptide sequence may be substituted with comparable amino acid residues. Such substitutions are well-known and are based the upon charge and structural characteristics of each amino acid. Derivatives include fragments of ST receptor binding peptides with deletions and/or insertions and/or conservative substitutions.

In some embodiments, ST receptor binding peptides comprise D amino acids. As used herein, the term "D amino acid peptides" is meant to refer to ST receptor binding peptides, fragments or derivatives which comprise at least one and preferably a plurality of D amino acids which are capable of binding to the ST receptor. The use of D amino acid peptides is desirable as they are less vulnerable to degradation and therefore have a longer half-life. D amino acid peptides comprising mostly all or consisting of D amino acids may comprise amino acid sequences in the reverse order of ST receptor binding peptides which are made up of L amino acids.

In some embodiments, ST receptor binding peptides, including D amino acid peptides, are conformationally restricted to present and maintain the proper structural conformation for binding to the ST receptor. The compositions may comprise additional amino acid residues required to achieve proper three dimensional conformation including residues which facilitate circularization or desired folding.

It is preferred that the ST receptor ligand used as the ST receptor binding moiety be as small as possible. Thus it is preferred that the ST receptor ligand be a non-peptide small molecule or small peptide, preferably less than 25 amino acids, more preferably less than 20 amino acids. In some embodiments, the ST receptor ligand which constitute the ST receptor binding moiety of a conjugated composition is less than 15 amino acids. ST receptor binding peptide comprising less than 10 amino acids and ST receptor binding peptide less than 5 amino acids may be used as ST binding moieties according to the present invention. It is within the scope of the present invention to include larger molecules which serve as ST receptor binding moieties including, but not limited to molecules such as antibodies, FAbs and F(Ab)2s which specifically bind to ST receptor.

An assay may be used to test both peptide and nonpeptide compositions to determine whether or not they are ST receptor ligands or, to test conjugated compositions to determine if they possess ST receptor binding activity. Such compositions that specifically bind to ST receptors can be identified by a competitive binding assay. The competitive binding assay is a standard technique in pharmacology which can be readily performed by those having ordinary skill in the art using readily available starting materials. Competitive binding assays have been shown to be effective for identifying compositions that specifically bind to ST receptors. Briefly, the assay consists of incubating a preparation of ST receptors (e.g. intestinal membranes from rat intestine, human intestine, T84 cells) with a constant concentration (1×10^{-10}M to 5×10^{-10}M) of ^{125}I-ST (any ST receptor ligand such as native STs SEQ ID NO:2, SEQ ID NO:3 or SEQ ID NO:5 may be used) and a known concentration of a test compound. As a control, a duplicate preparation of ST receptors are incubated with a duplicate concentration of ^{125}I-ST in the absence of test compound. Assays are incubated to equilibrium (2 hours) and the amount of ^{125}I-ST bound to receptors is quantified by standard techniques. The ability of the test compound to bind to receptors is measured as its ability to prevent (compete with) the ^{125}I-ST from binding. Thus, in assays containing the test compound which bind to the receptor, there will be less radioactivity associated with the receptors. This assay, which is appropriate for determining the ability of any molecule to bind to ST receptors, is a standard competitive binding assay which can be readily employed by those having ordinary skill in the art using readily available starting materials.

ST may be isolated from natural sources using standard techniques. Additionally, ST receptor binding peptides and conjugated compositions or portions thereof which are peptides may be prepared routinely by any of the following known techniques.

ST receptor binding peptides and conjugated compositions or portions thereof which are peptides may be prepared using the solid-phase synthetic technique initially described by Merrifield, in *J. Am. Chem. Soc.*, 15:2149–2154 (1963). Other peptide synthesis techniques may be found, for

example, in M. Bodanszky et al., (1976) *Peptide Synthesis*, John Wiley & Sons, 2d Ed.; Kent and Clark-Lewis in *Synthetic Peptides in Biology and Medicine*, p. 295–358, eds. Alitalo, K., et al. Science Publishers, (Amsterdam, 1985); as well as other reference works known to those skilled in the art. A summary of peptide synthesis techniques may be found in J. Stuart and J. D. Young, *Solid Phase Peptide Synthelia*, Pierce Chemical Company, Rockford, Ill. (1984), which is incorporated herein by reference. The synthesis of peptides by solution methods may also be used, as described in *The Proteins*, Vol. II, 3d Ed., p. 105–237, Neurath, H. et al., Eds., Academic Press, New York, N.Y. (1976). Appropriate protective groups for use in such syntheses will be found in the above texts, as well as in J. F. W. McOmie, *Protective Groups in Organic Chemistry*, Plenum Press, New York, N.Y. (1973), which is incorporated herein by reference. In general, these synthetic methods involve the sequential addition of one or more amino acid residues or suitable protected amino acid residues to a growing peptide chain. Normally, either the amino or carboxyl group of the first amino acid residue is protected by a suitable, selectively removable protecting group. A different, selectively removable protecting group is utilized for amino acids containing a reactive side group, such as lysine.

Using a solid phase synthesis as an example, the protected or derivatized amino acid is attached to an inert solid support through its unprotected carboxyl or amino group. The protecting group of the amino or carboxyl group is then selectively removed and the next amino acid in the sequence having the complementary (amino or carboxyl) group suitably protected is admixed and reacted with the residue already attached to the solid support. The protecting group of the amino or carboxyl group is then removed from this newly added amino acid residue, and the next amino acid (suitably protected) is then added, and so forth. After all the desired amino acids have been linked in the proper sequence, any remaining terminal and side group protecting groups (and solid support) are removed sequentially or concurrently, to provide the final peptide. The peptide of the invention are preferably devoid of benzylated or methylbenzylated amino acids. Such protecting group moieties may be used in the course of synthesis, but they are removed before the peptides are used. Additional reactions may be necessary, as described elsewhere, to form intramolecular linkages to restrain conformation.

ST receptor binding peptides and conjugated compositions or portions thereof which are peptides may also be prepared by recombinant DNA techniques. Provision of a suitable DNA sequence encoding the desired peptide permits the production of the peptide using recombinant techniques now known in the art. The coding sequence can be obtained from natural sources or synthesized or otherwise constructed using widely available starting materials by routine methods. When the coding DNA is prepared synthetically, advantage can be taken of known codon preferences of the intended host where the DNA is to be expressed.

To produce an ST receptor binding peptide which occurs in nature, one having ordinary skill in the art can, using well-known techniques, obtain a DNA molecule encoding the ST receptor binding peptides from the genome of the organism that produces the ST receptor binding peptide and insert that DNA molecule into a commercially available expression vector for use in well-known expression systems.

Likewise, one having ordinary skill in the art can, using well known techniques, combine a DNA molecule that encodes an ST receptor binding peptide, such as SEQ ID NO:1 and SEQ ID NO:4, which can be obtained from the genome of the organism that produces the ST, with DNA that encodes a toxin, another active agent that is a peptide or additionally, any other amino acid sequences desired to be adjacent to the ST receptor binding peptide amino acid sequence in a single peptide and insert that DNA molecule into a commercially available expression vector for use in well-known expression systems.

For example, the commercially available plasmid pSE420 (Invitrogen, San Diego, Calif.) may be used for recombinant production in *E. coli*. The commercially available plasmid pYES2 (Invitrogen, San Diego, Calif.) may be used for production in *S. cerevisiae* strains of yeast. The commercially available MaxBac™ (Invitrogen, San Diego, Calif.) complete baculovirus expression system may be used for production in insect cells. The commercially available plasmid pcDNA I (Invitrogen, San Diego, Calif.) may be used for production in mammalian cells such as Chinese Hamster Ovary cells.

One having ordinary skill in the art may use these or other commercially available expression vectors and systems or produce vectors using well-known methods and readily available starting materials. Expression systems containing the requisite control sequences, such as promoters and polyadenylation signals, and preferably enhancers, are readily available and known in the art for a variety of hosts. See e.g., Sambrook et al., *Molecular Cloning a Laboratory Manual*, Second Ed. Cold Spring Harbor Press (1989). Thus, the desired proteins can be prepared in both prokaryotic and eukaryotic systems, resulting in a spectrum of processed forms of the protein.

The most commonly used prokaryotic system remains *E. coli*, although other systems such as *B. subtilis* and Pseudomonas are also useful. Suitable control sequences for prokaryotic systems include both constitutive and inducible promoters including the lac promoter, the trp promoter, hybrid promoters such as tac promoter, the lambda phage P1 promoter. In general, foreign proteins may be produced in these hosts either as fusion or mature proteins. When the desired sequences are produced as mature proteins, the sequence produced may be preceded by a methionine which is not necessarily efficiently removed. Accordingly, the peptides and proteins claimed herein may be preceded by an N-terminal Met when produced in bacteria. Moreover, constructs may be made wherein the coding sequence for the peptide is preceded by an operable signal peptide which results in the secretion of the protein. When produced in prokaryotic hosts in this matter, the signal sequence is removed upon secretion.

A wide variety of eukaryotic hosts are also now available for production of recombinant foreign proteins. As in bacteria, eukaryotic hosts may be transformed with expression systems which produce the desired protein directly, but more commonly signal sequences are provided to effect the secretion of the protein. Eukaryotic systems have the additional advantage that they are able to process introns which may occur in the genomic sequences encoding proteins of higher organisms. Eukaryotic systems also provide a variety of processing mechanisms which result in, for example, glycosylation, carboxy-terminal amidation, oxidation or derivatization of certain amino acid residues, conformational control, and so forth.

Commonly used eukaryotic systems include, but are not limited to, yeast, fungal cells, insect cells, mammalian cells, avian cells, and cells of higher plants. Suitable promoters are available which are compatible and operable for use in each of these host types as well as are termination sequences and

enhancers, as e.g. the baculovirus polyhedron promoter. As above, promoters can be either constitutive or inducible. For example, in mammalian systems, the mouse metallothionene promoter can be induced by the addition of heavy metal ions.

The particulars for the construction of expression systems suitable for desired hosts are known to those in the art. For recombinant production of the protein, the DNA encoding it is suitably ligated into the expression vector of choice and then used to transform the compatible host which is then cultured and maintained under conditions wherein expression of the foreign gene takes place. The protein of the present invention thus produced is recovered from the culture, either by lysing the cells or from the culture medium as appropriate and known to those in the art.

One having ordinary skill in the art can, using well-known techniques, isolate the protein that is produced.

According to the present invention, the active moiety may be a therapeutic agent or an imaging agent. One having ordinary skill in the art can readily recognize the advantages of being able to specifically target metastasized colorectal cells with an ST receptor ligand and conjugate such a ligand with many different active agents.

Chemotherapeutics useful as active moieties which when conjugated to an ST receptor binding moiety are specifically delivered to metastasized colorectal cells are typically, small chemical entities produced by chemical synthesis. Chemotherapeutics include cytotoxic and cytostatic drugs. Chemotherapeutics may include those which have other effects on cells such as reversal of the transformed state to a differentiated state or those which inhibit cell replication. Examples of chemotherapeutics include common cytotoxic or cytostatic drugs such as for example: methotrexate(amethopterin), doxorubicin(adrimycin), daunorubicin, cytosinarabinoside, etoposide, 5-4 fluorouracil, melphalan, chlorambucil, and other nitrogen mustards (e.g. cyclophosphamide), cis-platinum, vindesine (and other vinca alkaloids), mitomycin and bleomycin. Other chemotherapeutics include: purothionin (barley flour oligopeptide), macromomycin. 1,4-benzoquinone derivatives and trenimon.

Toxins are useful as active moieties. When a toxin is conjugated to an ST receptor binding moiety, the conjugated composition is specifically delivered to a metastasized colorectal cell by way of the ST receptor binding moiety and the toxin moiety kills the cell. Toxins are generally complex toxic products of various organisms including bacteria, plants, etc. Examples of toxins include but are not limited to: ricin, ricin A chain (ricin toxin), Pseudomonas exotoxin (PE), diphtheria toxin (DT), *Clostridium perfringens* phospholipase C (PLC), bovine pancreatic ribonuclease (BPR), pokeweed antiviral protein (PAP), abrin, abrin A chain (abrin toxin), cobra venom factor (CVF), gelonin (GEL), saporin (SAP), modeccin, viscumin and volkensin. As discussed above, when protein toxins are employed with ST receptor binding peptides, conjugated compositions may be produced using recombinant DNA techniques. Briefly, a recombinant DNA molecule can be constructed which encodes both the ST receptor ligand and the toxin on a chimeric gene. When the chimeric gene is expressed, a fusion protein is produced which includes an ST receptor binding moiety and an active moiety. Protein toxins are also useful to form conjugated compounds with ST receptor binding peptides through non-peptidyl bonds.

In addition, there are other approaches for utilizing active agents for the treatment of cancer. For example, conjugated compositions may be produced which include an ST binding moiety and an active moiety which is an active enzyme. The ST binding moiety specifically localizes the conjugated composition to the tumor cells. An inactive prodrug which can be converted by the enzyme into an active drug is administered to the patient. The prodrug is only converted to an active drug by the enzyme which is localized to the tumor. An example of an enzyme/prodrug pair includes alkaline phosphatase/etoposidephosphate. In such a case, the alkaline phosphatase is conjugated to an ST receptor binding ligand. The conjugated compound is administered and localizes at the metastasized cell. Upon contact with etoposidephosphate (the prodrug), the etoposidephosphate is converted to etoposide, a chemotherapeutic drug which is taken up by the cancer cell.

Radiosensitizing agents are substances that increase the sensitivity of cells to radiation. Examples of radiosensitizing agents include nitroimidazoles, metronidazole and misonidazole (see: DeVita, V. T. Jr. in *Harrison's Principles of Internal Medicine*, p.68, McGraw-Hill Book Co., New York 1983, which is incorporated herein by reference). The conjugated compound that comprises a radiosensitizing agent as the active moiety is administered and localizes at the metastasized cell. Upon exposure of the individual to radiation, the radiosensitizing agent is "excited" and causes the death of the cell.

Radionuclides may be used in pharmaceutical compositions that are useful for radiotherapy or imaging procedures.

Examples of radionuclides useful as toxins in radiation therapy include: ^{47}Sc, ^{67}Cu, ^{90}Y, ^{109}Pd, ^{123}I, ^{125}I, ^{131}I, ^{186}Re, ^{188}Re, ^{199}Au, ^{211}At, ^{212}Pb and ^{212}B. Other radionuclides which have been used by those having ordinary skill in the art include: ^{32}P and ^{33}P, ^{71}Ge, ^{77}As, ^{103}Pb, ^{105}Rh, ^{111}Ag, ^{119}Sb, ^{121}Sn, ^{131}Cs, ^{143}Pr, ^{161}Tb, ^{177}Lu, ^{191}Os, ^{193M}Pt, ^{197}Hg, all beta negative and/or auger emitters. Some preferred radionuclides include: ^{90}Y, ^{131}I ^{211}At and $^{212}Pb/^{212}Bi$.

According to the present invention, the active moieties may be an imaging agent. Imaging agents are useful diagnostic procedures as well as the procedures used to identify the location of metastasized cells. Imaging can be performed by many procedures well-known to those having ordinary skill in the art and the appropriate imaging agent useful in such procedures may be conjugated to an ST receptor ligand by well-known means. Imaging can be performed, for example, by radioscintigraphy, nuclear magnetic resonance imaging (MRI) or computed tomography (CT scan). The most commonly employed radionuclide imaging agents include radioactive iodine and indium. Imaging by CT scan may employ a heavy metal such as iron chelates. MRI scanning may employ chelates of gadolinium or manganese. Additionally, positron emission tomography (PET) may be possible using positron emitters of oxygen, nitrogen, iron, carbon, or gallium. Example of radionuclides useful in imaging procedures include: ^{43}K, ^{52}Fe, ^{57}Co, ^{67}Cu, ^{67}Ga, ^{68}Ga, ^{77}Br, $^{81}Rb/^{81M}Kr$, ^{87M}Sr, ^{99M}Tc, ^{111}In, ^{113M}In, ^{123}I, ^{125}I, ^{127}Cs, ^{129}Cs, ^{131}I, ^{132}I, ^{197}Hg, ^{203}Pb and ^{206}Bi.

It is preferred that the conjugated compositions be non-immunogenic or immunogenic at a very low level. Accordingly, it is preferred that the ST receptor binding moiety be a small, poorly immunogenic or non-immunogenic peptide or a non-peptide. Likewise, it is preferred that the active moiety be a small, poorly-immunogenic or non-immunogenic peptide or a non-peptide. Native ST, being a small peptide, has been shown to poorly immunogenic. (See: Klipstein, F. A. et al. (1982) *Infect. Immun.* 37:550–557; Giannella, R. A. et al. (1981) *Infect. Immun.* 33:186; Bur-

gess, M. N. et al. (1978) *Infect. Immun.* 21:60; Evans, D. G. et al. (1973) *Infect. Immun.* 7:873; Gyles, C. L. (1979) *Ann. N.Y. Acad. Sci.* 16:314; and Sack, R. B. (1975) *Ann. Rev. Microbiol.* 29:333.) Similarly, fragments and amino acid substitute derivatives of native ST are poorly immunogenic. Accordingly, conjugated compositions which include all or part of the native ST as an ST receptor binding moiety are generally poorly immunogenic to the extent that the native ST is poorly immunogenic.

ST receptor ligands are conjugated to active agents by a variety of well-known techniques readily performed without undue experimentation by those having ordinary skill in the art. The technique used to conjugate the ST receptor ligand to the active agent is dependent upon the molecular nature of the ST receptor ligand and the active agent. After the ST receptor ligand and the active agent are conjugated to form a single molecule, assays may be performed to ensure that the conjugated molecule retains the activities of the moieties. The ST receptor binding assay described above may be performed using the conjugated compound to test whether it is capable of binding to the ST receptor. Similarly, the activity of the active moiety may be tested using various assays for each respective type of active agent. Radionuclides retain there activity, i.e. their radioactivity, irrespective of conjugation. With respect to active agents which are toxins, drugs and targeting agents, standard assays to demonstrate the activity of unconjugated forms of these compounds may be used to confirm that the activity has been retained.

Conjugation may be accomplished directly between the ST receptor ligand and the active agent or linking, intermediate molecular groups may be provided between the ST receptor ligand and the active agent. Crosslinkers are particularly useful to facilitate conjugation by providing attachment sites for each moiety. Crosslinkers may include additional molecular groups which serve as spacers to separate the moieties from each other to prevent either from interfering with the activity of the other.

In some preferred embodiments, the ST receptor ligand peptide is SEQ ID NO:2, SEQ ID NO:3, SEQ ID NOS:5–54 or fragments or derivatives thereof. It has been observed that conjugation to these molecules is preferably performed at the amino terminus of each respective peptide. In ST receptor ligand peptides comprising D amino acid sequences in the opposite order as SEQ ID NO:2, SEQ ID NO:3, SEQ ID NOS:5–54, conjugation preferably is performed at the carboxy terminus.

One having ordinary skill in the art may conjugate an ST receptor ligand peptide to a chemotherapeutic drug using well-known techniques. For example, Magerstadt, M. *Antibody Conjugates and Malignant Disease.* (1991) CRC Press, Boca Raton, USA, pp. 110–152) which is incorporated herein by reference, teaches the conjugation of various cytostatic drugs to amino acids of antibodies. Such reactions may be applied to conjugate chemotherapeutic drugs to ST receptor ligands, including ST receptor binding peptides, with an appropriate linker. ST receptor ligands which have a free amino group such as ST receptor binding peptides may be conjugated to active agents at that group. Most of the chemotherapeutic agents currently in use in treating cancer possess functional groups that are amenable to chemical crosslinking directly with proteins. For example, free amino groups are available on methotrexate, doxorubicin, daunorubicin, cytosinarabinoside, cis-platin, vindesine, mitomycin and bleomycin while free carboxylic acid groups are available on methotrexate, melphalan, and chlorambucil. These functional groups, that is free amino and carboxylic acids, are targets for a variety of homobifunctional and heterobifunctional chemical crosslinking agents which can crosslink these drugs directly to the single free amino group of ST. For example, one procedure for crosslinking ST receptor ligands which have a free amino group such as ST receptor binding peptides, as for example SEQ ID NO:2, SEQ ID NO:3, SEQ ID NO:5–54 to active agents which have a free amino group such as methotrexate, doxorubicin, daunorubicin, cytosinarabinoside, cis-platin, vindesine, mitomycin and bleomycin, or alkaline phosphatase, or protein- or peptide-based toxin employs homobifunctional succinimidyl esters, preferably with carbon chain spacers such as disuccinimidyl suberate (Pierce Co, Rockford, Ill.). In the event that a clearable conjugated compound is required, the same protocol would be employed utilizing 3,3'-dithiobis (sulfosuccinimidylpropionate; Pierce Co.).

In order to conjugate an ST receptor ligand peptide to a peptide-based active agent such as a toxin, the ST receptor ligand and the toxin may be produced as a single, fusion protein either by standard peptide synthesis or recombinant DNA technology, both of which can be routinely performed by those having ordinary skill in the art. Alternatively, two peptides, the ST receptor ligand peptide and the peptide-based toxin may be produced and/or isolated as separate peptides and conjugated using crosslinkers. As with conjugated compositions that contain chemotherapeutic drugs, conjugation of ST receptor binding peptides and toxins can exploit the ability to modify the single free amino group of an ST receptor binding peptide while preserving the receptor-binding function of this molecule.

One having ordinary skill in the art may conjugate an ST receptor ligand peptide to a radionuclide using well-known techniques. For example, Magerstadt, M. (1991) *Antibody Conjugates And Malignant Disease*, CRC Press, Boca Raton, Fla.,; and Barchel, S. W. and Rhodes, B. H., (1983) *Radioimaging and Radiotherapy*, Elsevier, NY, N.Y., each of which is incorporated herein by reference, teach the conjugation of various therapeutic and diagnostic radionuclides to amino acids of antibodies. Such reactions may be applied to conjugate radionuclides to ST receptor ligand peptides or to ST receptor ligands including ST receptor ligand peptides with an appropriate linker.

The present invention provides pharmaceutical compositions that comprise the conjugated compounds of the invention and pharmaceutically acceptable carriers or diluents. The pharmaceutical composition of the present invention may be formulated by one having ordinary skill in the art. Suitable pharmaceutical carriers are described in *Remington's Pharmaceutical Sciences*, A. Osol, a standard reference text in this field, which is incorporated herein by reference. In carrying out methods of the present invention, conjugated compounds of the present invention can be used alone or in combination with other diagnostic, therapeutic or additional agents. Such additional agents include excipients such as coloring, stabilizing agents, osmotic agents and antibacterial agents.

The conjugated compositions of the invention can be, for example, formulated as a solution, suspension or emulsion in association with a pharmaceutically acceptable parenteral vehicle. Examples of such vehicles are water, saline, Ringer's solution, dextrose solution, and 5% human serum albumin. Liposomes may also be used. The vehicle may contain additives that maintain isotonicity (e.g., sodium chloride, mannitol) and chemical stability (e.g., buffers and preservatives). The formulation is sterilized by commonly used techniques. For example, a parenteral composition suitable for administration by injection is prepared by dissolving

1.5% by weight of active ingredient in 0.9% sodium chloride solution.

The pharmaceutical compositions according to the present invention may be administered as either a single dose or in multiple doses. The pharmaceutical compositions of the present invention may be administered either as individual therapeutic agents or in combination with other therapeutic agents. The treatments of the present invention may be combined with conventional therapies, which may be administered sequentially or simultaneously.

The pharmaceutical compositions of the present invention may be administered by any means that enables the conjugated composition to reach the targeted cells. In some embodiments, routes of administration include those selected from the group consisting of intravenous, intraarterial, intraperitoneal, local administration into the blood supply of the organ in which the tumor resides or directly into the tumor itself. Intravenous administration is the preferred mode of administration. It may be accomplished with the aid of an infusion pump.

The dosage administered varies depending upon factors such as: the nature of the active moiety; the nature of the conjugated composition; pharmacodynamic characteristics; its mode and route of administration; age, health, and weight of the recipient; nature and extent of symptoms; kind of concurrent treatment; and frequency of treatment.

Because conjugated compounds are specifically targeted to cells with ST receptors, conjugated compounds which comprise chemotherapeutics or toxins are administered in doses less than those which are used when the chemotherapeutics or toxins are administered as unconjugated active agents, preferably in doses that contain up to 100 times less active agent. In some embodiments, conjugated compounds which comprise chemotherapeutics or toxins are administered in doses that contain 10–100 times less active agent as an active moiety than the dosage of chemotherapeutics or toxins administered as unconjugated active agents. To determine the appropriate dose, the amount of compound is preferably measured in moles instead of by weight. In that way, the variable weight of different ST binding moieties does not affect the calculation. Presuming a one to one ratio of ST binding moiety to active moiety in conjugated compositions of the invention, less moles of conjugated compounds may be administered as compared to the moles of unconjugated compounds administered, preferably up to 100 times less moles.

Typically, chemotherapeutic conjugates are administered intravenously in multiple divided doses.

Up to 20 gm IV/dose of methotrexate is typically administered in an unconjugated form. When methotrexate is administered as the active moiety in a conjugated compound of the invention, there is a 10- to 100-fold dose reduction. Thus, presuming each conjugated compound includes one molecule of methotrexate conjugated to one ST receptor binding moiety, of the total amount of conjugated compound administered, up to about 0.2–2.0 g of methotrexate is present and therefore administered. In some embodiments, of the total amount of conjugated compound administered, up to about 200 mg–2 g of methotrexate is present and therefore administered.

Methotrexate has a molecular weight of 455. One mole of the ST peptide-methotrexate conjugate weighs between about 1755–2955 depending on the ST peptide used. The effective dose range for ST peptide-methotrexate conjugate is between about 10 to 1000 mg. In some embodiments, dosages of 50 to 500 mg of ST peptide-methotrexate conjugate are administered. In some embodiments, dosages of 80 to 240 mg of ST peptide-methotrexate conjugate are administered.

Doxorubicin and daunorubicin each weigh about 535. Thus, ST peptide-doxorubicin conjugates and ST peptide-daunorubicin conjugates each have molecular weights of between about 1835–2553.5. Presuming each conjugated compound includes one molecule of doxorubicin or daunorubicin conjugated to one ST receptor binding moiety, the effective dose range for ST peptide-doxorubicin conjugate or ST peptide-daunorubicin conjugate is between about 40 to 4000 mg. In some embodiments, dosages of 100 to 1000 mg of ST peptide-doxorubicin conjugate or ST peptide-daunorubicin conjugate are administered. In some embodiments, dosages of 200 to 600 mg of ST peptide-doxorubicin conjugate or ST peptide-daunorubicin conjugate are administered.

Toxin-containing conjugated compounds are formulated for intravenous administration. Using this approach, up to 6 nanomoles/kg of body weight of toxin have been administered as a single dose with marked therapeutic effects in patients with melanoma (Spitler L. E., et al. (1987) *Cancer Res.* 47:1717). In some embodiments, up to about 11 micrograms of ST peptide-toxin conjugated compound/kg of body weight may be administered for therapy.

Presuming each conjugated compound includes one molecule of ricin toxin A chain conjugated to an ST receptor binding moiety, conjugated compositions comprising ricin toxin A chain are administered in doses in which the proportion by weight of ricin toxin A chain is 1–500 μg of the total weight of the conjugated compound administered. In some preferred embodiments, conjugated compositions comprising ricin toxin A chain are administered in doses in which the proportion by weight of ricin toxin A chain is 10–100 μg of the total weight of the conjugated compound administered. In some preferred embodiments, conjugated compositions comprising ricin toxin A chain are administered in doses in which the proportion by weight of ricin toxin A chain is 2–50 μg of the total weight of the conjugated compound administered. The molecular weight of ricin toxin A chain is 32,000. Thus, a conjugated compound that contains ricin A chain linked to an ST peptide has a molecular weight of about 33,300–34,500. The range of doses of such conjugated compounds to be administered are 1 to 500 μg. In some embodiments, 10 to 100 μg of such conjugated compounds are administered. In some embodiments, 20 to 50 μg of such conjugated compounds are administered.

Presuming each conjugated compound includes one molecule of diphtheria toxin A chain conjugated to an ST receptor binding moiety, conjugated compositions comprising diphtheria toxin A chain are administered in doses in which the proportion by weight of diphtheria toxin A chain is 1–500 μg of the total weight of the conjugated compound administered. In some preferred embodiments, conjugated compositions comprising diphtheria toxin A chain are administered in doses in which the proportion by weight of diphtheria toxin A chain is 10–100 μg of the total weight of the conjugated compound administered. In some preferred embodiments, conjugated compositions comprising diphtheria toxin A chain are administered in doses in which the proportion by weight of diphtheria toxin A chain is 40–80 μg of the total weight of the conjugated compound administered. The molecular weight of diphtheria toxin A chain is 66,600. Thus, a conjugated compound that contains diphtheria A chain linked to an ST peptide has a molecular weight of about 67,900–69,100. The range of doses of such

conjugated compounds to be administered tested are 1 to 500 μg. In some embodiments, 10 to 100 μg of such conjugated compounds are administered. In some embodiments, 40 to 80 μg of such conjugated compounds are administered.

Presuming each conjugated compound includes one molecule of Pseudomonas exotoxin conjugated to an ST receptor binding moiety, conjugated compositions comprising Pseudomonas exotoxin are administered in doses in which the proportion by weight of Pseudomonas exotoxin is 0.01–100 μg of the total weight of the conjugated compound administered. In some preferred embodiments, conjugated compositions comprising Pseudomonas exotoxin are administered in doses in which the proportion by weight of Pseudomonas exotoxin is 0.1–10 μg of the total weight of the conjugated compound administered. In some preferred embodiments, conjugated compositions comprising Pseudomonas exotoxin are administered in doses in which the proportion by weight of Pseudomonas exotoxin is 0.3–2.2 μg of the total weight of the conjugated compound administered. The molecular weight of Pseudomonas exotoxin is 22,000. Thus, a conjugated compound that contains Pseudomonas exotoxin linked to an ST peptide has a molecular weight of about 23,300–24,500. The range of doses of such conjugated compounds to be administered tested are 0.01 to 100 μg. In some embodiments, 0.1 to 10 μg of such conjugated compounds are administered. In some embodiments, 0.3 to 2.2 μg of such conjugated compounds are administered.

To dose conjugated compositions comprising ST receptor binding moieties linked to active moieties that are radioisotopes in pharmaceutical compositions useful as imaging agents, it is presumed that each ST receptor binding moiety is linked to one radioactive active moiety. The amount of radioisotope to be administered is dependent upon the radioisotope. Those having ordinary skill in the art can readily formulate the amount of conjugated compound to be administered based upon the specific activity and energy of a given radionuclide used as an active moiety. Typically 0.1–100 millicuries per dose of imaging agent, preferably 1–10 millicuries, most often 2–5 millicuries are administered. Thus, pharmaceutical compositions according to the present invention useful as imaging agents which comprise conjugated compositions comprising an ST receptor binding moiety and a radioactive moiety comprise 0.1–100 millicuries, in some embodiments preferably 1–10 millicuries, in some embodiments preferably 2–5 millicuries, in some embodiments more preferably 1–5 millicuries. Examples of dosages include: ^{131}I=between about 0.1–100 millicuries per dose, in some embodiments preferably 1–10 millicuries, in some embodiments 2–5 millicuries, and in some embodiments about 4 millicuries; ^{111}In=between about 0.1–100 millicuries per dose, in some embodiments preferably 1–10 millicuries, in some embodiments 1–5 millicuries, and in some embodiments about 2 millicuries; ^{99m}Tc=between about 0.1–100 millicuries per dose, in some embodiments preferably 5–75 millicuries, in some embodiments 10–50 millicuries, and in some embodiments about 27 millicuries. Depending upon the specific activity of the radioactive moiety and the weight of the ST receptor binding moiety the dosage defined by weight varies. ST peptides have molecular weights of between about 1300–2500. In the pharmaceutical composition comprising an ST peptide linked to a single ^{131}I in which the specific activity of ^{131}I-ST peptide is about 2000 Ci/mmol, administering the dose of 0.1–100 millicuries is the equivalent of 0.1–100 μg ^{131}I-ST peptide, administering the dose of 1–10 millicuries is the equivalent of 1–10 μg of ^{131}I-ST peptide, administering the dose of 2–5 millicuries is equivalent to giving 2–5 μg of ^{131}I-ST peptide and administering the dose of 1–5 millicuries is equivalent to giving 1–5 μg of ^{131}I-ST peptide. In the pharmaceutical composition comprising an ST peptide linked to a single ^{111}In in which the specific activity of ^{111}In-ST peptide is about 1 Ci/mmol, administering the dose of 0.1–100 millicuries is the equivalent of 0.2–200 mg ^{111}In-ST peptide, administering the dose of 1–10 millicuries is the equivalent of 2–20 mg of ^{111}In-ST peptide, administering the dose of 2–5 millicuries is equivalent to giving 4–10 mg of ^{111}In-ST peptide and administering the dose of 1–5 millicuries is equivalent to giving 2–10 mg of ^{111}In-ST peptide.

To dose conjugated compositions comprising ST receptor binding moieties linked to active moieties that are radioisotopes in pharmaceutical compositions useful as therapeutic agents, it is presumed that each ST receptor binding moiety is linked to one radioactive active moiety. The amount of radioisotope to be administered is dependent upon the radioisotope. Those having ordinary skill in the art can readily formulate the amount of conjugated compound to be administered based upon the specific activity and energy of a given radionuclide used as an active moiety. For therapeutics that comprise ^{131}I, between 10–1000 nM, preferably 50–500, more preferably about 300 nanomoles of ^{131}I at the tumor, per gram of tumor, is desirable. Thus, if there is about 1 gram of tumor, and about 0.1% of the administered dose binds to the tumor, 0.5–100 mg of ^{131}I-ST peptide conjugated compound is administered. In some embodiments, 1 to 50 mg of ^{131}I-ST peptide conjugated compound is administered. In some embodiments, 5 to 10 mg of ^{131}I-ST peptide conjugated compound is administered. Wessels B. W. and R. D. Rogus (1984) *Med. Phys.* 11:638 and Kwok, C. S. et al. (1985) *Med. Phys.* 12:405, both of which are incorporated herien by reference, disclose detailed dose calculations for diagnostic and therapeutic conjugates which may be used in the preparation of pharmaceutical compositions of the present invention which include radioactive conjugated compounds.

One aspect of the present invention relates to a method of treating individuals suspected of suffering from metastasized colorectal cancer. Such individuals may be treated by administering to the individual a pharmaceutical composition that comprises a pharmaceutically acceptable carrier or diluent and a conjugated compound that comprises an ST receptor binding moiety and an active moiety wherein the active moiety is a radiostable therapeutic agent. In some embodiments of the present invention, the pharmaceutical composition comprises a pharmaceutically acceptable carrier or diluent and a conjugated compound that comprises an ST receptor binding moiety and an active moiety wherein the active moiety is a radiostable active agent and the ST receptor binding moiety is a peptide. In some embodiments of the present invention, the pharmaceutical composition comprises a pharmaceutically acceptable carrier or diluent and a conjugated compound that comprises an ST receptor binding moiety and an active moiety wherein the active moiety is a radiostable active agent and the ST receptor binding moiety is selected from the group consisting of: SEQ ID NO:2, SEQ ID NO:3, SEQ ID NOS:5–54 and fragments and derivatives thereof. In some embodiments of the present invention, the pharmaceutical composition comprises a pharmaceutically acceptable carrier or diluent and a conjugated compound that comprises an ST receptor binding moiety and an active moiety wherein the active moiety is a radiostable active agent and the ST receptor binding moiety is selected from the group consisting of: SEQ ID NO:2, SEQ

ID NO:3, SEQ ID NO:5, SEQ ID NO:6 and SEQ ID NO:54. In some embodiments of the present invention, the pharmaceutical composition comprises a pharmaceutically acceptable carrier or diluent and a conjugated compound that comprises an ST receptor binding moiety and an active moiety wherein the active moiety is a radiostable therapeutic agent. In some embodiments of the present invention, the pharmaceutical composition comprises a pharmaceutically acceptable carrier or diluent and a conjugated compound that comprises an ST receptor binding moiety and an active moiety wherein the active moiety is a radiostable active agent selected from the group consisting of: methotrexate, doxorubicin, daunorubicin, cytosinarabinoside, etoposide, 5-4 fluorouracil, melphalan, chlorambucil, cis-platinum, vindesine, mitomycin, bleomycin, purothionin, macromomycin, 1,4 -benzoquinone derivatives, trenimon, ricin, ricin A chain, Pseudomonas exotoxin, diphtheria toxin, *Clostridium perfringens* phospholipase C, bovine pancreatic ribonuclease, pokeweed antiviral protein, abrin, abrin A chain, cobra venom factor, gelonin, saporin, modeccin, viscumin, volkensin, alkaline phosphatase, nitroimidazole, metronidazole and misonidazole. In some embodiments of the present invention, the pharmaceutical composition comprises a pharmaceutically acceptable carrier or diluent and a conjugated compound that comprises an ST receptor binding moiety and an active moiety wherein the ST receptor binding moiety is selected from the group consisting of: SEQ ID NO:2, SEQ ID NO:3, SEQ ID NOS:5–54 and fragments and derivatives thereof and the active moiety is a radiostable active agent selected from the group consisting of: methotrexate, doxorubicin, daunorubicin, cytosinarabinoside, etoposide, 5-4 fluorouracil, melphalan, chlorambucil, cis-platinum, vindesine, mitomycin, bleomycin, purothionin, macromomycin, 1,4-benzoquinone derivatives, trenimon, ricin, ricin A chain, Pseudomonas exotoxin, diphtheria toxin, *Clostridium perfringens* phospholipase C, bovine pancreatic ribonuclease, pokeweed antiviral protein, abrin, abrin A chain, cobra venom factor, gelonin, saporin, modeccin, viscumin, volkensin, alkaline phosphatase, nitroimidazole, metronidazole and misonidazole. In some embodiments of the present invention, the pharmaceutical composition comprises a pharmaceutically acceptable carrier or diluent and a conjugated compound that comprises an ST receptor binding moiety and an active moiety wherein the active moiety is a radiostable active agent selected from the group consisting of: methotrexate, doxorubicin, daunorubicin, cytosinarabinoside, cis-platin, vindesine, mitomycin and bleomycin, alkaline phosphatase, ricin A chain, Pseudomonas exotoxin and diphtheria toxin. In some embodiments of the present invention, the pharmaceutical composition comprises a pharmaceutically acceptable carrier or diluent and a conjugated compound that comprises an ST receptor binding moiety and an active moiety wherein the ST receptor binding moiety is selected from the group consisting of: SEQ ID NO:2, SEQ ID NO:3, SEQ ID NO:5, SEQ ID NO:6 and SEQ ID NO:54 and the active moiety is a radiostable active agent selected from the group consisting of: methotrexate, doxorubicin, daunorubicin, cytosinarabinoside, cis-platin, vindesine, mitomycin and bleomycin, alkaline phosphatase, ricin A chain, Pseudomonas exotoxin and diphtheria toxin. In some embodiments of the present invention, the pharmaceutical composition comprises a pharmaceutically acceptable carrier or diluent and a radiostable conjugated compound described in Example 1. The individual being treated may be diagnosed as having metastasized colorectal cancer or may be diagnosed as having localized colorectal cancer and may undergo the treatment proactively in the event that there is some metastasis as yet undetected. The pharmaceutical composition contains a therapeutically effective amount of the conjugated composition. A therapeutically effective amount is an amount which is effective to cause a cytotoxic or cytostatic effect on metastasized colorectal cancer cells without causing lethal side effects on the individual.

One aspect of the present invention relates to a method of treating individuals suspected of suffering from metastasized colorectal cancer. Such individuals may be treated by administering to the individual a pharmaceutical composition that comprises a pharmaceutically acceptable carrier or diluent and a conjugated compound that comprises an ST receptor binding moiety and an active moiety wherein the active moiety is a radioactive. In some embodiments of the present invention, the pharmaceutical composition comprises a pharmaceutically acceptable carrier or diluent and a conjugated compound that comprises an ST receptor binding moiety and an active moiety wherein the active moiety is a radioactive and the ST receptor binding moiety is a peptide. In some embodiments of the present invention, the pharmaceutical composition comprises a pharmaceutically acceptable carrier or diluent and a conjugated compound that comprises an ST receptor binding moiety and an active moiety wherein the active moiety is a radioactive and the ST receptor binding moiety is selected from the group consisting of: SEQ ID NO:2, SEQ ID NO:3, SEQ ID NOS:5–54 and fragments and derivatives thereof. In some embodiments of the present invention, the pharmaceutical composition comprises a pharmaceutically acceptable carrier or diluent and a conjugated compound that comprises an ST receptor binding moiety and an active moiety wherein the active moiety is a radioactive and the ST receptor binding moiety is selected from the group consisting of: SEQ ID NO:2, SEQ ID NO:3, SEQ ID NO:5, SEQ ID NO:6 and SEQ ID NO:54. In some embodiments of the present invention, the pharmaceutical composition comprises a pharmaceutically acceptable carrier or diluent and a conjugated compound that comprises an ST receptor binding moiety and an active moiety wherein the active moiety is a radioactive agent selected from the group consisting of: ^{47}Sc, ^{67}Cu, ^{90}Y, ^{109}Pd, ^{123}I, ^{125}I, ^{131}I, ^{186}Re, ^{188}Re, ^{199}Au, ^{211}At, ^{212}Pb, ^{212}B, ^{32}P and ^{33}P, ^{71}Ge, ^{77}As, ^{103}Pb, ^{105}Rh, ^{111}Ag, ^{119}Sb, ^{121}Sn, ^{131}Cs, ^{143}Pr, ^{161}Tb, ^{177}Lu, ^{191}Os, ^{193M}Pt, ^{197}Hg. In some embodiments of the present invention, the pharmaceutical composition comprises a pharmaceutically acceptable carrier or diluent and a conjugated compound that comprises an ST receptor binding moiety and an active moiety wherein the ST receptor binding moiety is selected from the group consisting of: SEQ ID NO:2, SEQ ID NO:3, SEQ ID NOS:5–54 and fragments and derivatives thereof and the active moiety is a radioactive agent selected from the group consisting of: ^{47}Sc, ^{67}Cu, ^{90}Y, ^{109}Pd, ^{123}I, ^{125}I, ^{131}I, ^{186}Re, ^{188}Re, ^{199}Au, ^{211}At, ^{212}Pb, ^{212}B, ^{32}P and ^{33}P, ^{71}Ge, ^{77}As, ^{103}Pb, ^{105}Rh, ^{111}Ag, ^{119}Sb, ^{121}Sn, ^{131}Cs, ^{143}Pr, ^{161}Tb, ^{177}Lu, ^{191}Os, ^{193M}Pt, ^{197}Hg, ^{32}P and ^{33}P, ^{71}Ge, ^{77}As, ^{103}Pb, ^{105}Rh, ^{111}Ag, ^{119}Sb, ^{121}Sn, ^{131}Cs, ^{143}Pr, ^{161}Tb, ^{177}Lu, ^{191}Os, ^{193M}Pt, ^{197}Hg, all beta negative and/or auger emitters. In some embodiments of the present invention, the pharmaceutical composition comprises a pharmaceutically acceptable carrier or diluent and a conjugated compound that comprises an ST receptor binding moiety and an active moiety wherein the active moiety is a radioactive agent selected from the group consisting of: ^{47}Sc, ^{67}Cu, ^{90}Y, ^{109}Pd, ^{123}I, ^{125}I, ^{131}I, ^{186}Re, ^{188}Re, ^{199}Au, ^{211}At, ^{212}Pb, ^{212}B, ^{32}P and ^{33}P, ^{71}Ge, ^{77}As, ^{103}Pb, ^{105}Rh, ^{111}Ag, ^{119}Sb, ^{121}Sn, ^{131}Cs, ^{143}Pr, ^{161}Tb, ^{177}Lu, ^{191}Os, ^{193M}Pt, ^{197}Hg. In some

embodiments of the present invention, the pharmaceutical composition comprises a pharmaceutically acceptable carrier or diluent and a conjugated compound that comprises an ST receptor binding moiety and an active moiety wherein the ST receptor binding moiety is selected from the group consisting of: SEQ ID NO:2, SEQ ID NO:3, SEQ ID NO:5, SEQ ID NO:6 and SEQ ID NO:54 and the active moiety is a radioactive agent selected from the group consisting of: ^{47}Sc, ^{67}Cu, ^{90}Y, ^{109}Pd, ^{123}I, ^{125}I, ^{131}I, ^{186}Re, ^{188}Re, ^{199}Au, ^{211}At, ^{212}Pb, ^{212}B, ^{32}P and ^{33}P, ^{71}Ge, ^{77}As, ^{103}Pb, ^{105}Rh, ^{111}Ag, ^{119}Sb, ^{121}Sn, ^{131}Cs, ^{143}Pr, ^{161}Tb, ^{177}Lu, ^{191}Os, ^{193M}Pt, ^{197}Hg. In some embodiments of the present invention, the pharmaceutical composition comprises a pharmaceutically acceptable carrier or diluent and a radioactive conjugated compound described in Example 1. The individual being treated may be diagnosed as having metastasized colorectal cancer or may be diagnosed as having localized colorectal cancer and may undergo the treatment proactively in the event that there is some metastasis as yet undetected. The pharmaceutical composition contains a therapeutically effective amount of the conjugated composition. A therapeutically effective amount is an amount which is effective to cause a cytotoxic or cytostatic effect on metastasized colorectal cancer cells without causing lethal side effects on the individual.

One aspect of the present invention relates to a method of detecting metastasized colorectal cancer cells in an individual suspected of suffering from metastasized colorectal cancer by radioimaging. Such individuals may be diagnosed as suffering from metastasized colorectal cancer and the metastasized colorectal cancer cells may be detected by administering to the individual, preferably by intravenous administration, a pharmaceutical composition that comprises a pharmaceutically acceptable carrier or diluent and a conjugated compound that comprises an ST receptor binding moiety and an active moiety wherein the active moiety is a radioactive and detecting the presence of a localized accumulation or aggregation of radioactivity, indicating the presence of cells with ST receptors. In some embodiments of the present invention, the pharmaceutical composition comprises a pharmaceutically acceptable carrier or diluent and a conjugated compound that comprises an ST receptor binding moiety and an active moiety wherein the active moiety is a radioactive and the ST receptor binding moiety is a peptide. In some embodiments of the present invention, the pharmaceutical composition comprises a pharmaceutically acceptable carrier or diluent and a conjugated compound that comprises an ST receptor binding moiety and an active moiety wherein the active moiety is a radioactive and the ST receptor binding moiety is selected from the group consisting of: SEQ ID NO:2, SEQ ID NO:3, SEQ ID NOS:5–54 and fragments and derivatives thereof. In some embodiments of the present invention, the pharmaceutical composition comprises a pharmaceutically acceptable carrier or diluent and a conjugated compound that comprises an ST receptor binding moiety and an active moiety wherein the active moiety is a radioactive and the ST receptor binding moiety is selected from the group consisting of: SEQ ID NO:2, SEQ ID NO:3, SEQ ID NO:5, SEQ ID NO:6 and SEQ ID NO:54. In some embodiments of the present invention, the pharmaceutical composition comprises a pharmaceutically acceptable carrier or diluent and a conjugated compound that comprises an ST receptor binding moiety and an active moiety wherein the active moiety is a radioactive agent selected from the group consisting of: radioactive heavy metals such as iron chelates, radioactive chelates of gadolinium or manganese, positron emitters of oxygen, nitrogen, iron, carbon, or gallium, ^{43}K, ^{52}Fe, ^{57}Co, ^{67}Cu, ^{67}Ga, ^{68}Ga, ^{77}Br, $^{81}Rb/^{81M}Kr$, ^{87M}Sr, ^{99M}Tc, ^{111}In, ^{113M}In, ^{123}I, ^{125}I, ^{127}Cs, ^{129}Cs, ^{131}I, ^{132}I, ^{197}Hg, ^{203}Pb and ^{206}Bi. In some embodiments of the present invention, the pharmaceutical composition comprises a pharmaceutically acceptable carrier or diluent and a conjugated compound that comprises an ST receptor binding moiety and an active moiety wherein the ST receptor binding moiety is selected from the group consisting of: SEQ ID NO:2, SEQ ID NO:3, SEQ ID NOS:5-54 and fragments and derivatives thereof and the active moiety is a radioactive agent selected from the group consisting of: radioactive heavy metals such as iron chelates, radioactive chelates of gadolinium or manganese, positron emitters of oxygen, nitrogen, iron, carbon, or gallium, ^{43}K, ^{52}Fe, ^{57}Co, ^{67}Cu, ^{67}Ga, ^{68}Ga, ^{77}Br, $^{81}Rb/^{81M}Kr$, ^{87M}Sr, ^{99M}Tc, ^{111}In, ^{113M}In, ^{123}I, ^{125}I, ^{127}Cs, ^{129}Cs, ^{131}I, ^{132}I, ^{197}Hg, ^{203}Pb and ^{206}Bi. In some embodiments of the present invention, the pharmaceutical composition comprises a pharmaceutically acceptable carrier or diluent and a conjugated compound that comprises an ST receptor binding moiety and an active moiety wherein the active moiety is a radioactive agent selected from the group consisting of: ^{43}K, ^{52}Fe, ^{57}Co, ^{67}Cu, ^{67}Ga, ^{68}Ga, ^{77}Br, $^{81}Rb/^{81M}Kr$, ^{87M}Sr, ^{99M}Tc, ^{111}In, ^{113M}In, ^{123}I, ^{125}I, ^{127}Cs, ^{129}Cs, ^{131}I, ^{132}I, ^{197}Hg, ^{203}Pb and ^{206}Bi. In some embodiments of the present invention, the pharmaceutical composition comprises a pharmaceutically acceptable carrier or diluent and a conjugated compound that comprises an ST receptor binding moiety and an active moiety wherein the ST receptor binding moiety is selected from the group consisting of: SEQ ID NO:2, SEQ ID NO:3, SEQ ID NO:5, SEQ ID NO:6 and SEQ ID NO:54 and the active moiety is a radioactive agent selected from the group consisting of: ^{43}K, ^{52}Fe, ^{57}Co, ^{67}Cu, ^{67}Ga, ^{68}Ga, ^{77}Br, $^{81}Rb/^{81M}Kr$, ^{87M}Sr, ^{99M}Tc, ^{111}In, ^{113M}In, ^{123}I, ^{125}I, ^{127}Cs, ^{129}Cs, ^{131}I, ^{132}I, ^{197}Hg, ^{203}Pb and ^{206}Bi. In some embodiments of the present invention, the pharmaceutical composition comprises a pharmaceutically acceptable carrier or diluent and a radioactive conjugated compound described in Example 1. The individual being treated may be diagnosed as having metastasized colorectal cancer or may be diagnosed as having localized colorectal cancer and may undergo the treatment proactively in the event that there is some metastasis as yet undetected. The pharmaceutical composition contains a diagnostically effective amount of the conjugated composition. A diagnostically effective amount is an amount which can be detected at a site in the body where cells with ST receptors are located without causing lethal side effects on the individual.

Another aspect of the invention relates to unconjugated compositions which comprise an ST receptor binding ligand and an active agent. For example, liposomes are small vesicles composed of lipids. Drugs can be introduced into the center of these vesicles. The outer shell of these vesicles comprise an ST receptor binding ligand. *Liposomes* Volumes 1, 2 and 3 CRC Press Inc. Boca Raton, Fla., which is incorporated herein by reference, disclose preparation of liposome-encapsulated active agents which include targeting agents that correspond to ST receptor ligand in the outer shell. Unconjugated compositions which comprise an ST receptor ligand in the matrix of a liposome with an active agent inside include such compostions in which the ST receptor ligand is selected from the group consisting of: SEQ ID NO:2, SEQ ID NO:3, SEQ ID NOS:5–54 and fragments and derivatives thereof and the active agent is selected from the group consisting of: methotrexate, doxorubicin, daunorubicin, cytosinarabinoside, etoposide, 5-4 fluorouracil, melphalan, chlorambucil, cis-platinum, vin-

desine, mitomycin, bleomycin, purothionin, macromomycin, 1,4 -benzoquinone derivatives, trenimon, ricin, ricin A chain, Pseudomonas exotoxin, diphtheria toxin, *Clostridium perfringens* phospholipase C, bovine pancreatic ribonuclease, pokeweed antiviral protein, abrin, abrin A chain, cobra venom factor, gelonin, saporin, modeccin, viscumin, volkensin, alkaline phosphatase, nitroimidazole, metronidazole and misonidazole.

Another aspect of the invention relates to unconjugated and conjugated compositions which comprise an ST receptor ligand used to deliver therapeutic nucleic acid molecules to cells that comprise an ST receptor such as normal cells of the intestinal tract as well as metastasized colorectal cancer cells. In some embodiments, the genetic material is delivered to metastasized tumor cells to produce an antigen that can be targeted by the immune system or to produce a protein which kills the cell or inhibits its proliferation. In some embodiments, the ST receptor ligand is used to deliver nucleic acids that encode nucleic acid molecules which replace defective endogenous genes or which encode therapeutic proteins. In some embodiments, the ST receptor ligand is thus used to deliver the active agent specifically to the cells lining the intestinal tract to treat diseases specific to this organ. According to this aspect of the invention, compositions comprise nucleic acid molecules which can replace defective genes. In some embodiments, the compositions are used in gene therapy protocols to deliver to individuals, genetic material needed and/or desired to make up for a genetic deficiency.

In some embodiments, the ST receptor ligand is combined with or incorporated into a delivery vehicle thereby converting the delivery vehicle into a specifically targeted delivery vehicle. For example, an ST receptor binding peptide may be integrated into the outer portion of a viral particle making such a virus an ST receptor-bearing cell specific virus. Similarly, the coat protein of a virus may be engineered such that it is produced as a fusion protein which includes an active ST receptor binding peptide that is exposed or otherwise accessible on the outside of the viral particle making such a virus an ST receptor-bearing cell-specific virus. In some embodiments, an ST receptor ligand may be integrated or otherwise incorporated into the liposomes wherein the ST receptor ligand is exposed or otherwise accessible on the outside of the liposome making such liposomes specifically targeted to ST receptor-bearing cells.

The active agent in the conjugated or unconjugated compositions according to this aspect of the invention is a nucleic acid molecule. The nucleic acid may be RNA or preferably DNA. In some embodiments, the nucleic acid molecule is an antisense molecule or encodes an antisense sequence whose presence in the cell inhibits production of an undesirable protein. In some embodiments, the nucleic acid molecule encodes a ribozyme whose presence in the cell inhibits production of an undesirable protein. In some embodiments, the nucleic acid molecule encodes a protein or peptide that is desirably produced in the cell. In some embodiments, the nucleic acid molecule encodes a functional copy of a gene that is defective in the targeted cell. The nucleic acid molecule is preferably operably linked to regulatory elements needed to express the coding sequence in the cell.

Liposomes are small vesicles composed of lipids. Genetic constructs which encode proteins that are desired to be expressed in ST receptor-bearing cells are introduced into the center of these vesicles. The outer shell of these vesicles comprise an ST receptor ligand, in some embodiments preferably an ST peptide. *Liposomes* Volumes 1, 2 and 3 CRC Press Inc. Boca Raton, Fla., which is incorporated herein by reference, disclose preparation of liposome-encapsulated active agents which include antibodies in the outer shell. In the present invention, an ST receptor ligand such as for example an ST peptide corresponds to the antibodies in the outer shell. Unconjugated compositions which comprise an ST receptor ligand in the matrix of a liposome with an active agent inside include such compositions in which the ST receptor ligand is selected from the group consisting of: SEQ ID NO:2, SEQ ID NO:3, SEQ ID NOS:5–54 and fragments and derivatives thereof.

In one embodiment for example, cystic fibrosis, a genetic disease in which there is a mutation of a specific gene encoding a chloride transport protein which ultimately produces abnormalities of function in many systems, most notably in the respiratory and intestinal tract, is treated by gene therapy techniques using ST receptor ligands to deliver the corrective gene to cells. Current therapy has been directed at replacing the mutant gene in the respiratory system with the normal gene by targeting these genes directly to the cells lining the respiratory tract using viruses which bind only to those cells. Similarly, the normal gene is packaged in liposomes targeted on their surface with ST receptor ligands and delivered to the intestinal tract. ST receptor ligands specifically target and direct the liposomes containing the normal gene to correct the lesion for cystic fibrosis to the specific cells lining the intestinal tract, from the duodenum to the rectum. Uptake of that genetic material by those cells should result in a cure of cystic fibrosis in the intestinal tract.

In another embodiment, the delivery of normal copies of the p53 tumor suppressor gene to the intestinal tract is accomplished using ST receptor ligand to target the gene therapeutic. Mutations of the p53 tumor suppressor gene appears to play a prominent role in the development of colorectal cancer in the intestinal tract. One approach to combatting this disease is the delivery of normal copies of this gene to the intestinal tract to cells expressing mutant forms of this gene. Genetic constructs that comprise normal p53 tumor suppressor genes are incorporated into liposomes that comprise an ST receptor ligand. The composition is delivered to the intestinal tract. ST receptor binding ligands specifically target and direct the liposomes containing the normal gene to correct the lesion created by mutation of p53 suppressor gene in intestinal cells.

Preparation of genetic constructs is with the skill of those having ordinary skill in the art. The present invention allows such construct to be specifically targeted by using the ST receptor ligands of the present invention. The compositions of the invention include an ST receptor ligand such as an ST peptide associated with a delivery vehicle and a gene construct which comprises a coding sequence for a protein whose production is desired in the cells of the intestinal tract linked to necessary regulatory sequences for expression in the cells. For uptake by cells of the intestinal tract, the compositions are administered orally or by enema whereby they enter the intestinal tract and contact cells which comprise ST receptors. The delivery vehicles associate with the ST receptor by virtue of the ST receptor ligand and the vehicle is internalized into the cell or the active agent/genetic construct is otherwise taken up by the cell. Once internalized, the construct can provide a therapeutic effect on the individual. One having ordinary skill in the art can readily formulate such compositions for oral or enema administration and determine the effective amount of such composition to be administered to treat the disease or disorder.

The following examples are illustrative but are not meant to be limiting of the present invention.

EXAMPLES

Example 1

The following are representative compounds according to the present invention. Whenever stated below, reference to a series of compounds is provided for efficiency and is meant to name each compound in the series including all the compounds in numerical order, such as for example "3-D1 to 3-D16" is meant to refer to compounds 3-D1, 3-D2, 3-D3, 3-D4, 3-D5, 3-D6, 3-D7, 3-D8, 3-D9, 3-D10, 3-D11, 3-D12, 3-D13, 3-D14, 3-D15 and 3-D16. Likewise, whenever stated below, reference to a series of SEQ ID NO:'s is provided for efficiency and is meant to name each SEQ ID NO: in the series including the all SEQ ID NO:'s in numerical order, such as for example SEQ ID NO:5 through SEQ ID NO:54 is meant to refer to SEQ ID NO:5, SEQ ID NO:6, SEQ ID NO:7, SEQ ID NO:8, SEQ ID NO:9, SEQ ID NO:10, SEQ ID NO:11, SEQ ID NO:12, SEQ ID NO:13, SEQ ID NO:14, SEQ ID NO:15, SEQ ID NO:16, SEQ ID NO:17, SEQ ID NO:18, SEQ ID NO:19, SEQ ID NO:20, SEQ ID NO:21, SEQ ID NO:22, SEQ ID NO:23, SEQ ID NO:24, SEQ ID NO:25, SEQ ID NO:26, SEQ ID NO:27, SEQ ID NO:28, SEQ ID NO:29, SEQ ID NO:30, SEQ ID NO:31, SEQ ID NO:32, SEQ ID NO:33, SEQ ID NO:34, SEQ ID NO:35, SEQ ID NO:36, SEQ ID NO:37, SEQ ID NO:38, SEQ ID NO:39, SEQ ID NO:40, SEQ ID NO:41, SEQ ID NO:42, SEQ ID NO:43, SEQ ID NO:44, SEQ ID NO:45, SEQ ID NO:46, SEQ ID NO:47, SEQ ID NO:48, SEQ ID NO:49, SEQ ID NO:50, SEQ ID NO:51, SEQ ID NO:52, SEQ ID NO:53 and SEQ ID NO:54. Similarly, whenever stated below, reference to a series of compounds is provided for efficiency and is meant to name each compound in the series including the all compounds in numerical order, such as for example "5-AP to 54-AP" is meant to refer to compounds 5-AP, 6-AP, 7-AP, 8-AP, 9-AP, 10-AP, 11-AP, 12-AP, 13-AP, 14-AP, 15-AP, 16-AP, 17-AP, 18-AP, 19-AP, 20-AP, 21-AP, 22-AP, 23-AP, 24-AP, 25-AP, 26-AP, 27-AP, 28-AP, 29-AP, 30-AP, 31-AP, 32-AP, 33-AP, 34-AP, 35-AP, 36-AP, 37-AP, 38-AP, 39-AP, 40-AP, 41-AP, 42-AP, 43-AP, 44-AP, 45-AP, 46-AP, 47-AP, 48-AP, 49-AP, 50-AP, 51-AP, 52-AP, 53-AP and 54-AP.

Compound 2-D1 comprises methotrexate (amethopterin) conjugated to SEQ ID NO:2.

Compound 2-D2 comprises doxorubicin (adrimycin) conjugated to SEQ ID NO:2.

Compound 2-D3 comprises daunorubicin conjugated to SEQ ID NO:2.

Compound 2-D4 comprises cytosinarabinoside conjugated to SEQ ID NO:2.

Compound 2-D5 comprises etoposide conjugated to SEQ ID NO:2.

Compound 2-D6 comprises 5-4 fluorouracil conjugated to SEQ ID NO:2.

Compound 2-D7 comprises melphalan conjugated to SEQ ID NO:2.

Compound 2-D8 comprises chlorambucil conjugated to SEQ ID NO:2.

Compound 2-D9 comprises cyclophosphamide conjugated to SEQ ID NO:2.

Compound 2-D10 comprises cis-platinum conjugated to SEQ ID NO:2.

Compound 2-D11 comprises vindesine conjugated to SEQ ID NO:2.

Compound 2-D12 comprises mitomycin conjugated to SEQ ID NO:2.

Compound 2-D13 comprises bleomycin conjugated to SEQ ID NO:2.

Compound 2-D14 comprises purothionin conjugated to SEQ ID NO:2.

Compound 2-D15 comprises macromomycin conjugated to SEQ ID NO:2.

Compound 2-D16 comprises trenimon conjugated to SEQ ID NO:2.

Compounds 3-D1 to 3-D16 are the same as compounds 2-D1 to 2-D16, respectively, except instead of comprising SEQ ID NO:2 as the ST receptor binding moiety, compounds 3-D1 to 3-D16 each comprise SEQ ID NO:3 as the ST receptor binding moiety.

Compounds 5-D1 to 5-D16 are the same as compounds 2-D1 to 2-D16, respectively, except instead of comprising SEQ ID NO:2 as the ST receptor binding moiety, compounds 5-D1 to 5-D16 each comprise SEQ ID NO:5 as the ST receptor binding moiety.

Compounds 6-D1 to 6-D16 are the same as compounds 2-D1 to 2-D16, respectively, except instead of comprising SEQ ID NO:2 as the ST receptor binding moiety, compounds 6-D1 to 6-D16 each comprise SEQ ID NO:6 as the ST receptor binding moiety.

Compounds 7-D1 to 7-D16 are the same as compounds 2-D1 to 2-D16, respectively, except instead of comprising SEQ ID NO:2 as the ST receptor binding moiety, compounds 7-D1 to 7-D16 each comprise SEQ ID NO:7 as the ST receptor binding moiety.

Compounds 8-D1 to 8-D16 are the same as compounds 2-D1 to 2-D16, respectively, except instead of comprising SEQ ID NO:2 as the ST receptor binding moiety, compounds 8-D1 to 8-D16 each comprise SEQ ID NO:8 as the ST receptor binding moiety.

Compounds 9-D1 to 9-D16 are the same as compounds 2-D1 to 2-D16, respectively, except instead of comprising SEQ ID NO:2 as the ST receptor binding moiety, compounds 9-D1 to 9-D16 each comprise SEQ ID NO:9 as the ST receptor binding moiety.

Compounds 10-D1 to 10-D16 are the same as compounds 2-D1 to 2-D16, respectively, except instead of comprising SEQ ID NO:2 as the ST receptor binding moiety, compounds 10-D1 to 10-D16 each comprise SEQ ID NO:2 as the ST receptor binding moiety.

Compounds 12-D1 to 12-D16 are the same as compounds 2-D1 to 2-D16, respectively, except instead of comprising SEQ ID NO:2 as the ST receptor binding moiety, compounds 12-D1 to 12-D16 each comprise SEQ ID NO:11 as the ST receptor binding moiety.

Compounds 12-D1 to 12-D16 are the same as compounds 2-D1 to 2-D16, respectively, except instead of comprising SEQ ID NO:2 as the ST receptor binding moiety, compounds 12-D1 to 12-D16 each comprise SEQ ID NO:12 as the ST receptor binding moiety.

Compounds 13-D1 to 13-D16 are the same as compounds 2-D1 to 2-D16, respectively, except instead of comprising SEQ ID NO:2 as the ST receptor binding moiety, compounds 13-D1 to 13-D16 each comprise SEQ ID NO:13 as the ST receptor binding moiety.

Compounds 14-D1 to 14-D16 are the same as compounds 2-D1 to 2-D16, respectively, except instead of comprising

SEQ ID NO:2 as the ST receptor binding moiety, compounds 14-D1 to 14-D16 each comprise SEQ ID NO:14 as the ST receptor binding moiety.

Compounds 15-D1 to 15-D16 are the same as compounds 2-D1 to 2-D16, respectively, except instead of comprising SEQ ID NO:2 as the ST receptor binding moiety, compounds 15-D1 to 15-D16 each comprise SEQ ID NO:15 as the ST receptor binding moiety.

Compounds 16-D1 to 16-D16 are the same as compounds 2-D1 to 2-D16, respectively, except instead of comprising SEQ ID NO:2 as the ST receptor binding moiety, compounds 16-D1 to 16-D16 each comprise SEQ ID NO:16 as the ST receptor binding moiety.

Compounds 17-D1 to 17-D16 are the same as compounds 2-D1 to 2-D16, respectively, except instead of comprising SEQ ID NO:2 as the ST receptor binding moiety, compounds 17-D1 to 17-D16 each comprise SEQ ID NO:17 as the ST receptor binding moiety.

Compounds 18-D1 to 18-D16 are the same as compounds 2-D1 to 2-D16, respectively, except instead of comprising SEQ ID NO:2 as the ST receptor binding moiety, compounds 18-D1 to 18-D16 each comprise SEQ ID NO:18 as the ST receptor binding moiety.

Compounds 19-D1 to 19-D16 are the same as compounds 2-D1 to 2-D16, respectively, except instead of comprising SEQ ID NO:2 as the ST receptor binding moiety, compounds 19-D1 to 19-D16 each comprise SEQ ID NO:19 as the ST receptor binding moiety.

Compounds 20-D1 to 20-D16 are the same as compounds 2-D1 to 2-D16, respectively, except instead of comprising SEQ ID NO:2 as the ST receptor binding moiety, compounds 20-D1 to 20-D16 each comprise SEQ ID NO:20 as the ST receptor binding moiety.

Compounds 22-D1 to 22-D16 are the same as compounds 2-D1 to 2-D16, respectively, except instead of comprising SEQ ID NO:2 as the ST receptor binding moiety, compounds 22-D1 to 22-D16 each comprise SEQ ID NO:21 as the ST receptor binding moiety.

Compounds 22-D1 to 22-D16 are the same as compounds 2-D1 to 2-D16, respectively, except instead of comprising SEQ ID NO:2 as the ST receptor binding moiety, compounds 22-D1 to 22-D16 each comprise SEQ ID NO:22 as the ST receptor binding moiety.

Compounds 23-D1 to 23-D16 are the same as compounds 2-D1 to 2-D16, respectively, except instead of comprising SEQ ID NO:2 as the ST receptor binding moiety, compounds 23-D1 to 23-D16 each comprise SEQ ID NO:23 as the ST receptor binding moiety.

Compounds 24-D1 to 24-D16 are the same as compounds 2-D1 to 2-D16, respectively, except instead of comprising SEQ ID NO:2 as the ST receptor binding moiety, compounds 24-D1 to 24-D16 each comprise SEQ ID NO:24 as the ST receptor binding moiety.

Compounds 25-D1 to 25-D16 are the same as compounds 2-D1 to 2-D16, respectively, except instead of comprising SEQ ID NO:2 as the ST receptor binding moiety, compounds 25-D1 to 25-D16 each comprise SEQ ID NO:25 as the ST receptor binding moiety.

Compounds 26-D1 to 26-D16 are the same as compounds 2-D1 to 2-D16, respectively, except instead of comprising SEQ ID NO:2 as the ST receptor binding moiety, compounds 26-D1 to 26-D16 each comprise SEQ ID NO:26 as the ST receptor binding moiety.

Compounds 27-D1 to 27-D16 are the same as compounds 2-D1 to 2-D16, respectively, except instead of comprising SEQ ID NO:2 as the ST receptor binding moiety, compounds 27-D1 to 27-D16 each comprise SEQ ID NO:27 as the ST receptor binding moiety.

Compounds 28-D1 to 28-D16 are the same as compounds 2-D1 to 2-D16, respectively, except instead of comprising SEQ ID NO:2 as the ST receptor binding moiety, compounds 28-D1 to 28-D16 each comprise SEQ ID NO:28 as the ST receptor binding moiety.

Compounds 29-D1 to 29-D16 are the same as compounds 2-D1 to 2-D16, respectively, except instead of comprising SEQ ID NO:2 as the ST receptor binding moiety, compounds 29-D1 to 29-D16 each comprise SEQ ID NO:29 as the ST receptor binding moiety.

Compounds 30-D1 to 30-D16 are the same as compounds 2-D1 to 2-D16, respectively, except instead of comprising SEQ ID NO:2 as the ST receptor binding moiety, compounds 30-D1 to 30-D16 each comprise SEQ ID NO:30 as the ST receptor binding moiety.

Compounds 32-D1 to 32-D16 are the same as compounds 2-D1 to 2-D16, respectively, except instead of comprising SEQ ID NO:2 as the ST receptor binding moiety, compounds 32-D1 to 32-D16 each comprise SEQ ID NO:31 as the ST receptor binding moiety.

Compounds 32-D1 to 32-D16 are the same as compounds 2-D1 to 2-D16, respectively, except instead of comprising SEQ ID NO:2 as the ST receptor binding moiety, compounds 32-D1 to 32-D16 each comprise SEQ ID NO:32 as the ST receptor binding moiety.

Compounds 33-D1 to 33-D16 are the same as compounds 2-D1 to 2-D16, respectively, except instead of comprising SEQ ID NO:2 as the ST receptor binding moiety, compounds 33-D1 to 33-D16 each comprise SEQ ID NO:33 as the ST receptor binding moiety.

Compounds 34-D1 to 34-D16 are the same as compounds 2-D1 to 2-D16, respectively, except instead of comprising SEQ ID NO:2 as the ST receptor binding moiety, compounds 34-D1 to 34-D16 each comprise SEQ ID NO:34 as the ST receptor binding moiety.

Compounds 35-D1 to 35-D16 are the same as compounds 2-D1 to 2-D16, respectively, except instead of comprising SEQ ID NO:2 as the ST receptor binding moiety, compounds 35-D1 to 35-D16 each comprise SEQ ID NO:35 as the ST receptor binding moiety.

Compounds 36-D1 to 36-D16 are the same as compounds 2-D1 to 2-D16, respectively, except instead of comprising SEQ ID NO:2 as the ST receptor binding moiety, compounds 36-D1 to 36-D16 each comprise SEQ ID NO:36 as the ST receptor binding moiety.

Compounds 37-D1 to 37-D16 are the same as compounds 2-D1 to 2-D16, respectively, except instead of comprising SEQ ID NO:2 as the ST receptor binding moiety, compounds 37-D1 to 37-D16 each comprise SEQ ID NO:37 as the ST receptor binding moiety.

Compounds 38-D1 to 38-D16 are the same as compounds 2-D1 to 2-D16, respectively, except instead of comprising SEQ ID NO:2 as the ST receptor binding moiety, compounds 38-D1 to 38-D16 each comprise SEQ ID NO:38 as the ST receptor binding moiety.

Compounds 39-D1 to 39-D16 are the same as compounds 2-D1 to 2-D16, respectively, except instead of comprising SEQ ID NO:2 as the ST receptor binding moiety, compounds 39-D1 to 39-D16 each comprise SEQ ID NO:39 as the ST receptor binding moiety.

Compounds 40-D1 to 40-D16 are the same as compounds 2-D1 to 2-D16, respectively, except instead of comprising

SEQ ID NO:2 as the ST receptor binding moiety, compounds 40-D1 to 40-D16 each comprise SEQ ID NO:40 as the ST receptor binding moiety.

Compounds 42-D1 to 42-D16 are the same as compounds 2-D1 to 2-D16, respectively, except instead of comprising SEQ ID NO:2 as the ST receptor binding moiety, compounds 42-D1 to 42-D16 each comprise SEQ ID NO:41 as the ST receptor binding moiety.

Compounds 42-D1 to 42-D16 are the same as compounds 2-D1 to 2-D16, respectively, except instead of comprising SEQ ID NO:2 as the ST receptor binding moiety, compounds 42-D1 to 42-D16 each comprise SEQ ID NO:42 as the ST receptor binding moiety.

Compounds 43-D1 to 43-D16 are the same as compounds 2-D1 to 2-D16, respectively, except instead of comprising SEQ ID NO:2 as the ST receptor binding moiety, compounds 43-D1 to 43-D16 each comprise SEQ ID NO:43 as the ST receptor binding moiety.

Compounds 44-D1 to 44-D16 are the same as compounds 2-D1 to 2-D16, respectively, except instead of comprising SEQ ID NO:2 as the ST receptor binding moiety, compounds 44-D1 to 44-D16 each comprise SEQ ID NO:44 as the ST receptor binding moiety.

Compounds 45-D1 to 45-D16 are the same as compounds 2-D1 to 2-D16, respectively, except instead of comprising SEQ ID NO:2 as the ST receptor binding moiety, compounds 45-D1 to 45-D16 each comprise SEQ ID NO:45 as the ST receptor binding moiety.

Compounds 46-D1 to 46-D16 are the same as compounds 2-D1 to 2-D16, respectively, except instead of comprising SEQ ID NO:2 as the ST receptor binding moiety, compounds 46-D1 to 46-D16 each comprise SEQ ID NO:46 as the ST receptor binding moiety.

Compounds 47-D1 to 47-D16 are the same as compounds 2-D1 to 2-D16, respectively, except instead of comprising SEQ ID NO:2 as the ST receptor binding moiety, compounds 47-D1 to 47-D16 each comprise SEQ ID NO:47 as the ST receptor binding moiety.

Compounds 48-D1 to 48-D16 are the same as compounds 2-D1 to 2-D16, respectively, except instead of comprising SEQ ID NO:2 as the ST receptor binding moiety, compounds 48-D1 to 48-D16 each comprise SEQ ID NO:48 as the ST receptor binding moiety.

Compounds 49-D1 to 49-D16 are the same as compounds 2-D1 to 2-D16, respectively, except instead of comprising SEQ ID NO:2 as the ST receptor binding moiety, compounds 49-D1 to 49-D16 each comprise SEQ ID NO:49 as the ST receptor binding moiety.

Compounds 50-D1 to 50-D16 are the same as compounds 2-D1 to 2-D16, respectively, except instead of comprising SEQ ID NO:2 as the ST receptor binding moiety, compounds 50-D1 to 50-D16 each comprise SEQ ID NO:50 as the ST receptor binding moiety.

Compounds 51-D1 to 51-D16 are the same as compounds 2-D1 to 2-D16, respectively, except instead of comprising SEQ ID NO:2 as the ST receptor binding moiety, compounds 51-D1 to 51-D16 each comprise SEQ ID NO:51 as the ST receptor binding moiety.

Compounds 52-D1 to 52-D16 are the same as compounds 2-D1 to 2-D16, respectively, except instead of comprising SEQ ID NO:2 as the ST receptor binding moiety, compounds 52-D1 to 52-D16 each comprise SEQ ID NO:52 as the ST receptor binding moiety.

Compounds 53-D1 to 53-D16 are the same as compounds 2-D1 to 2-D16, respectively, except instead of comprising SEQ ID NO:2 as the ST receptor binding moiety, compounds 53-D1 to 53-D16 each comprise SEQ ID NO:53 as the ST receptor binding moiety.

Compounds 54-D1 to 54-D16 are the same as compounds 2-D1 to 2-D16, respectively, except instead of comprising SEQ ID NO:2 as the ST receptor binding moiety, compounds 54-D1 to 54-D16 each comprise SEQ ID NO:54 as the ST receptor binding moiety.

Compound 2-T1 comprises ricin conjugated to SEQ ID NO:2.

Compound 2-T2 comprises ricin A chain (ricin toxin) conjugated to SEQ ID NO:2.

Compound 2-T3 comprises Pseudomonas exotoxin (PE) conjugated to SEQ ID NO:2.

Compound 2-T4 comprises diphtheria toxin (DT), conjugated to SEQ ID NO:2.

Compound 2-T5 comprises *Clostridium perfringens* phospholipase C (PLC) conjugated to SEQ ID NO:2.

Compound 2-T6 comprises bovine pancreatic ribonuclease (BPR) conjugated to SEQ ID NO:2.

Compound 2-T7 comprises pokeweed antiviral protein (PAP) conjugated to SEQ ID NO:2.

Compound 2-T8 comprises abrin conjugated to SEQ ID NO:2.

Compound 2-T9 comprises abrin A chain (abrin toxin) conjugated to SEQ ID NO:2.

Compound 2-T10 comprises cobra venom factor (CVF) conjugated to SEQ ID NO:2.

Compound 2-T11 comprises gelonin (GEL) conjugated to SEQ ID NO:2.

Compound 2-T12 comprises saporin (SAP) conjugated to SEQ ID NO:2.

Compound 2-T13 comprises modeccin conjugated to SEQ ID NO:2.

Compound 2-T14 comprises viscumin conjugated to SEQ ID NO:2.

Compound 2-T15 comprises volkensin conjugated to SEQ ID NO:2.

Compounds 3-T1 to 3-T15 are the same as compounds 2-T1 to 2-T15, respectively, except instead of comprising SEQ ID NO:2 as the ST receptor binding moiety, compounds 3-T1 to 3-T15 each comprise SEQ ID NO:3 as the ST receptor binding moiety.

Compounds 5-T1 to 5-T15 are the same as compounds 2-T1 to 2-T15, respectively, except instead of comprising SEQ ID NO:2 as the ST receptor binding moiety, compounds 5-T1 to 5-T15 each comprise SEQ ID NO:5 as the ST receptor binding moiety.

Compounds 6-T1 to 6-T15 are the same as compounds 2-T1 to 2-T15, respectively, except instead of comprising SEQ ID NO:2 as the ST receptor binding moiety, compounds 6-T1 to 6-T15 each comprise SEQ ID NO:6 as the ST receptor binding moiety.

Compounds 7-T1 to 7-T15 are the same as compounds 2-T1 to 2-T15, respectively, except instead of comprising SEQ ID NO:2 as the ST receptor binding moiety, compounds 7-T1 to 7-T15 each comprise SEQ ID NO:7 as the ST receptor binding moiety.

Compounds 8-T1 to 8-T15 are the same as compounds 2-T1 to 2-T15, respectively, except instead of comprising SEQ ID NO:2 as the ST receptor binding moiety, compounds 8-T1 to 8-T15 each comprise SEQ ID NO:8 as the ST receptor binding moiety.

Compounds 9-T1 to 9-T15 are the same as compounds 2-T1 to 2-T15, respectively, except instead of comprising SEQ ID NO:2 as the ST receptor binding moiety, compounds 9-T1 to 9-T15 each comprise SEQ ID NO:9 as the ST receptor binding moiety.

Compounds 10-T1 to 10-T15 are the same as compounds 2-T1 to 2-T15, respectively, except instead of comprising SEQ ID NO:2 as the ST receptor binding moiety, compounds 10-T1 to 10-T15 each comprise SEQ ID NO:2 as the ST receptor binding moiety.

Compounds 11-T1 to 11-T15 are the same as compounds 2-T1 to 2-T15, respectively, except instead of comprising SEQ ID NO:2 as the ST receptor binding moiety, compounds 11-T1 to 11-T15 each comprise SEQ ID NO:11 as the ST receptor binding moiety.

Compounds 12-T1 to 12-T15 are the same as compounds 2-T1 to 2-T15, respectively, except instead of comprising SEQ ID NO:2 as the ST receptor binding moiety, compounds 12-T1 to 12-T15 each comprise SEQ ID NO:12 as the ST receptor binding moiety.

Compounds 13-T1 to 13-T15 are the same as compounds 2-T1 to 2-T15, respectively, except instead of comprising SEQ ID NO:2 as the ST receptor binding moiety, compounds 13-T1 to 13-T15 each comprise SEQ ID NO:13 as the ST receptor binding moiety.

Compounds 14-T1 to 14-T15 are the same as compounds 2-T1 to 2-T15, respectively, except instead of comprising SEQ ID NO:2 as the ST receptor binding moiety, compounds 14-T1 to 14-T15 each comprise SEQ ID NO:14 as the ST receptor binding moiety.

Compounds 15-T1 to 15-T15 are the same as compounds 2-T1 to 2-T15, respectively, except instead of comprising SEQ ID NO:2 as the ST receptor binding moiety, compounds 15-T1 to 15-T15 each comprise SEQ ID NO:15 as the ST receptor binding moiety.

Compounds 15-T1 to 15-T15 are the same as compounds 2-T1 to 2-T15, respectively, except instead of comprising SEQ ID NO:2 as the ST receptor binding moiety, compounds 15-T1 to 15-T15 each comprise SEQ ID NO:15 as the ST receptor binding moiety.

Compounds 17-T1 to 17-T15 are the same as compounds 2-T1 to 2-T15, respectively, except instead of comprising SEQ ID NO:2 as the ST receptor binding moiety, compounds 17-T1 to 17-T15 each comprise SEQ ID NO:17 as the ST receptor binding moiety.

Compounds 18-T1 to 18-T15 are the same as compounds 2-T1 to 2-T15, respectively, except instead of comprising SEQ ID NO:2 as the ST receptor binding moiety, compounds 18-T1 to 18-T15 each comprise SEQ ID NO:18 as the ST receptor binding moiety.

Compounds 19-T1 to 19-T15 are the same as compounds 2-T1 to 2-T15, respectively, except instead of comprising SEQ ID NO:2 as the ST receptor binding moiety, compounds 19-T1 to 19-T15 each comprise SEQ ID NO:19 as the ST receptor binding moiety.

Compounds 20-T1 to 20-T15 are the same as compounds 2-T1 to 2-T15, respectively, except instead of comprising SEQ ID NO:2 as the ST receptor binding moiety, compounds 20-T1 to 20-T15 each comprise SEQ ID NO:20 as the ST receptor binding moiety.

Compounds 21-T1 to 21-T15 are the same as compounds 2-T1 to 2-T15, respectively, except instead of comprising SEQ ID NO:2 as the ST receptor binding moiety, compounds 21-T1 to 21-T15 each comprise SEQ ID NO:21 as the ST receptor binding moiety.

Compounds 22-T1 to 22-T15 are the same as compounds 2-T1 to 2-T15, respectively, except instead of comprising SEQ ID NO:2 as the ST receptor binding moiety, compounds 22-T1 to 22-T15 each comprise SEQ ID NO:22 as the ST receptor binding moiety.

Compounds 23-T1 to 23-T15 are the same as compounds 2-T1 to 2-T15, respectively, except instead of comprising SEQ ID NO:2 as the ST receptor binding moiety, compounds 23-T1 to 23-T15 each comprise SEQ ID NO:23 as the ST receptor binding moiety.

Compounds 24-T1 to 24-T15 are the same as compounds 2-T1 to 2-T15, respectively, except instead of comprising SEQ ID NO:2 as the ST receptor binding moiety, compounds 24-T1 to 24-T15 each comprise SEQ ID NO:24 as the ST receptor binding moiety.

Compounds 25-T1 to 25-T15 are the same as compounds 2-T1 to 2-T15, respectively, except instead of comprising SEQ ID NO:2 as the ST receptor binding moiety, compounds 25-T1 to 25-T15 each comprise SEQ ID NO:25 as the ST receptor binding moiety.

Compounds 26-T1 to 26-T15 are the same as compounds 2-T1 to 2-T15, respectively, except instead of comprising SEQ ID NO:2 as the ST receptor binding moiety, compounds 26-T1 to 26-T15 each comprise SEQ ID NO:26 as the ST receptor binding moiety.

Compounds 27-T1 to 27-T15 are the same as compounds 2-T1 to 2-T15, respectively, except instead of comprising SEQ ID NO:2 as the ST receptor binding moiety, compounds 27-T1 to 27-T15 each comprise SEQ ID NO:27 as the ST receptor binding moiety.

Compounds 28-T1 to 28-T15 are the same as compounds 2-T1 to 2-T15, respectively, except instead of comprising SEQ ID NO:2 as the ST receptor binding moiety, compounds 28-T1 to 28-T15 each comprise SEQ ID NO:28 as the ST receptor binding moiety.

Compounds 29-T1 to 29-T15 are the same as compounds 2-T1 to 2-T15, respectively, except instead of comprising SEQ ID NO:2 as the ST receptor binding moiety, compounds 29-T1 to 29-T15 each comprise SEQ ID NO:29 as the ST receptor binding moiety.

Compounds 30-T1 to 30-T15 are the same as compounds 2-T1 to 2-T15, respectively, except instead of comprising SEQ ID NO:2 as the ST receptor binding moiety, compounds 30-T1 to 30-T15 each comprise SEQ ID NO:30 as the ST receptor binding moiety.

Compounds 31-T1 to 31-T15 are the same as compounds 2-T1 to 2-T15, respectively, except instead of comprising SEQ ID NO:2 as the ST receptor binding moiety, compounds 31-T1 to 31-T15 each comprise SEQ ID NO:31 as the ST receptor binding moiety.

Compounds 32-T1 to 32-T15 are the same as compounds 2-T1 to 2-T15, respectively, except instead of comprising SEQ ID NO:2 as the ST receptor binding moiety, compounds 32-T1 to 32-T15 each comprise SEQ ID NO:32 as the ST receptor binding moiety.

Compounds 33-T1 to 33-T15 are the same as compounds 2-T1 to 2-T15, respectively, except instead of comprising SEQ ID NO:2 as the ST receptor binding moiety, compounds 33-T1 to 33-T15 each comprise SEQ ID NO:33 as the ST receptor binding moiety.

Compounds 34-T1 to 34-T15 are the same as compounds 2-T1 to 2-T15, respectively, except instead of comprising SEQ ID NO:2 as the ST receptor binding moiety, compounds 34-T1 to 34-T15 each comprise SEQ ID NO:34 as the ST receptor binding moiety.

Compounds 35-T1 to 35-T15 are the same as compounds 2-T1 to 2-T15, respectively, except instead of comprising SEQ ID NO:2 as the ST receptor binding moiety, compounds 35-T1 to 35-T15 each comprise SEQ ID NO:35 as the ST receptor binding moiety.

Compounds 36-T1 to 36-T15 are the same as compounds 2-T1 to 2-T15, respectively, except instead of comprising SEQ ID NO:2 as the ST receptor binding moiety, compounds 36-T1 to 36-T15 each comprise SEQ ID NO:36 as the ST receptor binding moiety.

Compounds 37-T1 to 37-T15 are the same as compounds 2-T1 to 2-T15, respectively, except instead of comprising SEQ ID NO:2 as the ST receptor binding moiety, compounds 37-T1 to 37-T15 each comprise SEQ ID NO:37 as the ST receptor binding moiety.

Compounds 38-T1 to 38-T15 are the same as compounds 2-T1 to 2-T15, respectively, except instead of comprising SEQ ID NO:2 as the ST receptor binding moiety, compounds 38-T1 to 38-T15 each comprise SEQ ID NO:38 as the ST receptor binding moiety.

Compounds 39-T1 to 39-T15 are the same as compounds 2-T1 to 2-T15, respectively, except instead of comprising SEQ ID NO:2 as the ST receptor binding moiety, compounds 39-T1 to 39-T15 each comprise SEQ ID NO:39 as the ST receptor binding moiety.

Compounds 40-T1 to 40-T15 are the same as compounds 2-T1 to 2-T15, respectively, except instead of comprising SEQ ID NO:2 as the ST receptor binding moiety, compounds 40-T1 to 40-T15 each comprise SEQ ID NO:40 as the ST receptor binding moiety.

Compounds 41-T1 to 41-T15 are the same as compounds 2-T1 to 2-T15, respectively, except instead of comprising SEQ ID NO:2 as the ST receptor binding moiety, compounds 41-T1 to 41-T15 each comprise SEQ ID NO:41 as the ST receptor binding moiety.

Compounds 42-T1 to 42-T15 are the same as compounds 2-T1 to 2-T15, respectively, except instead of comprising SEQ ID NO:2 as the ST receptor binding moiety, compounds 42-T1 to 42-T15 each comprise SEQ ID NO:42 as the ST receptor binding moiety.

Compounds 43-T1 to 43-T15 are the same as compounds 2-T1 to 2-T15, respectively, except instead of comprising SEQ ID NO:2 as the ST receptor binding moiety, compounds 43-T1 to 43-T15 each comprise SEQ ID NO:43 as the ST receptor binding moiety.

Compounds 44-T1 to 44-T15 are the same as compounds 2-T1 to 2-T15, respectively, except instead of comprising SEQ ID NO:2 as the ST receptor binding moiety, compounds 44-T1 to 44-T15 each comprise SEQ ID NO:44 as the ST receptor binding moiety.

Compounds 45-T1 to 45-T15 are the same as compounds 2-T1 to 2-T15, respectively, except instead of comprising SEQ ID NO:2 as the ST receptor binding moiety, compounds 45-T1 to 45-T15 each comprise SEQ ID NO:45 as the ST receptor binding moiety.

Compounds 46-T1 to 46-T15 are the same as compounds 2-T1 to 2-T15, respectively, except instead of comprising SEQ ID NO:2 as the ST receptor binding moiety, compounds 46-T1 to 46-T15 each comprise SEQ ID NO:46 as the ST receptor binding moiety.

Compounds 47-T1 to 47-T15 are the same as compounds 2-T1 to 2-T15, respectively, except instead of comprising SEQ ID NO:2 as the ST receptor binding moiety, compounds 47-T1 to 47-T15 each comprise SEQ ID NO:47 as the ST receptor binding moiety.

Compounds 48-T1 to 48-T15 are the same as compounds 2-T1 to 2-T15, respectively, except instead of comprising SEQ ID NO:2 as the ST receptor binding moiety, compounds 48-T1 to 48-T15 each comprise SEQ ID NO:48 as the ST receptor binding moiety.

Compounds 49-T1 to 49-T15 are the same as compounds 2-T1 to 2-T15, respectively, except instead of comprising SEQ ID NO:2 as the ST receptor binding moiety, compounds 49-T1 to 49-T15 each comprise SEQ ID NO:49 as the ST receptor binding moiety.

Compounds 50-T1 to 50-T15 are the same as compounds 2-T1 to 2-T15, respectively, except instead of comprising SEQ ID NO:2 as the ST receptor binding moiety, compounds 50-T1 to 50-T15 each comprise SEQ ID NO:50 as the ST receptor binding moiety.

Compounds 51-T1 to 51-T15 are the same as compounds 2-T1 to 2-T15, respectively, except instead of comprising SEQ ID NO:2 as the ST receptor binding moiety, compounds 51-T1 to 51-T15 each comprise SEQ ID NO:51 as the ST receptor binding moiety.

Compounds 52-T1 to 52-T15 are the same as compounds 2-T1 to 2-T15, respectively, except instead of comprising SEQ ID NO:2 as the ST receptor binding moiety, compounds 52-T1 to 52-T15 each comprise SEQ ID NO:52 as the ST receptor binding moiety.

Compounds 53-T1 to 53-T15 are the same as compounds 2-T1 to 2-T15, respectively, except instead of comprising SEQ ID NO:2 as the ST receptor binding moiety, compounds 53-T1 to 53-T15 each comprise SEQ ID NO:53 as the ST receptor binding moiety.

Compounds 54-T1 to 54-T15 are the same as compounds 2-T1 to 2-T15, respectively, except instead of comprising SEQ ID NO:2 as the ST receptor binding moiety, compounds 54-T1 to 54-T15 each comprise SEQ ID NO:54 as the ST receptor binding moiety.

Compounds 2-AP, 3-AP and 5-AP to 54-AP refer to the 51 conjugated compounds that comprise alkaline phosphatase conjugated to SEQ ID NO:2, SEQ ID NO:3 and SEQ ID NO:5 through SEQ ID NO:54, respectively.

Compounds 2-NIZ, 3-NIZ and 5-NIZ to 54-NIZ refer to the 51 conjugated compounds that comprise nitroimidazole conjugated to SEQ ID NO:2, SEQ ID NO:3 and SEQ ID NO:5 through SEQ ID NO:54, respectively.

Compounds 2-MEZ, 3-MEZ and 5-MEZ to 54-MEZ refer to the 51 conjugated compounds that comprise metronidazole conjugated to SEQ ID NO:2, SEQ ID NO:3 and SEQ ID NO:5 through SEQ ID NO:54, respectively.

Compounds 2-MIS, 3-MIS and 5-MIS to 54-MIS refer to the 51 conjugated compounds that comprise misonidazole conjugated to SEQ ID NO:2, SEQ ID NO:3 and SEQ ID NO:5 through SEQ ID NO:54, respectively.

Compounds 2-47Sc, 3-47Sc and 5-47Sc to 54-47Sc refer to the 51 conjugated compounds that comprise ^{47}Sc conjugated to SEQ ID NO:2, SEQ ID NO:3 AND SEQ ID NO:5 through SEQ ID NO:54, respectively.

Compounds 2-67Cu, 3-67Cu and 5-67Cu to 54-67Cu refer to the 51 conjugated compounds that comprise ^{67}Cu conjugated to SEQ ID NO:2, SEQ ID NO:3 AND SEQ ID NO:5 through SEQ ID NO:54, respectively.

Compounds 2-90Y, 3-90Y and 5-90Y to 54-90Y refer to the 51 conjugated compounds that comprise ^{90}Y conjugated to SEQ ID NO:2, SEQ ID NO:3 AND SEQ ID NO:5 through SEQ ID NO:54, respectively.

Compounds 2-109Pd, 3-109Pd and 5-109Pd to 54-109Pd refer to the 51 conjugated compounds that comprise ^{109}Pd

conjugated to SEQ ID NO:2, SEQ ID NO:3 AND SEQ ID NO:5 through SEQ ID NO:54, respectively.

Compounds 2-123I, 3-123I and 5-123I to 54-123I refer to the 51 conjugated compounds that comprise ^{123}I conjugated to SEQ ID NO:2, SEQ ID NO:3 AND SEQ ID NO:5 through SEQ ID NO:54, respectively.

Compounds 2-125I, 3-125I and 5-125I to 54-125I refer to the 51 conjugated compounds that comprise ^{125}I conjugated to SEQ ID NO:2, SEQ ID NO:3 AND SEQ ID NO:5 through SEQ ID NO:54, respectively.

Compounds 2-131I, 3-131I and 5-131I to 54-131I refer to the 51 conjugated compounds that comprise ^{131}I conjugated to SEQ ID NO:2, SEQ ID NO:3 AND SEQ ID NO:5 through SEQ ID NO:54, respectively.

Compounds 2-132I, 3-132I and 5-132I to 54-132I refer to the 51 conjugated compounds that comprise ^{132}I conjugated to SEQ ID NO:2, SEQ ID NO:3 AND SEQ ID NO:5 through SEQ ID NO:54, respectively.

Compounds 2-186Re, 3-186Re and 5-186Re to 54-186Re refer to the 51 conjugated compounds that comprise ^{186}Re, conjugated to SEQ ID NO:2, SEQ ID NO:3 AND SEQ ID NO:5 through SEQ ID NO:54, respectively.

Compounds 2-188Re, 3-188Re and 5-188Re to 54-188Re refer to the 51 conjugated compounds that comprise ^{188}Re, conjugated to SEQ ID NO:2, SEQ ID NO:3 AND SEQ ID NO:5 through SEQ ID NO:54, respectively.

Compounds 2-199Au, 3-199Au and 5-199Au to 54-199Au refer to the 51 conjugated compounds that comprise ^{199}Au, conjugated to SEQ ID NO:2, SEQ ID NO:3 AND SEQ ID NO:5 through SEQ ID NO:54, respectively.

Compounds 2-211At, 3-211At and 5-211At to 54-211At refer to the 51 conjugated compounds that comprise ^{211}At, conjugated to SEQ ID NO:2, SEQ ID NO:3 AND SEQ ID NO:5 through SEQ ID NO:54, respectively.

Compounds 2-212Pb, 3-212Pb and 5-212Pb to 54-212Pb refer to the 51 conjugated compounds that comprise ^{212}Pb conjugated to SEQ ID NO:2, SEQ ID NO:3 AND SEQ ID NO:5 through SEQ ID NO:54, respectively.

Compounds 2-212Bi, 3-212Bi and 5-212Bi to 54-212Bi refer to the 51 conjugated compounds that comprise ^{212}Bi conjugated to SEQ ID NO:2, SEQ ID NO:3 AND SEQ ID NO:5 through SEQ ID NO:54, respectively.

Compounds 2-203Pb, 3-203Pb and 5-203Pb to 54-203Pb refer to the 51 conjugated compounds that comprise ^{203}Pb conjugated to SEQ ID NO:2, SEQ ID NO:3 AND SEQ ID NO:5 through SEQ ID NO:54, respectively.

Compounds 2-206Bi, 3-206Bi and 5-206Bi to 54-206Bi refer to the 51 conjugated compounds that comprise ^{206}Bi conjugated to SEQ ID NO:2, SEQ ID NO:3 AND SEQ ID NO:5 through SEQ ID NO:54, respectively.

Compounds 2-32P, 3-32P and 5-32P to 54-32P refer to the 51 conjugated compounds that comprise ^{32}P conjugated to SEQ ID NO:2, SEQ ID NO:3 AND SEQ ID NO:5 through SEQ ID NO:54, respectively.

Compounds 2-33P, 3-33P and 5-33P to 54-33P refer to the 51 conjugated compounds that comprise ^{33}P conjugated to SEQ ID NO:2, SEQ ID NO:3 AND SEQ ID NO:5 through SEQ ID NO:54, respectively.

Compounds 2-71Ge, 3-71Ge and 5-71Ge to 54-71Ge refer to the 51 conjugated compounds that comprise ^{71}Ge conjugated to SEQ ID NO:2, SEQ ID NO:3 AND SEQ ID NO:5 through SEQ ID NO:54, respectively.

Compounds 2-77As, 3-77As and 5-77As to 54-77As refer to the 51 conjugated compounds that comprise ^{77}As conjugated to SEQ ID NO:2, SEQ ID NO:3 AND SEQ ID NO:5 through SEQ ID NO:54, respectively.

Compounds 2-103Pd, 3-103Pd and 5-103Pd to 54-103Pd refer to the 51 conjugated compounds that comprise ^{103}Pd conjugated to SEQ ID NO:2, SEQ ID NO:3 AND SEQ ID NO:5 through SEQ ID NO:54, respectively.

Compounds 2-105Rh, 3-105Rh and 5-105Rh to 54-105Rh refer to the 51 conjugated compounds that comprise ^{105}Rh conjugated to SEQ ID NO:2, SEQ ID NO:3 AND SEQ ID NO:5 through SEQ ID NO:54, respectively.

Compounds 2-111Ag, 3-111Ag and 5-111Ag to 54-111Ag refer to the 51 conjugated compounds that comprise ^{111}Ag conjugated to SEQ ID NO:2, SEQ ID NO:3 AND SEQ ID NO:5 through SEQ ID NO:54, respectively.

Compounds 2-119Sb, 3-119Sb and 5-119Sb to 54-119Sb refer to the 51 conjugated compounds that comprise ^{119}Sb conjugated to SEQ ID NO:2, SEQ ID NO:3 AND SEQ ID NO:5 through SEQ ID NO:54, respectively.

Compounds 2-121Sn, 3-121-Sn and 5-121Sn to 54-121Sn refer to the 51 conjugated compounds that comprise ^{121}Sn conjugated to SEQ ID NO:2, SEQ ID NO:3 AND SEQ ID NO:5 through SEQ ID NO:54, respectively.

Compounds 2-131Cs, 3-131Cs and 5-131Cs to 54-131Cs refer to the 51 conjugated compounds that comprise ^{131}Cs conjugated to SEQ ID NO:2, SEQ ID NO:3 AND SEQ ID NO:5 through SEQ ID NO:54, respectively.

Compounds 2-127Cs, 3-131Cs and 5-131Cs to 54-127Cs refer to the 51 conjugated compounds that comprise ^{127}Cs conjugated to SEQ ID NO:2, SEQ ID NO:3 AND SEQ ID NO:5 through SEQ ID NO:54, respectively.

Compounds 2-129Cs, 3-129Cs and 5-129Cs to 54-129Cs refer to the 51 conjugated compounds that comprise ^{129}Cs conjugated to SEQ ID NO:2, SEQ ID NO:3 AND SEQ ID NO:5 through SEQ ID NO:54, respectively.

Compounds 2-143Pr, 3-143Pr and 5-143Pr to 54-143Pr refer to the 51 conjugated compounds that comprise ^{143}Pr conjugated to SEQ ID NO:2, SEQ ID NO:3 AND SEQ ID NO:5 through SEQ ID NO:54, respectively.

Compounds 2-161Tb, 3-161Tb and 5-161Tb to 54-161Tb refer to the 51 conjugated compounds that comprise ^{161}Tb conjugated to SEQ ID NO:2, SEQ ID NO:3 AND SEQ ID NO:5 through SEQ ID NO:54, respectively.

Compounds 2-177Lu, 3-177Lu and 5-177Lu to 54-177Lu refer to the 51 conjugated compounds that comprise ^{177}Lu conjugated to SEQ ID NO:2, SEQ ID NO:3 AND SEQ ID NO:5 through SEQ ID NO:54, respectively.

Compounds 2-191Os, 3-191Os and 5-191Os to 54-191Os refer to the 51 conjugated compounds that comprise ^{191}Os conjugated to SEQ ID NO:2, SEQ ID NO:3 AND SEQ ID NO:5 through SEQ ID NO:54, respectively.

Compounds 2-193mPt, 3-193mPt and 5-193mPt to 54-193mPt refer to the 51 conjugated compounds that comprise ^{193M}Pt conjugated to SEQ ID NO:2, SEQ ID NO:3 AND SEQ ID NO:5 through SEQ ID NO:54, respectively.

Compounds 2-197Hg, 3-197Hg and 5-197Hg to 54-197Hg refer to the 51 conjugated compounds that comprise ^{197}Hg conjugated to SEQ ID NO:2, SEQ ID NO:3 AND SEQ ID NO:5 through SEQ ID NO:54, respectively.

Compounds 2-43K, 3-43K and 5-43K to 54-43K refer to the 51 conjugated compounds that comprise ^{43}K conjugated to SEQ ID NO:2, SEQ ID NO:3 AND SEQ ID NO:5 through SEQ ID NO:54, respectively.

Compounds 2-52Fe, 3-52Fe and 5-52Fe to 54-52Fe refer to the 51 conjugated compounds that comprise ^{52}Fe conju-

gated to SEQ ID NO:2, SEQ ID NO:3 AND SEQ ID NO:5 through SEQ ID NO:54, respectively.

Compounds 2-57Co, 3-57Co and 5-57Co to 54-57Co refer to the 51 conjugated compounds that comprise ^{57}Co conjugated to SEQ ID NO:2, SEQ ID NO:3 AND SEQ ID NO:5 through SEQ ID NO:54, respectively.

Compounds 2-67Ga, 3-67Ga and 5-67Ga to 54-67Ga refer to the 51 conjugated compounds that comprise ^{67}Ga conjugated to SEQ ID NO:2, SEQ ID NO:3 AND SEQ ID NO:5 through SEQ ID NO:54, respectively.

Compounds 2-68Ga, 3-68Ga and 5-68Ga to 54-68Ga refer to the 51 conjugated compounds that comprise ^{68}Ga conjugated to SEQ ID NO:2, SEQ ID NO:3 AND SEQ ID NO:5 through SEQ ID NO:54, respectively.

Compounds 2-77Br, 3-77Br and 5-77Br to 54-77Br refer to the 51 conjugated compounds that comprise ^{77}Br conjugated to SEQ ID NO:2, SEQ ID NO:3 AND SEQ ID NO:5 through SEQ ID NO:54, respectively.

Compounds 2-81Rb, 3-81Rb and 5-81Rb to 54-81Rb refer to the 51 conjugated compounds that comprise ^{81}Rb conjugated to SEQ ID NO:2, SEQ ID NO:3 AND SEQ ID NO:5 through SEQ ID NO:54, respectively.

Compounds 2-81mKr, 3-81mKr and 5-81mKr to 54-81mKr refer to the 51 conjugated compounds that comprise ^{81M}Kr conjugated to SEQ ID NO:2, SEQ ID NO:3 AND SEQ ID NO:5 through SEQ ID NO:54, respectively.

Compounds 2-87mSr, 3-87mSr and 5-87mSr to 54-87mSr refer to the 51 conjugated compounds that comprise ^{87M}Sr conjugated to SEQ ID NO:2, SEQ ID NO:3 AND SEQ ID NO:5 through SEQ ID NO:54, respectively.

Compounds 2-99mTc, 3-99mTc and 5-99mTc to 54-99mTc refer to the 51 conjugated compounds that comprise ^{99M}Tc conjugated to SEQ ID NO:2, SEQ ID NO:3 AND SEQ ID NO:5 through SEQ ID NO:54, respectively.

Compounds 2-111In, 3-111In and 5-111In to 54-111In refer to the 51 conjugated compounds that comprise ^{111}In conjugated to SEQ ID NO:2, SEQ ID NO:3 AND SEQ ID NO:5 through SEQ ID NO:54, respectively.

Compounds 2-113mIn, 3-113mIn and 5-113mIn to 54-113mIn refer to the 51 conjugated compounds that comprise ^{113M}In conjugated to SEQ ID NO:2, SEQ ID NO:3 AND SEQ ID NO:5 through SEQ ID NO:54, respectively.

The compounds described in this example are combined with a pharmaceutically acceptable carrier or diluent to produce pharmaceutical compositions according to the present invention. Radiostable compounds described herein are useful in pharmaceutical compositions as therapeutics in the treatment of individuals suspected of suffering from metastasized colorectal cancer including treatment of individuals diagnosed with localized colorectal cancer as a prophylactic/therapeutic before metastasis can be readily detected. When present in therapeutically effective amounts, radioactive compounds described herein are useful in pharmaceutical compositions as therapeutic agents in the treatment of individuals suspected of suffering from metastasized colorectal cancer including treatment of individuals diagnosed with localized colorectal cancer as a prophylactic/therapeutic before metastasis can be readily detected. When present in diagnostically effective amounts, radioactive compounds described herein are useful in pharmaceutical compositions as imaging agents in the diagnosis and identification of metastasized colorectal cancer in individuals.

Example 2

One procedure for crosslinking ST receptor ligands which have a free amino group such as ST receptor binding peptides, as for example SEQ ID NO:2, SEQ ID NO:3, and SEQ ID NOS:5–54 to active agents which have a free amino group such as methotrexate, doxorubicin, daunorubicin, cytosinarabinoside, cis-platin, vindesine, mitomycin and bleomycin, or alkaline phosphatase, or protein- or peptide-based toxin employs homobifunctional succinimidyl esters, preferably with chain carbon spacers such as disuccinimidyl suberate (Pierce Co, Rockford, Ill.). This approach of amino group derivatization has been employed successfully to crosslink native ST to biotin and, ultimately, to large agarose beads of micron-scale size, preserving the function of native ST (Hughes, M., et al. (1991) *Biochem.* 30:10738; Hakki, S., et al. (1993) *Int. J. Biochem.* 25:557; Almenoff, J. S., et al. (1992) *Mol. Micro.* 8:865; each of which is incorporated herein by reference).

An ST binding ligand with the free amino group such as an ST receptor binding peptide is incubated in the presence of the chemical crosslinking agent and an active agent which have a free amino group in equimolar quantities at room temperature for 15–30 min. Incubation is terminated by separating the reactants by gel permeation chromatography by HPLC. This technique separates the conjugated compounds from free active agents and free ST binding ligands, active agent-active agent conjugates and ST binding ligand-ST binding ligand conjugates. Homogeneous preparations of conjugated through their free amino groups and with a preferred molar ratio of 1:1 are obtained. As indicated above, complexing the free amino group of an ST peptide preserves receptor binding function.

Example 3

In the event that a cleavable conjugated compound is required, the same protocol as described above may be employed utilizing 3,3'-dithiobis (sulfosuccinimidylpropionate (SPDP); Pierce, Ill.). SPDP forms a sulfhydral group from a free amino group which may be used to conjugate a compound to another free amino group. For example, ST peptides such as SEQ ID NO:2, SEQ ID NO:3, SEQ ID NOS:5–54 are derivatized using established procedures employing N-succinimidyl-3 (2-pyridildithio)propionate (SPDP, Pharmacia-LKB, New Jersey). The ST peptide is incubated with a 5-fold molar excess of SPDP for 30 minutes at room temperature. The ST-pyridylthiopropionate conjugate is separated from unreacted reagents by gel permeation chromatography by HPLC. An active agent with a free amino group, such as a protein-based toxin, is prepared for conjugation by reduction with dithiothreitol for 4 hours at room temperature. Reduced active agent is incubated with a 2-fold molar excess of ST receptor ligand-PDP conjugate at pH 8.0 for 36 hours at 4°°C. Conjugate compound is purified from unreacted agents by gel permeation chromatography by HPLC.

This protocol for conjugation is particularly useful to conjugate ST peptides to diphtheria toxin A chains and Pseudomonas exotoxin as well as ricin toxin A chains (Magerstadt, M. *Antibody Conjugates and Malignant Disease.* (1991) CRC Press, Boca Raton, USA, pp. 110–152; Cawley, D. B. et al. (1980) Cell 22:563; Cumber, A. J., et al. (1985) *Meth. Enz.* 112:207; Gros, O. (1985) *J. Immunol. Meth.* 81:283; Worrell, N. R., et al. (1986) *Anti-Cancer Drug Design* 1:179; Thorpe, P. E. et al. (1987) *Cancer Res.* 47:5924, each of which is incorporated herein by reference).

Example 4

Active agents with a free amino group may be derivatized with SPDP as described above and conjugated with an ST

ligand that has a free amino group and that has been modified with the succinimidyl ester of iodoacetic acid (Pierce Co., Rockford, Ill.) (Magerstadt, M. (1991) *Antibody Conjugates And Malignant Disease*, CRC Press Boca Raton; Cumber, A. J. et al. (1985) *Meth. Enz.* 112:20, which are incorporated herein by reference). Conjugation relies on the selective reaction of iodoacetyl groups introduced into the amino terminal of the ST ligand with the thiol groups introduced into the active agent. As with the above protocol, this procedure avoids homopolymer formation. However, the product is conjugated through a central thioether linkage which cannot be reduced.

Example 5

An ST receptor ligand with a free amino group and active agents with free amino groups may be conjugated through a disulfide bond using iminothiolane (Pierce, Rockford, Ill.) (Fitzgerald, D. J. P. et al. (1983) *Cell* 32:607; Magerstadt, M. (1991) *Antibody Conjugates And Malignant Disease,* CRC Press, Boca Raton; Bjorn, M. J., et al. (1985) *Cancer Res.* 45:1214; Bjorn, M. J., et al. (1986) *Cancer Res.* 46:3262, which are incorporated herein by reference). The ST receptor ligand with a free amino group is derivatized at the amino terminal with iminothiolane and the active agent is derivatized with SPDP as described above. Reacting iminothiolane-derivatized ST receptor ligand with SPDP-derivatized active agent results in conjugation by a reducible disulfide bond. In addition, iminothiolane provides the versatility to conjugate these proteins through bonds other than disulfides. Thus, derivatization of active agents with the heterobifunctional agent sulfosuccinimidyl 4-(N-maleimidomethyl) cyclohexane (Pierce, Rockford, IL) and reaction with iminothiolane-derivatized ST receptor ligand will conjugate these peptides without formation of disulfides.

Example 6

Conjugated compounds according to the invention which comprise an active moiety that is a therapeutic agent specifically inhibit T84 cells in vitro. The following protocols may be used to demonstrate that the conjugated compounds according to the invention which comprise an active moiety that is chemotherapeutic or toxin specifically inhibit T84 cells in vitro. Inhibition of T84 cells is assessed by determining the effects of conjugated compounds on the ability of T84 cells to incorporate ^{35}S-leucine into protein, ^{3}H-thymidine into DNA, and to form colonies. The assessment of protein and DNA synthesis are classical techniques to determine the cytotoxicity of conjugated compounds in vitro. Inhibition of protein synthesis is measured because the toxins used as active moieties are specific inhibitors of this process. Therefore, these assays are the most sensitive measure of whether conjugated compounds are binding to and internalized into T84 cells. Inhibition of DNA synthesis is measured because some chemotherapeutics inhibit DNA synthesis and further, it is a cytotoxicity assay which correlates closely with the reproductive survivability of cells in culture. Cytotoxicity, or the disruption of normal cellular metabolic processes, may not always directly correlate with cell survivability. Therefore, assessment of colony formation will directly measure the ability of the experimental agents to decrease the survivability of tumor cells, which closely correlates with the impact of therapeutic agents on tumor viability in vivo. Controls include performing the same assay using the unconjugated form of the active agent and the unconjugated form of the ST receptor ligand of which the conjugated compound is comprised in place of the conjugated compound. The results obtained in the test assays and control assays are compared.

Conjugated compounds are assessed for their ability to inhibit protein and DNA synthesis in vitro and to inhibit survival and proliferation by measuring colony formation in monolayer culture by established protocols (Wilson, A. P. **(1987)** "Cytotoxicity and viability assays", Animal Cell Culture: A Practical Approach. Freshney, R. I., ed. pp. **183–216**, IRL Press, Oxford. which is incorporated herein by reference).

To assess the ability of a conjugated compound to inhibit protein synthesis in vitro, cells are plated in 200 μl of medium at a sub-confluent density of 1–2×10^{5} and allowed to attach to form a dividing cell monolayer over 12 hours at 37° C. Subsequently, the media is replaced with 200 μl of fresh media containing the appropriate concentration of conjugated compounds and cells incubated at 37° C. for various amounts of time. At the end of the indicated incubation period, cells is washed twice with medium and incubated at 37° C. in 0.5 ml of methionine-free medium supplemented with 0.5 μCi of L^{35}S-methionine (800 Ci/mmol). After incubation for another 2 hours at 37° C., the medium is aspirated, cells washed twice with medium containing 1 mg/ml of methionine, and then precipitated in 12% ice-cold TCA. Radioactivity recovered in TCA precipitates by centrifugation is quantified by liquid scintillation spectroscopy. In these studies, cells are maintained in log growth and assays are performed using triplicate wells. Data is expressed as a percentage of protein synthesis observed in the presence of experimental agents compared to untreated cells.

To assess the ability of a conjugated compound to inhibit DNA synthesis in vitro cells are plated as a subconfluent monolayer and incubated with experimental agents as described above. At the end of the incubation period, cells are washed twice and incubated at 37° C. in medium containing 2.5 μCi of ^{3}H-thymidine (5 Ci/mmol). After incubation for another hour, cells are processed with TCA, precipitates recovered, and radioactivity quantified as described above. As above, cells are maintained in log growth and assays is performed in triplicate. Data is expressed as a percentage of DNA synthesis observed in the presence of experimental agents compared to untreated cells.

To assess the ability of a conjugated compound to inhibit survival and proliferation by measuring colony formation in monolayer culture, cells are plated as a sub-confluent monolayer on 25 cm^{2} flasks and allowed to attach as described above. The medium is replaced with that containing various concentrations of experimental agents and incubated with cells for various amounts of time. At the end of the incubation, cells are recovered as a single cell suspension by trypsinization and replated to a density which will yield 100– 200 colonies per 6 cm plate. Cells are permitted to grow for 7 days, then fixed in methanol, stained with 1% crystal violet, and the number of colonies quantified. Assays are performed in duplicate and data is expressed as a percentage of colony formation observed in the presence of experimental agents compared to untreated cells. Results in our laboratory have demonstrated that T84 cells can be placed into single cell suspensions utilizing trypsin (10 μg/ml) with a plating efficiency of 40% and a doubling time of 18 hours.

Example 7

Radioactive iodine such as ^{123}I, ^{125}I, ^{131} I and ^{132}I, can be added to an ST receptor binding peptide such as an ST

peptide using a standard protocol well-known to those having ordinary skill in the art (Thompson, M. et al. (1985) *Analytical Biochemistry* 148:26, which is incorporated herein by reference). Radioactive iodine is conjugated directly to an ST peptide such as SEQ ID NO:2, SEQ ID NO:3 or SEQ ID NO:5 at tyrosine-5, tyrosine-4 or tyrosine-5, respectively.

Briefly, the ST peptide is produced in bacteria. For example, *E. coli* strain 431 is grown in culture and secretes ST into this culture. The culture media is then purified using routine techniques. ST can also be made by solid-phase synthesis as has been done previously, using standard techniques. (Dreyfus, L., et al. (1983) *Infec. Immun.* 42:539, which is incorporated herein by reference.

Ten micrograms of ST peptide are reacted with 2 milli-Curies of radioactive INa (Amersham Corporation, Massachusetts) in the presence of Iodobeads (Bio Rad Laboratories, California) and beta-D-glucose. These are reacted for 30 min after which the products are subjected to chromatography on a Sepak reversed-phase cartridge (Millipore Corp., Massachusetts) followed by separation on a C_{18}reversed-phase column by HPLC using a 20– 25% acetonitrile gradient. Conjugated compositions which comprise SEQ ID NO:2, SEQ ID NO:3 or SEQ ID NO:5 with the radioiodine attached to tyrosine-4 elutes at 45 min. These molecules retain full biochemical and pharmacological activity.

Example 8

^{125}I is conjugated directly to an ST peptide such as SEQ ID NO:13 at tyrosine-4.

SEQ ID NO:13 is produced by solid-phase synthesis as described above. Ten micrograms of SEQ ID NO:13 are reacted with 2 milliCuries of ^{125}INa (Amersham Corporation, Massachusetts) in the presence of Iodobeads (Bio Rad Laboratories, California) and beta-D-glucose. These are reacted for 30 min after which the products are subjected to chromatography on a Sepak reversed-phase cartridge (Millipore Corp., Massachusetts) followed by separation on a C_{18}reversed-phase column by HPLC using a 20– 25% acetonitrile gradient. ^{125}I-SEQ ID NO:13 conjugate with the radioiodine attached to tyrosine-4 elutes at 45 min. This molecule retains full biochemical and pharmacological activity.

Dosing of radioiodine for diagnostic imaging typically requires about 4 milliCuries/patient (Steinstraber, A., et al. (1988) *J. Nucl. Med.* 29:875; Wessels, B. W. and Rogus, R. D. (1984) *Med. Phys.* 11:638; Kwok, C. S., et al. (1985) *Med. Phys.* 12:405). For proteins labeled with a specific activity of 2,000 Curies/mmol, such as ST peptide, this would require about 10 micrograms of labeled peptide injected intravenously per patient for diagnostic imaging.

Example 9

^{131}I is conjugated directly to an ST peptide such as SEQ ID NO:13 at tyrosine-4.

SEQ ID NO:13 is produced by solid-phase synthesis as described above. Ten micrograms of SEQ ID NO:13 are reacted with 10 milliCuries of ^{131}INa (Amersham Corporation, Massachusetts) in the presence of Iodobeads (Bio Rad Laboratories, California) and beta-D-glucose. These are reacted for 30 min after which the products are subjected to chromatography on a Sepak reversed-phase cartridge (Millipore Corp., Massachusetts) followed by separation on a C_{18}reversed-phase column by HPLC using a 20– 25% acetonitrile gradient. ^{131}I-SEQ ID NO:13 conjugate with the radioiodine attached to tyrosine-4 elutes at 45 min. This molecule retains full biochemical and pharmacological activity.

Typically, for radioiodinated antibodies (MW=160,000 Da), about 150 nanomoles of protein (24 milligrams) labeled with a specific activity of 10,000 Curies/mmol are required per gram of tumor per patient (Humm, J. L. (1986) *J. Nucl. Med.* 27:1490). Thus, for proteins labeled with a specific activity of 2,000 Curies/mmol, with a molecular weight of 2,000 Da, such as ST peptide, about 3 milligrams would be required per gram of tumor per patient for intravenous infusion.

Example 10

In some embodiments, coupling of ST receptor ligands which have a free amino group, particularly ST receptor binding peptides such as ST peptides, and active agents with a free amino group such as protein-based toxins is performed by introducing a disulfide bridge between the 2 molecules. This strategy is particularly useful to conjugate ST peptides since the free amino terminal has been shown to be useful as a point of conjugation without affecting ST binding activity. This strategy is particularly useful to conjugate protein-based toxins since the free amino terminal is available on such molecules and for some conjugated compounds, most notably RTA conjugates, a disulfide bride which can be reduced to yield separate proteins has been demonstrated to be important in the construction of functional chimeras targeted by monoclonal antibodies (Magerstadt, M. (1991) *Antibody Conjugates And Malignant Disease,* CRC Press, Boca Raton; Bjorn, M. J., et al. (1985) *Cancer Res.* 45:1214; Bjorn, M. J., et al. (1986) *Cancer Res.* 46:3262; Masuho, Y., et al. (1982) *J. Biochem.* 91:1583, which are each incorporated herein by reference). While some toxins may be coupled to ST peptides using crosslinking agents which do not result in a reducible disulfide bridge between the individual components but retain functional cytotoxicity, ricin A chain toxin requires a reducible disulfide for cytotoxicity while Pseudomonas exotoxin, for example, does not.

Disulfide coupling is achieved using established procedures employing the heterobifunctional agent N-succinimidyl-3 (2-pyridyldithio)-proportionate (SPDP, Pharmacia-LKB, Piscataway, N.J.) (Magerstadt, M. (1991) *Antibody Conjugates And Malignant Disease*, CRC Press, Boca Raton; Cawley, D. B. et al. (1980) *Cell* 22:563; Cumber, A. J., et al. (1985) *Meth. Enz.* 112:20; Gros, O., et al. (1985) *J. Immunol. Meth.* 81:283; Worrell, N. R., (1986) *Anti-Cancer Drug Design* 1:19; Thorpe, P. E., et al. (1987) *Cancer Res.* 4:5924, which are incorporated herein by reference).

In some embodiments, toxins including the A chains of deglycosylated ricin toxin (RTA; Sigma Chemical Co., St. Louis, Mo.), diphtheria toxin A (DTA; Calbiochem, La Jolla, Calif.) and Pseudomonas exotoxin (PEA) are conjugated to ST peptides to produce conjugated compositions according to the present invention using this procedure. Deglycosylated RTA is employed since the glycosylated form of this toxin exhibits non-specific binding to liver cells. DTA is prepared from diphtheria toxin by an established procedure (Michel, A. and Drykx, J. (1975) *Biochem. Biophys. Acta* 365:15; Cumber, A. J., et al. (1985) *Meth. Enz.* 112:207, both of which are incorporated herein by reference). PEA

In some embodiments, ST peptides are conjugated to toxins by this procedure. For example, the ST peptide SEQ ID NO:3 which is produced as described above (see Drey-

fus, L., et al. (1983) *Infec. Immun.* 42:539, which is incorporated herein by reference).

Toxins are prepared for coupling by reduction with 0.1M dithiothreitol (DTT) for 4 hours at room temperature in 0.4M Tris-HCl, pH 8.0 and 1 mM EDTA. Reduced toxins are desalted on a Sephadex G-25 column equilibrated in TES buffer and mixed with a 2-fold molar excess of ST-PDP. Reactions are adjusted to pH 8.0 with TES and incubated at 4° C. for 36 hours. ST peptide-toxin conjugates are purified from unreacted products and homopolymers of ST peptides and toxins by gel filtration on Sephadex G-75 in 20 mM TES, pH 8.0 containing 0.1M NaCl. Chromatographic fractions are monitored by SDS-PAGE on 10% polyacrylamide gels under non-reducing conditions for the presence of 1:1 conjugates of ST peptides and toxins. Also, these conjugates are analyzed by 10% SDS-PAGE under reducing conditions, to insure that ST and cytotoxins are coupled by a reducible disulfide bond. Molar concentrations of the conjugate are calculated by quantifying radioactivity in these samples.

ST trace labeled with ^{125}I on tyrosine 4 (10 Ci/mmol) is used in order to follow the conjugate through various separation and chromatographic steps and to enable us to calculate the molar ratio of ST to cytotoxin in the final purified conjugate. ST trace labeled with ^{125}I is derivatized by incubating 1 mg/ml with a 5-fold molar excess of SPDP for 30 min at room temperature in Na phosphate buffer, pH 7.4. The ST-pyridylthiopropionate (ST-PDP) conjugate is purified from unreacted crosslinking agent by chromatography on Sephadex G-25 equilibrated with 20 mM N-Tris(hydroxymethyl)-methyl-2-aminoethane sulfonic acid (TES) buffer, pH 7.4. Preservation of receptor binding of conjugated ST peptides in human intestinal membranes is determined in competition assays of increasing concentrations of ST-PDP and ^{125}I-ST (5×10^{10}M), to insure that this process does not destroy the function of the ST receptor ligand.

The above coupling protocol has several advantages for conjugating the various toxins. First, it introduces a reducible disulfide bridge into the conjugated composition, important for RTA cytotoxicity. Also, this technique avoids the exposure of ST peptide to quantitative reduction with DTT which could interrupt its 3 intrachain disulfide bonds important for receptor binding activity. In addition, there is a single group available at the amino terminal of ST peptide for derivatization with SPDP and previous experiments have demonstrated that derivatization of that group preserves the binding properties of the ligand. Therefore, other configurations for conjugation which could result in inactivation of ST are not possible. Furthermore, PEA requires preactivation with DTT to achieve optimum cytotoxicity which will be accomplished utilizing the above protocol.

To produce a functional conjugated compound that comprises a toxin, it is essential that the receptor binding and enzyme activities of the moieties are preserved throughout the process of conjugation. Therefore, once such conjugate compounds are obtained, they are tested for the preservation of those functions. ST receptor binding activity of conjugated compounds is examined in competitive binding assays, as described above. In these studies, increasing concentrations of the conjugated compounds are incubated with a constant concentration (5×10^{10}M) of ^{125}I-ST and intestinal membranes (50–100 μg of protein) to achieve equilibrium. Parallel incubations contain excess (5×10^{7}M) unlabeled ST to assess non-specific binding. The concentration-dependent competitive displacement of radiolabeled ST by conjugated compounds is compared to the competitive displacement achieved by native ST. Displacement curves are employed to estimate the affinity of each conjugated compound (K_D) and compare that to the affinity of native ST measured by this technique. Control studies include evaluating the ability of unconjugated toxins to compete with native ST for receptor binding. These studies establish that the binding function of ST in the conjugated construct is preserved.

Preservation of toxin activity in conjugated compounds is also assessed. PEA and DTA induce toxicity by catalyzing the NAD-dependent ADP-ribosylation of elongation factor 2 (EF2), inhibiting protein synthesis. ADP-ribosyl transferase activity is assessed using an established assay (Chung, D. W. and Collier, R. J. *Infect. Immun.* 16:832; Fitzgerald, D. J. P. (1987) *Meth. Enz.* 151:139, which are both incorporated herein by reference). Reactions are conducted in 30 Mm Tris-HCl, pH 8.2 containing 40 mM DTT, 50 mCi ^{14}C-NAD, and 20 μl of rabbit reticulocyte lysate containing elongation factor 2 (EF-2; Promega, Madison, Wis.) in a total volume of 500 μl. Reactions are initiated by the addition of lysate, incubated for 30 minutes at 37° C., and terminated by the addition of ice-cold 12% TCA. Radioactivity in protein precipitates collected by centrifugation is quantified by liquid scintillation spectroscopy. The ability of the conjugated compounds that comprise DTA or PEA to catalyze the transfer of labeled ADP-ribose to EF-2 is compared to that catalyzed by similar quantities of unconjugated toxins. Control experiments include examining the ability of unconjugated toxins or ST to catalyze ADP-ribose transfer and the effects of ST on the enzymatic activity of unconjugated cytotoxins.

RTA inhibits protein synthesis by catalytically inactivating the 608 ribosomal subunit. The catalytic activity of conjugated compounds that comprise RTA is assessed by its ability to inhibit protein synthesis in cell-free assays using established procedures (Leonard, J. E. et al. (1985) *Cancer Res.* 45:5263 which is incorporated herein by reference). Assays contain 35 μl of nuclease-treated rabbit reticulocyte lysates, 1 μl of 1 mM mixed amino acids deficient in methionine, 2 μl of Brome mosaic RNA (Promega, Madison, Wis.) at 0.5 μg/μl, 7 μl of sterile water or conjugate solution, and 5 μCi of ^{35}S-methionine in a total volume of 50 μl. Reactions will be initiated by the addition of lysate, incubated at 30° C. for 30 minutes, and terminated by the use of addition of 12% TCA. Radioactivity in protein precipitates collected by centrifugation is quantified by liquid scintillation spectroscopy. Control experiments include examining the ability of unconjugated RTA or ST peptide to inhibit cell-free protein synthesis and the effects of ST peptide on the inhibitory activity of the unconjugated cytotoxin.

Example 11

Methotrexate is linked to SEQ ID NO:12 by the homobifunctional crosslinker succinimidyl esters with long chain carbon spacers such as disuccinimidyl suberate (Pierce, Ill.). SEQ ID NO:12 is incubated in the presence of the chemical crosslinking agent and methotrexate in equimolar quantities at room temperature for 15–30 min. Incubation is terminated by separating the reactants by gel permeation chromatography by HPLC. This technique separates the methotrexate/SEQ ID NO:12 conjugates from free drug, free ST peptide, drug-drug conjugates and ST peptide-ST peptide conjugates. Homogeneous preparations of SEQ ID NO:12-methotrexate conjugates coupled through their free amino groups and with a preferred molar ratio of 1:1 are obtained. Complexing the free amino group of ST preserves receptor binding function.

Example 12

^{111}In is coupled to SEQ ID NO:37 with functional amino groups using a chelator. The ST peptide has a free amino function at the amino terminal which may be modified without altering the ST receptor binding activity of the ST peptide. ^{111}In is rapidly and potently chelated by either EDTA (ethylenediaminetetraacetic acid) or DTPA (diethylenetriaminepetaacetic acid). DTPA is preferred over EDTA because the latter may be more unstable in vivo. The ^{113}In-DTPA is converted to a mixed N-hydroxysuccinimide ester which is reactive with free amino groups, mixed with ST, and the reaction products, including ^{111}In-SEQ ID NO:37 separated by HPLC (Bremer, K. H. and Schwarz, A. (1987) in *Safety And Efficacy Of Radiopharmaceuticals.* Kristensen, K. and Norbygaard, E., Eds. Martinius Nijhoff, Dordrecht, The Netherlands, P. 43; Krejcarek, G. E., and Tucker, K. L. (1977) *Biochem. Biophys. Res. Commun.* 77:581; Paxton, R. J., et al. (1985) *Cancer Res.* 45:5694; Richardson, A. P., et al. (1986) *Nucl. Med. Biol.* 14:569, which are each incorporated herein by reference).

Example 13

^{99m}Tc can be conjugated to SEQ ID NO:46 using an approach which is similar to that for indium. Thus, technetium can be chelated by DTPA which is converted to an anhydride, such as N-hydroxysuccinimide anhydride, and reacted with SEQ ID NO:46. The ST-technetium conjugate can then be separated using HPLC (Magerstadt, M. (1991) *Antibody Conjugates And Malignant Disease* CRC Press, Boca Raton; Eckelman, W. C. and Paik, C. H. (1986) *Nucl. Med. Biol.* 14:569)

Example 14

Diphtheria toxin A chain (DTA) is prepared from native diphtheria toxin by standard techniques. SEQ ID NO:22 is coupled to N-succinimidyl-3(2-pyridyldithio)-propionate (SPDP, Pharmacia-LKB, Piscataway, N.J.) and the SEQ ID NO:22-PDP conjugate is purified by HPLC by established procedures. DTA is reduced with dithiothreitol and incubated with SEQ ID NO:22-PDP. DTA-SEQ ID NO:22 is purified after conjugation using HPLC.

Example 15

Pseudomonas Exotoxin is prepared from native sources by standard techniques. SEQ ID NO:54 is coupled to N-succinimidyl-3(2-pyridyldithio)-propionate (SPDP, Pharmacia-LKB, Piscataway, N.J.) and the SEQ ID NO:54-PDP conjugate is purified by HPLC by established procedures. Pseudomonas Exotoxin is reduced with dithiothreitol and incubated with SEQ ID NO:54-PDP. Pseudomonas Exotoxin-SEQ ID NO:54 is purified after conjugation using HPLC.

Example 16

Doxorubicin is linked to SEQ ID NO:54 by the homobifunctional crosslinker succinimidyl esters with long chain carbon spacers such as disuccinimidyl suberate (Pierce, Ill.). SEQ ID NO:54 is incubated in the presence of the chemical crosslinking agent and doxorubicin in equimolar quantities at room temperature for 15–30 min. Incubation is terminated by separating the reactants by gel permeation chromatography by HPLC. This technique separates the doxorubicin/SEQ ID NO:54 conjugates from free doxorubicin, free ST peptide, drug-drug conjugates and ST peptide-ST peptide conjugates. Homogeneous preparations of SEQ ID NO:54-doxorubicin conjugates coupled through their free amino groups and with a preferred molar ratio of 1:1 are obtained. Complexing the free amino group of ST preserves receptor binding function.

Example 17

Daunorubicin is linked to SEQ ID NO:32 by the homobifunctional crosslinker succinimidyl esters with long chain carbon spacers such as disuccinimidyl suberate (Pierce, Ill.). SEQ ID NO:32 is incubated in the presence of the chemical crosslinking agent and daunorubicin in equimolar quantities at room temperature for 15–30 min. Incubation is terminated by separating the reactants by gel permeation chromatography by HPLC. This technique separates the daunorubicin/SEQ ID NO:54 conjugates from free daunorubicin, free ST peptide, drug-drug conjugates and ST peptide-ST peptide conjugates. Homogeneous preparations of SEQ ID NO:54-daunorubicin conjugates coupled through their free amino groups and with a preferred molar ratio of 1:1 are obtained. Complexing the free amino group of ST preserves receptor binding function.

SEQUENCE LISTING

(1) GENERAL INFORMATION:

(i i i) NUMBER OF SEQUENCES: 54

(2) INFORMATION FOR SEQ ID NO:1:

(i) SEQUENCE CHARACTERISTICS:
(A) LENGTH: 57 base pairs
(B) TYPE: nucleic acid
(C) STRANDEDNESS: double
(D) TOPOLOGY: both

(i i) MOLECULE TYPE: cDNA

(i x) FEATURE:

(A) NAME/KEY: CDS
(B) LOCATION: 1..57

(x i) SEQUENCE DESCRIPTION: SEQ ID NO:1:

```
AAC AAC ACA TTT TAC TGC TGT GAA CTT TGT TGT AAT CCT GCC TGT GCT    48
Asn Asn Thr Phe Tyr Cys Cys Glu Leu Cys Cys Asn Pro Ala Cys Ala
  1               5                  10                  15

GGA TGT TAT                                                      57
Gly Cys Tyr
```

(2) INFORMATION FOR SEQ ID NO:2:

(i) SEQUENCE CHARACTERISTICS:
(A) LENGTH: 19 amino acids
(B) TYPE: amino acid
(D) TOPOLOGY: linear

(i i) MOLECULE TYPE: protein

(x i) SEQUENCE DESCRIPTION: SEQ ID NO:2:

```
Asn Asn Thr Phe Tyr Cys Cys Glu Leu Cys Cys Asn Pro Ala Cys Ala
  1               5                  10                  15

Gly Cys Tyr
```

(2) INFORMATION FOR SEQ ID NO:3:

(i) SEQUENCE CHARACTERISTICS:
(A) LENGTH: 18 amino acids
(B) TYPE: amino acid
(D) TOPOLOGY: linear

(i i) MOLECULE TYPE: peptide

(x i) SEQUENCE DESCRIPTION: SEQ ID NO:3:

```
Asn Thr Phe Tyr Cys Cys Glu Leu Cys Cys Tyr Pro Ala Cys Ala Gly
1               5                  10                  15

Cys Asn
```

(2) INFORMATION FOR SEQ ID NO:4:

(i) SEQUENCE CHARACTERISTICS:
(A) LENGTH: 57 base pairs
(B) TYPE: nucleic acid
(C) STRANDEDNESS: double
(D) TOPOLOGY: both

(i i) MOLECULE TYPE: cDNA

(i x) FEATURE:
(A) NAME/KEY: CDS
(B) LOCATION: 1..57

(x i) SEQUENCE DESCRIPTION: SEQ ID NO:4:

```
AAT AGT AGC AAT TAC TGC TGT GAA TTG TGT TGT AAT CCT GCT TGT AAC    48
Asn Ser Ser Asn Tyr Cys Cys Glu Leu Cys Cys Asn Pro Ala Cys Asn
  1               5                  10                  15

GGG TGC TAT                                                      57
Gly Cys Tyr
```

(2) INFORMATION FOR SEQ ID NO:5:

(i) SEQUENCE CHARACTERISTICS:
(A) LENGTH: 19 amino acids
(B) TYPE: amino acid
(D) TOPOLOGY: linear

(i i) MOLECULE TYPE: protein

-continued

(x i) SEQUENCE DESCRIPTION: SEQ ID NO:5:

```
Asn Scr Scr Asn Tyr Cys Cys Glu Leu Cys Cys Asn Pro Ala Cys Asn
 1               5                  10                  15

Gly Cys Tyr
```

(2) INFORMATION FOR SEQ ID NO:6:

(i) SEQUENCE CHARACTERISTICS:
(A) LENGTH: 15 amino acids
(B) TYPE: amino acid
(D) TOPOLOGY: linear

(i i) MOLECULE TYPE: peptide

(x i) SEQUENCE DESCRIPTION: SEQ ID NO:6:

```
Pro Asn Thr Cys Glu Ile Cys Ala Tyr Ala Ala Cys Thr Gly Cys
 1               5                  10                  15
```

(2) INFORMATION FOR SEQ ID NO:7:

(i) SEQUENCE CHARACTERISTICS:
(A) LENGTH: 18 amino acids
(B) TYPE: amino acid
(D) TOPOLOGY: linear

(i i) MOLECULE TYPE: peptide

(x i) SEQUENCE DESCRIPTION: SEQ ID NO:7:

```
Asn Asn Thr Phe Tyr Cys Cys Glu Leu Cys Cys Asn Pro Ala Cys Ala
 1               5                  10                  15

Gly Cys
```

(2) INFORMATION FOR SEQ ID NO:8:

(i) SEQUENCE CHARACTERISTICS:
(A) LENGTH: 17 amino acids
(B) TYPE: amino acid
(D) TOPOLOGY: linear

(i i) MOLECULE TYPE: peptide

(x i) SEQUENCE DESCRIPTION: SEQ ID NO:8:

```
Asn Thr Phe Tyr Cys Cys Glu Leu Cys Cys Asn Pro Ala Cys Ala Gly
 1               5                  10                  15

Cys
```

(2) INFORMATION FOR SEQ ID NO:9:

(i) SEQUENCE CHARACTERISTICS:
(A) LENGTH: 16 amino acids
(B) TYPE: amino acid
(D) TOPOLOGY: linear

(i i) MOLECULE TYPE: peptide

(x i) SEQUENCE DESCRIPTION: SEQ ID NO:9:

```
Thr Phe Tyr Cys Cys Glu Leu Cys Cys Asn Pro Ala Cys Ala Gly Cys
 1               5                  10                  15
```

(2) INFORMATION FOR SEQ ID NO:10:

(i) SEQUENCE CHARACTERISTICS:
(A) LENGTH: 15 amino acids
(B) TYPE: amino acid
(D) TOPOLOGY: linear

(i i) MOLECULE TYPE: peptide

-continued

(x i) SEQUENCE DESCRIPTION: SEQ ID NO:10:

```
Phe Tyr Cys Cys Glu Leu Cys Cys Asn Pro Ala Cys Ala Gly Cys
 1               5                  10                  15
```

(2) INFORMATION FOR SEQ ID NO:11:

(i) SEQUENCE CHARACTERISTICS:
(A) LENGTH: 14 amino acids
(B) TYPE: amino acid
(D) TOPOLOGY: linear

(i i) MOLECULE TYPE: peptide

(x i) SEQUENCE DESCRIPTION: SEQ ID NO:11:

```
Tyr Cys Cys Glu Leu Cys Cys Asn Pro Ala Cys Ala Gly Cys
 1               5                  10
```

(2) INFORMATION FOR SEQ ID NO:12:

(i) SEQUENCE CHARACTERISTICS:
(A) LENGTH: 13 amino acids
(B) TYPE: amino acid
(D) TOPOLOGY: linear

(i i) MOLECULE TYPE: peptide

(x i) SEQUENCE DESCRIPTION: SEQ ID NO:12:

```
Cys Cys Glu Leu Cys Cys Asn Pro Ala Cys Ala Gly Cys
 1               5                  10
```

(2) INFORMATION FOR SEQ ID NO:13:

(i) SEQUENCE CHARACTERISTICS:
(A) LENGTH: 18 amino acids
(B) TYPE: amino acid
(D) TOPOLOGY: linear

(i i) MOLECULE TYPE: peptide

(x i) SEQUENCE DESCRIPTION: SEQ ID NO:13:

```
Asn Thr Phe Tyr Cys Cys Glu Leu Cys Cys Asn Pro Ala Cys Ala Gly
 1               5                  10                  15

Cys Tyr
```

(2) INFORMATION FOR SEQ ID NO:14:

(i) SEQUENCE CHARACTERISTICS:
(A) LENGTH: 17 amino acids
(B) TYPE: amino acid
(D) TOPOLOGY: linear

(i i) MOLECULE TYPE: peptide

(x i) SEQUENCE DESCRIPTION: SEQ ID NO:14:

```
Thr Phe Tyr Cys Cys Glu Leu Cys Cys Asn Pro Ala Cys Ala Gly Cys
 1               5                  10                  15

Tyr
```

(2) INFORMATION FOR SEQ ID NO:15:

(i) SEQUENCE CHARACTERISTICS:
(A) LENGTH: 16 amino acids
(B) TYPE: amino acid
(D) TOPOLOGY: linear

(i i) MOLECULE TYPE: peptide

-continued

(x i) SEQUENCE DESCRIPTION: SEQ ID NO:15:

Phe Tyr Cys Cys Glu Leu Cys Cys Asn Pro Ala Cys Ala Gly Cys Tyr
1 5 10 15

(2) INFORMATION FOR SEQ ID NO:16:

(i) SEQUENCE CHARACTERISTICS:
(A) LENGTH: 15 amino acids
(B) TYPE: amino acid
(D) TOPOLOGY: linear

(i i) MOLECULE TYPE: peptide

(x i) SEQUENCE DESCRIPTION: SEQ ID NO:16:

Tyr Cys Cys Glu Leu Cys Cys Asn Pro Ala Cys Ala Gly Cys Tyr
1 5 10 15

(2) INFORMATION FOR SEQ ID NO:17:

(i) SEQUENCE CHARACTERISTICS:
(A) LENGTH: 14 amino acids
(B) TYPE: amino acid
(D) TOPOLOGY: linear

(i i) MOLECULE TYPE: peptide

(x i) SEQUENCE DESCRIPTION: SEQ ID NO:17:

Cys Cys Glu Leu Cys Cys Asn Pro Ala Cys Ala Gly Cys Tyr
1 5 10

(2) INFORMATION FOR SEQ ID NO:18:

(i) SEQUENCE CHARACTERISTICS:
(A) LENGTH: 17 amino acids
(B) TYPE: amino acid
(D) TOPOLOGY: linear

(i i) MOLECULE TYPE: peptide

(x i) SEQUENCE DESCRIPTION: SEQ ID NO:18:

Asn Thr Phe Tyr Cys Cys Glu Leu Cys Cys Tyr Pro Ala Cys Ala Gly
1 5 10 15

Cys

(2) INFORMATION FOR SEQ ID NO:19:

(i) SEQUENCE CHARACTERISTICS:
(A) LENGTH: 16 amino acids
(B) TYPE: amino acid
(D) TOPOLOGY: linear

(i i) MOLECULE TYPE: peptide

(x i) SEQUENCE DESCRIPTION: SEQ ID NO:19:

Thr Phe Tyr Cys Cys Glu Leu Cys Cys Tyr Pro Ala Cys Ala Gly Cys
1 5 10 15

(2) INFORMATION FOR SEQ ID NO:20:

(i) SEQUENCE CHARACTERISTICS:
(A) LENGTH: 15 amino acids
(B) TYPE: amino acid
(D) TOPOLOGY: linear

(i i) MOLECULE TYPE: peptide

(x i) SEQUENCE DESCRIPTION: SEQ ID NO:20:

Phe Tyr Cys Cys Glu Leu Cys Cys Tyr Pro Ala Cys Ala Gly Cys

-continued

1 5 10 15

(2) INFORMATION FOR SEQ ID NO:21:

(i) SEQUENCE CHARACTERISTICS:
(A) LENGTH: 14 amino acids
(B) TYPE: amino acid
(D) TOPOLOGY: linear

(i i) MOLECULE TYPE: peptide

(x i) SEQUENCE DESCRIPTION: SEQ ID NO:21:

Tyr Cys Cys Glu Leu Cys Cys Tyr Pro Ala Cys Ala Gly Cys
1 5 10

(2) INFORMATION FOR SEQ ID NO:22:

(i) SEQUENCE CHARACTERISTICS:
(A) LENGTH: 13 amino acids
(B) TYPE: amino acid
(D) TOPOLOGY: linear

(i i) MOLECULE TYPE: peptide

(x i) SEQUENCE DESCRIPTION: SEQ ID NO:22:

Cys Cys Glu Leu Cys Cys Tyr Pro Ala Cys Ala Gly Cys
1 5 10

(2) INFORMATION FOR SEQ ID NO:23:

(i) SEQUENCE CHARACTERISTICS:
(A) LENGTH: 17 amino acids
(B) TYPE: amino acid
(D) TOPOLOGY: linear

(i i) MOLECULE TYPE: peptide

(x i) SEQUENCE DESCRIPTION: SEQ ID NO:23:

Thr Phe Tyr Cys Cys Glu Leu Cys Cys Tyr Pro Ala Cys Ala Gly Cys
1 5 10 15

Asn

(2) INFORMATION FOR SEQ ID NO:24:

(i) SEQUENCE CHARACTERISTICS:
(A) LENGTH: 16 amino acids
(B) TYPE: amino acid
(D) TOPOLOGY: linear

(i i) MOLECULE TYPE: peptide

(x i) SEQUENCE DESCRIPTION: SEQ ID NO:24:

Phe Tyr Cys Cys Glu Leu Cys Cys Tyr Pro Ala Cys Ala Gly Cys Asn
1 5 10 15

(2) INFORMATION FOR SEQ ID NO:25:

(i) SEQUENCE CHARACTERISTICS:
(A) LENGTH: 15 amino acids
(B) TYPE: amino acid
(D) TOPOLOGY: linear

(i i) MOLECULE TYPE: peptide

(x i) SEQUENCE DESCRIPTION: SEQ ID NO:25:

Tyr Cys Cys Glu Leu Cys Cys Tyr Pro Ala Cys Ala Gly Cys Asn
1 5 10 15

-continued

(2) INFORMATION FOR SEQ ID NO:26:

(i) SEQUENCE CHARACTERISTICS:
(A) LENGTH: 14 amino acids
(B) TYPE: amino acid
(D) TOPOLOGY: linear

(i i) MOLECULE TYPE: peptide

(x i) SEQUENCE DESCRIPTION: SEQ ID NO:26:

```
Cys Cys Glu Leu Cys Cys Tyr Pro Ala Cys Ala Gly Cys Asn
 1               5                  10
```

(2) INFORMATION FOR SEQ ID NO:27:

(i) SEQUENCE CHARACTERISTICS:
(A) LENGTH: 18 amino acids
(B) TYPE: amino acid
(D) TOPOLOGY: linear

(i i) MOLECULE TYPE: peptide

(x i) SEQUENCE DESCRIPTION: SEQ ID NO:27:

```
Asn Ser Ser Asn Tyr Cys Cys Glu Leu Cys Cys Asn Pro Ala Cys Thr
 1               5                  10                  15

Gly Cys
```

(2) INFORMATION FOR SEQ ID NO:28:

(i) SEQUENCE CHARACTERISTICS:
(A) LENGTH: 17 amino acids
(B) TYPE: amino acid
(D) TOPOLOGY: linear

(i i) MOLECULE TYPE: peptide

(x i) SEQUENCE DESCRIPTION: SEQ ID NO:28:

```
Ser Ser Asn Tyr Cys Cys Glu Leu Cys Cys Asn Pro Ala Cys Thr Gly
 1               5                  10                  15

Cys
```

(2) INFORMATION FOR SEQ ID NO:29:

(i) SEQUENCE CHARACTERISTICS:
(A) LENGTH: 16 amino acids
(B) TYPE: amino acid
(D) TOPOLOGY: linear

(i i) MOLECULE TYPE: peptide

(x i) SEQUENCE DESCRIPTION: SEQ ID NO:29:

```
Ser Asn Tyr Cys Cys Glu Leu Cys Cys Asn Pro Ala Cys Thr Gly Cys
 1               5                  10                  15
```

(2) INFORMATION FOR SEQ ID NO:30:

(i) SEQUENCE CHARACTERISTICS:
(A) LENGTH: 15 amino acids
(B) TYPE: amino acid
(D) TOPOLOGY: linear

(i i) MOLECULE TYPE: peptide

(x i) SEQUENCE DESCRIPTION: SEQ ID NO:30:

```
Asn Tyr Cys Cys Glu Leu Cys Cys Asn Pro Ala Cys Thr Gly Cys
 1               5                  10                  15
```

(2) INFORMATION FOR SEQ ID NO:31:

(i) SEQUENCE CHARACTERISTICS:
(A) LENGTH: 14 amino acids
(B) TYPE: amino acid
(D) TOPOLOGY: linear

(i i) MOLECULE TYPE: peptide

(x i) SEQUENCE DESCRIPTION: SEQ ID NO:31:

```
Tyr Cys Cys Glu Leu Cys Cys Asn Pro Ala Cys Thr Gly Cys
 1               5                  10
```

(2) INFORMATION FOR SEQ ID NO:32:

(i) SEQUENCE CHARACTERISTICS:
(A) LENGTH: 13 amino acids
(B) TYPE: amino acid
(D) TOPOLOGY: linear

(i i) MOLECULE TYPE: peptide

(x i) SEQUENCE DESCRIPTION: SEQ ID NO:32:

```
Cys Cys Glu Leu Cys Cys Asn Pro Ala Cys Thr Gly Cys
 1               5                  10
```

(2) INFORMATION FOR SEQ ID NO:33:

(i) SEQUENCE CHARACTERISTICS:
(A) LENGTH: 18 amino acids
(B) TYPE: amino acid
(D) TOPOLOGY: linear

(i i) MOLECULE TYPE: peptide

(x i) SEQUENCE DESCRIPTION: SEQ ID NO:33:

```
Ser Ser Asn Tyr Cys Cys Glu Leu Cys Cys Asn Pro Ala Cys Thr Gly
 1               5                  10                  15

Cys Tyr
```

(2) INFORMATION FOR SEQ ID NO:34:

(i) SEQUENCE CHARACTERISTICS:
(A) LENGTH: 17 amino acids
(B) TYPE: amino acid
(D) TOPOLOGY: linear

(i i) MOLECULE TYPE: peptide

(x i) SEQUENCE DESCRIPTION: SEQ ID NO:34:

```
Ser Asn Tyr Cys Cys Glu Leu Cys Cys Asn Pro Ala Cys Thr Gly Cys
 1               5                  10                  15

Tyr
```

(2) INFORMATION FOR SEQ ID NO:35:

(i) SEQUENCE CHARACTERISTICS:
(A) LENGTH: 16 amino acids
(B) TYPE: amino acid
(D) TOPOLOGY: linear

(i i) MOLECULE TYPE: peptide

(x i) SEQUENCE DESCRIPTION: SEQ ID NO:35:

```
Asn Tyr Cys Cys Glu Leu Cys Cys Asn Pro Ala Cys Thr Gly Cys Tyr
 1               5                  10                  15
```

(2) INFORMATION FOR SEQ ID NO:36:

(i) SEQUENCE CHARACTERISTICS:
(A) LENGTH: 15 amino acids
(B) TYPE: amino acid
(D) TOPOLOGY: linear

(i i) MOLECULE TYPE: peptide

(x i) SEQUENCE DESCRIPTION: SEQ ID NO:36:

```
Tyr Cys Cys Glu Leu Cys Cys Asn Pro Ala Cys Thr Gly Cys Tyr
 1               5                  10                  15
```

(2) INFORMATION FOR SEQ ID NO:37:

(i) SEQUENCE CHARACTERISTICS:
(A) LENGTH: 14 amino acids
(B) TYPE: amino acid
(D) TOPOLOGY: linear

(i i) MOLECULE TYPE: peptide

(x i) SEQUENCE DESCRIPTION: SEQ ID NO:37:

```
Cys Cys Glu Leu Cys Cys Asn Pro Ala Cys Thr Gly Cys Tyr
 1               5                  10
```

(2) INFORMATION FOR SEQ ID NO:38:

(i) SEQUENCE CHARACTERISTICS:
(A) LENGTH: 18 amino acids
(B) TYPE: amino acid
(D) TOPOLOGY: linear

(i i) MOLECULE TYPE: peptide

(x i) SEQUENCE DESCRIPTION: SEQ ID NO:38:

```
Asn Thr Phe Tyr Cys Cys Glu Leu Cys Cys Asn Pro Ala Cys Ala Gly
 1               5                  10                  15

Cys Tyr
```

(2) INFORMATION FOR SEQ ID NO:39:

(i) SEQUENCE CHARACTERISTICS:
(A) LENGTH: 18 amino acids
(B) TYPE: amino acid
(D) TOPOLOGY: linear

(i i) MOLECULE TYPE: peptide

(x i) SEQUENCE DESCRIPTION: SEQ ID NO:39:

```
Asn Thr Phe Tyr Cys Cys Glu Leu Cys Cys Ala Pro Ala Cys Ala Gly
 1               5                  10                  15

Cys Tyr
```

(2) INFORMATION FOR SEQ ID NO:40:

(i) SEQUENCE CHARACTERISTICS:
(A) LENGTH: 18 amino acids
(B) TYPE: amino acid
(D) TOPOLOGY: linear

(i i) MOLECULE TYPE: peptide

(x i) SEQUENCE DESCRIPTION: SEQ ID NO:40:

```
Asn Thr Phe Tyr Cys Cys Glu Leu Cys Cys Asn Ala Ala Cys Ala Gly
 1               5                  10                  15

Cys Tyr
```

(2) INFORMATION FOR SEQ ID NO:41:

-continued

(i) SEQUENCE CHARACTERISTICS:
(A) LENGTH: 17 amino acids
(B) TYPE: amino acid
(D) TOPOLOGY: linear

(i i) MOLECULE TYPE: peptide

(x i) SEQUENCE DESCRIPTION: SEQ ID NO:41:

```
Asn Thr Phe Tyr Cys Cys Glu Leu Cys Cys Asn Pro Ala Cys Ala Gly
  1               5                  10                  15

Cys
```

(2) INFORMATION FOR SEQ ID NO:42:

(i) SEQUENCE CHARACTERISTICS:
(A) LENGTH: 15 amino acids
(B) TYPE: amino acid
(D) TOPOLOGY: linear

(i i) MOLECULE TYPE: peptide

(x i) SEQUENCE DESCRIPTION: SEQ ID NO:42:

```
Tyr Cys Cys Glu Leu Cys Cys Asn Pro Ala Cys Ala Gly Cys Tyr
  1               5                  10                  15
```

(2) INFORMATION FOR SEQ ID NO:43:

(i) SEQUENCE CHARACTERISTICS:
(A) LENGTH: 14 amino acids
(B) TYPE: amino acid
(D) TOPOLOGY: linear

(i i) MOLECULE TYPE: peptide

(x i) SEQUENCE DESCRIPTION: SEQ ID NO:43:

```
Tyr Cys Cys Glu Leu Cys Cys Asn Pro Ala Cys Ala Gly Cys
  1               5                  10
```

(2) INFORMATION FOR SEQ ID NO:44:

(i) SEQUENCE CHARACTERISTICS:
(A) LENGTH: 14 amino acids
(B) TYPE: amino acid
(D) TOPOLOGY: linear

(i i) MOLECULE TYPE: peptide

(x i) SEQUENCE DESCRIPTION: SEQ ID NO:44:

```
Cys Cys Glu Leu Cys Cys Asn Pro Ala Cys Ala Gly Cys Tyr
  1               5                  10
```

(2) INFORMATION FOR SEQ ID NO:45:

(i) SEQUENCE CHARACTERISTICS:
(A) LENGTH: 13 amino acids
(B) TYPE: amino acid
(D) TOPOLOGY: linear

(i i) MOLECULE TYPE: peptide

(x i) SEQUENCE DESCRIPTION: SEQ ID NO:45:

```
Cys Cys Glu Leu Cys Cys Asn Pro Ala Cys Ala Gly Cys
  1               5                  10
```

(2) INFORMATION FOR SEQ ID NO:46:

(i) SEQUENCE CHARACTERISTICS:
(A) LENGTH: 25 amino acids

(B) TYPE: amino acid
(D) TOPOLOGY: linear

(i i) MOLECULE TYPE: peptide

(x i) SEQUENCE DESCRIPTION: SEQ ID NO:46:

```
Gln Ala Cys Asp Pro Pro Ser Pro Pro Ala Glu Val Cys Cys Asp Val
 1               5                  10                  15

Cys Cys Asn Pro Ala Cys Ala Gly Cys
            20                  25
```

(2) INFORMATION FOR SEQ ID NO:47:

(i) SEQUENCE CHARACTERISTICS:
(A) LENGTH: 16 amino acids
(B) TYPE: amino acid
(D) TOPOLOGY: linear

(i i) MOLECULE TYPE: peptide

(x i) SEQUENCE DESCRIPTION: SEQ ID NO:47:

```
Ile Asp Cys Cys Ile Cys Cys Asn Pro Ala Cys Phe Gly Cys Leu Asn
 1               5                  10                  15
```

(2) INFORMATION FOR SEQ ID NO:48:

(i) SEQUENCE CHARACTERISTICS:
(A) LENGTH: 18 amino acids
(B) TYPE: amino acid
(D) TOPOLOGY: linear

(i i) MOLECULE TYPE: peptide

(x i) SEQUENCE DESCRIPTION: SEQ ID NO:48:

```
Ser Ser Asp Trp Asp Cys Cys Asp Val Cys Cys Asn Pro Ala Cys Ala
 1               5                  10                  15

Gly Cys
```

(2) INFORMATION FOR SEQ ID NO:49:

(i) SEQUENCE CHARACTERISTICS:
(A) LENGTH: 19 amino acids
(B) TYPE: amino acid
(D) TOPOLOGY: linear

(i i) MOLECULE TYPE: peptide

(x i) SEQUENCE DESCRIPTION: SEQ ID NO:49:

```
Asn Ser Ser Asn Tyr Cys Cys Glu Leu Cys Cys Tyr Pro Ala Cys Thr
 1               5                  10                  15

Gly Cys Tyr
```

(2) INFORMATION FOR SEQ ID NO:50:

(i) SEQUENCE CHARACTERISTICS:
(A) LENGTH: 13 amino acids
(B) TYPE: amino acid
(D) TOPOLOGY: linear

(i i) MOLECULE TYPE: peptide

(x i) SEQUENCE DESCRIPTION: SEQ ID NO:50:

```
Cys Cys Asp Val Cys Cys Asn Pro Ala Cys Thr Gly Cys
 1               5                  10
```

(2) INFORMATION FOR SEQ ID NO:51:

-continued

(i) SEQUENCE CHARACTERISTICS:
(A) LENGTH: 14 amino acids
(B) TYPE: amino acid
(D) TOPOLOGY: linear

(i i) MOLECULE TYPE: peptide

(x i) SEQUENCE DESCRIPTION: SEQ ID NO:51:

```
Cys Cys Asp Val Cys Cys Tyr Pro Ala Cys Thr Gly Cys Tyr
  1               5                  10
```

(2) INFORMATION FOR SEQ ID NO:52:

(i) SEQUENCE CHARACTERISTICS:
(A) LENGTH: 14 amino acids
(B) TYPE: amino acid
(D) TOPOLOGY: linear

(i i) MOLECULE TYPE: peptide

(x i) SEQUENCE DESCRIPTION: SEQ ID NO:52:

```
Cys Cys Asp Leu Cys Cys Asn Pro Ala Cys Ala Gly Cys Tyr
  1               5                  10
```

(2) INFORMATION FOR SEQ ID NO:53:

(i) SEQUENCE CHARACTERISTICS:
(A) LENGTH: 14 amino acids
(B) TYPE: amino acid
(D) TOPOLOGY: linear

(i i) MOLECULE TYPE: peptide

(x i) SEQUENCE DESCRIPTION: SEQ ID NO:53:

```
Cys Cys Gln Leu Cys Cys Asn Pro Ala Cys Thr Gly Cys Tyr
  1               5                  10
```

(2) INFORMATION FOR SEQ ID NO:54:

(i) SEQUENCE CHARACTERISTICS:
(A) LENGTH: 15 amino acids
(B) TYPE: amino acid
(D) TOPOLOGY: linear

(i i) MOLECULE TYPE: peptide

(x i) SEQUENCE DESCRIPTION: SEQ ID NO:54:

```
Pro Gly Thr Cys Glu Ile Cys Ala Tyr Ala Ala Cys Thr Gly Cys
  1               5                  10                  15
```

I claim:

1. A method of imaging metastasized colorectal cancer cells in an individual comprising the steps of:

a) administering into the circulatory system of said individual, a diagnostically effective amount of a pharmaceutical composition comprising:

i) a pharmaceutically acceptable carrier or diluent, and,

ii) a conjugated compound comprising:

1) a ST receptor binding moiety; and,

2) an active moiety;

wherein said ST receptor binding moiety is a heat stable (ST) toxin peptide having less than 25 amino acids or fragments or derivatives thereof, wherein said heat stable toxin, fragments or derivatives thereof specifically bind to the ST receptor, and said active moiety is an imaging agent which can be detected in said individual's body; and

b) detecting localization and accumulation of said imaging agent in said individual's body.

2. The method of claim 1 wherein said pharmaceutical composition is administered to said individual intravenously.

3. A method of claim 1 wherein said imaging agent is radioactive.

4. The method of claim 3 wherein said ST receptor binding moiety has 13–25 amino acids.

5. The method of claim 3 wherein said ST receptor binding moiety is selected from the group consisting of: SEQ ID NO:2, SEQ ID NO:3, SEQ ID NO:5, SEQ ID NO:6 and SEQ ID NO:54.

6. The method of claim 3 wherein said active moiety is selected from the group consisting of: ^{43}K, ^{52}Fe, ^{57}Co, ^{67}Cu, ^{67}Ga, ^{68}Ga, ^{77}Br, $^{81}Rb/^{81M}Kr$, ^{87M}Sr, ^{99M}Tc, ^{111}In, ^{113M}In, ^{123}I, ^{125}I, ^{127}Cs, ^{129}Cs, ^{131}I, ^{132}I, ^{197}Hg, ^{203}Pb and ^{206}Bi.

7. The method of claim 3 wherein said active moiety is selected from the group consisting of: ^{99M}Tc, ^{111}In and ^{125}I.

8. The method of claim 3 wherein said active moiety is selected from the group consisting of: radioactive iodine and radioactive indium.

9. The method of claim 3 wherein said ST receptor binding moiety is selected from the group consisting of: SEQ ID NO:2, SEQ ID NO:3, SEQ ID NO:5, SEQ ID NO:6 and SEQ ID NO:54.

10. The method of claim 3 wherein said

ST receptor binding moiety is selected from the group consisting of: SEQ ID NO:2, SEQ ID NO:3, SEQ ID NO:5, SEQ ID NO:6 and SEQ ID NO:54; and

said active moiety is selected from the group consisting of: ^{43}K, ^{52}Fe, ^{57}Co, ^{67}Cu, ^{67}Ga, ^{68}Ga, ^{77}Br, $^{81}Rb/^{81M}Kr$, ^{87M}Sr, ^{99M}Tc, ^{111}In, ^{113M}In, ^{123}I, ^{125}I, ^{127}Cs, ^{129}Cs, ^{131}I, ^{132}I, ^{197}Hg, ^{203}Pb and ^{206}Bi.

11. The method of claim 3 wherein said

ST receptor binding moiety is selected from the group consisting of: SEQ ID NO:2, SEQ ID NO:3, SEQ ID NO:5, SEQ ID NO:6 and SEQ ID NO:54; and

said active moiety is selected from the group consisting of: ^{99M}Tc, ^{111}In and ^{125}I.

12. The method of claim 3 wherein said pharmaceutical composition is administered in a dose of 0.1–100 millicuries.

13. The method of claim 3 wherein said pharmaceutical composition is administered in a dose of 1–10 millicuries.

14. The method of claim 3 wherein said pharmaceutical composition is administered in a dose of 2–5 millicuries.

15. The method of claim 14 wherein said conjugated compound consists of ^{125}I linked to SEQ ID NO:13.

16. The method of claim 3 wherein said conjugated compound consists of ^{111}In linked to SEQ ID NO:37.

17. The method of claim 3 wherein said conjugated compound consists of ^{99m}Tc linked to SEQ ID NO:46.

18. A method of imaging metastasized colorectal cancer cells in an individual comprising the steps of:

a) administering into said individual's circulatory system, a diagnostically effective amount of a pharmaceutical composition comprising:

i) a pharmaceutically acceptable carrier or diluent, and,

ii) a conjugated compound comprising:

1) a ST receptor binding moiety; and,

2) an active moiety;

wherein said ST receptor binding moiety is a heat stable (ST) toxin peptide having less than 25 amino acids or fragments or derivatives thereof, wherein said heat stable toxin, fragments or derivatives thereof specifically bind to the ST receptor, and said active moiety is an imaging agent which can be detected in said individual's body by radioscintigraphy, nuclear magnetic resonance imaging, computed tomography or positron emission tomography; and

b) detecting localization and accumulation of said imaging agent in said individual's body by radioscintigraphy, nuclear magnetic resonance imaging, computed tomography or positron emission tomography.

19. The method of claim 18 wherein said pharmaceutical composition is administered to said individual intravenously.

20. The method of claim 18 wherein said ST receptor binding moiety has 13–25 amino acids.

21. The method of claim 18 wherein said ST receptor binding moiety is selected from the group consisting of: SEQ ID NO:2, SEQ ID NO:3, SEQ ID NO:5, SEQ ID NO:6 and SEQ ID NO:54.

22. A method of claim 18 wherein said imaging agent is detected by radioscintigraphy.

* * * * *

Proc. Natl. Acad. Sci. USA
Vol. 89, pp. 947–951, February 1992
Pharmacology

Guanylin: An endogenous activator of intestinal guanylate cyclase

(intestine/cyclic GMP/heat-stable enterotoxin/diarrhea/peptide)

MARK G. CURRIE*†, KAM F. FOK‡, JOHJI KATO*, ROSALYN J. MOORE*, FRANKLIN K. HAMRA*, KEVIN L. DUFFIN§, AND CHRISTINE E. SMITH¶

Departments of *Molecular Pharmacology, ‡Biological Chemistry, §Physical Sciences, and ¶Protein Biochemistry, Monsanto Corporate Research, Monsanto Company, St. Louis, MO 63167

Communicated by Philip Needleman, October 11, 1991

ABSTRACT **Intestinal guanylate cyclase mediates the action of the heat-stable enterotoxin to cause a decrease in intestinal fluid absorption and to increase chloride secretion, ultimately causing diarrhea. An endogenous ligand that acts on this guanylate cyclase has not previously been found. To search for a potential endogenous ligand, we utilized T84 cells, a human colon carcinoma-derived cell line, in culture as a bioassay. This cell line selectively responds to the toxin in a very sensitive manner with an increase in intracellular cyclic GMP. In the present study, we describe the purification and structure of a peptide from rat jejunum that activates this enzyme. This peptide, which we have termed guanylin, is composed of 15 amino acids and has the following amino acid sequence, PNTCEICAYAACTGC, as determined by automated Edman degradation sequence analysis and electrospray mass spectrometry. Analysis of the amino acid sequence of this peptide reveals a high degree of homology with heat-stable enterotoxins. Solid-phase synthesis of this peptide confirmed that it stimulates increases in T84 cyclic GMP levels. Guanylin required oxidation for expression of bioactivity and subsequent reduction of the oxidized peptide eliminated the effect on cyclic GMP, indicating a requirement for cysteine disulfide bond formation. Synthetic guanylin also displaces heat-stable enterotoxin binding to cultured T84 cells. Based on these data, we propose that guanylin is an activator of intestinal guanylate cyclase and that it stimulates this enzyme through the same receptor binding region as the heat-stable enterotoxins.**

Guanylate cyclase is comprised of a group of proteins that share a common enzymatic function of producing cyclic GMP but differ quite remarkably in their selectivity toward activation by ligands. The three major types of guanylate cyclase are the soluble, particulate, and intestinal [cytoskeletal-associated particulate or heat-stable enterotoxin (STa)-sensitive] forms and each is regulated by different ligands (1, 2). Activation of the soluble guanylate cyclase occurs in response to nitric oxide, whereas activation of the particulate enzyme occurs in response to the natriuretic peptides (atrial natriuretic peptide, brain natriuretic peptide, and C-type natriuretic peptide) (1, 2). An endogenous activator of the intestinal guanylate cyclase has not previously been identified. However, the STa from *Escherichia coli* is known to selectively activate this form of the enzyme (3, 4). The intestinal form is predominantly found in the intestinal epithelial cells with the largest number of receptors oriented toward the lumen (1, 2). Recently, it has been cloned and expressed from rat small intestinal mucosa (5). This enzyme is characterized by an extracellular receptor binding region, a transmembrane region, an intracellular protein kinase-like region, and a cyclase catalytic domain (5).

The publication costs of this article were defrayed in part by page charge payment. This article must therefore be hereby marked "*advertisement*" in accordance with 18 U.S.C. §1734 solely to indicate this fact.

Pathogenic strains of *E. coli* and other bacteria produce a family of heat-stable enterotoxins (STs) that activate intestinal guanylate cyclase. STs are acidic peptides that contain 18 or 19 amino acids with six cysteines and three disulfide bridges that are required for full expression of bioactivity (6). The increase of intestinal epithelial cyclic GMP elicited by STs is thought to cause a decrease in water and sodium absorption and an increase in chloride secretion (7, 8). These changes in intestinal fluid and electrolyte transport then act to cause secretory diarrhea. In developing countries, the diarrhea resulting from STs causes many deaths, particularly in the infant population (9). STs are also considered a major cause of traveler's diarrhea in developed countries (10). They have also been reported to be a leading cause of morbidity and death in domestic animals (11).

In the present study, we designed a bioassay to search for a potential endogenous ligand that activates the intestinal guanylate cyclase. This bioassay is based on the demonstration that T84 cells in culture respond to ST in a selective and sensitive manner with graded increases of intracellular cyclic GMP. This bioassay revealed that the intestine as well as the kidney possessed an active material. Purification of this material from the rat intestine was accomplished and the structure was determined to be a 15-amino acid peptide with 4 cysteines that must be disulfide-linked for bioactivity. The peptide, termed guanylin, also possesses a high degree of homology with STs.

MATERIALS AND METHODS

Cell Culture. A cultured human colon carcinoma cell line (T84) was obtained from the American Type Culture Collection at passage 52. Cells were grown to confluency in 24-well culture plates with a 1:1 mixture of Ham's F12 medium and Dulbecco's modified Eagle's medium (DMEM) supplemented with 10% fetal calf serum, 100 international units of penicillin per ml, and 100 μg of streptomycin per ml. Cells were used at passages 54–60.

Cyclic GMP Determination. Monolayers of T84 cells in 24-well plates were washed twice with 1 ml of DMEM per ml and then incubated at 37°C for 10 min with 0.5 ml of DMEM containing 1 mM isobutylmethylxanthine (IBMX), a cyclic nucleotide phosphodiesterase inhibitor. Agents and fractions were then added for the indicated time as described in *Results*. The media was then aspirated and the reaction was terminated by the addition of ice-cold 0.5 ml of 0.1 M HCl. Aliquots were then evaporated to dryness under nitrogen and resuspended in 5 mM sodium acetate buffer (pH 6.4). The

Abbreviations: IBMX, isobutylmethylxanthine; TFA, trifluoroacetic acid; C_{18}, octadecasilyl; STa, heat-stable enterotoxin; ST, heat-stable enterotoxin; DTT, dithiothreitol; PTH, phenylthiohydantoin.

†To whom reprint requests should be addressed at: Monsanto Company, Mail Zone T3P, 800 North Lindbergh Boulevard, St. Louis, MO 63167.

samples were subsequently measured for cyclic GMP by RIA as described by Steiner *et al.* (12).

Purification of Guanylin. Rat jejunums flushed of luminal contents with 50 ml of saline and immediately placed on dry ice were obtained from Bioproducts for Science (Indianapolis). The jejunums were thawed, minced, and boiled for 10 min in 1 M acetic acid. The extract was centrifuged at 20,000 × *g* for 20 min at 4°C. The resulting supernatant was filtered and applied to an octadecasilyl (C_{18}) Sep-Pak (Waters). The column was washed with 10% acetonitrile/0.1% trifluoroacetic acid (TFA)/H_2O and eluted with 60% acetonitrile/0.1% TFA/H_2O. The eluted peptide fraction was lyophilized and resuspended in 50 ml of distilled H_2O containing 0.8% ampholytes, pH range 3–10, and applied to a preparative isoelectric focusing cell (Rotofor, Bio-Rad). The sample was focused for 150 min at 12 W constant power. The fractions were harvested, pH determined, and bioassayed. The active fractions, which focused around pH 3.8, were then refocused under similar conditions and the resulting active fractions were lyophilized. The sample was then resuspended in 1 ml of 10% acetonitrile/0.1% TFA/H_2O, applied to a C_{18} semipreparative HPLC column (Vydac, Hesperia, CA), and eluted at a flow rate of 3 ml/min. The following gradient was used to fractionate the sample: 10% acetonitrile, 0.1% TFA to 30% acetonitrile, 0.1% TFA in 180 min. The active fraction was then determined by bioassay and lyophilized. This sample was resuspended in 1 ml of 10% acetonitrile/0.1% TFA/H_2O and applied to a phenyl analytical HPLC column (Vydac, Hesperia, CA). The conditions for elution were similar to that described above for the semipreparative column except the flow was 1 ml/min. The active fraction was lyophilized and then resuspended in 1 ml of 10% acetonitrile/0.1% TFA/H_2O. The sample was then applied to a C_{18} analytical HPLC column (Vydac) and eluted according to the above description for the phenyl column. The active fraction was identified by bioassay and lyophilized. The sample was reconstituted in 1 ml of 10% acetonitrile/0.1% TFA/H_2O, reapplied to the analytical C_{18} column, and eluted by a gradient of 10% acetonitrile/10 mM ammonium acetate/H_2O, pH 6.2, to 30% acetonitrile/10 mM ammonium acetate/H_2O, pH 6.2, in 180 min. The active fraction was lyophilized and reconstituted in 0.05 ml of 0.1% TFA/H_2O. The sample was then applied to a C_8 microbore column and eluted by an increasing gradient of 0.33%/min of acetonitrile/0.1% TFA/H_2O. Two separate batches of purified peptide were then subjected to sequence analysis.

N-Terminal Protein Sequence Analysis. Automated Edman degradation chemistry was used to determine the NH_2-terminal protein sequence. An Applied Biosystems model 470A gas-phase sequencer was employed for the degradations (13) using the standard sequencer cycle 03RPTH. The respective phenylthiohydantoin (PTH) amino acid derivatives were identified by reverse-phase HPLC analysis in an on-line fashion employing an Applied Biosystems model 120A PTH analyzer fitted with a Brownlee 2.1-mm i.d. PTH C_{18} column. On-sequencer pyridylethylation was performed as outlined by Kruft *et al.* (14). The PTH derivative of pyridylethylcysteine was identified by HPLC as eluting slightly prior to the PTH derivative of methionine.

Electrospray Mass Spectrometry. Individual samples of native and synthetic guanylin were purified by microbore C_8 reverse-phase HPLC (Brownlee Aquapore RP-300 7-μm column, P. J. Cobert, St. Louis, MO) and eluting fractions of the peptides were collected and concentrated to ≈8 pmol/μl for mass analysis. Sample solutions were introduced to the mass spectrometer via injection into a stream of acetonitrile/H_2O/TFA, 1000:1000:1, vol/vol/vol, which continuously flowed to the mass spectrometer at a flow of 10 μl/min. Three microliters of each of the concentrated guanylin samples was injected to obtain the results that are presented in this paper.

A Sciex API III triple-quadrupole mass spectrometer (Thornhill, Ontario, Canada) equipped with an atmospheric pressure ion source was used to sample positive ions produced from an electrospray interface (15). Mass analysis of sample ions was accomplished by scanning the first quadrupole in 1 atomic mass unit increments from 1000 to 2400 atomic mass units in ≈3 s and passing mass-selected ions through the second and third quadrupoles operated in the rf-only mode to the multiplier. For maximum sensitivity, the mass resolution of the quadrupole mass analyzer was set so that ion signals were ≈2 atomic mass units wide at half peak height, but the centroid of the ion signal still represented the correct mass of the ion. Comparison of the oxidized and reduced guanylin molecular ion region was made by scanning the quadrupole mass analyzer in 0.1 atomic mass unit steps from 1510 to 1525 atomic mass units in 2 s. Mass spectra of the guanylin samples were averaged over all of the scans that were acquired during elution of the 3-μl sample solution.

Binding Assay. ^{125}I-labeled STa (^{125}I-STa) was prepared by the Iodo-Gen method (16). T84 cell monolayers were washed twice with 1 ml of DMEM and then incubated for 30 min at 37°C in 0.5 ml of DMEM with ^{125}I-STa (amino acids 5–18) (100,000 cpm per well) and either guanylin or 100 nM STa. The cells were then washed four times with 1 ml of DMEM and solubilized with 0.5 ml of 1 M NaOH per well. This volume was transferred to tubes and assayed for radioactivity by a γ counter. Results are expressed as the percentage specifically bound.

Chemical Synthesis of Guanylin. Guanylin was synthesized by the solid-phase method (17) with an Applied Biosystems 430A peptide synthesizer on Cys(4-CH_3Bzl)-OCH_2-phenylacetamidomethyl resin using double coupling cycles to ensure complete coupling at each step. Coupling was effected with preformed symmetrical anhydride of *tert*-butoxycarbonyl amino acids (Applied Biosystems), and peptides were cleaved from the solid support in hydrogen fluoride/dimethylsulfide/anisole/*p*-thiocresol, 8:1:1:0.5, vol/vol/vol/wt, at 0°C for 60 min. Peptides were cyclized using dimethylsulfoxide as described by Tam *et al.* (18). Peptides were purified by successive reverse-phase chromatography on a 45 × 300 mm Vydac C_{18} column and on a 19 × 150 mm μBondapak C_{18} column, using a gradient of 10–30% acetonitrile in 0.5% TFA. The structures and purity of the synthetic peptides were verified by fast atom bombardment mass spectrometry, amino acid analysis, and gas-phase sequence analysis.

RESULTS

Initial characterization of the T84 cell response indicated that these cells were very sensitive to STa with a concentration of 10^{-10} M eliciting a 4-fold increase in cyclic GMP. The cells also displayed a remarkable range, with a maximal response of STa (10^{-7} M) eliciting a >1000-fold increase in cyclic GMP. Furthermore, we failed to detect an effect of either sodium nitroprusside (10^{-3} M) or atrial natriuretic peptide (10^{-6} M) on cyclic GMP levels, suggesting that the T84 serves as a selective bioassay for agents that activate the intestinal guanylate cyclase. Various rat tissues were surveyed as sources for T84 cell cyclic GMP agonist activity, and jejunum and kidney were found to possess activity while liver, brain, pancreas, spleen, lung, and testes lacked detectable activity (Fig. 1). We also observed that rat embryonic intestine possessed a similar activity. Treatment of the T84 cells with 10% of embryonic intestinal extract increased the cyclic GMP from a basal level of 120 ± 10 fmol per well to 270 ± 10 fmol per well (mean ± SE).

Purification of the adult rat jejunal bioactivity was accomplished by the processing scheme described in *Materials and Methods*. Briefly, following acid boiling and extraction by a

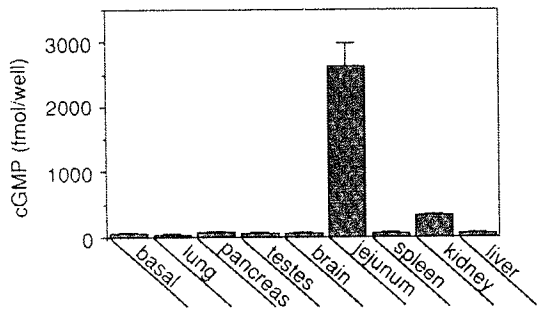

FIG. 1. Effect of extracts from various tissues on T84 cyclic GMP levels. Acid extracts were prepared from 1 g of tissue and 10% of each extract was applied to IBMX-treated cells. Values are means ± SE (n = 3).

C_{18} reverse-phase matrix, the material was fractionated on a preparative isoelectric focusing cell, which resulted in a 200-fold purification and indicated that the isoelectric point was about 3.8. Refocusing of the active fraction resulted in a further 5- to 10-fold purification. The active fraction was then purified to homogeneity by a series of reverse-phase HPLC steps, including a semipreparative C_{18} column, a phenyl column, two separations on a C_{18} column utilizing different ion-pairing reagents, and final purification on a microbore C_8 column (Fig. 2).

Preliminary experiments suggested that the material was a low molecular weight peptide; therefore the material was subjected to N-terminal protein sequence analysis and to electrospray mass spectrometric analysis. The combination of the data derived from these two techniques yielded the complete sequence for guanylin: Pro-Asn-Thr-Cys-Glu-Ile-Cys-Ala-Tyr-Ala-Ala-Cys-Thr-Gly-Cys. The N-terminal sequence through 14 places was determined by two independent gas-phase sequencing experiments. The C-terminal amino acid was deduced from data obtained by electrospray mass spectroscopy. The initial results yielded a sequence in which no PTH amino acid derivative was observed at positions 4, 7, and 12. Since cysteine residues cannot be positively identified during gas-phase sequencing without reduction and alkylation, the lack of a PTH amino acid derivative at these positions suggested the presence of cysteine residues. For complete verification, the putative cysteine residues of guanylin were pyridylethylated and the peptide was resequenced. The subsequent N-terminal gas-phase sequence analysis verified cysteine residues at positions 4, 7, and 12. Further primary structure information was obtained by electrospray mass spectrometry. The electrospray mass spectrum of native guanylin (Fig. 3*A*) contains an ion signal at m/z 1516 that corresponds to the protonated peptide. This assignment is 103 atomic mass units higher than the mass expected for the peptide whose sequence was obtained by gas-phase sequence analysis. This difference of 103 atomic mass units is consistent with an additional disulfide-linked cysteine or with a threonine at the C terminus of the peptide. Reduction of the disulfide bonds of guanylin with dithiothreitol (DTT) resulted in a 4 atomic mass unit increase in molecular weight of the peptide (Fig. 3 *B* and *C*), indicating that it contains two disulfide bonds. Therefore, since there are only three cysteines in the original 14 N-terminal amino acids, the 103 atomic mass unit difference must result from an additional C-terminal cysteine that is disulfide-linked to one of the other three cysteines in the guanylin sequence.

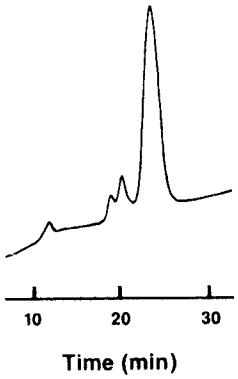

FIG. 2. Final purification of guanylin by C_8 reverse-phase microbore HPLC. Chromatographic peaks (A_{214}, 0.1 absorbance unit full scale) were collected and measured for activity. The active peak (55% of a full-scale response) is indicated by shading, with 1% of the fraction giving a 10-fold increase in cyclic GMP.

The resulting full amino acid sequence of the peptide was compared with all other proteins in the GenBank, National Biomedical Research Foundation, and SwissProt databases by a computer-based search. This search revealed that guanylin has homology with the STs, with the greatest homology identified in the cysteine-rich regions of the molecules (19, 20). The distinctive difference between guanylin and the STs is that guanylin possesses four cysteines with two disulfide-linked bridges while all of the known STs have six cysteines with three disulfide-linked bridges (Fig. 4).

Chemical synthesis of guanylin based on the experimentally derived sequence resulted in three different HPLC fractions following oxidation in air. Each of these fractions contained a peptide with the same molecular weight as native guanylin (1516 atomic mass units) as determined by mass spectrometric analysis. However, only one of these fractions exhibited potent bioactivity in the T84 cell bioassay consistent with guanylin. This fraction also exhibited a similar HPLC retention time to that of native guanylin. Since guanylin has four cysteine residues, the three fractions of synthetic guanylin probably represented the three possible different disulfide bridge alignments. Bioactive synthetic guanylin stimulated increases in cyclic GMP levels of T84 cells that were time and concentration dependent. Guanylin (10^{-8} M) caused a marked elevation of cyclic GMP after 1 min, which progressively increased through 30 min (Fig. 5*A*). Examination of the concentration–response curve shows that guanylin elicited an increase in cyclic GMP at 10^{-10} M and this response increased through the range of concentrations tested (Fig. 5*B*). To characterize the effect of treatment of reducing agents on the bioactivity of guanylin, we pretreated the peptide for 30 min with 1 mM DTT. The basal level of cyclic GMP for this experiment was 160 ± 50 fmol per well, which increased to 2820 ± 500 fmol per well after a 30-min treatment with guanylin (10^{-8} M). However, following the pretreatment of the peptide with DTT, the effect of the 30-min treatment with the peptide on cyclic GMP was almost completely abolished (250 ± 50 fmol per well). The action of DTT does not appear to be a direct effect of DTT on guanylate cyclase since treatment of the cells with 10 μM DTT (final concentration of DTT that the cells were exposed to in the experiment) failed to affect their responsiveness to STa treatment (data not shown). Finally, we examined in preliminary experiments the ability of guanylin to displace specifically bound ^{125}I-STa from T84 cells. In this experiment, guanylin caused a concentration-dependent displacement of labeled STa from the T84 cells (Fig. 6) with an IC_{50} of 5×10^{-8} M.

DISCUSSION

In the present study, we describe the purification and sequence of a rat intestinal peptide that possesses the properties consistent with an endogenous ligand for the intestinal guanylate cyclase. We have termed this peptide guanylin because of its ability to stimulate intestinal guanylate cyclase. Synthetic guanylin was found to increase cyclic GMP levels in T84 cells in a time- and concentration-dependent manner. Guanylin was also found to displace the specific binding of ^{125}I-STa from T84 cells. Therefore, these data support our proposal that guanylin is an endogenous activator of the

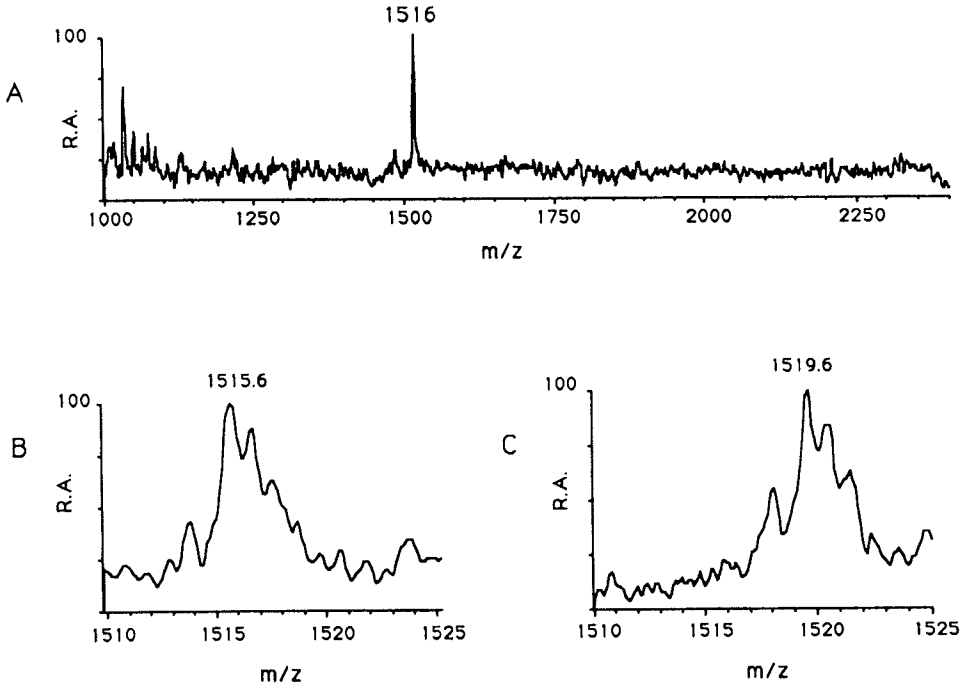

FIG. 3. Electrospray mass spectra of native guanylin. (*A*) Mass spectral analysis of native guanylin in a range of 1000–2400 atomic mass units shows the molecular weight to be 1516 atomic mass units. (*B* and *C*) Comparison of the mass spectra of oxidized (*B*) and reduced (*C*) native guanylin in the range 1510–1525 atomic mass units. R.A., relative abundance.

intestinal guanylate cyclase and suggest that this peptide may influence intestinal fluid and electrolyte transport.

Purification of guanylin was accomplished by capitalizing on the stable nature of this peptide, its acidic isoelectric point, and its characteristic elution on reverse-phase HPLC. Initially, we were concerned that the activity may result from bacterial contamination. To limit this possibility the purification was limited to jejunum, which in normal animals is considered unlikely to contain considerable bacterial contamination. Furthermore, we found in preliminary experiments that every individual rat intestine that we extracted possessed bioactivity. We also found that embryonic intestine, which is considered free of bacteria, exhibits similar activity, strongly suggesting that the intestine indeed possesses a unique ligand. The structure of guanylin further strengthens this proposal. However, definitive proof of the intestinal source of guanylin must await a thorough analysis of the tissue by immunological and molecular methods.

The unique structure of the 15-amino acid peptide guanylin is characterized by an N-terminal proline, a C-terminal cysteine, a glutamic acid, a total of four cysteines, and the absence of basic amino acids. The conditions under which guanylin was isolated may have given rise to a truncated form that possesses the properties required for bioactivity but is derived from a larger precursor. The synthetic peptide required cyclization for expression of bioactivity and this activity was abolished by treatment with the reducing agent DTT. Interestingly, during the purification of oxidized synthetic guanylin, we observed three major chromatographic peaks, each of which contained a peptide of the same molecular weight as native guanylin. Since guanylin has four cysteine residues, the three fractions of synthetic guanylin probably represent the three possible alignments of the disulfide bridges. It is likely that the two inactive fractions represent improperly folded peptide. The alignment of the

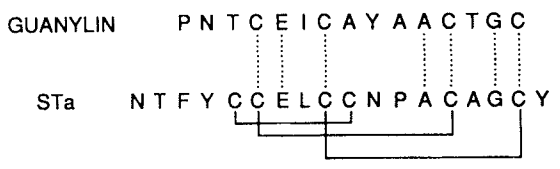

FIG. 4. Comparison of the structures of guanylin and STa. Identical amino acids are indicated by the dotted lines. The reported disulfide alignment for STa (20) is represented by the solid lines.

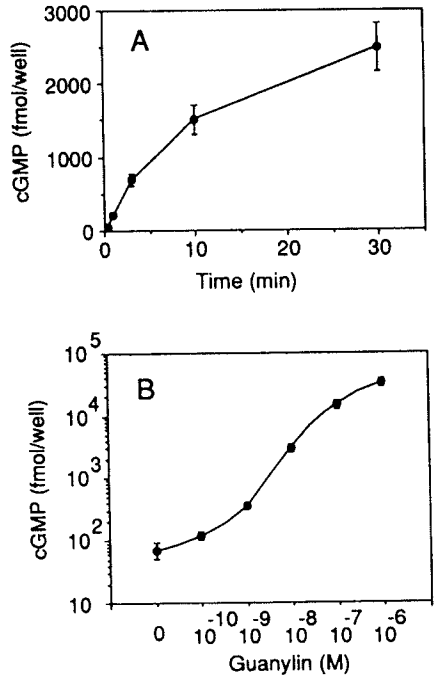

FIG. 5. Time course (*A*) and concentration–response (*B*) effect of synthetic guanylin on cyclic GMP levels in T84 cells. In the time course experiment, T84 cells were treated with 10^{-8} M guanylin for the indicated times. For the concentration–response, the cells were incubated with various concentrations of guanylin for 30 min. Cells for both experiments were treated with 1 mM IBMX. Values represent means ± SE (n = 4).

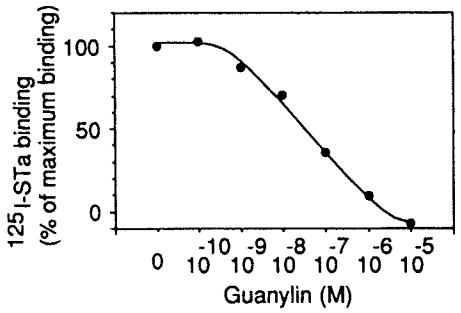

FIG. 6. Displacement of ^{125}I-STa specific binding from T84 cells by guanylin. Cells were incubated for 30 min at 37°C with labeled STa and various concentrations of guanylin. Specific binding (%) was determined by dividing the specifically bound ^{125}I-STa at each guanylin concentration by the specifically bound ^{125}I-STa in the absence of guanylin. Each point represents the mean of triplicates.

disulfide bridges at this time remains undetermined; however, a comparison of the conserved cysteines in guanylin with the known structure of STa (20) suggests that the disulfide bridge alignments may occur between positions 4 and 12 and between 7 and 15 (Fig. 4).

Guanylin appears to act in a manner similar to STs in stimulating cyclic GMP levels and presumably acts through the same extracellular binding region of the intestinal guanylate cyclase. This form of guanylate cyclase has recently been cloned, sequenced, and expressed (5). Intestinal guanylate cyclase was found to possess an extracellular domain that is thought to contain the STa binding region, a transmembrane domain, an intracellular protein kinase-like region, and a cyclase catalytic domain (5). The present study indicates that this protein serves as a receptor for guanylin and mediates the effect of guanylin to increase intracellular cyclic GMP levels. The major site of expression of this receptor appears to be the intestinal epithelial cell, but recent binding studies with ^{125}I-STa indicate that receptors coupled to guanylate cyclase activity exist in other epithelial cells in many different organs of the North American opossum (21, 22). This evidence indicates that this form of guanylate cyclase may be found in other cellular sites than the intestine and may be involved in the regulation of many different cellular functions, particularly epithelial transport. Thus, the actions of guanylin may ultimately extend to other tissues beside the intestine. Indeed, guanylin may possess previously undescribed subtypes of receptors that do not recognize STs.

The immediate physiologic and pathophysiologic implications of the discovery of guanylin primarily relate to the regulation of intestinal fluid and electrolyte transport. A target for guanylin is the intestinal guanylate cyclase and it is likely that this receptor acts to transduce many of the signals for this peptide. Since STa also targets this receptor, the actions of this toxin should serve as a model for the expected actions of guanylin. Guanylin, through its effect on guanylate cyclase and cyclic GMP, may act to decrease sodium and water permeability and to increase chloride secretion. An excess of guanylin would, therefore, be expected to elicit secretory diarrhea in a manner similar to STa. A key to understanding the role of guanylin will be the determination of the specific cell source(s) of guanylin. Thus, the discovery of guanylin should provide a foundation for future studies directed at determining the cellular source of this peptide and its action on epithelial function.

We thank Drs. Philip Needleman, William Moore, and Allen Nickols for their useful discussions and helpful advice.

1. Singh, S., Lowe, K. G., Thorpe, D. S., Rodriquez, H., Kuang, W.-J., Dangott, L. J., Chinkers, M., Goeddel, D. B. & Garbers, D. L. (1988) *Nature (London)* **334**, 708–712.
2. Waldman, S. A. & Murad, F. (1987) *Pharmacol. Rev.* **39**, 163–196.
3. Field, M., Graf, L. H., Laird, W. J. & Smith, P. L. (1978) *Proc. Natl. Acad. Sci. USA* **75**, 2800–2804.
4. Guerrant, R. L., Hughes, J. M., Chang, B., Robertson, D. C. & Murad, F. (1980) *J. Infect. Dis.* **142**, 220–228.
5. Schulz, S., Green, C. K., Yuen, P. S. T. & Garbers, D. L. (1990) *Cell* **63**, 941–948.
6. Yoshimura, S., Ikemura, H., Watanabe, H., Aimoto, S., Shimonishi, Y., Hara, S., Takeda, T., Miwatani, T. & Takeda, Y. (1985) *FEBS Lett.* **181**, 138–142.
7. Field, M., Rao, C. M. & Chang, E. B. (1989) *N. Engl. J. Med.* **321**, 879–883.
8. Guarino, A., Cohen, M., Thompson, M., Dharmsathaphorn, K. & Giannella, R. (1987) *Am. J. Physiol.* **253**, G775–G780.
9. Robins-Browne, R. M. (1987) *Rev. Infect. Dis.* **9**, 28–53.
10. Levine, M. M. (1987) *J. Infect. Dis.* **155**, 377–389.
11. Burgess, M. N., Bywater, R. J., Cowley, C. M., Mullan, N. A. & Newsome, D. M. (1978) *Infect. Immunol.* **21**, 526–531.
12. Steiner, A. L., Paghara, A. S., Chase, L. R. & Kipnis, D. M. (1972) *J. Biol. Chem.* **247**, 1114–1120.
13. Hunkapiller, M. W., Hewick, R. M., Dreyer, R. J. & Hood, L. E. (1983) *Methods Enzymol.* **91**, 399–413.
14. Kruft, V., Ulrike, K. & Wittmann-Liebold, B. (1991) *Anal. Biochem.* **193**, 306–309.
15. Bruins, A. P., Covey, T. R. & Henion, J. D. (1987) *Anal. Chem.* **59**, 2642–2651.
16. Fraker, P. & Speck, J. C. (1978) *Biochem. Biophys. Res. Commun.* **80**, 849–857.
17. Merrifield, R. B. (1963) *J. Am. Chem. Soc.* **85**, 2149–2154.
18. Tam, J. P., Wu, C.-R., Liu, W. & Zhang, J.-W. (1991) *J. Am. Chem. Soc.* **113**, 6657–6662.
19. Guzman-Verduzo, L. M. & Kupersztoch, Y. M. (1989) *Infect. Immunol.* **57**, 645–648.
20. Houghten, R. A., Ostresh, J. M. & Klipstein, F. A. (1984) *Eur. J. Biochem.* **145**, 157–162.
21. Krause, W. J., Freeman, R. H. & Forte, L. R. (1990) *Cell Tissue Res.* **260**, 387–394.
22. Forte, L. R., Krause, W. J. & Freeman, R. H. (1988) *Am. J. Physiol.* **257**, F1040–F1046.

ELSEVIER

European Journal of Pharmacology 343 (1998) 67–77

ejp

Characterization of binding sites of a new neurotensin receptor antagonist, [^{3}H]SR 142948A, in the rat brain

Catalina Betancur [a,*], Maryse Canton [b], Alain Burgos [b], Bernard Labeeuw [b], Danielle Gully [b], William Rostène [a], Didier Pélaprat [a]

[a] *INSERM U. 339, Hôpital Saint-Antoine, 184 rue du Faubourg Saint-Antoine, 75571 Paris Cedex 12, France*
[b] *Sanofi Recherche, 195 route d'Espagne, 31036 Toulouse Cedex, France*

Received 31 July 1997; revised 3 November 1997; accepted 7 November 1997

Abstract

The present study describes the characterization of the binding properties and autoradiographic distribution of a new nonpeptide antagonist of neurotensin receptors, [^{3}H]SR 142948A (2-{[5-(2,6-dimethoxyphenyl)-1-(4-(*N*-(3-dimethylaminopropyl)-*N*-methylcarbamoyl)-2-isopropylphenyl)-1H-pyrazole-3-carbonyl]-amino}-adamantane-2-carboxylic acid, hydrochloride), in the rat brain. The binding of [^{3}H]SR 142948A in brain membrane homogenates was specific, time-dependent, reversible and saturable. [^{3}H]SR 142948A bound to an apparently homogeneous population of sites, with a K_d of 3.5 nM and a B_{max} value of 508 fmol/mg of protein, which was 80% higher than that observed in saturation experiments with [^{3}H]neurotensin. [^{3}H]SR 142948A binding was inhibited by SR 142948A, the related nonpeptide receptor antagonist, SR 48692 (2-{[1-(7-chloroquinolin-4-yl)-5-(2,6-dimethoxyphenyl)-1H-pyrazole-3-carbonyl]amino}-adamantane-2-carboxylic acid) and neurotensin. Saturation and competition studies in the presence or absence of the histamine H_1 receptor antagonist, levocabastine, revealed that [^{3}H]SR 142948A bound with similar affinities to both the levocabastine-insensitive neurotensin NT_1 receptors (20% of the total binding population) and the recently cloned levocabastine-sensitive neurotensin NT_2 receptors (80% of the receptors) (K_d = 6.8 and 4.8 nM, respectively). The regional distribution of [^{3}H]SR 142948A binding in the rat brain closely matched the distribution of [^{125}I]neurotensin binding. In conclusion, these findings indicate that [^{3}H]SR 142948A is a new potent antagonist radioligand which recognizes with high affinity both neurotensin NT_1 and NT_2 receptors and represents thus an excellent tool to study neurotensin receptors in the rat brain. © 1998 Elsevier Science B.V.

Keywords: [^{3}H]SR 142948A; Neurotensin receptor; Nonpeptide receptor antagonist; Levocabastine; Receptor autoradiography; Brain

1. Introduction

Neurotensin is a 13-amino acid neuropeptide found in the central nervous system and peripheral tissues of numerous mammalian species (Emson et al., 1982; Mai et al., 1987). Neurotensin acts as a neurotransmitter–neuromodulator in a variety of physiological processes. In particular, neurotensin has been shown to play an important role in the modulation of midbrain dopamine transmission (Kasckow and Nemeroff, 1991); neurotensin is also involved in nociception, hypothermia and control of anterior pituitary hormone secretion (Rostène and Alexander, 1997). In the adult rat and mouse brain, neurotensin can bind to two different binding sites which can be distinguished by their affinity for neurotensin (Mazella et al., 1983), as well as by their sensitivity to levocabastine, a histamine H_1 receptor antagonist (Schotte et al., 1986). In other species, including humans, rabbits and guinea pigs, only levocabastine-insensitive sites have been detected in the brain (Schotte et al., 1986). Until recently, it was believed that the physiological effects of neurotensin were mediated through a single class of G protein-coupled receptors, corresponding to the levocabastine-insensitive binding sites, cloned from rat brain (Tanaka et al., 1990) and human adenocarcinoma HT-29 cell line (Vita et al., 1993). In contrast, it was assumed that levocabastine-sensitive neurotensin binding sites lacked signalling activity and were thus considered as acceptor sites, devoid of function. Very recently, however, a novel neurotensin receptor (called NT_2) sensitive to levocabastine was cloned in the rat hypothalamus (Chalon et al., 1996) and mouse brain (Mazella et al., 1996). It also belongs to the family of G protein-coupled receptors and has about 40% homology

* Corresponding author. Tel.: +33-1-49284688; fax: +33-1-43408270; e-mail: betancur@adr.st-antoine.inserm.fr

with the previously cloned rat and human neurotensin receptors (NT_1). The biological function of the neurotensin NT_2 receptor remains to be determined.

A major advancement in the field of neurotensin research was provided by the discovery of the first highly potent and selective nonpeptide neurotensin receptor antagonist, SR 48692 (Gully et al., 1993). SR 48692 is orally active, crosses the blood brain barrier and has a long-lasting action; it shows higher affinity for neurotensin NT_1 than for NT_2 receptors. This antagonist can counteract the effects of neurotensin in numerous in vitro and in vivo assays (Gully et al., 1993); however, SR 48692 is unable to inhibit neurotensin-induced hypothermia and analgesia in rats and mice (Dubuc et al., 1994). This compound also fails to reverse dopamine release in the nucleus accumbens evoked by neurotensin injection in the ventral tegmental area (Steinberg et al., 1994), as well as the hypolocomotion induced by intracerebroventricular administration of the peptide (Pugsley et al., 1995). These findings suggest that these effects of neurotensin could be mediated through a neurotensin receptor subtype which is insensitive to SR 48692 (Le et al., 1996).

Although SR 48692 has proved an important pharmacological tool for studying neurotensin receptors and for exploring the existence of possible neurotensin receptor subtypes, it has certain properties that could limit its usefulness. In particular, SR 48692 has very low aqueous solubility and 100 times lower affinity for the rat brain when compared to the guinea pig brain (Gully et al., 1993). Thus, the tritiated ligand derived from this antagonist, [^{3}H]SR 48692, bound with high affinity to the guinea pig brain ($K_d = 2$ nM) (Betancur et al., 1995) and to cells transfected with the rat neurotensin NT_1 receptor ($K_d = 3$ nM) (Labbé-Jullié et al., 1995), but exhibited high levels of nonspecific binding when tested in adult rat brain homogenates or sections (unpublished observation).

Recently, Sanofi developed a second nonpeptide antagonist of neurotensin receptors, SR 142948A, which is chemically related to SR 48692 but has better solubility and increased affinity in the rat brain (Gully et al., 1997). SR 142948A recognizes with similar affinity (in the nanomolar range) both neurotensin NT_1 and NT_2 receptors (Gully et al., 1997). Interestingly, in contrast to SR 48692, SR 142948A blocked the hypothermia and analgesia induced by central injection of neurotensin, revealing a wider spectrum of action, probably through inhibition of different neurotensin receptor subtypes (Gully et al., 1997).

In the present study, we examined the binding properties of a newly developed tritiated form of SR 142948A ([^{3}H]SR 142948A) in adult rat brain membrane homogenates. Furthermore, we studied the autoradiographic distribution of [^{3}H]SR 142948A binding sites in the rat brain and compared it with that of [^{125}I]neurotensin binding. [^{3}H]SR 142948A binding was studied in the presence or absence of levocabastine, in order to determine its binding properties to neurotensin NT_1 and NT_2 receptors.

2. Materials and methods

2.1. Chemicals

SR 142948A (2-{[5-(2,6-dimethoxyphenyl)-1-(4-(*N*-(3-dimethylaminopropyl)-*N*-methylcarbamoyl)-2-isopropylphenyl)-1H-pyrazole-3-carbonyl]-amino}-adamantane-2-carboxylic acid, hydrochloride) (Fig. 1) and SR 48692 (2-{[1-(7-chloroquinolin-4-yl)-5-(2,6-dimethoxyphenyl)-1H-pyrazole-3-carbonyl] amino} -adamantane-2-carboxylic acid) were synthesized at Sanofi Recherche (Montpellier, France). Both compounds were dissolved in dimethylsulfoxide and stored in aliquots at −20°C until the day of the experiment. [^{3}H]SR 142948A (83 Ci/mmol) was tritiated at Sanofi Recherche (Alnwick, Great Britain). [^{3}H]Neurotensin (104 Ci/mmol) was purchased from New England Nuclear (Les Ulis, France) and monoiodo-[^{125}I-Tyr^3]neurotensin (2000 Ci/mmol) was iodinated and purified as described previously (Sadoul et al., 1984). Unlabeled neurotensin was purchased from Neosystem Laboratories (Strasbourg, France). Levocabastine was kindly provided by Janssen Pharmaceutica (Beerse, Belgium) and was solubilized in ethanol.

2.2. Preparation of brain membrane homogenates

Male Sprague–Dawley rats (180–220 g, Charles River, Saint Aubain-les-Elboeuf, France) were killed by cervical dislocation. The whole brain (minus the cerebellum) was removed rapidly and homogenized in 10 volumes (original wet weight/volume) of 50 mM Tris–HCl ice-cold buffer (pH 7.4) for 30 s by using a polytron (setting 5). After 20 min of centrifugation at 50 000 × *g*, the pellet was washed and again centrifuged as above. The final pellet was resuspended in binding assay buffer containing 50 mM Tris–HCl (pH 7.4), 1 mM EDTA, 0.1% bovine serum albumin, 1 mM 1,10 orthophenanthroline (Sigma, Saint

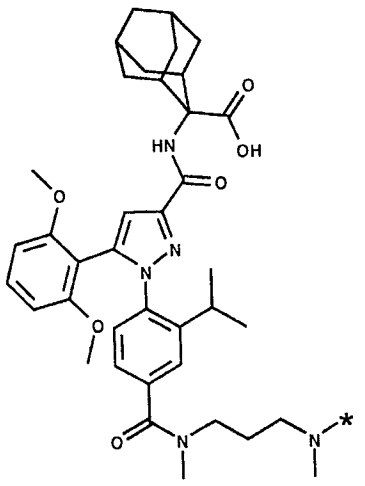

Fig. 1. Chemical structure of SR 142948A. *: location of the 3 tritium atoms.

Louis, MO), 5 mM dithiothreitol and 40 mg/l bacitracin and stored as aliquots in liquid nitrogen until used.

2.3. Binding assays in brain homogenates

Aliquots of brain membranes (300 μg/assay) were incubated in 0.5 ml (final volume) of binding assay buffer containing the appropriate concentrations of [^{3}H]SR 142948A and unlabeled drugs. After incubation at 20°C for 60 min, the assay medium was diluted with 4 ml of ice-cold 50 mM Tris–HCl buffer (pH 7.4) and filtered rapidly under reduced pressure through Whatman glass-fiber GF/B filters pretreated with 0.1% polyethylenimine. The filters were washed 3 times under the same conditions and transferred to vials containing 4 ml of scintillation cocktail. The bound radioactivity was determined by liquid scintillation counting. Nonspecific binding was determined in the presence of 1 μM unlabeled SR 142948A.

Saturation experiments were carried out with increasing concentrations of [^{3}H]SR 142948A (0.05 to 16 nM). In association kinetic experiments, rat brain homogenates were incubated with [^{3}H]SR 142948A (2 nM) for various time periods. For dissociation studies, [^{3}H]SR 142948A was incubated for 30 min with brain membranes, unlabeled SR 142948A was then added at a final concentration of 1 μM and incubations were stopped at the indicated times. Competition studies were conducted with a single concentration of [^{3}H]SR 142948A (2 nM) and at least 10 concentrations of unlabeled ligands. In addition, saturation and competition studies with [^{3}H]SR 142948A were performed in the presence of a constant concentration of levocabastine (10 μM), which selectively inhibits binding to neurotensin NT_2 receptors. The effect of guanyl nucleotides on [^{3}H]SR 142948A binding was examined by adding increasing concentrations of the nonhydrolyzable GTP analog 5′-guanylylimidodiphosphate (Gpp(NH)p) to the binding assay. [^{3}H]neurotensin binding to rat brain membranes was performed as described previously (Goedert et al., 1984), in the presence or absence of levocabastine (10 μM). Nonspecific binding was determined by incubation with 1 μM neurotensin. All experiments were performed 2 or 3 times in triplicate. Data from association, saturation and competition studies were analyzed by using a nonlinear regression program, LIGAND (Munson and Rodbard, 1980). K_i values were calculated according to the Cheng and Prusoff (1973) equation.

2.4. Autoradiography of [^{3}H]SR 142948A binding sites

Adult male rats were killed by decapitation, the brain was removed rapidly, frozen on dry ice and stored at −80°C. Coronal sections (20 μm thick) were cut on a cryostat at −16°C, mounted on slides (Superfrost plus, Menzel-Glaser, Madison, WI) and stored at −20°C until used. [^{3}H]SR 142948A binding was performed by incubating the sections for 60 min at room temperature with 300 μl of 2 nM [^{3}H]SR 142948A in 50 mM Tris–HCl buffer (pH 7.4), containing 1 mM EDTA, 0.1% bovine serum albumin, 40 mg/ml bacitracin and 0.5 mM 1,10 orthophenanthroline, in the presence or absence of 1 μM levocabastine. Additional sections were incubated with 10 μM SR 142948A for the determination of nonspecific binding. After incubation, the sections were washed 3 times for 10 min each at 4°C in 50 mM Tris–HCl buffer (pH 7.4), containing 1 mM EDTA and 0.1% bovine serum albumin. Slides were then dipped briefly in distilled water and dried under a stream of air. Sections were placed in X-ray cassettes, apposed to Hyperfilm-^{3}H (Amersham, France) for 3 weeks and developed by standard photographic procedures.

2.5. Autoradiography of [^{125}I]neurotensin binding sites

[^{125}I]Neurotensin binding was performed as described previously (Moyse et al., 1987). Briefly, slide-mounted brain sections were incubated for 60 min at 4°C with 300 μl of 0.3 nM [^{125}I]neurotensin in 50 mM Tris–HCl buffer (pH 7.4), containing 5 mM $MgCl_2$, 0.2% bovine serum albumin and 0.5 mM 1,10 orthophenanthroline, in the presence or absence of 1 μM levocabastine. Nonspecific binding was determined in the presence of 10 μM unlabeled neurotensin. The sections were washed 4 times for 2 min each at 4°C in 40 mM Tris–HCl buffer (pH 7.4), dipped briefly in distilled water and dried. Radiolabeled sections were exposed to Hyperfilm-βmax (Amersham) for 1 week.

2.6. Densitometric analysis

Quantitative optical density measurements of film autoradiographs were carried out with a computer-based image analysis system (HISTO-RAG, Biocom, Les Ulis, France). Optical densities of nonspecific binding were subtracted from total binding to obtain specific binding. Measurements were performed bilaterally on 4 brain sections per level. Values were expressed as nCi/mg tissue by using autoradiographic ^{3}H and ^{125}I micro-scales (Amersham) that were exposed together with the tissue sections. Brain structures were identified according to the atlas of Paxinos and Watson (1986).

3. Results

3.1. Biochemical profile of [^{3}H]SR 142948A binding to rat brain membrane homogenates

3.1.1. Tissue concentration linearity

Fig. 2 shows the total, nonspecific and specific binding of [^{3}H]SR 142948A to rat brain homogenates as a function of membrane protein concentration. The specific binding of [^{3}H]SR 142948A measured at 2 nM was linear with increasing protein concentration until 400 μg of protein/tube.

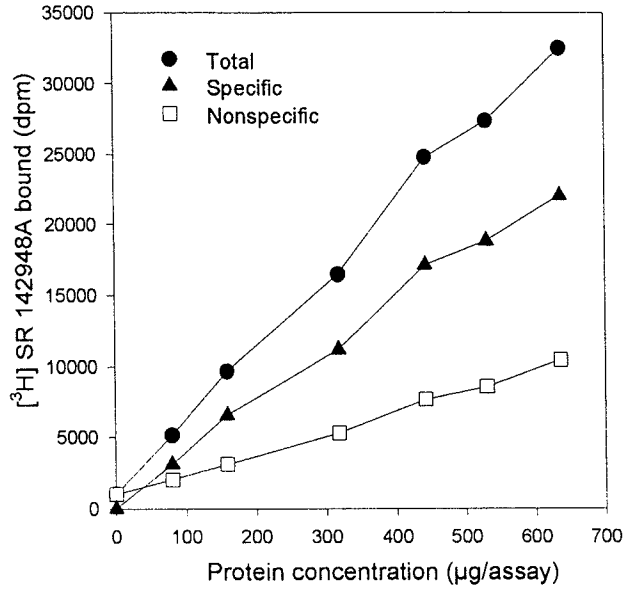

Fig. 2. [^{3}H]SR 142948A binding as a function of increasing protein concentrations. Various concentrations of rat brain membranes were incubated with 2 nM [^{3}H]SR 142948A for 60 min at 20°C. Nonspecific binding was determined with 1 μM unlabeled SR 142948A. Specific binding was defined as the difference between total and nonspecific binding. The data represent the mean of triplicate determinations.

3.1.2. Saturation studies

Fig. 3 shows a saturation isotherm of the binding of [^{3}H]SR 142948A to rat brain membranes. Analysis of the saturation curves by computer-assisted nonlinear regression or by Scatchard analysis (Fig. 3, inset) revealed a single class of high-affinity binding sites ($K_d = 3.48 \pm 0.22$ nM; mean ± S.E.M., $n = 3$) for radioligand concentrations ranging from 0.05 to 16 nM, with a maximal binding capacity (B_{max}) of 508.4 ± 45.0 fmol/mg of protein.

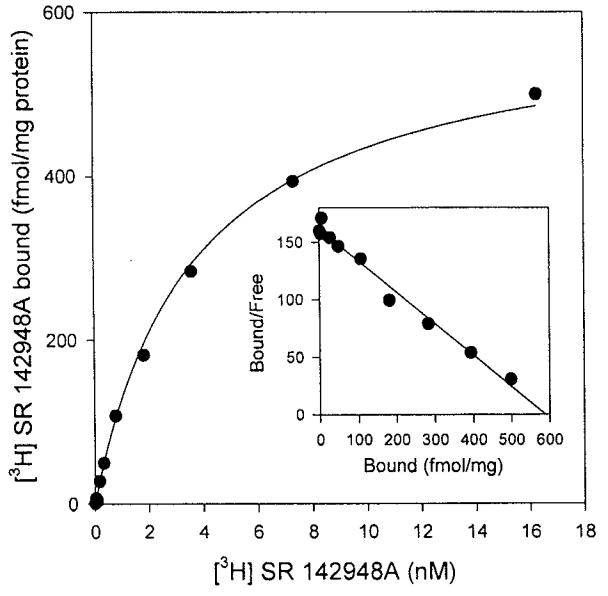

Fig. 3. Saturation analysis and Scatchard plot (inset) of [^{3}H]SR 142948A binding to rat brain membranes. Membranes were incubated for 60 min at 20°C over a concentration range of [^{3}H]SR 142948A (0.05 to 16 nM); nonspecific binding was defined with 1 μM unlabeled SR 142948A. The data shown are from one of 3 experiments performed in triplicate.

3.1.3. Kinetic studies

The specific binding of [^{3}H]SR 142948A to rat brain membranes was time dependent, reaching a steady state in about 60–80 min at 20°C (Fig. 4A). Fig. 4B illustrates the rate of dissociation, measured at various time intervals after addition of 1 μM unlabeled SR 142948A at equilibrium binding. The dissociation kinetics revealed a first-order process with a dissociation rate constant (k_{-1}) of 0.021 min^{-1} (mean, $n = 2$). The observed association rate constant (k_{obs}) was 0.033 min^{-1} and the kinetic association constant (k_1), calculated from the equation $k_1 = (k_{obs}$

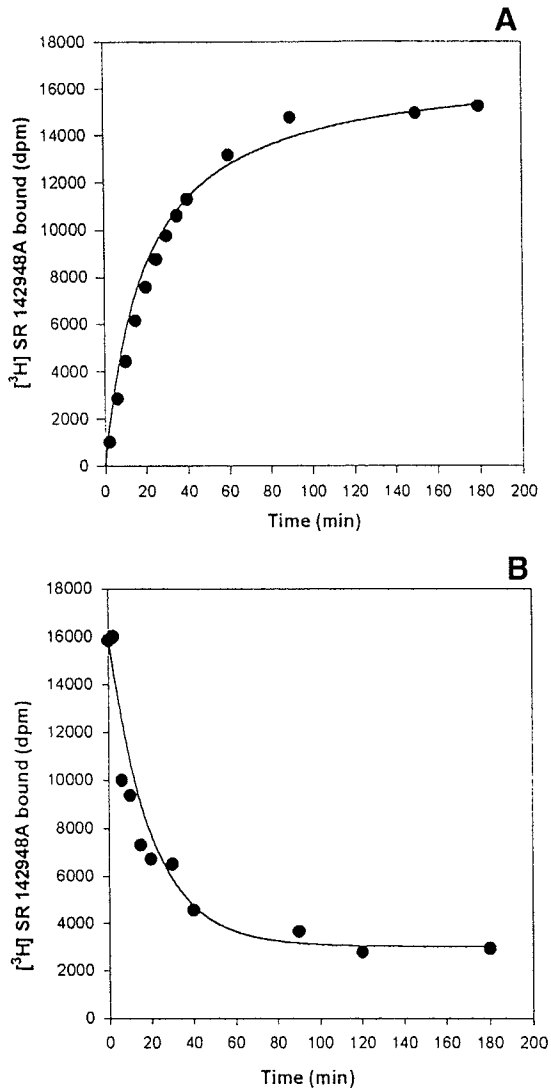

Fig. 4. Association (A) and dissociation (B) kinetics of specific [^{3}H]SR 142948A binding to rat brain membranes. (A) The association of 2 nM [^{3}H]SR 142948A binding was determined at various time intervals. (B) Time course of dissociation of [^{3}H]SR 142948A binding, initiated with 1 μM unlabeled SR 142948A. The points shown are means of triplicate determinations from a representative experiment.

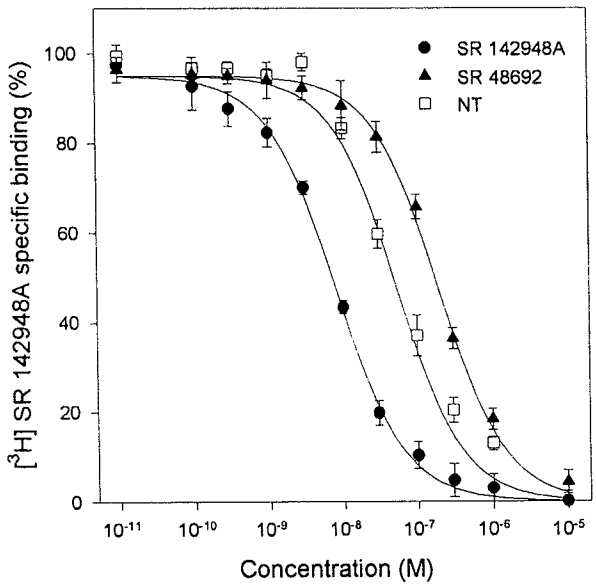

Fig. 5. Inhibition of specific [^{3}H]SR 142948A binding to rat brain membranes by increasing concentrations of SR 142948A, SR 48692 and neurotensin. Results represent the means ± S.E.M. of 3 independent experiments performed in triplicate.

$-k_1$)/([^{3}H]SR 142948A), was 0.006×10^9 M^{-1} min^{-1}. The dissociation constant (K_d) calculated from the ratio k_{-1}/k_1 was 3.5 nM, similar to the dissociation constant determined in saturation studies.

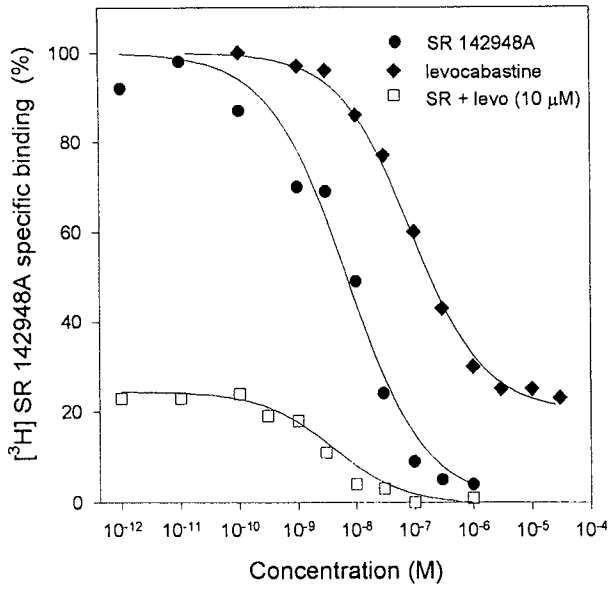

Fig. 6. Inhibition of specific [^{3}H]SR 142948A binding to rat brain membranes by SR 142948A, levocabastine and SR 142948A in the presence of a constant concentration of levocabastine (10 μM). Specific binding of [^{3}H]SR 142948A without levocabastine represents 100%. In the absence of levocabastine, SR 142948A (●) inhibited [^{3}H]SR 142948A binding to neurotensin NT_1 and NT_2 receptors. Levocabastine (◆) inhibited binding of [^{3}H]SR 142948A to NT_2 receptors (80% of the receptors). In the presence of 10 μM levocabastine, SR 142948A (□) inhibited [^{3}H]SR 142948A binding to NT_1 receptors (20% of the receptors). The data shown are from a single experiment performed in triplicate. The experiment was repeated 3 times with similar results.

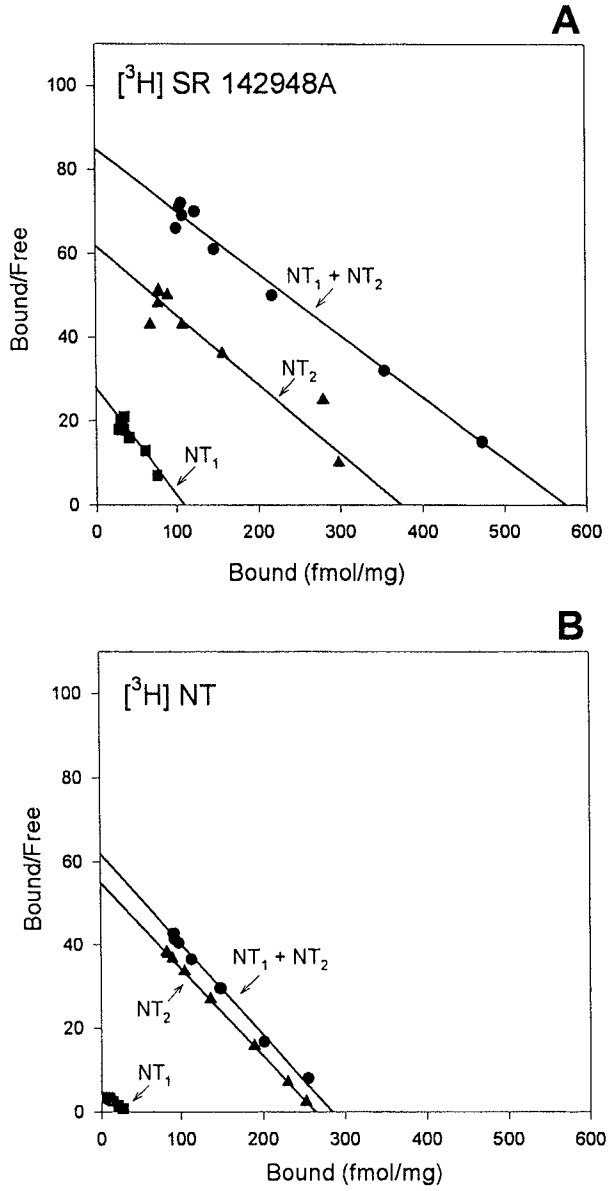

Fig. 7. Scatchard analysis of saturation of [^{3}H]SR 142948A (A) and [^{3}H]neurotensin (B) binding to rat brain membranes performed with or without 10 μM levocabastine. [^{3}H]SR 142948A and [^{3}H]neurotensin bound to neurotensin NT_1 and NT_2 receptors; the addition of 10 μM levocabastine to the binding assay blocked levocabastine-sensitive NT_2 receptors and revealed NT_1 receptors. The NT_2 receptor data were calculated as the difference between the results obtained in the absence and in the presence of levocabastine. The values are from typical experiments and represent the means of triplicate determinations.

3.1.4. Competition studies

Fig. 5 shows the inhibition of [^{3}H]SR 142948A binding by increasing concentrations of unlabeled SR 142948A, SR 48692 and neurotensin in rat brain homogenates. The K_i value obtained for unlabeled SR 142948A, 5.0 ± 0.4 nM, was close to the values determined in kinetic studies (Hill coefficient, $n_H = 0.98 \pm 0.01$). The binding of [^{3}H]SR 142948A to rat brain membranes was fully displaced by the natural ligand neurotensin, as well as by the previously described neurotensin receptor antagonist SR 48692, a

nonpeptide molecule chemically related to SR 142948A. These competition curves gave K_i values of 32.8 ± 5.9 nM (n_H = 0.99 ± 0.10) for neurotensin and 123.6 ± 15.7 nM (n_H = 0.95 ± 0.06) for SR 48692.

3.1.5. Effect of levocabastine on [^{3}H]SR 142948A and [^{3}H]neurotensin binding

The addition of increasing concentrations of levocabastine to the [^{3}H]SR 142948A binding assay resulted in progressive blockade of neurotensin NT_2 receptors (Fig. 6). Concentrations greater than 1 μM levocabastine completely inhibited the binding of [^{3}H]SR 142948A to NT_2 receptors, which constituted 80% of the whole population of sites. The presence of 10 μM levocabastine in the [^{3}H]SR 142948A binding assay revealed neurotensin NT_1 receptors, which were recognized by SR 142948A with an IC_{50} value of 4.0 ± 0.3 nM, in the same nanomolar range as for experiments without levocabastine (IC_{50} = 7.0 ± 1.5 nM).

Saturation experiments were also performed in the presence or absence of 10 μM levocabastine with a fixed concentration of [^{3}H]SR 142948A and increasing concentrations of unlabeled SR 142948A. Scatchard analysis of [^{3}H]SR 142948A binding data in the absence of levocabastine yielded a linear plot (Fig. 7A), indicating the presence of a homogeneous population of binding sites (K_d = 6.1 ± 1.6 nM, B_{max} = 527 ± 22 fmol/mg protein; n = 3). However, the parallel leftward shift of this straight line obtained in the presence of 10 μM levocabastine indicated binding to neurotensin NT_1 receptors (K_d = 3.4 ± 0.5 nM, B_{max} = 104 ± 8 fmol/mg protein) and, by difference, revealed neurotensin NT_2 receptors (K_d = 8.5 ± 4.1 nM,

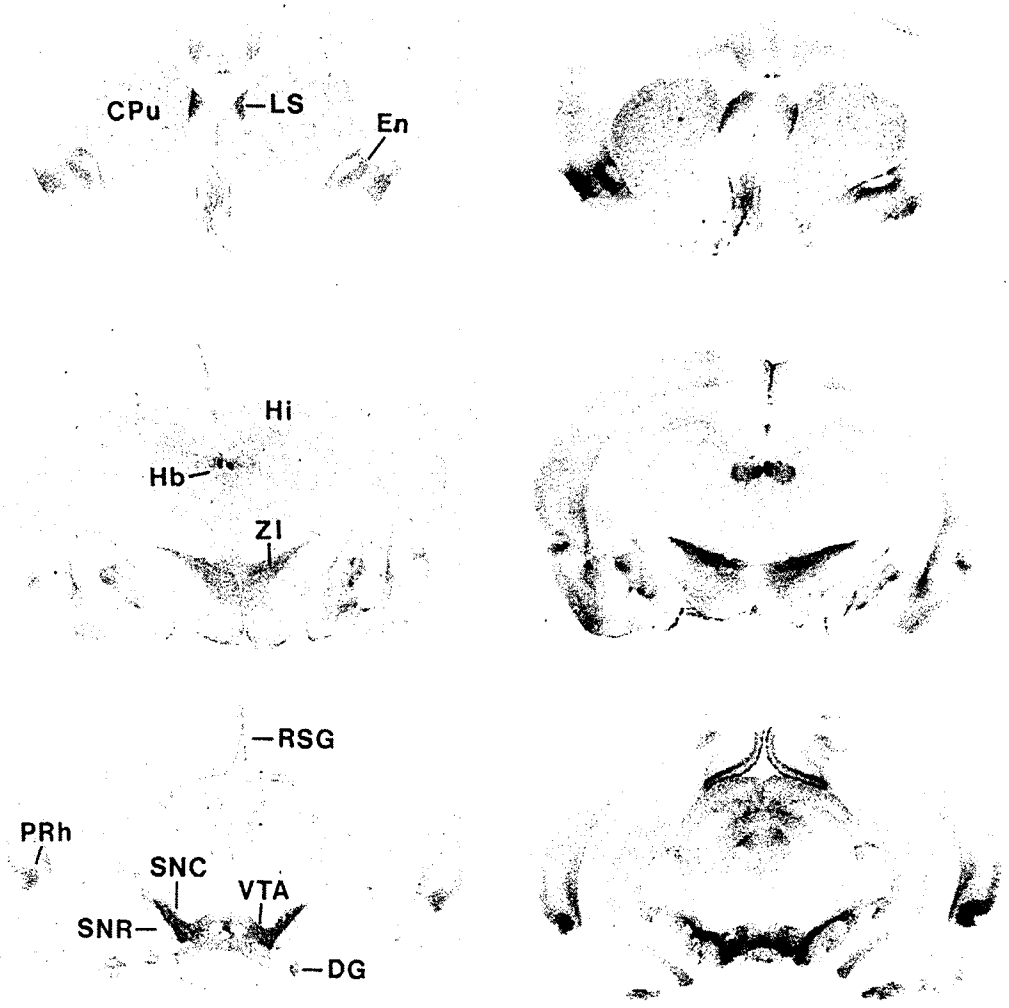

Fig. 8. Autoradiographic distribution of [^{3}H]SR 142948A (left) and [^{125}I]neurotensin (right) binding sites in coronal sections of the rat brain. Photographs show [^{3}H]SR 142948A and [^{125}I]neurotensin binding in the absence of levocabastine. Nonspecific binding was determined in the presence of 10 μM unlabeled SR 142948A or neurotensin, respectively, and was indistinguishable from background. Abbreviations: CPu = caudate putamen; DG = ventral dentate gyrus; En = endopirifom nucleus; Hb = habenula; Hi = hippocampus; LS = lateral septum; Prh = perirhinal area; RSG = retrosplenial granular cortex; SNC = substantia nigra, pars compacta; SNR = substantia nigra, pars reticulata; VTA = ventral tegmental area; ZI = zona incerta.

B_{max} = 422 ± 58 fmol/mg protein). These data confirmed that [^{3}H]SR 142948A exhibits similar affinities for the two subtypes of neurotensin receptors. Similar experiments performed with [^{3}H]neurotensin (Fig. 7B) revealed K_d values comparable to those of [^{3}H] SR 142948A (6.8 and 4.8 nM for NT_1 and NT_2 receptors, respectively). However, [^{3}H]neurotensin bound to a lower number of binding sites than [^{3}H]SR 142948A (B_{max} values of 32 and 265 fmol/mg for NT_1 and NT_2 receptors, respectively).

3.1.6. Effect of guanyl nucleotides on [^{3}H]SR 142948A binding

In order to determine whether the binding of [^{3}H]SR 142948A was sensitive to guanyl nucleotides, we examined the affinity of the radioligand in the presence of Gpp(NH)p, a nonhydrolyzable analog of GTP. The addition of Gpp(NH)p in concentrations up to 100 μM did not modify the specific binding of [^{3}H]SR 142948A to rat brain membranes (data not shown).

3.2. Autoradiographic localization of [^{3}H]SR 142948A binding sites in the rat brain: Comparison with [^{125}I]neurotensin binding

Preliminary experiments showed that the characteristics of [^{3}H]SR 142948A binding to rat midbrain sections were similar to those observed for brain membrane homogenates. [^{3}H]SR 142948A binding was saturable and reached a steady state by 60 min. Specific [^{3}H]SR 142948A binding was approximately 90% of the total binding, as

Table 1
Regional distribution of [^{3}H]SR 142948A and [^{125}I]neurotensin binding sites in the rat brain, in the presence or absence of levocabastine

Brain area	Specific binding			
	[^{3}H]SR 142948A		[^{125}I]neurotensin	
	− levo	+ levo	− levo	+ levo
Cerebral cortex				
Frontal cortex	1.91 ± 0.11	1.12 ± 0.02	0.39 ± 0.03	0.29 ± 0.01
Anterior cingulate cortex	6.61 ± 0.27	6.41 ± 0.14	2.01 ± 0.16	1.79 ± 0.14
Dorsal peduncular cortex	9.44 ± 0.18	7.67 ± 0.27	2.47 ± 0.39	1.80 ± 0.09
Agranular insular cortex	7.58 ± 0.21	5.66 ± 0.51	1.62 ± 0.19	1.05 ± 0.09
Dorsal endopiriform nucleus	5.06 ± 0.12	4.59 ± 0.09	1.82 ± 0.13	1.15 ± 0.07
Parietal cortex	1.84 ± 0.05	0.82 ± 0.05	0.40 ± 0.02	0.27 ± 0.01
Perirhinal area	10.54 ± 0.29	8.98 ± 0.22	2.51 ± 0.32	2.29 ± 0.05
Retrosplenial granular cortex	3.11 ± 0.09	1.98 ± 0.12	1.07 ± 0.03	0.84 ± 0.06
Temporal cortex	2.22 ± 0.05	1.01 ± 0.06	0.47 ± 0.01	0.33 ± 0.01
Forebrain				
Septohippocampal nucleus	5.90 ± 0.27	5.50 ± 0.29	2.09 ± 0.47	2.01 ± 0.17
Lateral septal nucleus, dorsal part	5.99 ± 0.25	4.65 ± 0.10	1.13 ± 0.02	1.02 ± 0.05
Basal ganglia				
Caudate putamen (striatum)	2.57 ± 0.13	2.12 ± 0.06	0.58 ± 0.02	0.51 ± 0.02
Accumbens nucleus, shell	2.62 ± 0.08	1.66 ± 0.07	0.52 ± 0.02	0.35 ± 0.01
Accumbens nucleus, core	2.39 ± 0.09	1.55 ± 0.06	0.55 ± 0.03	0.37 ± 0.01
Amygdala				
Central amygdaloid nucleus	5.00 ± 0.33	3.10 ± 0.09	1.29 ± 0.09	0.93 ± 0.02
Posteromedial cortical amygdaloid nucleus	9.17 ± 0.38	8.06 ± 0.26	1.83 ± 0.20	1.60 ± 0.12
Diencephalon				
Zona incerta	7.84 ± 0.14	5.67 ± 0.46	1.61 ± 0.06	1.32 ± 0.03
Lateral habenular nucleus	5.41 ± 0.20	4.01 ± 0.11	1.20 ± 0.06	0.80 ± 0.04
Medial habenular nucleus	10.68 ± 0.48	9.01 ± 0.50	2.63 ± 0.14	1.92 ± 0.07
Hippocampal formation				
Dentate gyrus, ventral part	8.41 ± 0.44	7.64 ± 0.31	1.19 ± 0.08	0.98 ± 0.14
Midbrain				
Substantia nigra, pars compacta	14.25 ± 1.08	11.34 ± 1.08	2.38 ± 0.10	2.05 ± 0.26
Substantia nigra, pars reticulata	3.21 ± 0.13	2.79 ± 0.14	0.99 ± 0.05	0.83 ± 0.07
Ventral tegmental area	15.10 ± 1.08	9.77 ± 0.97	2.18 ± 0.17	1.71 ± 0.19
Superficial gray layer of the superior colliculus	4.10 ± 0.13	2.28 ± 0.08	0.82 ± 0.03	0.64 ± 0.03

[^{3}H]SR 142948A and [^{125}I]neurotensin specific binding to neurotensin NT_1 and NT_2 receptors was determined on rat brain sections by autoradiography, in the presence (+ levo) or absence (− levo) of levocabastine (1 μM). The occlusion of neurotensin NT_2 receptors by levocabastine allowed detection of NT_1 receptors. The difference between binding in the absence and in the presence of levocabastine represents binding to NT_2 receptors. Optical densities were measured bilaterally on 4 brain sections per level and expressed as mean ± S.E.M. nCi/mg tissue.

determined with 2 nM radioligand. Analysis of competition studies performed on rat midbrain sections showed that SR 142948A, SR 48692 and neurotensin induced a dose-dependent and complete inhibition of [^{3}H]SR 142948A binding (data not shown).

Fig. 8 shows the regional distribution of [^{3}H]SR 142948A and [^{125}I]neurotensin binding sites in the rat brain. The highest density of [^{3}H]SR 142948A and [^{125}I]neurotensin binding was present in the midbrain, in the ventral tegmental area and substantia nigra pars compacta. Intense labeling was also observed in the perirhinal area as well as in the dorsal peduncular, anterior cingulate and agranular insular cortices, posteromedial cortical amygdaloid nucleus, medial habenula and ventral dentate gyrus. The endopiriform nucleus, septohippocampal nucleus, central amygdaloid nucleus and zona incerta exhibited moderate levels of binding. Finally, a low density of binding sites was observed in the frontal, parietal, temporal and retrosplenial granular cortices, caudate putamen, nucleus accumbens, lateral septum, hypothalamus, hippocampus, substantia nigra pars reticulata and in the superficial gray layer of the superior colliculus.

Table 1 shows the comparative distribution of [^{3}H]SR 142948A and [^{125}I]neurotensin binding sites in the rat brain, in the presence or absence of levocabastine. An excellent correlation between the regional distribution of the two ligands was observed, in agreement with the autoradiographic localization of neurotensin receptors in rat brain described previously (Moyse et al., 1987). The presence of levocabastine in the incubation buffer inhibited binding to neurotensin NT_2 receptors and decreased the amount of labeling with [^{3}H]SR 142948A and [^{125}I]neurotensin in all brain regions studied, indicating that both ligands labeled neurotensin NT_1 and NT_2 receptors. This result is in agreement with the ubiquitous distribution of NT_2 receptors in the rat brain (Schotte et al., 1986).

4. Discussion

The binding of the nonpeptide neurotensin receptor antagonist [^{3}H]SR 142948A to rat brain membranes was rapid, tissue concentration and time dependent, saturable and reversible. Scatchard analyses of saturation experiments indicated that [^{3}H]SR 142948A binds with high affinity ($K_d = 3.5$ nM) and apparently recognizes a single class of binding sites. The number of sites labeled by [^{3}H]SR 142948A ($B_{max} = 508$ fmol/mg protein) was 80% greater than the B_{max} value determined with [^{3}H]neurotensin under the same experimental conditions (297 fmol/mg protein). Competition experiments with unlabeled SR 142948A yielded a Hill coefficient near unity, further suggesting that the antagonist bound to an apparently homogeneous population of binding sites.

The potencies of the neurotensin receptor antagonists SR 142948A and SR 48692 in inhibiting specific [^{3}H]SR 142948A binding ($K_i = 5$ and 123.6 nM, respectively) were similar to their previously reported potencies in displacing [^{125}I]neurotensin binding in adult rat brain homogenates ($IC_{50} = 3.96$ and 82 nM for SR 142948A and SR 48692, respectively) (Gully et al., 1997). In contrast, the potency of the natural peptide agonist neurotensin for inhibiting [^{3}H]SR 142948A binding ($K_i = 32.8$ nM) was 10-fold lower than its potency in displacing [^{125}I]neurotensin binding ($IC_{50} = 3.2$ nM). This is consistent with results obtained with other receptor systems, demonstrating that estimates of agonist affinity are lower when an antagonist rather than an agonist radioligand is displaced. Indeed, a reduced potency for agonists to compete against radiolabeled antagonist ligands has been observed previously for neurotensin receptors in the guinea pig brain (Betancur et al., 1995), as well as for muscarinic cholinergic receptors (Waelbroeck et al., 1982), cholecystokinin CCK_A (Chang et al., 1986; Talkad et al., 1994) and CCK_B receptors (Chang et al., 1989), tachykinin NK_1 receptors (McLean et al., 1991) and 5-HT_2 receptors (Teitler et al., 1990). These findings have been interpreted as indicating the existence of different conformational states of the same receptor, with different affinities for agonist and antagonist ligands (Schwartz et al., 1995).

The higher number of receptors detected with [^{3}H]SR 142948A when compared with the number detected with the agonist radioligand, [^{3}H]neurotensin, also supports this hypothesis. The ability of radiolabeled nonpeptide antagonists to recognize a larger number of receptors, characterized by low affinity for the agonist, than agonist-derived radioligands appears to be a common phenomenon. For instance, we showed previously that in the guinea pig brain the number of binding sites labeled by the antagonist [^{3}H]SR 48692 exceeded by 20-fold the number of receptors labeled with the agonist [^{125}I]neurotensin (Betancur et al., 1995). The binding sites detected by [^{3}H]SR 48692 were characterized by a low affinity for neurotensin and were insensitive to GTP, suggesting that they represent the uncoupled form of the neurotensin receptor. These data, together with current hypotheses on the molecular interactions of ligands with their receptors, suggest that agonists bind with high affinity to the active receptor conformation, whereas antagonists bind with higher affinity to the inactive conformation (Schwartz et al., 1995). Thus, peptide agonists and nonpeptide antagonists act as allosteric competitive ligands by binding in a mutually exclusive fashion to sites occurring in different receptor conformations. In support of this model, recent site-directed mutational studies of the rat neurotensin NT_1 receptor showed that mutations in the N-terminal part eliminate neurotensin binding without affecting the binding of [^{3}H]SR 48692 (Labbé-Jullié et al., 1995). This finding suggests the existence of distinct agonist and antagonist binding domains on the neurotensin NT_1 receptor, similarly to what has been reported for several other neuropeptide receptors (for review, see Betancur et al., 1997).

Levocabastine is a nonpeptide antagonist of histamine H_1 receptors that is structurally unrelated to neurotensin (Stockbroekx et al., 1986), but binds also to neurotensin NT_2 receptors (Schotte et al., 1986). The recent cloning of the mouse NT_2 receptor and its expression in *Xenopus* oocytes indicated that levocabastine acts as an agonist in this system, since it triggers a Cl^- inward current, as does neurotensin (Mazella et al., 1996). Saturation and competition experiments performed with or without levocabastine indicated that [^{3}H]SR 142948A bound with high affinity to neurotensin NT_1 and NT_2 receptors (K_d = 3.4 and 8.5 nM, respectively). Indeed, the addition of levocabastine to the [^{3}H]SR 142948A binding assay caused a parallel leftward shift of the Scatchard plot, indicating the displacement of [^{3}H]SR 142948A binding from levocabastine-sensitive NT_2 receptors. The similar affinity of [^{3}H]SR 142948A for both subtypes of neurotensin receptors explains the apparently homogeneous population of binding sites detected with this ligand in the absence of levocabastine. Moreover, our results indicate that neurotensin NT_2 receptors constitute 80% of the whole population of sites labeled by [^{3}H]SR 142948A (B_{max} = 104 and 422 fmol/mg protein for NT_1 and NT_2 receptors, respectively) on rat brain membranes.

Guanyl nucleotides differentially affect agonist and antagonist binding in several neurotransmitter receptor systems. Accordingly, guanyl nucleotides have been reported to significantly reduce [^{125}I]neurotensin binding to NT_1 receptors, by interfering with the formation of the high-affinity agonist-receptor-G protein ternary complex (Hermans et al., 1996). In contrast, the present study showed that addition of Gpp(NH)p had no effect on specific [^{3}H]SR 142948A binding. This finding is consistent with previous data showing that antagonist ligands bind with high affinity to the G protein-uncoupled state of receptors (Teitler et al., 1990; Rosenkilde et al., 1994; Betancur et al., 1995). It should be noted, however, that the levocabastine-sensitive neurotensin binding site is insensitive to GTP (Vincent, 1995), although recent data indicate that the cloned mouse neurotensin NT_2 receptor is coupled functionally to phospholipase C when expressed in oocytes (Mazella et al., 1996). Other studies have shown that an absence of GTP-sensitive binding does not necessarily indicate failure to activate a second messenger cascade (Chung et al., 1988; Maeda et al., 1990; Hermans et al., 1996).

The different sensitivity to Gpp(NH)p of neurotensin NT_1 and NT_2 receptors is particularly interesting in view of the fact that the lowest homology between the two neurotensin receptors is in their third cytoplasmic loop and C-terminal domain (Chalon et al., 1996; Mazella et al., 1996), two regions implicated in the coupling to G proteins (Yamada et al., 1994; Hermans et al., 1996). Furthermore, it has been proposed that the extremely high number of Ser/Thr residues in the third intracytoplasmic loop and the C-terminal domain of the neurotensin NT_2 receptor protein could be associated with a basal phosphorylated state resulting in desensitization of the receptor (Mazella et al., 1996). This could result in a higher proportion of receptors in the uncoupled form expressed in the membrane and might explain the insensitivity of the NT_2 receptor to GTP analogs. The use of recently developed radiolabeled agonist ligands specific for the G protein-coupled state of neurotensin receptors (Gaudriault et al., 1996), in the presence or absence of levocabastine, could help to determine the different states of coupling of neurotensin NT_1 and NT_2 receptors.

The autoradiographic distribution of [^{3}H]SR 142948A binding in sections of rat brain was consistent with its selective binding to neurotensin receptors. The heterogeneous pattern of specific [^{3}H]SR 142948A binding closely matched the localization of [^{125}I]neurotensin binding observed in adjacent sections. The addition of levocabastine to the incubation buffer resulted in a small and diffuse reduction of [^{3}H]SR 142948A and [^{125}I]neurotensin binding in all brain structures studied, in agreement with previous studies indicating that neurotensin NT_2 receptors are distributed throughout the rat central nervous system (Schotte et al., 1986; Kitabgi et al., 1987) and are predominantly associated with glial cells (Schotte et al., 1988). The ubiquitous distribution of neurotensin NT_2 receptors contrasts with the highly regional localization of NT_1 receptors in the brain. Indeed, NT_1 receptors are particularly abundant in brain regions rich in dopamine neurons, such as the substantia nigra and the ventral tegmental area, as well as in certain cortical areas. These results are in agreement with the previously described distribution of [^{125}I]neurotensin binding (Moyse et al., 1987) and neurotensin NT_1 receptor mRNA (Nicot et al., 1994) observed in the rat brain.

The functional characterization of the actions of SR 142948A in the central nervous system showed that this compound, like the first-generation neurotensin receptor antagonist SR 48692, antagonizes the turning behavior induced by intrastriatal injection of neurotensin in mice as well as acetylcholine release evoked by neurotensin in the striatum (Gully et al., 1993, 1997). Neither compound modified dopamine release in the nucleus accumbens after injection of neurotensin into the ventral tegmental area (Steinberg et al., 1994; Gully et al., 1997). However, unlike SR 48692, SR 142948A blocked the hypothermia and analgesia induced by central injection of neurotensin in rodents (Gully et al., 1997). These results suggest that SR 142948A may interact with a neurotensin receptor subtype which is not blocked by SR 48692. It would be interesting to assess the potential involvement of the recently identified neurotensin NT_2 receptor in the mediation of the hypothermia and anti-nociceptive effects induced by neurotensin.

In conclusion, [^{3}H]SR 142948A represents a new potent nonpeptide antagonist radioligand specific for neurotensin receptors. The compound binds to rat neurotensin NT_1 and NT_2 receptors with nanomolar affinity, close to that of the

natural ligand neurotensin. The ligand previously described, [^{3}H]SR 48692, exhibits a higher affinity for NT_1 than for NT_2 receptors and has a low ratio of total binding to nonspecific binding in rat brain membranes and tissue sections, which limits its utility. Consequently, the availability of [^{3}H]SR 142948A provides a valuable tool for the study of neurotensin receptors in the central nervous system.

Acknowledgements

We thank A.M. Lhiaubet for labeling [^{125}I]neurotensin. C.B. is supported by a post-doctoral fellowship from INSERM (Institut National de la Santé et de la Recherche Médicale), France.

References

Betancur, C., Canton, M., Gully, D., Vela, G., Pélaprat, D., Rostène, W., 1995. Characterization and distribution of binding sites for a new neurotensin receptor antagonist ligand, [^{3}H]SR 48692, in the guinea pig brain. J. Pharmacol. Exp. Ther. 273, 1450–1458.

Betancur, C., Azzi, M., Rostène, W., 1997. Nonpeptide antagonists of neuropeptide receptors: Tools for research and therapy. Trends Pharmacol. Sci. 18, 372–386.

Chalon, P., Vita, N., Kaghad, M., Guillemot, M., Bonnin, J., Delpech, B., Le Fur, G., Ferrara, P., Caput, D., 1996. Molecular cloning of a levocabastine-sensitive neurotensin binding site. FEBS Lett. 386, 91–94.

Chang, R.S.L., Lotti, V.J., Chen, T.B., Kunkel, K.A., 1986. Characterization of the binding of [^{3}H]-(±)-L-364,718: A new potent, nonpeptide cholecystokinin antagonist radioligand selective for peripheral receptors. Mol. Pharmacol. 30, 212–217.

Chang, R.S.L., Chen, T.B., Bock, M.G., Freidinger, R.M., Chen, R., Rosegay, A., Lotti, V.J., 1989. Characterization of the binding of [^{3}H]L-365,260: A new potent and selective brain cholecystokinin (CCK-B) and gastrin receptor antagonist radioligand. Mol. Pharmacol. 35, 803–808.

Cheng, Y., Prusoff, W., 1973. Relationship between the inhibition constant (K_i) and the concentration of inhibitor which causes 50% inhibition (IC_{50}) of an enzymatic reaction. Biochem. Pharmacol. 22, 3099–3108.

Chung, F.Z., Wang, C.D., Potter, P.C., Venter, J.C., Fraser, C.M., 1988. Site-directed mutagenesis and continuous expression of human β-adrenergic receptors. J. Biol. Chem. 263, 4052–4055.

Dubuc, I., Costentin, J., Terranova, J.P., Barnouin, M.C., Soubrié, P., Le Fur, G., Rostène, W., Kitabgi, P., 1994. The nonpeptide neurotensin antagonist, SR 48692, used as a tool to reveal putative neurotensin receptor subtypes. Br. J. Pharmacol. 112, 352–354.

Emson, P.C., Goedert, M., Horsfield, P.M., Rioux, F., St. Pierre, S., 1982. The regional distribution and chromatographic characterization of neurotensin-like immunoreactivity in the rat central nervous system. J. Neurochem. 38, 992–999.

Gaudriault, G., Zsürger, N., Vincent, J.P., 1996. Radiolabeled ligands specific for the G protein-coupled state of neurotensin receptors. J. Neurochem. 67, 2590–2598.

Goedert, M., Pittaway, K., Williams, B.J., Emson, P.C., 1984. Specific binding of tritiated neurotensin to rat brain membranes: Characterization and regional distribution. Brain Res. 304, 71–81.

Gully, D., Canton, M., Boigegrain, R., Jeanjean, F., Molimard, J.C., Poncelet, M., Gueudet, C., Heaulme, M., Leyris, R., Brouard, A., Pélaprat, D., Labbé-Jullié, C., Mazella, J., Soubrié, P., Maffrand, J.P., Rostène, W., Kitabgi, P., Le Fur, G., 1993. Biochemical and pharmacological profile of a potent and selective nonpeptide antagonist of neurotensin receptor. Proc. Natl. Acad. Sci. USA 90, 65–69.

Gully, D., Labeeuw, B., Boigegrain, R., Oury-Donat, F., Bachy, A., Poncelet, M., Steinberg, R., Suaud-Chagny, M.F., Santucci, V., Vita, N., Pecceu, F., Labbé-Jullié, C., Kitabgi, P., Soubrié, P., Le Fur, G., Maffrand, J.P., 1997. Biochemical and pharmacological activities of SR 142948A, a new potent neurotensin receptor antagonist. J. Pharmacol. Exp. Ther. 280, 802–812.

Hermans, E., Octave, J.N., Maloteaux, J.M., 1996. Interaction of the COOH-terminal domain of the neurotensin receptor with a G protein does not control the phospholipase C activation but is involved in the agonist-induced internalization. Mol. Pharmacol. 49, 365–372.

Kaseow, J., Nemeroff, C.B., 1991. The neurobiology of neurotensin: Focus on neurotensin–dopamine interactions. Regul. Pept. 36, 153–164.

Kitabgi, P., Rostène, W., Dussaillant, M., Schotte, A., Laduron, P.M., Vincent, J.P., 1987. Two populations of neurotensin binding sites in murine brain: Discrimination by the antihistamine levocabastine reveals markedly different radioautographic distribution. Eur. J. Pharmacol. 140, 285–293.

Labbé-Jullié, C., Botto, J.M., Mas, M.V., Chabry, J., Mazella, J., Vincent, J.P., Gully, D., Maffrand, J.P., Kitabgi, P., 1995. [^{3}H]SR 48692, the first nonpeptide neurotensin antagonist radioligand: Characterization of binding properties and evidence for distinct agonist and antagonist binding domains on the rat neurotensin receptor. Mol. Pharmacol. 47, 1050–1056.

Le, F., Cusak, B., Richelson, E., 1996. The neurotensin receptor: Is there more than one subtype?. Trends Pharmacol. Sci. 17, 1–3.

Maeda, S., Lameh, J., Mallet, W.G., Philip, M., Ramachandran, J., Sadée, W., 1990. Internalization of the Hm1 muscarinic cholinergic receptor involves the third cytoplasmic loop. FEBS Lett. 269, 386–388.

Mai, J., Triepel, K.J., Metz, J., 1987. Neurotensin in the human brain. Neuroscience 22, 499–524.

Mazella, J., Poustis, C., Labbé, C., Cheeler, F., Kitabgi, P., Granier, C., Van Rietschoten, J., Vincent, J.P., 1983. Monoiodo Trp^{11}-neurotensin, a highly radioactive ligand of neurotensin receptors: Preparation, biological activity, and binding properties to rat brain synaptic membranes. J. Biol. Chem. 258, 3476–3481.

Mazella, J., Botto, J.M., Guillemare, E., Coppola, T., Sarret, P., Vincent, J.P., 1996. Structure, functional expression, and cerebral localization of the levocabastine-sensitive neurotensin/neuromedin N receptor from mouse brain. J. Neurosci. 16, 5613–5620.

McLean, S., Ganong, A.H., Seeger, T.F., Bryce, D.K., Pratt, K.G., Reynolds, L.S., Siok, C.J., Lowe, J.A. III, Heym, J., 1991. Activity and distribution of binding sites in brain of a nonpeptide substance P (NK_1) receptor antagonist. Science 251, 437–439.

Moyse, E., Rostène, W., Vial, M., Leonard, K., Mazella, J., Kitabgi, P., Vincent, J.P., Beaudet, A., 1987. Distribution of neurotensin binding sites in rat brain: A light microscopic radioautographic study using monoiodo [^{125}I]Tyr$_3$-neurotensin. Neuroscience 22, 525–536.

Munson, P.J., Rodbard, D., 1980. LIGAND: A versatile computerized approach for characterization of ligand-binding systems. Anal. Biochem. 107, 220–239.

Nicot, A., Rostène, W., Bérod, A., 1994. Neurotensin receptor expression in the rat forebrain and midbrain: A combined analysis by in situ hybridization and receptor autoradiography. J. Comp. Neurol. 341, 407–419.

Paxinos, G., Watson, C., 1986. The Rat Brain in Stereotaxic Coordinates, 2nd ed. Academic Press, Sydney.

Pugsley, T.A., Akunne, H.C., Whetzel, S.Z., Demattos, S., Corbin, A.E., Wiley, J.N., Wustrow, D.J., Wise, L.D., Heffner, T.G., 1995. Differential effects of the nonpeptide neurotensin antagonist, SR 48692, on the pharmacological effects of neurotensin agonists. Peptides 16, 37–44.

Rosenkilde, M.M., Cahir, M., Gether, U., Hjorth, S.A., Schwartz, T.W.,

1994. Mutations along transmembrane segment II of the NK-1 receptor affect substance P competition with non-peptide antagonists but not substance P binding. J. Biol. Chem. 269, 28160–28164.

Rostène, W.H., Alexander, M.J., 1997. Neurotensin and neuroendocrine regulation. Front. Neuroendocrinol. 18, 115.

Sadoul, J.L., Mazella, J., Amar, S., Kitabgi, P., Vincent, J.P., 1984. Preparation of neurotensin selectively iodinated on the tyrosine 3 residue. Biological activity and binding properties on mammalian neurotensin receptors. Biochem. Biophys. Res. Commun. 120, 812–819.

Schotte, A., Leysen, J.E., Laduron, P.M., 1986. Evidence for a displaceable non-specific [^{3}H]neurotensin binding site in rat brain. Naunyn Schmiedebergs Arch. Pharmacol. 333, 400–405.

Schotte, A., Rostène, W., Laduron, P.M., 1988. Different subcellular localization of neurotensin receptor and neurotensin acceptor sites in the rat brain dopaminergic system. J. Neurochem. 50, 1026–1031.

Schwartz, T.W., Gether, U., Schambye, H.T., Hjorth, S.A., 1995. Molecular mechanism of action of nonpeptide ligands for peptide receptors. Curr. Pharm. Design 1, 355–372.

Steinberg, R., Brun, P., Fournier, M., Souilhac, J., Rodier, D., Mons, G., Terranova, J.P., Le Fur, G., Soubrié, P., 1994. SR 48692, a non-peptide neurotensin receptor antagonist differentially affects neurotensin-induced behaviour and changes in dopaminergic transmission. Neuroscience 59, 921–929.

Stockbrockx, R.A., Luyckx, M.G., Willems, J.M., Janssen, M.A.C., Bracke, J.O.M.M., Joosen, B.L.P., Van Wauwe, J.P., 1986. Levocabastine (R 50 547), the prototype of a chemical series of compounds with specific H_1-antihistamine activity. Drug Dev. Res. 8, 87–93.

Talkad, V.D., Fortune, K.P., Pollo, D.A., Shah, G.N., Wank, S.A., Gardner, J.D., 1994. Direct demonstration of three different states of the pancreatic cholecystokinin receptor. Proc. Natl. Acad. Sci. USA 91, 1868–1872.

Tanaka, K., Masu, M., Nakanishi, S., 1990. Structure and functional expression of the cloned rat neurotensin receptor. Neuron 4, 847–854.

Teitler, M., Leonhardt, S., Weisberg, E.L., Hoffman, B.J., 1990. 4-[^{125}I]iodo-(2,5-dimethoxy)phenylisopropylamine and [^{3}H]ketanserin labeling of 5-hydroxytryptamine$_2$ ($5HT_2$) receptors in mammalian cells transfected with a rat $5HT_2$ cDNA: Evidence for multiple states and not multiple $5HT_2$ receptor subtypes. Mol. Pharmacol. 38, 594–598.

Vincent, J.P., 1995. Neurotensin receptors: Binding properties, transduction pathways and structure. Cell. Mol. Neurobiol. 15, 501–512.

Vita, N., Laurent, P., Lefort, S., Chalon, P., Dumont, X., Kaghad, M., Gully, D., Le Fur, G., Ferrara, P., Caput, D., 1993. Cloning and expression of a complementary DNA encoding a high affinity human neurotensin receptor. FEBS Lett. 317, 139–142.

Waelbroeck, M., Robberecht, P., Chatelain, P., Christophe, J., 1982. Rat cardiac muscarinic receptors. I. Effects of guanine nucleotides on high- and low-affinity binding sites. Mol. Pharmacol. 21, 581–588.

Yamada, M., Yamada, M., Watson, M.A., Richelson, E., 1994. Deletion of the putative third intracellular loop of the rat neurotensin receptor abolishes phosphoinositide hydrolysis but not cyclic AMP formation in CHO-K1 cells. Mol. Pharmacol. 46, 470–476.

Proc. Natl. Acad. Sci. USA
Vol. 90, pp. 65–69, January 1993
Pharmacology

Biochemical and pharmacological profile of a potent and selective nonpeptide antagonist of the neurotensin receptor

DANIELLE GULLY*†, MARYSE CANTON*, ROBERT BOIGEGRAIN‡, FRANCIS JEANJEAN‡, JEAN-CHARLES MOLIMARD‡, MARTINE PONCELET‡, CHRISTIANE GUEUDET‡, MICHEL HEAULME‡, ROGER LEYRIS‡, ALINE BROUARD§, DIDIER PELAPRAT§, CATHERINE LABBÉ-JULLIÉ¶, JEAN MAZELLA¶, PHILIPPE SOUBRIÉ‡, JEAN-PIERRE MAFFRAND*, WILLIAM ROSTÈNE§, PATRICK KITABGI¶, AND GÉRARD LE FUR*

Sanofi Recherche, *195 route d'Espagne, 31036 Toulouse Cédex, and ‡371 rue du Pr. J. Blayac, 34082 Montpellier Cédex, France; §Unité 339, Institut National de la Santé et de la Recherche Médicale, Hôpital St. Antoine, 184 rue du Fbg St. Antoine, 75571 Paris Cédex 12, France; and ¶Institut de Pharmacologie Moléculaire et Cellulaire du Centre National de la Recherche Scientifique, Université de Nice-Sophia Antipolis, Sophia Antipolis, 660 route des Lucioles, 06560 Valbonne, France

Communicated by Susan E. Leeman, August 6, 1992

ABSTRACT **We describe the characteristics of SR 48692, a selective, nonpeptide antagonist of the neurotensin receptor. *In vitro*, this compound competitively inhibits ^{125}I-labeled neurotensin binding to the high-affinity binding site present in brain tissue from various species with IC_{50} values of 0.99 ± 0.14 nM (guinea pig), 4.0 ± 0.4 nM (rat mesencephalic cells), 7.6 ± 0.6 nM (COS-7 cells transfected with the cloned high-affinity rat brain receptor), 13.7 ± 0.3 nM (newborn mouse brain), 17.8 ± 0.9 nM (newborn human brain), 8.7 ± 0.7 nM (adult human brain), and 30.3 ± 1.5 nM (HT-29 cells). It also displaces ^{125}I-labeled neurotensin from the low-affinity levocabastine-sensitive binding sites but at higher concentrations (34.8 ± 8.3 nM for adult mouse brain and 82.0 ± 7.4 nM for adult rat brain). In guinea pig striatal slices, SR 48692 blocks K^+-evoked release of [^{3}H]dopamine stimulated by neurotensin with a potency (IC_{50} = 0.46 ± 0.02 nM) that correlates with its binding affinity. In a cell line derived from a human colon carcinoma (HT-29), SR 48692 competitively antagonizes neurotensin-induced intracellular Ca^{2+} mobilization with a pA_2 ($-\log K_{app}$) values of 8.13 ± 0.03, which is consistent with results obtained in binding studies. Moreover, SR 48692 is devoid of any intrinsic agonist activity. This compound is also active *in vivo*, since it reverses at low dose (80 μg/kg) the turning behavior induced by intrastriatal injection of neurotensin in mice with similar potency whatever the route of administration (i.p. or orally) and with a long duration of action (6 hr). Thus, being a potent and selective neurotensin receptor antagonist, SR 48692 may be considered as a powerful tool for investigating the role of neurotensin in physiological and pathological processes.**

Neurotensin (<Glu-Leu-Tyr-Glu-Asn-Lys-Pro-Arg-Arg-Pro-Tyr-Ile-Leu) was discovered in bovine hypothalamus (1) and subsequently shown to be widely distributed in the central nervous system (2, 3) and in the digestive tract (2, 4) of mammals. Neurotensin acts as a neuromodulator in the brain (5) and, in particular, as a modulator of dopamine transmission in the nigrostriatal and mesocorticolimbic systems (6, 7). It has neuroendocrine actions such as the mediation of the preovulatory surge (8, 9). In addition, neurotensin exerts potent hypothermic and analgesic effects when injected into the central nervous system (10, 11). In the periphery, it acts as a paracrine and endocrine modulator of digestive functions (4, 12) and produces numerous effects on the cardiovascular system of mammals (13).

Neurotensin interacts with specific membrane receptors that have been characterized in a number of tissues and cell lines of peripheral and central origins (for a review, see ref. 14). So far, structure–activity studies have not provided conclusive evidence for the existence of neurotensin receptor subtypes (14). However, adult rat and mouse brains have been shown to contain, in addition to high-affinity neurotensin receptors, low-affinity levocabastine-sensitive binding sites (15, 16). Whether these sites could mediate some neurotensin effects remains to be elucidated (16). The main transduction system coupled to high-affinity neurotensin receptors in a variety of systems appears to be the guanine nucleotide-binding regulatory protein-dependent stimulation of phospholipase C leading to an increase in intracellular calcium (17). Recent cloning, sequencing, and expression of the high-affinity levocabastine-insensitive neurotensin receptor from rat brain has indeed revealed that it belongs to the family of guanine nucleotide-binding regulatory protein-coupled receptors (18).

Despite the synthesis of neurotensin analogues, none of these compounds exhibited antagonist properties (14). The present report describes the biochemical and pharmacological properties of SR 48692 {2-[(1-(7-chloro-4-quinolinyl)-5-(2,6-dimethoxyphenyl)pyrazol-3-yl)carbonylamino]tricyclo(3.3.1.1.^{3,7})decan-2-carboxylic acid},

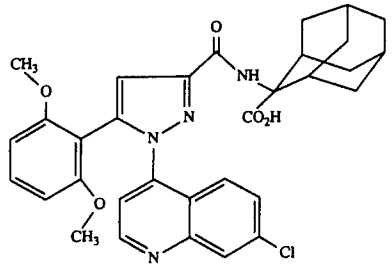

SR 48692

a potent and selective nonpeptide antagonist of neurotensin receptors, which was obtained by optimization of a lead compound discovered by random screening of several thousand chemicals.

MATERIALS AND METHODS

Materials. SR 48692 was synthesized at Sanofi Recherche (Montpellier, France) and solubilized in dimethyl sulfoxide for all experiments. Mono[^{125}I]iodo[Tyr^3]neurotensin(^{125}I-neurotensin; 2000 Ci/mmol; 1 Ci = 37 GBq) was prepared as

The publication costs of this article were defrayed in part by page charge payment. This article must therefore be hereby marked "*advertisement*" in accordance with 18 U.S.C. §1734 solely to indicate this fact.

Abbreviation: p.o., orally.
†To whom reprint requests should be addressed.

Table 1. IC_{50} values and Hill coefficients (n_H) for the inhibition of specific ^{125}I-neurotensin binding by unlabeled neurotensin and SR 48692 in various species

Sample	Neurotensin		SR 48692	
	IC_{50}, nM	n_H	IC_{50}, nM	n_H
Adult guinea pig brain	2.8 ± 1.6	0.95 ± 0.05	0.99 ± 0.14	1.15 ± 0.13
Adult rat brain	3.2 ± 0.5	0.89 ± 0.03	82.0 ± 7.4	0.67 ± 0.09
Rat mesencephalic cells	0.63 ± 0.16	0.89 ± 0.06	4.0 ± 0.4	0.91 ± 0.07
Transfected COS-7 cells	0.15 ± 0.02	0.74 ± 0.10	7.6 ± 0.6	0.95 ± 0.14
Newborn mouse brain	0.30 ± 0.02	0.86 ± 0.08	13.7 ± 0.3	0.97 ± 0.09
Adult mouse brain	2.0 ± 0.0	0.92 ± 0.06	34.8 ± 8.3	0.51 ± 0.08
Newborn human brain	0.31 ± 0.04	0.81 ± 0.09	17.8 ± 0.9	1.05 ± 0.12
Adult human brain	1.6 ± 0.4	0.75 ± 0.09	8.7 ± 0.7	0.83 ± 0.06
HT-29 cells	0.26 ± 0.04	0.75 ± 0.13	30.3 ± 1.5	1.01 ± 0.16

Each value represents the mean ± SE from at least three separate experiments performed in triplicate.

described (19). Neurotensin was purchased from Neosystem Laboratories. All other chemicals were from commercial sources.

Cell Culture. Mesencephalic cells from brains of embryonic Wistar rats (day 15) and the human colon carcinoma HT-29 and the mammalian fibroblast COS-7 cell lines were grown as described (20, 21).

Transfection of COS-7 Cells. The *Hin*dIII–*Not* I fragment coding for the high-affinity rat brain receptor (gift of S. Nakanishi; see ref. 18) was ligated into the *Hin*dIII–*Not* I cloning site of the CDM 8 vector and transfected into COS-7 cells by the DEAE-dextran precipitation method (22).

Preparation of Tissue Homogenates. Whole brain homogenates from 7-day-old and adult mice, guinea pig, adult rat, and newborn human (whole brain of a 32-day-old male infant who died from sudden infant death syndrome and dissected out less than 48 hr after death) and cortical regions of an adult male human brain (dissected 10 hr after death) were prepared as reported (23). Cell homogenates from confluent HT-29 cells were prepared as described (21). Membranes from COS-7 cells were prepared similarly 48–72 hr after transfection.

Binding Assays. All binding assays with tissue homogenates were carried out at 20°C in 50 mM Tris·HCl buffer (pH 7.5) containing 0.2% bovine serum albumin, and 1 mM 1,10-phenanthroline (newborn mouse and human brain, COS-7 cells, and HT-29 cells) or 0.1% bovine serum albumin, bacitracin (40 mg/liter), 1 mM EDTA, 5 mM dithiothreitol, and 1 mM 1,10-phenanthroline (guinea pig, adult rat, adult mouse, and adult human brain) in the presence of ^{125}I-neurotensin (0.05–0.10 nM) and various concentrations of protein (0.01–0.30 mg per tube). Total, nonspecific, and specific binding was measured at equilibrium by the filtration technique as described (19, 21). Binding experiments with rat mesencephalic neurons (500,000 cells per well) were carried out at 37°C as reported (20).

Autoradiographic Studies. Coronal sections (20 μm thick) from guinea pig midbrain were incubated with ^{125}I-neurotensin and processed for film autoradiography as reported for rat brain sections (24).

Superfusion Experiments. Striatal slices from male guinea pig (350 μm) were preincubated 30 min with 120 nM [^{3}H]dopamine in Krebs buffer containing 1 μM pargyline, 1 mM ascorbic acid, and 0.1 μM desipramine, saturated with 5% CO_2 in O_2, and then superfused in a chamber at a rate of 0.5 ml/min with Krebs buffer containing bacitracin (40 mg/liter), 5 mM dithiothreitol, and 0.1 mM 1,10-phenanthroline. After a 45-min wash period, two 3-min fractions were collected to measure basal release. Neurotensin was introduced during the fifth collection period and was present until the end of the experiment. SR 48692 (0.1–10 nM) was added 6 min prior to neurotensin. Release of [^{3}H]dopamine was stimulated by superfusion for 3 min with buffer containing 20 mM K^+.

Intracellular Ca^{2+} Measurements. Subconfluent plated HT-29 cells were loaded for 90 min at 37°C with 5 μM indo-1 AM in complete culture medium. The cells were trypsinized, washed, and diluted in incubation medium (140 mM NaCl/5 mM KCl/0.9 mM $MgCl_2$/1.8 mM $CaCl_2$/5 mM glucose, pH 7.4) to about 50,000 cells per ml. Indo-1 fluorescence was assayed by flow cytometry using an ATC 3000 cell sorter (Odam-Brucker, Wissembourg, France). The ratio of indo-1 violet/blue fluorescence was calculated for each individual cell. Neurotensin was added 1 min after 1% (vol/vol) dimethyl sulfoxide (final concentration) or SR 48692, and the

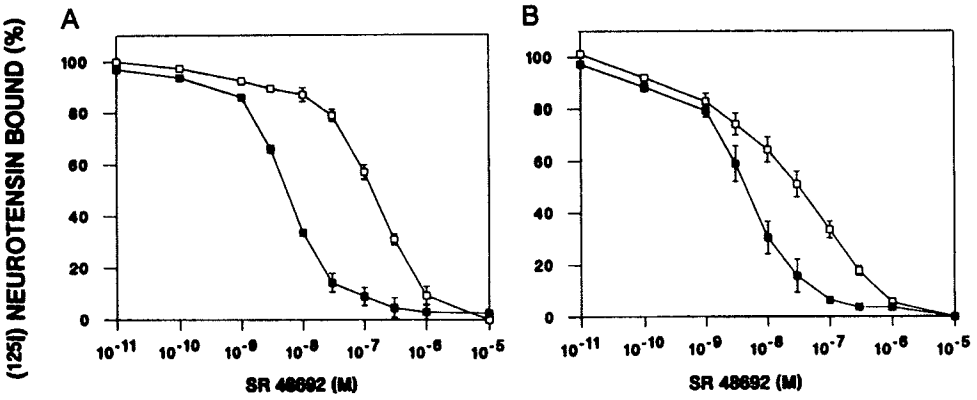

FIG. 1. Inhibition of ^{125}I-neurotensin-specific binding to adult rat brain membranes (*A*) and adult mouse brain membranes (*B*) by SR 48692. Each value is represented as the mean ± SE of three determinations in the absence (□) and in the presence (■) of 10^{-5} M levocabastine. In some cases, the SE values were smaller than the corresponding symbols.

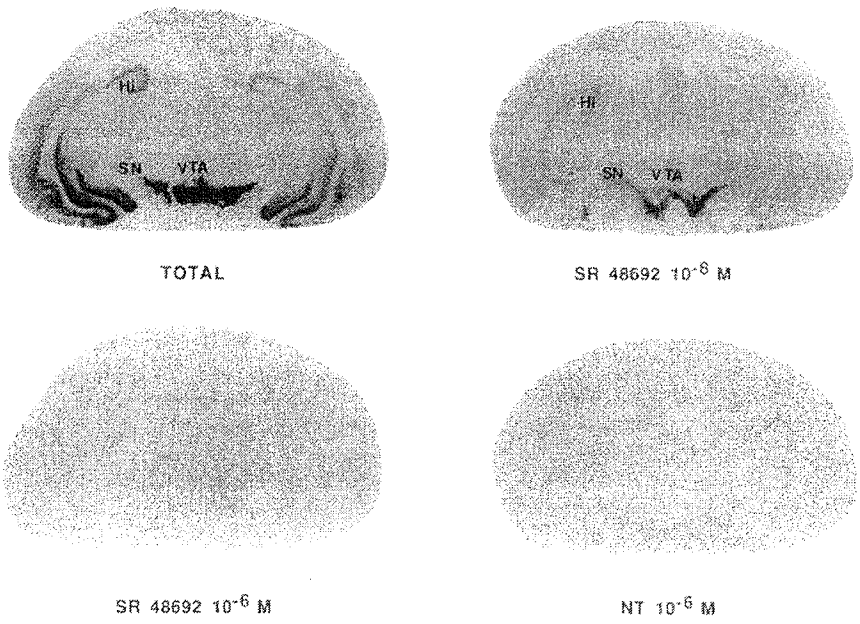

FIG. 2. SR 48692 antagonism of ^{125}I-neurotensin labeling on coronal sections from guinea pig midbrain. ^{125}I-Neurotensin (0.1 nM) was incubated in the absence (TOTAL) or in the presence of two concentrations of SR 48692 (10^{-8} and 10^{-6} M) or with unlabeled neurotensin (NT; 10^{-6} M). A light labeling is still visible in both the substantia nigra and ventral tegmental area in the presence of unlabeled neurotensin, whereas labeling has totally disappeared in the presence of the same concentration of SR 48692. SN, substantia nigra; VTA, ventral tegmental area; Hi, hippocampus.

maximal neurotensin-induced increase in the fluorescence ratio was determined.

Turning Behavior in Mice. Turning behavior induced by unilateral intrastriatal neurotensin injection (10 pg in 1 μl) was performed in conscious, female CD1 mice (Charles River Breeding Laboratories) according to Worms *et al.* (25). The number of complete contralateral rotations was visually recorded and accumulated over three periods of 2 min (3–5, 6–8, and 9–11 min) postinjection. SR 48692 (20, 40, and 80 μg/kg) was administered i.p. or orally (p.o.) 30 and 60 min before intrastriatal injection, respectively. In addition, a time-course study was performed with SR 48692 at 80 μg/kg (p.o.).

RESULTS

Binding Studies. SR 48692 totally inhibited the specific binding of ^{125}I-neurotensin to homogenates from adult guinea pig brain, rat mesencephalic cells, COS-7 cells transfected with the cDNA coding for the high-affinity rat brain neurotensin receptor, newborn mouse brain, newborn and adult human brains, and human colon carcinoma HT-29 cells. In these various models, SR 48692 exhibited IC_{50} values (means ± SE) ranging between 0.99 ± 0.14 nM (adult guinea pig brain membranes) and 30.3 ± 1.5 nM (HT-29 cell membranes), with Hill coefficients close to unity (Table 1). However, SR 48692 inhibited the specific binding of ^{125}I-neurotensin in adult rat brain and adult mouse brain with higher IC_{50} values (82.0 ± 7.4 and 34.8 ± 8.3 nM, respectively) and lower Hill coefficients (0.67 ± 0.09 and 0.51 ± 0.08), which are consistent with the recognition by SR 48692 of both high- and low-affinity sites in the adult rat and mouse brains. In the presence of 10 μM levocabastine, which recognizes only the low-affinity neurotensin sites, the IC_{50} obtained with SR 48692 in rat and mouse brain were much lower (5.0 ± 1.5 and 5.7 ± 1.5 nM, respectively), and Hill coefficients were close to unity, which indicates that this compound is more potent on the high-affinity than on the low-affinity binding sites in adult murine brains (Fig. 1). The high degree of selectivity of SR 48692 for neurotensin receptors was demonstrated by its lack of activity in several binding assays with nonpeptide (dopamine D_1 and D_2, α_1- and α_2-adrenergic, serotonin 5-HT_2, muscarinic M_1 and M_2, histamine H_1, and μ, δ, κ, and σ opiate receptors) and peptide (cholecystokinin A and B, [Arg^8]vasopressin, bradykinin, neuropeptide Y, and neurokinin 1 and 2) ligands (data not shown).

Autoradiographic Studies. Data presented in Fig. 2 show a high labeling of both substantia nigra pars compacta and ventral tegmental area by ^{125}I-neurotensin in the guinea pig brain. In the pars reticulata of the substantia nigra, several labeled processes seemed to radiate from cells in the pars compacta. Similar to what was observed in the rat (24), the most internal layers of the cortex, the cortical nucleus of the

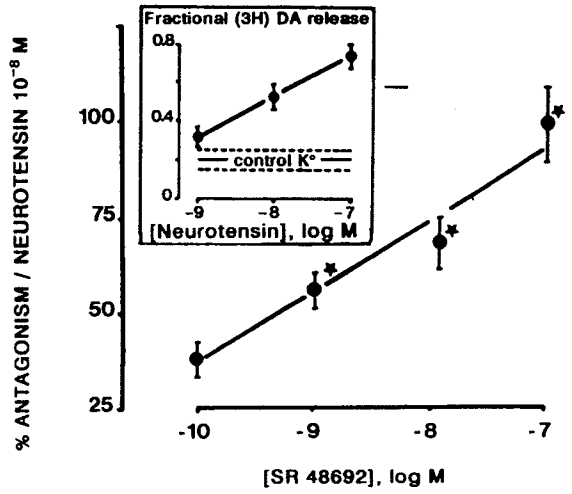

FIG. 3. SR 48692 antagonism of the stimulation by neurotensin of K^+-evoked release of [^{3}H]dopamine from striatal guinea pig slices. Results, expressed as percent inhibition of neurotensin effect, were the mean ± SE from three experiments performed in triplicate. (★, $P < 0.05$ vs. neurotensin group; Dunnett's test). (*Inset*) Dose–response curve for the neurotensin effect on 20 mM K^+-stimulated release of [^{3}H]dopamine. Dopamine release was expressed as percent of radioactivity present in the superfusion medium.

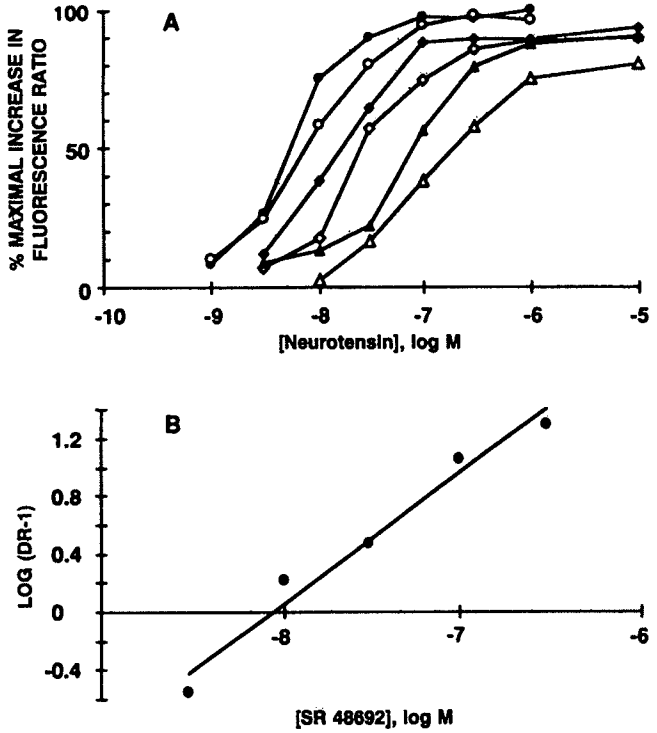

FIG. 4. Antagonism by SR 48692 of the neurotensin-induced calcium mobilization in HT-29 cells. (*A*) Concentration–response curves for neurotensin-induced calcium increase in HT-29 cells in the absence (●) or presence of SR 48692 at 3 (○), 10 (◆), 30 (◇), 100 (▲), and 300 nM (△). The results are expressed as the percent of the maximal increase over the basal fluorescence ratio induced by neurotensin. (*B*) Corresponding Schild plot for the antagonistic effect of SR 48692. The data are from a typical experiment. DR-1, dose ratio minus one.

amygdala as well as the pyramidal layer of the hippocampal formation and the granular cells of the dentate gyrus, mainly in its ventral portion, showed high densities of neurotensin binding sites. The addition of increasing concentrations of SR 48692 produced dramatic decreases in the density of the ^{125}I-neurotensin labeling in all structures. Incubation with either neurotensin or SR 48692 (1 μM) resulted in the complete loss of the labeling and, in contrast to what was observed with unlabeled neurotensin at the same concentration, autoradiograms are almost indiscernible from the film background (Fig. 2).

Stimulation of the K$^+$-Evoked Release of [^{3}H]Dopamine from Guinea Pig Striatal Slices. Addition of 1–100 nM neurotensin to the superfusion medium caused an enhancement of the K$^+$-stimulated (but not basal) release of [^{3}H]dopamine (Fig. 3 *Inset*). The stimulatory effect (132.7% ± 15.4%; mean ± SE) produced by 10 nM neurotensin was dose-dependently counteracted by SR 48692 (IC_{50} = 0.46 ± 0.02 nM; Fig. 4). Up to 100 nM SR 48692 did not significantly affect the spontaneous and K$^+$-evoked release of [^{3}H]dopamine by itself, indicating a lack of agonistic activity of the compound (data not shown).

Ca^{2+} Mobilization in HT-29 Cells. As previously reported (21, 26), neurotensin induced a concentration-dependent mobilization of Ca^{2+} in HT-29 cells. Increasing concentrations of SR 48692 produced parallel rightward shifts of the neurotensin dose–response curve (Fig. 4*A*). In the course of three experiments, EC_{50} values for neurotensin were 4.8 ± 0.7, 6.9 ± 0.9, 11.3 ± 2.2, 21.7 ± 0.3, 58.3 ± 4.4, and 140 ± 20 (mean ± SE in nM) in the absence and presence of 3, 10, 30, 100, and 300 nM SR 48692, respectively. Schild plot analysis of the data such as those shown in Fig. 4*B* yielded pA_2 ($-\log K_{app}$) and K_i values for SR 48692 of 8.13 ± 0.03 and 7.4 ± 0.6 nM, respectively, with a slope of 0.91 ± 0.07.

Turning Behavior. The mean number of contralateral rotations induced by 10 pg of intrastriatal injection of neurotensin was 13.1 ± 1.9. These rotations were found to be insensitive to spiroperidol and 6-hydroxydopamine lesions (data not shown). SR 48692 administered i.p. or p.o. reduced the neurotensin-induced turning; 80% antagonism was observed at 80 μg/kg (Fig. 5 *Inset*). The time-course study performed with SR 48692 at 80 μg/kg (p.o.) revealed a significant effect (−35%) as soon as 30 min after injection; maximal antagonism (−85%) was observed between 1 and 2 hr postinjection. Furthermore, SR 48692 did not reduce cholecystokinin-induced turning even at high concentrations (data not shown), indicating that the antagonistic effect of this compound was specific to neurotensin.

DISCUSSION

In the present study, we describe and characterize a potent and selective nonpeptide neurotensin antagonist: SR 48692. This compound potently inhibited ^{125}I-neurotensin binding in models in which only high-affinity neurotensin receptors are

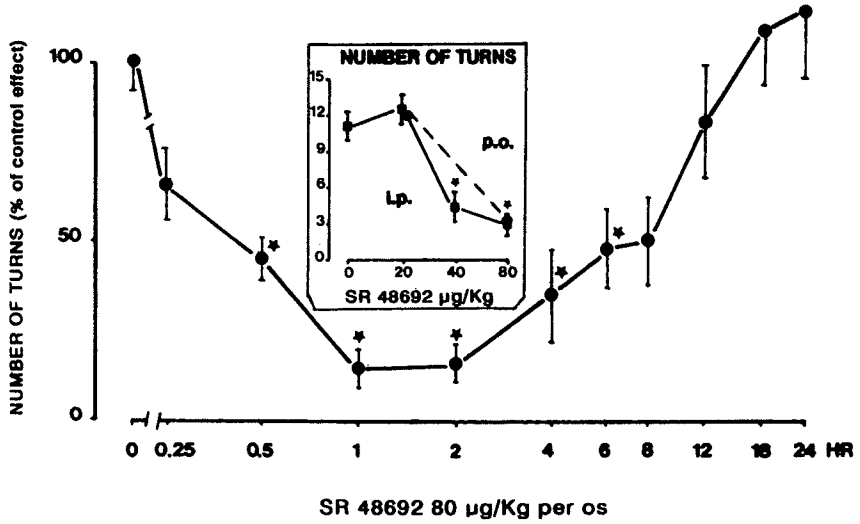

FIG. 5. Antagonism by SR 48692 of the turning behavior induced by intrastriatal injection of neurotensin (10 pg per mouse, 12 mice per group): dose–effect relationship (*Inset*) and time-course study after oral administration. Data are the mean ± SE (Dunnett's t-test; ⋆, $P < 0.05$).

present such as newborn mouse and human brain (27, 28), HT-29 cells (21), rat mesencephalic neurons (20), and COS-7 cells transfected with the cloned high-affinity rat brain receptor (18). SR 48692 also potently inhibited ^{125}I-neurotensin binding to the high-affinity binding sites in adult rat and mouse brain homogenates, whereas it was much less potent at the low-affinity, levocabastine-sensitive binding sites that are also present in these preparations (16). The IC_{50} of SR 48692 for binding to adult rat brain homogenates in the presence of levocabastine was similar to that for binding to the cloned high-affinity rat brain receptor. Finally, SR 48692 was even more potent than unlabeled neurotensin in binding to guinea pig brain tissues as shown by both radioreceptor assay and autoradiographic techniques.

Consistent with the existence of neurotensin binding sites on terminals of the nigrostriatal dopaminergic pathway (29, 30), neurotensin was shown to promote an increase in K^+-evoked release of [^{3}H]dopamine from rat, cat, and rabbit striatal slices (31–33). This observation was extended here to guinea pig striatal slices. SR 48692 was without effect on basal and K^+-evoked dopamine release, but completely antagonized the effect of neurotensin on K^+-stimulated dopamine release with a potency similar to its affinity for guinea pig brain receptors.

Neurotensin has previously been reported to stimulate Ca^{2+} mobilization through an increase in inositol phosphates in the human colon carcinoma HT-29 cell line (21, 26). Binding experiments and intracellular Ca^{2+} measurements showed that SR 48692 acted as a potent and full competitive antagonist of the neurotensin-induced Ca^{2+} response in this system.

Evidence suggests that neurotensin receptors located postsynaptically to, rather than on, dopamine neurons may be involved in some behavioral changes produced by central injection of neurotensin (34, 35). In a well-defined cholecystokinin model (25), we found that unilateral injection of neurotensin into the striatum of unrestrained mice produced dopamine-independent circling behavior. SR 48692 (80 μg/kg i.p. or p.o.) was able to antagonize this effect of neurotensin. These data demonstrate that SR 48692 has a good oral bioavailability and strongly support the conclusion that the antagonist can cross the blood–brain barrier.

In summary SR 48692, a nonpeptide antagonist of neurotensin receptor may be very useful in experiments to design the physiological and putative pathological roles of neurotensin.

We thank Nicole Zsurger and Antoine Coquerel for the gift of newborn human brain tissue, Shigetada Nakanishi for the gift of the rat brain neurotensin receptor cDNA, Dariush Farahifar for his help in cytometry experiments, Micheline Vial for her help in autoradiographic studies, and Anne-Marie Lhiaubet for the radiolabeled ligand preparation.

1. Carraway, R. E. & Leeman, S. E. (1973) *J. Biol. Chem.* **248,** 6854–6861.
2. Carraway, R. E. & Leeman, S. E. (1976) *J. Biol. Chem.* **251,** 7045–7052.
3. Emson, P. C., Goedert, M. & Mantyh, P. W. (1985) in *Handbook of Chemical Neuroanatomy: Vol. 4, GABA and Neuropeptides in the CNS*, Pt. 1, eds. Bjorklund, A. & Hökfelt, T. (Elsevier, Amsterdam), pp. 355–405.
4. Rosell, S. & Rökaeus, A. (1981) *Clin. Physiol.* **1,** 3–21.
5. Elliott, P. J. & Nemeroff, C. B. (1986) in *Neural and Endocrine Peptides and Receptors*, ed. Moody, T. W. (Plenum, New York), pp. 219–245.
6. Nemeroff, C. B. (1986) *Psychoneuroendocrinology* **11,** 15–37.
7. Kitabgi, P. (1989) *Neurochem. Int.* **14,** 111–119.
8. Ferris, C. F., Pan, J. X., Singer, E. A., Boyd, N. D., Carraway, R. E. & Leeman, S. E. (1984) *Neuroendocrinology* **38,** 145–151.
9. Alexander, M. J., Mahoney, P. D., Ferris, C. G., Carraway, R. E. & Leeman, S. E. (1989) *Endocrinology* **124,** 783–788.
10. Bissette, G., Nemeroff, C. B., Loosen, P. T., Prange, A. J., Jr., & Lipton, M. A. (1976) *Nature (London)* **262,** 607–609.
11. Clineschmidt, B. V., McGuffink, J. C. & Bunting, P. B. (1979) *Eur. J. Pharmacol.* **54,** 129–139.
12. Allescher, H. D. & Ahmad, S. (1991) in *Neuropeptide Function in the Gastrointestinal Tract*, ed. Daniel, E. E. (CRC, Boca Raton, FL), pp. 309–400.
13. Rioux, F., Kérouac, R., Quirion, R. & St.-Pierre, S. (1982) *Ann. N.Y. Acad. Sci.* **400,** 56–74.
14. Kitabgi, P., Checler, F., Mazella, J. & Vincent, J. P. (1985) *Rev. Clin. Basic Pharmacol.* **5,** 397–486.
15. Schotte, A., Leysen, J. E. & Laduron, P. M. (1986) *Naunyn-Schmiedeberg's Arch. Pharmacol.* **333,** 400–405.
16. Kitabgi, P., Rostène, W., Dussaillant, M., Schotte, A., Laduron, P. & Vincent, J. P. (1987) *Eur. J. Pharmacol.* **140,** 285–293.
17. Kostka, P. (1991) in *Neuropeptide Function in the Gastrointestinal Tract*, ed. Daniel, E. E. (CRC, Boca Raton, FL), pp. 249–271.
18. Tanaka, K., Masu, M. & Nakanishi, S. (1990) *Neuron* **4,** 847–854.
19. Sadoul, J. L., Mazella, J., Amar, S., Kitabgi, P. & Vincent, J. P. (1984) *Biochem. Biophys. Res. Commun.* **120,** 812–819.
20. Dana, C., Pelaprat, P., Vial, M., Brouard, A., Lhiaubet, A. M. & Rostène, W. (1991) *Dev. Brain Res.* **61,** 259–264.
21. Bozou, J. C., Rochet, N., Magnaldo, I., Vincent, J. P. & Kitabgi, P. (1989) *Biochem. J.* **264,** 871–878.
22. Luthman, H. & Magnusson, G. (1983) *Nucleic Acids Res.* **11,** 1295–1308.
23. Lugrin, D., Vecchini, F., Doulut, S., Rodriguez, M., Martinez, J. & Kitabgi, P. (1991) *Eur. J. Pharmacol.* **205,** 191–198.
24. Moyse, E., Rostène, W., Vial, M., Leonard, K., Mazella, J., Kitabgi, P., Vincent, J. P. & Beaudet, A. (1987) *Neuroscience* **22,** 525–536.
25. Worms, P., Gueudet, C. & Bizière, K. (1986) *Life Sci.* **39,** 2199–2208.
26. Turner, J., James-Kracke, M. R. & Camden, J. M. (1990) *J. Pharmacol. Exp. Ther.* **253,** 1049–1056.
27. Mazella, J., Chabry, J., Zsurger, N. & Vincent, J. P. (1989) *J. Biol. Chem.* **264,** 5559–5563.
28. Zsurger, N., Chabry, J., Coquerel, A. & Vincent, J. P. (1992) *Brain Res.* **586,** 303–310.
29. Quirion, R., Chiueh, C. C., Everist, H. D. & Pert, A. (1985) *Brain Res.* **327,** 385–389.
30. Herve, D., Tassin, J. P., Studler, J. M., Dana, C., Kitabgi, P., Vincent, J. P., Glowinski, J. & Rostène, W. (1986) *Proc. Natl. Acad. Sci. USA* **83,** 6203–6207.
31. De Quidt, M. E. & Emson, P. C. (1983) *Brain Res.* **274,** 376–380.
32. Battaini, F., Govoni, S., Di Giovine, S. & Trabuchi, M. (1986) *Naunyn-Schmiedeberg's Arch. Pharmacol.* **332,** 267–270.
33. Markstein, R. & Emson, P. (1988) *Eur. J. Pharmacol.* **152,** 147–152.
34. Kasckow, J. & Nemeroff, C. B. (1991) *Regul. Pept.* **36,** 153–164.
35. Rivest, R. & Masden, C. A. (1992) *Neuroscience* **47,** 341–349.

European Journal of Pharmacology, 140 (1987) 285–293
Elsevier

EJP 00877

Two populations of neurotensin binding sites in murine brain: discrimination by the antihistamine levocabastine reveals markedly different radioautographic distribution

Patrick Kitabgi [1,*], William Rostène [2], Monique Dussaillant [2], Alain Schotte [3], Pierre M. Laduron [4] and Jean-Pierre Vincent [1]

[1] *Centre de Biochimie du CNRS, Université de Nice, Faculté des Sciences, Parc Valrose, 06034 Nice Cédex, France,* [2] *Unité INSERM U 55, Hôpital St. Antoine, 75571 Paris Cédex 12, France,* [3] *Janssen Pharmaceutica, B-2340 Beerse, Belgium, and* [4] *Centre de Recherche Rhône Poulenc, BP 14, 94403 Vitry/Seine Cédex, France*

Received 2 March 1987, revised MS received 21 April 1987, accepted 26 May 1987

Monoiodo-[^{125}I-Tyr^3]neurotensin (NT) bound to a high affinity, low capacity binding component and a lower affinity, high capacity component in rat brain synaptic membranes. The antihistamine H_1 agent levocabastine, which bears no structural relationship to NT, selectively and totally inhibited NT binding to its low affinity binding sites. The IC_{50} for levocabastine was 7 nM. Lowering the temperature of the binding assay from 25 to 4°C markedly reduced the affinity of the high affinity NT binding site but did not affect the ability of levocabastine to discriminate between high and low affinity NT binding sites in rat brain membranes and tissue sections. Radioautographic studies of [^{125}I-Tyr^3]NT binding to rat brain tissue sections in the absence and presence of levocabastine revealed markedly different regional distributions of the two NT binding components. The levocabastine-sensitive NT binding site was present in membranes from rat and mouse brain but absent from rabbit brain membranes and from human brain tissue sections. It was also absent from mouse neuroblastoma N1E115 and human colonic adenocarcinoma HT29 cell membranes, two cell lines which have previously been shown to possess NT receptors functionally coupled to intracellular second messenger-generating systems. These findings are discussed in the light of the known properties of the high and low affinity NT binding sites in rat brain.

[^{125}I-Tyr^3]neurotensin binding; Radioautography; Levocabastine; H_1 histamine receptor; Brain; (Rat)

1. Introduction

Neurotensin (NT), a brain and gut tridecapeptide, fulfills all the major criteria that classify it as a neurotransmitter in the central nervous system (Elliott and Nemeroff, 1986). The demonstration that brain tissues contain specific NT receptors is central to this concept (Kitabgi et al., 1977; Uhl et al., 1977). In the past 10 years, there have been numerous radioreceptorassay and radioautographic studies on the pharmacological and biochemical properties and on the regional distribution of NT receptors in brain from various species including man (see Kitabgi et al., 1985 for review).

The recent development of radioiodinated NT ligands with high specific radioactivity, i.e. monoiodo-[^{125}I-Tyr^3,Trp^{11}]NT and monoiodo-[^{125}I-Tyr^3]NT has made it possible to detect in rat brain membranes two components of specific NT binding, a high affinity, low capacity, and a lower affinity, high capacity component (Mazella et al., 1983; Sadoul et al., 1984b). Both components were quite similar with respect to their structural requirements toward a variety of NT analogues (Mazella et al., 1983; Kitabgi et al., 1985). The only difference reported so far for these two popu-

* To whom all correspondence should be addressed.

lations of NT binding sites, apart from their affinity and binding capacity, was the greater sensitivity of the high affinity NT binding component to mono- and divalent cations and to guanyl nucleotides (Kitabgi and Vincent, 1986).

This high affinity, low capacity component had previously escaped detection with [^{3}H]NT as a ligand because of the relatively low specific radioactivity of this radiolabeled molecule (Kitabgi et al., 1977). However, it was recently reported that the potent antihistamine drug levocabastine was able to distinguish two components of [^{3}H]NT binding in rat brain membranes (Schotte et al., 1986). One component was displaced by submicromolar concentrations of levocabastine whereas the other component was insensitive to the drug. Obviously, it would be of great interest to know whether the levocabastine-sensitive and -insensitive [^{3}H]NT binding components bear any relation to the high and low affinity binding sites detected with radioiodinated NT. If so, levocabastine could represent a useful pharmacological tool for discriminating between high and low affinity NT binding sites and for characterizing further the properties of these two populations of sites. More generally, agents or conditions that would differentially affect high and low affinity NT binding sites, should prove useful in this regard.

The present study describes the effects of levocabastine and temperature on the binding of monoiodo-[^{125}I-Tyr^3]NT to rat brain membranes. It is shown that both agents affect NT binding to its high and low affinity binding sites differentially. The discriminative property of levocabastine toward the two populations of NT binding sites made it possible to compare their anatomical distribution in rat brain tissue sections by means of radioautographic techniques. Finally the effect of levocabastine on NT binding was investigated in brain tissues from various species including man and in cell lines that possess NT receptors.

2. Materials and methods

2.1. Drugs and peptides

Unlabeled NT was purchased from Peninsula Laboratories (California). Monoiodo-[^{125}I-Tyr^3]NT was prepared at a specific radioactivity of 2000 Ci/mmol as previously described (Sadoul et al., 1984b). Monoiodo-[Tyr^3]NT has been shown to behave identically to unlabeled NT in a variety of biological and binding assays, including radioreceptor assays with rat brain membranes (Sadoul et al., 1984b). Levocabastine (R 50547) (fig. 1), a novel potent histamine (H_1) antagonist, was from Janssen Pharmaceutica (Beerse, Belgium). All other reagents were of the best commercially available grade.

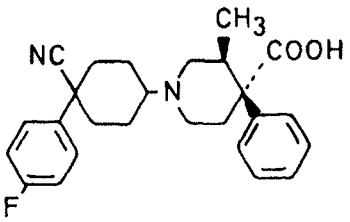

Fig. 1. Chemical structure of levocabastine.

2.2. Binding studies with rat brain membranes

Purified rat brain synaptic membranes from adult male rats were prepared according to Jones and Matus (1974) and incubated (0.3-0.4 mg/ml of protein) at equilibrium for 20 min at 25°C or 40 min at 4°C with [^{125}I-Tyr^3]NT and, when needed, with unlabeled NT and levocabastine in a final volume of 250 μl of 50 mM Tris HCl buffer pH 7.5 containing 0.2% bovine serum albumin. Bound (B) NT was separated from free (F) by filtration as previously described (Mazella et al., 1983). The saturation experiments at 25°C from which Scatchard plots were derived were performed by incubating four concentrations of [^{125}I-Tyr^3]NT ranging from 10 to 100 pM then by adding increasing concentrations of unlabeled NT ranging from 0.05 to 25 nM to the highest concentration (100 pM) of labeled peptide. Nonspecific binding for each concentration of radioligand was evaluated in separate incubations in the presence of an excess (1 μM) of unlabeled NT and was subtracted from total binding in order to obtain the specific binding. Saturation experiments at 4°C were performed similarly except that all concentrations of labeled and unlabeled NT were doubled. In competition experiments

with levocabastine, the concentration of labeled NT was 0.1 and 0.2 nM at 25 and 4°C, respectively. Curvilinear Scatchard plots were interpreted as indicating the existence of two populations of NT binding sites and were fitted by computer in order to obtain values for the binding parameters (dissociation constant K_d and maximal binding capacity B_m) for each class of sites (Mazella et al., 1983). For a given concentration of free ligand (L), the proportion p of bound NT associated with the high affinity binding sites could be calculated according to the relation

$$P = \frac{\frac{1}{K_{dh}+L}}{\frac{1}{K_{dh}+L} + \frac{B_{ml}/B_{mh}}{K_{dl}+L}} \quad \text{equation 1}$$

where (h) and (l) designate the binding parameters of the high and low affinity NT binding components, respectively. Linear Scatchard plots were fitted by linear regression analysis.

2.3. Binding studies with rat brain tissue sections

Coronal sections (thickness 20 μm) were cut from frozen adult male rat brains and processed for [^{125}I-Tyr^3]NT binding as previously described (Moyse et al., in press). Briefly, slide-mounted tissue sections were incubated at 4°C for 60 min with 0.1 nM monoiodo-[^{125}I-Tyr^3]NT, without or with 1 μM levocabastine in 50 mM Tris HCl buffer pH 7.5 containing 5 mM $MgCl_2$, 0.2% bovine serum albumin, 500 μM orthophenanthrolin and 50 μM bacitracin. Additional sections were incubated in the presence of 0.1 μM unlabeled NT for determination of non-specific binding. After incubation, the sections were washed for 8 min at 4°C in four consecutive baths containing 40 mM Tris HCl buffer, pH 7.4.

Film radioautograms were obtained by apposition of the sections to ^{3}H-Ultrofilm (LKB, France) for 3 weeks at room temperature in the dark. After development, quantitative optical density measurements were obtained and converted to femtomoles of NT bound per mg protein as described (Rostène and Mourre, 1985).

In some experiments, the binding of [^{125}I-Tyr^3]NT to tissue sections was measured at 25°C after a 30 min incubation in the presence of varying concentrations of labeled and unlabeled NT. Radioactivity measurements were performed by wiping off the sections from the slides with Schleicher and Schüll filters which were placed in plastic tubes and counted in a gamma counter (Rostène et al., 1986). Scatchard plots were analyzed as described above for brain membranes.

2.4. Binding studies with other tissues

Rabbit brain synaptic membranes were prepared as described above for rat brain membranes. The mouse brain particulate fraction was prepared as previously described for human brain (Sadoul et al., 1984b). Particulate fractions from neuroblastoma N1E115 cells and human colonic HT29 cells were prepared as previously reported (Bozou et al., 1985). Binding to human brain sections was obtained as previously described (Sadoul et al., 1984a). Binding experiments and Scatchard analysis were performed as described above for rat brain membranes.

3. Results

3.1. Effect of levocabastine on [^{125}I-Tyr^3]NT binding to rat brain membranes at 25°C

As mentioned in the Introduction, purified rat brain synaptic membranes have been shown to contain two classes of NT binding sites which differ in their affinity and binding capacity. The K_d and B_m values for each class of sites were averaged from the Scatchard analysis of 14 experiments performed over a period of two years with [^{125}I-Tyr^3]NT as the radioligand. These mean values as well as their range are shown in table 1.

Figure 2 shows the Scatchard plot of a typical binding experiment performed at 25°C with [^{125}I-Tyr^3]NT and rat brain synaptic membranes in the absence and presence of levocabastine. As expected, the Scatchard plot obtained in the absence of the drug was curvilinear and yielded binding parameters for the high and low affinity NT binding components (table 1) well within the normal range. A striking result is that in the presence of 1

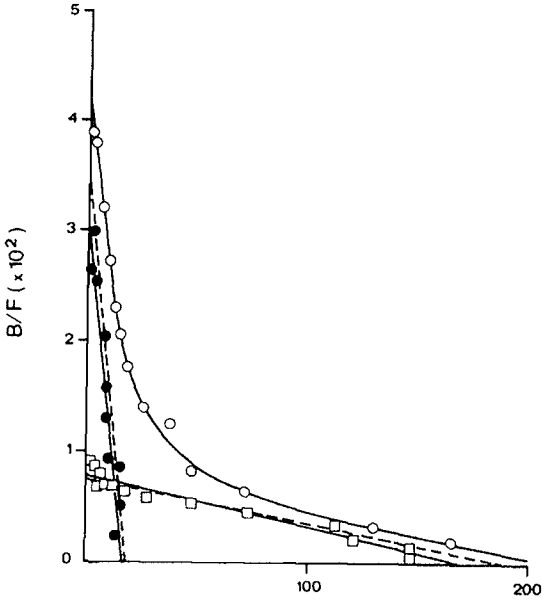

Fig. 2. Scatchard analysis of [^{125}I-Tyr^3]NT binding to rat brain synaptic membranes at 25° C in the absence (○) and presence (●) of 1 μM levocabastine, and at 4° C in the absence of levocabastine (□). The dashed lines represent the theoretical Scatchard plots of high and low affinity NT binding at 25° C in the absence of levocabastine. Points are from a typical experiment and are the means from triplicate determinations.

μM levocabastine, the Scatchard plot was linear and, moreover, virtually superimposed with the theoretical plot representing the high affinity component of [^{125}I-Tyr^3]NT binding (fig. 2). It was consistent with this that the binding parameters obtained in the presence of levocabastine were almost identical to those of the high affinity NT binding sites in the control experiment (table 1).

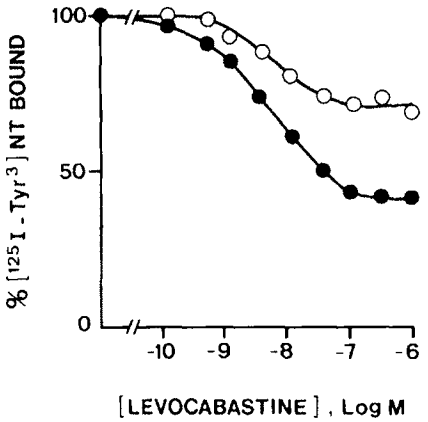

Fig. 3. Effect of increasing concentrations of levocabastine in inhibiting 0.1 nM [^{125}I-Tyr^3]NT specific binding to rat brain synaptic membranes at 25° C (○) and at 4° C (●). Points are from a typical experiment and are the means from triplicate determinations.

These data demonstrate that levocabastine 1 μM can totally inhibit the binding of [^{125}I-Tyr^3]NT to its low affinity sites without affecting the binding to the high affinity sites.

The effect of increasing concentrations of levocabastine on the binding of 0.1 nM [^{125}I-Tyr^3]NT to rat brain membranes at 25° C is shown in fig. 3. The antihistamine drug inhibited NT binding in a concentration-dependent manner. However only a fraction (28%) of the binding was inhibited at maximally effective concentrations (0.1-1 μM). Calculation according to equation 1 and based on the binding parameters shown in table 1 indicated that at 0.1 nM labeled ligand, 77 and 23% of bound ligand will be on the average associated with the high and low affinity NT binding components, respectively (see Materials and methods for

TABLE 1

Binding parameters of [^{125}I-Tyr^3]NT binding to rat brain synaptic membranes at 25° C in the absence or presence of levocabastine. Parameters were derived from Scatchard analysis of binding experiments such as that shown in fig. 2. Values are the means ± S.E.M. of n experiments. 'Range' represents the lowest and highest values obtained for each parameter in 14 experiments. h and l refer to the high and low affinity NT binding sites respectively.

Parameter	Mean values (n = 14)	Range	Control (n = 3)	Levocabastine, 1 μM (n = 3)
K_{dh}, nM	0.15 ± 0.02	0.06 – 0.29	0.16 ± 0.01	0.17 ± 0.015
B_{mh}, fmol/mg	15.5 ± 1.1	8.6 – 22	16.7 ± 1.9	16.6 ± 3.5
K_{dl}, nM	7.2 ± 0.9	3.4 – 16	6.1 ± 1.1	–
B_{ml}, fmol/mg	135.7 ± 11.6	97 – 212	191.0 ± 11.8	–

the details of the calculation). These results are consistent with an interaction of levocabastine exclusively with the low affinity NT binding component. The IC_{50} value for levocabastine in inhibiting [^{125}I-Tyr^3]NT binding to the low affinity sites was 7 ± 0.8 nM (n = 3).

3.2. Effect of temperature on [^{125}I-Tyr^3]NT binding to rat brain membranes and tissue sections

Figure 2 illustrates a typical Scatchard plot of [^{125}I-Tyr^3]NT binding to rat brain membranes at 4°C and compares it to that obtained at 25°C. It is striking that the plot was essentially linear and looked as though the high affinity binding component of NT was no longer detectable at 4°C. Linear regression analysis of data derived from three experiments at 4°C and similar to that shown in fig. 2 yielded a K_d value of 7.1 ± 0.8 nM and a B_m value of 154.7 ± 9.7 fmol/mg protein. These values resembled closely those found for the low affinity component of NT binding at 25°C (table 1).

This result could mean either that high affinity NT binding sites were lost at 4°C or that their affinity decreased in such a way that they could not be distinguished from the low affinity sites by Scatchard analysis. Levocabastine was used to test these two possibilities. In the first case, levocabastine should have been able to totally inhibit [^{125}I-Tyr^3]NT binding, while in the second case there should have remained a levocabastine-insensitive component of [^{125}I-Tyr^3]NT binding. The results in fig. 3 show that the latter hypothesis was correct. Levocabastine inhibited in a concentration-dependent manner ($IC_{50} = 7 \pm 1$ nM, n = 3) the binding of 0.2 nM [^{125}I-Tyr^3]NT to rat brain synaptic membranes at 4°C. Although the antihistamine drug inhibited a larger fraction of binding at 4°C than at 25°C (fig. 3) there still remained a significant proportion (40%) that was insensitive to the drug. Assuming that this proportion represents the fraction of bound ligand associated with the high affinity NT binding sites and that high and low affinity sites are present in the same ratio in membranes at 25 and 4°C, an average K_d value of 1 nM could be calculated from equation 1 (see Materials and methods) for the high affinity sites at 4°C. This increase in K_d value (bringing it closer to that of the low affinity sites) together with a low binding capacity could account for the difficulty of detecting the high affinity (levocabastine insensitive) NT binding sites at 4°C by Scatchard analysis.

Previous studies of monoiodo-[^{125}I-Tyr^3]NT binding to rat brain tissue sections indicated that, at 4°C, the peptide apparently bound to one population of sites (linear Scatchard plot) with K_d and B_m values of 7.7 ± 0.3 nM and 74 ± 4 fmol/mg protein, respectively (Moyse et al., 1987). The Scatchard plots obtained when binding of [^{125}I-Tyr^3]NT to tissue sections was studied at 25°C were curvilinear (not shown). Computer analysis of the plots yielded K_d and B_m values (n = 2) of, respectively, 0.19 nM and 7.7 fmol/mg protein for the high affinity binding component, and 15.6 nM and 60 fmol/mg protein for the low affinity component. These results, which are similar to those obtained with brain membranes, indicate that rat brain tissue sections contain both high and low affinity NT binding sites and that the high affinity sites are no longer detectable by Scatchard analysis at 4°C.

3.3. Radioautographic studies

Figure 4 shows radioautograms of [^{125}I-Tyr^3]NT binding to rat midbrain sections incubated without or with 1 μM levocabastine. Table 2 presents quantitative radioautographic measurements of [^{125}I-Tyr^3]NT binding to sections made at different brain levels. The distribution pattern of NT binding sites in the absence of antihistamine agent (fig. 4A, table 2) was quite similar to that previously observed with [^{3}H]NT and [^{125}I-Tyr^3]NT (Young and Kuhar, 1981; Quirion et al., 1982; Moyse et al., 1987).

It is apparent that, in the presence of levocabastine, [^{125}I-Tyr^3]NT binding was decreased in wide brain areas including most of the cortex, the dorsal hippocampus, the thalamus and the globus pallidus (fig. 4B, table 2). In these brain areas, which display low to moderate levels of [^{125}I-Tyr^3]NT binding, levocabastine reduced the binding to almost background levels. A few discrete regions with higher levels of NT binding e.g. the

various layers of the superior colliculus showed a partial (about 50%) decrease in labeling intensity in the presence of levocabastine (fig. 4B; table 2). In contrast, NT labeling in discrete regions rich in NT binding sites such as the external plexiform layer of the olfactory bulbs, the rhinal sulcus, the posterior cortical amygdaloid nucleus, the ventral dentate gyrus, the substantia nigra and the ventral tegmental area was not affected by 1 μM levocabastine (fig. 4B, table 2).

3.4. Effect of levocabastine on [^{125}I-Tyr^3]NT binding in various species and cell lines

Scatchard analysis of NT binding to mouse brain membranes revealed two populations of sites, one with high and one with low affinity. The K_d values were 0.13 and 2.2 nM, and the respective B_m values were 85 and 160 fmol/mg protein (n = 2). Note the higher proportion of high affinity sites in mouse than in rat brain membranes. As in the rat brain membranes however, levocabastine 1 μM completely inhibited NT binding to the low affinity site without affecting binding to the high affinity site.

In contrast, rabbit brain membranes contained a single levocabastine-insensitive population of NT binding sites with K_d and B_m values of 0.5 nM and 107 fmol/mg protein, respectively.

A similar situation was found with membranes prepared form the mouse neuroblastoma N1E115 or the human colonic adenocarcinoma HT29 cell lines which both displayed a single population of high affinity NT binding sites (K_d values of 0.06

TABLE 2

Regional discribution of levocabastine-insensitive and -sensitive NT binding sites in rat brain.

Brain region	[^{125}I-Tyr^3]NT binding *		Brain region	[^{125}I-Tyr^3]NT binding *	
	Control	Levocabastine, 1 μM		Control	Levocabastine, 1 μM
Olfactory bulb			*Hippocampal formation*		
External plexiform layer	45.2 ± 2.6	51.4 ± 4.2	CA_1, pyramidal layer	7.3 ± 0.3	4.3 ± 0.2 [b]
			molecular layer	7.1 ± 0.7	3.8 ± 0.2 [b]
Cerebral cortex			CA_3, pyramidal layer	6.9 ± 0.5	5.9 ± 0.5
Prefrontal cortex	6.7 ± 0.9	4.7 ± 0.9	Dorsal subiculum	4.7 ± 0.3	2.1 ± 0.2 [b]
Frontoparietal cortex,			Dorsal dentate gyrus	8.7 ± 0.7	10.0 ± 0.9
layers I-II	6.7 ± 0.5	3.3 ± 0.3 [b]	Ventral dentate gyrus	68.9 ± 5.2	59.2 ± 5.2
layers III-IV	10.9 ± 1.0	3.1 ± 0.2 [b]			
layers V-VI	8.5 ± 0.7	3.3 ± 0.3 [b]	*Diencephalon*		
Parietal cortex,			Hypothalamus	10.2 ± 0.5	10.6 ± 0.9
layers I-II	7.3 ± 0.3	2.6 ± 0.2 [b]	Red thalamic nucleus	4.0 ± 0.3	2.8 ± 0.3 [a]
layers III-IV	7.8 ± 0.5	2.8 ± 0.2 [b]	Pretectal thalamic nucleus	12.6 ± 1.6	4.7 ± 1.6 [b]
layers V-VI	7.3 ± 0.3	2.9 ± 0.2 [b]	Lateral geniculate		
Temporal cortex,			thalamic nucleus	9.2 ± 0.7	3.8 ± 0.2 [b]
layers I-II	4.5 ± 0.5	2.9 ± 0.2 [b]			
layers III-IV	5.2 ± 0.5	2.9 ± 0.2 [b]	*Midbrain*		
layers V-VI	5.0 ± 0.3	2.9 ± 0.2 [b]	Substantia nigra,		
Cingulate cortex	84.3 ± 9.7	86.3 ± 7.6	pars compacta	100.0 ± 8.0	102.9 ± 0.7
Occipital cortex	8.0 ± 0.5	5.0 ± 0.5 [b]	pars reticulata	33.4 ± 3.6	28.4 ± 2.4
Rhinal sulcus	32.4 ± 3.6	26.8 ± 5.4	Ventral tegmental area	94.6 ± 8.0	102.4 ± 8.3
Retrosplenial cortex	25.3 ± 2.2	24.2 ± 2.9	Superior colliculus,		
			layer I	34.6 ± 2.4	19.2 ± 2.1 [b]
Basal ganglia			layer II	20.9 ± 1.4	10.4 ± 1.6 [b]
Caudate-putamen	18.9 ± 2.2	20.3 ± 1.4	layer III	39.6 ± 3.1	14.7 ± 1.9 [b]
Globus pallidus	5.0 ± 0.3	2.9 ± 0.5 [b]	Dorsal raphe	14.4 ± 1.7	12.6 ± 1.6
Nucleus accumbens	12.3 ± 0.9	12.6 ± 0.5			

* Binding was determined by densitometry on film radioautograms and is expressed relative to NT binding in the substantia nigra, pars compacta taken as 100. NT binding in this region was 9.7 ± 0.3 fmol/mg protein. Values are the means ± S.E.M. of 8 determinations and were compared by means of Student's t-test. [a] $P < 0.05$ and [b] $P < 0.01$ compared to control.

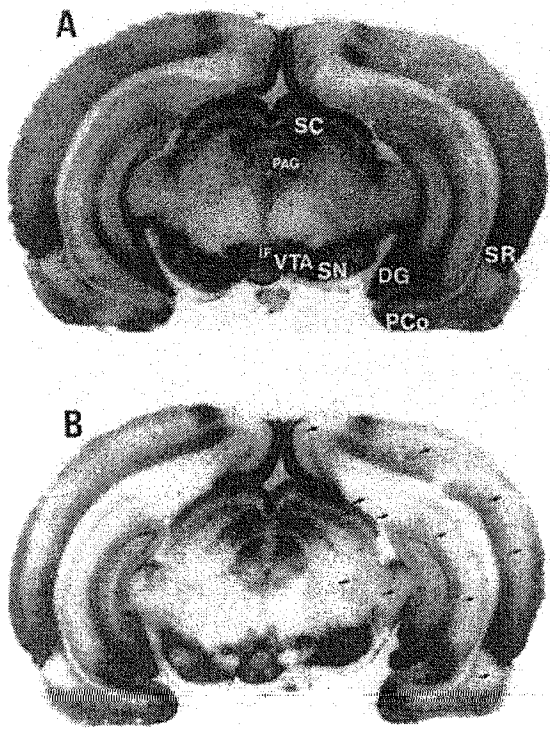

Fig. 4. Radioautographic distribution of [^{125}I-Tyr^3]NT binding in rat midbrain sections, (A) in the absence or (B) in the presence of 1 μM levocabastine. Arrows denote regions where NT binding was reduced by levocabastine. Abbreviations: DG, dentate gyrus; IF, interfascicularis nucleus; PAG, periaqueductal gray; PCo, posterior cortical amygdaloid nucleus; SC: superior colliculus; SN, substantia nigra; SR, rhinal sulcus; VTA, ventral tegmental area.

nM for N1E115 cells and 0.26 nM for HT29 cells) that were completely insensitive to 1 μM levocabastine. Both cell lines have been shown to respond to NT by an increase in intracellular inositol phosphate levels (Amar et al., 1986; Snider et al., 1986; Amar et al., in press). As expected, levocabastine had no effect on inositol phosphate levels in either cell line (not shown).

Finally, in sections from human post-mortem brains incubated at 4°C with 0.1 nM [^{125}I-Tyr^3]NT, 1 μM levocabastine had no significant effect on NT binding densities in various regions as evaluated by quantitative radioautography (not shown).

4. Discussion

The present study demonstrated clearly that the high and low affinity NT binding sites previously characterized in rat brain membranes with iodinated NT derivatives (Mazella et al., 1983; Sadoul et al., 1984b), correspond respectively to the levocabastine insensitive and sensitive [^{3}H]NT binding sites recently described (Schotte et al., 1986). We propose, for the rest of the Discussion, to designate site H the high affinity (levocabastine-insensitive) NT binding site, and site L the low affinity (levocabastine-sensitive) NT binding site.

It is remarkable that levocabastine does not affect [^{125}I-Tyr^3]NT binding to site H at concentrations at which it totally inhibits ligand binding to site L. Such a selectivity of levocabastine for one class of NT binding sites is in contrast with the previous finding that a variety of NT partial sequences and analogues displayed quite similar relative binding potencies for sites H and L in rat brain membranes (Mazella et al., 1983; Kitabgi et al., 1985). This and the fact that levocabastine, an H_1 antihistamine agent, has no structural similarity to NT (fig. 1), suggests that the drug is not a true competitive inhibitor of NT binding, but rather binds to a separate site that can modulate NT binding to site L. This site could belong either to the low affinity NT receptor molecule itself or to a levocabastine binding molecule present in its vicinity. Whatever the mechanism by which levocabastine selectively modulates NT binding to site L, the antihistamine agent represents a useful tool for discriminating between the two classes of NT binding sites in rat brain.

Other agents can differentially affect NT binding to sites H and L in rat brain. These include divalent cations such as Mg^{2+} and Mn^{2+} and guanyl nucleotides like GTP which respectively increase and decrease the affinity of NT for site H without affecting NT binding to site L (Kitabgi and Vincent, 1986). In the present study we show that low temperature also selectively decreased NT binding affinity for site H in rat brain membranes and tissue sections. This finding, together with the low binding capacity of site H, explains why the latter could not be distinguished from site

L by Scatchard analysis of binding experiments performed at 0-4°C with rat brain tissue sections (Young and Kuhar, 1981; Quirion et al., 1982; Moyse et al., in press). It is interesting that divalent cations, guanyl nucleotides and temperature all selectively affect NT binding to site H. Thus, levocabastine represents the only agent known so far that selectively modulates NT binding to site L. It should be noted that levocabastine inhibits [^{125}I-Tyr^3]NT binding to site L almost as potently as NT.

These exceptional features of levocabastine made it possible to compare the anatomical distribution of sites H and L in rat brain tissue sections with radioautographic techniques. Marked differences were observed. Site H was almost exclusively found in discrete brain regions that have been described in previous radioautographic studies as rich in NT receptor (Young and Kuhar, 1981; Quirion et al., 1982; Moyse et al., in press). In most cases, these brain areas were devoid of significant amounts of site L. Conversely, site L was distributed diffusely with a moderate density over wide brain areas including most of the cortex, the dorsal hippocampus and the thalamus. These regions did not seem to contain site H since levocabastine reduced NT binding to virtually background levels. Such a distribution of site L is compatible with the fact that rat brain tissues contain overall about tenfold higher amounts of site L than site H. In general, there seemed to be no overlap of sites H and L except in a few areas such as the superior colliculus. It should be noted that in brain areas rich in site H, small amounts of site L, 10% or less, may have escaped detection due to experimental uncertainty. These results confirm and extend at a better level of resolution those of a previous study on the distribution of levocabastine-sensitive [^{3}H]NT binding in dissected rat brain regions (Schotte et al., 1986). However, significant levels (30-45%) of levocabastine-sensitive [^{3}H]NT binding sites have been reported for brain regions that we now found to be devoid of site L such as the substantia nigra or the nucleus accumbens. This difference may have arisen from the difficulty of dissecting such small brain areas without taking surrounding tissues that could contain significant amounts of site L.

Site L was present in membranes from rat and mouse brain and, in contrast, was absent from rabbit brain membranes. Furthermore, levocabastine did not affect [^{125}I-Tyr^3]NT binding to human brain tissue sections. These results confirm and extend previous data (Schotte et al., 1986) showing that [^{3}H]NT binding in homogenates from guinea-pig, cat, dog and human brain was insensitive to levocabastine (Schotte et al., 1986). It should be noted however that in guinea-pig and human brain membranes, [^{125}I-Tyr^3]NT binds to two populations of sites that display binding parameters similar to those of rat brain membranes (Sadoul et al., 1984a,b). Such a species difference regarding the ability of levocabastine to inhibit NT binding to its low affinity site is in contrast with the finding that the antihistamine agent exhibits the same activity profile at peripheral and central H_1 histamine receptors in all the mammalian species tested including man (unpublished observations). Furthermore, the rank order of potency of levocabastine and its enantiomers to inhibit [^{3}H]NT binding in rat brain (Schotte et al., 1986) parallels closely that at the H_1 histamine receptor (unpublished data). These observations raise interesting questions regarding a possible relationship between the H_1 receptor and the levocabastine binding site through which the antihistamine drug inhibits NT binding to site L in murine species. The possibility remains, as for other species, that molecules different from levocabastine could modulate NT binding to its low affinity binding site. In any case, caution should be exerted before extrapolating to other species binding data obtained in the rat.

The present work does not directly address the question of the physiological relevance of the two types of NT binding sites described here. This problem could be better studied in biological systems which possess either type of site and to which a clear NT-induced cellular response could be assigned. Such is the case for site H which is present alone in the N1E115 and HT29 cell lines. The NT receptor in these cell lines has been shown to be coupled to an increase in intracellular levels in inositol phosphates (Amar et al., 1986; Snider et al., 1986; Amar et al., in press) and cGMP (Amar et al., 1985; Gilbert et al., 1986),

and t
(Bozo
lackir

[redacted]

DELFIA® Eu-labeled bombesin

AD0227 - 150 pmol
AD0228 - 600 pmol

For Research Use Only

INTENDED USE

This DELFIA® Eu-labeled bombesin is intended for use in ligand receptor binding assays.

INTRODUCTION

Bombesin is a 14 amino acid long peptide, isolated from the skin of the amphibian frog *Bombina bombina*. The mammalian homologues to bombesin consist of various forms of gastrin-releasing peptide and neuromedin B. So far, four subtypes of bombesin receptors have been cloned; BB1, BB2, BB3 and BB4. Upon receptor ligand binding, the receptor transmit extracellular signals across membranes by activating specific signal-transducing heterotrimeric G-proteins, which in turn regulate a variety of intracellular effectors. The mammalian bombesin-like peptides contribute to diverse biological functions in the central nervous system and peripheral tissues, which include e.g. thermoregulation, satiety, smooth muscle contraction, stimulation of pancreatic secretion and gastrointestinal hormone release.

DELFIA europium (Eu)-labeled bombesin is a synthetic peptide, similar to amphibian bombesin with a europium chelate coupled to the amino end of the peptide. The sequence of DELFIA Eu-labeled bombesin is Ac-Eu^{3+}-Ahx-PQRLGNQWAVGHLM-NH_2. DELFIA Eu-labeled bombesin binds with high affinity to mammalian BB1 and BB2 receptors and is a useful tool to study the function of these receptors.

PRODUCT USE

The DELFIA Eu-labeled bombesin binding assay is based on dissociation-enhanced time-resolved fluorescence. DELFIA Eu-labeled bombesin and the ligand specific receptor are incubated on an AcroWell[1] filter plate (when using e.g. membrane preparations or whole cells), on a coated plate (e.g. soluble receptors, membrane preparations or whole cells) or on a cell culture plate (e.g. adherent cells), after which unbound labeled ligand is removed. Eu is dissociated from the bound ligand by using DELFIA Enhancement Solution. Dissociated Eu creates highly fluorescent complexes, which are measured in a multilabel counter with TRF option.

During the development phase, the biological activity of the DELFIA Eu-labeled bombesin has been demonstrated on AcroWell filtration based assays.

DELFIA is a registered trademark of PerkinElmer, Inc.
[1] AcroWell is a trademark of Pall Corporation.

CONTENTS

Figures in parentheses refer to the 600 pmol package.

Component	Quantity	Storage
DELFIA Eu-labeled bombesin 150 pmol (600 pmol)	1 vial, lyophilized	+2 - +8°C

The lyophilized DELFIA Eu-labeled bombesin contains Tris-HCl buffered salt solution, bovine serum albumin (BSA) and Dextran T-40.

NOTE: The powder contains sodium azide (< 1 %) as preservative and it is harmful by inhalation, in contact with skin and if swallowed.

PREPARATION OF REAGENT

Reagent	Storage and reconstituted stability
DELFIA Eu-labeled bombesin	Keep the vial on ice. Stable for 5 days at +2 - +8°C. For longer periods, aliquot and store at -20°C. Avoid freezing and thawing. Stable for at least one month at -20°C.

Reconstitute the lyophilized DELFIA Eu-labeled bombesin by adding 150 µL (600 µL) of distilled water to yield a DELFIA Eu-labeled bombesin concentration of 1000 nmol/L and mix gently. Allow to stand for at least 30 minutes on ice before use to ensure that all solid material is dissolved.

NOTE: The powder contains sodium azide (< 1 %) as preservative and it is harmful by inhalation, in contact with skin and if swallowed. The dissolved ligand contains < 0.1 % sodium azide and is not considered harmful.

MATERIALS REQUIRED BUT NOT SUPPLIED WITH THE REAGENT

The DELFIA Eu-labeled bombesin filtration based assay requires the following items, which are available from PerkinElmer Life and Analytical Sciences or its distributors.

1. Time-resolved fluorometer, e.g. 2100 EnVision™, 1420 VICTOR™ or Fusion™ Multilabel Reader
2. Automatic shaker - DELFIA Plateshake (prod. no. 1296-003/004)

EnVision, VICTOR and Fusion are trademarks of PerkinElmer, Inc.

3. Pipette for dispensing the DELFIA Enhancement Solution - Eppendorf Multipette (prod. no. 1296-014) with 5 mL Combitips (prod. no. 1296-016) or alternatively the DELFIA Plate Dispense (prod. no. 1296-041)
4. DELFIA L*R binding buffer concentrate (10x) (prod. no. CR134-250)
5. DELFIA L*R wash concentrate (25x) (prod. no. CR135-250)
6. DELFIA Enhancement Solution (prod. no. 1244-104 for 50 mL; 1244-105 for 250 mL and 4001-0010 for 1000 mL)
7. AcroWell Filter Plate (prod. no. P5020)
8. Membrane preparation from bombesin receptor expressing cell line, e.g. human BB1 (prod. no. RBHBS1M) or BB2 (prod. no. RBHBS2M)

In addition to the DELFIA system the following are required:

- Unlabeled bombesin (e.g. Bachem, prod. no. H-2155)
- Saponin (e.g. Calbiochem, prod. no. 558255)
- Distilled water
- Filterplate washing manifold: Multiscreen Vacuum Manifold, Millipore
- Precision pipettes for dispensing microliter volumes
- Pipettes for dispensing milliliter volumes
- Glass or polypropylene tubes

PROCEDURAL NOTES

1. The binding buffer composition in ligand receptor assays is usually receptor specific. To achieve the best results in a DELFIA assay, the buffer should contain BSA to avoid non-specific binding, and low concentrations of a chelator, e.g. EDTA (ethylenediaminetetraacetic acid), to keep the fluorescence background low. The recommended binding buffer (see section "EXAMPLE OF FILTRATION BASED ASSAY CONDITIONS") is optimized to be used with human BB2 receptor in DELFIA assay.

2. Some receptor preparations may require an addition of a protease inhibitor, e.g. phenylmethylsulfonyl fluoride (PMSF), in the binding buffer.

3. When filtering the plate, ensure that each well is washed thoroughly, e.g. four times with 300 µL of recommended wash solution (see section "EXAMPLE OF FILTRATION BASED ASSAY CONDITIONS"). After washing the plate, check that the wells are dry. Remove any remaining moisture by blotting the plate on absorbent paper.

4. When using the Millipore manifolder/vacuum unit, the AcroWell Filter Plate may not fit tightly on the manifolder/vacuum frame. The plate will fit better on the frame if the metal grid is removed from the top of the frame. The black rubber part should, however, be left on the frame in order to prevent problems with vacuum leakage.

5. For optimal results, flush the pipette tips or the dispenser tips and tubing thoroughly with DELFIA Enhancement Solution. We recommend using plastic vials instead of glass vials.

EXAMPLE OF FILTRATION BASED ASSAY CONDITIONS

Binding buffer: DELFIA L*R binding buffer concentrate (10x), diluted 1:10 containing the following reagents as final concentrations:

50 mmol/L Tris-HCl, pH 7.5
5 mmol/L $MgCl_2$
25 µmol/L EDTA
0.2 % BSA

supplemented with 50 µg/mL saponin

Wash solution: DELFIA L*R wash concentrate (25x), diluted 1:25 containing the following reagents as final concentrations:

50 mmol/L Tris-HCl, pH 7.5
5 mmol/L $MgCl_2$

Binding protocol: Binding assays are performed in 100 µL total volume according to the following conditions. All the dilutions are prepared in binding buffer.

1. Pipetting:	25 µL binding buffer (total binding) OR unlabeled ligand (non-specific binding) 25 µL Eu-labeled ligand 50 µL diluted receptor
2. Incubation:	shake the plate slowly for 15 seconds, then incubate the plate for 90 minutes at room temperature
3. Washing:	four times with 300 µL of wash solution
4. Eu enhancement:	200 µL DELFIA Enhancement Solution/well, incubate for 15 minutes at room temperature with slow shaking
5. Measurement:	time-resolved fluorometer with Eu-filter

CALCULATION OF RESULTS

$$S/B = \frac{\text{Total values}}{\text{Non-specific values}}$$

$$Z' = 1 - \frac{3 \times SD_{total} + 3 \times SD_{non\text{-}specific}}{\text{Mean signal}_{total} - \text{Mean signal}_{non\text{-}specific}}$$

SD = standard deviation

K_d and K_i values are calculated using GraphPad Prism® [2] software.

[2] GraphPad Prism is a registered trademark of GraphPad Software Inc.

RESULTS

Saturation curve

Figure 1 shows typical data for measuring the saturation binding. The saturation experiment was performed with increasing amounts of DELFIA Eu-labeled bombesin in the presence of 0.2 µg of human BB2 receptor (B_{max} 9.3 pmol/mg protein) per well. Non-specific binding was determined in the presence of 500 nmol/L unlabeled bombesin. A typical K_d value for DELFIA Eu-labeled bombesin is around 0.5 nmol/L. See Product Information Sheet for lot specific K_d value.

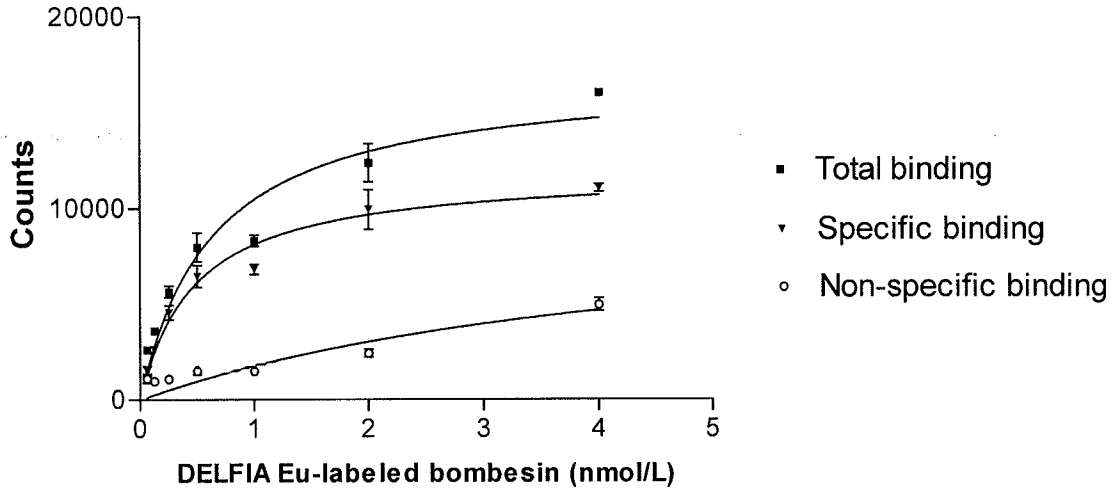

Figure 1. A K_d value of 0.47 nmol/L was obtained using the human BB2 receptor. The assay was performed as described in "EXAMPLE OF FILTRATION BASED ASSAY CONDITIONS". The fluorescence was measured with VICTOR^2. The values represent the mean ±SD from triplicate wells.

In addition, a K_d value of 0.56 nmol/L was obtained using 0.4 µg of human BB1 receptor (B_{max} 3.4 pmol/mg protein); data not shown.

Competition curve

The competition between the DELFIA Eu-labeled bombesin and unlabeled bombesin is shown in Figure 2. The displacement curve was performed with 0.5 nmol/L of DELFIA Eu-labeled bombesin and increasing amounts of unlabeled bombesin in the presence of 0.2 µg of human BB2 receptor (B_{max} 9.3 pmol/mg protein) per well. A typical K_i value is around 0.2 nmol/L.

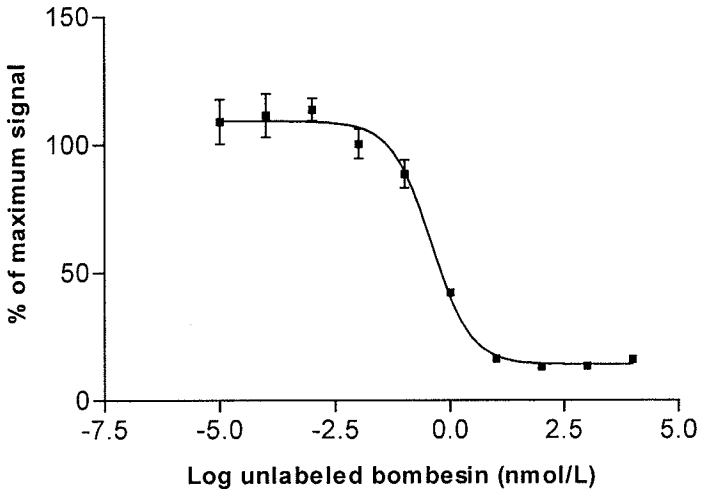

Figure 2. A K_i value of 0.19 nmol/L was obtained using the human BB2 receptor. The assay was performed as described in "EXAMPLE OF FILTRATION BASED ASSAY CONDITIONS". The fluorescence was measured with VICTOR^2. The values represent the mean ±SD from triplicate wells.

In addition, a K_i value of 0.24 nmol/L was obtained using 0.4 µg of human BB1 receptor (B_{max} 3.4 pmol/mg protein) in the presence of 0.5 nmol/L DELFIA Eu-labeled bombesin (data not shown).

S/B ratio and Z' value

Typical readings, S/B ratios and Z' values using VICTOR^2 and EnVision (n = 12) are shown in Table 1. S/B and Z' were calculated using a concentration of DELFIA Eu-labeled bombesin close to the K_d value. Decreasing the number of flashes in EnVision shortens the measurement time at the expense of counts.

Table 1. S/B and Z' were calculated using a concentration of 0.5 nmol/L DELFIA Eu-labeled bombesin.

	VICTOR	EnVision	EnVision	EnVision
Flash		100	50	10
Time / plate		1 min 7 sec	55 sec	45 sec
Total binding	8530	6466	3202	623
CV%	7.9	7.1	6.3	6.3
Non-specific binding	1103	760	369	73
CV%	12.8	17.3	17.7	21.4
S/B	8	9	9	8
Z'	0.67	0.69	0.72	0.70

WARNINGS AND PRECAUTIONS

DELFIA Eu-labeled bombesin is intended for research use only.

Lyophilized DELFIA Eu-labeled bombesin contains sodium azide (NaN_3) as a preservative. The powder is harmful by inhalation, in contact with skin and if swallowed. Sodium azide may react with lead and copper plumbing to form highly explosive metal azides. On disposal, flush with a large volume of water to prevent azide build-up.

To avoid Eu-contamination that can result in a high fluorescence background in assays, high standard pipetting and washing techniques are required. Avoid contaminating pipettes with Eu-labeled reagents.

Disposal of all waste should be in accordance with local regulations.

WARRANTY

Purchase of the product gives the purchaser the right to use this material in his own research, development, and investigational work. The product is not to be injected into humans or used for diagnostic procedures. PerkinElmer Life and Analytical Sciences, Wallac Oy reserves the right to discontinue or refuse orders to any customer who plans to use these products for any other purposes.

PerkinElmer Life and Analytical Sciences, Wallac Oy does not warrant or guarantee that the product is merchantable or satisfactory for any particular purpose, nor free from any claim of foreign or domestic patent infringement by a third party, and there are no warranties, expressed or implied, to such effect. PerkinElmer Life and Analytical Sciences, Wallac Oy will not be liable for any incidental, consequential or contingent damages involving their use including damages to the property or personal injuries.

All information supplied with the product and technical assistance given is believed to be accurate, but it remains the responsibility of the investigator to confirm all technical aspects of the application. We appreciate receiving any additions, corrections, or updates to information supplied to the customer.

LITERATURE

Zhang, J.H., Chung, T.D.Y. and Oldenburg, K.R. (1999): A simple statistical parameter for use in evaluation and validation of high throughput screening assays. J. Biomol Screen **4,** 67-73.

DELFIA® Ligands Guide 006783
To download pdf file: www.perkinelmer.com/delfia

June 2003

Manufactured by:

PerkinElmer Life and Analytical Sciences,
Wallac Oy
P.O. Box 10
FIN-20101 Turku
FINLAND

PerkinElmer®
precisely.

Niosomes and Polymeric Chitosan Based Vesicles Bearing Transferrin and Glucose Ligands for Drug Targeting

Christine Dufes,[1,4] Andreas G. Schätzlein,[2] Laurence Tetley,[3] Alexander I. Gray,[1] Dave G. Watson,[1] Jean-Christophe Olivier,[4] William Couet,[4] and Ijeoma F. Uchegbu[1,5]

Received March 11, 2000; accepted July 7, 2000

Purpose. To prepare polymeric vesicles and niosomes bearing glucose or transferrin ligands for drug targeting.

Methods. A glucose-palmitoyl glycol chitosan (PGC) conjugate was synthesised and glucose-PGC polymeric vesicles prepared by sonication of glucose-PGC/ cholesterol. N-palmitoylglucosamine (NPG) was synthesised and NPG niosomes also prepared by sonication of NPG/ sorbitan monostearate/ cholesterol/ cholesteryl poly-24-oxyethylene ether. These 2 glucose vesicles were incubated with colloidal concanavalin A gold (Con-A gold), washed and visualised by transmission electron microscopy (TEM). Transferrin was also conjugated to the surface of PGC vesicles and the uptake of these vesicles investigated in the A431 cell line (over expressing the transferrin receptor) by fluorescent activated cell sorter analysis.

Results. TEM imaging confirmed the presence of glucose units on the surface of PGC polymeric vesicles and NPG niosomes. Transferrin was coupled to PGC vesicles at a level of 0.60 ± 0.18 g of transferrin per g polymer. The proportion of FITC-dextran positive A431 cells was 42% (FITC-dextran solution), 74% (plain vesicles) and 90% (transferrin vesicles).

Conclusions. Glucose and transferrin bearing chitosan based vesicles and glucose niosomes have been prepared. Glucose bearing vesicles bind Con-A to their surface. Chitosan based vesicles are taken up by A431 cells and transferrin enhances this uptake.

KEY WORDS: polymeric vesicles; glucose vesicles; transferrin vesicles.

[1] Department of Pharmaceutical Sciences, University of Strathclyde, Strathclyde Institute for Biomedical Sciences, 27 Taylor Street, Glasgow G4 0NR, United Kingdom.

[2] Department of Medical Oncology, University of Glasgow, Garscube Estate, Switchback Road, Glasgow G61 1BD, United Kingdom.

[3] Institute of Biomedical and Life Sciences, University of Glasgow, Joseph Black Building, Glasgow G12 8QQ, United Kingdom.

[4] Laboratoire de Pharmacie Galénique et Biopharmacie, Faculté de Médecine et Pharmacie, 34 rue du Jardin des Plantes, 86000 Poitiers, France.

[5] To whom correspondence should be addressed. (e-mail: i.f.uchegbu@strath.ac.uk)

ABBREVIATIONS: Con A-gold, concanavalin A gold; DMSI, dimethylsuberimidate; DMSO, dimethylsulphoxide; FACS, Fluorescent activated cell sorter; FITC-dextran, fluorescein isothiocyanate dextran; PGC, palmitoyl glycol chitosan; NPG, N-palmitoyl glucosamine; PBS, phosphate buffered saline; TEM, transmission electron microscopy; TF, transferrin.

INTRODUCTION

Actively targeted therapies have demonstrated their potential in the tumour targeting of polymeric gene delivery systems (1), the central nervous system targeting of peptide analgesics (2) and the targeting of oligonucleotides to the liver hepatocytes and macrophages (3). In our laboratories polymeric vesicles for drug delivery have been developed from a specially designed amphiphilic chitosan derivative-palmitoyl glycol chitosan (PGC) (4). While the passive targeting of anti-cancer phospholipid vesicles (liposomes) (5,6) and non-ionic surfactant vesicles (niosomes) (7) to solid tumours has been well documented, liposomes for gene delivery are predominantly passively targeted to the lung endothelium (8,9). Hence, depending on their potential use it will be necessary to elucidate active targeting strategies for vesicular systems. Additionally the targeting of large hydrophilic molecules across the blood brain barrier (BBB) is invariably problematic. Transferrin bearing proteins however may be targeted across the blood brain barrier when administered via the carotid artery (10) and the exploitation of the BBB glucose transporter, GLUT-1 (11,12), using glucose peptide conjugates results in peptide delivery to the central nervous system (2). The GLUT-1 receptor is also over expressed in some tumour tissue (13,14), hence a glucose targeting ligand may be useful for targeting anti-cancer genes to tumour tissue. It is possible that the active targeting of polymeric vesicles for drug/ gene delivery may be accomplished with targeting ligands. This work reports on the preparation and characterisation of polymeric vesicles and niosomes bearing targeting ligands.

MATERIALS AND METHODS

Materials

Palmitic acid N-hydroxysuccinimide, glucosamine, sorbitan monostearate (Span 60), cholesterol, glycol chitosan (Mw = 164,000), concanavalin A gold (Con A-gold, 20nm), β-D-glucopyranosyl phenylisothiocyanate, N-N-diisopropylethylamine, dimethyl-suberimidate (DMSI), triethanolamine, fluorescein isothiocyanate dextran (FITC-dextran), phosphate buffered saline (PBS, pH = 7.4) tablets, iron-saturated human transferrin (TF), Folin Ciocalteu's reagent, uranylformate, sodium carbonate, sodium potassium tartrate and cupric sulphate, were all purchased from Sigma Aldrich Co, UK. Dialysis tubing was obtained from Medicell International, UK. Chloroform, isopropanol, dimethylsulphoxide (DMSO) and diethylether were all purchased from Merck, UK. Cholesteryl poly-24-oxyethylene ether (Solulan C24) was kindly donated by D.F. Anstead, UK. All tissue culture reagents were obtained from Gibco, UK.

Preparation of Glucose-Bearing Niosomes

Synthesis of N-Palmitoyl Glucosamine (NPG)

This was prepared in a similar manner to that described for the glycoside palmitoyl muramic acid (15) and was derived from the method of Lapidot and others (16). Glucosamine (86.3mg) was dissolved in dimethylsulphoxide (15mL) and triethanolamine (93μL). To this was added palmitic acid N-

0724-8741/00/1000-1250$18.00/0

hydroxysuccinimide (283mg) dissolved in chloroform (4mL). The mixture was stirred at room temperature for 48 h, protected from light. Chloroform was evaporated off at room temperature and the remaining liquid freeze-dried. The resulting powder was purified by washing consecutively with water (200 ml), chloroform (50 ml), and ether (200 ml) and then was freeze-dried again. NPG (Figure 1) was obtained as a white powder.

^1H NMR Analysis of NPG

^1H NMR (with integration) and ^1H correlation spectroscopy experiments (Bruker AMX 400MHz spectrometer, Bruker Instruments, UK) were performed on NPG solutions in deuterated DMSO.

Mass Spectrometry

Analysis of NPG was carried out by mass spectrometry (fast atom bombardment–FAB on a JEOL AX505 mass spectrometer, Jeol Instruments, UK).

Preparation of NPG Niosomes

Niosomes were prepared by shaking a mixture of NPG (16mg), Span 60 (65mg), cholesterol (58mg) and Solulan C24 (54mg) in water (5mL) at 90°C for 1h, followed by probe sonication (Soniprobe Instruments, UK) for 4 minutes with the instrument set at 20% of its maximum capacity.

Synthesis of the PGC- Glucose Conjugate

Palmitoyl glycol chitosan (PGC) (Fig. 2) was synthesised by the reaction of glycol chitosan with palmitic acid N-hydroxysuccinimide in a 4:1 sugar monomer, palmitic acid molar ratio and characterised by ^1H NMR analysis as previously described (4). PGC - glucose conjugate was prepared using methods described previously (17). PGC (5mg), β-D-glucopyranosyl phenylisothiocyanate (5mg) and N-N-diisopropylethylamine (4μl) were dissolved in DMSO (5mL). The reaction mixture was stirred at room temperature for 24h, diluted with water (25mL), exhaustively dialysed against 1L of water (over a 24h period with 6 changes), and finally freeze-dried.

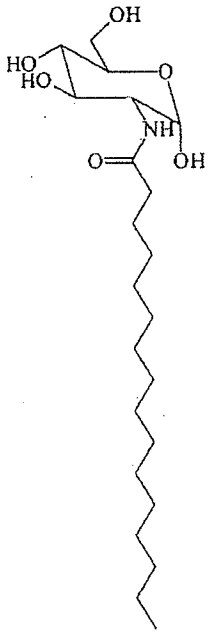

Fig. 1. Chemical structure of N-palmitoyl glucosamine (N-PG).

Preparation of Polymeric Glucose Vesicles

Vesicles were prepared by probe sonicating the PGC-glucose conjugate (4mg) and cholesterol (2mg) in water (4mL) for 4 min with the instrument set at 20% of its maximum output. The temperature of the probe sonicated formulation reached a maximum temperature of ~ 60°C. The vesicle dispersion was then filtered through a 0.45 μm filter.

Preparation Of Control Span 60 Niosomes

Vesicles were prepared by shaking a mixture of Span 60 (73mg), cholesterol (65mg), Solulan C24 (54mg) in water (5mL) at 90°C for 1h followed by probe sonication for 4 minutes with the instrument set at 20% of its maximum capacity.

Transmission Electron Microscopy (TEM)

The presence of glucose on the vesicle surface was evaluated by incubation with a colloidal dispersion of Con A-gold thus exploiting the affinity of the lectin concanavalin A for glucose (18). Glucose bearing vesicles and control plain Span 60 niosome suspensions (0.1mL) were shaken with the Con A-gold dispersion (0.1mL) at 60°C for 1h. To separate unbound Con A-gold from bound Con A-gold, the mixture was then centrifuged (1,000g for 10 min, Beckman L8-55 ultracentrifuge, Beckman Instruments, UK) and the pelleted unbound Con A-gold discarded. Vesicles bearing the bound gold were then imaged by TEM as follows. Droplets of the vesicle preparation were mixed in equal (20 μl) volumes with 1% uranylformate (pH 4.8) on a specimen support grid and immediately dried down using filter paper. The negatively stained grid samples were then imaged on a LEO 902 energy filtering electron microscope at 80 kV.

Preparation of TF-Bearing Polymeric Vesicles Entrapping the Fluorescent Marker FITC-Dextran

Preparation of Plain PGC Vesicles

PGC vesicles were prepared from PGC and cholesterol as previously described (4), by probe sonicating PGC (10mg) and cholesterol (4mg) in PBS (pH = 7.4, 2mL) for 4 min with the instrument set at 20% of its maximum capacity.

Conjugation of TF to PGC Vesicles (TF-PGC)

TF was linked with PGC vesicles by using DMSI as a cross-linking reagent (19) in a similar manner to that reported for TF-coated liposomes (20). To 2mL of the vesicle suspension (2mL), obtained from above (5mg mL^{-1}), was added TF (12mg) and DMSI (24mg) in triethanolamine HCl buffer (pH 7.4, 2mL). The coupling reaction was allowed to take place at room temperature for 2h whilst stirring. Free TF was then removed by ultracentrifugation (2 × 150,000g for 1h). After each ultracentrifugation step the pelleted vesicles were resuspended in PBS (pH = 7.4, 2mL).

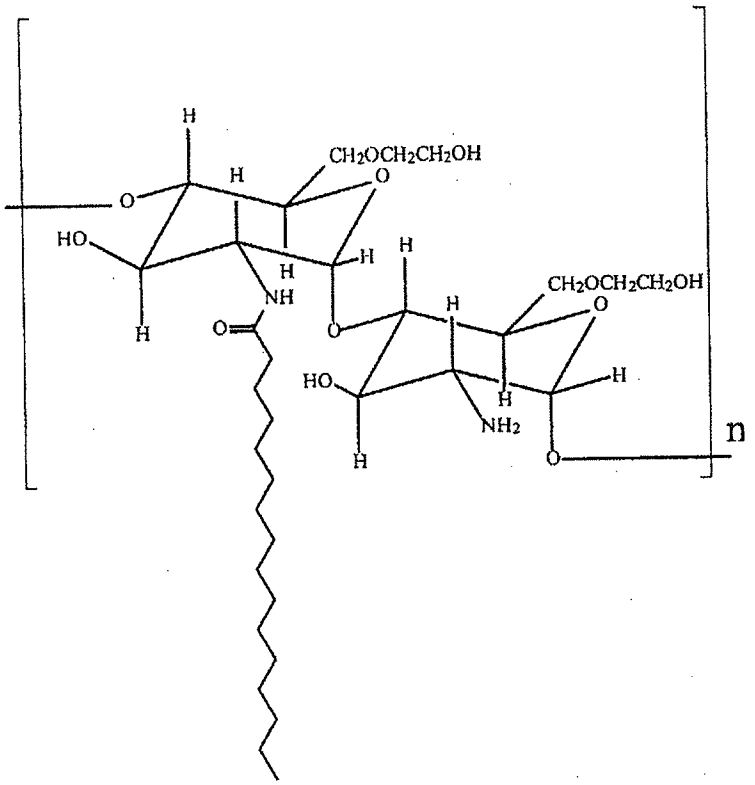

Fig. 2. Chemical structure of palmitoyl glycol chitosan (PGC).

Assay for Conjugated TF

The amount of conjugated TF was determined using the Lowry method (21). TF bearing vesicle suspensions, blank vesicles bearing no TF and vesicle suspensions carried through the TF conjugation reaction but without the cross-linking agent DMSI were used in this assay. The latter vesicles were used to ensure that TF was not merely adsorbed to the vesicle surface. To sodium carbonate solution (25mL, 2%w/v in NaOH 0.1M) was added sodium potassium tartrate (0.5mL, 2%w/v) and cupric sulphate (0.5mL, 1%w/v) with constant stirring to avoid precipitation. To 1mL of this solution (freshly prepared) was added 100μl of each of the vesicle suspensions (5mg mL^{-1} PGC) or the standard TF solutions (0–0.5mg mL^{-1}) and the mixture allowed to stand for 10min. To these samples was then added Folin Ciocalteu's reagent (100μL) with immediate vortexing. All samples were subsequently left to stand for 30min and the colour reaction quantified by measuring the absorbance at 750nm (UV-1, Unicam Ltd., UK). The sample derived from the blank vesicles not containing TF was used in the reference cell, when measuring the absorbance of the vesicle samples. The amount of protein associated with the vesicles was determined with reference to the standard TF solutions.

Loading of FITC-Dextran TF-PGC Vesicles

FITC-dextran loaded TF-PGC vesicles were prepared by probe sonicating on ice TF-coated vesicles, obtained as described above in a solution of FITC-dextran (2mL, 6mg mL^{-1}). Unentrapped FITC-dextran was removed by ultracentrifugation (150,000g × 1h) and the FITC-dextran loaded vesicle pellet resuspended in PBS (2mL).

Assay for the Amount of FITC-Dextran Entrapped by TF- PGC Vesicles

PGC vesicles were disrupted by adding the vesicle suspension (0.1mL) to isopropanol (1mL). This solution was then diluted to 10mL with PBS (pH = 7.4) and the fluorescence measured (Perkin Elmer LS-50 fluorescence spectrometer, Perkin-Elmer Instruments, UK.) at an excitation wavelength of 480nm and an emission wavelength of 560nm. The amount FITC-dextran was computed with reference to standard solutions of FITC-dextran (11μg mL^{-1}–11mg mL^{-1}) in an isopropanol, PBS (pH = 7.4) mixture (10: 90).

Vesicle Sizing

Vesicle sizing was performed by photon correlation spectroscopy on a Malvern Zetasizer 1 (Malvern Instruments, UK.).

Cellular Uptake of FITC-Dextran Loaded TF- PGC Vesicles

The A431-human epidermoid carcinoma cell line (ATCC CRL-1555) (22,23) was grown as a monolayer culture at 37°C in 5% CO_2 and maintained by regular passages in Dulbecco's medium supplemented with 10% foetal bovine serum, L-glutamine (1%w/v). Plated A 431 cells (10^5 cells/well) were incubated (37°C for 4 h) with transferrin-bearing vesicles (0.2 mL, 104μg mL^{-1} PGC) loaded with FITC-dextran (24μg mL^{-1}), blank FITC-dextran vesicles or with FITC-dextran solution. The concentration of FITC-dextran was the same for all the samples.

For the microscopic studies cells were grown and exam-

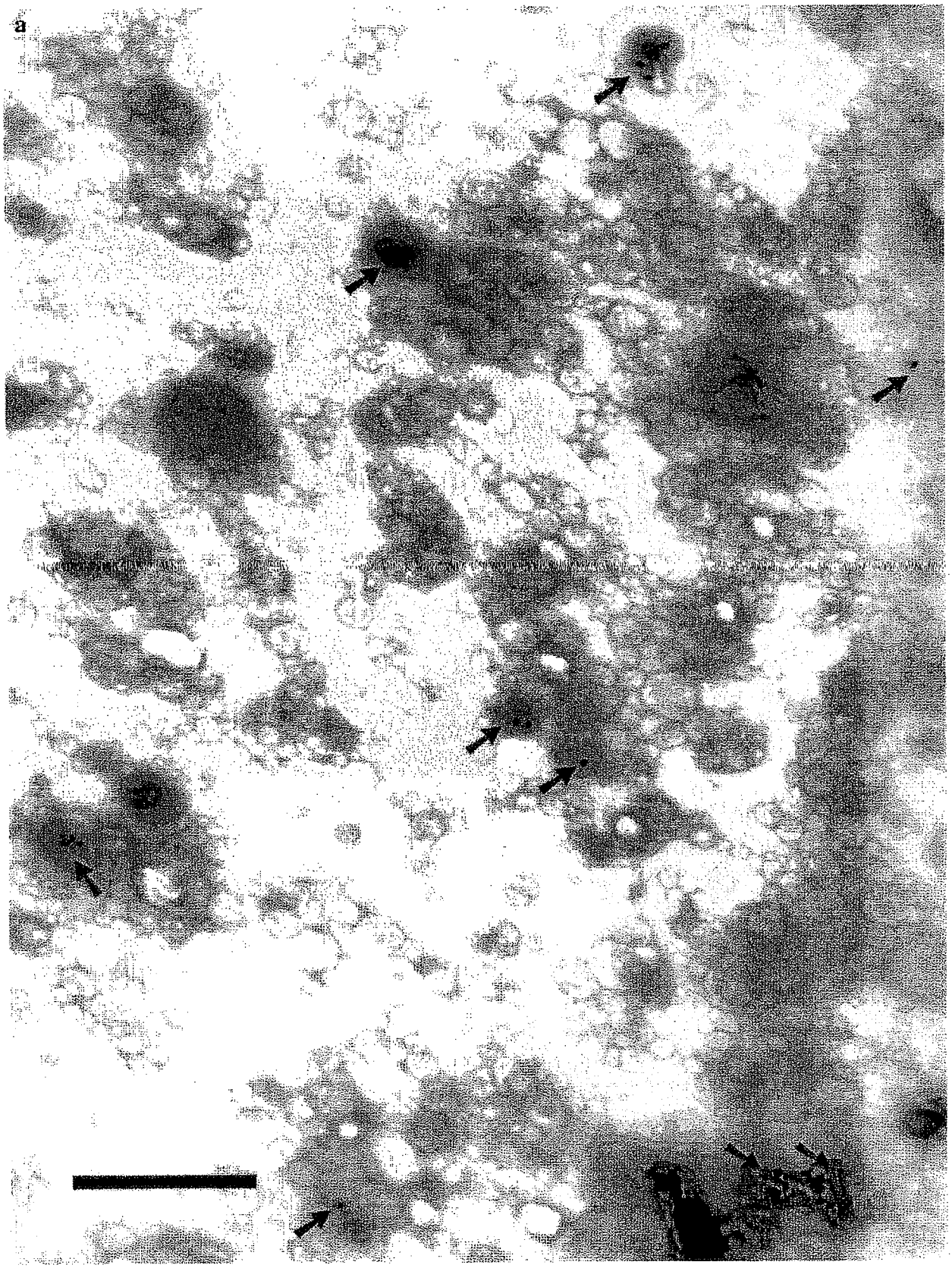

Fig. 3. Continued on facing page.

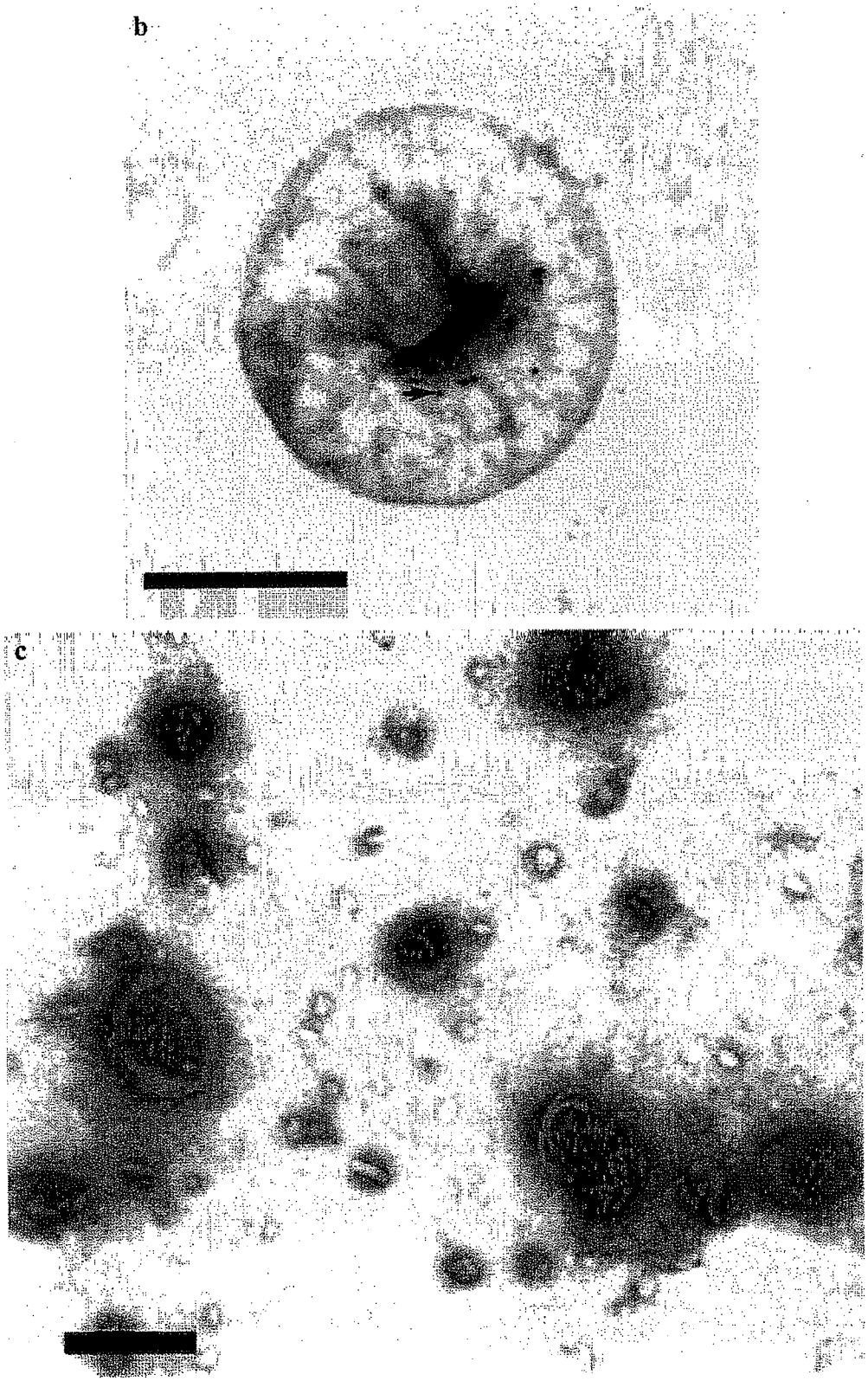

Fig. 3. Transmission electron micrographs with negative staining of Con A-gold (20 nm) associated with a) N-PG vesicles, b) PGC- glucose vesicles, and c) plain Span 60 niosomes. Gold particles are indicated by arrow , bar = 100nm.

ined on coverslips. At the end of the incubation period, cells were washed with PBS (pH = 7.4), transferred to a holder where the cells were immersed in PBS (pH = 7.4) and examined using confocal microscopy (λ_{ex} = 488 nm, Biorad 600 confocal microscope, Biorad, UK). For flow cytometry studies, the cells were trypsinised after the incubation period, washed (PBS , pH = 7.4) and pelleted (1,000g) twice. Cellular FITC-dextran uptake was examined on a FACStar flow cytometer (Becton-Dickinson Instruments, UK). The forward scatter (FSC) and sideward scatter (SSC) of a control cell suspension was used to discriminate cells and debris. 20,000 cells (gated events) were counted for each sample. FITC–dextran fluorescence was detected with logarithmic settings (FL1, λ_{em} = 515–545 nm). Cells were counted as positive when their fluorescence (FL1) was higher than that of 95% of cells from an untreated cell suspension, (i.e. channel 198 to 1024)

RESULTS

Glucose Bearing Vesicles

NPG Niosomes

The characterisation of PGC was as previously described (4). Proton assignments by ^{1}H NMR of NPG were as follows: δ 0.86 ppm = CH3 (palmitoyl), δ 1.25 ppm = CH2 (palmitoyl), δ 1.89 ppm – CII2 (palmitoyl shielded by carbonyl), δ 2.14 ppm = CH2 (adjacent to carbonyl protons), δ 2.71 ppm = CH (C2 sugar proton), δ 3.3–4.0 ppm = non-exchangeable sugar protons. Mass spectrometry data yielded one main peak corresponding to the mass ion 418 (100%, M^+) and further minor peaks 400 (72.75 %, M^+ -OH) and 432 (24.43%, M^+ + OH). These results indicate that NPG was successfully prepared.

Stable vesicles could be formed from NPG, sorbitan monostearate, cholesterol, Solulan C24 (10: 40: 40: 10 mole%). Higher levels of NPG resulted in unstable formulations with the NPG crystallising out of the formulation within hours. Glucose niosomes prepared from NPG had a z-average mean diameter of 164nm.

Glucose-PGC Vesicles

Polymeric (PGC) glucose bearing vesicles had a z-average mean diameter of 155nm.

Con-A Gold Binding

Both types of vesicles effectively bound Con A-gold while the control plain vesicles (devoid of glucose) did not (Figure 3), indicating the presence of accessible glucose units on the surface of these niosomes and polymeric vesicles.

Transferrin Bearing PGC Vesicles

Transferrin was successfully conjugated to PGC in these vesicles, as determined by the Lowry assay at a level of 0.60 ± 0.18g of TF per g polymer (50 ± 15% of the initial transferrin used). FITC-dextran was entrapped in the transferrin bearing vesicles (0.23g per g polymer, corresponding to 10% of the initial FITC-dextran) and in the plain chitosan based vesicles (0.32g per g polymer, corresponding to 13% of the initial FITC-dextran). Plain PGC vesicles had a z-average mean diameter of 420nm, while TF-PGC vesicles had a z-average size of 458nm and TF-PGC vesicles loaded with FITC-dextran had a z-average size of 740nm.

Cellular Uptake of Fluorescently Labelled TF-PGC Vesicles

Fluorescence microscopy images showed a brighter fluorescence (more fluorescently labelled vesicles) associated with cells incubated with the transferrin bearing vesicles when compared to the plain vesicles (Figure 4). Flow cytometry data (Fig. 5) also indicated that there was the greater percentage of positive cells when the transferrin bearing vesicles were incubated with the cells. However it is interesting to note that the polymeric vesicles without TF also associated to a greater degree with the cells than the fluorescent marker (FITC-dextran) in solution. This is indicative of the fact that these latter vesicles are also taken up by the cells or at least enhance the uptake of the fluorescent polymer.

DISCUSSION

This work is the first report of the preparation of polymeric chitosan based vesicles bearing targeting ligands. In addition the synthesis of a new surfactant NPG is described. The synthesis is a simple one-step procedure unlike the synthetic methods previously reported (24). Stable vesicles could not be produced from this surfactant alone or in the presence of cholesterol and the incorporation of more than 10mole% NPG into the bilayer of niosomes resulted in NPG crystallising out within hours. 6-O-alkanoyl-α-D glucose amphiphiles also crystallise out of niosomes prepared with these agents and cholesterol within 3–4 weeks (25). Small niosomes in the colloidal size range may be formed with this new amphiphile, NPG. 1-alkyl glucosides have been reported to form large unilamellar niosomes by Kiwada and others (26). These latter niosomes are 1μm in diameter and were reported to be stable when stored in the dark for up to 25 weeks. The production of colloidal dispersions of the 1-alkyl glucoside niosomes was not however reported by these authors. To our knowledge this is the first report of the production of sub-micron glucose vesicles in which the glucose units are found to be recognisable by the glucose specific lectin-con A. Con A served as a model for the glucose specific receptor.

The PGC-glucose conjugate produced vesicles with a smaller z-average mean diameter than vesicles produced from plain PGC (155nm vs 420nm). The conjugation of glucose to PGC probably resulted in an increase in the size of the hydrophilic portion of the molecule relative to the hydrophobic portion of the molecule. An increase in the hydrophilic head group of an amphiphile or mixture of amphiphiles would result in an increase in vesicle curvature and hence a decrease in vesicle size (27). It appears that with amphiphilic pendant like polymers, a similar increase in the hydrophilic head group area also decreases vesicle size. Vesicles incorporating only 10 mole % of NPG are able to bind Con A, as do vesicles prepared from the PGC-glucose conjugate (Figure 3). This indicates that the glucose units were accessible on the vesicle surface and may be accessible to glucose receptors in vivo. Because human cancer cells have an enhanced need for glucose and hence frequently over express the GLUT receptors

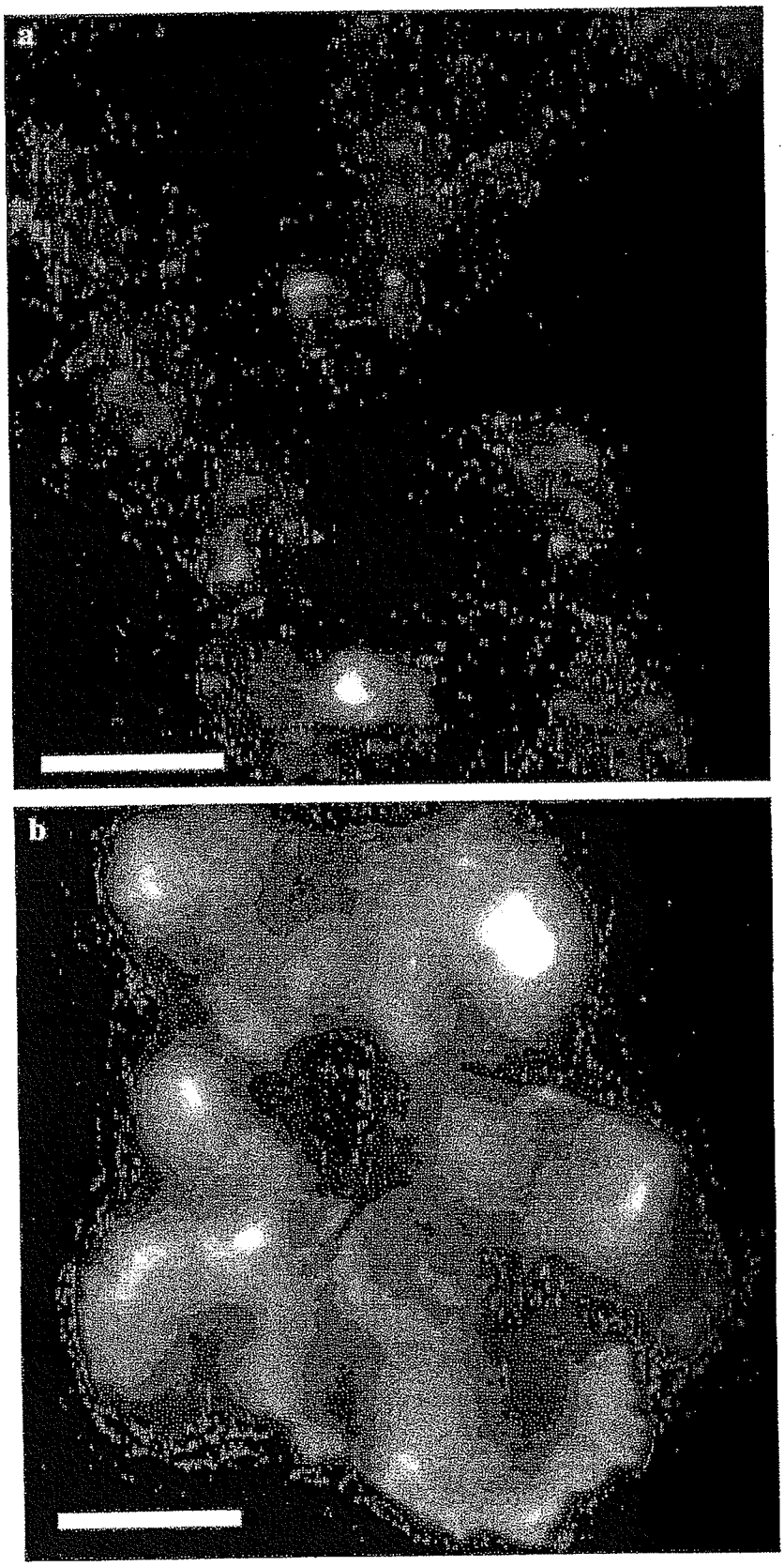

Fig. 4. Fluorescence micrographs of A 431 tumour cells treated with a) plain FITC-dextran loaded vesicles (without transferrin) and b) transferrin bearing FITC-dextran loaded vesicles. bar = 100 nm.

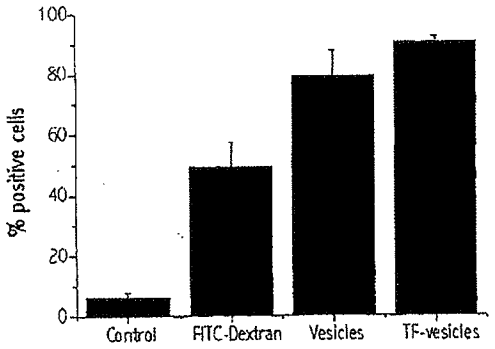

Fig. 5. FACS analysis of the uptake of FITC-D solution ("solution"), FITC-D vesicles without Tf ("vesicles"), and Tf-bearing vesicles loaded with FITC-D ("TF vesicles"), by A 431 cells. "Control": untreated cells. Cells were counted as FITC positive when their fluorescence was higher than that of 95 % of cells from an untreated cell suspension. n = 3.

(14), these glucose bearing vesicles may prove useful as gene targeting agents to tumour cells over-expressing the GLUT receptor isoforms. In addition the presence of GLUT 1 receptors at the BBB (28) may potentially be exploited with these carriers, causing them to increase the transfer of large hydrophilic molecules across the BBB.

Transferrin was coupled to the surface of the polymeric vesicles and appeared to be accessible to the TF receptor in the A431 cell line (Figures 4 and 5). Transferrin receptors are also over expressed on the surface of many proliferating cells (29) and their presence may be exploited for the targeting of gene expression to tumours (1). In addition the administration of transferrin-protein conjugates via the carotid artery resulted in the enhanced transfer of large proteins across the BBB (10). These transferrin bearing vesicles may thus find a use in the targeting to the central nervous system.

CONCLUSION

Glucose niosomes and glucose or transferrin bearing polymeric vesicles have been successfully prepared for drug targeting. The accessibility of these targeting ligands to the glucose specific lectin Con A or to the transferrin receptor have been demonstrated. In addition the encapsulation of FITC-dextran within polymeric vesicles has been shown to promote the uptake of the fluorescent marker. Further studies on the usefulness of these new vesicles in vivo are planned for the very near future.

ACKNOWLEDGMENTS

This work was supported by a University of Strathclyde New Lecturer Starter Grant to IFU.

REFERENCES

1. M. Ogris, S. Brunner, S. Schuller, R. Kircheis, and E. Wagner. PEGylated DNA/transferrin-PEI complexes: Reduced interaction with blood components, extended circulation in blood and potential for systemic gene delivery. *Gene Ther.* **6**:595–605 (1999).
2. R. Polt, F. Porreca, L. Z. Szabo, E. J. Bilsky, P. Davis, T. J. Abbruscato, T. P. Davis, R. Horvath, H. I. Yamamura, and V. J. Hruby. Glycopeptide enkephalin analogs produce analgesia in mice—Evidence for penetration of the blood-brain-barrier. *Proc. Natl. Acad. Sci. USA* **91**:7114–7118 (1994).
3. R. I. Mahato, S. Takemura, K. Akamatsu, M. Nishikawa, Y. Takakura, and M. Hashida. Physicochemical and disposition characteristics of antisense oligonucleotides complexed with glycosylated poly(L-lysine). *Biochem. Pharmacol.* **53**:887–895 (1997).
4. I. F. Uchegbu, A. G. Schatzlein, L. Tetley, A. I. Gray, J. Sludden, S. Siddique, and E. Mosha. Polymeric chitosan-based vesicles for drug delivery. *J. Pharm. Pharmacol.* **50**:453–458 (1998).
5. D. Papahadjopoulos, T. M. Allen, A. Gabizon, E. Mayhew, K. Matthay, S. K. Huang, K. D. Lee, M. C. Woodle, D. D. Lasic, and C. Redemann. Sterically stabilized liposomes: Improvements in pharmacokinetics and antitumor therapeutic efficacy. *Proc. Natl. Acad. Sci. USA* **88**:11460–11464 (1991).
6. F. Yuan, M. Leunig, S. K. Huang, D. A. Berk, D. Papahadjopoulos, and R. K. Jain. Microvascular permeability and interstitial penetration of sterically stabilized (stealth) liposomes in a human tumor xenograft. *Cancer Res.* **54**:3352–3356 (1994).
7. I. F. Uchegbu, J. A. Double, J. A. Turton, and A. T. Florence. Distribution, metabolism and tumoricidal activity of doxorubicin administered in sorbitan monostearate (Span 60) niosomes in the mouse. *Pharm. Res.* **12**:1019–1024 (1995).
8. Y. K. Song and D. X. Liu. Free liposomes enhance the transfection activity of DNA/lipid complexes in vivo by intravenous administration. *Biochim. Biophys. Acta* **1372**:141–150 (1998).
9. L. G. Barron, L. Gagne, and F. C. Szoka, Jr. Lipoplex-mediated gene delivery to the lung occurs within 60 minutes of intravenous administration. *Human Gene Ther.* **10**:1683–1694 (1999).
10. R. D. Broadwell, B. J. Baker-Cairns, P. M. Friden, C. Oliver, and J. C. Villegas. Transcytosis of protein through the mammalian cerebral epithelium and endothelium. III. Receptor-mediated transcytosis through the blood-brain barrier of blood-borne transferrin and antibody against the transferrin receptor. *Experimental Neurol.* **142**:47–65 (1996).
11. C. L. Farrell and W. M. Pardridge. Blood-brain-barrier glucose transporter is asymmetrically distributed on brain capillary endothelial lumenal and ablumenal membranes—An electron-microscopic immunogold study. *Proc. Natl. Acad. Sci. USA* **88**: 5779–5783 (1991).
12. W. M. Pardridge. Molecular regulation of blood-brain barrier GLUT1 glucose transporter. In J.Greenwood, D. J. Begley and M. B. Segal (eds.), *New Concepts of a blood brain barrier,* Plenum Press, New York, 1995, pp. 81–88.
13. T. Higashi, N. Tamaki, T. Honda, T. Torizuka, T. Kimura, T. Inokuma, G. Ohshio, R. Hosotani, M. Imamura, and J. Konishi. Expression of glucose transporters in human pancreatic tumors compared with increased FDG accumulation in PET study. *J. Nucl. Med.* **38**:1337–1344 (1997).
14. T. A. D. Smith. Facilitative glucose transporter expression in human cancer tissue. *Br. J. Biomed. Sci.* **56**:285–292 (1999).
15. I. F. Uchegbu. The biodistribution of novel 200nm palmitoyl muramic acid vesicles. *Int. J. Pharm.* **162**:19–27 (1998).
16. Y. Lapidot, N. D. Groot, and I. Fry-Shafrir. II A general method for the preparation of acylaminoacyl-tRNA. *Biochim. Biophys. Acta* **145**:292–299 (1967).
17. C. R. McBroom, C. H. Samanen, and I. J. Goldstein. Carbohydrate antigens: Coupling of carbohydrates to proteins by diazonium and phenylisothiocyanate reaction. *Meth. Enzymol.* **28**:212–219 (1972).
18. M. Monsigny, A. C. Roche, and P. Midoux. Uptake of neoglycoproteins via membrane lectins of L1210 cells evidenced by quantitative flow cytofluorometry and drug targeting. *Biol. Cell* **51**: 187–196 (1984).
19. N. Benhamou and G. B. Ouellette. Ultrastructural-localization of glycoconjugates in the fungus ascocalyx-abietina, the scleroderris canker agent of conifers, using lectin gold complexes. *J. Histochem. Cytochem.* **34**:855–867 (1986).
20. G. E. Davies and G. R. Stark. Use of dimethyl suberimidate, a cross-linking agent in studying the subunit structure of oligomeric proteins. *Proc. Natl. Acad. Sci. USA* **66**:651–656 (1970).
21. J. C. Stavridis, G. Deliconstantinos, M. C. Psallidopoulos, N. A. Armenakas, D. J. Hadjiminas, and J. Hadjiminas. Construction of transferrin-coated liposomes for in vivo transport of exogenous DNA to bone marrow erythroblasts in rabbits. *Exp. Cell Res.* **164**:568–572 (1986).
22. O. H. Lowry, N. J. Rosenburgh, A. L. Farr, and R. J. Randall.

0013-7227/92/1312-0799$03.00/0
Endocrinology

Vol. 131, No. 2
Printed in U.S.A.

Expression of Recombinant Human Follicle-Stimulating Hormone Receptor: Species-Specific Ligand Binding, Signal Transduction, and Identification of Multiple Ovarian Messenger Ribonucleic Acid Transcripts*

JONATHAN L. TILLY†, TOSHIHIKO AIHARA‡, KEIJI NISHIMORI, XIAO-CHI JIA, HAKAN BILLIG, KIM I. KOWALSKI, E. A. PERLAS, AND AARON J. W. HSUEH

Division of Reproductive Biology, Department of Gynecology and Obstetrics, Stanford University School of Medicine, Stanford, California 94305–5317

ABSTRACT

The ligand specificity and biochemical properties of the human (h) FSH receptor are poorly characterized due to the low abundance of these receptors and the limited availability of human tissues. Using a fragment of rat FSH receptor cDNA, we screened a human testicular cDNA library and obtained a FSH receptor cDNA covering the entire amino acid-coding region. After transfection of a human fetal kidney cell line (293) with the hFSH receptor cDNA, radioligand receptor analysis revealed the presence of high affinity (K_d, 1.7×10^{-9} M) FSH-binding sites on the plasma membrane. Both recombinant and wild-type hFSH displaced [^{125}I]hFSH binding, with ED_{50} values of 25 and 70 ng/ml, respectively, whereas hLH, hCG, and hTSH were ineffective. Although human, rat (r), and ovine FSH as well as equine CG competed for rat testicular FSH receptor binding, only hFSH and rFSH interacted effectively with the recombinant hFSH receptor, suggesting that species-specific ligand recognition exists between human and rodent receptors. After incubation of transfected cells with hFSH, but not recombinant hLH or hCG, a dose-dependent increase (ED_{50}, 10 ng/ml) in extracellular cAMP accumulation was observed, indicating a functional coupling of the expressed human receptor with the endogenous adenyl cyclase. In cells cotransfected with the FSH receptor expression plasmid and a luciferase reporter gene driven by the promoter of a cAMP-responsive gene, treatment with hFSH, but not hCG, resulted in a dose-dependent increase in luciferase activity. Northern blot analysis using a cRNA probe derived from the human receptor cDNA indicated the presence of multiple FSH receptor mRNA transcripts (7.0, 4.2, and 2.5 kilobases) in RNA prepared from human follicular phase ovary, but not from human corpus luteum or placenta. Additionally, two FSH-binding sites of 76 and 112 kilodaltons were detected in transfected 293 cells after ligand/receptor cross-linking and sodium dodecyl sulfate-polyacrylamide gel electorphoresis analysis. These results demonstrate the expression of functional hFSH receptor with unique ligand specificity and provide new data on the biochemical properties of the human receptor at the mRNA and protein levels. (*Endocrinology* **131**: 799–806, 1992)

FSH IS a member of the glycoprotein hormone family that also comprises LH, CG, and TSH (1, 2). Hormones of this family are dimers consisting of a common α-subunit and hormone-specific β-subunits joined together by noncovalent binding (3). As with the other glycoprotein hormones, FSH binding to target cells increases adenyl cyclase activity through interaction with membrane-associated G-proteins (4), thus classifying the FSH receptor to the G-protein-coupled receptor family (5–7). The hallmark of G-protein-coupled receptors is the presence of seven transmembrane-spanning segments that possess a homologous cluster of six or seven amino acid residues located on the carboxyl-terminal region of the third cytoplasmic loop. Recent molecular cloning of rat LH and FSH receptors have indicated that this conserved region, which has been implicated in G-protein coupling of the β-adrenergic receptor (8–10) and TSH receptor (11), is also present in the third cytoplasmic loop of gonadotropin receptors (12, 13).

Although the importance of FSH in testicular and ovarian development and reproductive function has been unequivocally established (for review, see Refs. 14–16), the limited availability of human gonadal tissues as well as the paucity of gonadal FSH-binding sites have precluded the study of human (h) FSH receptors. Recent studies from our laboratory have indicated that the ligand specificity of human *vs.* rat (r) LH receptors is dramatically different, suggesting that the properties of human gonadotropin receptors may differ from those of experimental animal models (17). To more clearly elucidate the properties of hFSH receptors, we report here the expression of a functional recombinant hFSH receptor with unique ligand specificity. Furthermore, the distribution of FSH receptor mRNA in human reproductive tissues and the biochemical properties of the expressed receptor are presented.

Received February 7, 1992.

Address all correspondence and requests for reprints to: Dr. Aaron J. W. Hsueh, Division of Reproductive Biology, Department of Obstetrics and Gynecology, Stanford University School of Medicine, 300 Pasteur Drive, Stanford, California 94305–5317.

* This work was supported by NIH Grant HD-23273.

† Postdoctoral fellow supported by the Lalor Foundation.

‡ On leave from the Department of Obstetrics and Gynecology, Hokkaido University, Sapporo, Japan.

Materials and Methods

Reagents and hormones

Restriction enzymes were obtained from Bethesda Research Laboratories (BRL; Gaithersburg, MD), Boehringer-Mannheim (Indianapolis, IN), and Stratagene (La Jolla, CA). A λgt11 human testicular cDNA

library was obtained from Clontech (Palo Alto, CA). The eukaryotic expression vector pCMX was a gift from Dr. K. Umesono of The Salk Institute (San Diego, CA). The recombinant human gonadotropin preparations were derived from serum-free conditioned medium of Chinese hamster ovary (CHO) cell lines transfected with human gonadotropin genes. The recombinant hLH contains a deletion of seven hydrophobic amino acids at the carboxyl-terminus and a substitution of Trp to Arg at position eight of the β-subunit for efficient dimerization and secretion from CHO cells (18). The recombinant hFSH has biological activity and chromatofocusing profiles similar to those of purified pituitary FSH (19). The concentrations of the recombinant gonadotropins were estimated in RIAs using purified pituitary preparations as standards (hLH, hLH I-3, 5,900 IU/mg; hFSH, hFSH I-3, 3,100 IU/mg by the hCG augmentation assay). hFSH (I-3), hCG (CR-127; 14,900 IU/mg), hLH (B1; 4,015 IU/mg), hTSH (B1; 15 IU/mg), rFSH (I-7; 4,714 IU/mg), and ovine (o) FSH (oFSH-17; 25 IU/mg) were obtained from the National Hormone and Pituitary Distribution Program (Bethesda, MD); recombinant hTSH was obtained from Genzyme (Cambridge, MA); equine (e) CG (PMSG; 2,530 IU/mg) was obtained from Calbiochem (La Jolla, CA); and porcine (p) FSH was the gift of Dr. H. Papkoff (University of California-San Francisco). Reagents required for the luciferase assay were purchased from Analytical Luminescence Laboratory (San Diego, CA).

cDNA library screening

A fragment of rFSH receptor cDNA, corresponding to bases 621–1031 of the published sequence (13), was obtained by reverse transcription-polymerase chain reaction of RNA prepared from PMSG-primed rat ovaries (20). This cDNA fragment was radiolabeled by the random priming method (21) and used to screen the human testicular cDNA library (22). Eight positively hybridizing phage clones ranging in size from 1.8–2.2 kilobases (kb) were isolated, subcloned into the pBluescript II SK plasmid (Stratagene), and sequenced using the dideoxy chain termination method (23) with a DNA sequencing kit (U.S. Biochemical Corp., Cleveland, OH) and specific primers. Individual fragments obtained from two separate clones (H37 and G3) were prepared by *Bam*HI restriction enzyme digestion and ligated at nucleotide position 686 to yield the final hFSH receptor cDNA construct containing the entire amino acid-coding region. Clone H37 contains 75-basepairs (bp) of 5′-untranslated region plus 1562 bp of open reading frame, but lacks the 3′-end and polyadenylation signal. Clone G3 starts at 168 bp of the open reading frame and covers the entire amino acid-coding region to the termination codon plus 26 bp of the 3′-untranslated region. These clones contain a 1394-bp overlapping region with identical nucleotide sequence, the identity of which was further confirmed by sequence analysis of the remaining six clones. The DNA sequence of the final clone was determined on both strands and compared to the published sequence of a cloned, but not expressed, human ovarian FSH receptor cDNA (24). Sequence comparison indicated seven individual basepair substitutions between our and the reported clone, resulting in five different amino acids at the following positions: 112 (Thr to Asn), 197 (Ala to Glu), 198 (Val to Leu), 307 (Ala to Thr), and 680 (Ser to Asn).

Expression of full-length cDNA in eukaryotic cells

An *Eco*RI linker (Promega, Madison, WI) was inserted into the *Eco*RV restriction site of the pCMX expression vector (17) to generate a plasmid (designated pCME) containing an *Eco*RI cloning site. The cDNA construct coding for the entire hFSH receptor (−75 to 2085 bp plus 26 bp of the 3′-untranslated region) was then subcloned into the *Eco*RI site of the pCME vector and partially sequenced to determine the orientation of the cDNA insert. Exponentially growing 293 cells derived from human fetal kidney were transiently transfected in 5 ml Dulbecco's Modified Eagle's Medium (DMEM; supplemented with 5% fetal calf serum, 2 mM L-glutamine, 100 U/ml penicillin, and 100 μg/ml streptomycin sulfate; Gibco, Santa Clara, CA) with the expression plasmid (designated pCME-hFSHR) using the calcium phosphate precipitation method (25) used routinely in our laboratory (17). Twenty-four hours after transfection, FSH receptor binding studies were performed by incubating cells (2 × 10^5/0.4 ml) with [^{125}I]hFSH at 22 C for 20 h or as indicated. Iodination of hFSH (I-3) was performed using the lactoperoxidase method (26). The specific activity and maximal binding of [^{125}I]hFSH, as determined by radioligand receptor assay using rat testicular membranes, were 99,000–110,000 cpm/ng and 7%, respectively. Nonspecific binding was determined by inclusion of a 1,000-fold excess of unlabeled ligand (Pergonal, Serono Laboratories, Randolph, MA). Similar procedures were used to analyze the ligand specificity of FSH-binding sites in testicular homogenates prepared from 15-day-old Sprague-Dawley rats (Johnson Labs, Bridgeview, IL). For cAMP analysis, transfected 293 cells (2 × 10^5/culture dish) were treated with various gonadotropins in the presence of 0.25 mM 3-isobutyl-1-methylxanthine (MIX; Sigma Chemical Co., St. Louis, MO) for 2 h at 37 C. After incubation, extracellular cAMP levels were determined by specific RIA, using [^{125}I]cAMP (ICN, Costa Mesa, CA) as the labeled ligand and a commercially available cAMP antiserum (ICN) (27). The intra- and interassay coefficients of variation were 6% and 10%, respectively.

Luciferase reporter gene

A 654-bp fragment of the 5′-flanking sequence of the rat tissue plasminogen activator (tPA) gene ligated to the luciferase gene plasmid p19LUC (28) was used (designated ptPA-LUC) (29). This portion of the tPA promoter region contains a cAMP-responsive element capable of mediating gonadotropin-stimulated tPA gene transcription (29). Exponentially growing 293 cells were transiently transfected in 5 ml DMEM with pCME-hFSHR and ptPA-LUC plasmids (at a ratio of 0.8:0.2; 7.5 μg total DNA). After transfection, cells were collected, counted, and dispensed into 12 × 75-mm culture tubes (5 × 10^4 cells/tube). The total volume was brought to 0.3 ml with DMEM containing 0.25 mM MIX with hFSH or hCG, and cells were incubated for 18 h at 37 C. After incubation, cells were lysed by the addition of 0.3 ml/tube 2 × lysis buffer [50 mM Tris-phosphate (pH 7.8), 4 mM dithiothrietol, 4 mM 1,2-diaminocyclohexane-*N*,*N*,*N*′,*N*′-tetraacetic acid, 20% glycerol, and 2% Triton X-100] at 22 C for 15 min. For estimation of luciferase activity, 10 μl cell lysate mixture were combined with 100 μl assay reagent [20 mM tricine, 1.07 mM $(MgCO_3)_4$ $Mg(OH)_2$–$5H_2O$, 2.67 mM $MgSO_4$, 0.1 mM EDTA, 33.3 mM dithiothrietol, 270 μM coenzyme-A, 470 μM luciferin, and 530 μM ATP], and light production was immediately measured for 10 sec in a luminometer (Monolight 2010, Analytical Luminescence Laboratory).

Preparation of nucleic acid probe for hFSH receptor mRNA

A fragment of the hFSH receptor cDNA, corresponding to bases 744–1026, was isolated after digestion of the hFSH receptor cDNA with the *Hin*cII restriction enzyme. This fragment, which possesses less than 50% nucleotide sequence homology to the hLH receptor cDNA (17), was subcloned into the pGEM4z vector (Promega). The plasmid clone was linearized with the *Sal*I restriction enzyme and served as a template for the production of a cRNA probe using T7 RNA polymerase (BRL) and [α-^{32}P]CTP (3000 Ci/mmol; Amersham, Arlington Heights, IL), as previously described (30).

Northern blot analysis

Human ovarian and placental tissues were provided by Dr. T. Tanaka (Hokkaido University, Sapporo, Japan) and Dr. A. Murphy (University of California-San Diego), respectively. Total RNA was extracted from human tissues using the guanidinium thiocyanate-phenol-chloroform extraction procedure (31). Total RNA samples were enriched for poly(A) mRNA by a single round of oligo(dT) column chromatography (Pharmacia LKB Biotechnology, Piscataway, NJ) and electrophoresed through 1% agarose-2.2 M formaldehyde gels. Samples were blotted onto nitrocellulose membranes (Schleicher and Schuell, Keene, NH) by overnight capillary electrophoresis and covalently cross-linked using a UV cross-linker (Stratagene). Membranes were then prehybridized for 2–4 h at 65 C in the presence of 50% formamide under standard conditions, followed by hybridization with the radiolabeled hFSH receptor cRNA probe at the same temperature for 18–20 h (20, 32, 33). Membranes were washed in 2 × sodium chloride-sodium citrate (SSC)-0.1% sodium dodecyl sulfate (SDS) for 10 min at room temperature, followed by two or three consecutive 15- to 20-min washes in 0.1 × SSC-0.1% SDS at

65 C, and exposed to Kodak X-Omat film (Eastman Kodak, Rochester, NY) for 1–5 days at −70 C.

Ligand receptor cross-linking

Cross-linking of [^{125}I]hFSH to binding sites in transfected 293 cells and rat testicular homogenates was performed using disuccinimidyl suberate (Pierce, Rockford, IL), as previously described (34). Briefly, 6 × 10^6 transfected 293 cells or homogenate from 10 immature rat testes were incubated with 8 × 10^5 cpm [^{125}I]hFSH in the absence or presence of a 1000-fold excess of unlabeled hormone at 22 C for 20 h in a total volume of 0.4 ml. After incubation, cells or homogenates were diluted with 1 ml wash solution (Dulbecco's PBS containing 0.1% BSA, 5 mM EDTA, and 5 mM *N*-ethylmaleimide), pelleted by centrifugation, washed, and recentrifuged. Pellets were then resuspended in 0.5 ml incubation buffer (D-PBS containing 10% dimethylsulfoxide), and disuccinimidyl suberate (freshly prepared in dimethylsulfoxide) was added to a final concentration of 1.5 mM. Cross-linking was carried out at 0 C for 30 min, and the reaction was stopped by the addition of 1 ml termination buffer [50 mM Tris-HCl (pH 7.5) and 100 mM NaCl]. The reaction tubes were centrifuged, and pellets were resuspended in 0.1 ml solubilization buffer [50 mM Tris-HCl (pH 7.5) and 1% Triton X-100]. Solubilization was performed by incubation at 0 C for 60 min, with mixing of samples every 15 min. The samples were centrifuged for 5 min at 13,000 × *g*, and the resultant supernatants were resolved by SDS-polyacrylamide gel electrophoresis (SDS-PAGE), using 8.5% polyacrylamide gels. The gels were then subjected to autoradiography at −70 C for 2–14 days.

Results

Expression and binding kinetics of hFSH receptors in eukaryotic cells

Cells derived from a human fetal kidney cell line (293) were transfected with the plasmid pCME-hFSHR. After a 24-h incubation, cells were analyzed by radioligand receptor binding (Fig. 1). A dose-dependent increase in specifically bound [^{125}I]hFSH was detected in transfected cells incubated with increasing concentrations of labeled FSH, whereas no specific binding was observed in nontransfected cells (data not shown). Analysis of receptor binding indicated a K_d value of 1.7 × 10^{-9} M.

To study the effects of incubation time and temperature on the kinetics of FSH receptor binding, transfected 293 cells were incubated with [^{125}I]hFSH at 4, 22, or 37 C for increasing lengths of time, after which specific binding was determined (Fig. 2). A time-dependent increase in the levels of specific FSH binding was observed in cells incubated at 22 and 37 C, whereas low levels of [^{125}I]hFSH binding were detected at 4 C. Maximal FSH binding was highest in cells incubated at 22 C, although the time required to reach maximal ligand binding was considerably longer in incubations conducted at 22 *vs.* 37 C (Fig. 2).

Interaction of hFSH receptor with recombinant and pituitary/urinary-derived human gonadotropins and TSH

To test the binding specificity of the expressed hFSH receptor for human gonadotropins, transfected 293 cells were incubated with [^{125}I]hFSH in the absence or presence of increasing doses of unlabeled urinary-derived hCG, or hFSH, hLH, or hTSH of both pituitary and recombinant origin. Displacement of labeled FSH from its binding sites was expressed relative to the total amount of specifically bound [^{125}I]hFSH (Fig. 3). Both recombinant and pituitary FSH preparations competed with [^{125}I]hFSH for FSH receptors expressed in 293 cells (ED_{50}: recombinant, 25 ng/ml; pituitary-derived, 70 ng/ml), whereas human pituitary LH and

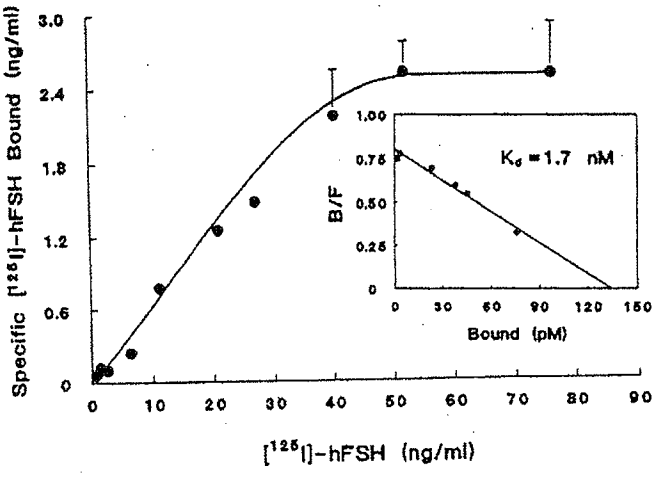

FIG. 1. Binding of [^{125}I]hFSH to hFSH receptors expressed in eukaryotic cells. 293 cells were transfected with the hFSH receptor plasmid pCME-hFSHR, and binding of radiolabeled hFSH was determined 24 h later. Cells (2 × 10^5/tube × 0.4 ml) were incubated with increasing concentrations of [^{125}I]hFSH in the absence or presence of a 1000-fold excess of unlabeled ligand. Levels of specifically bound [^{125}I]hFSH are shown together with the derived Scatchard plot (*inset*; B/F, bound to free ratio). Data are the mean ± SEM of triplicate determinations from a representative experiment.

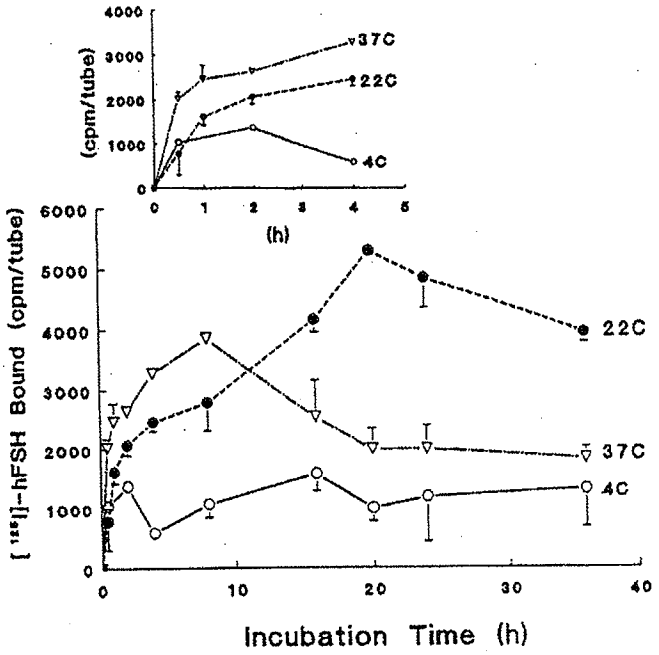

FIG. 2. Effects of incubation time and temperature on rate and extent of [^{125}I]hFSH binding to 293 cells. Transfected 293 cells (2 × 10^5/tube) expressing hFSH receptors were incubated with radiolabeled hFSH in the absence or presence of a 1000-fold excess of ligand at 4, 22, or 37 C for increasing lengths of time, after which levels of specifically bound [^{125}I]hFSH were calculated (mean ± SEM of triplicate determinations from a representative experiment). An enlarged figure for the first 4 h of incubation is presented in the *inset*.

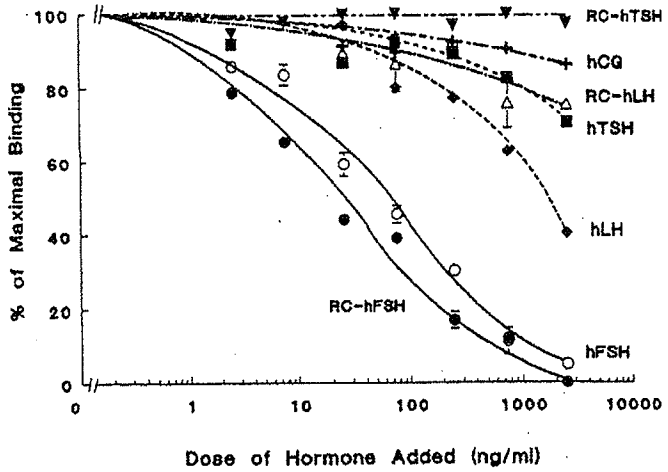

FIG. 3. Interaction of recombinant (RC) and pituitary/urinary-derived human gonadotropins and TSH with hFSH receptors expressed in transfected 293 cells. Displacement of [^{125}I]hFSH binding to hFSH receptors by hFSH, hLH, hCG, or hTSH was determined in radioligand receptor assays (mean ± SEM of three replicate experiments).

TSH were effective only at high doses. In contrast, negligible interaction of hCG or recombinant hLH or hTSH with the expressed FSH receptors was observed (Fig. 3).

Ligand specificity of human vs. rat FSH receptors

To assess the ligand specificity of the hFSH receptor, 293 cells expressing human receptors were incubated with [^{125}I] hFSH in the absence or presence of increasing doses of eCG (PMSG) or FSH from human, rat, ovine, and porcine origin. Displacement of [^{125}I]hFSH by unlabeled hormone in the human receptor was compared to that of testicular homogenates from 15-day-old rats (Fig. 4). hFSH and rFSH preparations were effective in binding to the recombinant hFSH receptor (ED_{50}: hFSH, 70 ng/ml; rFSH, 125 ng/ml), whereas only minimal interaction of oFSH, pFSH, or eCG with hFSH receptors was observed (Fig. 4A). In contrast, FSH from rat, human, and ovine origin as well as eCG effectively competed with radiolabeled FSH for binding sites in rat testicular homogenates (hFSH = rFSH > oFSH > eCG); however, pFSH was effective only at high doses (Fig. 4B).

Gonadotropin stimulation of cAMP production and tPA promoter-luciferase reporter gene by transfected 293 cells expressing hFSH receptors

The functional capacity of the recombinant hFSH receptor was tested based on gonadotropin stimulation of cAMP production by transfected 293 cells. Treatment of cells with human pituitary FSH caused a dose-dependent increase in cAMP formation (ED_{50}, 10 ng/ml), with a maximal 13-fold increase observed in response to 100 ng/ml FSH (Fig. 5A). Human pituitary LH also increased cAMP production at doses of 100 (4-fold) and 1000 (6.6-fold) ng/ml, whereas neither hCG nor recombinant hLH altered cAMP levels compared to control values (Fig. 5A).

Our earlier data demonstrated the stimulation of rat tPA

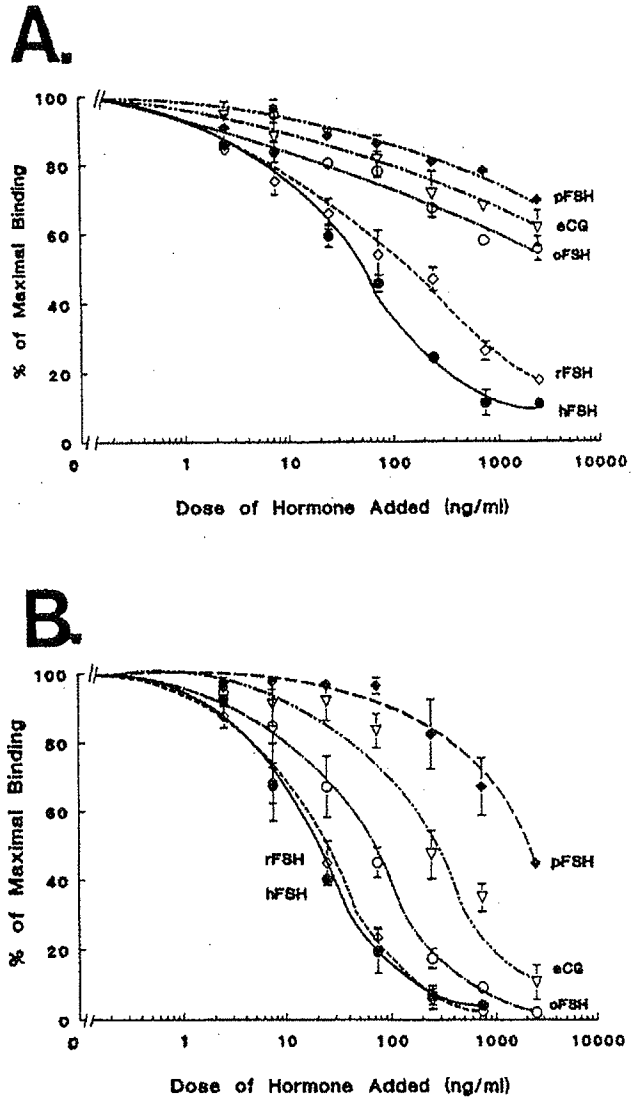

FIG. 4. Displacement of [^{125}I]hFSH binding to human and rat FSH receptors by human, rat, ovine, equine, and porcine gonadotropins. Transfected 293 cells expressing hFSH receptors (A) or rat testicular homogenates (B) were incubated with [^{125}I]hFSH in the absence or presence of hFSH, rFSH, oFSH, or pFSH as well as eCG. Displacement curves are presented as a percentage of maximal binding at each dose of unlabeled hormone (mean ± SEM of three replicate experiments).

gene expression in ovarian granulosa cells (32). In granulosa cells transfected with a luciferase reporter gene driven by a cAMP-responsive region of the rat tPA gene promoter, treatment with FSH increases luciferase expression (29). Using this tPA-luciferase reporter plasmid, we evaluated the ability of human gonadotropins to induce luciferase activity in 293 cells transfected with plasmids for both hFSH receptor and the reporter constructs. Treatment of cells with increasing doses of FSH, but not hCG, caused a dose-dependent increase in luciferase activity, with an estimated ED_{50} of 8 ng/ml and a maximal 2-fold increase at 100 ng/ml (Fig. 5B). These findings demonstrate a functional linkage of recombinant hFSH receptors to the tPA gene.

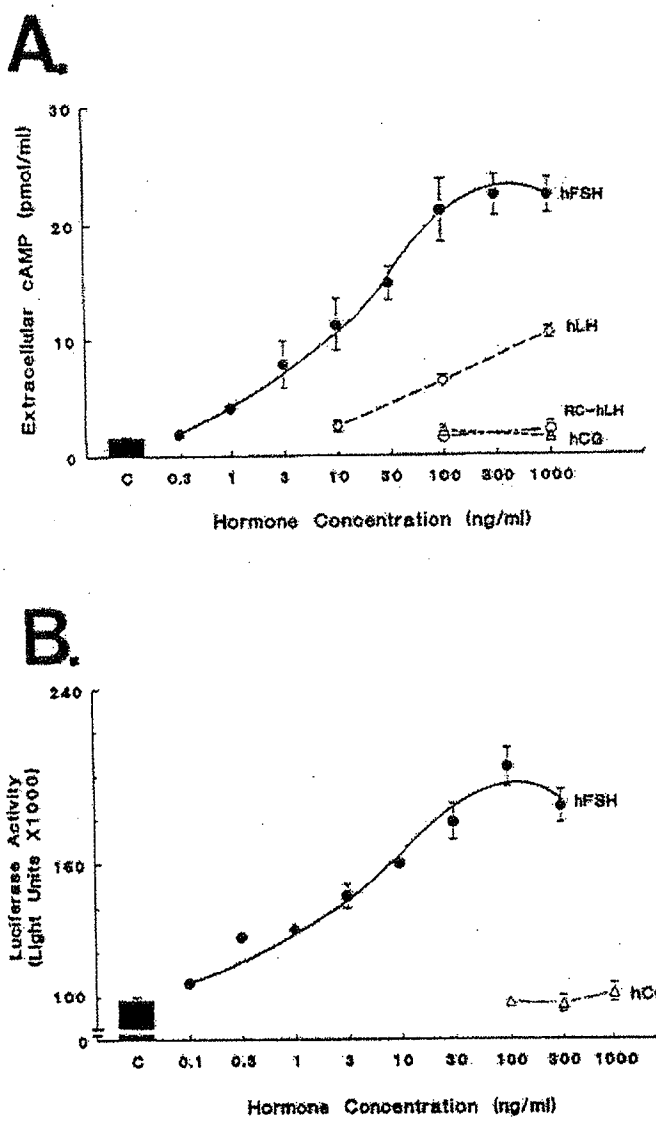

FIG. 5. Gonadotropin stimulation of cAMP production (A) and luciferase activity (B) by 293 cells expressing hFSH receptors. A, Extracellular cAMP accumulation was measured after incubation of transfected 293 cells (2×10^5/culture dish) for 2 h at 37 C with 0.25 mM MIX in the absence or presence of hFSH, hLH, or hCG. Data are the mean ± SEM of six cultures from three replicate experiments (RC, recombinant). B, Dose-dependent stimulation of luciferase activity by hFSH, but not hCG, in 293 cells cotransfected with the hFSH receptor plasmid and a tPA promoter-luciferase reporter gene construct (note the break in the y-axis). Data are the mean ± SEM of triplicate determinations from a representative experiment.

Northern blot analysis of FSH receptor mRNAs in human reproductive tissues

To study the expression of hFSH receptor mRNA, RNA was extracted from human reproductive tissues and analyzed by Northern blot, using a radiolabeled cRNA probe corresponding to the extracellular region of cDNA from our cloned hFSH receptor (Fig. 6). Analysis of poly(A)-enriched mRNA prepared from human follicular phase ovary indicated the existence of three mRNA transcripts (7.0, 4.2, and 2.5 kb) that were not detected in an equivalent amount of mRNA prepared from corpus luteum (day 21 of the menstrual cycle) or placenta (week 19 of pregnancy; Fig. 6).

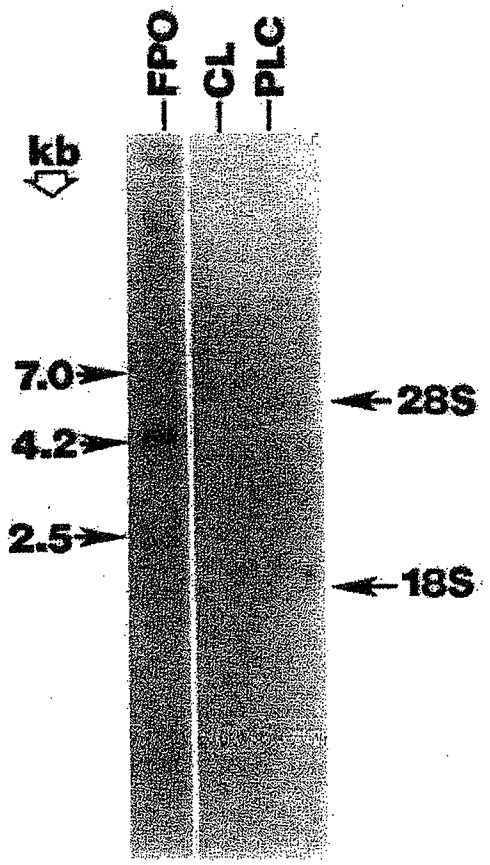

FIG. 6. Northern blot analysis of hFSH receptor mRNAs in human reproductive tissues. Poly(A)-enriched RNA samples prepared from human follicular phase ovary (FPO), 21-day-old corpora lutea (CL), or 19-week-old placenta (PLC) (2 μg/lane) were resolved through denaturing agarose gels, transferred to nitrocellulose filters, and hybridized to a ^{32}P-labeled hFSH receptor cRNA probe. Filters were washed and exposed to photographic films for 5 days at −70 C. Migration distances of the 28S and 18S ribosomal RNAs of a parallel total RNA sample from human ovary are indicated.

Cross-linking of [^{125}I]hFSH to FSH-binding sites in transfected cells and immature rat testes

To estimate the molecular size of the recombinant hFSH receptor, [^{125}I]hFSH was cross-linked to FSH-binding sites in transfected 293 cells using disuccinimidyl suberate, followed by SDS-PAGE analysis (Fig. 7). A predominant autoradiographic band of protein, with an estimated molecular mass of 109 kilodaltons (kDa; 76 kDa for the binding protein after correction for mass attributed to the ligand) was detected in transfected cells expressing hFSH receptors, whereas a 1000-fold excess of ligand completely blocked [^{125}I]hFSH binding (Fig. 7). A less abundant protein band of approximately 145 kDa (112 kDa for the binding protein) was also present. These findings were comparable to those observed for FSH

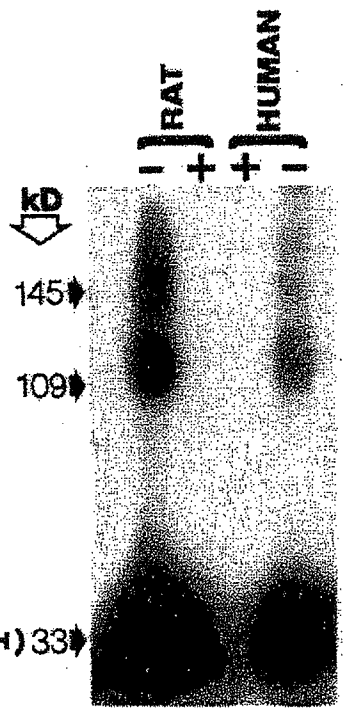

FIG. 7. Cross-linking of hFSH- and rFSH-receptors to [125I]hFSH. Radiolabeled hFSH was cross-linked to FSH receptors in transfected 293 cells expressing hFSH receptors (HUMAN) or rat testicular homogenates (RAT) using disuccinimidyl suberate. Proteins were separated through 8.5% polyacrylamide gels and analyzed by autoradiography (14 days at −70 C). The sizes of the proteins were estimated by comparison to migration distances of known protein mol wt standards. Symbols indicate the absence (−) or presence (+) of a 1000-fold excess of ligand (Pergonal) during the binding incubation period before the cross-linking reaction.

receptors found in testicular homogenates of immature rats under the same experimental conditions (Fig. 7).

Discussion

We report here the ligand specificity and biochemical properties of the recombinant hFSH receptor. Our data indicate that hFSH, but not LH or CG, competes with [125I] hFSH for binding to the recombinant FSH receptor. In addition, hFSH stimulates cAMP production in 293 cells expressing the human receptor, whereas recombinant hLH and hCG are without effect. As a result of stimulation of endogenous cAMP levels by FSH, a tPA promoter-driven luciferase reporter gene was also activated. Similar to the species-specific ligand binding recently reported for the hLH receptor (17), the recombinant hFSH receptor interacts with hFSH and rFSH, but only minimally with eCG or FSH of ovine and porcine origins. We also report here the first identification of FSH receptor mRNA in human ovaries as well as the determination of the molecular size of the recombinant hFSH receptor through ligand cross-linking analysis.

Comparison of the present human testicular FSH receptor cDNA with an ovarian cDNA clone recently reported (24) indicated seven individual basepair substitutions throughout the receptor sequence, resulting in five amino acid changes. Although we are uncertain of the basis for the observed disparity between our and the reported clone, our FSH receptor cDNA could be expressed, whereas no expression data were reported for the ovarian clone. Additionally, four of the five variant amino acids are identical between our hFSH and the reported rFSH receptor sequence (13). The ability of 293 cells transfected with our cDNA to express high affinity FSH receptors coupled to the endogenous adenyl cyclase and a luciferase reporter gene indicates that our clone encodes for a functional protein.

The availability of a cell line that expresses recombinant hFSH receptors has provided an unlimited source of the human receptor and enabled us to perform analysis of the ligand specificity of the human receptor. Radioligand receptor assays demonstrated that the hFSH receptor does not interact with hCG or recombinant hLH or hTSH at physiological or supraphysiological concentrations. However, highly purified human pituitary LH and TSH did cross-react with recombinant FSH receptors, suggesting that the pituitary hormone preparations contain minor FSH contamination. Furthermore, unlike the ability of rat testicular FSH receptors to recognize gonadotropin preparations from diverse species (Ref. 35 and the present study), the human receptor interacted preferentially with human and rat FSH. These findings coupled with a similar species-specific ligand binding of hLH receptors (17) indicate significant evolutionary changes in both human gonadotropin receptors. Alternatively, we cannot rule out subtle differences in posttranslational processing of the receptor in 293 cells *vs.* gonadal cells that may influence its binding characteristics. However, the ligand specificity of hLH-binding sites expressed in 293 cells (17) is identical to that of native LH receptors present in human corpus luteum (36), suggesting that the properties of these recombinant proteins are similar to those of endogenous gonadal receptors.

Saturation binding and Scatchard analysis demonstrated that the recombinant FSH-binding site has an estimated K_d of 1.7 nM, comparable to that reported for FSH receptors in human testes (37). In addition, the effects of incubation time and temperature on the rate and extent of [125I]hFSH binding by recombinant hFSH receptors were similar to those reported for rat testicular FSH (35) and LH (38) receptors. Recombinant hFSH receptors occupied by gonadotropin are also capable of interacting with the endogenous G-proteins of the 293 cells to increase cAMP formation, thus providing a useful model to study FSH-activated signal transduction. Additionally, the use of a luciferase reporter gene driven by the cAMP-responsive promoter of the rat tPA gene (29) has indicated that transfected cells expressing hFSH receptors respond to FSH with increased luciferase activity. These findings provide evidence that FSH-induced signal transduction in cells expressing recombinant hFSH receptors is coupled to the activation of genes that are regulated by gonadotropins under physiological conditions within gonadal cells (32). However, the relatively small magnitude of the FSH response using the luciferase system (compared to cAMP) suggests a potential limitation of this assay in its present form. The reasons for this observation are unclear, but may

be related to the lack of gonadal cell-specific transcription factors in 293 cells that limit the activation of the luciferase reporter gene construct. Nonetheless, future modifications of the present cell model and the cAMP-driven luciferase gene reporter system should provide a useful and sensitive bioassay for hFSH.

The availability of hFSH receptor cDNA enabled us to study FSH receptor mRNA transcripts within human reproductive tissues. Northern blot analysis revealed the existence of several FSH receptor mRNAs within human follicular phase ovary, consistent with those reported for multiple FSH receptor mRNA transcripts in rat gonadal tissues (20, 39, 40). However, RNA prepared from human corpora lutea did not contain detectable levels of this message, suggesting that ovarian FSH receptor mRNA levels undergo up- and down-regulation during the human menstrual cycle in a manner similar to that reported for experimental animal models (20, 41).

Based on the deduced amino acid sequence of the hFSH receptor cDNA, the calculated molecular mass of the mature protein is approximately 75.6 kDa, consistent with the size estimation of recombinant FSH receptor based on ligand cross-linking and SDS-PAGE and comparable to that observed for FSH receptors in immature rat testes. Of interest was the finding of a less abundant 112-kDa FSH-binding site in both transfected 293 cells and rat testes, presumably resulting from posttranslational glycosylations of the protein. Alternatively, the smaller FSH-binding site may arise from proteolytic cleavage of the larger 112-kDa protein, as has been suggested by previous studies on hCG-binding sites in rat gonadal tissues (42).

Previous studies using nonreducing PAGE followed by ligand blotting have estimated the size of the FSH receptor in bovine and rat testicular membranes to be approximately 240 kDa (43, 44), possibly resulting from receptor aggregation and dimer formation. Moreover, photoaffinity labeling of the pFSH receptor revealed the presence of a major cross-linked complex of 104 kDa, which could be reduced with dithiothrietol into two smaller complexes of 75 and 61 kDa (45). Although the reasons for the discrepancy between our and earlier findings are unclear, they may result from varying methodologies (*e.g.* ligand-receptor cross-linking *vs.* ligand blotting) or species differences. Our data, however, suggest that binding of FSH does not require prior dimerization of its receptor on the plasma membrane, although it is possible that receptor aggregation may be important for receptor stability and/or signal transduction (46).

Expression of the hFSH receptor provides unlimited material for future studies of clinical interest. Additionally, the ability to measure cAMP production and luciferase reporter gene activity in a cell line expressing hFSH receptors should allow the establishment of a sensitive bioassay for human gonadotropins and for screening new FSH agonists and antagonists. Because earlier reports have suggested the presence of circulating antibodies against FSH receptor in patients with premature ovarian failure (47–49), the etiology of pathophysiological conditions associated with gonadotropin receptor dysfunction may also be more clearly elucidated.

Note Added in Proof

Amplification of human ovarian and testicular mRNA by reverse transcription polymerase chain reaction with oligonucleotide primers specific for human FSH receptor cDNA sequences, followed by direct sequencing of resultant PCR products after T7 gene 6 exonuclease treatment (50), indicated 100% sequence identity of this human FSH receptor cDNA with our clone obtained by cDNA library screening. Furthermore, independent cloning of human FSH receptor cDNA by R. Dijkema and R. de Leeuw (Organon, Oss, the Netherlands) also indicated 100% sequence identity with our cDNA clone (personal communication). Accession no. M95489.

Acknowledgments

The authors thank Dr. T. Ny (University of Umea, Umea, Sweden) for the rat tPA promoter-luciferase reporter gene; Drs. M. Oikawa and P. S. LaPolt for polymerase chain reaction analysis of the rFSH receptor cDNA; Dr. I. Boime (Washington University, St. Louis, MO) for provision of CHO cells secreting human LH and FSH; Dr. K. Umesono (The Salk Institute, San Diego, CA) for the pCMX expression vector and 293 cell line; Dr. T. Tanaka (Hokkaido University, Sapporo, Japan) for human ovarian tissues; Dr. A. Murphy (University of California-San Diego) for human placental tissue; Dr. H. Papkoff (University of California-San Francisco) for the gift of pFSH; and the National Hormone and Pituitary Distribution Program (Bethesda, MD) for hFSH, hLH, hCG, hTSH, rFSH, and oFSH.

References

1. **Pierce JG, Parsons TF** 1981 Glycoprotein hormones: structure and function. Annu Rev Biochem 50:465–495
2. **Ryan RJ, Charlesworth MC, McCormick DJ, Milius RP, Keutmann HT** 1988 The glycoprotein hormones: recent studies of structure-function relationships. FASEB J 2:2661–2669
3. **Kourides IA, Gurr JA, Wolf O** 1984 The regulation and organization of thyroid stimulating hormone genes. Recent Prog Horm Res 40:79–120
4. **Reichert Jr LE, Dattatreyamurty B** 1989 The follicle-stimulating hormone (FSH) receptor in testis: interaction with FSH, mechanism of signal transduction, and properties of the purified receptor. Biol Reprod 40:13–26
5. **Keinanen KP, Rajaniemi HJ** 1986 Rat ovarian lutropin receptor is a transmembrane protein. Biochem J 239:83–87
6. **Lefkowitz RJ, Caron MG** 1988 Adrenergic receptors. Models for the study of receptors coupled to guanine nucleotide regulatory proteins. J Biol Chem 263:4993–4996
7. **Birnbaumer L, Abramowitz J, Brown AM** 1990 Receptor-effector coupling by G proteins. Biochim Biophys Acta 1031:163–224
8. **Kobilka B** 1992 Adrenergic receptors as models for G protein-coupled receptors. Annu Rev Neurosci 15:87–114
9. **Strader CD, Dixon RAF, Cheung AH, Candelore MR, Blake AD, Sigal IS** 1977 Mutations that uncouple the β-adrenergic receptor from Gs and increase agonist efficiency. J Biol Chem 262:16439–16443
10. **Kobilka BK, Kobilka TS, Daniel K, Regan JW, Caron MC, Lefkowitz RJ** 1988 Chimeric α2 and β2-adrenergic receptors: delineation of domains involved in effector coupling and ligand binding specificity. Science 240:1310–1316
11. **Chazenbalk GD, Nagayama Y, Russo D, Wadsworth HL, Rapoport B** 1990 Functional analysis of the cytoplasmic domains of the human thyrotropin receptor by site-directed mutagenesis. J Biol Chem 265:20970–20975
12. **McFarland KC, Sprengel R, Phillips HS, Kohler M, Rosemblit N, Nikolics K, Segaloff DL, Seeburg PH** 1989 Lutropin-chorionogonadotropin receptor: an unusual member of the G protein-coupled receptor family. Science 245:494–499
13. **Sprengel R, Braun T, Nikolics K, Segaloff DL, Seeburg PH** 1990 The testicular receptor for follicle-stimulating hormone: structure and functional expression of cloned cDNA. Mol Endocrinol 4:525–

530
14. **Means AR, Fakunding JL, Huckins C, Tindall DJ, Vitale R** 1976 Follicle-stimulating hormone, the Sertoli cell, and spermatogenesis. Recent Prog Horm Res 32:477–527
15. **Richards JS** 1980 Maturation of ovarian follicles: actions and interactions of pituitary and ovarian hormones on follicular cell development. Physiol Rev 60:51–89
16. **Hsueh AJW, Bicsak TA, Jia X-C, Dahl KD, Fauser BCJM, Galway AB, Czekala N, Pavlou SN, Papkoff H, Keene J, Boime I** 1989 Granulosa cells as hormone targets: the role of biologically active follicle-stimulating hormone in reproduction. Recent Prog Horm Res 45:209–277
17. **Jia X-C, Oikawa M, Bo M, Tanaka T, Ny T, Boime I, Hsueh AJW** 1991 Expression of human luteinizing hormone (LH) receptor: interaction with LH and chorionic gonadotropin from human but not equine, rat, and ovine species. Mol Endocrinol 5:759–768
18. **Matzuk MM, Spangler MM, Camel M, Suganuma N, Boime I** 1989 Mutagenesis and chimeric genes define determinants in the β subunits of human chorionic gonadotropin and lutropin for secretion and assembly. J Cell Biol 109:1429–1438
19. **Keene JL, Matzuk MM, Otani T, Fauser BCJM, Galway AB, Hsueh AJW, Boime I** 1989 Expression of biologically active human follitropin in Chinese hamster ovary cells. J Biol Chem 264:4769–4775
20. **LaPolt PS, Tilly JL, Aihara T, Nishimori K, Hsueh AJW** 1992 Gonadotropin-induced up- and down-regulation of ovarian FSH receptor gene expression: effects of PMSG, hCG and recombinant FSH. Endocrinology 130:1289–1295
21. **Feinberg AP, Vogelstein B** 1983 A technique for radiolabeling DNA restriction endonuclease fragments to high specific activity. Anal Biochem 132:6–13
22. **Maniatis T, Fritsch EF, Sambrook J** 1982 Molecular Cloning–A Laboratory Manual. Cold Spring Harbor Laboratory, Cold Spring Harbor
23. **Hattori M, Sakai Y** 1986 Dideoxy sequencing method using denatured plasmid templates. Anal Biochem 15:232–238
24. **Minegish T, Nakamura K, Takakura Y, Ibuki Y, Igarashi M** 1991 Cloning and sequencing of human FSH receptor cDNA. Biochem Biophys Res Commun 175:1125–1130
25. **Chen C, Okayama H** 1987 High efficiency transformation of mammalian cells by plasmid DNA. Mol Cell Biol 7:2745–2752
26. **Miyachi Y, Vaitukaitis JL, Nieschlag E, Lipsett MB** 1972 Enzymatic radioiodination of gonadotropins. J Clin Endocrinol Metab 34:23–28
27. **Davoren JB, Hsueh AJW** 1985 Vasoactive intestinal peptide: a novel stimulator of steroidogenesis by cultured rat granulosa cells. Biol Reprod 33:37–52
28. **De Wet JR, Wood KV, DeLuca M, Helinski DR, Subramani S** 1987 Firefly luciferase gene: structure and expression in mammalian cells. Mol Cell Biol 7:725–737
29. **Feng P, Ohlsson M, Ny T** 1990 The structure of the TATA-less rat tissue-type plasminogen activator gene. J Biol Chem 265:2022–2027
30. **Melton DA, Krieg PA, Rebagliati MR, Maniatis T, Zinn K, Green MR** 1984 Efficient *in vitro* synthesis of bioactive RNA and RNA hybridization probes from plasmids containing a bacteriophage SP6 promoter. Nucleic Acids Res 12:7035–7056
31. **Chomczynski P, Sacchi N** 1987 Single-step method of RNA isolation by acid guanidinium thiocyanate-phenol-chloroform extraction. Anal Biochem 162:156–159
32. **Ohlsson M, Hsueh AJW, Ny T** 1988 Hormonal regulation of tissue-type plasminogen activator ribonucleic acid levels in rat granulosa cells: mechanism of induction by follicle-stimulating hormone and gonadotropin-releasing hormone. Mol Endocrinol 2:854–861
33. **LaPolt PS, Oikawa M, Jia X-C, Dargan C, Hsueh AJW** 1990 Gonadotropin-induced up- and down-regulation of rat ovarian LH receptor message levels during follicular growth, ovulation and luteinization. Endocrinology 126:3277–3279
34. **Mathews LS, Vale WW** 1991 Expression cloning of an activin receptor, a predicted transmembrane serine kinase. Cell 65:973–982
35. **Means AR, Vaitukaitis J** 1972 Peptide hormone "receptors:" specific binding of ^{3}H-FSH to testis. Endocrinology 90:39–46
36. **Cole FE, Weed JC, Schneider GT, Holland JB, Geary WL, Levy DL, Huseby RA, Rice BF** 1976 The specificity of gonadotropin binding by the human corpus luteum. Fertil Steril 27:921–928
37. **Wahlstrom T, Huhtaniemi I, Hovatta O, Seppala M** 1983 Localization of luteinizing hormone, follicle-stimulating hormone, prolactin, and their receptors in human and rat testis using immunocytochemistry and radioreceptor assay. J Clin Endocrinol Metab 57:825–830
38. **Catt KJ, Tsuruhara T, Dufau L** 1972 Gonadotropin binding sites of the rat testis. Biochim Biophys Acta 279:194–201
39. **Heckert LL, Griswold MD** 1991 Expression of follicle-stimulating hormone receptor mRNA in rat testis and Sertoli cells. Mol Endocrinol 5:670–677
40. **Tilly JL, LaPolt PS, Hsueh AJW** 1992 Hormonal regulation of follicle-stimulating hormone receptor messenger RNA levels in cultured rat granulosa cells. Endocrinology 130:1296–1302
41. **Camp TA, Rahal JO, Mayo KE** 1991 Cellular localization and hormonal regulation of follicle-stimulating hormone and luteinizing hormone receptor mRNAs in the rat ovary. Mol Endocrinol 5:1405–1417
42. **Roche PC, Ryan RJ** 1989 Purification, characterization, and amino-terminal sequence of the ovarian receptor for luteinizing hormone/human choriogonadotropin. J Biol Chem 264:4636–4641
43. **Dattatreyamurty B, Zhang S-B, Reichert Jr LE** 1990 Purification of follitropin receptor from bovine calf testes. J Biol Chem 265:5494–5503
44. **Reichert Jr LE, Dattatreyamurty B, Grasso P, Santa-Coloma TA** 1991 Structure-function relationships of the glycoprotein hormones and their receptors. Trend Pharmacol Sci 12:199–203
45. **Shin J, Ji TH** 1985 Photoaffinity labeling of the follitropin receptor. J Biol Chem 260:14020–14025
46. **Podesta EJ, Solano AR, Attar R, Sanchez ML, Molina-Veda L** 1983 Receptor aggregation induced by antilutropin receptor antibody and biological response in rat testis Leydig cells. Proc Natl Acad Sci USA 80:3986–3990
47. **Dias JA, Gates SA, Reichert Jr LE** 1982 Evidence for the presence of follicle-stimulating hormone receptor antibody in human serum. Fertil Steril 38:330–338
48. **Chiauzzi V, Cigorra S, Escobar ME, Rivarola MA, Charreau EH** 1982 Inhibition of follicle-stimulating hormone receptor binding by circulating immunoglobulin. J Clin Endocrinol Metab 54:1221–1228
49. **van Weissenbruch MM, Hoek A, van Vliet-Bleeker I, Schoemaker J, Drexhage H** 1991 Evidence for the existence of immunoglobulins that block ovarian granulosa cell growth *in vitro*. A putative role in resistant ovary syndrome. J Clin Endocrinol Metab 73:360–367
50. **Shon M, Gerimo J, Bastia D** 1982 The nucleotide sequence of replication origin β of the plasmid R6K. J Biol Chem 257:13823–13827

Br. J. Pharmacol. (1992), **106**, 61–66

Combined dose-ratio analysis of cholecystokinin receptor antagonists, devazepide, lorglumide and loxiglumide in the guinea-pig gall bladder

*[1]L.A. Bishop, V.P. Gerskowitch, R.A.D. Hull, N.P. Shankley & J.W. Black

James Black Foundation, 68 Half Moon Lane, London SE24 9JE and *Department of Analytical Pharmacology, King's College School of Medicine & Dentistry, The Rayne Institute, 123 Coldharbour Lane, London SE5 9NU

1 Interactions between cholecystokinin octapeptide (CCK-8) and CCK_A-receptor antagonists derived from benzodiazepines (devazepide) and glutamic acid (lorglumide and loxiglumide) have been examined in an improved bioassay using the guinea-pig, isolated, gall bladder preparation.

2 The presence of CCK_B-receptors in the assay was provisionally-ruled out on the basis of the low potency of pentagastrin in the assay. By applying analyses of both agonism and antagonism, pentagastrin was shown to behave as a partial agonist at the CCK_A-receptor.

3 Devazepide, lorglumide and loxiglumide behaved as simple competitive antagonists of CCK_A-receptors and pK_B values of 9.98, 7.59 and 7.07 were estimated, respectively.

4 Application of a combined dose-ratio analysis to the interactions between CCK-8 and combinations of devazepide/lorglumide and devazepide/loxiglumide indicated that these molecules behave as syntopic, competitive, antagonists at the CCK_A-receptor.

5 We conclude that the guinea-pig gall bladder assay contains a homogeneous population of CCK_A-receptors and offer an explanation for the differences between our results and those obtained recently by Maubach *et al.* (1991) which were taken as preliminary evidence for CCK_A-receptor heterogeneity.

Keywords: Receptor, cholecystokinin; muscle, smooth, gall bladder; pentagastrin; devazepide; lorglumide; loxiglumide

Introduction

The pharmacological classification of cholecystokinin (CCK)/gastrin receptors as CCK_A and CCK_B was proposed on the basis of the behaviour of selective agonists and antagonists in both radioligand binding studies and functionally-intact bioassays (see Woodruff & Hughes, 1991). Among the most frequently-used antagonists for testing and developing this classification are the benzodiazepine derivative, devazepide (Evans *et al.*, 1986) and the glutamic acid derivatives lorglumide (Makovec *et al.*, 1987) and loxiglumide (Setnikar *et al.*, 1987). Devazepide, lorglumide and loxiglumide are reported to be selective, competitive, antagonists for CCK_A-receptors with pK_D values of $\sim$ 10.1, 7.7 and 6.5, respectively as compared with pK_D values at CCK_B-receptors of $\sim$ 6.6, 5.6 and 5.0, respectively (Setnikar *et al.*, 1987; Lotti & Chang, 1989). These pK_B values have been estimated on the assumption that the agonist-antagonist interactions are competitive. If these ligands are to be used to prove the homogeneity of hormone receptors, then the assumption that the competitive behaviour is due to mutual exclusivity at a common site, so called syntopic behaviour, must be made.

However, 'competitive' behaviour can be found for example in bioassays involving high efficacy agonists and functional antagonists and in ligand binding assays involving agonists and allosteric antagonists.

There are marked differences in chemical structure and physico-chemical properties between the benzodiazepine and glutamic acid derivatives and the peptide hormone itself. Consequently, it seemed pertinent to question whether these ligands compete for the same site at the CCK_A-receptor. We have applied a combined dose-ratio analysis (Paton & Rang, 1965; Black *et al.*, 1986; Shankley *et al.*, 1988) which, as far as we are aware, provides the only currently available test for behaviour consistent with a syntopic, competitive mechanism of action. The experiments were performed on the guinea-pig gall bladder assay which has conventionally been considered to contain a single population of CCK_A-receptors. We found that it was necessary to improve the existing assay so that it met the generally-accepted criteria for quantitative analysis (Furchgott, 1972; Black & Shankley, 1985). However, during the course of these studies Maubach *et al.* (1991) presented data which, they concluded, provided preliminary evidence for CCK_A-receptor heterogeneity in the guinea-pig gall bladder. Our findings are discussed in the light of their conclusions.

Methods

Guinea-pig gall bladder assay

The assay was based on the method described by La Morte *et al.* (1981). In brief, four longitudinal strips of smooth muscle were dissected from each gall bladder taken from male Dunkin-Hartley guinea-pigs (250–500 *g*) and suspended in 20 ml organ baths maintained at 29°C ± 0.5 in modified (low Ca^{2+}) Krebs-Henseleit solution (mM: Na^+ 143, K^+ 5.9, Ca^{2+} 0.5, Mg^{2+} 1.2, Cl^- 128, HPO_4^{2-} 1.2, SO_4^{2+} 1.2, D-glucose 10, HCO_3^- 25) and gassed with 95% O_2 and 5% CO_2. Following the application of a single 1 g load, the tissues were allowed to relax until a stable baseline was produced. Tension, expressed in grams, was continuously recorded with an isometric transducer.

Experimental protocols

A stable baseline was achieved after an initial 20–40 min relaxation period at which time the bathing solution was replaced and tissues incubated for a further 60 min period in

[1] Author for correspondence.

the absence of an antagonist or appropriate vehicle. In preliminary studies it was found, following a primary CCK-8 concentration-effect (E/[A]) curve, that there was a residual degree of CCK_A-receptor stimulation even though the tissue had been subject to multiple washes (6 washes at 5 min intervals). Therefore, only a single, cumulative, agonist E/[A] curve was obtained in each tissue. Experiments were allocated to a randomised block design so that 4–8 replicates were obtained for each treatment group.

Data analysis

Logistic curve-fitting E/[A] data from individual preparations were fitted to a general logistic function to provide estimates of the midpoint slope parameter (p), midpoint location ($\log[A_{50}]$) and upper asymptote (α) of the curves. These parameters, expressed as mean ± s.e.mean, were used for subsequent analysis and display of data (see Black & Shankley, 1985 for details).

Competitive analysis Competitive analysis was performed according to the procedure described previously (Black *et al.*, 1985a). When no significant differences in values of p and α were found by one-way ANOVA, then the $\log[A_{50}]$ values in the absence and presence of antagonist (B) were directly fitted to the following derivation of the Schild equation,

$$\log[A_{50}]_B = \log[A_{50}] + \log\left(1 + \frac{[B]^b}{10^{\log K_B}}\right).$$

When the Schild slope parameter (b) was not significantly different from unity, then the data were re-fitted with b constrained to unity so that the antagonist equilibrium dissociation constant could be estimated as $\log K_B \pm$ s.e. For purposes of display, conventional Schild plots have been constructed with slopes of unity which intersect the abscissa scale at the pK_B calculated by the method above.

Combined dose-ratio analysis This analysis was performed according to the procedure developed by Shankley *et al.* (1988). In brief, when two antagonists act syntopically, that is, at the same site, then their combined dose-ratio is given by:

$$r_{(B+C)} = r_B + r_C - 1$$

where r_B and r_C are the dose-ratios obtained independently in the presence of the antagonists B and C, respectively. This relationship can be re-written in terms of the experimentally-estimated $\log[A_{50}]$ values,

$$S_A = \log[A_{50}]_{B+C} - \log([A_{50}]_B + [A_{50}]_C - [A_{50}]),$$

where S_A is the test statistic for the model which will have a value of zero when the data comply with the model. Similarly, when two antagonists act independently, that is, allotopically, their combined dose ratios multiply,

$$r_{(B+C)} = r_B.r_C$$

This relationship may also be expressed in terms of $\log[A_{50}]$ values,

$$S_M = \log[A_{50}]_{B+C} - \log[A_{50}]_B - \log[A_{50}]_C + \log[A_{50}],$$

so that S_M, the test statistic, will have a value of zero when the data complies with this model.

Analysis of agonism The agonism expressed by pentagastrin was analysed by direct model-fitting of the concentration-effect curve data to the following equation which describes the behaviour of an agonist in a single receptor-effector system (Black & Leff, 1983):

$$E = \frac{E_M[A]^n\tau^n}{(K_A + [A])^n + [A]^n\tau^n}$$

The fit was performed using the BMDP derivative-free, non-linear regression, programme (Dixon, 1990) on a VAX 3200 computer. The parameters for the maximum effect (E_M) and the slope parameter of the transducer function (n) were constrained to numeric values (see Results) and estimates made of the equilibrium dissociation constant (K_A) and the operational efficacy (τ) (for further details see Black *et al.*, 1985b).

Compounds

Compounds were obtained and prepared as follows: the sulphated octapeptide of cholecystokinin (CCK-8) and pentagastrin were obtained from Cambridge Biochemicals Ltd., UK. CCK-8 was dissolved in 10% absolute ethanol to provide a final stock solution of 2 mM concentration. Pentagastrin was dissolved in 100% dimethylformamide (DMF) to give a 100 mM stock. Devazepide, also known as L364718 (a gift from Merck, Sharpe & Dohme Ltd, U.S.A.), was dissolved in DMF to give a 0.12 mM stock concentration. Lorglumide (CR1409) and loxiglumide (CR1505) (Rotta Spa, Milan) were dissolved in an aqueous solution of NaOH (pH = 8) to give a 12 mM stock concentration. All compounds were subsequently diluted in distilled water. The maximum volume of DMF and distilled water added to any one 20 ml organ bath was 20 µl and 500 µl, respectively. Neither the vehicles nor the antagonists were found to produce significant effects on baseline tone.

Results

Analysis of CCK-8 concentration-effect (E/[A]) curve data in guinea-pig gall bladder

Assay problems were encountered when cholecystokinin octapeptide (CCK-8) was used as agonist on the guinea-pig gall bladder assay prepared according to the method of La Morte *et al.* (1981) who used it for studying the effects of histamine. Although concentration-dependent responses were obtained, the assay was prone to agonist-induced spontaneous activity and, as shown previously (Nieber *et al.*, 1988), unstable response profiles (Figure 1a). This behaviour made the determination of precise response levels uncertain. In addition, an unacceptably high variation was found in the shape and location ($\log[A_{50}]$) of the E/[A] curves (Figure 1a).

The spontaneous activity was eliminated by reducing the temperature from 37°C to 29°C and by lowering the $[Ca^{2+}]$ from 2.5 mM to 0.5 mM (Figure 1a). A reduction in variability was obtained by the use of very small (3 × 1 mm) strips cut from the body of the gall bladder (Figure 1a). These changes had the effect of reducing the standard deviation about the mean $\log[A_{50}]$ from 0.79 to 0.39 ($n = 21$, $n = 24$, respectively) and increasing the potency of CCK-8 by almost one log unit. Moreover, under the improved assay conditions the E/log[A] curves were consistently monotonic and symmetrical around the $\log[A_{50}]$. Therefore, it was possible, objectively, to analyse the data by fitting it to the three-parameter logistic function (see Methods) to obtain the parameter values like those shown in Table 1.

Analysis of pentagastrin concentration-effect (E/[A]) curve data in guinea-pig gall bladder

CCK-8 is reported to be a powerful stimulant of not only CCK_A-receptors but also CCK_B-receptors (Lotti *et al.*, 1986). Therefore, it was possible that the analysis of the antagonists could be confounded by the presence of CCK_B-receptors which might also be coupled to smooth muscle contraction in the gall bladder. This was investigated with pentagastrin as agonist because it is a selective agonist with nM potency in those tissues classified as containing CCK_B-receptors (Lotti *et al.*, 1986) but only µM potency in those now classified as

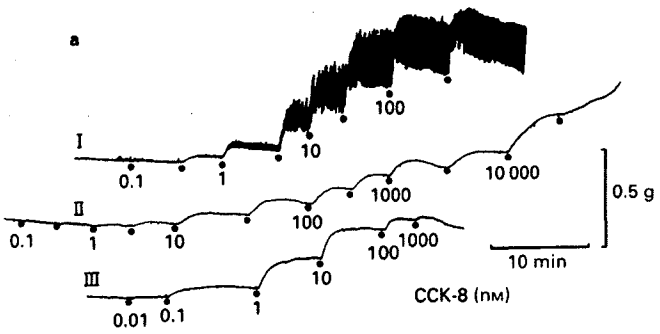

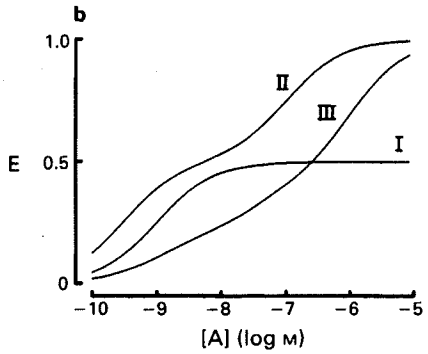

Figure 1 Development of the guinea-pig gall bladder assay. (a) Experimental traces showing cholecystokinin octapeptide (CCK-8) E/[A] curves obtained by cumulative dosing. Traces showing, (I) spontaneous activity observed when the assay was prepared according to La Morte *et al.*, 1981, (II) a complex curve following the reduction of both temperature, from 37°C to 29°C, and $[Ca^{2+}]$ from 2.5 mM to 0.5 mM and (III) a monotonic curve following the additional reduction in the size of the preparation (see Results for details) (b) Simulations showing theoretical E/[A] curves obtained from a mathematical model which describes the summation of effects from multiple units of tissue within a single bioassay preparation. Each unit is assumed to produce E as a simple rectangular hyperbolic function of [A], so that the total effect is given by,

$$E = \frac{\alpha_1.[A]}{[A_{50}]_1 + [A]} + \frac{\alpha_2.[A]}{[A_{50}]_2 + [A]} + \frac{\alpha_2.[A]}{[A_{50}]_3 + [A]}$$

The potency ($[A_{50}]$) of A and the maximum effect (α) can vary in each unit. In the simulations, assays are assumed to consist of (I) one functional unit ($[A_{50}]_1 = 1$ nM, $\alpha_1 = 0.5$), (II) two functional units with $\log[A_{50}]$ values separated by 2 log units ($[A_{50}]_1 = 0.3$ nM, $[A_{50}]_2 = 100$ nM) and equal contributions to the total effect ($\alpha_1 = \alpha_2 = 0.5$), (III) three functional units with $\log[A_{50}]$ values separated by 1.5 log unit intervals ($[A_{50}]_1 = 1$ nM, $[A_{50}]_2 = 30$ nM, $[A_{50}]_3 = 1$ μM) and unequal contributions to the total effect ($\alpha_1 = 0.20$, $\alpha_2 = 0.20$, $\alpha_3 = 0.60$).

Table 1 Analysis of cholecystokinin octapeptide (CCK-8) and pentagastrin E/[A] curves on the guinea-pig gall bladder assay

		logistic curve-fitting parameters[3]		
	n	$\log[A_{50}]$	p	α (force:g)
CCK-8	4	−8.63 ± 0.13	0.63 ± 0.05	0.42 ± 0.12
Pentagastrin	4	−5.38 ± 0.11	0.87 ± 0.18	0.16 ± 0.05[1]

	Agonism model-fitting[2]	
	pK_A	τ
Pentagastrin	4.86 ± 0.52	0.34 ± 0.24

[1]Significantly different from the value of α for the CCK-8 E/[A] curve, $P < 0.05$. [2]CCK-8 was assumed to be a high efficacy agonist in the assay to permit estimation of pK_A and τ values for pentagastrin (see text for details). [3]See Methods for details.

containing CCK_A-receptors (Williams *et al.*, 1978).

Although pentagastrin produced concentration-dependent increases in tension, it was 10000 fold less potent than CCK-8 and the maximum of the pentagastrin E/[A] curve (α) was significantly less than that obtained with CCK-8 (Figure 2a and Table 1). To determine whether pentagastrin was acting as a partial agonist at CCK_A-receptors, two further experiments were performed. First, pentagastrin E/[A] curves were obtained in the presence of a concentration (0.1 μM) of the selective CCK_A-receptor antagonist, devazepide, which is ~1000 fold higher than its K_B at CCK_A-receptors but ~2.5 fold lower than its reported K_B at CCK_B-receptors. Second, CCK-8 E/[A] curves were obtained in the absence and presence of 100 μM pentagastrin which was pre-incubated for 30 min.

The results (Figure 2b) were consistent with pentagastrin behaving as a partial agonist at CCK_A-receptors; that is, devazepide totally abolished the response to pentagastrin and pentagastrin produced a small (1.13 ± 0.18 log unit) significant shift of the CCK-8 E/log[A] curve in quantitative agreement with expectations for the interaction between a low efficacy and high efficacy agonist competing for a common receptor (Barlow *et al.*, 1967). This conclusion was supported by the results of directly-fitting the individual pentagastrin E/[A] data to the model of agonism described by Black & Leff (1983) (see Methods). A good fit was obtained, as judged-by-eye, and estimates were made of the equilibrium dissociation constant, K_A, and the efficacy parameter, τ, for pentagastrin at the CCK_A-receptor (Table 1 and Figure 2a).

The model fitting was only possible by making the, as yet untestable, assumption that CCK-8 was a high efficacy agonist in the assay. Thus, the value of α for CCK-8 could be taken to be equal to the model parameter for the maximum possible agonist effect in the system (E_M) and the midpoint slope parameter (p) of the CCK-8 concentration-effect curve taken to be equal to the midpoint slope of the transducer function (n). Importantly, the pK_B (5.10 ± 0.18, d.f. = 7), estimated for pentagastrin from the single shift competition experiment using CCK-8 as agonist, was not significantly different from the equilibrium dissociation constant value ($pK_A = 4.86 \pm 0.52$, d.f. = 13) estimated by the analysis of the agonism produced by pentagastrin.

Therefore, the presence of potentially-confounding responses due to activation of CCK_B-receptors could be provisionally ruled-out.

Analysis of competitive antagonism

Devazepide, loxiglumide and lorglumide produced concentration-dependent inhibition of the CCK-8-induced contractions resulting in parallel, rightward, displacement of the E/log[A] curves. Subsequent analysis of the $\log[A_{50}]$ values indicated that the compounds behaved as simple competitive antagonists over the range of concentrations used and pK_B values were estimated (Table 2 and Figure 3).

Combined dose-ratio analysis

The combined dose-ratio analysis experiments were designed to test whether the three antagonists, the glutamic acid derivatives (lorglumide and loxiglumide) and the benzodiazepine derivative (devazepide) acted syntopically at the CCK_A-receptor. The optimum discrimination between the multiplicative and additive models is achieved, theoretically, when large dose-ratios are used in the test. However, in practice, we were restricted to a maximum shift of 2–2.5 log units of the CCK-8 E/[A] curve by the limited solubility of CCK-8 itself. Therefore, antagonist concentrations were chosen which were predicted to produce log dose-ratios of approximately 1.7. Thus, if addition of dose-ratios occurred then the predicted combined log dose-ratio of 2 would have been fully-quantifiable. Clearly, if the dose-ratios multiplied then the CCK-8 E/[A] curves would have been displaced to

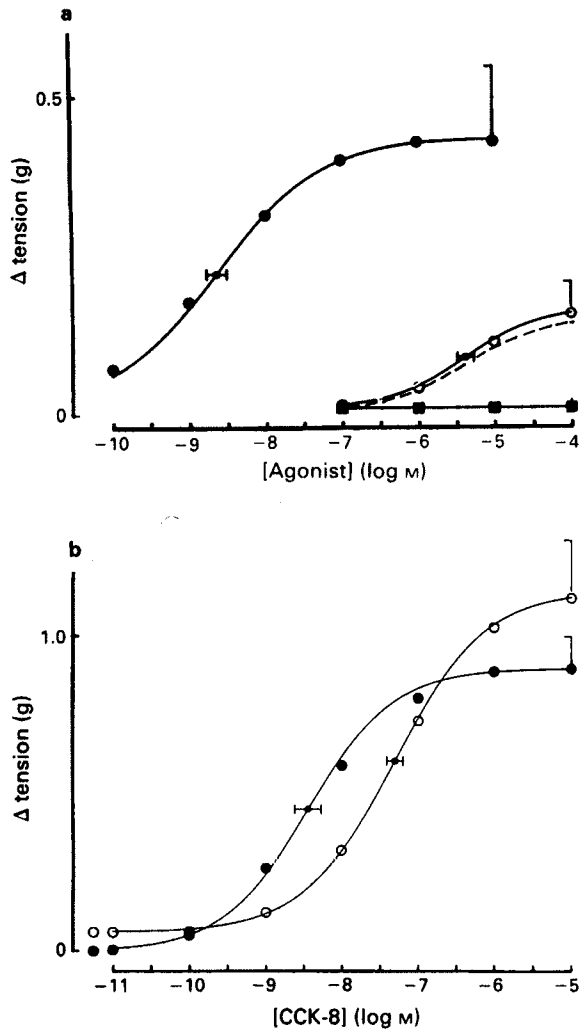

Figure 2 (a) E/[A] curves obtained using cholecystokinin octapeptide (CCK-8) (●), pentagastrin (○) and pentagastrin in the presence of 100 nM L-364718 (■) in the guinea-pig gall bladder assay. Data from individual preparations ($n = 4$) were fitted to a general logistic function and the midpoint slope location ($\log[A_{50}]$) and upper asymptote (α) of the curves expressed as mean ± s.e.mean. The hatched line shown superimposed on the pentagastrin E/[A] data was drawn using the parameters estimated by fitting the Black & Leff (1983) model of agonism (see text for details). (b) CCK-8 E/[A] curves in the absence (●) and presence (○) of 100 μM pentagastrin preincubated for 30 min.

Table 2 Analysis of cholecystokinin octapeptide (CCK-8) antagonist interactions on the guinea-pig gall bladder assay

Compound	*b* (s.e.)	pK_B (s.e.)	*n*
Lorglumide	1.05 (0.23)	7.59 (0.21)	64
Loxiglumide	1.27 (0.16)	7.07 (0.21)	64
Devazepide	1.19 (0.09)	9.98 (0.13)	22

such an extent (log dose-ratio = 3.4) that only threshold CCK-8 responses would have been visible. The data obtained in both experiments were consistent with the additive, syntopic, model and allowed rejection of the multiplicative, allotopic, model (Figure 4 and Table 3). Thus, lorglumide was concluded to be acting syntopically with devazepide which, in turn, was found to act syntopically with loxiglumide.

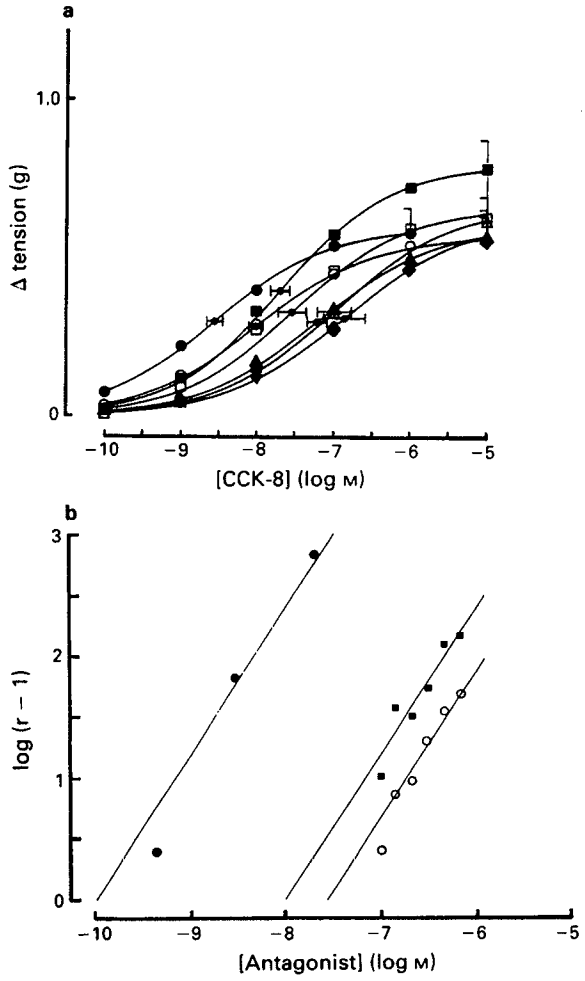

Figure 3 Analysis of competitive antagonism: (a) cholecystokinin octapeptide (CCK-8) E/[A] curves ($n = 6/8 \pm$ s.e.mean) in the guinea-pig gall bladder assay in the absence (●) and presence of (○) 0.4, (■) 0.6, (□) 1, (▲) 1.5, (△) 2.5, (◆) 4 μM loxiglumide. (b) Schild plots for the interaction between CCK-8 and devazepide (●), loxiglumide (■) and lorglumide (□) on the guinea-pig gall bladder assay.

Discussion

The primary aim of the study was to determine if the benzodiazepine derivative, devazepide, and the glutamic acid derivatives, loxiglumide and lorglumide, act syntopically and competitively at CCK_A-receptors in the guinea-pig gall bladder. Although this preparation has been previously described (La Morte *et al.*, 1981), in practice, we found it was necessary to improve the existing techniques for CCK_A-receptor bioassay. We wanted to apply models of agonism and antagonism, based on the applicability of the Law and Mass Action to the ligand-receptor interactions. These require for simplicity that measurements of effect are made when the agonist response achieves a clearly-defined, sustained plateau. This steady-state condition is usually assumed to indicate an underlying equilibrium condition at the receptors.

In addition to improving the signal-to-noise ratio and reducing spontaneous activity in the tissues to allow accurate, response measurement, the technical changes provided the bonus of increasing the apparent potency of the CCK-8. This allows the behaviour of the antagonists to be studied over a wider range of concentrations, with the E/[A] curves fully-defined, than would have otherwise been possible due to the limited solubility and cost of the peptide agonist, CCK-8.

No evidence for CCK_B-receptors was found in the im-

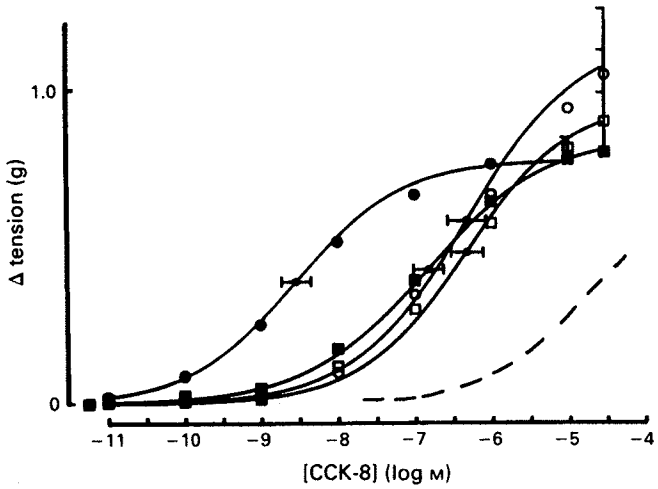

Figure 4 Combined dose-ratio analysis: cholecystokinin octapeptide (CCK-8) E/[A] curves in the absence (●) and presence of 6 nM devazepide (○), 1 μM loxiglumide (■) and a combination of 6 nM devazepide and 1 μM loxiglumide (□). The dashed line shows the location of the CCK-8 E/[A] curve which was predicted by assuming that the antagonists acted independently.

Table 3 Combined dose-ratio analysis

B C (1 μM)	*Devazepide* (6 nM) + *lorglumide* (1 μM)	*Devazepide* (6 nM) + *loxiglumide*
Observed log r_B	1.68	1.20
Observed log r_C	2.18	1.84
Multiplication:		
Expected log $r_{(B+C)}$	3.87	3.04
Addition:		
Expected log $r_{(B+C)}$	2.30	1.92
Observed log $r_{(B+C)}$	2.19	1.99
$S_A \pm$ s.e.	0.11 ± 0.26	0.01 ± 0.21
$S_M \pm$ s.e.	1.68 ± 0.42*	1.14 ± 0.30*

*Significantly different from zero, $P < 0.05$.

proved assay and it was shown that the benzodiazepine derivative, devazepide, and the glutamic acid derivatives, loxiglumide and lorglumide, behaved syntopically and competitively at CCK_A-receptors. From a medicinal chemistry point of view, this result suggests that a molecular model of the CCK_A-receptor requires receptor binding homology for these different chemical structures and the peptide hormone, CCK-8, itself. In addition, we did not find any evidence for CCK_A-receptor heterogeneity as judged by the finding that the CCK-8 E/[A] curves were symmetrical and monotonic in the absence and presence of the antagonists and that the Schild plots were linear over a wide range of antagonist, and, therefore, agonist concentrations.

Recently, Maubach *et al.* (1991) published, in abstract form, data from the analysis of the interactions between, *inter alia*, CCK-8 and two of the antagonists used in this study, devazepide and lorglumide, in an assay also prepared from the guinea-pig gall bladder. In their study, a Schild plot slope significantly greater than unity was obtained with devazepide. The CCK-8 E/[A] curves, in both the absence and presence of the antagonists, were referred to as 'extended' because increases in tension were obtained over 5 log cycles of CCK-8 concentration. Maubach *et al.* (1991) concluded that this was preliminary evidence for CCK_A-receptor heterogeneity. Clearly, our results do not support this view. There are several obvious technical differences between their studies and ours; they incubated antagonists for 30 min rather than 60 min; their experiments were conducted at 37°C whereas we used 29°C; consecutive CCK-8 E/[A] curves were obtained on each preparation rather than a single one; the assay consisted of half gall bladders rather than short, thin strips. Our experience with long strips of tissue suggests that CCK-8 E/[A] curves could be flat with associated high variance if the muscle was taken from a relatively large area of the gall bladder (Figure 1).

We have considered one explanation for these 'extended' curves which may have general applicability to the development and interpretation of other bioassays. Regional variation of hormone receptor concentration is recognised within physiological structures such as the urinary bladder (Taira, 1972). The operational model of agonism (Black & Leff, 1983), in common with other models (Furchgott, 1966), predicts that this variation would have the effect of changing the potency of high efficacy agonists. It was possible to simulate the various profiles of 'extended' CCK E/[A] curves shown in Figure 1 by assuming that the assays prepared from larger pieces of muscle contain several operational units of muscle. Thus, although the receptors in the units are the same, each unit has a different sensitivity to the agonist. The total effect measured in an assay was assumed to be given by the summation of the effects produced by the individual units (Figure 1b). In terms of this model, it is as though, by choosing to use small strips of muscle taken from the central section of the gall bladder, that we have selected a homogeneous muscle unit set with high CCK_A-receptor concentration, so that potent, monotonic CCK-8 E/[A] curves were obtained.

We gratefully acknowledge the skilled technical assistance of Alexander Gerskowitch and Matthew Wilson.

References

BARLOW, R.B., SCOTT, N.C. & STEPHENSON, R.P. (1967). The affinity and efficacy of onium salts on the frog rectus abdominis. *Br. J. Pharmacol.*, **31**, 18–196.

BLACK, J.W., GERSKOWITCH, V.P., LEFF, P. & SHANKLEY, N.P. (1986). Analysis of competitive antagonism when this property occurs as part of a pharmacological resultant. *Br. J. Pharmacol.*, **89**, 547–555.

BLACK, J.W. & LEFF, P. (1983). Operational models of pharmacological agonism. *Proc. R. Soc. B.*, **220**, 141–162.

BLACK, J.W., LEFF, P. & SHANKLEY, N.P. (1985a). Further analysis of anomalous pK_B values for histamine H_2-receptor antagonists on the isolated mouse stomach assay. *Br. J. Pharmacol.*, **86**, 581–587.

BLACK, J.W., LEFF, P., SHANKLEY, N.P. & WOOD, D. (1985b). An operational model of pharmacological agonism: the effect of E/[A] curve shape on agonist dissociation constant estimation. *Br. J. Pharmacol.*, **84**, 561–581.

BLACK, J.W. & SHANKLEY, N.P. (1985). The isolated stomach preparation of the mouse: a physiological unit for pharmacological analysis. *Br. J. Pharmacol.*, **86**, 571–579.

BOCK, M.G., DIPARDO, R.M., EVANS, B.E., RITTLE, K.E., WHITTER, W.L., VEBER, D.F., ANDERSON, P.S. & FREIDINGER, R.M. (1989). Benzodiazepine gastrin and brain cholecystokinin receptor antagonists. *J. Med. Chem.*, **32**, 13–16.

DIXON, W.J. (1990). ed: *BMDP Statistical Software*. Berkeley, Los Angeles & London. University of California Press.

EVANS, E., RITTLE, K.E., BOCK, M.G., DIPARDO, M., WHITTER, W.L., VEBER, D.F., ANDERSON, P.S. & FREIDINGER, R.M. (1986). Design of potent, orally effective nonpeptidal antagonists of the peptide hormone cholecystokinin. *Proc. Natl. Acad. Sci. U.S.A.*, **83,** 4918–4922.

FURCHGOTT, R.F. (1972). The classification of adrenoceptors (adrenergic receptors). An evaluation from the standpoint of receptor theory. *Handb. Exp. Pharmakol.*, **33,** 283–335.

LOTTI, V.J., CHANG, R.S.L., KLING, P.J. & CERINO, D.J. (1986). Evidence that cholecystokinin octapeptide (CCK-8) acts as a potent, full agonist on gastrin receptors for acid secretion in the isolated mouse stomach: lack of antagonism by the specific CCK antagonist asperlicin. *Digestion*, **35,** 170–174.

LOTTI, V.J. & CHANG, R.S.L. (1989). A new potent and selective non-peptide gastrin antagonist and brain cholecystokinin receptor (CCK-B) ligand: L365260. *Eur. J. Pharmacol.*, **162,** 273–280.

MAKOVEC, F., BANI, M., CEREDA, R., CHISTE, R., PACINI, M.A., REVEL, L., ROVATI, L.A. & SETNIKAR, I. (1987). Pharmacological properties of lorglumide as a member of a new class of cholecystokinin antagonists. *Arz.-Forsch.*, **37,** 1265–1268.

MAUBACH, K., PATEL, M. & SPRAGGS, C.F. (1991). Interaction of gastrin/cholecystokinin agonists and antagonists on guinea-pig gall bladder. *Br. J. Pharmacol.*, **104,** 142P.

LA MORTE, W.W., HINGSTON, S.J. & WISE, W.E. (1981). pH-dependent activity of H_1- and H_2-histamine receptors in guinea-pig gall bladder. *J. Pharmacol. Exp. Ther.*, **217,** 638–644.

NIEBER, K., MILENOV, K., RAKOVSKA, A., HENKLEIN, P. & OEHME, P. (1988). Responses of guinea-pig gastric, ileal and gall bladder smooth muscle to desamino-cholecystokinin octapeptide (CCK 7). *Meth. Find. Exp. Clin. Pharmacol.*, **10,** 513–520.

PATON, W.D.M. & RANG, H.P. (1965). The uptake of atropine and related drugs by intestinal smooth muscle of the guinea pig in relation to acetylcholine receptors. *Proc. R. Soc. B.*, **183,** 1–44.

SETNIKAR, I., BANI, M., CEREDA, R., CHISTE, R., MAKOVEC, F., PACINI, M.A., REVEL, L., ROVATI, L.C. & ROVATI, L.A. (1987). Pharmacological characterisation of a new potent and specific nonpolypeptide cholecystokinin antagonist. *Arz.-Forsch.*, **37,** 703–707.

SHANKLEY, N.P., BLACK, J.W., GANELLIN, C.R. & MITCHELL, R.C. (1988). Correlation between log $P_{OCT/H20}$ and pK_B estimates for a series of muscarinic and histamine H_2-receptor antagonists. *Br. J. Pharmacol.*, **94,** 264–274.

TAIRA, N. (1972). The autonomic pharmacology of the bladder. *Annu. Rev. Pharmacol.*, **12,** 197–208.

WILLIAMS, J.A., KORC, M. & DORMER, R.L. (1978). Action of secretagogues on a new preparation of functionally intact, isolated pancreatic acini. *Am. J. Physiol.*, **235,** E517–E524.

WOODRUFF, G.N. & HUGHES, J. (1991). Cholecystokinin antagonists. *Annu. Rev. Pharmacol. Toxicol.*, **31,** 469–501.

(Received November 20, 1991
Revised January 7, 1992
Accepted January 13, 1992)

Brain Research, 628 (1993) 254–262
Elsevier Science Publishers B.V.

BRES 19437

Effects of CCK_8 and of the CCK_B-selective agonist BC264 on extracellular dopamine content in the anterior and posterior nucleus accumbens: a microdialysis study in freely moving rats

Nathalie Ladurelle [a], Gérard Keller [b], Bernard P. Roques [a], Valérie Daugé [a,*]

[a] *Département de Pharmacochimie Moléculaire et Structurale, U 266 INSERM, URA D 1500 CNRS,* [b] *Département de Chimie Minérale Structurale, URA 200 CNRS, Université René Descartes (Paris V), Faculté des Sciences Pharmaceutiques et Biologiques, 4 avenue de l'Observatoire, 75270 Paris Cedex 06, France*

(Accepted 29 June 1993)

Key words: Nucleus accumbens; Cholecystokinin; Local perfusion; Dopamine release; Microdialysis; Freely moving rat

The effects of the local administration of cholecystokinin octapeptide (CCK_8) in the posterior nucleus accumbens (N. Acc.) and of BC264 (a selective CCK_B agonist) in the anterior N. Acc. on dopamine (DA) neurotransmission were studied in awake rats. Microdialysis was used to quantify the extracellular contents of DA and its two metabolites, 3,4-dihydroxyphenylacetic acid (DOPAC) and homovanillic acid (HVA). In the posterior N. Acc., a perfusion of 10^{-5} M CCK_8 for 40 min (i.e. 25 pmol) increased the extracellular levels of DA, DOPAC and HVA. In contrast, 10^{-4} M BC264 perfused for 40 min (i.e. 350 pmol) into the anterior N. Acc. reduced extracellular DA but did not modify DOPAC and HVA levels. These findings suggest that the CCK-DA interactions are different in various regions of the N. Acc. and emphasize the functional heterogeneity of the N. Acc., issuing in part from its particular DA innervation (mixed CCK-DA terminals only in the posterior region) but also from the distribution of the CCK fibers and binding sites in this nucleus. This microdialysis study, using perfusions of CCK compounds in the N. Acc. of freely moving rats, shows that the CCK system might play an important regulatory role in limbic DA function.

INTRODUCTION

The carboxy-terminal sulfated cholecystokinin octapeptide (CCK_8) is one of the most abundant peptides in the brain. It acts as a neurotransmitter and/or a neuromodulator via two CCK receptor subtypes, the CCK_A receptors or peripheral type and the CCK_B receptors or central type. In 1980, Hökfelt et al.[17] showed that CCK_8 is present in a subpopulation of rat mesencephalic dopaminergic neurones. In rodents, as well as in primates and humans, these mixed CCK-DA neurones are localized mainly in the ventral tegmental area (VTA), but also in the substantia nigra pars compacta[18,33]. In rodents, it has been shown that these neurones project to different limbic structures, such as the medial septum, the medial olfactory tubercule and the postero-medial nucleus accumbens (N. Acc.)[17,19,20,35]. This latter region also contains CCK_8 afferents issuing from the nucleus tractus solitarius[45]. In contrast, the anterior part of the N. Acc. receives DA terminals from the VTA and CCK_8 afferent fibers, probably originating from neurones of the frontal cortex and amygdala[11,47]. Moreover, the distribution of CCK binding sites was shown to be heterogenous in the N. Acc., CCK_B receptors being more abundant in the rostral region than in the caudal region[29] which probably also contains CCK_A receptors[1].

In agreement with this neuroanatomical organisation, dopaminergic transmission is clearly modulated by the CCKergic system, as illustrated by the CCK_8-induced increase in the firing of the DA neurones of the rat VTA[21,46]. In previous release experiments performed in rats, CCK_8 was found either to have no effect on DA release[15] or to increase and decrease basal and K^+-evoked DA release, respectively[42–44]. Furthermore, a reduction of the K^+-evoked release of DA following treatment by CCK_8 has been reported[25] while an increase has also been shown[41]. These discrepancies cannot be explained by taking into account the heterogeneity of the N. Acc. Ruggeri et al.[32] have shown, by microdialysis experiments in anesthetized

* Corresponding author. Fax: (33) (1) 43 26 69 18.

rats, that CCK_8 increases DA release in the anterior N. Acc. but has no effect in the posterior region. On the other hand, CCK_8 was shown to decrease the K^+-induced DA release from slices of the anterior N. Acc., possibly through CCK_B receptor activation, and to increase this evoked release by CCK_A receptor stimulation in the posterior N. Acc.[26]. These apparently inconsistent modulatory effects of CCK in the N. Acc. could be due to differences in the dopaminergic innervation (colocalization or not CCK-DA) and/or to tonic or phasic activity of the dopaminergic system. Accordingly, different behavioral responses can be observed, depending of the injection site of CCK_8 and analogues in the N. Acc. and of the emotional state of the animals[4,6,8,9,39,40].

The aim of the present study was therefore to analyse the effects of CCK_8 on the extracellular contents of DA and its two metabolites homovanillic acid (HVA) and 3,4-dihydroxyphenylacetic acid (DOPAC) in the N. Acc. by microdialysis in freely moving rats[38]. The use of awake animals is important, since anaesthesia could modify DA release in rats[34]. For this study, microdialysis probes were first implanted in the median N. Acc. and biochemical and behavioural controls were carried out after intraperitoneal (i.p.) injection of D/L-amphetamine, a classical DA releaser which induces notably a hyperactivity in animals. CCK_8, a mixed CCK_A/CCK_B agonist or BC264, a highly potent and selective CCK_B agonist[2] were locally administered through the probes in the posterior and the anterior N. Acc., respectively, at doses corresponding to those previously shown to induce behavioural modifications[6,8]. Moreover, the choice of the compounds and of their injection sites (i.e. BC264 in the anterior N. Acc. and CCK_8 in the posterior N. Acc.) was made on the basis of previous studies, showing that CCK_8 but not BC264 produced a behavioral effect after injection into the posterior N. Acc.[7]. A lack of effect of CCK_B agonists (unsulfated CCK_8, pentagastrin) in this region has also been reported on DA release from slices of N. Acc.[26]. In contrast, both CCK_8 and BC264 administered in the anterior N. Acc. had similar effects on rat behavior[8]. Moreover, CCK_8 or unsulfated CCK_8 modified DA release from slices of anterior N. Acc.[26]. Finally, the CCK_B receptor antagonists did not suppress the behavioral effects of CCK_8 in the posterior N. Acc., in contrast to their action in the anterior N. Acc.[5].

MATERIALS AND METHODS

Animals

Male Wistar rats (Elevage Depré, France) weighing about 200 g at the time of surgery were used. They were housed in groups of four in a temperature and humidity controlled environment and had free access to food and water.

Surgery

Rats were anesthetized by an i.p. injection of chloral hydrate (400 mg/kg), mounted in a stereotaxic apparatus (Unimécanique, France) and implanted with an unilateral stainless steel cannula guide (20 gauge, i.e., 0.9 mm in diameter) 1.5 mm above the N. Acc., according to the atlas of Paxinos and Watson[28]. For the D/L-amphetamine experiment, the coordinates were: rostral: +1.7 mm; lateral: +1.6 mm and ventral: −8 mm relative to bregma and skull surface. For the BC264 experiment, implantations in the anterior N. Acc. were: rostral: +2.1 mm; lateral: +1.6 mm and ventral: −8 mm and for the CCK_8 perfusion in the posterior N. Acc., the coordinates were: rostral: +1.2 mm; lateral: +1.2 mm and ventral: −8 mm.

After implantation, the animals were treated with Extencilline® (0.3 MUI/kg, intramuscular) to prevent infection. They were tested 7 days after surgery.

Brain microdialysis procedure

The dialysis probes were constructed according to Robinson and Whishaw[31] with 3 mm of active membrane (Spectrum, Medical Industries Inc.). The outer diameter of the dialysis membranes was 0.25 mm and their molecular weight cut-off was 6000 Da.

The probes were inserted into the rat N. Acc. via a connector that controlled the depth of penetration and were fixed onto the chronically implanted cannula guide by a locking screw. The connector was attached to a liquid swivel located on a balance beam to minimize discomfort to the rat. A polyethylene tubing was connected to the swivel and attached to a 2.5-ml syringe (CMA, Carnegie Medicin). The animals were implanted with the probes the night prior to the experiment and placed in individual black boxes (40 × 40 × 40 cm). This period allowed the animals to become accustomed to the system and minimized disturbances due to the insertion of the probe. The following day, the polyethylene tubing was connected to a microinfusion pump (CMA/100, Carnegie Medicin) and rats were continuously perfused for 2 h at 2 μl/min with dialysis buffer (120 mM NaCl; 5 mM KCl; 1.8 mM $CaCl_2$; 1.2 mM $MgCl_2$; 0.2 mM phosphate-buffered saline pH 7.4 with a final sodium concentration of 120.7 mM) in order to reach a steady state. The perfusate was then collected in small tubes containing 15 μl of the HPLC mobile phase (for the composition see below) with the addition of 5 μl of an antioxydant solution (EDTA 0.04% in 0.1 M perchloric acid). In order to determine the basal efflux of the amines, 3 baseline samples (20 min each) were collected, the animals were then treated either by a 40 min perfusion of CCK compounds or by an i.p. injection of D/L-amphetamine; nine additional 20-min dialysis samples were then collected. The change in perfusion medium from saline to CCK_8 or BC264 solutions was carried out by hand, taking care to not introduce bubbles in the tubing.

Behavior monitoring

To evaluate the duration of the global activity of the animals during the experiments, their behavior was recorded by a video processor analysis system (Videotrack 512, View Point, Lyon, France) consisting of a video camera placed above the individual animal boxes and linked to a computer. The displacement of the center of gravity of the animals was calculated to quantify the activity of the rats. All the ambulatory movements (i.e. movements towards a given point) and the non-ambulatory movements (i.e. little movements without deplacement of the animals, such as rearing or grooming) were considered as activity periods. The total duration of these movements was measured for each 20-min session of sample collection.

Determination of the in vitro recovery

To estimate the in vitro recovery of the three monoamines (DA, DOPAC, HVA), the same protocol was used as for the in vivo experiments. The extremity of the probes was placed in an eppendorf containing the monoamines dissolved in dialysis buffer (10^{-6} M for DOPAC and HVA; 10^{-7} M for DA). The probes were perfused at

37 ± 1°C at a flow rate of 2 μl/min with dialysis buffer free of monoamines. The perfusate was collected at 20-min intervals in the same mixture as mentioned above. The percentage of recovery was estimated for each molecule by the following ratio: *concentration of the monoamine in dialysis samples / concentration of the monoamine in the outside medium*. The recovery was $9.87 \pm 0.92\%$ for DA, $9.96 \pm 0.40\%$ for DOPAC and $11.10 \pm 0.70\%$ for HVA, $n = 12$.

In order to estimate the in vitro recovery of the perfusion of CCK_8 and BC264 through the dialysis membrane, probes were placed into an eppendorf containing 1 ml of dialysis buffer and were perfused (2 μl/min; 37 ± 1°C) with the same solution containing either 10^{-6} M CCK_8 with 500 cpm/μl of [^{3}H]pCCK_8 added as tracer or 10^{-6} M BC264 with 500 cpm/μl of [^{3}H]pBC264 added as tracer. The eppendorf tube was replaced every 20 min and the radioactivity was counted in a liquid scintillation β-counter (1209 Rackbeta, LKB Wallac). The recovery was determined by the following ratio: *radioactivity counted in the tube / radioactive drug perfused through the probe during 20 min*. The recovery was $3.25 \pm 0.34\%$ for CCK_8, $n = 7$ and $4.47 \pm 0.43\%$ for BC264, $n = 8$.

Neurochemical measurements

DA, DOPAC and HVA were quantified by HPLC with electrochemical detection. The HPLC system consisted of an isocratic Knauer 64 pump linked to an automatic sample injector (Wisp 710B, Waters). A C_{18} column (100 mm × 2.3 mm, 3 μm particle size; Catecholamine, Europhor, France) was used to separate the biogenic amines. They were detected by a coulometric electrochemical system (Coulochem ESA, model 5100A) using three electrodes (a guard cell, model 5020 ESA and an analytical cell containing two electrodes in series, model 5011 ESA). The guard cell was set at +0.4 V and placed before the injector to decrease background noise resulting from oxidizable compounds in the mobile phase. The working electrodes were set at +0.35 V and −0.23 V, respectively. The mobile phase (0.015 M sodium acetate, 0.015 M citric acid, 1.2–1.7 mM sodium octane sulfonate, 0.2 mM EDTA and 12.5% methanol, pH 3.8) was delivered at a flow rate of 0.9 ml/min. The 3 monoamines were eluted within 10 min and the peaks were monitored by a data processor (CR5A, Shimadzu). Standard samples containing DA, DOPAC and HVA and standard curves ranging from 0 to 2000 pg were used to quantify each compound. The limit of detection of these molecules was around 15 pg per sample.

Histology

Rats were sacrificed with an overdose of chloral hydrate. The brains were removed, frozen and cut in a cryostat. The slices (50 μm) were stained with cresyl violet and the location of the implantation site was determined according to the atlas of Paxinos and Watson[28] (Fig. 1). Probes that traversed more than 70% of the N. Acc. were considered to be correctly placed. The anteriority was estimated in regard to the islands of Calleja and the laterality relative to the anterior commissure. Approximately 7% of rats were not correctly implanted and were eliminated from the data calculations.

Drugs and treatments

To evaluate the sensitivity of the DA fibers in the N. Acc. under our experimental conditions, the classical DA releaser D/L-amphetamine sulfate (Calaire chimie, Calais, France) was dissolved in 0.9% saline and administered at doses of 0.5 and 2 mg/kg i.p.

Cholecystokinin octapeptide sulfate (CCK_8) and the CCK_B agonist BC264 (Boc-Tyr(SO_3H)-gNle-mGly-Trp-(NMe)Nle-Asp-Phe-NH_2) synthesized in the laboratory as previously described by Charpentier et al.[3], were dissolved in dialysis buffer. BC264 was perfused for 40 min at either 10^{-5} and 10^{-4} M. Given the percentage of recovery obtained in vitro, it was estimated that, under these conditions, 35 and 350 pmol of BC264, respectively, reached the N. Acc. CCK_8 was also perfused for 40 min at doses of 10^{-9}, 10^{-7} and 10^{-5} M i.e. 2.5, 250 fmol and 25 pmol, respectively, when taking into account its percentage of recovery.

[^{3}H]pBC264 was synthesized in the laboratory[3] and [^{3}H]pCCK_8 was from Amersham (Buckinghamshire, England).

The pH value (7.4) was controlled for each solution before use in the experiments.

Data analysis

The results for each rat were first converted to the percentage of change from the average of the three baseline measurements taken before treatment and the mean and the S.E.M. were then calculated.

TABLE I

Average basal extracellular levels, uncorrected for recovery, of DA, DOPAC and HVA in the median, posterior and anterior N. Acc. of rats

Data are given in pg/20 min sample and in nanomolar concentrations *(between parenthesis)* and expressed as means ± S.E.M. of the three basal microdialysis samples taken before drug treatment. Statistical comparison of the means (ANOVA one way): DA: $F_{2,74} = 4.901$, $P = 0.0100$; DOPAC: $F_{2,74} = 6.141$, $P = 0.0034$; HVA: $F_{2,74} = 6.034$, $P = 0.0037$.

	DA		*DOPAC*		*HVA*	
Median N. Acc.						
Saline ($n = 5$)	34.1 ± 4.7	*(4.5 ± 0.6)*	920.9 ± 201.3	*(137.0 ± 29.9)*	641.0 ± 126.5	*(88.0 ± 17.4)*
D/L-Amph. 0.5 mg/kg ($n = 5$)	33.9 ± 5.5	*(4.5 ± 0.7)*	909.0 ± 158.5	*(135.2 ± 23.6)*	615.7 ± 90.0	*(84.5 ± 12.3)*
D/L-Amph. 2.0 mg/kg ($n = 6$)	40.3 ± 5.1	*(5.3 ± 0.7)*	1222.7 ± 216.0	*(181.8 ± 32.1)*	724.7 ± 124.3	*(99.4 ± 17.1)*
Mean ($n = 16$)	39.5 ± 4.2	*(5.2 ± 0.5)*	1047.1 ± 145.8	*(155.7 ± 21.7)*	676.9 ± 98.9	*(92.9 ± 13.6)*
Posterior N. Acc.						
Saline ($n = 9$)	47.1 ± 6.6	*(6.2 ± 0.9)*	1590.9 ± 204.4	*(236.6 ± 30.4)*	1037.0 ± 169.1	*(142.3 ± 23.2)*
CCK_8 10^{-5} M ($n = 9$)	58.3 ± 7.7	*(7.7 ± 1.0)*	1623.0 ± 201.4	*(241.4 ± 30.0)*	949.7 ± 93.2	*(130.3 ± 12.8)*
CCK_8 10^{-7} M ($n = 8$)	49.2 ± 7.2	*(6.5 ± 0.9)*	1554.8 ± 207.7	*(231.2 ± 30.9)*	964.7 ± 100.2	*(132.4 ± 13.7)*
CCK_8 10^{-9} M ($n = 8$)	51.8 ± 11.1	*(6.8 ± 1.5)*	1522.0 ± 224.9	*(226.4 ± 33.4)*	1009.3 ± 164.8	*(138.5 ± 22.6)*
Mean ($n = 34$)	51.5 ± 3.7	*(6.8 ± 0.5)* [a,d]	1574.7 ± 100.0	*(230.2 ± 14.9)* [b,c]	991.2 ± 64.5	*(136.0 ± 8.9)* [a,c]
Anterior N. Acc.						
Saline ($n = 9$)	36.5 ± 7.5	*(4.8 ± 1.0)*	1217.6 ± 176.7	*(181.1 ± 26.3)*	693.0 ± 85.0	*(95.1 ± 11.7)*
BC 264 10^{-4} M ($n = 9$)	35.7 ± 4.3	*(4.7 ± 0.6)*	1110.3 ± 107.2	*(165.1 ± 15.9)*	756.6 ± 67.8	*(103.8 ± 9.3)*
BC 264 10^{-5} M ($n = 9$)	33.4 ± 3.7	*(4.4 ± 0.5)*	1228.5 ± 127.2	*(182.7 ± 18.9)*	702.5 ± 51.5	*(96.4 ± 7.1)*
Mean ($n = 27$)	35.1 ± 2.8	*(4.6 ± 0.4)*	1188.6 ± 80.7	*(176.8 ± 12.0)*	731.6 ± 38.2	*(100.4 ± 5.2)*

[a] $P < 0.01$ vs. anterior N. Acc.; [b] $P < 0.05$ vs. anterior N. Acc.; [c] $P < 0.01$ vs. median N. Acc.; [d] $P < 0.05$ vs. median N. Acc., Newman–Keuls test.

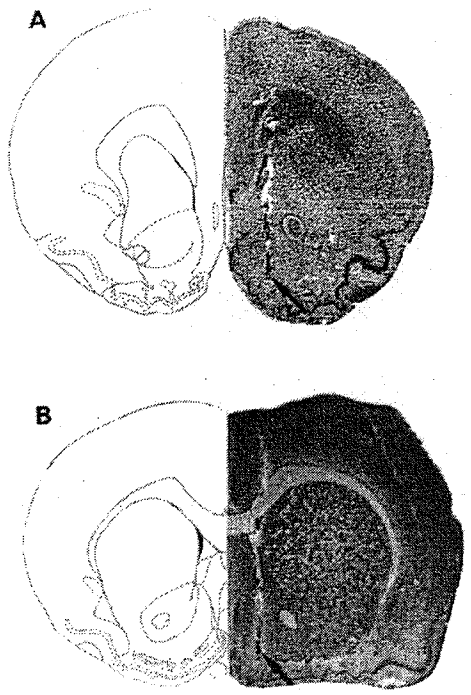

Fig. 1. Histological control of brain slices (50 μm). The right side of the figures represents a trace of a typical implantation site and the left side is from the atlas of Paxinos and Watson[28]. Arrows show the tip of the probes. A: microdialysis probe placement into the anterior N. Acc. B: microdialysis probe placement into the posterior N. Acc.

The dialysis time-course data were analysed using a two-way repeated measure (treatment and time) analysis of variance (ANOVA). When this analysis was significant, one-way (treatment) ANOVA was followed by a Dunnett's t-test. A statistical comparison of the global basal levels of DA, DOPAC and HVA in the anterior, median and posterior N. Acc. was made by a Newman–Keuls test. The 5% level for statistical significance was chosen a priori.

RESULTS

Effects of acute D/L*-amphetamine*

The effects of acute D/L-amphetamine were investigated in order to verify the sensitivity of the N. Acc. DA fibers under our experimental conditions.

No difference was found in the basal levels of DA and its metabolites in the medial N. Acc. of rats before D/L-amphetamine treatment versus saline treatment (Table I).

Acute D/L-amphetamine increased DA outflow between 40 and 80 min after administration: 172.0 ± 14.1% and 275.0 ± 29.8% of the basal efflux at 0.5 and 2.0 mg/kg i.p., respectively, $F_{2,13\ \text{treatment}} = 8.421$ $P = 0.0045$, $F_{8,104\ \text{time}} = 8.506$ $P = 0.0001$, $F_{16,104\ \text{interaction}} = 3.040$ $P = 0.0003$. On the other hand, for both doses, a reduction in metabolite levels was observed. For DOPAC: 71.8 ± 1.5% and 49.7 ± 5.8% of baseline at 0.5 and 2.0 mg/kg, respectively; $F_{2,13\ \text{treatment}} = 4.193$ $P = 0.0393$, $F_{8,104\ \text{time}} = 3.297$ $P = 0.0022$, $F_{16,104\ \text{interaction}} = 0.593$ $P = 0.8825$. For HVA: 73.1 ± 4.2% and 50.3 ± 8.6% of baseline at 0.5 and 2.0 mg/kg, respectively; $F_{2,13\ \text{treatment}} = 4.095$ $P = 0.0418$, $F_{8,104\ \text{time}} = 5.408$ $P = 0.0001$, $F_{16,104\ \text{interaction}} = 1.397$ $P = 0.1576$.

Effects of CCK_8 *perfused in the posterior nucleus accumbens*

There was no difference in the basal levels of DA, DOPAC and HVA between the treated groups and the saline group before treatment (Table I).

After treatment, two-way ANOVA showed a significant increase in extracellular DA efflux following a 40-min perfusion of 10^{-5} M CCK_8 (i.e. 25 pmol) (Fig. 2). This effect was maximum at the start of the perfusion (164.3 ± 11.9% of basal), and the DA levels returned to basal concentrations at the end of the perfusion. A clear but not significant increase in extracellular DOPAC and HVA levels was also observed.

Effect of BC264 perfused in the anterior nucleus accumbens

Before treatment, there was no difference in the basal levels of DA, DOPAC and HVA between the treated groups and the saline group (Table I).

After treatment, the data analysis showed a significant difference between the treated groups and the saline group for extracellular DA outflow (Fig. 3). BC264 produced a significant decrease to 55.4 ± 5.6% of basal levels when perfused for 40 min at a concentration of 10^{-4} M (i.e. 350 pmol). This decrease appeared at the end of the perfusion and was still significant 60 min later. On the other hand, the treatment had no significant effect on the extracellular levels of either DOPAC or HVA.

Comparison of the basal levels of DA, DOPAC and HVA between the two parts of the nucleus accumbens

As previously discussed, before treatment there was no difference in the basal levels of the three monoamines between the four groups of rats implanted in the posterior N. Acc. (i.e. saline, CCK_8 10^{-9} M, CCK_8 10^{-7} M and CCK_8 10^{-5} M groups; Table I). Similary, there was no difference in the basal levels between the three groups of rats implanted in the anterior N. Acc. (i.e. saline, BC264 10^{-4} M and BC264 10^{-5} M groups; Table I) and between the three groups implanted in the median N. Acc. (i.e. saline, D/L-amphetamine 0.5 mg/kg and D/L-amphetamine 2.0 mg/kg groups; Table I). The global means of the basal levels of DA, DOPAC and HVA were then calculated by grouping, for each molecule, the values measured before treatment in all the rats implanted (1) in the

median N. Acc. ($n = 16$), (2) in the posterior N. Acc. ($n = 34$) and (3) in the anterior N. Acc. ($n = 27$). These calculations are reported in Table I. The statistical analysis showed that these global basal levels were significantly higher in the posterior than in the anterior or the median portions of the N. Acc.

Behavioral effects

After treatment by 0.5 or 2.0 mg/kg D/L-amphetamine i.p., the locomotor activity of the rats

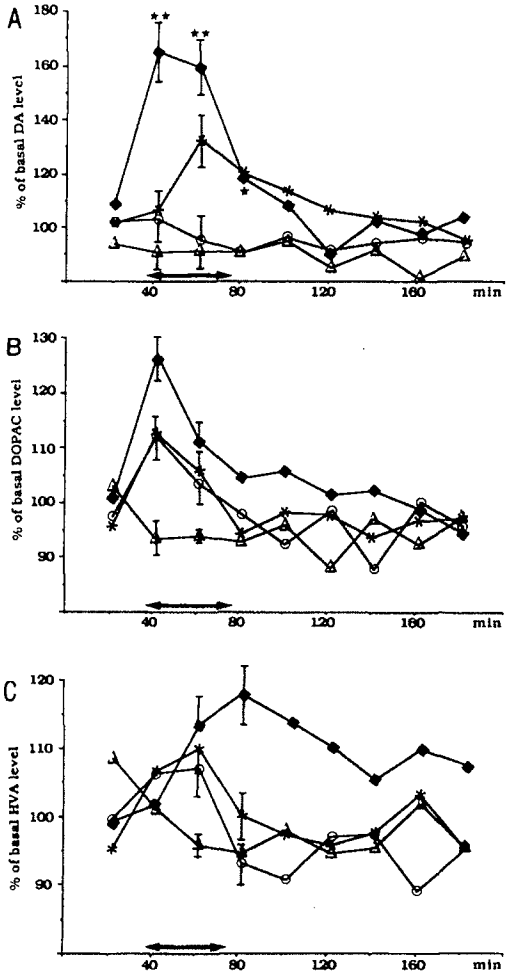

Fig. 2. Time-course effects of a 40-min local perfusion of CCK_8 on the extracellular levels of DA (A), DOPAC (B) and HVA (C), uncorrected for recovery, in the posterior N. Acc. The presence of CCK_8 in the N. Acc. shown in the figures by the black arrows, was estimated taking into account of the dead volume of the perfusion system and shown in the figures by the black arrows. The 100% value represents the mean of the three baseline dialysis samples taken before drug administration and the results are expressed as the percentage of this mean; bars are S.E.M. In order to not overload the figures, only a few S.E.M. bars are shown. Two-way ANOVA: DA: $F_{3,27\ \text{treatment}} = 9.099$, $P = 0.0003$; $F_{8,216\ \text{time}} = 8.409$, $P = 0.0001$; $F_{24,216\ \text{interaction}} = 3.707$, $P = 0.0001$. DOPAC: $F_{3,27\ \text{treatment}} = 0.849$, $P = 0.4556$; $F_{8,216\ \text{time}} = 3.257$, $P = 0.0015$; $F_{24,216\ \text{interaction}} = 0.982$, $P = 0.4912$. HVA: $F_{3,27\ \text{treatment}} = 1.617$, $P = 0.2069$; $F_{8,216\ \text{time}} = 0.691$, $P = 0.6996$; $F_{24,216\ \text{interaction}} = 1.009$, $P = 0.4548$. *, $P < 0.05$; **, $P < 0.01$; Dunnett's t-test. △ Saline; ○ CCK8 10^{-9} M; * CCK8 10^{-7} M; ♦ CCK8 10^{-5} M.

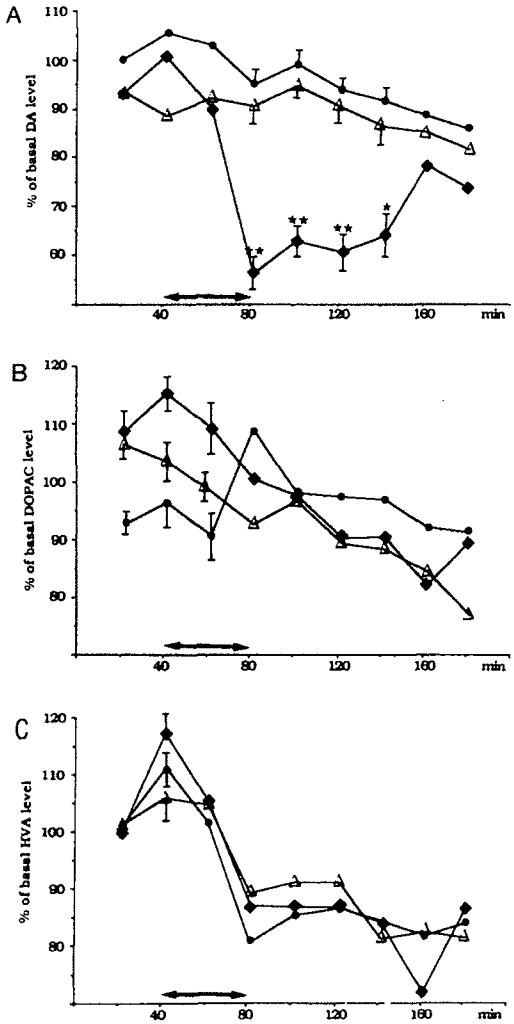

Fig. 3. Time-course effects of a 40 min local perfusion of BC264 on the extracellular levels of DA (A), DOPAC (B) and HVA (C), uncorrected for recovery, in the anterior N. Acc. The presence of BC264 in the N. Acc. shown in the figures by the black arrows, was estimated taking into account of the dead volume of the perfusion system and shown in the figures by the black arrows. The 100% value represents the mean of the three baseline dialysis samples taken before drug administration and the results are expressed as the percentage of this mean; bars are S.E.M. In order to not overload the figures, only a few S.E.M. bars are shown. Two way ANOVA: DA: $F_{2,23\ \text{treatment}} = 10.881$, $P = 0.0005$; $F_{8,184\ \text{time}} = 6.497$, $P = 0.0001$; $F_{16,184\ \text{interaction}} = 2.968$, $P = 0.0002$. DOPAC: $F_{2,23\ \text{treatment}} = 0.461$, $P = 0.6358$; $F_{8,184\ \text{time}} = 4.086$, $P = 0.0002$; $F_{16,184\ \text{interaction}} = 1.441$, $P = 0.1257$. HVA: $F_{2,23\ \text{treatment}} = 0.044$, $P = 0.9569$; $F_{8,184\ \text{time}} = 11.426$, $P = 0.0001$; $F_{16,184\ \text{interaction}} = 0.448$, $P = 0.9670$. *, $P < 0.05$; **, $P < 0.01$; Dunnett's t-test. △ Saline; ● BC264 10^{-5} M; ♦ BC264 10^{-4} M.

was increased by approximately 150 and 250%, respectively, as compared to the saline animals, which moved for about 7 min/20 min session; $F_{2,13\ \text{treatment}} = 10.123$ $P = 0.0002$, $F_{8,104\ \text{time}} = 9.305$ $P = 0.0001$, $F_{16,104\ \text{interaction}} = 0.943$ $P = 0.3715$.

In contrast, none of the CCKergic perfusions modified the global activity of the animals. Without treatment, the rats implanted in the posterior N. Acc. spent about 3 min/session in movements; the perfusion of

CCK_8 did not modify this time: $F_{3,27\ \text{treatment}} = 1.217$ $P = 0.3190$, $F_{8,216\ \text{time}} = 1.296$ $P = 0.2245$, $F_{24,216\ \text{interaction}} = 1.015$ $P = 0.4486$. When implanted in the anterior region, the control animals, as well as those treated with BC264, moved about 6 min/session: $F_{2,23\ \text{treatment}} = 0.616$ $P = 0.5491$, $F_{8,184\ \text{time}} = 1.531$ $P = 0.121$, $F_{16,184\ \text{interaction}} = 0.599$ $P = 0.9228$.

Even though it is not statistically significant, it is interesting to note the differences in the duration of movements as a function of the localization of the implantation site of the dialysis probe. Animals implanted in the posterior N. Acc. (+1.2 mm/bregma) seemed less active (3 min of activity) than those implanted in the median (+1.7 mm/bregma; 7 min of activity) or the rostral parts (+2.1 mm/bregma; 6 min of activity).

DISCUSSION

In the present study we have determined the effects of CCK compounds on DA neurotransmission in the N. Acc. by using intracerebral microdialysis applied to freely moving rats. Extracellular basal dialysate levels of DA and its two metabolites DOPAC and HVA were of the same order as those obtained in several previous studies[16,23,32]. The responsiveness of the DA fibers in the N. Acc. was verified by i.p. administration of 0.5 and 2.0 mg/kg of D/L-amphetamine. The respective 172% and 275% increases of DA outflow and the decrease in the extracellular levels of DOPAC and HVA measured in the N. Acc. were in good agreement with the well known facilitation of DA release and inhibition of monoamine oxydase induced by D/L-amphetamine[12,16]. Furthermore, as expected, these biochemical modifications were associated with the classical behavioral effect of D/L-amphetamine i.e. a drastic increase in rat motor activity following the drug administration.

In the posterior N. Acc., the highest dose of CCK_8 (10^{-4} M) perfused during 40 min, i.e. 25 pmol, induced a measurable effect on DA neurotransmission by increasing the extracellular levels of DA for 40 min while DOPAC and HVA were slightly but not significantly increased. This effect could result from two phenomena: an enhancement of DA release and/or an inhibition of its reuptake. These results were in good agreement with the recent in vitro studies of Marshall et al.[26] showing an increase of DA release in slices of N. Acc. under CCK_8 superfusion. Our results give support to the proposed potentiation of the effects of DA by CCK_8 in the posterior N. Acc.[4]. On the other hand, under the experimental conditions used, no modification of motor activity was observed, even with the highest dose of CCK_8 which produced a 64% increase of DA levels in the perfusate.

In general an increase of DA release in the N. Acc. is associated with a hyperactivity[36], however, several explanations can be proposed for the lack of behavioral modification following local CCK_8 treatment. First, the DA release induced by CCK_8 is perhaps too low to produce a behavioral effect, although 0.5 mg/kg of D/L-amphetamine, which induced a comparable increase of DA in the N. Acc., was able to induce a hyperactivity. However, the CCK_8 was administered locally in the posterior N. Acc. while the D/L-amphetamine was given i.p. and then could act on many other neuronal systems to produce its locomotor effect (anterior part of the N. Acc., dorsal striatum). Another hypothesis is that the DA release observed after CCK_8 treatment could be restricted to a category of DA neurones which are not involved in hyperlocomotion. Accordingly, anatomical studies have shown ultrastructural differences suggesting distinct subpopulations of mesencephalic DA neurones projecting to the rat N. Acc.[48]. A third possibility is that the lack of change in global activity after local CCK_8 perfusion into the posterior N. Acc. could be due to the habituation of the rats to their environment, since they were placed in the boxes the day prior experiments. Indeed, certain behavioral effects can only be observed under certain experimental conditions, for instance, CCK8 was shown to induce a hypoexploration measured in the four hole box or in the open field, only in rats non accustomed to these tests[6]. In our study, the habituation could possibly explain the absence of behavioral effects. Experiments are in progress to evaluate the importance of the environment on the DA release induced by CCK_8 and its link with the behavioral effects.

Finally, if the effect of CCK_8 is physiologically significant, this could indicate that the peptide behaves as a positive feed-forward modulator of DA release, since CCK_8 contained in the mixed CCK/DA neurones was shown to be co-released with DA after amphetamine or potassium treatments. This CCK release would increase that of DA. Nevertheless, this hypothesis is not the only one possible, since recent anatomical data have shown that CCK terminals issuing from neurones of the nucleus tractus solitarius are also present in the posterior N. Acc.[45].

In the anterior N. Acc., the 40 min perfusion of 10^{-4} M of the selective CCK_B agonist BC264 (i.e. 350 pmol) decreased significantly the extracellular DA outflow for 60 min following the end of the perfusion. A similar decrease in DA release has been recently reported from slices of anterior N. Acc.[26]. On the other

hand, no modification of the metabolite levels was observed. Although the extracellular levels of metabolites are not necessarily a good reflection of the neuronal enzymatic activity, this lack of effect on the extracellular levels of DOPAC and HVA could be due to a compensatory modification of catabolic activities (monoamine oxydase and catecholamine-*O*-methyl transferase) in order to maintain a constant level of metabolites despite the reduced DA release. However, this hypothesis would need further investigation to be validated. Finally, the lack of quantitative change in the global motor activity of animals is in agreement with a previous study, showing a qualitative, but not a quantitative, modification of locomotor activity after intra-accumbens injection of BC264. A decrease of the spontaneous alternation but not of the number of arm visits (measured in the Y-maze) has been reported after the administration of BC264 in the anterior N. Acc. in the same picomolar dose range as used in this study[8]. It is interesting to note that a 6-hydroxydopamine lesion in the N. Acc., which decreases the DA content, also induced a decrease in the spontaneous alternation behaviour of rats[10,37].

This study provides evidence that CCK_8 and BC264 modify DA neurotransmission in the N. Acc. and leads to an important question: what part of the synapse (i.e. pre or postsynaptic element) is involved in the effects of CCK_8 and BC264? A direct action on DA terminals was suggested, since tetrodotoxin (a voltage-dependent sodium channels blocker) was unable to block the CCK_8-induced modifications of DA efflux from slices of N. Acc.[26]. Nevertheless, no modification in the density of CCK binding sites was found in the N. Acc. after 6-hydroxydopamine lesions of mesolimbic and nigrostriatal DA neurones[13]. One possible reason for this discrepancy might be due to a low density of CCK receptors on the DA terminals, which would mean that the reduction of binding following lesioning would not be significant. Another possibility could be an action of CCK_8 on terminal fibers coming from other structures which act on DA terminals such as glutamatergic fibers from the hippocampus or amygdala or GABAergic fibers.

Finally, the differences observed between the basal levels of DA, DOPAC and HVA in the anterior, median and posterior N. Acc. on one hand and between the locomotor activity of the rats implanted in these three regions on the other hand are interesting. In the caudal region of the N. Acc., the basal release of the three biogenic amines appeared to be higher than in the other regions. A similar region specific difference in DA release has also been shown to occur in superfused slices of anterior and posterior N. Acc. under conditions of K^+-evoked release[26]. Moreover, the global DA content was also shown to be different in the N. Acc. with DA innervation being more important in the caudal part than in the rostral one[14]. In agreement with these findings, our data show that the rats implanted in the posterior N. Acc. have a slight, although not significant, reduction in their locomotor activity. On the other hand, it cannot be excluded that the implantation of the probe in the various parts of the N. Acc. induced lesions of neural networks differently involved in the control of locomotion.

This paper reports the first microdialysis results showing modifications of the extracellular levels of DA in various parts of the N. Acc. by CCK compounds in freely moving rats. These data suggest that the modulation of the DAergic function of the N. Acc. involves two different mechanisms in the anterior and the posterior regions of this structure. In the rostral region, the DA release is reduced via the activation of CCK_B receptors while DOPAC and HVA levels were not changed, indicating a possible metabolic compensation. In contrast, in the caudal region, an increase in extracellular DA and its metabolites was observed. Thus, this functional antagonism between the two regions of the N. Acc. may explain the numerous discrepancies reported in the literature (opposite effects or lack of effect). Finally, the lack of quantitative modification of the global motor activity of the rats following treatment with both CCK agonists could be explained by an habituation of the animals to their environment. It could be interesting to study whether the CCK-induced modification of DA neurotransmission is identical or not in rats submitted to a novel environment or placed in stressful conditions.

In conclusion, these results underline the importance of CCK-DA interactions in the N. Acc. The CCK system might play an important regulatory role in limbic DA function, which is disturbed in several psychiatric disorders. Indeed, several studies in animals and some clinical trials have implicated the CCK system in anxiety[22,30] and in schizophrenia[27]. These interactions between the two systems are all the more interesting, since a reduction of D/L-amphetamine-evoked DA release has been found in the rat anterior N. Acc. after *peripheral* administration of ceruletide, a mixed CCK_A/CCK_B receptor agonist[24]. Increasing our knowledge in this field could lead to the possibility of modulating certain DAergic treatments by CCK agonists or antagonists.

Acknowledgments. We wish to thank Dr. A. BEAUMONT for the stylistic revision of the paper and C. DUPUIS for her assistance in preparing it. We also wish to acknowledge P. Kalivas, C. Durieux

and M. Orosco for their circumspect advices concerning the microdialysis and the HPLC technics.

REFERENCES

1 Barrett, W.R., Steffey, M.E. and Wolfram, A.W., Type A cholecystokinin binding sites in the cow brain: characterization using (−) [^{3}H]L364718 membrane binding assays, *Mol. Pharmacol.*, 36 (1989) 285–290.

2 Charpentier, B., Durieux, C, Pélaprat, D., Dor, A., Reibaud, M., Blanchard, J.C. and Roques, B.P., Enzyme-resistant CCK analogs with high affinities for central receptors, *Peptides*, 9 (1988) 835–841.

3 Corringer, P.J., Durieux, C., Ruiz-Gayo, M. and Roques, B.P., Tritium labelling of two selective agonists for CCK-B receptors: [^{3}H]propionyl-Tyr(SO_3Na)-gNle-mGly-Trp-(N-Me)Nle-Asp-Phe-NH_2 ([^{3}H]pBC264) and [^{3}H]propionyl-γD.Glu-Tyr(SO_3H)-Nle-D.Lys-Trp-Nle-Asp-Phe-NH_2 ([3H]pBC254), *J. Labelled Compounds Radiopharm.*, 31 (1992) 459–468.

4 Crawley, J.N., Hommer, D.W. and Skirboll, L.R., Topographical analysis of nucleus accumbens sites at which cholecystokinin potentiates dopamine-induced hyperlocomotion in the rat brain, *Brain Res.*, 335 (1985) 337–341.

5 Crawley, J.N., Subtype-selective cholecystokinin receptor antagonists block cholecystokinin modulation of dopamine-mediated behaviors in the rat mesolimbic pathway, *J. Neurosci.*, 12 (1992) 3380–3391.

6 Daugé, V., Steimes, P., Derrien, M., Beau, N., Roques, B.P. and Féger, J., CCK8 effects on motivational and emotional states of rat involve CCK-A receptors of the postero-median part of the nucleus accumbens, *Pharmacol. Biochem. Behav.*, 34 (1989) 157–163.

7 Daugé, V., Böhme, G.A., Crawley, J.N., Durieux, C., Stutzmann, J.M., Féger, J., Blanchard, J.C. and Roques, B.P., Investigation of behavioral and electrophysiological responses induced by selective stimulation of CCK-B receptors by using a new highly potent CCK analog, BC 264, *Synapse*, 6 (1990) 73–80.

8 Daugé, V., Derrien, M., Blanchard, J.C. and Roques, B.P., The selective CCK-B agonist, BC 264 injected in the antero-lateral part of nucleus accumbens, reduces the spontaneous alternation behaviour of rats, *Neuropharmacology*, 31 (1992) 67–75.

9 De Witte, P., Heidbreder, C., Roques, B.P. and Vanderhaeghen, J.J., Opposite effects of cholecystokinin octapeptide (CCK8) and tetrapeptide (CCK4) after injection into the caudal part of the nucleus accumbens or the rostral part and the cerebral ventricles, *Neurochem. Int.*, 10 (1987) 473–479.

10 Derrien, M., Durieux, C., Daugé, V. and Roques, B.P., Involvement of D2 dopamine receptors in the emotional and motivational responses induced by injection of CCK8 in the posterior part of the nucleus accumbens, *Brain Res.*, 617 (1993) 181–188.

11 Fallon, J.H. and Seroogy, K.B., The distribution and some connections of the cholecystokinin neurons in the rat brain, *Ann. NY Acad. Sci.*, 448 (1985) 121–132.

12 Fuxe, K. and Ungerstedt, U., Histochemical studies on the effect of (+)-amphetamine, drugs of the imipramine group and tryptamine on central catecholamine and 5-hydroxytryptamine neurones after intraventricular injection of catecholamines and 5-hydroxytryptamine, *Eur. J. Pharmacol.*, 4 (1968) 135–144.

13 Gaudreau, P., Saint-Pierre, S., Pert, C.B. and Quirion, R., Cholecystokinin receptors in mammalian brain. A comparative characterization and visualization, *Ann. NY Acad. Sci.*, 448 (1985) 198–219.

14 Groenewegen, H.J., Meredith, G.E., Berendje, H.W., Voorn, P. and Volters, J.G., The compartmental organization of ventral striatum in the rat. In Crossmann and Sambrook (Eds.), *Neuronal Mechanisms in Disorders of Movements, Vol. 9*, London Libbey, 1989, pp. 45–54.

15 Hamilton, M., Sheehan, M.J., De Belleroche, J., Herberg, L.J., The cholecystokinin analogue caerulein does not modulate dopamine release or dopamine induced locomotor activity in the nucleus accumbens of the rat, *Neurosci. Lett.* 44 (1984) 77–82.

16 Hernandez, L., Lee, F. and Hoebel, B.G., Simultaneous microdialysis and amphetamine infusion in the nucleus accumbens and striatum of freely moving rats: increase in extracellular dopamine and serotonin, *Brain Res. Bull.*, 19 (1987) 623–628.

17 Hökfelt, T., Skirboll, L., Rehfeld, J.F., Goldstein, M., Markey, K. and Dann, O., A subpopulation of mesencephalic dopamine neurones projecting to limbic areas containing a cholecystokinin-like peptide: evidence from immunochemistry combined with retrograde tracing, *Neuroscience*, (1980) 2093–2124.

18 Hökfelt, T., Skirboll, L., Everitt, B.J., Meister, B., Brownstein, M., Jacobs, T., Faden, A., Kuga, S., Goldstein, M., Markstein, R., Dockray, G. and Rehfeld, J., Distribution of cholecystokinin-like immunoreactivity in the nervous system: Co-existence with classical neurotransmitters and other neuropeptides, *Ann. NY Acad. Sci.*, 448 (1985) 255–274.

19 Hökfelt, T., Holets, V.R., Staines, W., Meister, B., Melander, T., Schalling, M., Schultzberg, M., Freedman, J., Bjorklund, H., Olson, L., Lindh, B., Elfvin, L.G., Lundberg, J.M., Lindgren, J.A., Samuelsson, B., Pernow, B., Terenius, L., Post, C., Everitt, B. and Goldstein, M., Co-existence of neuronal messengers-an overview. In T. Hökfelt, K. Fuxe and B. Pernow (Eds.), *Progress in Brain Research, Vol. 68, Ch. 4*, Elsevier Science Publishers, Amsterdam/New York, 1986, pp. 33–70.

20 Hökfelt, T., Herrera-Marschitz, M., Seroogy, K., Ju, G., Staines, W.A., Holets, V., Schalling, M., Ungerstedt, U., Post, C., Rehfeld, J.F., Frey, P., Fischer, J., Dockray, G., Hamaoka, T., Walsh, J.H. and Goldstein, M., Immunohistochemical studies on cholecystokinin (CCK)-immunoreactive neurons in the rat using sequence specific antisera and with special reference to the caudate nucleus and primary sensory neurons, *J. Chem. Neuroanat.*, 1 (1988) 11–52.

21 Hommer, D., Stoner, G., Crawley, J.N., Paul, S.N. and Skirboll, L.R., Cholecystokinin-dopamine co-existence: electrophysiological actions corresponding to cholecystokinin receptor subtype, *J. Neurosci.*, 6 (1986) 3039–3043.

22 Hughes, J., Boden, P., Costall, B., Domeney, A., Kelly, E., Horwell, D.C., Hunter, J.C., Pinnock, R.D. and Woodruff, G.N., Development of a class of selective cholecystokinin type B receptor antagonists having potent anxiolytic activity, *Proc. Natl. Acad. Sci. USA*, 87 (1990) 6728–6732.

23 Kalivas, P.W., Duffy, P. and Eberhardt, H., Modulation of A10 dopamine neurons by γ-aminobutyric acid agonists, *J. Pharmacol. Exp. Ther.*, 253 (1990) 858–866.

24 Kihara, T., Masato, I., Katsuaki, M. and Matsushita, A., Differential effects of ceruletide on amphetamine-induced behaviors and regional dopamine release in the rat, *Eur. J. Pharmacol.*, 230 (1993) 271–277.

25 Marshall, F.H., Barnes, S., Pinnock, R.D. and Hughes, J., Characterization of cholecystokinin octapeptide stimulated endogenous dopamine release from the rat nucleus accumbens in vitro, *Br. J. Pharmacol.*, 99 (1990) 845–848.

26 Marshall, F.H., Barnes, S., Hughes, J., Woodruff, G.N. and Hunter, J.C., Cholecystokinin modulates the release of dopamine from the anterior and posterior nucleus accumbens by two differents mechanisms, *J. Neurochem.*, 56 (1991) 917–922.

27 Nair, N.P.V., Lal, S. and Bloom, D.M., Cholecystokinin peptides, dopamine and schizophrenia-A review, *Prog. Neuro-Psychopharmacol. Biol. Psychiat.*, 9 (1985) 515–524.

28 Paxinos, G. and Watson, C., *The Rat Brain in Stereotaxic Coordinates*, 2nd edn., Academic Press, New York, 1986.

29 Pélaprat, D., Boer, Y., Studler, J.M., Peschanski, M., Tassin, J.P., Glowinski, J., Rostene, W. and Roques, B.P., Autoradiography of CCK receptors in the rat brain using [^{3}H]Boc(Nle$^{28-31}$) CCK_7 and [^{125}I]Bolton Hunter CCK_8. Functional significance of subregional distribution, *Neurochem. Int*, 10 (1987) 495–508.

30 Ravard, S. and Dourish, C.T., Cholecystokinin and anxiety, *Trends Pharmacol. Sci.*, 11 (1990) 271–273.

31 Robinson, T.E. and Whishaw, I.Q., Normalization of extracellular dopamine in striatum following recovery from a partial unilateral 6-OHDA lesion of the substantia nigra: a microdialysis study in freely moving rats, *Brain Res.*, 450 (1988) 209–224.

32 Ruggeri, M., Ungerstedt, U., Agnati, L.F., Mutt, V., Härfstrand,

A. and Fuxe, K., Effect of cholecystokinin peptides and neurotensin on dopamine release and metabolism in the rostral and caudal part of the nucleus accumbens using intracerebral dialysis in the anaesthesized rat, *Neurochem. Int.*, 10 (1987) 509–520.

33 Schalling, H., Friberg, K., Seroogy, K., Riederer, P., Bird, E., Schiffmann, S.N., Mailleux, P., Vanderhaeghen, J.J., Kuga, S., Goldstein, M., Kitahama, K., Luppi, P.H., Jouvet, M. and Hökfelt, T., Analysis of expression of cholecystokinin in dopamine cells in the ventral mesencephalon of several species and in humans with schizophrenia, *Proc. Natl. Acad. Sci. USA* 87 (1990) 8427–8431.

34 Stahle, L., Collin, A.K. and Ungerstedt, U., Effect of halothane anaesthesia on extracellular levels of dopamine, dihydroxyphenylacetic acid, homovanillic acid and 5-hydroxyindolacetic acid in rat striatum: a microdialysis study, *Naunyn Schmiedeberg Arch. Pharmacol.*, 342 (1990) 136–140.

35 Studler, J.M., Simon, H., Cesselin, F., Legrand, J.C., Glowinski, J. and Tassin, J.P., Biochemical investigation of the localization of cholecystokinin octapeptide in dopaminergic neurons originating from the ventral tegmental area of the rat, *Neuropeptides*, 2 (1981) 131–139.

36 Swerdlow, N.R., Vaccarino, F.J., Amalric, M. and Koob, G.F., The neural substrate for the motor-activating properties of psychostimulants: a review of recent findings, *Pharmacol. Biochem. Behav.*, 25 (1986) 233–248.

37 Taghzouti, K., Louilot, A., Herman, J.P., Le Moal, M. and Simon, H., Alternation behaviour, spatial discrimination and reversal disturbances following 6-OHDA lesions in the nucleus accumbens of the rat, *Behav. Neural. Biol.* 44 (1985) 354–363.

38 Ungerstedt, U., Herrera-Marschitz, M., Jungnelius, U., Stahle, L., Tossman, U. and Zetterström, T., Dopamine synaptic mechanisms reflected in studies combining behavioral recordings and brain dialysis, *Adv. Biosci.*, 37 (1982) 219–231.

39 Vaccarino, F.J. and Randkin, J., Nucleus accumbens cholecystokinin (CCK) can either attenuate or potentiate amphetamine-induced locomotor activity: evidence for rostro-caudal differences in accumbens CCK functions, *Behav. Neurosci.*, 103 (1989) 831–836.

40 Vaccarino, F.J. and Vaccarino, A.L., Antagonism of CCK function in the rostral and caudal nucleus accumbens: differential effect on brain stimulation reward, *Neurosci. Lett.*, 97 (1989) 151–156.

41 Vickroy, T.W. and Bianchi, B.R., Pharmacological and mechanistic studies of cholecystokinin facilitated [^{3}H]dopamine efflux from rat nucleus accumbens, *Neuropeptides*, 13 (1989) 43–50.

42 Voigt, M.M. and Wang, R.Y., In vivo release of dopamine in the nucleus accumbens of the rat: modulation by cholecystokinin, *Brain Res.*, 296 (1984) 189–194.

43 Voigt, M.M., Wang, R.Y. and Westfall, T.C., The effects of cholecystokinin on the in vitro release of newly synthesized [^{3}H]dopamine from the nucleus accumbens of rat, *J. Neurosci.* 5 (1985) 2744–2749.

44 Voigt, M.M., Wang, R.Y. and Westfall, T.C., Cholecystokinin octapeptides alter the release of endogenous dopamine from the rat nucleus accumbens in vitro, *J. Pharmacol. Exp. Ther.*, 237 (1986) 147–153.

45 Wang, Z.J., Rao, Z.R. and Shi, J.W., Tyrosine hydroxylase, neurotensin or cholecystokinin-containing neurons in the nucleus tractus solitari send projection fibers to the nucleus accumbens in the rat, *Brain Res.* 578 (1992) 347–350.

46 White, F.J. and Wang, R.Y., Interactions of cholecystokinin octapeptide and dopamine on nucleus accumbens neurons, *Brain Res.*, 300 (1984) 161–166.

47 Zaborsky, L., Alheid, G.H., Beinfeld, M.C., Eiden, L.E., Helmer, L. and Palkovits, M., Cholecystokinin innervation of the ventral striatum: a morphological and radioimmunological study, *Neuroscience*, 14 (1985) 427–453.

48 Zahm, D.S. and Brog, J.S., On the significance of subterritories in the 'accumbens' part of the rat ventral striatum, *Neuroscience*, 50 (1992) 751–767.

(3*R*)-*N*-(1-(*tert*-Butylcarbonylmethyl)-2,3-dihydro-2-oxo-5-(2-pyridyl)-1*H*-1,4-benzodiazepin-3-yl)-*N*'-(3-(methylamino)phenyl)urea (YF476): A Potent and Orally Active Gastrin/CCK-B Antagonist

Graeme Semple,*[†] Hamish Ryder,[†] David P. Rooker,[†] Andrzej R. Batt,[†] David A. Kendrick,[†] Michael Szelke,[†] Mitsuaki Ohta,[‡] Masato Satoh,[‡] Akito Nishida,[‡] Shinobu Akuzawa,[‡] and Keiji Miyata[‡]

Ferring Research Institute, Chilworth Research Centre, Chilworth, Southampton SO16 7NP, U.K., and Institute for Drug Discovery Research, Yamanouchi Pharmaceutical Co., Ltd., 21, Miyukigaoka, Tsukuba, Ibaraki 305, Japan

Received September 25, 1996[⊗]

A number of new 1,4-benzodiazepin-2-one-based gastrin/CCK-B receptor antagonists related to the archetypal analogue L-365,260, and more closely to the recently reported compound YM022, have been synthesized and evaluated for biological activity. The compounds were screened for their ability to inhibit the binding of [^{125}I]CCK-8 to gastrin/CCK-B receptors prepared from rat brains and that of [^{3}H]L-364,718 to CCK-A receptors from rat pancreas, and were shown to be potent and selective ligands for the gastrin/CCK-B receptor. Functional studies *in vivo* demonstrated the compounds to be antagonists of the receptor as evidenced by their ability to inhibit pentagastrin-induced gastric acid secretion in anesthetized rats. More extensive evaluation *in vivo* included determination of ED_{50} values in the rat acid secretion model for selected compounds and an examination of the effect of these compounds on pentagastrin-induced gastric acid secretion in Heidenhain pouch dogs following oral and intravenous administration. Two compounds, i.e. (3*R*)-*N*-[1-[(*tert*-butylcarbonyl)methyl]-2,3-dihydro-2-oxo-5-(2-pyridyl)-1*H*-1,4-benzodiazepin-3-yl]-*N*'-[3-(methylamino)phenyl]urea, **15c** (YF476), and (3*R*)-*N*-[1-[(*tert*-Butylcarbonyl)methyl]-2,3-dihydro-2-oxo-5-(2-pyridyl)-1*H*-1,4-benzodiazepin-3-yl]-*N*'-[3-(dimethylamino)phenyl]urea hydrochloride, **15d**, showed potent dose-dependent effects in both models with the former showing excellent oral bioavailability and an ED_{50} of 21 nmol/kg po in dogs. **15c** is currently under clinical investigation for the treatment of gastro-oesophagal reflux disease (GORD).

Introduction

Gastric acid secretion is controlled by the action of (H^+,K^+)-ATPase (the proton pump) in response to stimulation of muscarinic (M_3), histamine (H_2), or gastrin receptors by their respective agonists. H_2 receptor antagonists and proton pump inhibitors are highly effective in reducing acid secretion[1−3] and have been the treatments of choice for peptic ulcer disease for a number of years. However, prolonged inhibition of secretion with either of these agents causes continuous stimulation of G-cells, resulting in hypergastrinaemia which is believed to lead to hyperplasia of the oxyntic mucosa[4,5] and the so-called acid rebound phenomenon. In addition, long-term administration of omeprazole, the prototypical proton pump inhibitor, results in the growth of gastric carcinomas in rats,[6] although such an effect has not been observed in humans.[7]

With the discovery of evidence for the involvement of the pathogen *Helicobacter pylori* in the majority of peptic ulcer cases, clinical prescribing regimens have changed. The increasing use of combination therapies has meant that antisecretory drugs are given for much shorter periods of time and any rebound effect is less important. However, *Helicobacter pylori* is not implicated in the pathogenesis of gastro-oesophagal reflux disease (GORD), and with longer treatment courses required with existing antisecretory drugs for treatment of this disorder, hypergastrinaemia, acid rebound, and relapse again present a problem.

Gastrin-17 is a heptadecapeptide hormone which acts as a physiological mediator of acid secretion in response to meals. It is closely related to cholecystokinin (CCK), the C-terminal pentapeptide portion being identical. Cloning of the gastrin and CCK receptors, designated CCK-A (the peripheral receptor) and CCK-B (the central receptor), has shown the gastrin and CCK-B receptors to be identical.[8] More recently there has been convincing evidence for a second gastrin receptor, which can bind the glycine-extended form of gastrin-17 and which appears to be responsible for the mitogenic effects of gastrin.[9]

With the above in mind, we decided to investigate inhibitors of the gastrin/CCK-B receptor as an alternative method of reducing gastric acid secretion, or indeed as an adjunct to longer term treatment with known inhibitors of acid secretion, which would avoid gastrin-mediated side effects and hence provide a useful new treatment for GORD and other gastrointestinal disorders.

We have recently described the discovery of a potent series of 1,4-benzodiazepin-2-one gastrin/CCK-B receptor antagonists related to the archetypal analogue L-365,260 (**1**, Figure 1) with sub-nanomolar affinities for the receptor, the compound YM022 (**2**)[10] being the optimal structure in our series.[11] Further improvement of the *in vivo* activity and bioavailability of these derivatives by incorporation of 1-alkylcarbonylmethyl and 5-(2-pyridyl) substituents has been communicated in preliminary form.[12,13]

In this paper we would like to present the structure−activity relationship studies which led us to the discovery of (3*R*)-*N*-[1-[(*tert*-Butylcarbonyl)methyl]-2,3-dihydro-

[†] Ferring Research Institute.
[‡] Yamanouchi Pharmaceutical Co., Ltd.
[⊗] Abstract published in *Advance ACS Abstracts*, January 1, 1997.

S0022-2623(96)00669-3 CCC: $14.00

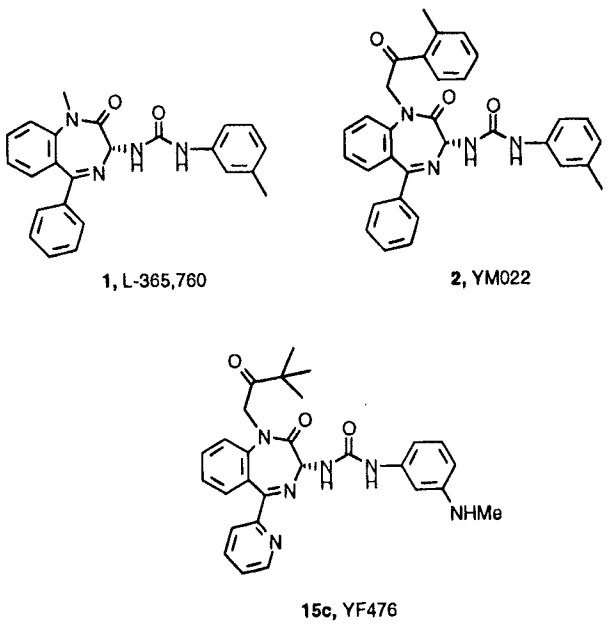

Figure 1. Structures of benzodiazepine-based gastrin/CCK-B ligands.

2-oxo-5-(2-pyridyl)-1*H*-1,4-benzodiazepin-3-yl]-*N*'-[3-(methylamino)phenyl]urea, (**15c**, YF476), a novel, potent gastrin/CCK-B antagonist incorporating a combination of these and other modifications and which is currently undergoing clinical trials.

Chemistry

Two approaches have previously been applied successfully to the synthesis of 3-substituted 1,4-benzodiazepines. The first involves construction of the parent heterocycle, followed by functionalization. In the case of 3-amino derivatives, this has been best achieved by formation of an oxime at the 3-position of the 1-alkylated 1,4-benzodiazepine, followed by catalytic hydrogenation.[14] As previously reported, YM022 was readily prepared using this procedure.[11] This method turned out not to be generally applicable, however, as attempts to adapt the chemistry for use in compounds with a 5-(2-pyridyl) substituent on the benzodiazepine scaffold failed at the final stage (Figure 2) when imine isomerization to give **8** was observed in addition to the desired oxime reduction.

The alternative strategy for the synthesis of 3-substituted 1,4-benzodiazepin-2-ones requires N-acylation of a 2-aminobenzoyl derivative with a carboxylic acid containing a suitable masked amine group X at the α-position (Figure 3). The amine functionality is eventually revealed and the intermediate cyclized to give the desired benzodiazepine.

This approach has been used to provide 3-amino-substituted benzodiazepines in good yield by coupling of 2-aminobenzophenone to α-(isopropylthio)-*N*-(benzyloxycarbonyl)glycine[15] (i.e. Figure 3, X = isopropylthio), followed by mercuric chloride-induced displacement of the thioether group with ammonia and finally acid-catalyzed cyclization to provide the desired benzodiazepine.[16] In our hands, this method proved very useful for the small-scale preparation of a wide range of protected 3-amino-5-arylbenzodiazepines and was highly amenable to producing series of analogues with 1-, 3-, and 5-position variations. Scale-up reactions, however,

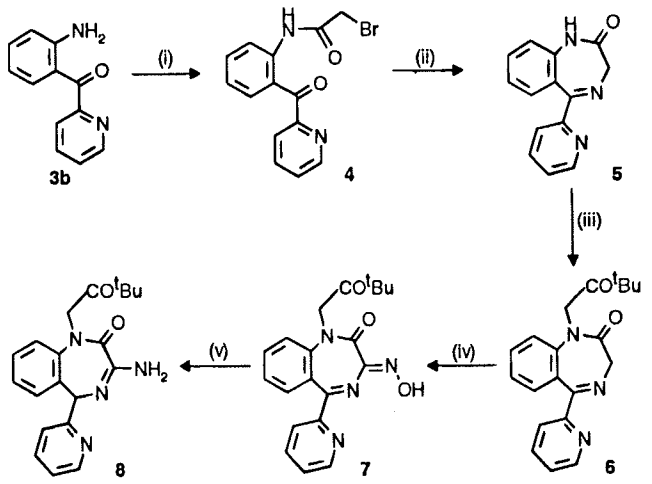

Figure 2. Synthesis of 3-amino-1-[(*tert*-butylcarbonyl)-methyl]-2,5-dihydro-5-(2-pyridyl)-1*H*-1,4-benzodiazepin-2-one. Reagents and conditions: (i) $BrCH_2COBr$, AcOH; (ii) (a) NH_3, (b) AcOH; (iii) (a) NaH, DMF, (b) $^tBuCOCH_2Br$; (iv) (a) KO^tBu, (b) ^iAmONO; (v) H_2/5% Ru on C, 60 °C, 20 kg/cm^2.

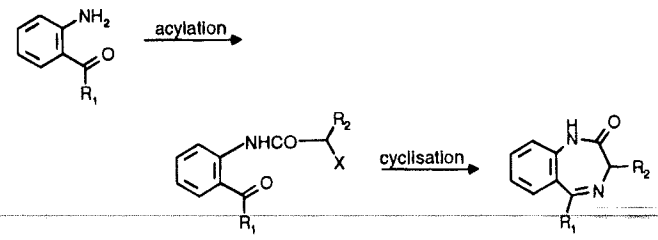

Figure 3. General strategy for benzodiazepine synthesis.

gave variable yields, and large-scale use of thioethers and highly toxic mercury salts is clearly undesirable. We were, however, able to make use of the same strategy for the construction of the benzodiazepine ring by using benzotriazole as the displaceable group (Figure 4) as reported recently by ourselves[17] and others.[18] The benzyl carbamate of α-(1-benzotriazolyl)glycine[19] (**9**) was coupled to the requisite (2-aminobenzoyl)aryl derivative in excellent yield, the benzotriazole moiety was then displaced with ammonia under mild conditions, and the ring synthesis was completed by brief acid treatment to form the benzodiazepine **11**. High yields of crystallizable products were obtained in this way under mild conditions and without the use of toxic reagents, and this route became our method of choice.

Conversion of **11** to the key intermediate **13** was accomplished by 1-alkylation with 1-bromopinacolone, followed by removal of the carbamate protecting group. In the 5-phenyl series the alkylated compound **12a** could be readily deprotected by hydrogenolysis of its benzyl carbamate (Z) protecting group. However, attempted removal of the Z-group from the 5-(2-pyridyl) analogue **12b** under the same conditions resulted in concomitant reduction and/or isomerization of the benzodiazepine imine function, depending on the hydrogenation conditions. The deprotection could, however, be effected in this case by treatment of **12b** with dry HBr in DCM. With carbamate protecting groups other than Z, a cleaner conversion to **13b** was achieved by treatment with TMSI.[17]

It is well documented that the opposite enantiomers of benzodiazepine-based gastrin/CCK-B ligands behave quite differently towards the receptor, with the (3*R*)-isomer being consistently the more active species.[11,20]

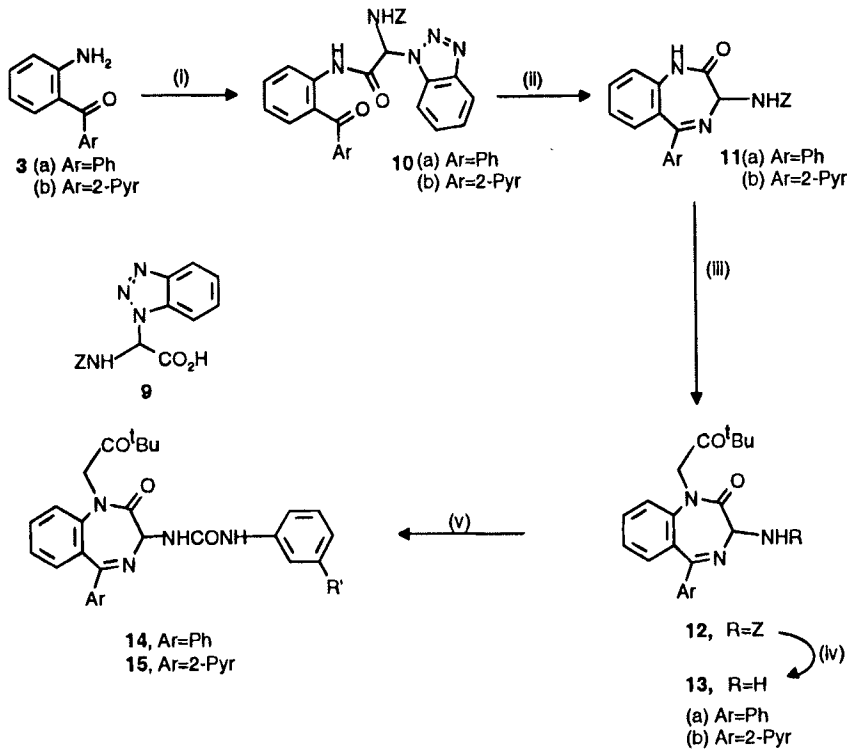

Figure 4. Benzotriazole-mediated synthesis of 5-phenyl- and 5-(2-pyridyl)-1,4-benzodiazepin-2-ones. Reagents and conditions: (i) EDC, **9**, 0 °C to room temperature; (ii) (a) NH_3/MeOH, (b) AcOH; (iii) (a) NaH, DMF, (b) $^tBuCOCH_2Br$; (iv) Ar=Ph, H_2/5% Pd on C; Ar=2-Pyr, HBr in DCM, 0 °C; (v) 3-R′-PhNCO.

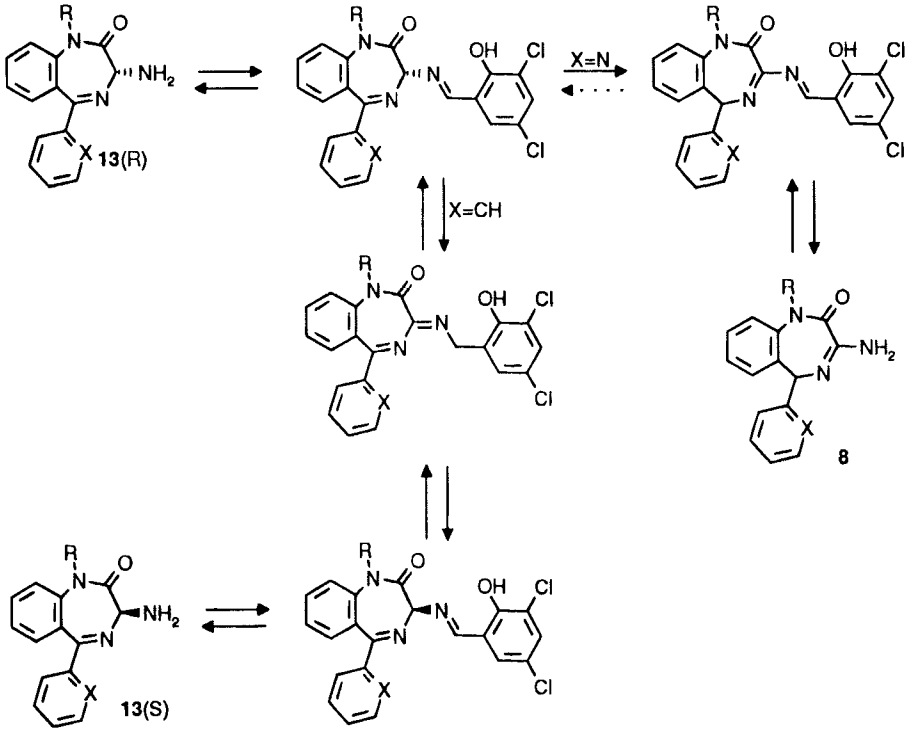

Figure 5. Interconversion of isomeric benzodiazepines *via* 3,5-dichlorosalicyl imines.

Where appropriate, we prepared the more active enantiomers of **14** and **15** by resolution of the 3-amino derivatives **13** followed by reaction of the resultant homochiral amine intermediate with the required isocyanate. The amine **13a** was readily resolved using a resolution–racemization method,[21] but under the same conditions, the analogue **13b** was converted to the isomeric 3-amino-2,5-dihydro-5-(2-pyridyl)-1*H*-1,4-benzodiazepin-2-one (**8**) obtained previously, and we were only able to resolve **13b** by classical fractional crystallization of its (*R*)- and (*S*)-mandelate salts.[17]

The resolution–racemization process operates through the interconversion of a series of imine intermediates which reversibly epimerize the 3-amino center (Figure 5, X = CH). However it appears that when the 5-substituent is a 2-pyridyl group (Figure 5, X = N) the favored isomerization is for the imino function within the benzodiazepine ring to move into conjugation with

the external imine and not *vice versa*. This process does not appear to be reversible when X = N, and so the eventual hydrolysis of the salicyl imine in this case gave the mandelic acid salt of **8** as the only isolable product. As with the differences in the hydrogenolysis products between the two series, the formation of this alternative product can only be ascribed to the differing electronic properties of the 5-phenyl and 5-(2-pyridyl) substituents adjacent to the benzodiazepine imine function.

Biology

The methods used for measuring binding of [^{125}I]CCK-8 to rat brains and that of [^{3}H]L-364,718 to rat pancreas were essentially identical to those described previously.[22] Specific binding was defined as the difference between total binding and nonspecific binding in the presence of 1 mM CCK-8 or L-364,718.

For *in vivo* screening studies, gastric acid secretion was measured in anesthetized rats as reported previously.[10] Acid secretion was measured at pH 7.0 using the pH-stat method with the addition of 0.025 N NaOH to the reservoir. Approximately 30 min after basal secretion had stabilized, pentagastrin at a rate of 20 nmol/kg/h was infused through the femoral vein. Test compounds were dissolved with polyethylene glycol 300 and injected iv 1 h after the start of pentagastrin infusion.

In the secondary *in vivo* test system, male beagle dogs with a Heidenhain pouch were used. One month after preparation of the pouch, secretory experiments were performed once a week in each animal throughout the experiments. Acidity of the gastric juice was measured by automatic titration of the gastric juice with 0.05 M NaOH to pH 7.0. Pentagastrin was infused at a rate of 8 μmol/kg/h through the femoral vein. Test compounds were administered po or iv at 3 h after the start of pentagastrin infusion.

Results and Discussion

A major drawback associated with the early benzodiazepine-based gastrin/CCK-B receptor antagonists was their lack of oral efficacy. This is exemplified by L-365,260, which is only sparingly soluble in water and has very limited oral bioavailability unless dosed as a solution in PEG 600.[23] We have previously shown that incorporation of a (*tert*-butylcarbonyl)methyl group at the 1-position[12] or a 2-pyridyl group at the 5-position[13] of the parent benzodiazepine structure provides a significant increase in absorption. Similar results have been achieved by incorporation of either a cyclohexyl group[24] or a cyclic amine to form an amidino functionality in the 5-position.[25] Other attempts to improve aqueous solubility have included introducing acidic groups,[26] or lipophilic surrogates thereof,[27] into the 3-position of the aryl urea portion of either the 1,4-benzodiazepin-2-one parent system or closely related structures.[28] We have recently shown that the opposite strategy, introducing basic amino substituents into the same region of the YM022 series, can provide an improvement in selectivity for the gastrin/CCK-B receptor over the CCK-A receptor. More significantly perhaps, increased inhibition of pentagastrin-induced gastric acid secretion in rats following intraduodenal administration was also observed for these compounds when compared to either the (3-methylphenyl)- or (3-carboxyphenyl)urea derivatives.[29] We can now report that when combinations of the above modifications are incorporated into the same molecule, the improvements in the *in vivo* effects are essentially additive, resulting eventually in the identification of **15c** which has potent oral antisecretory activity in Heidenhain pouch dogs.

We initially examined the effect of incorporating neutral, acidic, or basic groups in the 3-position of the phenylurea substituent of the 1-[(*tert*-butylcarbonyl)-methyl]-1,3-dihydro-5-phenyl-2*H*-1,4-benzodiazepin-2-one core structure as shown in Table 1. We observed that the incorporation of a 3-carboxy substituent, to give **14b**, did not improve binding to the rat gastrin/CCK-B receptor, although some *in vivo* antisecretory activity was still observed at 0.1 μmol/kg iv in our rat screening model. It is important to note that basal levels of acid secretion in this model are typically around 25−30% of the pentagastrin-induced peak; hence a figure of 75−80% inhibition represents the return of acid secretion to basal levels or below.

The (3-aminophenyl)urea derivative **14f** was essentially equipotent with the parent 3-tolylurea derivative **14a** both *in vitro* and *in vivo* in rats. However, when alkylated amino groups were incorporated into the same position (**14g−j**), there was a significant improvement in the compounds' affinities for the gastrin/CCK-B receptor, which was accompanied in most cases by improved receptor selectivity. In addition, all of the [3-(alkylamino)phenyl]urea analogues showed significant inhibition of pentagastrin-induced gastric acid secretion *in vivo* in rats at the screening dose of 0.1 μmol/kg iv.

We next examined the effect of introducing the 5-(2-pyridyl) substituent, which we had previously shown conferred improved bioavailability when incorporated as a single change to the parent structure,[13] into the [3-(alkylamino)phenyl]urea series. As can be seen in Table 1, all of the resulting compounds with the exception of the 3-(1-piperidyl)phenyl urea analogue **15h** showed comparable or improved affinity and selectivity for the gastrin/CCK-B receptor when compared to the parent 3-tolylurea derivative **15a**. In addition, the active compounds in this second [3-(alkylamino)phenyl]-urea series again showed potent inhibition of pentagastrin-induced gastric acid secretion *in vivo* in rats at the screening dose of 0.1 μmol/kg iv. No significant advantage was observed by either increasing the size of the alkyl groups on the amino nitrogen or incorporating them into a ring.

Several compounds from the two series were selected for more extensive evaluation *in vivo* (Table 2) according to the methods previously described.[30] ED_{50} values were determined for the inhibition of pentagastrin-induced gastric acid secretion in rats following iv administration of the test compound, and as expected, all of the analogues tested showed potency comparable to that of the original parent compound YM022 in this model.

We next examined the effect of the compounds on pentagastrin-induced gastric acid secretion in Heidenhain pouch dogs. As we were searching for compounds with significant oral activity, for our first screening point we selected an oral dose of 3 μmol/kg and all of the compounds tested showed a significant effect at this dose. There was already an indication that the incor-

Table 1. Structure–Activity Relationships of 3-Substituted Phenylurea Derivatives of 2,3-Dihydro-1*H*-1,4-benzodiazepin-2-ones **14** and **15**

compd no.	config	R′	CCK-B[a] (nM)	CCK-A[b] (nM)	ratio (CCK-A/CCK-B)	*in vivo* screening (% inhibition of H^+ secretion in rats at 0.1 μmol/kg iv)[c]
2			0.11 (0.10–0.11)	146 (120–170)	1327	ED_{50} = 8.3 nmol/kg (6.1–10.9)
14a	*R*	Me	0.52 (0.43–0.63)	111 (85–146)	213	77[d]
14b	*RS*	CO_2H	3.29 (2.41–4.50)	2059 (1594–2659)	626	56
14c	*RS*	NO_2	0.16 (0.10–0.28)	589 (527–658)	3681	76
14d	*RS*	CN	1.29 (0.25–6.70)	700 (631–776)	542	65
14e	*RS*	NHCHO	0.59 (0.28–1.21)	561 (521–605)	951	74
14f	*R*	NH_2	0.50 (0.38–0.67)	953 (807–1125)	1906	75
14g	*R*	NHMe	0.11 (0.08–0.15)	120 (88–164)	1091	80
14h	*R*	NMe_2	0.21 (0.18–0.29)	89 (73–108)	423	65
14i	*R*	NEt_2	0.14 (0.11–0.18)	558 (421–741)	3986	82
14j	*R*	1-pyrrolidyl	0.17 (0.13–0.22)	157 (145–171)	923	79
15a	*R*	Me	0.44 (0.33–0.59)	470 (361–611)	1068	78
15b	*R*	NH_2	0.43 (0.35–0.54)	1820 (1699–1949)	4233	62
15c	*R*	NHMe	0.10 (0.08–0.13)	502 (434–581)	5020	87
15d	*R*	NMe_2	0.20 (0.15–0.26)	113 (82–156)	565	65[d]
15e	*S*	NMe_2	1.26 (0.83–1.91)	572 (486–674)	454	nd
15f	*R*	NEt_2	0.11 (0.07–0.19)	301 (230–395)	2736	74
15g	*R*	1-pyrrolidyl	0.11 (0.10–0.12)	253 (188–342)	2300	75
15h	*R*	1-piperidyl	0.84 (0.79–0.88)	944 (759–1173)	1124	55

[a] IC_{50} value for displacement of [^{125}I]CCK-8 from gastrin/CCK-B receptors from rat brain (95% confidence limits). [b] IC_{50} value for displacement of [^{3}H]L-364,718 from CCK-A receptors from rat pancreas (95% confidence limits). [c] Inhibition of pentagastrin-induced gastric acid secretion in anethsetized rats (0.1 μmol/kg iv). [d] Percent inhibition at a dose of 0.03 μmol/kg.

Table 2. Further *in Vivo* Evaluation of New Gastrin/CCK-B Antagonists. Inhibition of Pentagastrin-Induced Gastric Acid Secretion in Rats and Heidenhain Pouch Dogs

compd	SD rat (iv) ED_{50} (μmol/kg)	inhibition of pentagastrin-induced gastric acid secretion in Heidenhain pouch dogs (po)	inhibition of pentagastrin-induced gastric acid secretion in Heidenhain pouch dogs (iv)
YM022 (**2**)	0.0078	72% at 3 μmol/kg 26% at 1 μmol/kg ED_{50} = 1.9 μmol/kg (1.0–2.9)[a]	ED_{50} = 0.026 μmol/kg (0.008–0.051)
14a	0.0057	53% at 3 μmol/kg	nd
14h	0.012	99% at 3 μmol/kg	nd
15a	0.016	97% at 3 μmol/kg 7% at 0.3 μmol/kg	nd
15c	0.008	100% at 0.1 μmol/kg 65% at 0.03 μmol/kg ED_{50} = 0.021 μmol/kg (0.013–0.029)	ED_{50} = 0.018 μmol/kg (0.013–0.027)
15d	0.011	98% at 0.1 μmol/kg 77% at 0.03 μmol/kg	ED_{50} = 0.014 μmol/kg (0.009–0.033)

[a] Figures in parentheses represent 95% confidence limits. nd = not determined.

poration of an alkylated amino group conferred beneficial effects on oral absorption, as **14h** was considerably more potent than **14a** at this preliminary oral dose level.

All three analogues which incorporated a 5-(2-pyridyl) substituent showed complete inhibition of acid secretion at the first screening dose. Lowering the dose allowed us to show that the combination of a 5-(2-pyridyl) group and a 3-(alkylamino) substituent on the urea portion provided highly potent orally active compounds. **15c** and **15d** were essentially equipotent in this dog model, and an ED_{50} value of 21 nmol/kg (~0.01 mg/kg) was determined for **15c**,[30] thus showing this compound to be about 90 times more potent than YM022 after oral administration. In addition, the inhibiton curves (Figure 6) showed that both compounds had an excellent duration of action, maintaining complete inhibiton of acid secretion for more than 6 h following oral administration at the 100 nmol/kg dose level.

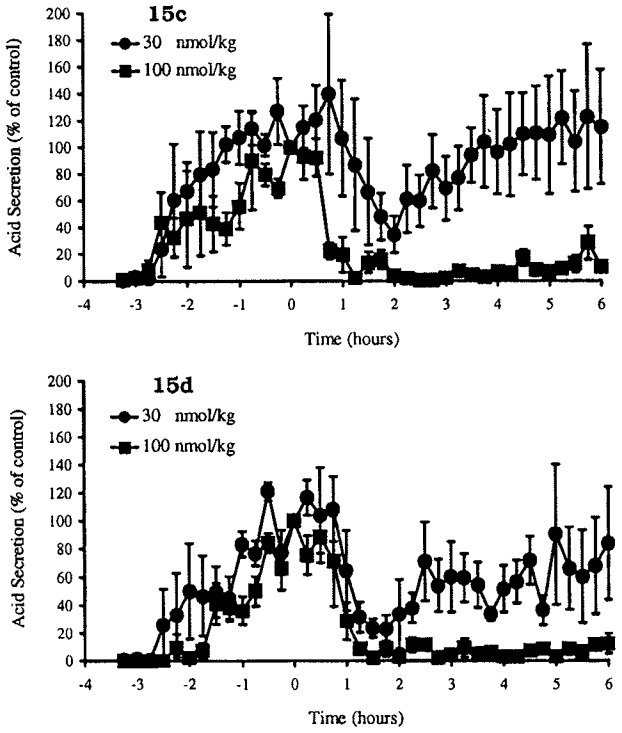

Figure 6. Inhibition of pentagastrin-induced gastric acid secretion in Heidenhain pouch dogs by oral administration of **15c** and **15d**. Pentagastrin 8 μmol/kg/h was infused from 3 h before, until 6 h after drug administration (t = 0), and acid secretion was measured by automatic titration. Each point is represented as a percentage of values observed immediately before drug administration and is the mean ± SEM (five animals per group).

To obtain an indication of the magnitude of the advantage provided by our new analogues in terms of oral bioavailability, we determined the ability of YM022, **15c**, and **15d** to inhibit pentagastrin-induced gastric acid secretion in Heidenhain pouch dogs following iv administration, and as expected all three compounds showed potent effects *via* this route (Table 2). When compared to their effects following oral dosing, we observed that compounds **15c** and **15d** showed only a modest difference in activity between oral and iv administration, whereas YM022 was around 70 times less potent following oral administration than by the iv route. These data indicated that both **15c** and **15d**, but not YM022, have excellent oral bioavailibility in dogs, and this together with their long duration of action *in vivo* suggested that we had identified two possible clinical candidates for the treatment of GORD and other gastrointestinal disorders.

Finally we conducted physicochemical studies on the two potential clinical candidates to determine their stability in the crystalline form. Gratifyingly, **15c** was obtained in a single-crystal form when isolated as its free base and remained stable even after 3 months at 40 °C and 75% relative humidity (no imine bond tautomerization was observed under these conditions). This compound, given the code number YF476, was selected for further development and is currently under clinical investigation for the treatment of GORD.

Experimental Section

Analytical and spectroscopic data for test compounds are included in the Supporting Information. Melting points were determined using a Yanaco MP-500D instrument and are uncorrected. Optical rotations were measured using a Perkin-Elmer 241 polarimeter and are uncorrected. ^{1}H NMR spectra were obtained using either a JEOL FX-90Q, a JEOL EX-270, or a JEOL JNN-EX-400 spectrometer. ^{13}C NMR spectra were obtained using a JEOL EX-270 spectrometer. Carbon atom types were determined by 90- and 135-DEPT experiments. Chemical shifts are reported in ppm (δ) downfield of tetramethylsilane as an internal reference (δ 0.0). Positive FAB mass spectra were recorded in glycerol or thioglycerol matrix either at the Michael Barber Centre for Mass Spectrometry, UMIST, Manchester, U.K., or by the Analytical Department of Yamanouchi Pharmaceutical Co. Elemental analyses were determined either by Elemental Microanalysis Ltd., Okehampton, Devon, U.K. or by the Analytical Department of Yamanouchi Pharmaceutical Co. and are within ±0.4% of calculated values. All reagents were obtained from commercial sources and used without further purification unless otherwise noted.

2-[2-[2-Bromoacetyl)amino]benzoyl]pyridine (4)[31]. **3b**[17,32] (2.5 g, 12.63 mmol) was taken up in acetic acid (25 mL) and the mixture stirred at 4 °C. Bromoacetyl bromide (1.1 mL, 12.8 mmol) was added dropwise over 20 min, and stirring continued for a further 15 min at 4 °C. The mixture was then evaporated, and the residue was partitioned between EtOAc (50 mL) and 0.5 M NaOH (50 mL). The organic portion was washed with water and brine, dried over Mg_2SO_4, and evaporated. The title compound was crystallized from EtOAc/hexane as a pale brown solid (3.25 g, 81%): mp 92−94 °C; ^{1}H NMR (400 MHz, $CDCl_3$) δ 11.67 (br s, 1H), 8.73 (d, 1H, J = 5Hz), 8.64 (d, 1H, J = 8Hz), 7.96−7.90 (m, 2H), 7.82 (dd, 1H, J_1 = 8 Hz, J_2 = 2 Hz), 7.61 (m, 1H), 7.51 (ddd, 1H, J_1 = 7 Hz, J_2 = 5 Hz, J_3 = 2 Hz), 7.17 (t, 1H, J = 8 Hz), 4.03 (s, 2H) ppm. Anal. ($C_{14}H_{11}N_2O_2Br$) C, H, N, Br.

2,3-Dihydro-5-(2-pyridyl)-1*H*-1,4-benzodiazepin-2-one (5). The title compound was prepared directly from **3b** without purification of the bromoacetylated intermediate **4** as described:[31] mp 245−246 °C (lit.[31] mp 232−234 °C); ^{1}H NMR (400 MHz, $CDCl_3$) δ 9.08 (br s, 1H), 8.64 (dd, 1H, J_1 = 5 Hz, J_2 = 1 Hz), 7.95 (d, 1H, J = 8 Hz), 7.81 (dt, 1H, J_t = 8 Hz, J_d = 2Hz), 7.37 (dd, 1H, J_1 = 7 Hz, J_2 = 5 Hz), 7.33 (dd, 1H, J_1 = 8 Hz, J_2 = 1 Hz), 7.15 (t, 1H, J = 8 Hz), 7.08 (d, 1H, J = 8 Hz), 4.37 (s, 2H) ppm. Anal. ($C_{14}H_{11}N_3O$) C, H, N.

1-[(*tert*-Butylcarbonyl)methyl]-2,3-dihydro-5-(2-pyridyl)-1*H*-1,4-benzodiazepin-2-one (6). **5** (8.3 g, 35 mmol) was azeotroped with DMF and the residue dissolved in dry DMF (300 mL) at 4 °C under nitrogen. Sodium hydride (1.4 g, 80% dispersion in oil, 46.6 mmol) was added portionwise with stirring, and the mixture was stirred for 40 min at 4 °C. 1-Bromopinacolone (6.0 mL, 46 mmol) was added, and the mixture was stirred at 4 °C to room temperature over 2 h. The mixture was evaporated to dryness and partitioned between EtOAc and water. The organic portion was washed with brine, dried ($MgSO_4$), and evaporated. The residue was crystallized from EtOAc/hexane to provide a colorless solid (8.65 g, 74%): mp 180−183 °C; ^{1}H NMR (400 MHz, $CDCl_3$) δ 8.63 (dd, 1H, J_1 = 5 Hz, J_2 = 1 Hz), 8.08 (d, 1H, J = 8 Hz), 7.81 (dt, 1H, J_t = 8 Hz, J_d = 2 Hz), 7.48 (dt, 1H, J_t = 8 Hz, J_d = 2 Hz), 7.38−7.33 (m, 2H), 7.21 (m, 1H), 7.08 (d, 1H, J = 8Hz), 5.09 (d, 1H, J = 18 Hz), 4.86 (d, 1H, J = 10 Hz), 4.36 (d, 1H, J = 18 Hz), 3.98 (d, 1H, J = 10 Hz), 1.28 (s, 9H) ppm; FAB-MS (M + H)$^+$ = 336. Anal. ($C_{20}H_{21}N_3O_2$) C, H, N.

1-[(*tert*-Butylcarbonyl)methyl]-2,3-dihydro-3-oximido-5-(2-pyridyl)-1*H*-1,4-benzodiazepin-2-one (7). The title compound was prepared using a modified version of the previously described procedure.[14,11] **6** (2.00 g, 6.0 mmol) was suspended in dry toluene (72 mL) at −20 °C under nitrogen. KO^{t}Bu (2.68 g, 23.9 mmol) was added portionwise to the stirring mixture so that the internal temperature did not rise above −10 °C, and stirring continued for a further 30 min at −20 °C. Isoamyl nitrite (2.10 g, 3equiv) was added, and the mixture was stirred at −20 to −5 °C over 3 h and then poured into a mixture of ice (100 g), AcOH (5 mL), and EtOAc (100 mL). The aqueous portion was basified and extracted with EtOAc (50 mL), and the combined organic portions were washed with brine, dried (Mg_2SO_4), and evaporated. The residue was crystallized from hot EtOAc (70 mL) as a pale

yellow solid (1.10 g, 51%): mp 262–264 °C dec; ^{1}H NMR (400 MHz, DMSO-d_6) δ 11.17 (1H, s), 8.65 (d, 1H, J = 8 Hz), 8.22 (d, 1H, J = 8 Hz), 8.05 (dt, 1H, J_t = 8 Hz, J_d = 2 Hz), 7.63–7.58 (m, 2H); 7.40 (d, 1H, J = 6 Hz), 7.30–7.24 (m, 2H), 5.03 (d, 1H, J = 18 Hz), 4.91 (d, 1H, J = 18 Hz), 1.17 (s, 9H) ppm; FAB-MS $(M + H)^+$ = 365. Anal. ($C_{20}H_{20}N_4O_3$) C, H, N.

3-Amino-1-[(*tert*-butylcarbonyl)methyl]-2,5-dihydro-5-(2-pyridyl)-1*H*-1,4-benzodiazepin-2-one (8). 7 (500 mg, 1.36 mmol) was taken up in MeOH (25 mL). The solution was degassed and treated with 5% Ru/C (Lancaster Synthesis, 150 mg). The mixture was hydrogenated in a Parr apparatus (20 kg/cm^2 H_2, 60 °C, 24 h) and then filtered and the catalyst well washed with methanol. The solvent was removed by evaporation, and the title compound was obtained by chromatography on silica (eluant 5% MeOH in $CHCl_3$) as a colorless solid (446 mg, 93%): ^{1}H-NMR (400 MHz, $CDCl_3$) δ 8.65 (d, 1H, J = 4 Hz), 7.97 (d, 1H, J = 8 Hz), 7.81 (m, 1H), 7.26 (m, 1H), 7.19 (m, 1H), 7.01 (m, 2H), 6.44 (d, 1H, J = 8 Hz), 5.98 (s, 1H), 5.15 (d, 1H, J = 18 Hz), 4.89 (br s, 2H), 4.70 (d, 1H, J = 18 Hz), 1.31 (s, 9H) ppm; FAB-MS $(M + 1)^+$ = 351.

Preparation of 3-Substituted Carboxylic Acids and Isocyanates. 3-(Formylamino)benzoic Acid. Acetic anhydride (76 mL) was added to 98% formic acid (130 mL), and the mixture was stirred at room temperature for 30 min. 3-Aminobenzoic acid (15 g, 109.5 mmol) was then added. The mixture was stirred at room temperature for 1 h and then treated with water (1.3 L) and stirring continued overnight. The resultant white precipitate was collected, washed with water, and dried *in vacuo* over P_2O_5 (15.4 g, 85%): ^{1}H NMR (270 MHz, MeOH-d_4) δ 8.45–8.3 (m, 2H), 8.0–7.5 (m, 4H) ppm.

3-(*N*-Formylmethylamino)benzoic Acid. A solution of 3-(formylamino)benzoic acid (2.28 g, 13.8 mmol) in DMF (25 mL) was added dropwise to a suspension of sodium hydride (1.05 g, 80% dispersion in oil) in DMF (15 mL) at 0 °C. The mixture was allowed to warm to room temperature over 1 h, and then iodomethane (0.95 ml) was added. A second portion of iodomethane (0.95 mL) was added after 1 h, and the mixture was stirred at room temperature overnight. The solvent was removed by evaporation, and the residue was partitioned between ethyl acetate and 1 M HCl. The organic layer was washed with brine, filtered (Whatman 1 PS phase separator), and evaporated. The residue was chromatographed on silica (eluant 60% EtOAc in hexane) to provide the methyl ester of the title compound as a colorless solid (2.30 g, 86%). A portion of this ester (900 mg, 4.66 mmol) was taken up in dioxane/water (2/1, v/v, 30 mL) and treated with LiOH·H_2O (378 mg, 9 mmol) at room temperature with stirring overnight. The mixture was acidified with 1 M HCl and extracted twice with EtOAc. The combined extracts were washed with brine, filtered (Whatman 1 PS phase separator), and evaporated. The title compound (420 mg, 50%) was used in the next step without further purification: ^{1}H NMR (270 MHz, $CDCl_3$) δ 8.52 (s, 1H), 8.0–7.85 (m, 2H), 7.5–7.35 (m, 2H), 3.36 (s, 3H) ppm.

3-(1-Pyrrolidyl)benzoic Acid. *m*-Aminobenzoic acid (13.7 g, 0.1 mol) was taken up in methanol (150 mL) and cooled to 0 °C. Acetyl chloride (10 mL) was added dropwise, and then the mixture was heated at reflux under nitrogen for 1 h. The mixture was cooled, evaporated, and partitioned between EtOAc and 5% $KHCO_3$. The organic portion was washed with brine, filtered (Whatman 1PS phase separator) and evaporated to provide methyl *m*-aminobenzoate as a brown oil which crystallized on standing (13.2 g, 88%). A portion of this amino ester (5.45 g, 36.1 mmol) was taken up in dry DMF (70mL) and treated with sodium hydride (3.78 g, 80% dispersion in oil, 126 mmol) at 0 °C under nitrogen for 14 h. 1,4-Dibromobutane (14.05 g, 65 mmol) and potassium iodide (0.6 g, 3.7 mmol) were added, and the mixture was heated at 80 °C for 72 h. The mixture was cooled, evaporated, and partitioned between EtOAc and 5% $KHCO_3$. The organic portion was washed with brine, filtered (Whatman 1PS phase separator), and evaporated. The residue was chromatographed on silica (eluant 8% EtOAc in hexane) to provide methyl 3-(1-pyrrolidyl)benzoate as a pale yellow solid (1.70 g, 23%). The solid was taken up in dioxane/water (40 mL) and treated with LiOH·H_2O (1.75 g, 5 equiv) at room temperature for 10 min, then at 40 °C for 30 min. Acetic acid (10 mL) was added, and the mixture was evaporated, azeotroped with toluene, and crystallized from AcOH/water/dioxane to provide a pale brown solid (1.26 g, 80%) which was dried *in vacuo* over P_2O_5: ^{1}H NMR (270 MHz, $CDCl_3$) δ 7.4–7.2 (m, 3H), 6.78 (m, 1H), 3.35 (m, 4H), 2.02 (m, 4H) ppm.

Methyl 3-(4-Pentenoylamino)benzoate. Methyl 3-aminobenzoate (4.5 g, 29.8 mmol) was taken up in DCM (10 mL) and pyridine (1 mL) at 0 °C. 4-Pentenoyl chloride (freshly prepared from 4-pentenoic acid (3.0 g, 29.97 mmol) and thionyl chloride (6.6 mL) at room temperature for 1 h, evaporated and azeotroped with DCM) was added dropwise in DCM (3 mL). The mixture was allowed to warm to room temperature, stirred overnight, and then evaporated. The residue was partitioned between EtOAc and 1 M HCl. The organic portion was washed with 5% $KHCO_3$ and brine, filtered (Whatman 1PS phase separator), and evaporated. The residue was chromatographed (eluant 30% EtOAc in hexanes) to provide a colorless oil (2.20 g, 32%): ^{1}H NMR (270 MHz, $CDCl_3$) δ 8.05 (t, 1H, J = 1.5 Hz), 7.93 (d, 1H, J = 8 Hz), 7.79 (d, 1H, J = 8 Hz), 7.56 (br s, 1H), 7.42 (t, 1H, J = 8 Hz), 5.92 (m, 1H), 5.2–5.0 (m, 2H), 3.93 (s, 3H), 2.51 (m, 4H) ppm.

Methyl 3-[(5-Bromopentanoyl)amino]benzoate. Methyl 3-(4-pentenoylamino)benzoate (1.7 g, 7.3 mmol) was taken up in dry THF (25 mL) at room temperature under nitrogen. 9-BBN (20 mL, 0.5M solution) was added, and the mixture was stirred at room temperature for 3 h. NaOH 1 M, (8 mL) was then added followed by 27% hydrogen peroxide (2.5 mL, dropwise). Stirring was continued at 40 °C for 1 h, and then the mixture was evaporated, taken up in EtOAc, and washed with 5% $KHCO_3$ and brine. The organic portion was filtered (Whatman 1PS phase separator), evaporated, and chromatographed (eluant 95% EtOAc in hexanes) to provide methyl 3-[(5-hydroxypentanoyl)amino]benzoate as a mixture with borates. The crude product was taken up in DCM (120 mL) and treated with triphenylphosphine (5 g) and carbon tetrabromide (6.2 g) at room temperature for 2 h with stirring. The mixture was then evaporated and chromatographed (eluant 40% EtOAc in hexanes) to provide the title compound as a colorless oil which solidified to a wax on standing (1.54 g, 67%). ^{1}H NMR (270 MHz, $CDCl_3$) δ 9.62 (br s, 1H), 8.26 (t, 1H, J = 1.5 Hz), 7.95–7.8 (m, 2H), 7.4 (m, 1H), 3.96 (s, 3H), 3.44 (m, 2H), 2.66 (m, 2H), 1.98 (m, 4H) ppm.

Methyl 3-(2-Oxo-1-piperidinyl)benzoate. Methyl 3-[(5-bromopentanoyl)amino]benzoate (1.50 g, 4.88 mmol) was taken up in dry DMF (40 mL) and treated with NaH (160 mg, 80% dispersion in oil, 5.33 mmol) at 0 °C. The mixture was stirred at room temperature under nitrogen for 10 min, KI (80 mg) was added, and the mixture was heated at 70 °C for 4 h. The mixture was evaporated and partitioned between EtOAc and 1 M HCl. The organic portion was washed with 5% $KHCO_3$ and brine, filtered (Whatman 1 PS phase separator), and evaporated. The residue was chromatographed (eluant 2% MeOH in EtOAc) to provide the title compound as a colorless oil (640 mg, 56%): ^{1}H NMR (270 MHz, $CDCl_3$) δ 8.1–7.95 (m, 2H), 7.60–7.50 (m, 2H), 3.98 (s, 3H), 3.75 (m, 2H), 2.64 (m, 2H), 2.03 (m, 4H) ppm.

3-(1-Piperidinyl)benzoic Acid. Methyl 3-(2-oxo-1-piperidinyl)benzoate (640 mg, 2.75 mmol) was dissolved in dry THF (30 mL), and borane–tetrahydrofuran complex (5 mL, 1 M solution in THF) was added. The mixture was stirred under nitrogen at reflux for 1 h, then cooled, and evaporated. The residue was taken up in MeOH/acetic acid (6/1, v/v, 70 mL) and heated at reflux for 3 h, then evaporated, and chromatographed (eluant 10% EtOAc in hexane) to provide the methyl ester of the title compound as a colorless oil (540 mg, 90%): ^{1}H NMR (270 MHz, $CDCl_3$) δ 7.59 (t, 1H, J = 1.5 Hz), 7.46 (dd, 1H, J_1 = 8 Hz, J_2 = 1.5 Hz), 7.28 (t, 1H, J = 8 Hz), 7.11 (m, 1H), 3.89 (s, 3H), 3.18 (m, 4H), 1.75–1.62 (m, 4H), 1.61–1.55 (m, 2H) ppm. The oil was dissolved in dioxane (12 mL) and water (8 mL). LiOH·H_2O (300 mg, 7.143 mmol) was added, and the mixture was stirred at 40 °C for 1 h, then acidified with acetic acid, evaporated, and azeotroped with toluene. The residue was chromatographed on silica (eluant 60:40:2, EtOAc/hexanes/AcOH, v/v/v) to provide the title compound as a colorless solid (450 mg, 90%): ^{1}H NMR (270 MHz, $CDCl_3$) δ 7.66 (s, 1H), 7.54 (d, 1H, J = 8 Hz), 7.32 (t,

1H, J = 8 Hz), 7.17 (dd, 1H, J_1 = 8 Hz, J_2 = 1.5 Hz), 3.22 (m, 4H), 1.72 (m, 4H), 1.61 (m, 2H) ppm.

3-[(*tert*-Butyloxycarbonyl)amino]benzoic Acid. 3-Aminobenzoic acid (24.69 g, 180 mmol) was taken up in 2 M KOH (180 mL) and dioxane (180 mL) and treated with di-*tert*-butyl dicarbonate (53.03 g, 243 mmol) at room temperature overnight. Dioxane was removed by evaporation, and the solution was diluted with 1 M KOH (300 mL). The aqueous portion was washed with ether (200 and 300 mL) and acidified to pH 4 with concentrated HCl. The resultant white precipitate was collected by filtration, washed with water, and dried *in vacuo* (P_2O_5) to give the title compound (38.97 g, 91%): ^{1}H NMR (90 MHz, DMSO-d_6) δ 9.52 (br s, 1H), 8.13 (m, 1H), 7.7–7.3 (m, 3H), 1.49 (s, 9H) ppm.

3-[N-(*tert*-Butyloxycarbonyl)methylamino]benzoic Acid. Sodium hydride (18.33 g, 60% dispersion in oil, 458.3 mmol) was added portionwise to a solution of 3-[(*tert*-butyloxycarbonyl)amino]benzoic acid (43.48 g, 183.3 mmol) in DMF (600 mL) below 10 °C, and the mixture was allowed to warm to room temperature with stirring over 1 h. MeI (84.54 g, 595.6 mmol) was added dropwise to the solution over 30 min at 5 °C, and the mixture was stirred at room temperature for 2 h. The mixture was evaporated, and the residue was partitioned between EtOAc (1.2 L) and water (600 mL). The organic portion was washed with saturated $NaHCO_3$ (100 mL) and water (5 × 200 mL), dried (Mg_2SO_4), and evaporated. The residual oil was taken up in methanol (1 L), 1 M LiOH (185 mL) was added to the solution at 5 °C, and the mixture was stirred at room temperature for 12 h. A further portion of 1 M LiOH (90 mL) was added, and the mixture was stirred for 1 h. The solution was concentrated to remove methanol, diluted with water and washed with EtOAc/hexane (1:2, v/v, 300 and 150 mL). The aqueous portion was acidified to pH 4 with concentrated HCl and extracted with EtOAc (400 and 200 mL). The combined organic portions were washed with brine, dried ($MgSO_4$), and evaporated. The residue was recrystallized from EtOAc/hexane (1:20 v/v, 420 mL) to give the title compound (36.08 g, 78%): ^{1}H NMR (90 MHz, $CDCl_3$) δ 8.0–7.9 (m, 2H), 7.5–7.4 (m, 2H), 3.31 (s, 3H), 1.47 (s, 9H) ppm.

3-[*N*-(*tert*-Butyloxycarbonyl)methylamino]phenyl Isocyanate. Et_3N (3.71 g, 36.7 mmol) and a solution of ethyl chloroformate (4.31 g, 39.7 mmol) in acetone (10 mL) were successively added dropwise to a solution of 3-[*N*-(*tert*-butyloxycarbonyl)methylamino]benzoic acid (8.0 g, 31.8 mmol) in acetone (64 mL) below 5 °C. After the solution was stirred for 30 min, a solution of NaN_3 (3.1 g, 47.7 mmol) in water (10 mL) was added below 5 °C. The mixture was stirred at the same temperature for a further 1 h and then poured into toluene (80 mL) and water (160 mL). The organic portion was washed with brine, refluxed for 2 h, and evaporated. The residue was distilled (100–105 °C/0.9–1.0 mmHg) to afford the title compound (6.2 g, 78%) as a yellow oil.

3-(Dimethylamino)phenyl Isocyanate. 3-(Dimethylamino)benzoic acid (350 g, 2.12 mol) was dissolved in acetone (2.8 L). Et_3N (249 g, 2.46 mol) was added dropwise to the solution below 10 °C, followed by the addition of a solution of ethyl chloroformate (287 g, 2.65 mol) in acetone (875 mL) below 5 °C. After the mixture was stirred for 30 min, a solution of NaN_3 (201 g, 3.18 mol) in water (570 mL) was added dropwise below 5 °C. The reaction mixture was stirred at 0–5 °C for a further 1 h and then poured into toluene–ice water (2:3, 11 L). The aqueous portion was extracted with a small amount of toluene, and the combined organic portions were washed with water and brine and dried ($MgSO_4$). After $MgSO_4$ was removed by filtration, the filtrate was added dropwise to hot toluene (1.5 L). The mixture was refluxed for 1 h and then evaporated, and the residue was distilled (0.6–0.8 mmHg, 74–77 °C) to afford the isocyanate (252 g, 74%) as a pale yellow oil.

(*RS*)-3-[(Benzyloxycarbonyl)amino]-2,3-dihydro-5-(2-pyridyl)-1*H*-1,4-benzodiazepin-2-one (11b). 3b[17] (660 mg, 3.33 mmol) and **9**[19] (1.63 g, 5 mmol) were mixed together in DCM (30 mL) at 0 °C under nitrogen. Water soluble carbodiimide (EDC, 1 g, 5 mmol) and DMAP (30 mg) were added, and the mixture was stirred at 0 °C for 10 min and at room temperature for 10 min. The resulting pale brown solution was poured into a mixture of 5% $KHCO_3$ (100 mL) and EtOAc (150 mL). The organic portion was washed with 5% $KHCO_3$, water, and brine, dried, and evaporated. (The intermediate **10b** could be isolated at this stage by chromatography on silica (eluant 55% EtOAc in hexanes) to provide the pure compound as a yellow oil in 93% yield: ^{1}H NMR ($CDCl_3$, 270 MHz) δ 11.65 (br s, 1H), 8.54 (d, 1H, J = 5.5 Hz), 8.50 (d, 1H, J = 8 Hz), 8.03 (d, 1H, J = 8 Hz), 7.75 (m, 3H), 7.5–7.08 (m, 12H), 6.98 (br m, 1H),; 5.05 (m, 2H) ppm.) The resultant crude product was treated with an ice-cold saturated solution of ammonia in methanol (30 mL), and the mixture was stoppered and stirred at room temperature for 1 h, then cooled, and evaporated. The residue was treated with a solution of ammonium acetate in acetic acid (0.1 g/mL, 30 mL) at room temperature for 1 h. The mixture was evaporated and partitioned between $CHCl_3$ and 1 M NaOH. The organic portion was washed with brine, dried, and evaporated, and the product was crystallized from EtOAc/hexane. The product was recrystallized from EtOAc/hexane to afford the title compound as a colorless solid (1.01 g, 79%): ^{1}H NMR ($CDCl_3$, 270 MHz) δ 9.0 (br s, 1H), 8.60 (d, 1H, J = 6 Hz), 8.07 (d, 1H, J = 8 Hz), 7.82 (dt, 1H, J_t = 8 Hz, J_d = 1 Hz), 7.4–7.2 (m, 9H), 6.98 (d, 1H, J = 8 Hz), 6.65 (d, 1H, J = 8 Hz), 5.37 (d, 1H, J = 8 Hz), 5.16 (m, 2H) ppm.

(*RS*)-3-[(Benzyloxycarbonyl)amino]-1-[(*tert*-butylcarbonyl)methyl]-2,3-dihydro-5-(2-pyridyl)-1*H*-1,4-benzodiazepin-2-one (12b). 11b (7.3 g, 18.9 mmol) was taken up in dry DMF (73 mL) at 0 °C. Sodium hydride (740 mg, 80% dispersion in oil, 1.3 equiv) was added portionwise keeping the internal temperature below 5 °C, and the mixture was stirred at room temperature 1 h. The mixture was recooled to 0 °C, and 1-bromopinacolone (10.21 g, 57 mmol) was added dropwise keeping the internal temperature below 10 °C, and stirring was continued at room temperature for a further 1 h. The mixture was evaporated, taken up in DCM (73 mL), and washed with 5% $NaHCO_3$ and brine. The organic portion was evaporated and recrystallized from EtOAc/hexane (1:1 v/v, ca. 150 mL) to provide the title compound as a white solid (7.31 g, 80%): ^{1}H NMR ($CDCl_3$, 270 MHz) δ 8.60 (d, 1H, J = 4 Hz), 8.14 (d, 1H, J = 8 Hz), 7.80 (dt, 1H, J_t = 7.5 Hz, J_d = 1.5 Hz), 7.50 (dt, 1H, J_t = 8.5 Hz, J_d = 1.5 Hz), 7.4–7.2 (m, 8H), 7.11 (d, 1H, J = 8 Hz), 6.72 (d, 1H, J = 8 Hz), 5.51 (d, 1H, J = 8 Hz), 5.12 (m, 2H), 5.0 (d, 1H, J = 17.8 Hz), 4.48 (d, 1H, J = 17.8 Hz), 1.25 (s, 9H) ppm; ^{13}C NMR ($CDCl_3$, 67.8 MHz) δ 208.2 (q), 166.7 (q), 166.2 (q), 155.7 (q), 148.6 (CH), 142.1 (q), 136.7 (CH), 136.2 (q), 132.0 (CH), 130.9 (CH), 128.4 (CH), 128.0 (CH), 124.8 (CH), 124.7 (CH), 124.3 (CH), 124.2 (q), 121.6 (CH), 68.8 (CH), 66.8 (CH_2), 54.2 (CH_2), 43.4 (q), 26.3 (CH_3) ppm.

(*RS*)-3-Amino-1-[(*tert*-butylcarbonyl)methyl]-2,3-dihydro-5-(2-pyridyl)-1*H*-1,4-benzodiazepin-2-one (13b). 12b (2.45 g, 5.12 mmol) was taken up in DCM (100 mL) at 0 °C, and the solution was saturated with dry HBr gas. The mixture was then stoppered and stirred at 0 °C for 4 h. EtOAc (100 mL) was then added, and the ice-cold mixture was filtered. The resultant hygroscopic pale yellow solid was washed well with EtOAc and then taken up in water (200 mL) and washed with ether (50 mL). The aqueous portion was basified with 5% $KHCO_3$ to pH 8 and extracted with chloroform (3 × 100 mL). The combined chloroform extracts were washed with brine, dried, and evaporated to give a near colorless foam (1.68 g, 93%): TLC (E. Merck; Kieselgel silica plates) single spot, R_f = 0.25 (eluant $CHCl_3$/MeOH/AcOH, 20:2:1, v/v/v); ^{1}H NMR ($CDCl_3$, 270 MHz) δ 8.62 (d, 1H, J = 5 Hz), 8.18 (d, 1H, J = 8 Hz), 7.80 (dt, 1H, J_t = 8 Hz, J_d = 1 Hz), 7.48 (dt, 1H, J_t = 8 Hz, J_d = 1 Hz), 7.37 (m, 2H), 7.20 (t, 1H, J = 8 Hz), 7.09 (d, 1H, J = 8 Hz), 5.07 (d, 1H, J = 18 Hz), 4.66 (s, 1H), 4.45 (d, 1H, J = 18 Hz) ppm; ^{13}C NMR ($CDCl_3$, 67.8 MHz) δ 208.9 (q), 169.9 (q), 155.9 (q), 148.8 (CH), 142.5 (q), 136.7 (CH), 131.8 (CH), 130.5 (CH), 128.7 (q), 124.5 (CH), 124.3 (CH), 124.1 (CH), 124.4 (CH), 70.4 (CH), 54.1 (CH_2), 44.0 (q), 26.4 (CH_3) ppm.

Attempted Racemization–Resolution of 13b. Crude **13b** (380 mg, 1.056 mmol) was taken up in MeCN (4 mL) and treated with (*S*)-mandelic acid (170 mg, 1.2 mmol). 3,5-Dichlorosalicaldehyde (10 mg) was added to the stirring mixture, and the mixture was cooled to 0 °C. Precipitation was observed, and stirring was continued at 0 °C overnight.

The resultant white solid was collected by filtration and washed with small portions of cold MeCN to provide the mandelate salt of **8** (304 mg, 58%). A portion of the salt (156 mg, 0.311 mmol) was partitioned between 5% $KHCO_3$ and $CHCl_3$ and the organic portion was washed with brine, filtered (Whatman 1 PS phase separator), and evaporated to give the free amine of **8** (110 mg, 98%). The analytical data for the free amine was identical to that described above for **8**.

Optical Resolution of 3-Amino-1-[(*tert*-butylcarbonyl)-methyl]-2,3-dihydro-5-(2-pyridyl)-1*H*-1,4-benzodiazepin-2-one (13b) by Fractional Crystallization. Crude **13b** (14 g, 40 mmol) was taken up in acetonitrile (50 mL) at −5 °C. (*R*)-Mandelic acid (3.2 g, 21 mmol) was added, and the mixture was stirred at −5 °C. A thick precipitate was formed, and acetonitrile (20 mL) was added dropwise to enable easier filtration. After 1 h at −5 °C the mixture was filtered and washed with small portions of cold MeCN. The resultant white precipitate was recrystallized from MeCN. (Anal. for mandelate salt ($C_{28}H_{30}N_4O_5 \cdot 0.5H_2O$) C, H, N.) The salt was partitioned between 5% $KHCO_3$ and $CHCl_3$, and the organic portion was washed with brine and filtered (Whatman 1 PS phase separator) to give the free (*R*)-amine (4.42 g, 32%): $[\alpha]_D$ = +212.6° (c = 0.715, $CHCl_3$); ^1H NMR and ^{13}C NMR data were identical to those for the racemic compound.

The filtrate from above was washed with base and taken up in MeCN (30 mL). Addition of (*S*)-mandelic acid afforded the (*S*)-amine salt in a similar manner. This was recrystallized from MeCN and washed with base to provide the free (*S*)-amine (3.87 g, 28%): $[\alpha]_D$ = −213.4° (c = 0.671, $CHCl_3$).

(*RS*)-3-[(Benzyloxycarbonyl)amino]-2,3-dihydro-5-phenyl-1*H*-1,4-benzodiazepin-2-one (11a). The title compound was prepared from 2-aminobenzophenone and (benzyloxycarbonyl)(1-benzotriazolyl)glycine as described above for **11b** in 79% yield. Analytical data were identical to literature values.[14]

Preparation of (*RS*)-3-[(Benzyloxycarbonyl)amino]-1-[(*tert*-butylcarbonyl)methyl]-2,3-dihydro-5-phenyl-1*H*-1,4-benzodiazepin-2-one (12a). The title compound was prepared by alkylation of **11a** with 1-bromopinacolone as described above for **12b** in 86% yield: ^1H NMR ($CDCl_3$, 270 MHz) δ 7.8−7.2 (m, 14H), 6.74 (d, 1H, J = 8 Hz), 5.53 (d, 1H, J = 8 Hz), 5.23 (s, 2H), 5.05 (d, 1H, J = 18 Hz), 4.77 (d, 1H, J = 18 Hz), 1.33 (s, 9H) ppm.

Preparation of (*RS*)-3-Amino-1-[(*tert*-butylcarbonyl)-methyl]-2,3-dihydro-5-phenyl-1*H*-1,4-benzodiazepin-2-one (8a). The title compound was prepared from **12a** by hydrogenolysis of the benzyl carbamate group in essentially quantitative yield as previously described:[16] ^1H NMR ($CDCl_3$, 270 MHz) δ 7.60 (d, 2H, J = 8 Hz), 7.5−7.0 (m, 7H), 4.96 (d, 1H, J = 17 Hz), 4.55 (m, 3H), 2.82 (br s, 2H), 1.18 (s, 9H) ppm.

Resolution of 3-Amino-1-[(*tert*-butylcarbonyl)methyl]-2,3-dihydro-5-phenyl-1*H*-1,4-benzodiazepin-2-one (13a) by Resolution−Racemization Procedure. 13a was resolved using minor modifications to the resolution−racemization procedure previously described.[11,21] Racemic **13a** (7.7 g, 22.95 mmol) was taken up in acetonitrile (20 mL) at −5 °C, and (*S*)-mandelic acid (3.44 g, 22.63 mmol) was added to the stirred solution, followed 30 min later by 3,5-dichlorosalicaldehyde (65 mg). After the mixture was stirred overnight at −5 °C, the resultant precipitate was collected by suction filtration, washed with small portions of cold acetonitrile and ether, and recrystallized from acetonitrile to give the (*S*)-mandelate salt of the (*R*)-isomer title compound as a white solid (6.70 g, 59%). A portion of this solid (460 mg, 0.897 mmol) was partitioned between $CHCl_3$ and 0.5 M NaOH. The organic portion was washed with brine, filtered (Whatman 1PS phase separator), and evaporated to provide the title compound as a colorless foam (^1H NMR identical to racemate). The chiral integrity of the amine was examined by coupling to Boc-Phe-OH using water soluble carbodiimide/HOBT in DMF. Analytical HPLC (Spherisorb C-18, 4.6 × 100 mm, 5 μm column, linear gradient of 40−90% 0.1%TFA/acetonitrile in 0.1%TFA/water, flow rate 0.8 mL/min) of the crude product showed only a single diasteromer peak at 17.7 min, whereas the racemic amine produced a 1:1 mixture of diastereomers under the same conditions (retention times 17.4 and 17.7 min).

General Procedures for the Preparation of 3-Amino-1-[(*tert*-butylcarbonyl)methyl]-2,3-dihydro-1*H*-1,4-benzodiazepin-2-one Urea Derivatives (14 or 15). Procedure A. Reaction of the Amine and the Pure Isocyanate. The required 3-amino-2,3-dihydro-1*H*-1,4-benzodiazepin-2-one (1 mmol) was taken up in DCM (25 mL) at 0 °C. To this solution was added the pure isocyanate (1.02 mmol, either from commercial sources or prepared as described above), and stirring was continued at room temperature for 2 h. The solvent was evaporated *in vacuo*, and the crude product was purified by flash chromatography on silica. Compounds **14a**, **14c**, **14d**, **14h**, **15a**, **15d**, and **15e** were prepared using this general method.

Procedure B. Reaction of the Amine and the Isocyanate Prepared *in Situ* from the Benzoic Acid. To a solution of the requisite benzoic acid (3 mmol, either from commercial sources or prepared as described above) in toluene (5 mL) was added diphenyl phosphoazidate (825 mg, 3 mmol) and Et_3N (303 mg, 3 mmol). The mixture was stirred at room temperature for 2 h, heated at reflux for 3 h, and cooled to 0 °C. A solution of the required 3-amino-2,3-dihydro-1*H*-1,4-benzodiazepin-2-one (1 mmol) in toluene (5 mL) was added, and the mixture was stirred at room temperature overnight, then evaporated, taken up in EtOAc, washed with 5% $KHCO_3$, H_2O, and brine, filtered (Whatman 1PS phase separator), and evaporated, and the crude product was purified by flash chromatography on silica. Compounds **14e**, **14i**, **14j**, **15f**, **15g**, and **15h** were prepared using this general method.

Specific Procedures for the Preparation of Urea Derivatives (14 or 15). *N*-[(3*RS*)-1-[(*tert*-butylcarbonyl)-methyl]-2,3-dihydro-2-oxo-5-phenyl-1*H*-1,4-benzodiazepin3-yl]-*N*'-(3-carboxyphenyl)urea (14b). (*RS*)-**13a** (600 mg, 1.72 mmol) was taken up in dry THF (8 mL) and Et_3N (0.26 mL, 1.9 mmol) and the solution cooled to 0 °C. The mixture was treated with a solution of *p*-nitrophenyl chloroformate (0.38 g, 1.9 mmol) in THF (4 mL), stirred at room temperature for 1 h, evaporated, and chromatographed (eluant EtOAc/hexane, 60:40, v/v) to provide an off-white solid (670 mg, 76%). The solid was taken up in DMF (10 mL) and *m*-aminobenzoic acid (245 mg, 1.75 mmol) added. The mixture was stirred at 45 °C for 18 h, cooled, and evaporated, and the residue was chromatographed (eluant EtOAc/hexane/AcOH, 60:40:2 v/v/v). The title compound was isolated as a colorless solid by recrystallization from acetonitrile (328 mg, 49%).

(3*R*)-*N*-[1-[(*tert*-Butylcarbonyl)methyl]-2,3-dihydro-2-oxo-5-phenyl-1*H*-1,4-benzodiazepin-3-yl]-*N*'-(3-aminophenyl)urea (14f). 14e (700 mg, 1.37 mmol) was taken up in acetone (10 mL) and treated with 4 M HCl at room temperature for 62 h. The mixture was partially evaporated to remove the acetone and partitioned between DCM and 5% $KHCO_3$. The organic portion was washed with brine, dried ($MgSO_4$), and evaporated. The residue was chromatographed on silica (eluant $CHCl_3$/MeOH/AcOH, 100:2:1, v/v/v), and the title compound was recrystallized from acetonitrile to provide a colorless solid (320 mg, 48%).

(3*R*)-*N*-[1-[(*tert*-Butylcarbonyl)methyl]-2,3-dihydro-2-oxo-5-phenyl-1*H*-1,4-benzodiazepin-3-yl]-*N*'-[3-(methylamino)phenyl]urea (14g). (3*R*)-*N*-[1-[(*tert*-Butylcarbonyl)-methyl]-2,3-dihydro-2-oxo-5-phenyl-1*H*-1,4-benzodiazepin-3-yl]-*N*'-[3-(*N*-formylmethylamino)phenyl]urea was prepared from (*R*)-**13a** and 3-(*N*-formylmethylamino)benzoic acid using general procedure B, and the product was partially purified by chromatography (eluant 75% EtOAc in hexane; 960 mg, 65%). The residue was taken up in acetone (15 mL) and the stirring solution treated with 4 M HCl at room temperature for 3 days. The mixture was partially evaporated to remove acetone, and the residue was partitioned between 5% $KHCO_3$ and DCM. The organic portion was washed with brine, filtered (Whatman 1PS phase separator), and evaporated, and the crude product was purified by flash chromatography on silica (eluant $CHCl_3$/MeOH/AcOH, 120:2:1, v/v/v). The title compound was isolated as a colorless solid by recrystallization from MeCN (400 mg, 45%).

(3*R*)-*N*-[1-[(*tert*-Butylcarbonyl)methyl]-2,3-dihydro-2-oxo-5-(2-pyridyl)-1*H*-1,4-benzodiazepin-3-yl]-*N*'-(3-aminophenyl)urea (15b). (3*R*)-*N*-[1-[(*tert*-Butylcarbonyl)methyl]-

2,3-dihydro-2-oxo-5-(2-pyridyl)-1*H*-1,4-benzodiazepin-3-yl]-*N'*-[3-[(*tert*-butyloxycarbonyl)amino]phenyl]urea was prepared from (*R*)-**13b** (850 mg, 2.43 mmol) and 3-[(*tert*-butyloxycarbonyl)amino]benzoic acid (1.19 g, 5 mmol) using general procedure B. The crude urea was taken up in DCM (10 mL) and treated with TFA (30 mL) at room temperature for 30 min under nitrogen. The mixture was evaporated and azeotroped with $CHCl_3$. The residue was partitioned between DCM and 5% $KHCO_3$, and the organic portion was washed with brine, dried ($MgSO_4$), and evaporated. The residue was chromatographed on silica (eluant 6% MeOH in EtOAc). The residue was taken up in 1:1 EtOAc/ether (40 mL) at −10 °C and treated dropwise with 4 M HCl in dioxane (0.5 mL). The mixture was stirred at −10 °C for 30 min, and the resultant precipitate was collected by filtration, washed with ether, and dried over NaOH to provide the hydrochloride salt of the title compound as a colorless solid (845 mg, 67%).

(3*R*)-*N*-[1-[(*tert*-Butylcarbonyl)methyl]-2,3-dihydro-2-oxo-5-(2-pyridyl)-1*H*-1,4-benzodiazepin-3-yl]-*N'*-[3-(methylamino)phenyl]urea (15c). 3-[*N*-[(*tert*-Butyloxycarbonyl)-methyl]amino]phenyl isocyanate (19.30 g, 77.7 mmol) was added dropwise to a solution of (*R*)-**13b** (27.19 g, 77.6 mmol) in DCM (200 mL) below 20 °C, and the mixture was stirred at room temperature for 30 min and then evaporated. The residue was taken up in EtOAc (200 mL) and water (100 mL), concentrated HCl (120 mL) was then added dropwise to the mixture below 20 °C, and the mixture was stirred for 3 h. The aqueous phase was separated, added to DCM (500 mL), and then basified to pH 10 with 20% NaOH while the temperature was maintained below 20 °C. The resultant organic portion was washed with brine (300 mL), and evaporated, and the residue was crystallized from ethanol. The resultant solid was recrystallized from ethanol (1.8 L) to provide the title compound as a white crystalline solid (27.30 g, 72%), mp 243−246 °C.

(3*R*)-*N*-[1-[(*tert*-Butylcarbonyl)methyl]-2,3-dihydro-2-oxo-5-(2-pyridyl)-1*H*-1,4-benzodiazepin-3-yl]-*N'*-[3-(dimethylamino)phenyl]urea Hydrochloride (15d·HCl). 15d (70 g, 136.6 mmol, prepared as described in general method A but not chromatographed) was taken up in ethanol (1 L), and 2.26 M HCl/ethanol (63.5 mL, 143.4 mmol) was added dropwise. The mixture was warmed to 50 °C to afford a clear solution, which was seeded, cooled to 0 °C, and stirred at the same temperature overnight. The resultant precipitate was collected by filtration to provide the title compound as a white crystalline solid (62.4 g, 82%), mp 181−184 °C.

Measurement of Binding Affinity for CCK-B/Gastrin Receptors. About 100 Sprague−Dawley (SD) rats were decapitated without anesthesia, the whole brain was immediately excised from each of the rats and homogenized in a 10-fold volume of 0.32 M aqueous solution of sucrose by the use of a Teflon-coated homogenizer, the homogenate thus obtained was centrifuged for 10 min at 900*g* by the use of a cooled centrifuge, and the supernatant was further centrifuged for 15 min at 11500g. The pellet thus obtained was dispersed in 50 mM Tris-HCl buffer (pH 7.4) containing 0.08% Triton X-100. This suspension was allowed to stand for 30 min and again centrifuged for 15 min at 11500*g*. The precipitate thus obtained was washed twice with 5 mM Tris-HCl buffer and twice with 50 mM Tris-HCl buffer in that order with centrifugal separation. The washed precipitate was suspended in 50 mM Tris-HCl buffer, and the suspension thus obtained was stored at −80 °C until the membrane preparation was required. For the assay the membrane preparations were warmed to room temperature, diluted with 10 mM HEPES buffer (containing 130 mM NaCl, 5 mM $MgCl_2$, 1 mM EDTA, and 0.25 mg/mL bacitracin; pH 6.5), incubated at 25 °C for 120 min in the presence of [^{125}I]BH-CCK-8 and the test compound (dissolved in DMSO), and then separated by suction filtration. Nonspecific binding was determined in the presence of 1 mM CCK-8. The amount of labeled ligand bound to the receptor was measured by the use of a γ-counter. IC_{50} values were determined, being that concentration of test compound required to inhibit specific binding by 50%.

Measurement of Binding Affinity for CCK-A Receptors. The pancreas of an SD rat was homogenized in a 20-fold volume of 50 mM Tris-HCl buffer (pH 7.7) by the use of a Polytrone-type homogeniser, the homogenate was twice centrifuged for 10 min at 50000*g* by the use of an ultracentrifuge, the pellet thus obtained was suspended in a 40-fold volume of 50 mM Tris-HCl buffer (containing 0.2% BSA, 5 mM $MgCl_2$, 0.1 mg/mL bacitracin and 5 mM DTT; pH 7.7), and the suspension was stored at −80 °C until the membrane preparations were required. The membrane preparations were then warmed to room temperature, diluted 1:10 with the buffer, and incubated at 37 °C for 30 min in the presence of [^{3}H]L-364, 718, and the test compound was then separated by suction filtration. Nonspecific binding was determined in the presence of 1 mM L-364,718. Test compounds were dissolved in DMSO. The amount of labeled ligand bound to the receptor was measured by the use of a liquid scintillation counter; IC_{50} values were determined, being that concentration of test compound required to inhibit specific binding by 50%.

Measurement of Inhibition of Pentagastrin-Stimulated Gastric Acid Secretion in Rats. A cannula was inserted into the trachea of a rat anesthetized with urethane (intraperitoneally administered, 1.25 g/kg), the abdominal wall was incised to expose the gastric and duodenal portions, and a polyethylene cannula was set in the anterior stomach after ligation of the cardia. The duodenum was then subjected to slight section, a polyethylene cannula was inserted from the incised portion toward the stomach, and the pylorus was ligated to fix the cannula. Physiological saline (with pH adjusted to 7.0) was perfused from the anterior stomach toward the pylorus at a rate of 3 mL/min, and the gastric acid secretion was measured by continuous titration of the perfusate by the use of a pH-stat (AUT-201; Toa Electronics, Ltd.). The continuous titration was carried out by using 25 mM NaOH solution until the pH reached 7.0, and the result was expressed as the amount of gastric acid secreted for every 10 min (mequiv/10 min). Pentagastrin was intravenously administered at a rate of 15 mg/kg/h. The secretion of gastric acid increased upon administration of pentagastrin, reaching the maximum level after 60 min, after which time the level was stably maintained. A test drug was then intravenously administered, and the secretion of gastric acid was measured. ED_{50} values were determined for some examples, this being the amount of the drug required to reduce the amount of secreted gastric acid down to 50% of the maximum level.

Measurement of Inhibition of Gastric Acid Secretion in Heidenhain Pouch Dogs. Male beagle dogs with Heidenhain pouch were used.[33] One month after preparation of the pouch, secretory experiments were performed once a week in each animal throughout the course of the investigation. Dogs were deprived of food for 18 h prior to experiments but allowed free access to water. A polyethylene tube was intubated through the femoral vein to infuse pentagastrin at a rate of 8 μmol/kg/h. Test compounds were administered po or iv at 3 h after the start of pentagastrin infusion. Gastric juice was collected every 15 min and the volume measured. The acidity of the gastric juice was measured by automatic titration with 0.05 N NaOH to pH 7.0. In the case of iv injection, test compounds were dissolved in DMF.

Supporting Information Available: Spectroscopic data for test substances (1 page). Ordering information is given on any current masthead page.

References

(1) Larsson, H.; Carlsson, E.; Junggren, U.; Olbe, L.; Sjostrand, S. E.; Skanberg, I.; Sundell, G. Inhibition of Gastric Acid Secretion by Omeprazole in the Dog and Rat. *Gastroenterology* **1983**, *85*, 900−907.

(2) Lind, T.; Cederberg, C.; Ekenved, G.; Haglund, U.; Olbe, L. Effect of Omeprazole - A Gastric Proton Pump Inhibitor - on Pentagastrin Stimulated Acid Secretion in Man. *Gut* **1983**, *24*, 270−276.

(3) Wallmark, B.; Larsson, H.; Humble, L. The Relationship between Gastric Acid Secretion and Gastric H^+,K^+-ATPase Activity. *J. Biol. Chem.* **1985**, *260*, 13681−13684.

(4) Betton, G. R.; Dormer, C. S.; Wells, T.; Pert, P.; Price, C. A.; Buckley, P. Gastric ECL-cell Hyperplasia and Carcinoids in Rodents Following Chronic Administration of H2-antagonists SK&F 93479 and Oxmetidine and Omeprazole. *Toxicol. Pathol.* **1988**, *16*, 288−298.

(5) Carney, J. A.; Go, V. L.; Fairbanks, V. F.; Moore, S. B.; Alpont, E. C.; Nora, F. E. The Syndrome of Gastric Argyrophil Carcinoid Tumors and Nonantral Gastric Atrophy. *Ann. Intern. Med.* **1983**, *99*, 761–766.
(6) Ekman, L.; Hansson, E.; Havu, N.; Carlsson, E.; Lundberg, C. Toxicological Studies on Omeprazole. *Scand. J. Gastroenterol.* **1985**, *20*, Suppl. 108, 53–69.
(7) (a) Brunner, G.; Lamberts, R.; Creutzfeldt, W. Efficacy and Safety of Omeprazole in the Long-term Treatment of Peptic Ulcer and Reflux Oesophagitis Resistant to Ranitidine. *Digestion* **1990**, *47*, Suppl. 1, 64–68. (b) Berlin, R. G. Omeprazole: Gastrin and Gastric Endocrine Cell Data from Clinical Studies. *Dig. Dis. Sci.* **1991**, *36*, 129–136.
(8) Lee, Y. M.; Beinborn, M.; McBride, E. W.; Lu, M.; Kolakowski, L. F.; Kopin, A. S. The Human Brain Cholecystokinin-B/Gastrin Receptor. *J. Biol. Chem.* **1993**, *268*, 8164–8169.
(9) Singh, P.; Owlia, A.; Espeijo, R.; Dai, B. Novel Gastrin Receptors Mediate Mitogenic Effects of Gastrin and Processing Intermediates on Swiss 3T3 Fibroblasts. Absence of Detectable Cholecystokinin (CCK)-A and CCK-B Receptors. *J. Biol. Chem.* **1995**, *270*, 8429–8438.
(10) Nishida, A.; Miyata, K.; Tsutsumi, R.; Yuki, H.; Akuzawa S.; Kobayashi. A.; Kamato, T.; Ito, H.; Yamano, M.; Katuyama, Y.; Ohta, M.; Honda, K. Pharmacological Profile of (R)-1-[2,3-Dihydro-1-{2′-methylphenacyl)-2-oxo-5-phenyl-1*H*-1,4-benzodiazepin-3-yl]-3-(3-methylphenyl)urea (YM022), a New Potent and Selective Gastrin/Cholecystokinin-B Receptor Antagonist *in Vitro* and *in Vivo*. *J. Pharmacol. Exp. Ther.* **1994**, *269*, 725–731.
(11) Satoh, M.; Kondoh, Y.; Okamoto, Y.; Nishida, A.; Miyata, K.; Ohta, M.; Mase T.; Murase, K. New 1,4-Benzodiazepin-2-one Derivatives as Gastrin/Cholecystokinin-B Antagonists. *Chem. Pharm. Bull.* **1995**, *43*, 2159–2167.
(12) Semple, G.; Ryder, H.; Kendrick, D. A.; Szelke, M.; Ohta, M.; Satoh, M.; Nishida, A.; Akuzawa S.; Miyata, K. Synthesis and Biological Activity of 1-Alkylcarbonylmethyl Analogues of YM022. *Bioorg. Med. Chem. Lett.* **1996**, *6*, 51–54.
(13) Semple, G.; Ryder, H.; Kendrick, D. A.; Szelke, M.; Ohta, M.; Satoh, M.; Nishida, A.; Akuzawa S.; Miyata, K. Synthesis and Biological Activity of 5 Hetoroaryl Benzodiazepines: Analogues of YM022. *Bioorg. Med. Chem. Lett.* **1996**, *6*, 55–59.
(14) Bock, M. G., DiPardo, R. M., Evans, B. E., Rittle, K. E., Veber,.D. F., Freidinger, R. M., Hirschfield, J.; Springer, J. P. Synthesis and Resolution of 3-Amino-1,3-dihydro-5-phenyl-2*H*-1,4-benzodiazepin-2-ones. *J. Org. Chem.* **1987**, *52*, 3232–3239.
(15) Zoller, U.; Ben-Ishai, D. Amidoalkylation of Mercaptans with Glyoxylic Acid Derivatives. *Tetrahedron* **1975**, *31*, 863–866.
(16) Bock, M. G., DiPardo, R. M., Evans, B. E., Rittle, K. E., Veber, D. F.; Freidinger, R. M. An Expedient Synthesis of 3-Amino-1,3-dihydro-5-phenyl-2*H*-1,4-benzodiazepin-2-one. *Tetrahedron Lett.* **1987**, *28*, 939–942.
(17) Semple,G.; Ryder, H.; Ohta, M.; Satoh, M. A Facile Large Scale Synthesis of Optically Active 3-Amino-5-(2 pyridyl) 1,4-benzodiazepin-2-one Derivatives. *Synth. Commun.* **1996**, *26*, 721–727.
(18) Sherrill, R. G.; Sugg, E. E. An Improved Synthesis and Resolution of 3-Amino-1,3-dihydro-5-phenyl-2*H*-1,4-benzodiazepin-2-ones. *J. Org. Chem.* **1995**, *60*, 730–734.
(19) Katritzky, A. R.; Urogdi, L.; Mayence, A. Benzotriazole Assisted Synthesis of Monoacyl Aminals and Their Peptide Derivatives. *J. Org. Chem.* **1990**, *55*, 2206–2214.
(20) Bock, M. G.; DiPardo, R. M.; Evans, B. E.; Rittle, K. E.; Whitter, W. L.; Garsky, V. M.; Gilbert, K. F.; Leighton, J. L.; Carson, K. L.; Mellin, E. C.; Veber, D. F.; Chang, R. S. L.; Lotti, V. J.; Freedman, S. B.; Smith, A. J.; Patel, S.; Anderson, P. S.; Freidinger, R. M. Development of 1,4-Benzodiazepine Cholecystokinin Type B Antagonists. *J. Med. Chem.* **1993**, *36*, 4276–4292.
(21) Reider, P. J.; Davis, P.; Hughes, D. L.; Grabowski, E. J. J. Crystallisation-Induced Assymetric Transformation: Stereospecific Synthesis of a Potent Peripheral CCK Antagonist. *J. Org. Chem.* **1987**, *52*, 955–957.
(22) Chang, R. S. L.; Lotti V. J. Biochemical and Pharmacological Characterization of an Extremely Potent and Selective Nonpeptide Cholecystokinin Antagonist. *Proc. Natl. Acad. Sci. U.S.A.* **1986**, *83*, 4923–4926.
(23) Lin, J. H.; Storey, D. E.; Chen, I.-W.; Xu, X. Improved Oral Absorption of L-365,260, A Poorly Soluble Drug. *Biopharm. Drug Disposit.* **1996**, *17*, 1–15.
(24) Chambers, M. S.; Hobbs, S. C.; Fletcher, S. R.; Matassa, V. G.; Mitchell, P. J.; Watt, A. P.; Baker, R.; Freedman, S. B.; Patel, S.; Smith, A. J. L-708,474: The C5-Cyclohexyl Analogue of L-365,260, a Selective High Affinity Ligand for the CCK-B/Gastrin Receptor. *Bioorg. Med. Chem. Lett.* **1993**, *3*, 1919–1924.
(25) (a) Showell, G. A.; Bourrain, S.; Neduvelil, J. G.; Fletcher, S. R.; Baker, R.; Watt, A. P.; Fletcher, A. E.; Freedman, S. B.; Kemp, J. A.; Marshall, G. R.; Patel, S.; Smith, A. J.; Matassa, V. G. High Affinity and Potent, Water-Soluble 5-Amino-1,4-benzodiazepine CCK-B/Gastrin Receptor Antagonists Containing a Cationic Solublizing Group. *J. Med. Chem.* **1994**, *37*, 719–721. (b) Showell, G. A.; Bourrain, S.; Fletcher, S. R.; Neduvelil, J. G.; Fletcher, A. E.; Freedman, S. B.; Patel, S.; Smith, A. J.; Marshall, G. R.; Graham, M. I.; Sohal, B.; Matassa, V. G. C5-Piperazinyl-1,4-benzodiazepines. Water Soluble, Orally Bioavailable CCK-B/Gastrin Receptor Antagonists. *Bioorg. Med. Chem. Lett.* **1995**, *5*, 3023–3026.
(26) Bock, M. G.; DiPardo, R. M.; Mellin, E. C.; Newton, R. C.; Veber, D. F., Freedman, S. B.; Smith, A. J.; Patel, S.; Kemp, J. A.; Marshall, G. R.; Fletcher, A. E.; Chapman, K. L.; Anderson, P. S.; Freidinger, R. M. Second-Generation Benzodiazepine CCK-B Antagonists. Development of Sub-nanomolar Analogues with Selectivity and Water Solubility. *J. Med. Chem.* **1994**, *37*, 722–724.
(27) Chambers, M. S.; Hobbs, S. C.; Graham, M. I.; Watt, A. P.; Fletcher, S. R.; Baker, R.; Freedman, S. B.; Patel, S.; Smith, A. J. Matassa, V. G. Potent, Selective Water-Soluble Bezodiazepine-Based CCK-B Receptor Antagonists that Contain Lipophilic Carboxylate Surrogates. *Bioorg. Med. Chem. Lett.* **1995**, *5*, 2303–2308.
(28) Lowe, J. A.; Drozda, S. E.; McLean, S.; Bryce, D. K.; Crawford, R. T.; Zorn, S.; Morrone, J.; Appleton, T. A.; Lombardo, F. A Water Soluble Benzazepine Cholecystokinin-B Receptor Antagonist. *Bioorg. Med. Chem. Lett.* **1995**, *5*, 1933–1936.
(29) Satoh, M.; Okamoto, Y.; Koshio, H.; Ohta, M.; Nishida, A.; Akuzawa, S.; Miyata, K.; Mase T.; Semple, G. Biological Activity of Analogues of YM022. Novel (3-Amino Substituted Phenyl)-urea Derivatives of 1,4-Benzodiazepin-2-one as Gastrin/Cholecystokinin-B Receptor Antagonists. *Chem. Pharm. Bull.* **1996**, *44*, 1412–1414.
(30) Takinami, Y.; Yuki, H.; Nishida, A.; Akuzawa, S.; Uchida, A.; Takemoto, Y.; Ohta, M.; Satoh, M.; Semple, G.; Miyata, K. (R) 1-[2,3-Dihydro-2-oxo-1-pivaloylmethyl-5-(2′-pyridyl)-1*H*-1,4-benzodiazepin-3-yl]-3-(3-methylaminophenyl) Urea (YF476) is a New Potent and Selective Gastrin/Cholecystokinin (CCK)-B Receptor Antagonist *In Vitro* and *In Vivo*. *Aliment. Pharmacol. Ther.*, 1996, in press.
(31) Fryer, R. I.; Schmidt, R. A.; Sternbach, L. H. Quinazolines and 1,4-Benzodiazepines XVII. Synthesis of 1,3-Dihydro-5-pyridyl-2*H*-1,4-benzodiazepine Derivatives. *J. Pharm. Sci.* **1964**, *53*, 264–268.
(32) van der Werth, A.; Lederer, F. German Patent No. 2,256,614, 1973.
(33) Heidenhain, R. *Pflugers Arch.* **1879**, *19*, 148.

JM960669+